THE PHYSICS OF PARTICLE SIZE ANALYSIS

A Conference arranged by
The Institute of Physics
and held in the University of Nottingham
from the 6 to 9 April, 1954

BRITISH JOURNAL OF
APPLIED PHYSICS

SUPPLEMENT NO. 3

LONDON
THE INSTITUTE OF PHYSICS
1954

BRITISH JOURNAL OF APPLIED PHYSICS

Editorial Note

In January 1952 Mr. R. L. Brown, of The British Coal Utilisation Research Association, informed the Board of The Institute of Physics that he and some of his colleagues felt that "the time may be ripe for a Conference to be convened on the measurement of particle size, particularly in the sub-sieve range." They believed that the fundamental physics behind the various techniques that had been developed in recent years required further consideration. Moreover, they knew that a number of different approaches to the problems had been made by different organizations and an exchange of views and experience would, they thought, be beneficial. The Board was in full agreement with these ideas and appointed an organizing Committee under the chairmanship of Mr. F. I. G. Rawlins; Mr. Brown was appointed Honorary Secretary of the Conference.

The Committee soon found that the interest in the subject was very wide, ranging over many industries, and decided to invite selected individuals "to prepare scientific papers containing original work which would almost certainly involve new experimental work before the Conference."

By permission of the Council, the Conference was held in the University of Nottingham from April 6–9, 1954. There were eight sessions and the papers are here presented in the same groups. At the Conference they were presented in summary only (advance proofs being available) or were taken as read, and the discussions were on the groups of papers corresponding to the Sessions (F and G being taken together). In this Supplement, however, I have as far as possible put the (edited) comments on each paper immediately after that paper together with the author's or authors' reply. Where, however, contributions do not specifically relate to any particular paper they are printed at the end of the relevant group of papers as "general discussion." Thus the discussion is not reported in the same order as it occurred and contributors who did not send in a copy of their remarks in writing are not reported. As the organizing Committee was unable, in the time available, to devise a complete system of agreed nomenclature and symbols for the subject, no serious attempt has been made to impose one.

Demonstrations of automatized particle counting and sizing machines were given during the Conference and a brief account of these will be found on p. S 210.

The Conference was opened by Professor Sir Geoffrey Taylor, who pointed out that the separation of particles was really a very old subject. "In fact," he said, "I suppose the oldest separation process is that in which the chaff is elutriated from the wheat." He pointed out that the scientific study of the processes now used on a large and growing scale in industry had, however, only started in recent years. Sir Geoffrey said that new and valuable contributions would be found in all the papers to be presented. From those concerned with automatic scanning processes for measurement of particle size, it was evident that great difficulties had been encountered and were being overcome, and considerable progress is reported in the papers. The discussion of the different approaches to the solution of these difficulties formed an

important feature of the Conference. In the course of his opening remarks, Sir Geoffrey also said: "There is to be a session devoted to that ever present and empirical but necessary subject of shape factors. The papers follow the lines one would expect. Shape factors are defined and a statistical examination of the distribution of these shape factors in ground coal, glass and dust is made. Another section deals with methods for determining the size of particles by their effect on transmitted or reflected light. Here the theories have gone a long way beyond the simple, but erroneous idea that each particle acts as an opaque obstacle according to the theory of geometrical optics. Two sessions are to deal with the reactions between particles and the surrounding fluid. One paper is, I think, a gallant effort on the part of a mathematician to descend into our arena of practical affairs. I think he should be encouraged to descend a little further still. Another paper is an interesting attempt to deal with the Stokes' diameter of an aggregate of spheres. The case when the aggregate is two spheres of different sizes is dealt with completely. Then there are some interesting papers on the flow of gas over finely divided solids."

All the papers submitted were refereed and a careful selection made, and I wish to record here the Institute's grateful thanks to the referees for the conscientious way in which they carried out their difficult task and to the authors for revising and even re-writing their scripts in accordance with referees' suggestions. It is a pleasure, once again, to place on record my thanks to the printers, Messrs. Unwin Brothers Ltd., The Gresham Press, for their help in producing the advance proofs in time for the Conference and for their co-operation in the production of this supplement. Its publication will, it is hoped, adequately record the present state of our knowledge of the underlying physics of the various methods of particle size analysis and serve to indicate the directions in which further work is most likely to succeed.

H. R. LANG
Secretary and Editor

The Institute of Physics, London
April 1954

CONTENTS

Session A. Relative motion of particles and fluids: size separation

Paper		*Page*
	Survey of the relative motion of particles and fluids. By P. G. W. HAWKSLEY, British Coal Utilisation Research Association	S 1
A.1.	The effective viscosity of suspensions. By Prof. G. J. KYNCH, D.I.C., Ph.D., University College of Wales, Aberystwyth	S 5
A.2.	The terminal velocity and structure of airborne aggregates of microscopic spheres. By V. TIMBRELL, B.Sc., A.R.C.S., D.I.C., Ph.D., Pneumoconiosis Research Unit	S 12
A.3.	Dust shadows below a cylinder containing a suction orifice and deposition of particles upon the cylinder. By C. N. DAVIES, D.Sc., F.Inst.P., and V. PEETZ, B.Sc., Medical Research Council	S 17
A.4.	A comparison of methods for particle size analysis. By B. A. JARRETT, Ph.D., A.M.I.Mech.E., and H. HEYWOOD, A.C.G.I., D.Sc., M.I.Mech.E., M.I.Chem.E., Imperial College of Science and Technology	S 21
A.5.	Theory of size classification of airborne dust clouds by elutriation. By W. H. WALTON, B.Sc., F.Inst.P., Scientific Department, National Coal Board	S 29
	General discussion on Session A	S 39

Session B. Relative motion of particles and fluids: molecular phenomena

B.1.	The measurement of surface area of finely divided solids by the flow of gases through them. By Prof. R. M. BARRER, D.Sc., Sc.D., F.R.I.C., F.R.S.E., University of Aberdeen	S 41
B.2.	An examination of the behaviour of adsorbed molecules by the flow of gases through microporous media. By Prof. R. M. BARRER, D.Sc., Sc.D., F.R.I.C., F.R.S.E., University of Aberdeen	S 49
B.3.	The flow of gases through packed beds of colloidal carbon blacks. By H. W. DAVIDSON, B.Sc., and B. M. TURK, Research Laboratories, The General Electric Co. Ltd., England	S 55
B.4.	Electroviscosity in dilute heterodisperse suspensions. By G. A. H. ELTON, Ph.D., F.R.I.C., Battersea Polytechnic, London, and F. G. HIRSCHLER, Ph.D., Deering Products Ltd.	S 60

Session C. Scattering and absorption of light by particles

	Survey of scattering and absorption of light by particles. By C. N. DAVIES, D.Sc., F.Inst.P., Medical Research Council	S 64
C.1.	Light scattering by polydisperse dust clouds. By J. MCK. ELLISON, B.A., Ph.D., Medical Research Council	S 66
C.2.	Photoextinction measurements on spherical particles. By P. C. LEWIS, B.Sc., and G. F. LOTHIAN, M.A., F.Inst.P., University College, Exeter	S 71
	General discussion on Session C	S 74

Session D. Particle shape factors

Paper		*Page*
D.1.	The shape of ground petroleum coke particles. By T. BEIRNE and J. M. HUTCHEON, B.Sc., Atomic Energy Research Establishment, Harwell	S 76
D.2.	The significance and application of shape factors in particle size analysis. By W. H. M. ROBINS, B.Sc., Scientific Department, National Coal Board	S 82
D.3.	The terminal velocity and size of airborne dust particles. By V. TIMBRELL, B.Sc., A.R.C.S., D.I.C., Ph.D., Pneumoconiosis Research Unit	S 86
D.4.	The relation between free-falling speed and particle size of airborne dusts. By R. J. HAMILTON, B.Sc., A.Inst.P., Scientific Department, National Coal Board	S 90
	General discussion on Session D	S 95

Session E. Visual counting and sizing of microscopic particles

E.1.	Inter-laboratory checks on the counting of coal dust particles on thermal precipitator slides. By J. F. HOLDSWORTH, M.A., F. HENLEY PRICE and R. C. TOMLINSON, D.I.C., M.A., Scientific Department, National Coal Board	S 96
E.2.	Factors in the design of a microscope eyepiece graticule for routine dust counts. By R. J. HAMILTON, B.Sc., A.Inst.P., J. F. HOLDSWORTH, M.A., and W. H. WALTON, B.Sc., F.Inst.P., Scientific Department, National Coal Board	S 101
E.3.	A particle-profile test strip for assessing the accuracy of sizing irregularly shaped particles with a microscope. By H. H. WATSON, B.Sc., F.Inst.P., and D. F. MULFORD, Suffield Experimental Station, Alberta	S 105
E.4.	The electron microscopy of airborne dusts. By J. CARTWRIGHT, Safety in Mines Research Establishment	S 109
	General discussion on Session E	S 120

Session F. Automatized counting and sizing: theory

	Survey of the automatic counting and sizing of particles. By W. H. WALTON, B.Sc., F.Inst.P., Scientific Department, National Coal Board	S 121
F.1.	Theory of particle sizing and counting by track scanning. By P. G. W. HAWKSLEY, British Coal Utilisation Research Association	S 125
F.2.	Some fundamental aspects of particle counting and sizing by line scans. By J. W. PHILLIPS, B.Sc., Scientific Department, National Coal Board	S 133

Session G. Automatized counting and sizing: photoelectronic machines

G.1.	A photoelectronic instrument for counting and sizing aerosol particles. By Prof. F. T. GUCKER, JR., Ph.D., and D. G. ROSE, M.A., Ph.D., University of Indiana	S 138
G.2.	The automatic size analysis of dust deposits by means of an illuminated slit. By L. LE BOUFFANT and J. L. SOULÉ, Centre d'Etudes et Recherches des Charbonnages de France	S 143
G.3.	The automatic counting of red blood cells. By E. H. COOKE-YARBOROUGH, M.A., A.M.I.E.E., and R. E. WHYARD, B.Sc., Atomic Energy Research Establishment, Harwell	S 147

Paper		*Page*
G.4.	Stages in the development of an arrested scan type microscopic particle counter. By H. A. DELL, A.R.C.S., D.I.C., Ph.D., The Mullard Research Laboratories	S 156
G.5.	Testing a counting machine. By R. J. COURSHEE, B.Sc., National Institute of Agricultural Engineering	S 161
G.6.	The design and construction of a photoelectronic scanning machine for sizing microscopic particles. By P. G. W. HAWKSLEY and J. H. BLACKETT, British Coal Utilisation Research Association; E. W. MEYER and A. E. FITZSIMMONS, Casella (Electronics) Ltd.	S 165
G.7.	An automatic system for obtaining particle size distributions with the aid of the flying spot microscope. By W. K. TAYLOR, M.Sc., University College, London	S 173
	General discussion on Sessions F and G	S 175

Session H. General

H.1.	The application of methods of particle size and surface area measurement to whiting. By G. E. BESSEY, M.Sc., F.R.I.C., and D. C. SOUL, B.Sc., A.R.I.C., A.R.C.S., British Whiting Research Laboratories	S 181
H.2.	A microscope method of measuring thicknesses of fine particles. By W. H. M. ROBINS, B.Sc., Scientific Department, National Coal Board	S 189
H.3.	Some methods of dispersing difficult powders. By M. G. HARWOOD, B.Sc., A.Inst.P., Philips Electrical Ltd.	S 193
H.4.	The adhesion of dust particles. By D. W. JORDAN, B.Sc., Medical Research Council	S 194
H.5.	The aggregation of aerosols. By Prof. J. M. DALLAVALLE, Sc.D., CLYDE ORR, JR., Ph.D., and B. L. HINKLE, Ph.D., The Georgia Institute of Technology	S 198
	General discussion on Session H	S 206

Summary of conference and concluding remarks

	By H. HEYWOOD, A.C.G.I., D.Sc., M.I.Mech.E., M.I.Chem.E., Imperial College of Science and Technology, London	S 209
	THE DEMONSTRATIONS	S 210
	Subject index	S 211
	Name index	S 215

INDEX TO THE PHYSICS OF PARTICLE SIZE ANALYSIS

SUBJECT INDEX

Absorption of light particles, scattering and S 64–S 75
Accuracy (*see also under* Errors *and* Statistical uncertainties)
, absolute S 152
check of microscope method of measuring thickness of fine particles with microscopic spheres S 191
of a particle sizing and counting machine, measuring the S 161
of counting S 99
of particle sizing and counting by eye S 161
of sizing irregularly shaped particles, particle-profile test strip for assessing the, with a microscope S 105
, some considerations of S 99, S 136
Adhesion of dust particles S 194
Adsorbed
films, concentration dependence of D_s in S 53
molecule S 45
molecules, examination of the behaviour of, by flow of gases through microporous media S 49
molecules, properties of, by the time-lag method S 50
Adzumi's method S 43
Aerosol particles, counting and sizing *see under* Particles, aerosol
Aerosols, aggregation of S 198
Aggregate, determination of the
structure of an S 13
terminal velocity of an S 13
Aggregates
, airborne, of microscopic sphere, terminal velocity and structure of S 12
, determination of frequency distribution of S 14
, mechanism of mutual adhesion of dust, to form S 194
, orientation of, during sedimentation S 14
Aggregation
, methods for evaluating S 20
of aerosols S 198
, re-definition of S 98
Airborne dust
particles, terminal velocity and size of S 86
samples, collection of S 109
Airborne dusts
, electron microscopy of S 109
, relation between free falling speed and particle size of S 90
Air permeability, determinations of specific surface of whitings by S 185
Approximations
, Mecke S 66
, Rayleigh-Gans S 66
Area
projected, determination of S 76
, surface *see under* Surface area
Arnell's equation S 44
Arrested scan type microscopic particle counter, stage in the development of an S 156
Aspiration of dust S 17
Automatic
, continuous, recording of size distribution of falling raindrops S 176
counting and size analysis of dust deposits by means of an illuminated slit S 143
counting and sizing machines, intermediate photography as an aid to S 175
counting and sizing of particles, survey of S 121
counting of neps in carded fibre webs S 178, S 210
counting of red blood cells S 147, S 210
particle counter S 210
particle size analysis of dust deposits, development of techniques for S 156
system for obtaining particle size distributions with the aid of the flying spot microscope S 173
Automatized counting and sizing:
photoelectronic machines S 138–S 180
theory S 121–S 137
Bahco analyser S 207
Beds, packed
, of colloidal carbon blacks, flow of gases through S 55
, permeability of S 4, S 55
Blood cells, red, automatic counting of S 147, S 210
Boddy's
crushing technique S 189, S 192
size analyser and concentration recorder S 118
Capillaries and microporous media, equations of flow in S 42
Capillary model and porous beds S 42, S 48
Carbon blacks, colloidal
, estimation of surface area of S 55
, flow of gases through packed beds of S 55
Carman-Arnell equation S 56, S 57, S 60
Centrifugal classifier S 207
Centrifuge cell design, recent development in S 39
Charge analysis, aerosol, apparatus, technique and results S 198
Checks, inter-laboratory, on the counting of coal dust particles, on thermal precipitator slides S 96
Chord intercept sizing S 162, S 210
Cloud
of opaque circular disks, Kirchhoff diffraction by S 69
settling, aspiration of S 17
Clouds, dust (*see under* Dust clouds)
, sedimenting, inertia-less, theorems relating to S 29
Coagulation S 62
Coal dust
, examination of S 91
particles on thermal precipitator slides, inter-laboratory checks on the counting of S 96
particles, photomicrographs of S 176
particles, shape factors of S 82
particles, size of S 92, S 172
Coarse particles: sieve residues S 181
Coke particles, the shape of ground petroleum S 76
Conifuge S 16, S 86, S 90
Construction
and performance of apparatus for measurement of surface area S 145
, design and, of photoelectronic scanning machine for sizing microscopic particles S 165
of apparatus for automatic counting of red blood cells S 149, S 210
Contamination, effects of S 63
Comparison and training of different observers S 96, S 105, S 106, S 108, S 119, S 163
Counter(s) particle *see under* Particle counter(s)
Counter, photoelectronic S 138, S 210
Counting
and sizing, aerosol particles, photoelectronic instrument for S 138
and sizing, automatized *see under* Automatized counting and sizing
and sizing, by frequency of interception S 135
and sizing, by line scans, some fundamental aspects of particle S 133
and sizing, by track scanning, theory of particle S 125
and sizing, of particles, photoelectronic machines for S 165
and sizing, of particles, survey of automatic S 121
and sizing, visual, of microscopic particles S 96
losses S 49
machine, testing a S 161
of particles S 78, S 96

Counting—*continued*
of particles, accuracy of S 99
of particles, comparison of optical and electron microscope methods S 109, S 112
, particle, compensation of errors in S 143
Counts
, routine dust, factors in the design of a microscope eyepiece graticule for S 101
, star, and particle, relation between S 177
Criteria of association S 135, S 157

Data, presentation of S 185
Demonstrations S 210
Densing, effect of, on permeability of carbon blacks S 58
Design
and construction of a photoelectronic scanning machine for sizing microscopic particles S 165
of a microscope eyepiece graticule for routine dust counts, factors in S 101
Diffusion surface *see under* Surface diffusion
Dispersing difficult powders, some methods of S 193
Doublets, experimental results on Stokes' diameter of S 15
Drop size distribution S 162
Dust(s) airborne *see under* Airborne dust(s)
Dust
clouds, airborne, theory of size classification by elutriation S 29
clouds, generation of S 87
clouds, motion under gravity of S 10
clouds, polydisperse, light scattering by S 66
clouds, types of, examined S 91
coal *see under* Coal dust
counts, routine, factors in the design of a graticule for S 101
deposits, automatic size analysis of, by means of an illuminated slit S 143
particles, adhesion of S 194
particles, airborne, terminal velocity and size of S 86
particles, detailed analysis of S 156
sampler, the gravitational terminal velocity S 12, S 86
sampling instruments, efficiency of S 194
shadows below a cylinder containing a suction orifice and deposition of particles upon the cylinder S 17
, test, preparation and properties of S 23, S 24
Dusts, asbestos, coal, cotton, rock, examination of S 91

Edge effects, elimination of S 123
Einstein equation S 61
Electrification and foreign vapours, influence on aggregation S 198
Electron microscopy of airborne dusts S 109
Electronic
circuits, of automatic blood cell counter S 150
system of photo-counter S 139, S 170
Electroviscosity in dilute heterodisperse suspensions S 60, S 62
Elliptical particles, extension to, of theoretical treatments for circular particles S 164
Elutriation
, air, methods of S 93, S 207
, continuous S 20
, theory of size classification of airborne dust clouds by S 29
Elutriators
, conical S 32
, cylindrical S 31
, horizontal S 33, S 37
, vertical S 30, S 38
Equation(s)
, Arnell S 44
, Carman-Arnell S 56, S 57, S 60
, consistency of S 8
, Einstein S 61
, Knudsen S 57
, Kozeny S 47, S 55, S 56, S 58
, Mie S 66
, of flow in capillaries and microporous media S 42
, permeability S 10
, Stokes-Navier S 6
, viscous, solution of S 6

Errors (*see also under* Accuracy *and* Statistical uncertainty)
due to indented edges S 175
involved in automatic blood cell counting and their minimization S 147
involved in particle counting by illuminated slit methods S 143
of analysis and measurement S 163
, particle counting, statistical compensation of S 143
, sampling S 168, S 179

Fick's Law S 42, S 49, S 53
Films, dilute adsorbed, lifetime of molecules in S 50
Flow
data, steady state, surface area determinations from S 43
experiments, measurement of the amount sorbed by S 51
in capillaries and microporous media, equations of S 42
Knudsen S 41, S 42, S 46, S 56
of gases through microporous media, examination of the behaviour of adsorbed molecules by the S 49
of gases through packed beds of colloidal carbon blacks S 55
of gases through them, measurement of surface area of finely divided solids by S 41
, orifice S 42
, Poiseuille S 41, S 42, S 44, S 46, S 56
, slip S 44
, steady state S 44, S 49
, streamline, with slip S 42
, surface S 41, S 60
, surface areas by, basis of further methods of measuring S 45
, transient S 44, S 45
, turbulent S 42
, viscous *see under* Viscous flow
Fluidization S 4
Fluid
motion in a suspension of particles *see under* Suspension of particles
, survey of relative motion of particles and S 1
Fluids, relative motion of particles and
: molecular phenomena S 41–S 63
: size separation S 1–S 40
Flying spot
arrested scan type particle sizer S 210
microscope, automatic system for obtaining particle size distributions with the aid of the S 173

G, statistical calculation of S 8
Gases, flow of *see under* Flow of gases
Graticule
for direct reading of particle thickness S 190
, globe and circle method S 105
Graticules
, comparison of S 103
, microscope eyepiece factors in the design of, for routine dust counts S 101
Guard spot S 122, S 135, S 161

Henry's Law S 45, S 49, S 50, S 53
Heterodisperse suspensions, dilute, electroviscosity in S 60

Irregularly shaped particles, a particle-profile test strip for assessing the accuracy of sizing, with a microscope S 105

Kirchhoff's diffraction theory S 66, S 67, S 69
Knudsen
equation S 57
flow *see under* Flow, Knudsen
Kozeny
constant S 48, S 49
equation S 47, S 55, S 56, S 58

Light scattering
and absorption of particles S 64–S 75
by polydisperse dust clouds S 66
by spheres S 66
techniques for assessing aggregation S 201

Machine
, counting, testing a S 161
, photoelectronic scanning, for sizing microscopic particles, design and construction of S 165

Magnetic materials, method of making microscopic slides with S 193
Manometer methods for particle size analysis, open and closed S 24
Mecke's approximation S 66
Membrane-coated cover glasses, preparation of S 110
Memory methods S 124, S 157, S 158, S 161
Meteorologists' techniques for collecting atmospheric aerosol S 120
Methods of particle size analysis
, comparative tests of equipment for S 24
, comparison of S 21, S 177, S 208
Methods of particle size analysis investigated:
air elutriation S 207
analysis of sedimentation velocities S 39
automatic *see under* Automatic counting and sizing
decanting S 22, S 24
"diver" glass S 21, S 24
"diver" roof S 21, S 24
electrical resistance S 23
electron microscope S 109
electrostatic S 176
extinction angle S 39
flow birefringence S 39
hydrometer S 22, S 24
individual S 135
manometric S 22, S 24
microscopic examination S 79, S 82, S 90, S 101, S 104, S 105
photoextinction S 24, S 207
pipette S 21, S 27
pipette (Andreasen) S 24, S 182
relation between optical and electron microscopic S 109
sedimentation S 39, S 40, S 207
statistical S 133
ultrasonic S 74
X-ray S 27, S 28
Microscope
blood count S 149
counts, relation between optical and electron S 109
eyepiece graticule for routine dust counts, factors in the design of S 101
, flying spot, automatic system for obtaining particle size distributions with the aid of the S 173
method of measuring thicknesses of fine particles S 189
methods of assessing aggregates S 201
particle-profile test strip for assessing the accuracy of sizing irregularly shaped particles with a S 105
Microscopic
particle counter, arrested scan type, stages in the development of S 156
particles, the design and construction of a photoelectronic scanning machine for sizing S 165
particles, visual counting and sizing of S 96–S 120
slides of difficult powders, methods of making S 193
spheres S 191
Microscopists, training of, in size analysis S 105, S 108
Microscopy, electron *see under* Electron microscopy
Microporous media
capillaries and equations of flow in S 42
, examination of the behaviour of adsorbed molecules by the flow of gases through S 49
Mie theory and equations. S 64, S 66, S 71, S 138, S 141
Molecular
phenomena: relative motion of particles and fluids S 41
streaming S 42
Molecules
, adsorbed *see under* Adsorbed molecules
, lifetime of, in dilute adsorbed films S 50

n, measurement of S 72
Nitrogen absorption, determination of specific surface of whiting by S 185
Notation *see under* Symbols, list of

Observers, comparison and training of S 96, S 105, S 108, S 119, S 163
Optical method of determining specific surface of whitings S 185
Orifice, suction, dust shadows below a cylinder containing a S 17

Packed beds *see under* Beds, packed
Packing
characteristics and shape constant, relation between S 80
spheres S 197
Particle
adhesion S 194, S 197
counter, arrested scan type microscopic, stages in the development of a S 156
counters, automatic S 210
counting errors S 143
counting and sizing *see under* Counting and sizing
density S 79
, effect of one, on velocity distribution S 8
exploration with arrested scan sizer, suggested methods of S 159
in uniform velocity gradient S 7
profile test strip for assessing accuracy of sizing of irregularly shaped particles with a microscope S 105
, projected area of a, determination of S 76
shape *see under* Shape, particle
, single, in an infinite fluid S 1
, single, in, a fluid of finite extent S 1
size, a function of ultimate or "equilibrium" electrification of aerosol particles S 205
size analysis by selective sampling S 19
size analysis, comparison of methods for S 21, S 208
size analysis errors, apart from instrumental S 23
size analysis, methods of *see under* Methods of particle size analysis
size analysis, shape factors in *see under* Shape factors
size analysis, training microscopists for S 105, S 108
size analysis, waveform for S 174
size and permeability relation for undensed carbon blacks S 55
size and shape, definitions of S 82
size and Stokes' diameter S 93
size and surface area measurement, the application of methods of, to whiting S 181
size distribution, effect of, on angular distribution of Rayleigh-Gans scattering S 68
size distributions with the aid of the flying spot microscope, automatic system of obtaining S 173
size of airborne dusts, relation between free falling speed and S 90
size of suspensions, and light scattering S 66
size, types of scattering measurements sensitive to S 66
trajectory characteristic k S 18
volume, determination of S 77
with a hole drilled through it S 7
Particles
, aerosol, photoelectronic instrument for counting and sizing S 138
, airborne dust, terminal velocity and size of S 86
and fluids, relative motion of: molecular phenomena S 41–S 63
and fluids, relative motion of: size separation S 1–S 40
and fluids, survey of the relative motion of S 1
, assessing the accuracy of sizing irregularly shaped S 105
, cloud of, in an infinite fluid S 2
, coal dust *see under* Coal dust particles
, coarse, sieve residues S 181
, counting of S 78, S 96
, deposition of, on a cylinder S 17
, fine, microscopic method of measuring thicknesses of S 189
, fluid motion in a suspension of *see under* Suspension of particles
, microscopic *see under* Microscopic particles
, non-circular, extension to, of methods based on frequency interception S 135
of all shapes, extension of flow equations to S 10
of given Stokes' diameter, mean weight of S 89
, scattering and absorption of light by S 64–S 75
, spherical, photoextinction measurements on S 71
, Stokes' diameter-frequency distribution of S 87

Particles—*continued*
, suspension(s) of *see under* Suspension(s) of particles
, total effect of, on velocity distribution S 8
, two, in a fluid of infinite extent S 2
Permeability
measurement, and surface area of pores, discussion of S 47
of packed beds S 4, S 55
Photoelectronic
instrument for counting and sizing aerosol particles S 138
machines, automatized counting and sizing S 138–S 180
scanning machine, comparison with visual sizing of coal particles S 172
scanning machine for sizing microscopic particles, design and construction of a S 165
scanning machine, performance of S 171
Photoextinction
equipment for particle size analysis S 24, S 207
measurements on spherical particles S 71
Photographic methods of assessing aggregation S 201
Photosedimentometer S 207
Poiseuille flow S 41, S 42, S 44, S 46, S 56
Pore
properties by Adzumi's method S 43
properties, time lag method of studying S 44
size and permeability, discussion of S 47
Pores, size distribution of, in a permeable packing S 48
Porosity
and permeability, relation between S 55
function S 58, S 60
Porous beds, capillary models and S 42, S 48
Powders, some methods of dispersing difficult S 193
Psychological aspects of particle counting S 108

Radon concentration, measurement of S 208
Raindrops, recording size distribution of falling S 176
Rayleigh-Gans
approximation S 66
scattering S 68
Respirability of particles S 90, S 92

Sampling
for electron microscope S 109
in still air S 207
, selective, by elutriation S 29
, selective, particle size analysis by S 19
Scanning
a line S 133, S 148
, arrested, technique S 156, S 158
by a double spot S 157
by a flat pencil of light, comparison of methods of S 143
by a flying spot S 157, S 173
by a path of finite width S 133
by a slit S 122, S 156, S 210
by a spot S 121, S 156
by mechanical oscillation of a microscope stage S 147
by television type raster S 173
, guard spot method S 122, S 135, S 161
, line S 167
machines, photoelectronic *see under* Photoelectronic scanning machines
methods of S 124, S 129, S 148
, track S 166
, track, theory of particle counting and sizing by S 125
Scan type microscopic particle counter, arrested, stages in the development of S 156
Scans, line, some fundamental aspects of particle counting and sizing by S 133
Scattering
and absorption of light by particles S 64–S 75
and absorption of light by particles: survey of S 64
, light, by polydisperse dust clouds S 67
measurements, types which are sensitive to particle size S 67
, Rayleigh-Gans S 66, S 68
Sedimentation
, Andreasen method S 182
, centrifugal S 182, S 187
meniscus, formation of a sharp S 60
, orientation of aggregates during S 14
, particle size distributions by S 182
, rapid routine analysis by S 21
rate measurements for assessing aggregation S 201
velocities S 39, S 60
Sedimenting inertia-less clouds, theorems relating to S 29
Settling cloud, aspiration of S 17
Shadow-casting S 82, S 92
Shape
constant and packing characteristics, relation between S 80
factors in different particle size groups, frequency distribution of S 85
factors in particle size analysis, significance and application of S 82
factors, particle S 76–S95, S 189
factors, particle, variation of S 83
of ground petroleum coke particles S 76
, particle S 2
, particle, physical characteristics and S 181
, quantitative definition of S 76
Shapes of aggregates, effect of electrification on S 198, S 205
Sieve
analysis S 181, S 187, S 188
residue determinations S 181, S 187
Signal generation and measurement S 162
Size
analysis, automatic, of dust deposits, by means of an illuminated slit S 143
analysis: scanning methods S 144
classification of airborne dust clouds by elutriation, theory of S 29
distribution S 145
distribution of coal particles: comparison of visual count and photoelectronic scanning machine S 165
distribution of falling raindrops S 176
distribution of pores in a permeable packing S 48
distribution, particle, by sedimentation S 182
distributions, particle, automatic system for obtaining, with the aid of the flying spot microscope S 173
of airborne dust particles, terminal velocity and S 86
, particle *see under* Particle size
range, micron, velocity of sedimentation of particles in the S 60
separation: relative motion of particles and fluids S 1–S 40
Sizer, particle
, chord intercept S 210
, flying spot, arrested scan type S 210
, slit scanning S 210
Sizing
, by intercept height S 123
, chord intercept S 162
, counting and *see under* Counting and sizing
irregularly shaped particles, assessing the accuracy of S 105
microscopic particles, design and construction of a photoelectronic machine for S 165
Slip-flow S 44
Slit
, illuminated, automatic size analysis of dust deposits by means of an S 143
scanning particles sizer S 210
Solid surfaces, mechanism of adhesion of dust to S 194
Solids, measurement of surface area of finely divided, by flow of gases through them S 41
Speed, free falling, and particle size of airborne dusts, relation between S 90
Sphere, velocity near a S 58
Spheres
, calculation of forces between S 194, S 197
, light scattering by S 66
, microscopic, terminal velocity and structure of airborne aggregates of S 12

Spheres—*continued*
, production of S 91
, refractive index of S 71
, water content of S 71
Spherical particles *see under* Particles, spherical
Spray
deposit measurements S 163
deposits, factors influencing the effectiveness of S 165
Stages in the development of an arrested scan type microscopic particle counter S 156
Star counting and particle counting, relation between S 177
Statistical
calculation of G S 8
uncertainties S 149 (*see also under* Errors *and* Accuracy)
Steady state flow data, surface area determinations from S 43
Stokes'
diameter and particle size S 93
diameter and projected diameter, relation between S 88, S 93
diameter-frequency distribution S 87
diameter, mean weight of particles of given S 89
diameter of doublets, experimental results on S 15
law S 7, S 39, S 184
law, simple derivation of S 5
–Navier equation S 6
Structure
of airborne aggregates of microscopic spheres, terminal velocity and S 12
of an aggregate, determination of the S 13
Sub-sieve analyses, general recommendations for S 26
Suction orifice, dust shadows below a cylinder containing a S 17
Summary of Conference S 209
Surface
area, construction and performance of an apparatus for the measurement of S 145
area determinations from steady state flow data S 43, S 49
area measurement, the application of methods of particle size and, to whiting S 181
area of colloidal carbons S 55
area of finely divided solids, the measurement of, by flow of gases through them S 41
area of particle and projected diameter, relation between S 177
areas by flow, basis of further methods of measuring S 45
areas by time lag method S 45
diffusion S 51–S 55
flow *see under* Flow, surface
Survey of the automatic counting and sizing of particles S 121
Suspension
, heterodisperse S 61
, homodisperse S 61
of particles, fluid motion in a S 7
of particles, viscous flow of a S 5
Suspensions
, dilute heterodisperse, electroviscosity in S 60
, effective viscosity of S 5
, settling of S 3
, uniform, preparation of S 72
Suspensions—*cantinued*
, viscosity of S 2, S 5
Symbols and notation S ii, S 41, S 49, S 55, S 126

Terminal velocity
and size of airborne dust particles S 86
and structure of airborne aggregates of microscopic spheres S 12
dust sampler, the gravitational S 12
of an aggregate, determination of S 13
Test
dust, preparation of S 24
dust, properties of S 23
strip, particle profile S 105
Testing a counting machine S 161
Tests of new photoelectronic counter S 141
Theory of
particle sizing and counting by track scanning S 125
size classification of airborne dust clouds by elutriation S 29
Thermal precipitator S 109
Thermal precipitator, slides, inter-laboratory checks on the counting of coal dust particles on S 196
Thicknesses of fine particles, microscopic method of measuring S 189
Time lag method
of studying pore properties S 44
, properties of adsorbed molecules by the S 50
, surface areas by S 45
Tortuosity factor S 45, S 47
Total scattering coefficient k, measurement of S 71
Track scanning *see under* Scanning, track

Ultrasonic technique for size analysis in sedimentation S 74

Vapours, foreign, influence on aggregation S 198
Velocity
distribution, effect of one particle on S 8
distribution, total effect of particles on S 8
near a sphere S 8
, terminal *see under* Terminal velocity
Viscosity
, effective S 8
of suspensions *see under* Suspension, viscosity of
Viscous
equations, solution of S 6
flow of suspensions of particles S 5
Visual count, comparison with photoelectronic scanning machine S 165
Volume, particle, determination of S 77

Whiting
application to methods of particle size and surface area measurement to S 181
, electron micrographs S 184
, particle size distribution, by sedimentation S 182
, presentation of size distribution data of S 185

NAME INDEX TO THE PHYSICS OF PARTICLE SIZE ANALYSIS

Abraham, R. P. S 197
Acton, R. A. *see under* Thompson, W.E.
Adler, C. R., Mark, A. M., Marshall, W. R., and Parent, R. J. S 165, S 173
Adzumi, H. S 41, S 43, S 47
Andreasen, A. H. M. S 74
Andreasen, A. H. M., Krebs, K., Dalsgaard-Pederson, N., Camradt-Petersen and Kjaer, B. S 183, S 186
Anrep J. S 100, S 118
Aoi, T. *see under* Tomotika, S.
Armitage, P. S 132, S 146
Armitage, P. *see under* Irwin, J. O.
Arnell J. C. S 41, S 47, S 56, S 59
Arnell, J. C. and Henneberry, G. O. S 58, S 60
Arnell, J. C. *see under* Carman, P. C.
Artemov, I. S. S 205, S 206
Arthur, J. R., Linnett, J. W., Raynor, E. J., and Sington, E. P. C. S 55, S 59, S 77, S 81
Aylward *see under* Davies

Bahco S 207
Barbier S 146
Bareford, C. F., and Dell, H. A. S 159
Barkas, W. W., S 54
Barker, O'Connor and Winder S 37
Barnes, M. D., and La Mer, V. K. S 143
Barnes, M. D. *see under* La Mer, V. K.
Barrer, R. M. S 41–S 55
Barrer, R. M., and Barrie, J. A. S 44–S 49, S 50, S 54
Barrer, R. M., and Grove, D. M. S 41, S 47, S 50, S 54. S 58, S 60
Barrer, R. M., Mackenzie, N., and MacLeod, D. S 41, S 47
Beadle, D. G. S 119

Beard, D. S. S 120
Behrens, D. J. *see under* Wolff, H. S.
Beirne, T., and Hutcheon, J. M. S 76, S 81
Beirne, T. *see under* Hutcheon, J. M.
Beischer, D. S 194, S 197
Berg, S. S 21, S 26
Berns, E. G. S 208
Bessey, G. E., and Soul, D. C. S 27, S 181, S 188
Biggs and MacMillan S 120
Birks, J. S 47
Blackett, J. H. *see under* Hawksley, P. G. W.
Blackett, J. H. *see under* Meyer, E.
Blankenstein, E. S 43, S 47
Boddy, R. G. H. B. S 118, S 189, S 191, S 192
Boring S 108
Bradburd, E. M. S 159
Bradley, R. S. S 194, S 197
Bricard, J. S 65
Brinkman, H. C. S 3, S 5, S 11
Brockelsby, C. F. *see under* Dell, H. A.
Bronowski, J. S 138, S 177
Brooks and Purcell S 47, S 49
Brown, Callaway S 184, S 186
Brown, G. S. *see under* Hazen, H. L.
Brown, J. F., and Skrebowski, J. K. S 27
Brunauer, S. S 41, S 47
Brunauer, S., Emmett, P. H., and Teller, E. S 185, S 186
Bueche, A. M. *see under* Debye, P.
Burgers, J. M. S 2, S 3, S 4, S 5, S 10
Busby, T. S. S 81

Callcott, T. G. S 117, S 187
Camradt-Petersen, E. *see under* Andreasen, A. H. M.
Carey, W. F., and Stairmand, C. J. S 186
Carman, P. C. S 41, S 47, S 49, S 53–S 59, S 81
Carman, P. C., and Arnell, J. C. S 43, S 44, S 47, S 56–S 59
Carman, P. C., and Malherbe, P. le R. S 50, S 54, S 58–S 60, S 185, S 186
Carman, P. C., and Raal, F. A. S 50, S 54
Carman, P. C. *see under* Kozeny, J.
Carpenter and Dietz S 187
Carslaw, H. S., and Jaeger, J. C. S 37
Cartwright, J. S 109, S 119
Caspersson, T. O. S 72, S 74
Cassell, H. M. S 65
Cawood, W. *see under* Patterson, H. S.
Cerf and Sheraga S 39, S 40
Chalker, W. R. *see under* Houghton, H. G.
Chamberlain, N. H. S 177, S 210
Chappel, F. P. *see under* Lothian, G. F.
Choate, S. P. *see under* Hatch, T.
Christiansen, E. B. *see under* Pettyjohn, E. S.
Chugunova, O. K. *see under* Radushkevich, L. V.
Clausing, P. S 42, S 47
Clyde Orr, Jr. *see under* DallaValle, J. M.
Colwill, D. J. S 193
Cooke-Yarborough, E. H. S 129, S 147, S 154, S 160
Cooke-Yarborough, E. H., and Whyard, R. E. S 122, S 147, S 165, S 173, S 210
Cooke-Yarborough, E. H., and Wolff, H. S. S 159
Cornell and Katz S 48, S 49
Courshee, R. J. S 100, S 122, S 161, S 165, S 173
Courshee, R. J. *see under* Trickett, E. S.
Coutts, J. R. H. S 27
Crofton, M. W. S 126, S 132
Cruise, A. J. *see under* Watson, H. H.
Cunningham, E. S 3, S 5
Czuber, E. S 126, S 132

DallaValle, J. M., Clyde Orr, Jr., and Hinkle, B. L. S 198, S 206
Dalsgaard-Pedersen, N. *see under* Andreasen, A. H. M.
Darcy S 3
Das Varma *see under* Guruswamy, S.
Davidson, H. W. S 77, S 81
Davidson, H. W., and Turk, B. M. S 55, S 60
Davies, Aylward and Leacey S 196 S 197
Davies, C. N. S 1, S 4, S 17, S 32, S 37, S 64, S 93, S 95, S 117, S 206
Davies, C. N., and Peetz, V. S 17, S 28
Davies, C. N. *see under* Irwin, J. O.
Dawes, J. G. S 37, S 156, S 159, S 173
Dawes, J. G., Maguire, B. A., and Tye, D. L. S 117
Dawes, J. G. *see under* Wynn, A. H. A.
Debye, P., and Bueche, A. M. S 3, S 5, S 11
Delfosse, P. S 181, S 186
Dell, H. A. S 123, S 130, S 135, S 137, S 156, S 159, S 161, S 165, S 173, S 175, S 210
Dell, H. A., and Brockelsby, C. F. S 159
Dell, H. A., and Jones, E. S 135, S 137, S 159
Dell, H. A. *see under* Bareford, C. F.
Derjaguin, B. S 44, S 47
Derjaguin, B., and Kusakov S 63
Dietz *see under* Carpenter
Dinnerstein *see under* Köhler
Domentianova, Z. M. *see under* Fedoseev, V. A.
Donat S 55, S 59
Donoghue, J. K. S 94
Dorain, P. S 141
Dorain, P. *see under* Thatcher, H. C.
Doyle, G. J. S 141, S 143
Drake, L. C. S 77, S 81
Drake, L. C. *see under* Ritter, H. L.
Drinker, P., and Hatch, T. F. S 69, S 71
Drummond, D. G. S 109, S 117
Dulin, C. I. S 63
Dulin, C. I., and Elton, G. A. H. S 62, S 63

Eames, T. A. S 100
Edsall S 39, S 40
Eilers, H. S 3, S 5
Einstein, H. S 2, S 3, S 5, S 61
Eirich, F. R. S 2, S 5, S 11, S 39, S 62
Eirich, F. R., Mark and Huber S 11
Eirich, R. F., and Riseman S 11
Ellison, J. McK. S 65, S 66
Elmore, W. C. S 141, S 143
Elmore, W. C., and Sands. M. L. S 143, S 170, S 173
Elton, G. A. H. S 62, S 63
Elton, G. A. H., and Hirschler, F. G. S 60, S 62
Elton, G. A. H., and Mitchell S 63
Elton, G. A. H. *see under* Dulin, C. I.
Emery *see under* Köhler
Emmett, P. H. *see under* Brunauer, S.
Ergun, S. S 58, S 60, S 77, S 81
Ergun, S., and Orning, E. G. S 77, S 81
Ergun, S., and Owen, J. S 81
Essenhigh, R. H. S 10, S 11, S 48
Evans S 63
Evans and Ewers S 63
Ewers *see under* Evans

Fair, G. M. S 55, S 59
Fairbrother and Mastin S 63
Fairs, G. L. S 54, S 85, S 100, S 104, S 108, S 190, S 191
Faxen, H. S 2, S 5, S 16
Fedoseev, V. A., Manakin, B. A., and Domentianova, Z. M. S 203, S 206
Fitzsimmons, A. E. *see under* Hawksley, P. G. W.
Flood, E. A., Tomlinson, R. H., and Leger, A. E. S 42, S 43, S 47, S 50, S 54
Franklin, R. E. S 81
French, C. C. J. *see under* Rose, H. E.
Frölich, H. and Sack, R. S 5, S 10
Frost-Jones, R. E. U., and Yardley, J. T. S 186
Fujitani, V. S 198, S 206
Fuoss and Strauss S 63

Gaede, W. S 42, S 47
Gammon, J. S 119
Gans, R. S 15
Gendron, P. R. *see under* La Mer, V. K.
Gerke, R. H. *see under* Wells, P. V.
German, W. L. *see under* Leech, L. G.
Gibbs, W. E. S 201, S 206
Gilchrist, J. D., and Taylor, J. S 77, S 81
Gillespie, T. S 198, S 206
Gillespie, T., and Langstroth, G. O. S 198, S 206
Gillings, D. W. S 124, S 157, S 159, S 177
Girifalco, L. A. *see under* Kraus, G.
Gold *see under* Guth, E.
Goldberg, B., and Penndorf, R. S 142, S 143
Goldstein S 1, S 4, S 39, S 40
Gonell S 207
Goyer, G. *see under* La Mer, V. K.
Green, H. L. S 76
Grove, D. M. *see under* Barrer, R. M.
Gruen, R. *see under* La Mer, V. K.
Grundy, P. M. S 164
Gucker, F. T. Jr. S 64, S 177
Gucker, F. T., Jr., and O'Konski, C. T. S 143, S 177, S 180
Gucker, F. T., Jr., O'Konski, C. T., Pickard, H. B., and Pitts, J. N., Jr. S 143
Gucker, F. T., Jr., and Rose, D. G. S 121, S 138
Gumprecht, R. O., and Sliepcevich, C. M. S 65
Guruswamy, S. S 81
Guruswamy, S., Roy, Das Varma, and Srinivasan S 81
Guth, E. S 63
Guth, E., and Gold S 11
Guth, E., and Simha, R. S 5
Guyton S 176, S 177, S 180

Hagerman, T. H. S 126, S 132
Hamaker, H. C. S 194, S 197
Hamilton, R. J. S 36, S 37, S 90, S 95, S 119
Hamilton, R. J., Holdsworth, J. F., and Walton, W. H. S 101
Hamington and Schachman S 39, S 40
Hansen, J. W. *see under* Kunkel, W. B.
Hardy, G. H. S 71

Harkins, W. D., and Jura, G. S 41, S 44, S 47
Harnwell, G. P. S 200, S 206
Harris, W. J. *see under* Walton, W. H.
Harwood, M. G. S 193, S 194
Hatch, L. P. *see under* Fair, G. M.
Hatch, T. F. *see under* Drinker, P.
Hatch T., and Choate, S. P. S 185, S 186
Haul, R. S 50, S 54
Hawksley, P. G. W. S 1–S 5, S 72, S 74, S 76, S 81, S 82, S 85, S 123, S 125, S 128, S 132, S 133, S 137, S 146, S 156, S 159, S 164, S 165, S 173, S 179
Hawksley, P. G. W., Blackett, J. H., Meyer, E. W., and Fitzsimmons, A. G. S 123, S 165
Hazen, H. L., Jaeger, J. J., and Brown, G. S. S 159
Henley Price, F. *see under* Holdsworth, J. F.
Henneberry, G. O. *see under* Arnell, J. C.
Hermans and Overbeck S 63
Hermges, F. G. S 175
Heywood, H. S 26, S 37, S 76, S 81, S 85, S 93, S 95, S 102, S 104, S 105, S 108, S 120, S 177, S 181, S 187, S 197, S 209
Heywood, H. *see under* Jarrett, B. A.
Hill, D. G. *see under* White, L.
Hinkle, B. L. *see under* DallaValle, J. M.
Hirschler, F. G. S 62
Hirschler, F. G. *see under* Elton, G. A. H.
Hoare, E. R. S 165, S 173
Holdsworth, J. F., Henley Price, F., and Tomlinson, R. C. S 96, S 100
Holdsworth, J. F. *see under* Hamilton, R. J.
Holl, H. S 74
Hoppner, K. S 183, S 186
Houghton, H. G., and Chalker, W. R. S 74
Huber *see under* Eirich, F. R.
Hutcheon, J. M. S 81
Hutcheon, J. M., and Beirne, T. S 210
Hutcheon, J. M. *see under* Beirne, T.
Huttig, G. S 41, S 47

Inn, E. C. Y. S 143
Inn, E. C. Y. *see under* La Mer, V. K.
Irwin, J. O., Armitage, P., and Davies, C. N. S 117

Jacobsen, H. E., and Sullivan, W. F. S 184, S 186
Jaeger, J. J. *see under* Hazen, H.
Jaeger, J. C. *see under* Carslaw, H. S.
Jarrett, B. A., and Heywood, H. S 21, S 28
Jeffrey *see under* Stimson
Johnson, J. C. S 65
Johnson, R. S 26, S 62, S 187
Jones, E. *see under* Dell, H. A.
Jones, R. V. *see under* Paul, W.
Joos, G. S 186
Jopling, D. W. S 185, S 186
Jordan, D. W. S 194
Juhola, A. J., and Wiig, E. O. S 81
Jura, G. *see under* Harkins, W. D.

Kallenbach, R. *see under* Wicke, E.
Katchalsky *see under* Kuhn
Katz *see under* Cornell
Keily, D. P. S 65
Kermack, W. O., M'Kendrick, A. G., and Ponder, E. S 3, S 5
Kilburn, T. *see under* Williams, F. C.
Kinosita, K. S 5
Kirkwood and Riseman S 11
Kjaer, B. *see under* Andreasen, A. H. M.
Klinkenberg S 48, S 49
Klose, W. S 42, S 47
Knudsen, M. S 42, S 47, S 54, S 56
Köhler and Dinnerstein S 108
Köhler and Emery S 108
Köhler and Wallach S 108
Kozeny, J. S 55–S 59
Kozeny, J., and Carman S 4
Kozhukhova, O. S. *see under* Samokvalov, K.
Krasny-Ergen S 62
Kraus, G., Ross, J. W., and Girifalco, L. A. S 41, S 47, S 58, S 60
Kraus, G., and Ross, J. W. S 41, S 47
Krebs, K. *see under* Andreasen, A. H. M.
Kruger, J. *see under* La Mer, V. K.
Krumbein, W. C., and Pettijohn, F. J. S 126, S 132
Kuenzle *see under* Kuhn
Kuhn, Kuenzle and Katchalsky S 63
Kunkel, W. B. S 2, S 5, S 176, S 180, S 195, S 197, S 198, S 206
Kunkel, W. B., and Hansen, J. W. S 177, S 180, S 198, S 206
Kusakov *see under* Derjaguin, B.
Kynch, G. J. S 2, S 5, S 10, S 11, S 37

Labeyrie, J. S 208
Ladenberg S 2
Lagercrantz, C. S 129, S 132, S 146, S 147, S 148, S 149, S 154, S 165, S 173
La Mer, V. K. S 72, S 74, S 141, S 143, S 200, S 206
La Mer, V. K., and Barnes, M. D. S 72, S 74
La Mer, V. K., and Gendron, P. R. S 143
La Mer, V. K., Goyer, G., Gruen, R., and Kruger, J. S 201, S 206
La Mer, V. K., Inn, E. C. Y., and Wilson, I. B. S 143
La Mer, V. K., and Sinclair, D. S 143
La Mer, V. K. *see under* Barnes, M. D.
La Mer, V. K. *see under* Sinclair, D.
Lamb, H. S 4, S 16
Lane, W. R. S 197
Langstroth, G. O. *see under* Gillespie, T.
Lea, F. M., and Nurse, R. W. S 56, S 59
Leacey *see under* Davies
Le Bouffant, L., and Saillard, P. S 146
Le Bouffant, L., and Soulé, J. L. S 122, S 143, S 146
Leech, L. G., Ratcliffe, S. W., and German, W. L. S 185, S 186
Leger, A. E. *see under* Flood, E. A.
Lennard-Jones S 194, S 197
Lewis, P. C., and Lothian, G. F. S 64, S 71
Lin, P. N. *see under* McNown, J. S.
Lincoln, B. S 16
Linnett, J. W. *see under* Arthur, J. R.
Lorenz S 2
Lothian, G. F., and Chappel, F. P. S 74
Lothian, G. F. *see under* Lewis, P. C.
Lowan, A. N. S 74
Lowe, H. T., and Lucas, D. H. S 195, S 197, S 198
Lucas, D. H. S 93, S 197
Lucas, D. H. *see under* Lowe, H. T.

Mackenzie, N. *see under* Barrer, R. M.
MacLeod, D. *see under* Barrer, R. M.
MacMillan *see under* Biggs
MacFarlane, R. G. S 129
MacFarlane, R. G., and Poole, J. F. C. S 165, S 173
McBain, J. W. S 46, S 47
McNown, J. S., and Lin, P. N. S 3, S 5
M'Kendrick, A. G. *see under* Kermack, W. O.

Mack, G. W. S 187
Maguire, B. A. *see under* Dawes, J. G.
Malherbe, P. le R. *see under* Carman, P. C.
Manakin, B. A. *see under* Fedoseev, V. A.
Margenau, H., and Murphy, G. M. S 132
Mark, A. M. *see under* Adler, C. R.
Mark *see under* Eirich, F. R.
Marshall, W. R. *see under* Adler, C. R.
Martin, G. S 81
Mason, B. J. S 120, S 176
Mason, B. J., and Ramanadhan S 180
Mastin *see under* Fairbrother
May, K. R. S 101, S 104
Melmore S 198
Meyer, E. W. S 108, S 129, S 159, S 176
Meyer, E. W., and Blackett, J. H. S 210
Meyer, E. W. *see under* Hawksley, P. G. W.
Mie, G. S 71, S 74, S 138, S 143
Millikan, R. S 43, S 47
Mitchell *see under* Elton, G. A. H.
Moody, N. F. *see under* Williams, F. C.
Mooney S 3, S 5
Morgan, V. T. S 48, S 207
Mulford, D. F. *see under* Watson, H. H.
Murphy, B. *see under* Scott, W. E.
Murphy, G. M. *see under* Margenau, H.

Neiburger, M., and Wurtele, M. G. S 203, S 206
Newton, H. E. S 159
Nobel, A. P. P. *see under* Van Heerden, C.
Nurse, R. W. *see under* Lea, F. M.

Odquist, K. G. S 126, S 132
Oldroyds S 11
O'Konski, C. T. S 141, S 143
O'Konski, C. T. *see under* Gucker, F. T., Jr.
Onsager S 63
Orning, E. G. *see under* Ergun, S.
Oseen S 1, S 5
Oster, G. S 67, S 71
Overbeck *see under* Hermans
Owen, J. *see under* Ergun, S.

Parent, R. J. *see under* Adler, C. R.
Patterson, H. S., and Cawood, W. S 104
Patterson, H. S., Whytlaw-Gray, R., and Cawood, W. S 201, S 206
Patterson, H. S. *see under* Whytlaw-Gray, R.
Paul, W., and Jones, R. V. S 74
Pedersen S 63
Peetz, V. *see under* Davies, C. N.
Peletier, L. A. S 207
Penndorf, R. *see under* Goldberg, B.
Perkins, W. M. T. S 27
Petryanov, I. V. S 198, S 206
Pettijohn, F. J. *see under* Krumbein, W. C.
Pettyjohn, E. S., and Christiansen, E. B. S 2, S 5
Phillips, J. W. S 100, S 119, S 122, S 133
Phillips, J. W., Thomas, D. G. A., and Walton, W. H. S 137

Phillips, J. W. *see under* Walton, W. H.
Pickard, H. B. *see under* Gucker, F. T., Jr.
Pigford, R. L. S 128, S 132, S 165, S 173
Pitts, J. H., Jr. *see under* Gucker, F. T., Jr.
Poiseuille S 42, S 46, S 56
Pollard, W. G., and Present, R. D. S 42, S 47
Ponder, E. *see under* Kermack, W. O.
Poole, J. F. C. *see under* MacFarlane, R. G.
Present, R. D. *see under* Pollard, W. G.
Purcell *see under* Brooks

Raal, F. A. *see under* Carman, P. C.
Radcliffe, A. S 93, S 108
Radushkevich, L. V., and Chugunova, O. K. S 198, S 236
Ramanadhan, *see under* Mason, B. J.
Ratcliffe, S. W. *see under* Leech, L. G.
Rawlins, F. I. G. S 96, S 121
Raynor, E. J. *see under* Arthur, J. R.
Reeves, E. V. S 179
Reynolds S 1, S 2
Richardson, E. G. S 74
Richardson, J. F., and Zaki, W. N. S 4, S 5
Rigden, P. J. S 41, S 47, S 56, S 58, S 59
Riseman, J. S 65
Riseman *see under* Eirich, F. R.
Riseman *see under* Kirkwood
Ritter, H. L., and Drake, L. C. S 77, S 81
Roberts, F. S 157, S 159
Roberts, F., and Young, J. Z. S 124, S 130, S 132, S 165, S 173
Roberts, F. *see under* Young, J. Z.
Robins, W. H. M. S 82, S 85, S 189, S 191, S 192
Rollason, E. C. *see under* Sharratt, E.
Roscoe, R. S 3, S 5
Rose, H. E. S 55, S 59, S 185, S 186
Rose, H. E., and French, C. C. J. S 185, S 186
Rose, W. *see under* Wyllie, M.
Rosebery S 101
Ross, J. W. *see under* Kraus, G.
Rotblat, J., Sayle, E. A., and Thomas, D. G. A. S 150, S 154
Rothman *see under* Weissberg
Roy *see under* Guruswamy, S.

Sack, R. *see under* Fröhlich, H.
Sadron S 39, S 40
Saillard, P. *see under* Le Bouffant, L.
Samokvalov, K. S 198, S 206
Samokvalov, K., and Kozhukhova, O. S. S 198, S 206
Sands, M. L. *see under* Elmore, W. C.
Sawyer, K. F., and Walton, W. H. S 85, S 90, S 93
Sayles, E. A. *see under* Rotblat, J.
Schachman *see under* Hamington
Schwartz, F. A. S 58, S 60
Scott, W. E., and Murphy, B. S 159
Sharratt, E., Van Someren, E. H. S., and Rollason, E. C. S 185, S 186
Sheraga *see under* Cerf
Simha, R. S 3, S 4, S 5, S 11
Simha, R. *see under* Weissberg
Sinclair, D. S 63, S 142, S 143, S 201, S 206
Sinclair, D., and La Mer, V. K. S 141, S 143
Sington, E. P. C. *see under* Arthur, J. R.
Skrebowski, J. K. *see under* Brown, J. F.
Sliepcevich, C. M. *see under* Gumprecht, R. O.
Smirnov, L. V., and Solntseva, V. H. S 198, S 206
Smoluchowski, M. von S 2, S 3, S 5, S 42, S 45, S 63, S 65
Solntseva, V. H. *see under* Smirnov, L. V.
Soper, A. K. S 120
Soulé, J. L. S 15
Soulé, J. L. *see under* Le Bouffant, L.
Srinivasan *see under* Guruswamy, S.
Stairmand, C. J. S 27, S 182, S 187, S 188, S 206
Stairmand, C. J. *see under* Carey, W. F.
Steinour, H. S 5
Stimson and Jeffrey S 2, S 5, S 15, S 16
Stokes S 1–S 7, S 12–S 15
Storey, M. G. *see under* Wolff, H. S.
Strauss *see under* Fuoss
Strivens, M. A. S 176
Sullivan, W. F. *see under* Jacobsen, H. E.
Svensson S 63

Taylor, C. S 121
Taylor, C. J. S 173
Taylor, Sir G. S 1, S 37, S 121
Taylor, J. *see under* Gilchrist, J. D.
Taylor, W. K. S 173, S 175
Teller, E. *see under* Brunauer, S.
Thatcher, H. C. S 65
Thatcher, H. C., and Dorain S 65
Thomas, A. L., and White, Locke, Jr. S 140, S 143
Thomas, D. G. A. *see under* Phillips, J. W.
Thomas, D. G. A. *see under* Rotblat, J.
Thomas, D. G. A. *see under* Walton, W. H.
Thomas, W. D. E. S 37
Thompson, W. E., and Acton, R. A. S 164
Thouless S 108
Timbrell, V. S 2, S 5, S 12, S 15, S 16, S 37, S 86, S 90, S 94, S 119
Tiselius S 63
Tolman S 63
Tomlinson, R. C. *see under* Holdsworth, J. F.
Tomlinson, R. H. *see under* Flood, E. A.
Tomotika, S., and Aoi, T. S 1, S 16
Trickett, E. S. S 210
Trickett, E. S., and Courshee, R. J. S 164
Trickett, E. S., and Wheeler, L. K. S 164
Trickett, E. S. *see under* Wheeler, L. K.
Turk, B. M. *see under* Davidson, H. W.
Tye, D. L. *see under* Dawes, J. G.

Vand, V. S 3, S 5, S 10, S 11
van de Hulst, H. C. S 64, S 65, S 71, S 74
Van Heerden, C., Nobel, A. P. P., and Van Krevelen, D. W. S 81
Van Krevelen, D. W. S 81
Van Krevelen, D. W. *see under* Van Heerden, C.
van Kreveld, A. S 93, S 120
Van Someren, E. H. S. *see under* Sharratt, E.
Vouk, V. B. S 65, S 66, S 71

Wagner, L. A. S 185, S 186
Wainwright, T., and Walton, W. H. S 109, S 117
Wales S 39, S 40
Walkenhorst, W. von S 109, S 117
Walker, J. R. D. S 37
Wallach *see under* Köhler
Walton, W. H. S 5, S 29, S 37, S 74, S 85, S 90, S 94, S 100, S 104, S 119, S 121, S 126, S 132, S 137, S 146, S 154, S 159, S 173, S 175, S 206, S 207
Walton, W. H., and Harris, W. J. S 109, S 117
Walton, W. H., Thomas, D. G. A., and Phillips, J. W. S 137, S 159
Walton, W. H. *see under* Hamilton, R. J.
Walton, W. H. *see under* Phillips, J. W.
Walton, W. H. *see under* Sawyer, K. F.
Warburg, G. S 42, S 45
Ward, A. N. S 10
Ward, S. G., and Whitmore, R. L. S 5
Washburn, E. W. S 77, S 81
Watson, H. H. S 16, S 37, S 81, S 85, S 90, S 94, S 95, S 100, S 101, S 104
Watson, H. H., and Cruise S 108
Watson, H. H., and Mulford, D. F. S 105
Weiner, C. S 65
Wells, P. V., and Gerke, R. H. S 198, S 206
Weissberg, Simha, R., and Rothman S 11
Wheeler, L. K., and Trickett, E. S. S 165, S 173
Wheeler, L. K. *see under* Trickett, E. S.
White, L., and Hill, D. G. S 198, S 206
White, Locke, Jr. *see under* Thomas, A. L.
Whitmore, R. L. *see under* Ward, S. G.
Whyard, R. E. *see under* Cooke-Yarborough, E. H.
Whytlaw-Gray, R., and Patterson, H. S. S 198, S 206
Whytlaw-Gray, R. *see under* Patterson, H. S.
Wicke, E., and Kallenbach, R. S 50, S 54
Wicksell, S. S 126, S 132, S 165, S 173
Wiig, E. O. *see under* Juhola, A. J.
Williams, F. C., and Kilburn, T. S 159
Williams, F. C., and Moody, N. F. S 159
Williams, P. S. S 117
Williamson, B. S 126, S 132
Willis, T. F. S 126, S 132
Wilson, I. B. *see under* La Mer, V. K.
Winder *see under* Barker
Wolff, H. S. S 129, S 132, S 147, S 154, S 159, S 165, S 173
Wolff, H. S., Storey, M. G., and Behrens, D. J. S 147, S 154
Wolff, H. S. *see under* Cooke-Yarborough, E. H.
Wright, B. M. S 38, S 90
Wurtele, M. G. *see under* Neiburger, M.
Wyllie, M., and Rose, W. S 44, S 47, S 49
Wynn, A. H. A., and Dawes, J. G. S 15

Yardley, J. T. *see under* Frost-Jones, R. E. U.
Young, J. Z., and Roberts, F. S 157, S 159, S 165, S 173
Young, J. Z. *see under* Roberts, F.

Zaba, J. B. J. S 62, S 63
Zaki, W. N. *see under* Richardson, J. F.

PRINTED IN GREAT BRITAIN BY UNWIN BROTHERS LIMITED, WOKING AND LONDON

SESSION A. RELATIVE MOTION OF PARTICLES AND FLUIDS: SIZE SEPARATION

Chairman: Prof. Sir Geoffrey Taylor, M.A., F.R.S.

Survey of the relative motion of particles and fluids

By P. G. W. Hawksley, The British Coal Utilisation Research Association, Leatherhead, Surrey

The relative motion of particles and fluid is discussed in terms of the hydrodynamic interference between particles in a suspension, which ranges from a small effect in the dilute suspensions used in particle size analysis to a decisive magnitude in the permeability of packed beds of particles. The behaviour of clouds of particles, sedimentation and viscosity of concentrated suspensions, hindered settling and fluidization are briefly mentioned.

There have been several comprehensive and detailed reviews[1,2] of the behaviour of particles in fluids. It is proposed here to discuss the subject in a rather general way to emphasize the essential unity of the phenomena of sedimentation, elutriation, hindered settling, permeability and so on. The theme of this survey is the mutual fluid-dynamic interference between particles, which ranges from a negligible effect in the settling of the extremely dilute suspensions recommended for particle size analysis to a phenomenon of overwhelming importance in the permeability to flow of a bed of particles in contact. The motion of a single particle and the resistance of a packed bed represent two extremes of size analysis measurements. Where there is negligible interference, each particle registers its individual vote according to its size and sedimentation, elutriation, impaction, etc., provide methods of obtaining the particle size distribution. At the other extreme the mutual interference is so severe that the system tends to behave as a whole; a concentrated suspension settles with little differential motion except between particles of very different sizes. The permeability of a packed system is governed very largely by the total surface area and total volume of the particles and is little affected by their size distribution.

A further reason for discussing the subject in this way is that particle size analysis is incidental to a study of the size dependent process operating in some particular application. A size distribution measurement is rarely of interest in itself; perhaps the only cases arise in investigations of theories of breakage or comminution and of the converse phenomena of condensation, crystal growth or aggregation. In the majority of cases the size measurement serves only to characterize the material employed in some size dependent process. Often such characterization amounts to little more than testing the material in a small scale version of the industrial or natural process. For example, the course of sedimentation of a suspension of colloidal fuel is used to characterize the tendency for the coal particles to separate from the oil when the fuel is left in storage tanks.

SINGLE PARTICLE IN AN INFINITE FLUID

We start with the case of a single particle moving in a viscous fluid of infinite extent. The particle pulls fluid along with it, although only very slowly at any appreciable distance. Nevertheless, the whole of the fluid travels with the particle. The drag D of the fluid on the particle can be calculated in a few simple cases. When the motion is so slow that the inertial terms may be dropped from the general differential equations of fluid motion, the resulting Stokes' equations can be solved and the drag and flow pattern calculated. The calculations[3] have been carried out only for the ellipsoid and its limiting shapes of sphere, infinitely long cylinder and flat blade, and infinitely thin disk. The drag may be written in the form

$$D = 3\pi\eta u d_d \qquad (1)$$

where η is the viscosity of the fluid, u the velocity of the particle and d_d is a linear dimension of the particle, which is termed[2] the drag diameter and is defined as the diameter of a sphere having the same drag as the particle for the same values of η and u. The drag diameter depends on the orientation of the particle relative to direction of motion; for example, a disk moving edge on has a drag diameter $16/9\pi$ times its diameter compared with $24/9\pi$ when moving broadside on. The drag diameter depends also on the rigidity of the particle; for a spherical liquid droplet of viscosity η_d, the drag diameter is smaller than the droplet diameter by the factor $(3\eta_d + 2\eta)/(3\eta_d + 3\eta)$. For a bubble of gas in a liquid ($\eta_d \ll \eta$), the factor is 2/3; for a liquid droplet in a liquid of the same viscosity ($\eta_d = \eta$), the factor is 5/6. The above expressions are valid only for very slow motion when the Reynolds' number $\rho u d_d/\eta$ is negligible compared with unity. Oseen's hydrodynamics provide a second starting point and yield expressions for the drag valid up to Reynolds' numbers as large as 4. Goldstein[4] obtained in 1929 an exact solution of Oseen's equations for the case of a sphere; and Tomotika and Aoi[5] have very recently solved the problem for an elliptic cylinder.

For other shapes of particles and higher Reynolds' numbers the drag must be obtained experimentally from tests in suitably large containing vessels. The drag coefficient C_D, defined as the ratio of the drag to the impact force (impact pressure times cross-sectional area of particle) is, for any given shape and proportions in a fixed orientation, a unique function of the Reynolds' number R_e. For the important case of spherical particles, many empirical expressions relating C_D and R_e have been reported in the literature; the most exhaustive analysis of the available data is that of Davies.[6]

SINGLE PARTICLE IN FLUID OF FINITE EXTENT

When the fluid is contained by walls, there are two effects: the fluid pulled along by the particle must produce a return flow since it cannot pass through the walls; and since the fluid is stationary at a finite distance from the particle, there is a distortion of the flow pattern which reacts back on the particle. Both effects increase the drag but the second is the more important, at least in the larger containing vessels, and has been investigated theoretically for spherical particles at

low Reynolds' numbers. To a first order the drag is increased by the factor $1/(1 - k'd_o/l)$ where k' is a numerical constant, d_o is the diameter of the sphere and $\frac{1}{2}l$ is the distance of the wall (for motion parallel to the wall). For a single wall k' is 0·563 (Lorenz[7]); for two walls 1·004 (Faxen[8]); for a circular cylinder, i.e. four walls, 2·104 (Faxen [9]). Obviously each extra wall increases the drag by an approximately proportionate amount. Consequently the settling velocity of a sphere in a cylinder, for example, is much the same over quite a large part of the central area; the increased retardation experienced by a particle displaced towards one side of the vessel is partly offset by a reduced retarding effect from the more distant opposite walls. The experimental data on the wall effect are not consistent (this has been discussed elsewhere[2]); most of the experiments were designed to test Ladenburg's theory for the case of a circular cylinder which contains an incorrect numerical constant.

TWO PARTICLES IN A FLUID OF INFINITE EXTENT

When two particles move through an extensive viscous fluid, each of them helps the other forward so that the drag of the fluid on either is less than if the other particle were absent. The common reduction in drag for a pair of spheres, first investigated by Smoluchowski[10] and Faxen[11] has been examined in detail by Stimson and Jeffrey.[12] The effect is surprisingly large. Even at 10 diameters apart, the reduction for spheres of the same size settling side by side amounts to some 7%, and at two diameters it is about 25%. The change in drag is not independent of the position of the two spheres, the reduction being greatest when their line of centres lie in the direction of motion. Furthermore, there is a component directed towards the leading sphere so that both spheres are equally deflected from the direction of the driving force.

CLOUD OF PARTICLES IN AN INFINITE FLUID

The mathematical difficulties of determining the drag when there are more than two particles present are very great, and approximate solutions have been obtained only by considering somewhat artificial models. In general, however, the mutual interference in a cloud of particles, each of which carries fluid with it, results in substantial reduction in the drag. Burgers[13] for example, has shown that a spherical cloud of diameter L behaves as if it were a liquid droplet of the same diameter and of viscosity equal to that of the fluid. The total drag is thus $(5/2).\pi\eta uL$. The settling velocity of a cloud of volume concentration c will thus exceed the Stokes' velocity of an individual particle of diameter d_o by the factor $(6/5)c(L/d_o)^2$. From the approximation made in the derivation, this factor is applicable only if it exceeds unity; it might otherwise appear that a cloud of sufficiently low concentration or small size would settle at a rate less than the Stokes' velocity. On the other hand in an earlier paper, Smoluchowski[10] found that the settling rate depended also on the arrangement of particles within the cloud and allowed the possibility that with some arrangements the cloud could settle at the Stokes' rate or even more slowly.

Where the cloud size or concentration is such that the factor appreciably exceeds unity it is likely that inertia effects (neglected in Burger's analysis) will become important both within the cloud and in the surrounding fluid; the cloud (which, for slow motion preserves its shape and size) may then be deformed or broken up.

There are two aspects of particular interest in Burger's analysis. In the first place, the cloud may be expected (for reasons discussed below) to have an effective viscosity η_c in excess of that of the pure fluid η_o. But since the drag of rigid sphere in a fluid of viscosity η is only 6/5 times greater than that of a liquid sphere of the same viscosity, any increase in the effective viscosity of the cloud can result at most in a 20% increase in drag. Secondly, Burger's detailed discussion shows that the fluid within the cloud moves at exactly the same speed as the particles. Whilst the complete impermeability is a consequence of the approximations made, it is true that assemblies of particles are relatively impermeable, providing the walls of the container are at a great distance. Eirich[14] has reported experiments on porous solids showing that the liquid inside, or contained in undulations at the surface, is carried with the solid. The concept of immobile or stagnant layers of fluid at rough surfaces is a prominent feature in some theories of the viscosity[15,16] and sedimentation[17] of suspensions. Kynch[18] also remarks, in his paper to this Conference, on the same phenomena for the liquid contained in a hole drilled through a sphere. A consequence in particle size analysis is that the cloud tends to carry smaller particles along with it and there is little differential sedimentation.

PARTICLE SHAPE

At this point we digress for a moment on the question of particle shape. Since a cloud of porous particles tends to carry fluid with it, it is to be expected that the drag of non-spherical particles and especially of rough-surfaced particles will be governed by the size of an enveloping surface. It is suggested here, as nothing more than a convenient approximation, that the drag diameter can be equated with the diameter Δ of a sphere having the same external surface area as the particle. For ellipsoid and disk this is a good approximation; taking an averaged orientation, it is correct within 5 to 10%. It also fits within 5% or so the extensive experimental data reported by Pettyjohn and Christiansen[19] for cubes, octahedra and tetrahedra (after allowance is made for a wall effect present in their tests) and also for Kunkel's data[20] on pairs, chains and clusters of spheres. It would also seem to agree with the data reported to this conference by Timbrell[21] on the settling of pairs of spheres of various sizes.

Since the effect of particle shape is usually discussed in terms of the Stokes' diameter d_s (that of a sphere having the same terminal velocity as the particle under the same conditions), it is worth remarking that the drag diameter is the more fundamental quantity. The Stokes' diameter is the ratio $\sqrt{(\delta^3/d_d)}$, δ being the volume diameter or size of sphere having the same volume as the particle.

VISCOSITY OF SUSPENSIONS

The presence in a fluid of rigid particles that cannot fully take part in any deformations of the fluid, results in an increased resistance to shear and a suspension has an apparent viscosity exceeding the viscosity of the suspending fluid. The relative viscosity η_r of the suspension (ratio of apparent η_c to pure fluid η_o viscosities) increases with the volume concentration c of the particles. For sufficiently dilute systems, it is given by the Einstein equation

$$\eta_r = 1 + kc \qquad (2)$$

where k is a numerical constant whose value depends on the rigidity, shape and orientation of the particles.[22] For a system of spheres (of any size distribution) Einstein[23] obtained the value $k = 5/2$. The presence of a single sphere

results in a disturbance of the whole fluid, perceptible even at large distances such that the total retardation is constant for all planes of shear; and the net effect for a number of point spheres, taken additively, is given by the above expression. The calculation neglects the mutual interactions between the fields of flow of the individual spheres, and also any "shielding" effects that the finite volumes of the spheres may have on the "transmission" of the interactions.

Attempts have been made to extend the theory to higher concentrations. It is possible to calculate the first order effect due to mutual interactions for point particles and this gives[24,25] an additional term of magnitude $12c^2$. Experimental data, however, indicate a less severe increase in relative viscosity and also a dependence on the size distribution of the spheres, the relative viscosity being higher for closely sized systems than for suspensions containing a wide range of sizes.[16] Clearly account must be taken of the finite volume of the particles. Brinkman[26] and independently Roscoe[27] derived the expression

$$\eta_r = (1 - c)^{-k} \tag{3}$$

for a system of particles covering a wide size range. They assumed that the addition to a suspension of an extra particle of very different size would change the viscosity by an incremental amount given by Einstein's equation (2) and the integrations of the resulting difference equation yields the above expression. The derivation is thus based on the supposition that the existing suspension behaves towards the additional particle as would a pure fluid; we return to this point in the following section. Vand[15] attempted the calculation of the relative viscosity allowing for the mutual interactions and obtained the result

$$\eta_r = \exp(kc/1 - Qc) \tag{4}$$

where Q is 39/64. The derivation is open to question but it would appear that it also assumes the suspension behaves towards any representative particle as if it were a pure fluid. There is close numerical agreement between equations (3) and (4) even at 50% concentration; and they both fit tolerably well Eilers' experimental data,[28] up to 35% concentration, on the viscosity of wide size range suspensions.

Since particles tend to carry fluid with them, there have been several attempts to account for the viscosity of concentrated suspensions by supposing that the immobilization of fluid between clumps of particles results in an increase in effective concentration. Roscoe[27] replaced c in equation (3) by $c3\sqrt{(2)}/\pi$, $\pi/3\sqrt{(2)}$ being the fractional solid content in closest (rhombohedral) packing of equal spherical particles; and argued that this represented the behaviour of concentrated suspensions of equal sized particles. Vand extended equation (4) in a similar manner. The same consideration led Mooney[29] to the expression (4) in which Q was an adjustable constant of order $1\frac{1}{2}$ for equal sized suspensions and less than unity for particles covering a wide size range. This type of approach is only an approximation, the immobilization of fluid corresponding to the shielding effect of particles on their hydrodynamic interaction. An attempt at a more rigorous treatment by Simha,[25] again leads to an expression containing an adjustable constant dependent on the manner of shielding and thus the arrangement and size distribution of the particles.

SETTLING OF SUSPENSIONS

It was mentioned earlier that as a consequence of the transport of fluid by particles there must be a return flow when the container is of finite size. This exaggerates the retarding influence of the walls so that both a single particle and a cloud will settle more slowly in containers of smaller diameter. When a cloud fills the entire vessel the whole return flow must go through the cloud. This results in a drag that invariably exceeds that of the individual particles. In addition the rigidity arising from the presence of the particles acts as a further and more serious retarding influence. Thus if we consider a single particle in the system, it behaves as if it were settling in an upward flowing fluid of higher viscosity, both the upward velocity and the apparent viscosity depending upon the concentration of the surrounding particles. Although this is undoubtedly an artificial picture of the situation, it has, nevertheless, provided a useful simplification. Working on these lines Burgers[13] has provided an approximate expression for the rate of settling of dilute suspensions. The relative velocity U_r, defined as the ratio of the settling rate of the suspension to the Stokes' velocity of a constituent particle, is according to Burgers,

$$U_r = 1 - 6\tfrac{3}{4}c \tag{5}$$

Several earlier attempts at the same problem by Cunningham,[30] Smoluchowski[10] and Kermack, M'Kendrick and Ponder,[31] indicated first-order effects of the same magnitude. Recently McNown and Lin,[32] have extended Smoluchowski's treatment to include inertia terms; their results indicate a retardation of appreciably larger magnitude than previous experimental work would suggest. There is lack of consistency in published experimental data but, to give an indication of the magnitude, the retardation at 1% concentration appears to lie between 4 and 7%.

A particular feature of all these attempts is that the numerical constant depends on the assumed arrangement of particles in the suspension. It is possible that the initial arrangement, whatever it may be, will be preserved during settling. This is consistent with the experimental observation[17] that settling seems to proceed at a uniform rate, but that repeated tests at the same concentration show a wide scatter in settling rates, as if slight differences in initial arrangement were maintained and resulted in different settling rates. On the other hand, there are lateral components which, it might be supposed, would lead, as a result of the settling process, to the establishment of a particle arrangement giving a maximum rate of settling. This would imply an acceleration from the start of settling.

This difference distinguishes attempts to provide a theory applicable at higher concentrations. Brinkman[33] and independently Debye and Bueche[34] developed an interpolation formula between the Darcy permeability region and the viscous flow region for a single sphere and obtained

$$U_r = 1 + \frac{3c}{4}\left[1 - \sqrt{\left(\frac{8}{c} - 3\right)}\right] \tag{6}$$

This assumes in effect that the particles in a suspension have the same arrangement as in a packed bed. On the other hand, Hawksley[35] derived an expression based on the assumption that the particles take up an equilibrium arrangement giving a maximum rate of settling

$$U_r = (1 - c)^2/\eta_r \tag{7}$$

where η_r denotes the effective relative viscosity of the suspension. For η_r, Vand's result, equation (4) above, was employed. Alternatively and with perhaps more theoretical justification, we can use Brinkman's and Roscoe's equation (3) since by its derivation it assumes that the remaining suspension

behaves towards a given particle as if it were a pure fluid. Numerically there is little difference between them and the resulting expression

$$U_r = (1 - c)^{9/2} \tag{8}$$

has the advantage of simplicity. Richardson and Zaki,[36] who have recently derived expressions for the relative velocity of various assumed initial arrangements, have shown experimentally that U_r is proportional to the 4·65 power of $(1 - c)$. For low concentrations (7) and (8) reduces to

$$U_r = 1 - 4\tfrac{1}{2}c \tag{9}$$

which indicates faster settling for an equilibrium process than for a fixed arrangement [equation (5)].

As remarked above the experimental evidence is conflicting, but it would seem that Burgers' and Brinkman's equations (5) and (6) set an upper limit and Hawksley's equations (7) and (8) set a lower limit to the relative velocity. It is suggested that settling in the absence of inter-particle forces tending to maintain the initial arrangement, will lie nearer the lower limit, whilst the settling of a flocculated system lies nearer the upper limit.

PERMEABILITY OF PACKED BEDS AND FLUIDIZATION

Notwithstanding the success of the Kozeny–Carman capillary analogy in accounting for the permeability of packed beds to fluid flow, it seems more natural to treat a bed as a collection of particles each subject to the drag of fluid rather than as a system of tortuous pores of varying cross-section. In any case the process of flow through a packed system must be essentially the same as the settling of a concentrated suspension, since it makes no difference whether particles or fluid move provided their spatial arrangement is the same. Brinkman[33] and others have regarded the processes as identical. But according to the discussion in the preceding section, a difference is to be expected in the arrangement of particles. In the formation of a packed bed the particles take up positions of lowest potential energy and fall into the spaces between others, giving a maximum resistance to flow, whilst in a settling suspension they may be expected to sort themselves out into an arrangement of minimum resistance. If this is the case, it can be shown[35] that at the concentrations found in packed systems, the drag for the packed bed will be some $1\frac{1}{2}$ times that of the suspension at the same concentration. This seems to be in accordance with experiment and is consistent with observations on fluidized beds (the just expanded bed can be maintained with only 2/3 the velocity that is needed to lift it). Thus, in addition to the Kozeny–Carman voidage function $(1 - c)^3/c^2$, we have that of Brinkman and also, from equation (8), the form $(1 - c)^{9/2}/c$, all three of which are in tolerable agreement.

Although a discussion of fluidization is beyond the scope of this survey a few general remarks may be made. As the velocity is increased through a packed bed, the pressure drop rises until it equals the weight per unit area when the bed should be lifted. In fact, what happens depends on the state of the bed packing and the relative size of the container. A coarse powder forms an interlocking structure; a fine powder is often sticky and in either case the pressure drop usually has to exceed the weight before the bed is lifted. In a narrow tube the interlocking structure will often lead to the bodily lifting of the bed but in a wide tube there is enough give for the bed to break up. With a suitable fine powder that is not sticky or which has been well aerated there may be a gentle expansion. The process of expansion involves a rearrangement of the particles from an aggregated to a dispersed condition. The just expanded bed behaves like a suspension and the effect of concentration can be calculated in the same way. But there is a fundamental difference between fluidization and hindered settling. In fluidization the fluid friction at the walls produces a velocity gradient and the particles circulate up at the axis and down at the walls. Thus as the velocity is increased beyond the just expanded state, the system behaves less and less like a settling suspension and attempts to apply sedimentation or permeability theories must fail. As the velocity is increased, the concentration decreases, and we pass through the regime of pneumatic conveying to elutriation. This brings the survey back to the starting point. But even here there is a difference. The drag of a single sphere in a non-linear velocity field is not identical with the Stokes' drag. In a parabolic velocity distribution it is slightly smaller as discussed by Simha.[37]

CONCLUSION

It will be apparent from the above discussion that the effective particle size changes as we go from the case of settling of single particles *via* clouds and suspensions, to flow through packed beds and then by way of fluidization and pneumatic conveying to the case of elutriation. This must be remembered in applying the results of size analyses made by sedimentation at very low dilutions. Then it seems likely that, even at low overall concentrations, there may arise clusters or clumps of particles which in consequence of the hydrodynamic interaction tend to behave as a whole. This may even be a prominent feature in such processes as gas cleaning. Cyclones, for example, are more efficient than would be expected from theoretical considerations, some of the finest particles being removed with the coarser sizes. On the other hand, size classifiers are frequently ineffective, even allowing for the inevitable ragged cut,[38] and it is possible that improvements are obtainable if a uniform low concentration could be maintained at all places in the gas stream. Another aspect that may be of practical interest is that rapid settling, which is the objective of thickening processes, depends on a free return flow. The high settling rate of a cloud or a flocculated aggregate is not lost until the walls are moderately close. Conversely an empty space near the walls allows a suspension to settle more rapidly; this happens, for example, if the container is tilted,[39] or if it has inclined walls. Particles falling away from the walls provide a clear space for a return flow; other factors are involved as well but this is the essential feature.

Thus, whilst it is necessary to consider carefully whether the particle size measured under ideal conditions is the operative size of immediate interest, there is at least a fair background of knowledge to assess the nature and magnitude of the errors involved.

REFERENCES

(1) Davies, C. N. *Symposium on Particle Size Analysis*, p. 25, *Suppl. to Trans Instn Chem. Engrs*, **25** (1947).
(2) Hawksley, P. G. W. *Brit. Coal Utilisation Res. Assoc., Bull.*, **15**, p. 105 (1951); **16**, pp. 117, 181 (1952).
(3) Lamb, H. *Hydrodynamics*, 6th ed., p. 604 (London: Cambridge University Press, 1932).
(4) Goldstein, S. *Proc. Roy. Soc. A*, **123**, p. 225 (1929).
(5) Tomotika, S., and Aoi, T. *Quart. J. Mech. Appl. Math.*, **6**, p. 290 (1953); **3**, p. 140 (1950); **4**, p. 401 (1951).
(6) Davies, C. N. *Proc. Phys. Soc.* [*London*], **57**, p. 259 (1945).

(7) LORENZ, H. *Abh. u. th. phys.*, **1**, p. 23 (1906).
(8) FAXEN, H.: *Ann. Phys.* [*Leipzig*], **68**, 89 (1922).
(9) FAXEN, H. *Ark. Mat. Astron. Fys.*, **17**, No. 27 (1922).
(10) SMOLUCHOWSKI, M. S. *Bull. Acad. Sci. Cracow*, **1a**, p. 28 (1911); also *Proc. 5th Internat. Congress of Mathematicians*, **2**, p. 192 (1912).
(11) FAXEN, H. *Ark. Mat. Astron. Fys.*, **19**, p. 13 (1925).
(12) STIMSON, M., and JEFFREY, G. B. *Proc. Roy. Soc. A*, **111**, p. 126 (1926).
(13) BURGERS, J. M. *Proc. K. Ned. Akad. Wetensch.*, **44**, pp. 1045, 1177 (1941); **45**, pp. 9, 126 (1942).
(14) EIRICH, F. *Rep. Progr. Phys.*, **7**, p. 329 (1940).
(15) VAND, V. *J. Phys. Coll. Chem.*, **52**, p. 277 (1948).
(16) WARD, S. G., and WHITMORE, R. L. *Brit. J. Appl. Phys.*, **1**, pp. 286, 325 (1950).
(17) STEINOUR, H. *Industr. Engng Chem.*, **36**, pp. 618, 840 and 901 (1944).
(18) KYNCH, G. J. This Supplement: Paper A.1.
(19) PETTYJOHN, E. S., and CHRISTIANSEN, E. B. *Chem. Engng. Progr.*, **44**, p. 157 (1948).
(20) KUNKEL, W. B. *J. Appl. Phys.*, **19**, p. 1056 (1948).
(21) TIMBRELL, V. This Supplement: Paper A.2.
(22) BURGERS, J. M. *2nd Rep. on Viscosity and Plasticity. K. Ned. Akad., Verhand.* (*Eerste Sectie*), D1, **16**, p. 113 (1938).
(23) EINSTEIN, A. *Ann. Phys.* [*Leipzig*], **19**, p. 289 (1906); **34**, p. 591 (1911).
(24) GUTH, E., and SIMHA, R. *Kolloidzsche*, **74**, p. 266 (1936); see also SIMHA, R. *J. Res. Nat. Bur. Stand., Wash.*, **42**, p. 409 (1949).
(25) SIMHA, R. *J. Appl. Phys.*, **23**, p. 1020 (1952).
(26) BRINKMAN, H. C. *J. Chem. Phys.*, **20**, p. 571 (1952).
(27) ROSCOE, R. *Brit. J. Appl. Phys.*, **3**, p. 267 (1952).
(28) EILERS, H. *Kolloid Z.*, **97**, p. 313 (1941).
(29) MOONEY, M. *J. Colloid Sci.*, **6**, p. 162 (1951).
(30) CUNNINGHAM, E. *Proc. Roy. Soc. A*, **83**, p. 357 (1910).
(31) KERMACK, W. O., M'KENDRICK, A. G., and PONDER, E. *Proc. Roy. Soc. Edinburgh*, **44**, p. 170 (1928–9).
(32) MCNOWN, J. S., and LIN, P. N. *Proc. Ind. Mid-Western Conf. Fluid Mechanics*, p. 401 (1952).
(33) BRINKMAN, H. C. *Appl. Sci. Res. A*, **1**, p. 81 (1948).
(34) DEBYE, P., and BUECHE, A. M. *J. Chem. Phys.*, **16**, p. 573 (1948).
(35) HAWKSLEY, P. G. W. Some Aspects of Fluid Flow, p. 114 (London: Edward Arnold and Co., 1951).
(36) RICHARDSON, J. F., and ZAKI, W. N. *Chem. Engng Sci.*, **3**, p. 65 (1954).
(37) SIMHA, R. *Kolloid Z.*, **76**, p. 16 (1936).
(38) WALTON, W. H. This Supplement: Paper A.5.
(39) KINOSITA, K. *J. Colloid Sci.*, **4**, p. 525 (1949).

Paper A.1

The effective viscosity of suspensions

By G. J. KYNCH, D.I.C., Ph.D., University College of Wales, Aberystwyth

A method is given for solving exactly the equations for slow, steady flow of an incompressible fluid containing a number of particles. These equations have been solved statistically for a suspension of spheres at low concentrations, and it is shown that Einstein's formula is not justified at concentrations above 1%. The procedure for larger concentrations is suggested, though not completed.

1. INTRODUCTION

In an attempt to find a simple derivation of Stokes' law it was noticed that the viscous equations for slow flow have a simple particular integral, and the remaining equation can then be solved by standard methods. The velocity at any point of the fluid is calculated by adding contributions from every point on the boundary, the contribution per unit area being the product of an effective boundary velocity and a propagation function.

In this paper we shall discuss various problems of viscous flow in terms of this form of solution, and especially the viscous flow of a suspension of particles which by this technique gives no more trouble than many other simpler problems. By this we mean, not that the mathematics is very simple, quite the contrary, but that it is possible to give a physical picture of what is happening so that the nature of any approximations can be clearly seen.

The problem of the viscous flow of a suspension is very important experimentally and is a fascinating challenge to the applied mathematician because of its complexity, which suggests to him that a simple approach should be possible using statistical methods. The first calculation by Einstein[1] showed that the apparent viscosity of a suspension of incompressible spheres in a liquid of viscosity μ was given by the formula

$$\mu_c = \mu(1 + 2{\cdot}5c) \qquad (1)$$

where c is the volume fraction of spheres, provided c is small so that the interactions of the spheres could be neglected. Since then a number of other authors have tackled the problem by various methods in order to extend the results. Fröhlich and Sack[2] used a method of a self-consistent type so that they could consider elastic or plastic particles. They assumed that the bulk of the fluid has viscosity μ leaving a sphere of viscosity μ_0 around each sphere whose volume is the average occupied by a particle. They could satisfy the boundary conditions to the first order in c and obtained for rigid spheres the same result as Einstein. Burgers'[3] who was more interested in the settling of suspensions, evolved a method where the effect of the motion of a particle on the fluid is replaced by an equivalent set of forces. To prevent divergence in some of his results he introduced a cut-off radius to this effect suggested by Oseen's solution of the viscous equations including the inertia terms.

More recently, Vand[4] has obtained formulae for large concentrations by considering the reaction of one spherical particle on another. The approximations are severe but evaluable, and his results have been widely quoted in the literature. Other authors have considered particles of non-spherical shape.

A good deal of experimental work has also been done on these problems using artificially made spheres of known size, or approximately known size, to discover the effect of various factors on the effective viscosity. It seems clear now that Einstein's result breaks down at concentrations of the order of 1% and that the effective viscosity[5] $1/\mu$ gives a straight

line when plotted against the concentration c: thus μ becomes infinite when c reaches the value c_0 which is close to the concentration for close packing. These results for spheres may not be correct for other shapes, nor other circumstances where interactions of a non-viscous type take place, but it seems reasonable to assume that they are not very wrong. There also seem to be considerable boundary effects for some form of apparatus and with certain methods of measuring the viscosity.

The theoretician has therefore enough problems in hand to keep him busy for some time, although he would probably like far more experimental data to help him in his work. Although we cannot answer more than one of these problems in this paper, we believe that the method outlined here may suggest new ideas and new approaches to these problems. This is possible because of the nature of the propagation function mentioned in the first paragraph. There is an electrostatic analogue to our problem where the particles and the apparatus boundaries are all replaced by bodies which are earthed or at given potentials. The propagation function to give the velocity at any point P of the fluid appears as the charge induced at any point on the boundary when a unit electric charge is placed at P and all the boundaries are earthed.

We avoid mathematics as far as possible, as it is intended to present the details elsewhere, and confine ourselves to a description of points which may be of interest.

2. SOLUTION OF THE VISCOUS EQUATIONS

The steady, slow viscous flow of an incompressible fluid is governed by the Stokes–Navier equation and the continuity equation

$$\mu\nabla^2\boldsymbol{u} = \operatorname{grad} p \tag{2}$$

$$\operatorname{div}\boldsymbol{u} = 0 \tag{3}$$

when inertia terms are neglected, p being the pressure. It follows that

$$\nabla^2 p = 0 \tag{4}$$

Because of equation (4) there is simple particular integral of equation (2)

$$\boldsymbol{u} = (\boldsymbol{r}p/2\mu) \tag{5}$$

where $\boldsymbol{r}$ is the position vector of the point, with Cartesian components (x, y, z). We therefore write

$$\boldsymbol{u} = (\boldsymbol{r}p/2\mu) + \boldsymbol{v} \tag{6}$$

where $\boldsymbol{v}$ satisfies the equations

$$\nabla^2\boldsymbol{v} = 0 \tag{7}$$

$$-2\mu\operatorname{div}\boldsymbol{v} = 3p + \boldsymbol{r}\operatorname{grad} p = 3p + r(\partial p/\partial r). \tag{8}$$

This separation of the velocity into two terms may seem unwise since, wherever the origin is chosen, the term in $\boldsymbol{r}p$ becomes large at large distance from the origin. This is true for the motion of pure liquid with the usual infinite boundaries and does lead to some difficulties, but it is not true with boundaries at a finite distance, and it is shown later that it is this term which is important for many of the problems we have in mind.

If $\boldsymbol{u}_b$ is the velocity on any of the boundaries, the boundary condition on $\boldsymbol{v}$ is that

$$\boldsymbol{v} = \boldsymbol{u}_b - (\boldsymbol{r}p/2\mu), \text{ on the boundary,} \tag{9}$$

the pressure p being unknown for the moment.

The solution of equation (7), which breaks down into three equations, one for each component of $\boldsymbol{v}$, is a familiar result of electrostatics, and can be obtained in various ways. In the electrostatic analogue the electric potential satisfies the equation $\nabla^2 V = 0$ and has given values on the boundaries. One method of solution involves a Green's function $G_p(\boldsymbol{r})$ which is a solution of the equation $\nabla^2 G = 0$ which is zero on the boundaries and reduces to the form $G = 1/4\pi R$ near the point P, where R is the distance from P.

The solution of equation (7) is then

$$\boldsymbol{v}_P = \int\int [\boldsymbol{u}_b - (\boldsymbol{r}p/2\mu)]\frac{\partial G_P}{\partial n}dS. \tag{10}$$

The integration extends over all elements dS on the boundaries, and $\partial G_P/\partial n$ is the derivative of G normal to these boundaries into the fluid. Similarly because of equation (4) the pressure satisfies the identity

$$p_P = \int\int p\frac{\partial G}{\partial n}dS \tag{11}$$

and it is easily verified by combining equations (10) and (11) that a change of origin which affects $\boldsymbol{r}$ on the boundaries leaves the total velocity $\boldsymbol{u}$ unaltered although it changes $\boldsymbol{v}$.

The solution of any problem is then to express $\boldsymbol{v}$ in terms of p, using equation (10), and then to adjust p so that the continuity equation (8) is satisfied. This adjustment is easily done using the method of successive approximation if the main term in p on the boundary is known or can be guessed.

If equation (8) is substituted into equation (10) an integral equation for p is obtained.

$$\left(3p + r\frac{\partial p}{\partial r}\right)_P = \int\int (2\mu\boldsymbol{u}_b - \boldsymbol{r}p)\cdot\operatorname{grad}_P\left(\frac{\partial G_P}{\partial n}\right)dS. \tag{12}$$

These equations can be simplified formally by choosing the origin at P. Then the term in $\boldsymbol{r}$ vanishes at P.

$$\left.\begin{aligned} \boldsymbol{u}_P &= \boldsymbol{v}_P, \quad -2\mu(\operatorname{div}\boldsymbol{v})_P = 3p_P \\ \boldsymbol{v}_P &= \int\int [\boldsymbol{u}_b - (\boldsymbol{R}p/2\mu)]\frac{\partial G_P}{\partial n}dS \\ 3p_P &= \int\int (2\mu\boldsymbol{u}_b - \boldsymbol{R}p)\cdot\operatorname{grad}_P(\partial G_P/\partial n)dS \end{aligned}\right\} \tag{13}$$

We have mentioned that infinite boundaries cause a little trouble in these equations. Moreover the problems under discussion involve the change of flow due to the insertion of one or more particles. Thus, in dealing with problems involving flow between parallel plates or along a circular tube, we separate $\boldsymbol{u}$ in a different way.

If $\boldsymbol{U}_0$ is the main flow between and along the apparatus boundaries which satisfies the boundary conditions and the viscous equations, we write

$$\boldsymbol{u} = \boldsymbol{U}_0 + \boldsymbol{r}p/2\mu + \boldsymbol{v} \tag{14}$$

where p is now the extra pressure due to the disturbance, and $\boldsymbol{v}$ is also due to the disturbance. The effect of this is to leave all our equations unchanged except that

$$\boldsymbol{u}_b \to \boldsymbol{u}_b' = \boldsymbol{u}_b - \boldsymbol{U}_0 \text{ on boundaries.} \tag{15}$$

Since the apparatus boundaries usually move in the same way before and after the disturbance, $\boldsymbol{u}_b' = 0$ on them, and

the integrals only extend over the extra boundaries of the extra bodies disturbing the flow.

3. FORCES ON PARTICLES

Equation (6) leads to simple expressions for the force and couple on a particle in a fluid. If a sphere of radius R is drawn in the fluid around the particle, the pressure p and velocity $\boldsymbol{v}$ can be expanded in spherical harmonics on and just outside the sphere, since

$$\nabla^2 p = \nabla^2 \boldsymbol{v} = 0.$$

Since the motion is steady, the forces on the particle can be calculated by summing the stresses on the sphere, and the calculation is independent of the radius of the sphere. A force only arises from a term in p of the form $\boldsymbol{\lambda} \cdot \boldsymbol{r}/r^3$, and a term in $\boldsymbol{v}$ of the form $\boldsymbol{\beta}/r$, where $\boldsymbol{r}$ is the position vector using the centre of the sphere as origin. Because of equation (8) it follows that $\boldsymbol{\lambda} = 2\mu\boldsymbol{\beta}$ and the force on the particle is

$$\boldsymbol{F} = -4\pi\boldsymbol{\lambda}. \tag{16}$$

A similar calculation of the moment of the forces about the centre of the sphere shows that this only arises from terms in $\boldsymbol{v}$ of the form $\boldsymbol{\omega} \wedge \boldsymbol{r}/r^3$, there being no analogous terms in the pressure. As one might expect, since $\boldsymbol{\omega}$ corresponds to rotation of the fluid, the couple on the particle is

$$\boldsymbol{M} = -8\pi\mu\boldsymbol{\omega}. \tag{17}$$

4. SIMPLE PROBLEMS

(*a*) *Stokes' Law.* In the case of Stokes' law for fluid flowing past a stationary sphere the existence of a force on the sphere implies a pressure term $p = Az/r^3$ when the flow is in the z-direction and the origin is at the centre of the sphere.

The function G_P for this problem is the potential due to a point charge at P in the presence of an earthed sphere. It is well known that this is equivalent to the charge at P and an image charge at the image of P in the sphere.

Substitution of these two results into equations (10), (15) and (12) soon shows that no other pressure term is needed and that

$$A = \frac{3}{2}\mu U_a$$

where U is the speed of flow at a distance and a is the radius of the sphere. The force is therefore $4\pi A = 6\pi\mu a U$.

(*b*) *Particle in uniform velocity gradient.* The problem of the flow with uniform velocity gradient

$$U_z = 2\lambda x, \quad U_y = 0, \quad U_z = 0 \tag{18}$$

past a sphere of radius a is just as easily dealt with. The force on the sphere is zero if it moves with the fluid, and the couple is zero if has an angular velocity $\omega_y = \lambda$, the vorticity of the fluid. Thus

$$(u_b')_x = -\lambda z, \quad (u_b')_y = 0, \quad (u_b')_z = -\lambda x \tag{19}$$

A first approximation to $\boldsymbol{v}$ suggests that the pressure has the form

$$p = A\lambda a^3 \frac{xz}{r^5}. \tag{20}$$

From equation (10) we obtain for the velocity $\boldsymbol{v}$ the components

$$\left.\begin{aligned}
v_x &= -\lambda a^3\Big(1 + \frac{A}{10\mu}\Big)\Big(\frac{\partial G_0}{\partial x}\Big)_A \\
&\quad - \frac{\lambda a^5 A}{30\mu}\frac{\partial}{\partial x}\Big(\frac{\partial^2 G_0}{\partial x \partial z}\Big)_A - \frac{\lambda a^3 A}{6\mu} x_A \Big(\frac{\partial^2 G_0}{\partial x \partial z}\Big)_A \\
v_y &= -\frac{\lambda a^5 A}{30\mu}\frac{\partial}{\partial y}\Big(\frac{\partial^2 G_0}{\partial x \partial z}\Big)_A - \frac{\lambda a^3 A}{6\mu} y_A \Big(\frac{\partial^2 G_0}{\partial x \partial z}\Big)_A \\
v_z &= -\lambda a^3\Big(1 + \frac{A}{10\mu}\Big)\Big(\frac{\partial G_0}{\partial x}\Big)_A \\
&\quad - \frac{\lambda a^5 A}{30\mu}\frac{\partial}{\partial z}\Big(\frac{\partial^2 G_0}{\partial x \partial z}\Big)_A - \frac{\lambda a^3 A}{6\mu} z_A \Big(\frac{\partial^2 G_0}{\partial x \partial z}\Big)_A
\end{aligned}\right\} \tag{21}$$

where $G_0 = 1/R = [(x - x_P)^2 + (y - y_P)^2 + (z - z_P)^2]^{-\frac{1}{2}}$ is the potential due to a unit charge at P (*not* with image charge). The derivatives of G_0 are calculated at A, the centre of the sphere.

This general expression is inserted for later use. In fact the last term vanishes as the origin is at $A (x_A = y_A = z_A = 0)$.

It is now necessary to satisfy equation (8). Using equations (21) with $G_0 = 1/R$ we find $-(\operatorname{div} \boldsymbol{v}) = -2\lambda a^3\Big(1 + \frac{A}{10\mu}\Big)\frac{xz}{r^5}$ at P.

It has been assumed that $p = A\lambda a^3 xz/r^5$ on the surface of the sphere, and outside, so that $3p + r(\partial p/\partial r) = -\operatorname{div} \boldsymbol{v} = 0$

$$\text{i.e. } A = -10\mu. \tag{22}$$

The vanishing of $(3p + r\partial p/\partial r)$ is peculiar to expressions where

$$\alpha p \propto r^{-3}, \tag{23}$$

at large distances, so it is easily verified that we have not omitted any possibilities.

With this value of A the usual expressions for the velocities are obtained.

(*c*) *Particle with a hole drilled through it.* A qualitative discussion of this problem serves as an introduction to our main problem. If a hole is drilled through a sphere and the sphere falls through a viscous fluid it is found that the fluid in the hole hardly moves and falls with the sphere even when the size of the hole is an appreciable fraction of the radius of the sphere. This fact appears at first sight rather odd, but can easily be explained. In terms of our solution the explanation takes the following form. The velocity at any point P in the hole is a sum of contributions from the boundaries, each weighted with a factor $\partial G/\partial n$, the normal field on earthed boundaries due to a charge at P. Now the rest of the sphere, when earthed, effectively screens P from the outside of the sphere and from the boundary of the apparatus, so that $\partial G/\partial n$ is small except on the surface of the hole, which almost surrounds P. This boundary merely carries the fluid along with it as a rigid body.

The same argument shows that the motion of the fluid outside the sphere is not very much affected by the creation of the hole.

5. FLUID MOTION IN A SUSPENSION OF PARTICLES

The fluid motion of a suspension of particles can be divided into two parts: a mean velocity U and a local velocity around each particle which is necessary to satisfy the boundary conditions. We assume that the mean velocity U is that of a fluid of viscosity μ flowing between the walls. By this we mean either that the force of the walls equals μ times the normal velocity gradient calculated from U, or that the rate

of dissipation of energy calculated with viscosity μ and velocity U equals the actual dissipation.

According to equation (10) the correction to the velocity at any point P due to the presence of the spheres or other particles appears first in the form of integrals over the boundaries of the particles of an effective boundary velocity $(\boldsymbol{u}_b - \boldsymbol{r}p/2\mu)$, multiplied by the weight factor $\partial G/\partial n$, and secondly through an alteration in the form of the function G. To a first approximation the effective boundary velocity and pressure can be assumed to be those obtained in Section 4(*b*), and further corrections are then calculated.

The function G is considerably changed. Using the electrostatic analogy it is now the potential due to a unit positive charge at P, when all the boundaries are earthed, i.e. in the presence of a cloud of earthed particles. These earthed particles have an induced negative charge, and the effect of all these charges is to reduce the field and therefore the potential away from the point P. Thus the effect on the velocity at P due to particles some way away from P, which are shielded from it, is reduced considerably. This shielding effect becomes more noticeable as the concentration rises. When the particles touch, the shielding of P is complete. The motion of the fluid at P is calculated entirely from the motion of the boundaries nearest to it. This condition arises for quite low concentrations: at a concentration of 10% the average gap between the nearest particles is little more than their linear dimensions. Thus any calculation which assumes that the effects of the particles on one another is additive is not only incorrect but gives an incorrect picture. The reaction of a sphere back on to another, which was considered by Vand,[4] now appears as an approximate substitute for the method of images.

(*a*) *Statistical calculation of G.* The value of the function G near any one particle A can be written

$$4\pi G = G_0 + G_1 \tag{24}$$

where G_0 is the potential due to the charge at P and the charges induced on all the boundaries except that of A itself, and G_1 is the potential due to the charge on A.

When the concentration is low G_0 can be calculated statistically. At large distance the main effect of the charge on A is approximately that due to the total induced charge. For a particle in a uniform field with potential V this induced charge would be of the form $-\alpha V_A$, where V_A is the potential at its centre and α is a characteristic length. In so far as G_0 is a uniform field the same formula can be used. Consequently, except for a region near A, G_0 itself is due approximately to a charge at P and a charge density $-n\alpha G_0$ over the fluid, where n is the number of particles per unit volume. Hence Poisson's equation asserts that

$$\nabla^2 G_0 = k^2 G_0 \quad (k^2 = 4\pi n\alpha) \tag{25}$$

The solution of this equation which corresponds to a unit charge at P is

$$G_0 = e^{-kr}/r \tag{26}$$

at a distance r from P. The new feature is the introduction of the cut-off radius $(1/k)$ into this expression for G_0.

The range of validity of this approximation is given by the condition that $(1/k)$ should be greater than the mean distance $2b_0$ between particles. Defining b_0 by the equation $4\pi n b_0^3/3 = 1$, this gives for spheres, where the length α is the radius of the spheres a, that

$$kb_0 = 3^{\frac{1}{3}} c^{\frac{1}{3}} < 1$$

where $c = 4\pi n a^3/3$ is the volume concentration. This implied that c should be less than 1%.

With these limitations the function G_0 can be regarded as a continuous function of the position of the centre of the particle A. For higher concentrations from 1 to 10% the same assumption can be made but a more careful calculation of G_0 must be made.

Near each particle A the calculation of G_0 should allow for the detailed positions of neighbouring particles, and this effect increases with the concentration. As long as $kb < 1$ it does not matter very much, and we assume that A is in a sphere of pure liquid of radius $b \simeq 2a < b_0$ inside a fluid containing a continuous distribution of centres of particles.

(*b*) *Effect of one particle on velocity distribution.* The total function G is obtained from G_0 by adding to it the function G_1 so that the sum

$$4\pi G = G_0 + G_1 = 0 \tag{27}$$

on the surface of the particle A. This is quite simply done for a sphere.

In applying this in equation (10) some assumption must be made about the pressure distribution on the surface of the particle. The simplest assumption is that it is the same in form as for a single particle, i.e. $p = A\lambda xz/a^2$, although it may be necessary to change the constant A. If this should prove to be incorrect, the fresh terms will appear as corrections from the equation for div $\boldsymbol{v}$.

For a sphere, such a calculation as this leads to an expression for the velocity at P due to a moving sphere A with small concentrations which is that given by equations (21) with a new expression for G_0, appropriate to the new problem.

(*c*) *Total effect of particles on the velocity distribution.* We now have to sum over all the particles and add the integrals over the apparatus walls in order to obtain the velocity at P. The latter can be dismissed quickly. For these problems $\boldsymbol{u}_b' = 0$ on the walls and the excess pressure is zero certainly for flow between parallel plates and also for flows where the radius of curvature of the walls is greater than $(1/k)$.

Provided G_0 is a continuous function of the co-ordinates of the centre of the particle A, the sum over the particle boundaries can be replaced by an integral, except for a small region near the point P. Instead of particles A at discrete positions, it is assumed that there is a continuous distribution of centres, a volume dv_A containing $n dv_A$ particles. The approximation is the same as that made in the molecular theory of liquids.

Assuming that n is a constant, and using equations (21), the result can be expressed as a surface integral over the walls and over the surface of the excluded region near P. The former gives only a small contribution because $G_0 = 0$ on the walls for the parallel plate apparatus, and is certainly very small when P is a distance greater than $(1/k)$ from the walls.

Hence the expression for the velocity reduces to an integral over the surface of a small region near P, and a sum of terms due to such particles as lie within it. Partly for simplicity and partly because we are really discussing a time average over random positions of the spheres we assume this region is just large enough to contain the particle nearest to P when it lies well within the fluid, and when P is close to a wall we assume that this region consists of a very thin layer close to the wall. The result is not sensitive to the size of this region as long as its dimensions are less than $(1/k)$.

(*d*) *Velocity near a sphere.* By the method just described it is found that the assumption $p = A\lambda xz/a^2$ is adequate near a sphere, without extra terms, with

$$A = -10\mu(1 + c) \tag{28}$$

To a first approximation the velocity is that given by equations

(21) with $G_0 = (1/R)$ as for an isolated particle, with the new value of A.

To a higher approximation the velocity components are rather different. The value of A is

$$A = -10\mu(1 + \alpha c) \tag{29}$$

and the velocity components are

$$\left.\begin{aligned}
v_x + \frac{xp}{2\mu} &= -\frac{\lambda z a^5}{r^5} + \alpha\lambda cz\left(1 - \frac{a^5}{r^5}\right) \\
&\quad + \lambda'\beta z\left(\frac{r^2}{a^2} - \frac{a^5}{r^5}\right) \\
&\quad + 5\lambda'\frac{x^2 z}{a^2}\left[\frac{a^5}{r^5}\left(\frac{a^2}{r^2} - 1\right) - \frac{4\beta}{25}\left(1 - \frac{a^5}{r^5}\right)\right] \\
v_y + \frac{yp}{2\mu} &= 5\lambda'\frac{xyz}{a^2}\left[\frac{a^5}{r^5}\left(\frac{a^2}{r^2} - 1\right) - \frac{4\beta}{25}\left(1 - \frac{a^5}{r^5}\right)\right] \\
v_z + \frac{zp}{2\mu} &= -\frac{\lambda x a^5}{r^5} + \alpha\lambda cx\left(1 - \frac{a^5}{r^5}\right) \\
&\quad + \lambda'\beta x\left(\frac{r^2}{a^2} - \frac{a^5}{r^5}\right) \\
&\quad + 5\lambda'\frac{x^2 z}{a^2}\left[\frac{a^5}{r^5}\left(\frac{a^2}{r^2} - 1\right) - \frac{4\beta}{25}\left(1 - \frac{a^5}{r^5}\right)\right]
\end{aligned}\right\} \tag{30}$$

where $\lambda'(1 - \beta) = \lambda(1 + \alpha c)$, and the pressure is

$$p = -10\mu\lambda'\frac{xz}{a^2}\left[\left(1 - \frac{4}{25}\beta\right)\frac{a^5}{r^5} - \frac{21}{25}\beta\right] \tag{31}$$

The two parameters α and β depend on the concentration

$$\alpha = \frac{(1 + kb + \frac{1}{2}k^2b^2)}{(1 + kb + \frac{1}{2}k^2b^2) - \frac{1}{3}ck^2b^2} \simeq 1 \tag{32}$$

only differs from unity by 5% when $kb = 1{\cdot}4$, which is a large value. It should be remembered that $(kb_0)^2 = 3(a/b_0) = 3c^{\frac{1}{3}}$ and $(ka)^2 = 3c$.

$$\left(\frac{b}{a}\right)^7\beta = \frac{k^2b^2(1 + kb + \frac{1}{2}k^2b^2)}{35(1 + kb + \frac{3}{4}k^2b^2 + \frac{2}{21}k^3b^3 + \frac{1}{105}k^4b^4)} \tag{33}$$

This is a very small number, and is no larger than $0{\cdot}05$ when $kb = 1{\cdot}4$.

The interesting feature of these expressions is the appearance of terms which increase with distance from the sphere. If these expressions are used up to $r = b$ the new terms are of the same order of magnitude as the main terms. For example, whereas the terms in $\alpha\lambda cz$ are negligible for $r \simeq a$, they become the dominant terms when $r = b$. These remarks should not be taken to imply that these expressions are valid up to $r = b$. Midway between particles it is certainly necessary to consider the effects of at least three particles in detail whereas we have only considered the effect of one.

However, the small variation in α and the size of β makes one hope that the expressions may be valid for concentrations larger than a few per cent although we have no positive evidence of this.

(*e*) *The effective viscosity.* The effective viscosity is calculated either from the rate of dissipation of energy or the velocity gradient near the walls. If the second method is used it is necessary to calculate the velocity at points near the wall. We exclude from the region of continuous centres a thin layer of thickness d on the boundary, not covering the whole boundary but of radius r_0 sufficiently large for G_0 to be practically zero along its narrow rim. By the method of images we now calculate G and G_0, removing the boundary and substituting a negative charge at the image of P. The distance of P from the boundary is $\rho < d$. The integrals involved are over the curved rim of the layer and its flat surface at a distance d from the wall.

Neglecting the term in $\nabla^2 G_0$ which is small of order c, the only term that remains is in v_z and this is

$$v_z = n\lambda a^3\left(1 - \frac{A}{15\mu}\right)\iint G_0 dS \tag{34}$$

over the flat surface of the layer. Assuming that the value of G_0 in the bulk of the fluid does not depend on the existence of this thin layer, the necessary expression for it is a term in e^{-kR}/R due to the charge at P and a similar term due to the image. The integration then gives, when $kd \ll 1$

$$v_z = n\lambda a^3\left(1 - \frac{A}{15\mu}\right)4\pi\frac{\sinh k\rho}{k} \tag{35}$$

with a velocity gradient at the boundary, assuming that $A = -10\mu$, of

$$\left(\frac{\partial v_z}{\partial \rho}\right)_0 = 5\lambda c \tag{36}$$

Thus the total velocity gradient near the boundary is

$$\frac{\partial U}{\partial x} + \frac{\partial v_z}{\partial x} = 2\lambda(1 + 2{\cdot}5c) \tag{37}$$

as originally obtained by Einstein.

This method of deriving the effective viscosity is rather insensitive to the method of deriving G_0, which is only introduced at the very end, although it does depend on the replacement of the summation over particle boundaries by an integration. To improve the value it is necessary to have a more accurate expression for G_0 than we are using, and it should include the term in $\nabla^2 G_0$ which was ignored.

(*f*) *Consistency of equations.* The consistency of the several approximations which have been made can be checked quite simply by calculating from the various equations the results for the simplest flow. If the liquid is flowing with uniform velocity in the z-direction, the particles also move along with it with this velocity. In order to obtain this result using our approximations [cf. equation (25)],

$$k^2 = 4\pi n\alpha\left(\frac{\sinh kb}{kb}\right) \tag{38}$$

which reduces to the simpler expression $k^2 = 4\pi na$ for spheres at low concentrations.

6. DISCUSSION

The preceding calculations may seem to have done little more than define the region of validity of the Einstein expression for the effective viscosity. In fact they have done more than that, since there are many other problems which can be treated along similar lines.

Although some of the details of the preceding work in Section 4 assume that the flow is between parallel plates, the results apply in general to other motions, provided that the velocity gradient is uniform over a region rather greater than the cut-off radius ($1/k$) and that the particle concentration is uniform. The cut-off radius is usually quite small, even for low concentrations. For particles of size 2 μ its value at a concentration of only 0·01% is no more than 100 μ.

Similarly, any variations in the particle concentration do not matter if they are inappreciable over a distance ($1/k$),

but we have to consider the possibility that they are greater than this, particularly near the wall. The calculation of the effective viscosity from the velocity gradient near the wall is especially vulnerable to this effect as we have assumed that the concentration there is the same as the average concentration in the fluid. It has not been found possible yet to devise any rule by means of which the variation of concentration can be deduced, but an attempt has been made to calculate the effect of any variation. Assuming a decrease near the wall rapid enough to affect the calculations, it was shown that the effect on the effective viscosity due to this decrease was compensated by terms in the equations due to the concentration gradient, so that the final result was the same as if the concentration in the bulk of the fluid had been used.

For large concentrations where particles are close together the shielding effect is so important that each particle must be discussed on its own. From a diagram showing a number of spheres close together it would seem that the motion of the fluid up to a distance b_0 from the centre of a particle might approximate to that of fluid between a sphere A rotating with angular velocity λ and an outer rigid envelope of radius $(2b_0-a)$ rotating in the opposite sense with an angular velocity $\omega_1 = a\lambda/(2b_0-a)$, together with a uniform shearing motion of the envelope. This model, however, seems a little crude and does not give very good results at present.

An alternative approach would be to assume that the velocity distribution outside the sphere is that given by equation (30) with one or two adjustable parameters, since this expression has the merit of giving zero velocity components in the right places. However, it breaks down in the dead regions equidistant from three or more particles.

Finally it should be added that the method can be extended to include particles of all shapes. At first sight this appears very difficult in view of the integrals over the boundaries. For any shape, except a sphere, these are bound to be difficult, if not impossible. That this is not a real limitation follows from the observation, that in the original formulation, the boundaries were not necessarily real boundaries, i.e. they are surfaces drawn in the fluid, the values of u_b being the fluid velocity on these surfaces. The equations then become conditions which the fluid flow must satisfy, and it is possible to deduce fluid flows of the usual types by a self-consistent calculation of the velocity using these equations.

To calculate the effect of non-spherical particles, therefore, we surround each particle by a sphere large enough to contain the particle, but so small that the velocity of the fluid inside is due almost entirely to the particle inside. From this we can deduce the velocity of the fluid on the surface of the enclosing sphere from the single particle problem, and use the result as the value of u_b in a calculation which now proceeds on lines identical with that of the spheres. Among the parameters involved are those defining the orientation of the particle. To allow for this G_0 is calculated as an average overall orientation of the other particles, and this is correct as long as there is not correlation between the motion of the particles. Similarly in the subsequent summations over boundaries an average over orientations is to be taken. It is hoped to give the results of such calculations in later papers.

REFERENCES

(1) EINSTEIN, A. *Ann. Phys.* [*Leipzig*], **19**, p. 289 (1906); **34**, p. 591 (1911).
(2) FRÖHLICH, H., and SACK, R. *Proc. Roy. Soc. A*, **185**, p. 415 (1946).
(3) BURGERS, J. M. *Proc. K. Ned. Akad. Wetensch.*, **44**, p. 1177 (1941); **45**, p. 9 (1942).
(4) VAND, V. *J. Phys. Coll. Chem.*, **52**, 277 (1948).
(5) WARD, A. N. Private communication.

DISCUSSION

Mr. R. H. Essenhigh: At the Safety in Mines Research Establishment we have been concerned recently with the motion under gravity of dust clouds at medium concentrations which are confined in a vertical Pyrex tube of 16 ft length and 3 in. diameter. This represents a sedimentary system and we have carried out a semi-empirical analysis using the permeability equations as suggested by Professor Kynch[1] in 1952. This analysis has been adequate for our immediate purpose, but the equations obtained involve three rather arbitrary constants and we should be interested to know whether Professor Kynch thinks that his equations could be adapted to our experimental conditions and used to predict the values of the three constants.

To obtain the equations we assumed that the interaction between particles was sufficient to prevent significant elutriation and the dust cloud could then be regarded as a continuous porous body. The vertical tube is open at the bottom and effectively closed at the top so that the air is stationary. There is a continuous dust feed mechanism at the top of the tube and the effect produced is that of an infinite porous piston in continuous steady motion which therefore creates a small but measurable drop in pressure at the top of the tube.

For analytical purposes, a thin horizontal element of the porous body is considered and this may be regarded as equivalent to a set of capillaries. This provides three major forces affecting the motion of the element: (i) gravity, acting downwards; (ii) friction of the air as it is forced through the equivalent capillaries, acting upwards; (iii) friction of the containing tube on the porous body, acting upwards. When these forces balance, the porous body is moving downwards at constant velocity and a negative pressure gradient is established up the tube.

Applying the permeability equations to this system the following relations were obtained:

$$\Delta y = H(1 - 2K_2/ag)D \tag{1}$$

$$D = (K_1/K_2)^{1/(n+1)}(M'/A)^{n/(n+1)} \tag{2}$$

$$F_s = K_1 V_c^n = K_2 D \tag{3}$$

where K_1, K_2 and n are the three arbitrary constants, and

D = dust cloud density;
Δy = pressure drop at top of tube (cm of water gauge);
M' = rate of feed of dust;
H = height of pressure point from bottom of tube;
a = tube radius;
g = gravitational constant;
A = cross-sectional area of tube;
F_s = frictional force of dust cloud on containing tube;
V_c = terminal velocity of the dust cloud.

The first two equations have been verified experimentally and the proportionality of Δy with D is illustrated in the figure. For this, cork dust was used over the concentration range 0·02 to 2 g/litre (volume concentration range 0·01% to 1%).

Equation (3) is important in that it gives the relation between the terminal or settling velocity of the cloud and the cloud concentration.

So far, three different cork dust samples have been examined. They all have a considerable particle size distribution but with a decreasing fraction of fines. The values of the constants for the three fractions are given in the table.

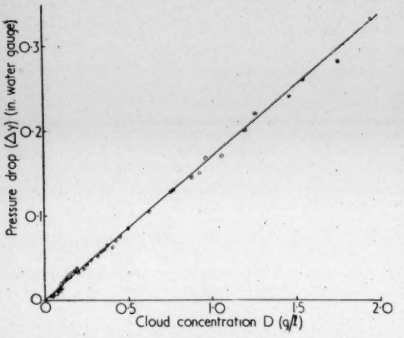

Relation of pressure drop (Δy) to cloud concentration (D). Experimental error in D, $\pm 0{\cdot}01$ g/l, and in Δy, $\pm 0{\cdot}005$ in. water gauge

Values of constants for different cork dust samples

Dust sample	K_1	K_2	n	$n/(n+1)$
fine	$1{\cdot}5 \times 10^{-4}$	331	2	0·667
medium	$6{\cdot}34 \times 10^{-13}$	200·5	7·33	0·88
coarse	—	271	∞	1·00

The importance of K_2 is that it also involves the specific surface of the dust cloud S by the relation

$$SF_c/g = (1 - 2K_2/ag) \qquad (4)$$

where F_c is the frictional force of the air in the capillary and if we know F_c, S can then be calculated.

This application of the permeability equations might be of value in analysis of other sedimentary systems.

Prof. F. R. Eirich: Prof. Kynch's lucid analysis is a welcome contribution to the general understanding of the flow behaviour of suspensions, presenting a convenient basis for the approach to a large variety of problems. It should be pointed out, however, that a number of problems stated in Prof. Kynch's paper have been satisfactorily treated before.

Of the papers quoted, the one by Vand on concentration effects is mathematically correct but suffers from an unacceptable physical premise. The papers by Guth and Gold,[2] and by Weissberg, Simha, and Rothman[3] have not been mentioned. The latter paper, in particular, treats in detail the shielding effect pointed out by Prof. Kynch. Simha has also discussed the conditions under which Einstein's law may be expected to hold in capillaries. Together with Mark and Huber,[4] and with Riseman,[5] earlier papers of mine deal with the behaviour of perforated bodies and with concentration effects analysed in terms of hydrodynamics designed to deal with swarms of particles. The latter method has been worked out simultaneously by Brinkman[6] and by Debye and Bueche,[7] and has been further developed and extensively employed by Kirkwood and Riseman.[8]

Author's reply: In the paper referred to by Mr. Essenhigh, the suggestion was made that the assumption that D is a function of V_c, in his notation, might be used to analyse experimental data on sedimentation. His equation (3) is a special form of this, which may be true over a limited range of concentrations, or in the turbulent conditions probably existing in a cloud of fine particles. It would be interesting to know whether n is negative for very coarse particles.

It is doubtful whether these constants could be calculated at present. My paper is an attempt to make such calculations under much simpler conditions.

Since my remarks on Vand's work may be misinterpreted, I should like to add that I do not accept his methods, especially that of the incremental increase in concentration. On the other hand, the form of his results is suggestive, plausible and useful, provided the numerical estimates are not taken too seriously.

I am grateful to Professor Eirich for pointing out to me (in oral discussion) that Simha[9] has already made calculations along the lines suggested in Section 6. He assumes that each particle is contained in a spherical cell of radius $b (\sim b_0)$ the boundary of which is fixed, and obtains reasonable agreement with experiment. The fact that I failed to obtain agreement with a model almost identical to his seems to be due to a numerical mistake on my part. It seems to me, however, that all these theories, although interesting, must be judged by their use in throwing light on more complicated questions such as the effect of variations in particle size and variation of concentration at boundaries and variable gradients.

(*Added subsequently.*) In reply to Prof. Eirich's written contribution, the aspect of my paper which seemed to me to be important was the demonstration of the shielding effect, which suggests quite different approximations at low and high concentrations. Apart from the paper of Weissberg, Simha and Rothman,[3] of which I was unaware until Prof. Eirich mentioned it, the papers which he mentions do not discuss this aspect and, rightly or wrongly, I omitted mention of them to avoid an extensive and complete bibliography of the whole field. I am glad that Prof. Eirich has pointed out this omission. Important work has been done by all the authorities he quotes. If I might add to his list, it would include Prof. Oldroyd, who has sought the equations of flow of concentrated suspensions.

REFERENCES

(1) Kynch. *Trans. Farad. Soc.*, **48**, p. 166 (1952).
(2) Guth and Gold. *Phys. Rev.*, **53**, p. 322 (1938).
(3) Weissberg, Simha and Rothman. *J. Res. Nat. Bur. Stand.*, **47**, p. 298 (1951).
(4) Eirich, Mark and Huber. *Der Papier-Fabrikant*, **27**, p. 251 (1937).
(5) Eirich and Riseman. *J. Polym. Sci.*, **4**, p. 417 (1949).
(6) Brinkman. *Physica*, **13**, p. 447 (1947).
(7) Debye and Bueche. *J. Chem. Phys.*, **16**, p. 573 (1948).
(8) Kirkwood and Riseman. *J. Polym. Sci.*, **4**, p. 417 (1949).
(9) Simha. *J. Appl. Phys.*, **23**, p. 1020 (1952).

Paper A.2

The terminal velocity and structure of airborne aggregates of microscopic spheres

By V. Timbrell, B.Sc., A.R.C.S., D.I.C., Ph.D., Pneumoconiosis Research Unit, Llandough Hospital, Nr. Penarth, Glam.

The terminal velocity of aggregates of spheres is determined by means of a dust sampling instrument which deposits them at sites on a collecting plate related to their terminal velocity; the size and relative positions of the spheres in an aggregate are determined microscopically. A test is applied to decide whether an aggregate examined was airborne in the same state or formed by juxtaposition of two or more airborne units at the same site. The free-fall orientation of an aggregate can be inferred from its orientation on the collecting plate. Results are given for the relationship between the Stokes' diameter of a doublet and the size of the components.

The parameter of a dust particle on which its motion in air depends is its terminal velocity. Whereas the terminal velocity of an irregular particle is determined by more than one dimension of the particle, the terminal velocity of a solid sphere of given density is related in a known way to the diameter which can be readily measured microscopically. Artificial clouds of spheres are therefore particularly useful in the laboratory for a number of purposes, including the determination of the collecting efficiency of dust sampling instruments and for studying the process of aggregation.

Aggregates are formed in such a cloud by collisions between spheres sedimenting at different rates. The collisions may also be the consequence of motion imparted to the air to give good mixing of the cloud, or imparted with the intention of increasing the proportion of aggregates.

If the effect of aggregation, and particularly if the process of aggregation is being investigated, it is desirable to know the terminal velocity of an aggregate as well as its structure, i.e. the size and relative positions of its component spheres.

Information about the structures of the aggregates can be obtained by microscopic examination of the deposit provided by one of a number of dust sampling instruments, e.g. by a sedimentation cell. The information thus obtained is subject to error, however, because no distinction can be made between "true" aggregates, which are seen in the deposit in the same state as when airborne, and so-called "synthetic"(1) aggregates which are formed by juxtaposition in the deposit of separately sampled spheres and true aggregates. Moreover the microscopic appearance of an aggregate in the deposit does not *per se* indicate its terminal velocity.

This paper describes a method of investigating the relationship between the terminal velocity and structure of aggregates of different types, e.g. doublets, triplets, etc. The method can also be used to determine the frequency distribution of the aggregates in a cloud on the basis of terminal velocity.

In any subsequent study of the state of aggregation of a cloud either the method described here may be used directly, or another technique of sampling the cloud which only provides information on the structure of the aggregates may be employed and the terminal velocities of the aggregates estimated from their structures by means of the results of the present investigation.

METHOD OF THE INVESTIGATION

It would be difficult to investigate the relation of the terminal velocity to the structure of aggregates with components 1–20 μ in diameter by first constructing the aggregates and then timing their fall. An easier method is to sample an aggregated cloud of spheres by means of an instrument in which the particles are deposited at distances along a collecting plate related to their terminal velocities. By microscopic examination of the deposit the terminal velocity of an aggregate can be determined from its site in the deposit, and its structure also investigated.

To carry out the investigation in this manner it is clearly desirable that the cloud should contain a high proportion of aggregates so that even in a deposit sparse enough to avoid forming many synthetic aggregates there will be sufficient true aggregates of different types.

Glass spheres are particularly suitable for the investigation and can be produced by fusing irregular Pyrex glass particles of the appropriate size in an air-acetylene flame, the particles being carried into the flame by the air supply. Although aggregates of irregular particles may be plentiful in the incident air, they fuse on passing through the flame to form single spheres, and with the large additional quantities of air that must be supplied to ensure a non-explosive atmosphere in the chamber containing the cloud, the subsequent spontaneous aggregation is insufficient. A well-aggregated cloud can be generated by collecting a quantity of spheres produced in this manner and re-dispersing them into a confined space.

THE GRAVITATIONAL TERMINAL VELOCITY DUST SAMPLER

The sampling instrument used in the investigation is described in another paper to this conference. Briefly, airborne particles are allowed to settle from a fixed height in a horizontal duct through which clean "winnowing" air flows at a constant rate. The particles fall at their individual terminal velocities and have a common horizontal velocity equal to that of the winnowing air. The lower the terminal velocity of a particle the further the particle is carried along the duct before being deposited on a glass collecting plate. The particles of the same terminal velocity lie on a line across the deposit at a distance along the deposit strictly related to the terminal velocity.

The good quality of the separation is demonstrated by the uniformity of size of isolated solid glass spheres in the deposit at any one site. Fig. 1 shows a photomicrograph of a small

Fig. 1. Photomicrograph of solid glass spheres at a site in the deposit where the mean diameter is 10 μ

area in the deposit at a site where the mean diameter of the spheres is 10 μ, and Fig. 2 shows the shape of the corresponding relative frequency distribution curve of the ratio (actual diameter of a sphere)/(mean diameter of the spheres) at the same site; the standard deviation of the distribution is about 0·02. The size separation of spheres in any other part of the deposit is of similar quality.

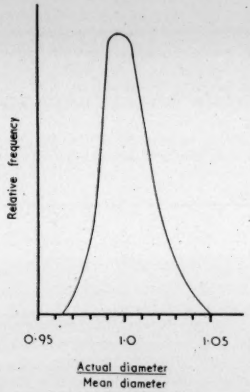

Fig. 2. Typical graph showing the spread in the diameter of solid glass spheres at a given site in the deposit

DETERMINATION OF THE TERMINAL VELOCITY OF AN AGGREGATE

An aggregate is classified by the sampling instrument as if it were a sphere of the same terminal velocity. The Stokes' diameter of the aggregate can therefore be determined from the diameters of the isolated spheres of the same density at the same site in the deposit. Whereas the Stokes' diameter is taken to be equal to the mean value of the diameters of these spheres the true value has a possible spread similar to that of the diameters of these spheres.

To enable the Stokes' diameter of an aggregate to be immediately determined from its site in the deposit, the deposit is calibrated by measuring a large number of isolated spheres at each of a number of sites along the deposit and a calibration curve is drawn showing the mean diameter of the isolated spheres against the distance along the deposit; the diameters are measured by a microscope attachment described elsewhere[2] with an error of about 1% at 10 μ and about 3% at 1 μ. Subsequently, the Stokes' diameter of an aggregate seen at any site in the deposit can be ascertained from the calibration curve, and its terminal velocity then evaluated from the existing data on the terminal velocity of spheres of specified density and diameter. Since this paper is concerned with only one material, glass (density 2·25 g/cm^3), Stokes' diameter will be employed as a measure of terminal velocity.

Some of the glass spheres, especially the large ones, produced by the method outlined, contain gas bubbles. When calibrating the instrument it is necessary to ensure that such spheres are discounted. One advantage of glass over other materials is that the presence of gas bubbles is readily detected.

DETERMINATION OF THE STRUCTURE OF AN AGGREGATE

The determination of the structure of an aggregate in the deposit, which entails measuring the diameter of each component and ascertaining the positions of the components relative to one another, is carried out under the microscope using mainly a 4 mm objective.

The diameter of a component sphere can be measured by means of the microscope attachment mentioned earlier or by means of a filar micrometer. The relative positions of the components in three dimensions can be ascertained from the diameters of the components, and the horizontal and vertical distances between their centres, the vertical distances being measured by means of the graduated fine-focus control on the microscope. In the case of the more complex aggregates a micro-manipulator may be needed to separate the components.

Occasionally, a gas bubble in a sphere has the appearance of an attached sphere but, by determining the diameters and relative depths of the major sphere and minor sphere or bubble, the true state can be ascertained. Fig. 3 is a photomicrograph showing a sphere containing a gas bubble which might be mistaken for a doublet. That it is a single sphere containing a bubble is evident in this case because its diameter is appreciably larger than that of the neighbouring solid

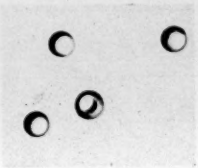

Fig. 3. Photomicrograph of a sphere containing a gas bubble, and some solid spheres

spheres, whereas the experimental results show that each sphere of a true doublet is smaller than the Stokes' diameter of the doublet.

In the present investigation since it is assumed that the density of all spheres equals the bulk density and that a sphere is completely specified by its diameter, aggregates containing spheres which are not solid are discounted.

A test can be applied to an aggregate in the deposit to decide whether it is true or synthetic. The test depends on the fact that if an aggregate is synthetic the simpler aggregates and/or single spheres which were sampled separately and deposited in juxtaposition, must have Stokes' diameters consistent with the site of the aggregate within the deposit. Any aggregate of interest is therefore mentally subdivided in all possible ways, with the condition that the relative positions of the component spheres in a subdivision must be the same as in the main aggregate; from the results already obtained on the simpler aggregates the Stokes' diameter of each subdivision is estimated from its structure. The aggregate can only be synthetic if the estimated Stokes' diameters of the subdivisions are close to the value of Stokes' diameter corresponding to the site of the aggregate in the deposit. Separation by the instrument must be good, firstly so that the data accumulated on the simpler aggregates allow an accurate estimate to be made of the Stokes' diameter of a subdivision, and secondly, so that there is little scatter in

the value of Stokes' diameter corresponding to the site in the deposit. Because of the good separation that has been achieved it is possible, for this test, to take the diameter of any isolated sphere at the same site as the aggregate as a measure of the Stokes' diameter corresponding to the site.

Fig. 4 is a photomicrograph of two similar true doublets and one synthetic doublet. The true doublets can be recognized because the diameters of the components of each are

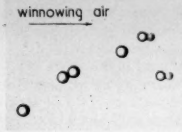

Fig. 4. Photomicrograph of two similar true doublets, one synthetic doublet, and isolated spheres

too small for them to have been deposited separately at the same site as the isolated spheres. The third doublet is clearly synthetic on account of the equality of the diameters of its components and of the isolated spheres.

As more information is accumulated on the relation of the Stokes' diameter of true aggregates to their structure, so the test can be applied to aggregates of increasing complexity.

In Fig. 5 some complicated aggregates are shown in two dimensions for simplicity and the diameters therefore must

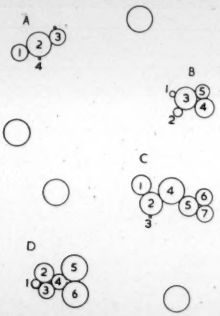

Fig. 5. Diagrammatic representation of complicated aggregates at a site in the deposit. *A* and *B* are true aggregates; *C* and *D* are synthetic aggregates

not be taken as exact. Aggregates *A* and *B* are true aggregates since all the possible subdivisions have estimated Stokes' diameters which indicate that had they been sampled separately, they would have been deposited elsewhere. Aggregate *C* is synthetic, being composed of a true triplet (1, 2, 3), a single sphere (4), and a true triplet (5, 6, 7). Aggregate *D* is also a synthetic being composed of a quadruplet (1, 2, 3, 4) and two single spheres (5, 6).

ORIENTATION OF AGGREGATES DURING SEDIMENTATION

The orientation that an aggregate takes up with respect to the vertical while falling freely in infinite space can be inferred to some extent from the orientation of the aggregate on the glass collecting plate. The following considerations are pertinent:

(i) The strength of the forces which tend to prevent an aggregate changing its orientation once it has made contact with the collecting plate is evident from the many aggregates that are seen in positions other than those of maximum stability. Also, in the case of synthetic doublets, the axis through the centres of the component spheres is often inclined at a large angle to the vertical, indicating that the lower sphere does not roll readily under the impact and weight of the second sphere of the same size.

(ii) The distances between a falling aggregate and the vertical walls of the duct between which it settles in the sampling instrument are so large compared with the dimensions of the aggregate that the walls are unlikely to have much effect on the orientation of the aggregate.

(iii) An aggregate before being deposited on the collecting plate passes through a layer of winnowing air in which the horizontal velocity decreases downwards; thus the upper part of the aggregate is under a greater drag than the lower.

It has been observed that true doublets are deposited with the smaller component (unless it is very small compared with the other) uppermost and with the axis of symmetry through the centres of the components inclined to the vertical in the direction of flow of the winnowing air as shown in Fig. 4. The greater the size of the upper component relative to the lower, the greater is the angle of inclination. This can be explained by presuming that a doublet normally falls freely in infinite space with the axis of symmetry vertical and that the axis inclines in the direction of flow of the winnowing air when the doublet passes through the layer mentioned in consideration (iii). When one component of a doublet is very small compared with the other, the axis of symmetry on the collecting plate has almost any orientation with respect to the vertical and to the winnowing air, indicating that if the doublet prefers a vertical axis of symmetry when falling freely, this is only taken up very slowly and also that the layer mentioned in (iii) has little effect on the orientation.

Gans[3] has shown that a particle that has three mutually perpendicular planes of symmetry will not change its initial orientation when falling, whatever this may be. Doublets consisting of two equal spheres possess such symmetry but, so far, the restricted conclusion that can be drawn from the present observations is that a doublet takes up the preferred orientation described above if the diameter of one sphere is not very small but less than 90% of the diameter of the other.

The effect of the layer mentioned in (iii) on more complicated aggregates is probably the same as the effect on doublets, so that their preferred orientation during sedimentation can also be inferred from their orientation on the collecting plate.

DETERMINATION OF THE FREQUENCY DISTRIBUTION OF AGGREGATES

The frequency distribution according to Stokes' diameter either of all aggregates or of aggregates of specified type (doublets, triplets, etc.), can be obtained from the deposit. At various distances along the deposit counts are made of the number of aggregates seen in microscopic traverses along the lines of constant Stokes' diameter; the range of Stokes' diameter corresponding to a traverse is equal to the product

of the width of the traverse and the gradient of the calibration curve at the point appropriate to the position of the traverse. The frequency of the aggregates occurring within a given small increment of Stokes' diameter, at any value of Stokes' diameter, is thus obtained by dividing the number counted in the corresponding traverse by the width of the traverse and by the gradient of the calibration curve. The relative frequencies are obtained by making the increments of Stokes' diameter equal over the whole range.

EXPERIMENTAL RESULTS ON STOKES' DIAMETER OF DOUBLETS

The description of the geometry of an aggregate rapidly becomes very complicated as the number of components increases. For example, doublets are uniquely described by the diameters of the two component spheres. Triplets are only uniquely described by the diameters of the three component spheres if the spheres are in mutual contact, otherwise an infinite number of possible configurations exist. The geometry of aggregates with a larger number of components is correspondingly more complicated.

It follows from the uniqueness of the geometry of a doublet that the Stokes' diameter is uniquely dependent on the size of the components, assuming equal densities. Only the quantitative experimental results of the investigation of doublets will be dealt with here.

Each doublet is specified by three parameters, the diameters D_1 and D_2 of the component spheres and the Stokes' diameter D_s. The problem is to determine the relationship between these three.

For a fixed D_s,

$$\frac{D_2}{D_s} = f_s\left(\frac{D_1}{D_s}\right)$$

The diameters of the components of a large number (about 200) of doublets in a small range of D_s were measured and the value of D_s of each doublet was determined from the calibration curve mentioned earlier. The ratios D_1/D_s and D_2/D_s were then plotted against one another and the curve of the type shown in Fig. 6 drawn through the points; these points showed some scatter because of the imperfect separation achieved by the sampling instrument. The curve is, of course, symmetrical about $D_1/D_s = D_2/D_s$ since either component may be called D_1.

By repeating this procedure at a number of different values of D_s in the range 3–20 μ the relationship between D_1/D_s and D_2/D_s was found to be independent of D_s within the limits of experimental error, i.e. for fixed D_s

$$\frac{D_2}{D_s} = f\left(\frac{D_1}{D_s}\right) \text{ for all } D_s.$$

This relationship is illustrated in Fig. 6.

Alternatively, it may be inquired: what is the effect on D_s of adding to a sphere of fixed diameter D_1, a sphere of varying diameter D_2? The relationship is shown in Fig. 7 and demonstrates that the Stokes' diameter of a doublet is determined mainly by the diameter of the larger component.

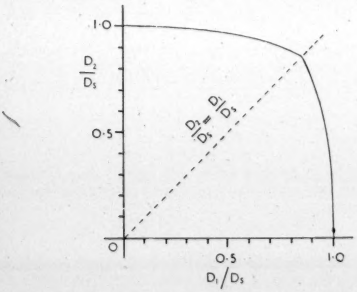

Fig. 6. Graphical relationship between the diameters of the components of a doublet of fixed Stokes' diameter

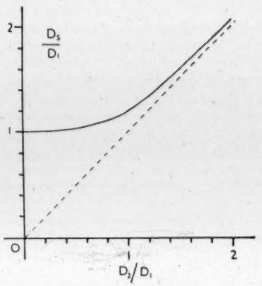

Fig. 7. Graphical relationship between the Stokes' diameter of a doublet and the diameter of one component, when the diameter of the other component is fixed

ACKNOWLEDGEMENT

I wish to express my thanks to Mr. S. R. Morgan for preparing the photographs and diagrams.

REFERENCES

(1) WYNN, A. H. A., and DAWES, J. G. *Min. of Fuel and Power Research Report*, No. 28 (Aug. 1951).
(2) TIMBRELL, V. *Nature* [*London*] **170**, p. 318 (1952).
(3) GANS, R. *Sitz Ak. Wiss. München*, p. 191 (1911).

DISCUSSION

M. J. L. Soulé: It may be interesting to compare the experimental results given by Dr. Timbrell on the terminal velocity of the aggregates with the values derived from the hydrodynamic theory. An exact calculation is possible for a doublet composed of two spheres. Stimson and Jeffery[1] have given exact formulae for the resistance acting upon two spheres which are a known distance apart. Faxen[2] has derived the limit of the formula for two equal spheres, when they touch each other. I have applied his method to the case of two unequal spheres.

According to Faxen, for two spheres of unit diameter the Stokes' diameter is 1·245. For example, if the ratio of the diameters is 1·5, I have calculated that the Stokes' diameter is 1·622. The calculated Stokes' diameter is just a little

smaller than the diameter of a sphere having the same volume as the doublet (at the utmost, it is inferior to it by 1·2%).

According to the measurements made by Dr. Timbrell, a doublet falls noticeably more slowly than is shown by the mathematical treatment (effective Stokes' diameter can be 6 or 7% smaller than the calculated diameter). Among the possible reasons explaining this difference, the following (to which Dr. le Bouffant drew my attention) seems to be plausible: the velocity is calculated for the steady orientation, namely in such an orientation that the smaller particle is exactly above the larger particle; but in practice oscillations take place during the fall, and as the other orientations all give lower velocities, the effective average velocity is then finally reduced in comparison with the theoretical velocity.

Mr. H. H. Watson: The size separation achieved by Dr. Timbrell in his apparatus appears to be very good. Can he say how it compares with that obtained with a Conifuge?

Is it possible to infer the orientation of an aggregate while airborne from its orientation on the glass collecting surface?

Mr. B. Lincoln: The main emphasis in the papers presented at this Conference has been on the application of Stokes' law to the motion of particles of shapes often other than spherical. In some cases, indeed, the retention of Stokes' law is made possible by introducing suitable correction factors; but in instances where the nearest approximating geometrical model is other than spherical, it is desirable to investigate the possibility of calculating the drag coefficient of the most suitable model. For example, as a result of the work of Lamb[3] and of Tomotika and Aoi[4] such a procedure may be adopted for the motion of a cylinder perpendicular to its longitudinal axis. The data of the latter workers is compared in the figure with the observed rate of fall of cylindrical particles

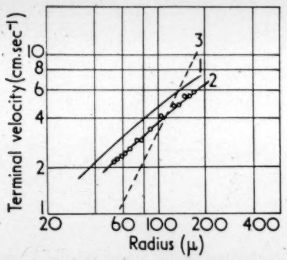

Terminal velocity of cylindrical particles in a viscous medium

Curve 1: theoretical; curve 2: experimental; curve 3: Stokes' radius.

in water and it is evident that the agreement is such as to encourage further work along these lines. The curve for the Stokes' radius (defined as the radius of a sphere of the same material having the same terminal velocity) is included for comparison. However, since the terminal velocity of these particles is predicted (and observed) to be independent of the length of the particle, the concept of Stokes' radius is not a satisfactory way of estimating the mass or volume of the particle.

Some other points relating to the motion of sedimenting particles may now be mentioned. The orientation of the particles in the above experiments was in all cases such that the longitudinal axis was horizontal. This is evidently the most stable configuration, and in general it will be conditions of stability, rather than maximum drag, that will determine the orientation of a falling particle. By applying the principles of the dynamics of rigid bodies, the forces acting on a sedimenting particle may be considered as affecting the translational motion of the mass-centre, and the rotation of the particle about this point. If the particle is of uniform density, the forces to be considered are the apparent weight acting at the mass-centre, and the resultant drag force which need not initially act through the mass-centre. The conditions for equilibrium of the rotational configuration are then that the weight and drag should be co-linear and that small angular displacements should produce a restoring couple. In some cases, e.g. cylinders at high Reynolds' numbers, a "street" of vortices, if formed in the wake of the particle, would cause it to undergo an oscillatory rotation as a result of the periodic displacement of the line of action of the resultant drag force.

Author's reply: In reply to M. Soulé I must point out that a discussion on the difference between the experimental and theoretical values for the Stokes' diameter of a doublet has been omitted from the present paper because of the many possible explanations, including the one put forward by M. Soulé, that have to be considered. Some of the difference must be due to experimental error in the measurement of the microscopic spheres, and to imperfection in the size-separation by the instrument. The fact that the difference between the two values increases as the two components of the doublet become more nearly equal suggests observer error in not discounting all synthetic doublets; the test to distinguish synthetic doublets from true ones needs to be most critical when the components of a doublet are nearly equal and neither is very different from the single spheres deposited at the same site. The hydrodynamic theory does not take account of the discontinuous nature of air. There may well be a difference between the "slip" correction for doublets, especially for the smaller ones, and that for the single spheres deposited at the same site which are used as a measure of the Stokes' diameter.

I have no information on the Conifuge to use for comparison, in answering Mr. Watson. In the paper, an attempt has been made to relate the orientation of a doublet on the collecting surface to its airborne orientation. The inferred orientation is the same as the orientation observed for a larger doublet settling in liquid.

REFERENCES

(1) Stimson and Jeffery. *Proc. Roy. Soc. A*, **111**, p. 110 (1927).
(2) Faxen. *Z. Angew. Math. Mech.*, **7**, p. 79 (1927).
(3) Lamb, H. *Hydrodynamics*, 5th edn., p. 583 (Cambridge: The University Press, 1930).
(4) Tomotika, S., and Aoi, T. *Quart. J. Mech. Appl. Math.*, **6**, p. 290 (1953).

Paper A.3

Dust shadows below a cylinder containing a suction orifice and deposition of particles upon the cylinder

By C. N. Davies, D.Sc., F.Inst.P., and V. Peetz, B.Sc., Medical Research Council's Environmental Hygiene Research Unit, London School of Hygiene and Tropical Medicine, London, W.C.1

A study is made of the aspiration of dust, suspended in an ideal fluid, into a bulky sampling head with an orifice in the top. The behaviour of the particles is characterized by the value of a parameter k which is proportional to the square of the particle size divided by the rate of suction.

When k is greater than 2, gravity governs the movement of the particles and when it is less than $1/(3 + 2\sqrt{2})$ the influence of suction predominates. For values exceeding $1/(3 + 2\sqrt{2})$ a shadow free from dust extends to infinity below the head and particles settle on the top. For smaller values of k there is no deposition on the head and the shadow area is finite.

An indication is given of the way in which the system could be employed for particle size analysis by selective sampling.

When dusty air is drawn into a suction orifice in a sampling head, there exists a region which is free from particles because it is screened by the head. On top of the head a deposit may collect owing to gravitational settlement of particles. The shape of the dust shadow region below, and the extent to which particles deposit on top, depend on particle size, rate of suction and air movement. Quite a number of intricate systems could exist which would be difficult to analyse, but it has been found possible, as a start, to come to definite conclusions regarding the suction of particles into an orifice in the top of a bulky sampling head in air which is at rest, apart from movement induced by the suction.

NEGLECT OF INERTIA

When a cloud of particles suspended in a fluid is sucked into an orifice, the inertia of the particles may cause their velocities to differ from that of the surrounding fluid. The magnitude of the effects due to this is indicated by the value of the particle parameter, $P = Ud^2\rho/9\eta D$, where U is the mean velocity in the orifice, d is the diameter of the particles, ρ their density, η the viscosity of the fluid and D the diameter of the orifice. This is valid unless the rate of suction is so violent that the drag of the particles is greater than is given by Stokes' law, when the inertia of the fluid has to be taken into account as well as that of the particles.

For values of P less than about $\frac{1}{3}$, the inertia of the particles can be neglected, but their course into the sampling orifice does not follow the streamlines of flow if they possess an appreciable sedimentation velocity due to gravity. These conditions are quite common when sampling airborne dust particles over $2\,\mu$ in size, or for rather coarser particles suspended in liquids.

ASPIRATION OF A SETTLING CLOUD

If a sampling head approximates to a point sink, it collects a true sample no matter how fast the particles settle or how slow may be the rate of suction.* The concentration of particles at any point is unaffected by the act of sampling.

A bulky object, however, casts a dust shadow when placed in a cloud of particles settling under gravity; within the shadow the concentration is zero. The purpose of this paper is to study the shape assumed by the dust shadow cast by a large sampling head sucking at various rates through a small orifice in the top.

The problem is dealt with in two dimensions, taking steady, ideal fluid flow. The system considered is a horizontal cylindrical sampling head, centre O, with a line sink A along the top (Fig. 1). If the slit absorbs Q c.c. of fluid per sec

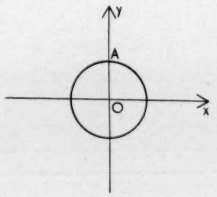

Fig. 1. Co-ordinate system

per cm length, it can be shown, by using a complex variable, that the resolutes of fluid velocity, U', V', outside the cylinder are given by

$$\left.\begin{aligned} U' &= -\frac{Q}{2\pi}\frac{x'(r'^2 - a^2 + 2ay')}{r'^2(r'^2 + a^2 - 2ay')} \\ V' &= -\frac{Q}{2\pi}\frac{y'(r'^2 - a^2) - 2ax'^2}{r'^2(r'^2 + a^2 - 2ay')} \end{aligned}\right\} \quad (1)$$

The accents attached to the variables indicate that they are normal dimensional quantities. Unaccented symbols will be used for dimensionless variables. The radius of the cylindrical head is a and $r'^2 = x'^2 + y'^2$; the direction of y' increasing is upwards and x' increases to the right.

If v_0 is the rate of settlement of the particles, which are supposed to be identical, the velocity resolutes of a particle are $(U', V' - v_0)$. The equations can be expressed in dimensionless variables by measuring lengths in units of a and velocities in units of v_0. This gives the resolutes of particle velocity as

$$\left.\begin{aligned} u &= -\frac{1}{k}\frac{x(r^2 - 1 + 2y)}{r^2(r^2 + 1 - 2y)} \\ v &= -\frac{1}{k}\frac{y(r^2 - 1) - 2x^2}{r^2(r^2 + 1 - 2y)} - 1 \end{aligned}\right\} \quad (2)$$

where all the symbols represent pure numbers and $k = 2\pi v_0 a/Q$.

This last quantity characterizes the pattern of the particle trajectories in the field and the shape of the shadow region; it is inversely proportional to the rate of aspiration.

* Davies, C. N. *Symposium on Particle Size Analysis, Suppl. to Trans Instn Chem. Engrs*, **25**, p. 25 (1947).

THE PARTICLE TRAJECTORY CHARACTERISTIC, k

The equation of a particle trajectory is

$$\frac{v}{u} = \frac{dy}{dx} = \frac{y}{x} - \frac{r^2}{x} \cdot \frac{2 - k(r^2 + 1 - 2y)}{(r^2 - 1 + 2y)} \qquad (3)$$

Particles move vertically when $x = 0$, $y = \pm\infty$, or $r^2 - 1 + 2y = 0$. The last condition defines a circle of radius $\sqrt{2}$ with centre $(0, -1)$. This is called the vertical circle; it is independent of k because ideal fluid motion was assumed. Inside the vertical circle particles move in the direction of x increasing and outside they have a decreasing x-co-ordinate.

The trajectories are horizontal when

$$4y = 1 - r^2(1 - 2k) \pm \sqrt{[r^4(1 - 12k + 4k^2) + 2r^2(7 - 2k) + 1]} \qquad (4)$$

This expression defines the neutral locus on which particles neither rise nor fall. Inside the neutral locus particles move upwards, outside they move downwards. The neutral locus meets the cylinder when $r = 1$, which gives $y = (k - 1)$ or 1. When k is greater than 2, the neutral locus does not exist because the rate of suction is too low.

The neutral locus and vertical circle intersect when $r^2 = 1/k$ and $y = \frac{1}{2}(1 - 1/k)$. The particle velocity is zero at points of intersection. There is no intersection for slow aspiration corresponding to $k > 1$; at $k = 1$ they meet on the sampling head at $(1, 0)$. For $1 > k > 1/(3 + 2\sqrt{2})$ intersection occurs when y is negative and at $k = 1/(3 + 2\sqrt{2})$ there is a single intersection on the y-axis. For higher rates of aspiration intersection does not take place, which means that particles are stationary where the neutral locus meets the y-axis below the head.

At a point of intersection certain limiting particle trajectories meet. The only other place where trajectories meet is at the orifice. The limiting particle trajectories divide the field into regions which specify the ultimate destination of the particles in them.

Direct integration of equation (3) has not been achieved but a number of limiting particle trajectories has been worked out by stepwise calculation for different values of k. They are illustrated in Fig. 2. The general course of other particle trajectories, which have not been evaluated, is easily inferred from the limiting ones illustrated.

$k = \infty$. This means that there is no aspiration and particles fall freely in a vertical direction. A shadow zone exists underneath the head bounded by particle trajectories which touch it at $x' = \pm a$. Particles fall on the upper surface of the head, the total number being $2acv_0$ particles/sec cm where c is the number of particles per cm^3.

$k > 2$. Decrease of k, by starting gentle suction into the orifice, causes a slight bulge to develop on the trajectories defining the shadow zone but there is no change in their points of contact with the head. There is no neutral locus; all particles move downwards.

Two limiting trajectories exist. One defines the boundary between particles which enter the orifice and those which settle on the head. The second divides particles which settle on the head from those which miss it and becomes the edge of the shadow when y is negative.

$k = 2$. At $k = 2$ the first limiting trajectory becomes horizontal as it approaches the orifice and this condition holds for all smaller values of k. The head, the vertical circle, and the limiting trajectories and their asymptotes are shown for $k = 2$ in Fig. 2(*a*). The field is divided into four regions within which the particle trajectories run as follows: (i) enter the orifice; (ii) terminate on the head; (iii) miss the head; and (iv) shadow zone, free from particles.

$k \geqslant 1$. As soon as k falls below 2, a neutral locus begins to develop between the orifice and points on top of the head where $y = (k - 1)$. Particles which cross the neutral surface move upwards between it and the top of the head and deposit on the head.

The first limiting particle trajectory, enclosing particles which enter the orifice, has an asymptote $x_1 = \pi/k$. This is true for all values of k.

The rate of settlement of particles on the head is determined by the radial component of particle velocity, $-y/r$, and is equal to

$$\int_{y=0}^{1} 2acv_0 y \, ds \text{ particles/sec cm}$$

where ds is an element of the circumference of the head equal to $dy/\sqrt{(1 - y^2)}$. This expression integrates to $2acv_0$ showing that the rate of deposition on the head is constant for $k \geqslant 1$ and independent of the rate of suction.

The second limiting trajectory separates the particles settling on the head from those which miss it altogether and has the asymptote x_2', where

$$2cv_0 x_2' = 2acv_0 + Qc \qquad (5)$$

giving

$$x_2'/a = x_2 = \pi/k + 1 \qquad (6)$$

This holds as long as $k \geqslant 1$.

The asymptotes of the shadow boundaries below the head are $x_3 = \pm 1$. The limiting width of the shadow is not affected by suction as long as $k \geqslant 1$, though a slight bulge develops below the head. The shadow boundaries meet the head at $(\pm 1, 0)$ and for $k > 1$ are continuous with the second limiting trajectory.

$1 > k \geqslant 1/(3 + 2\sqrt{2})$. As k decreases below unity the shadow climbs up over the top of the head. Deposition of particles takes place only on an area near the orifice; the peripheral part of the head is clear of deposit over an area which increases as k decreases.

The neutral locus forms a pair of cusps on the vertical circle which approach one another and unite on the y-axis when $k = 1/(3 + 2\sqrt{2})$.

The half-width, x_3, of the shadow at $y = -\infty$ is equal to $(x_2 - x_1)$. The x-co-ordinate of the point on the top of the cylinder up to which the shadow climbs has the same value, and the rate of deposition of particles on the sampling head is therefore $2cv_0(x_2 - x_1)$.

x_1 is always equal to π/k and x_2 approaches x_1 as k decreases until, at $k = 1/(3 + 2\sqrt{2})$, x_2 and x_1 coincide and the shadow fines away to nothing below $y = -(1 + \sqrt{2})$. There remains a finite, pendulous shadow hanging below and enclosing the sampling head right up to the orifice. No deposition on the head takes place for this and lower values of k and region (ii) of the field has disappeared.

$1/(3 + 2\sqrt{2}) > k > 0$. Further increase of the rate of suction causes the pendant shadow to close in on the cylinder and to vanish when k becomes zero. The neutral locus splits horizontally from the point of contact of the cusps to form inner and outer loci.

The inner locus meets the shadow at $x = 0$ and shrinks on to the cylinder to vanish with k. The outer locus meets the limiting particle trajectory on the y-axis and expands as k diminishes. Finally, at $k = 0$, it becomes infinite with the asymptote $y = 2$. Particle trajectories for $k = 0$ coincide with the streamlines of fluid flow.

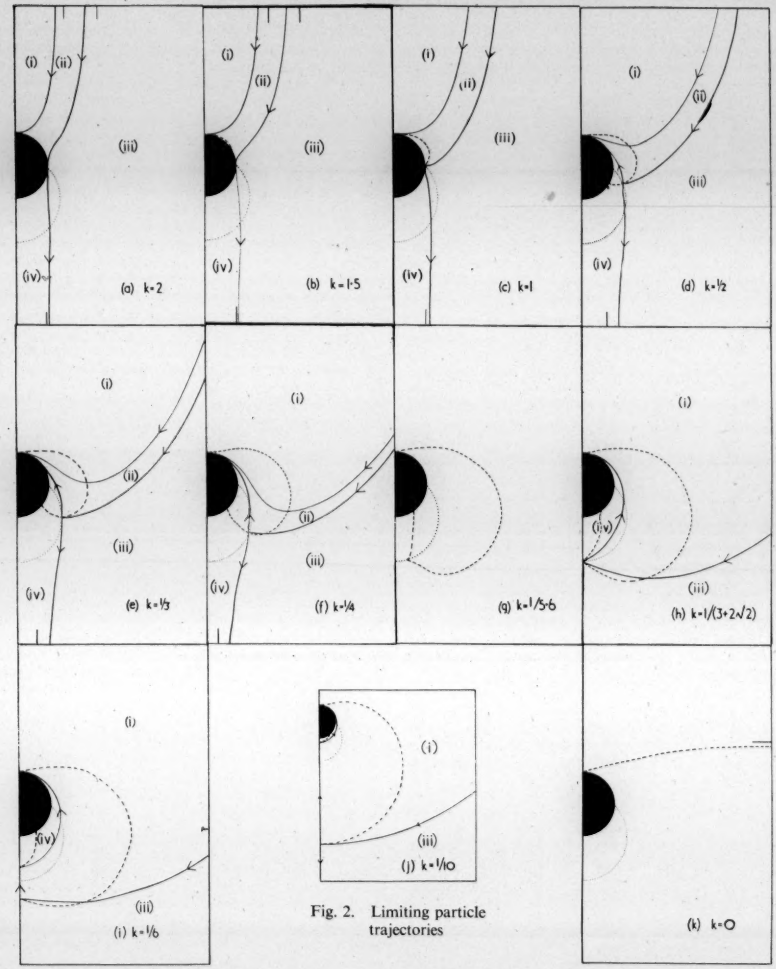

Fig. 2. Limiting particle trajectories

All particles in region (i) enter the orifice; those in region (ii) settle on the head; particles in region (iii) miss the head altogether; region (iv) is the dust shadow free from particles

– – – – neutral locus.
. . . . . vertical circle.
——— limiting particle trajectories for the range of values which can be taken by k.

APPLICATIONS TO PARTICLE SIZE ANALYSIS

The problem has been idealized by assuming the fluid to be without viscosity and the orifice to be infinitely narrow. A real fluid, owing to its viscosity, cannot slip over the surface of the cylinder. The tangential and normal resolutes of fluid velocity are therefore, in reality, both zero, whereas the equations expressing the flow field are based on the assumption that only the normal resolute vanishes at the surface.

In real fluids, all particles of negligible inertia must be travelling vertically when they fall on the cylinder. The real neutral locus cannot, therefore, meet the surface of the

cylinder but must turn away, close to it, and form a closed surface as indicated in Fig. 3. The rate of settlement of particles on the cylinder is not affected by the angle at which they approach, so neglect of viscosity cannot alter the rate on this account.

For the same reason the shadow boundary, which is, of course, a particle trajectory, cannot be tangential to the cylinder except when $y = 0$. For values of k below unity, therefore, it must curve round very near to where it meets the cylinder to become vertical at the point of contact. This

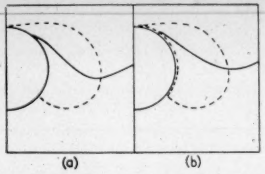

Fig. 3. The neutral locus and trajectory of a particle which settles on the head (*a*) in ideal fluid, (*b*) in real fluid

would not make much difference in the rate of deposition on the area near the orifice nor upon the size of the area shadowed.

Appreciable changes in the flow pattern at low rates of aspiration, when viscous forces in the bulk of the fluid are significant, would modify the course of the particle trajectories but could not alter the general nature of the dependence on aspiration rate which is illustrated in the sequence of figures in Fig. 2. Similar modifications would result if a different shape of sampling head was employed.

It is considered that findings for a cylindrical head in ideal fluid give a good qualitative idea of the form of dust shadows and the settlement of dust on a suction head of any shape having an upwards facing orifice.

If the orifice is finite in size, having a width α when projected on the x-axis, an error arises because the actual velocity with which particles enter is equal to the fluid velocity plus the sedimentation velocity. For steady suction over a period, this results in the concentration of airborne dust being estimated as

$$c\,(1 + v_0\alpha/Q) \text{ particles/cm}^3$$

instead of c. This error is negligible when $v_0\alpha/Q$ is small.

Now, $v_0 a/Q = k/2\pi$ and when $k < 1/(3 + 2\sqrt{2})$ there is no deposition of dust on the head. Hence, as long as

$$2v_0 a/Q < 1/(3 + 2\sqrt{2})\pi$$
$$< 1/18$$

no dust collects around the orifice.

The width of the orifice, α, cannot exceed $2a$, the width of the head. It is clear, then, that the observation that the speed of suction suffices to prevent deposition on the head adjacent to the orifice provides an indication that the concentration determined by analysis of the sample cannot be in error by more than 100/18 or about 5%.

Dust clouds normally contain particles of different sizes so that a and Q are fixed when sampling and all sizes are collected simultaneously. Variation of k is then due to the range of v_0 and a picture of what is going on is provided by superimposing the parts of Fig. 2.

The coarse particles which enter the orifice come from a narrow region above the orifice and the fine ones from a wide region. The widths of the regions are defined by the values of $x_1 = \pm \pi/k$ where k is proportional to v_0, that is to the square of the particle size.

By placing a horizontal screen above the orifice, extending between the first limiting trajectories, all large particles which would otherwise enter the orifice will settle on top of the screen. Only a small proportion of small particles would be caught in this way, however; the rest would enter the orifice to provide a selected sample containing only particles smaller than a certain size.

A particle size analysis could be achieved by using a number of suction heads fitted with differently sized baffle plates. The size of baffle depends on its height above the orifice. If it is placed far above, the interference with the flow pattern would be negligible but disturbances due to external air currents might be troublesome.

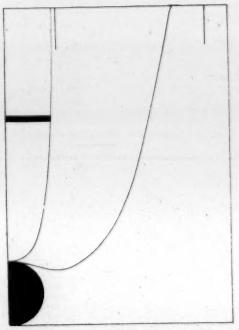

Fig. 4. Limiting particle trajectories to enter the orifice for $k = 2$ and $k = \frac{1}{2}$. The baffle shown cuts out all the larger particles and about 25% of the smaller ones

Apart from such considerations, it is easy to see how the proportion of fine particles collected depends on their size when a baffle, designed to cut out all particles greater than a certain diameter D, is used. If d is the diameter of the fine particles then the proportion, E, collected is calculated from the values of x_1 which are inversely proportional to the squares of the respective diameters (Fig. 4). Hence,

$$E = (1/d^2 - 1/D^2)/(1/d^2)$$
$$= 1 - (d/D)^2 \qquad (7)$$

This is the same square law of selective sampling which holds for continuous elutriation.*

* Davies, C. N. *Proc. Instn Mech. Engrs*, *B* **1**, p. 185 (1952).

Paper A.4

A comparison of methods for particle size analysis*

By B. A. Jarrett, Ph.D., A.M.I.Mech.E., and H. Heywood, A.C.G.I., D.Sc., M.I.Mech.E., M.I.Chem.E.,
Imperial College of Science and Technology, London, S.W.7

The research was undertaken to make comparative tests on equipment for particle size analysis with the special object of devising methods suitable for rapid routine analyses by sedimentation. A special test dust, having a controlled grading, was used for the comparative tests. The authors' recommendations for suitable methods of size analysis are given, with the probable degree of error and the range of particle size to which the various methods are applicable.

The work described in this paper was undertaken, firstly, to make comparative tests with existing sedimentation forms of particle size analysis equipment, over the range of 53 to 2 μ; and secondly, to devise methods suitable for the rapid testing of relatively coarse dusts over the size range 76 to 20 μ. The specific problem involved in this latter range of sizes is the relatively high velocity of fall in water. The measuring device must therefore be free from inertia effects in order that the particle concentration as observed will not lag behind the true value being measured.

The ideal method of analysis would measure the particle concentration at a given depth in a suspension, but in practice the mean concentration is measured over a small range of depths, and this mean value of concentration assumed to occur at the mean sampling depth. This is not valid unless the relation between depth and concentration is linear over the sampling range, and an error will be introduced into the calculation of particle size corresponding to the measured concentration. The ratio of sampling range to maximum sampling depth is a measure of the inaccuracy due to this factor in particle size determination, a feature which is inherent in any piece of equipment, and will be termed the "discrimination factor." Theoretical considerations show that the sampling range can be as much as one-fifth of the maximum sampling depth before the error in concentration determination approaches 0·5%, for a dust having a size distribution that is smooth and free from discontinuities.

A convenient method of defining the initial dust concentration of a uniform suspension is by the increase in density caused by the introduction of the particles, since this simplifies calculation of the results. Thus the term "0·01 suspension" indicates a uniformly dispersed suspension in which the concentration of dust particles is such that the density is 0·01 g/cm^3 higher than that of the pure dispersing liquid. Preliminary tests had shown that higher concentrations introduced particle interference, and lower concentrations would greatly increase the difficulty of measurements.

METHODS INVESTIGATED

Some of the methods given below are well known, and are therefore not described in detail. The methods which were specifically developed during the course of the research are more fully described.

All the methods of analysis investigated were of the so-called incremental type, i.e. the concentration of particles is measured within a range of depths that is small compared with the mean depth below the surface level of the sampling point. The cumulative methods, such as the single manometer tube and the sedimentation balance, were not investigated because these all suffer from the inherent inability to distinguish sudden but slight discontinuities in the size-distribution curve.[1] Such discontinuities may, however, be an important characteristic of particulate systems, and therefore cumulative methods of analysis are inadequate for certain lines of research, though they may be satisfactory for other purposes. The discrimination factor is 1 for all cumulative methods of analysis; for the incremental methods finally recommended the discrimination factor is less than 0·2, being zero for the ideal case.

Pipette method. Andreasen's form of the pipette equipment was used, the vessels being housed in a thermally insulated cabinet.[2]

Hydrometer method. The density of the suspension was measured by a hydrometer bulb having a stream-line form. The method is simple and has been standardized for the particle size analysis of soils.[3]

The "diver" method. This method was developed by S. Berg,[4] and makes use of small glass "divers" [Fig. 1(*a*)] of known density which are inserted into the suspension and

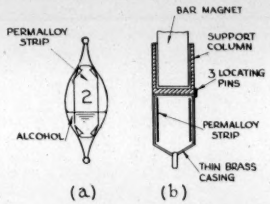

Fig. 1. (*a*) Glass "diver"; (*b*) Roof "diver"

settle at the level at which the density is equal to that of the diver. They continue to sink at this density level as sedimentation progresses. Each diver contains a Permalloy strip, and is weighted to the required density with alcohol. A number of divers are required since each diver gives only one point on the size-distribution curve. The divers are small and no stem breaks the surface, so that the error due to surface tension is eliminated. The rate of dust deposition on the diver is slower than occurs on a hydrometer, and results from the horizontal displacement of the suspension as the diver sinks through it, making readings for the larger particle sizes inaccurate.

The divers are not visible in the suspension, and Berg located them by attraction to the wall of the glass sedimentation tube by means of a magnet. An alternating current inductance-resistance bridge was used as a detector in the work described here. A high permeability alloy strip in the diver destroyed the balance of the bridge when a thin search coil surrounding the sedimentation tube was moved past the diver.

If dust is prevented from settling on the diver then this

* For fuller details of some of the experiments and apparatus see Ph.D. thesis submitted to the University of London in 1949 by one of the authors (B. A. J.).

method will be accurate for all particle sizes. The method of fitting stationary divers at the foot of a vertical column immersed at a known depth in the suspension was developed during this work [Fig. 1(*b*)] and has been called the "roof diver" method. The diver falls from the column when the density of the surrounding suspension becomes less than that of the diver. The diver was made of brass, and contained a Permalloy strip; it was held on to a hollow brass column while being inserted in the suspension by means of a magnetic rod which was afterwards withdrawn. Any tendency for the diver to stick to the column was minimized by gently vibrating or tapping the column about twice per second, which could be accomplished electrically. The initial movement of the diver was detected by the search coil and bridge circuit mentioned above.

In the equipment used, only one diver was fitted under the column, but a series of cylindrical divers of varying density and one below the other could be used.

Decanting method. The procedure consists of repeated sedimentations and decantings until all particles below a certain size have been removed from the suspension. This method is used for the preparation of sized fractions, but it is very tedious as a method of size analysis. The theory has been described elsewhere.[1]

Manometric method. Existing forms of equipment consist of two tubes containing the pure liquid, connected to, or immersed in, the sedimentation column at different levels, whereby a slight hydrostatic difference in level occurs which is proportional to the mean density of the suspension between the two levels. Thus if the difference in level before the largest particle has reached the sampling level is X, and the difference at some time later is x, then the weight of particles in the sampling range is $(100x/X)\%$ of the original concentration. Although simple in theory, many difficulties are

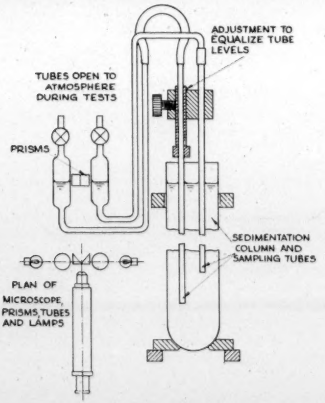
ADJUSTMENT TO EQUALIZE TUBE LEVELS
TUBES OPEN TO ATMOSPHERE DURING TESTS
PRISMS
SEDIMENTATION COLUMN AND SAMPLING TUBES
PLAN OF MICROSCOPE, PRISMS, TUBES AND LAMPS

Fig. 2. Open manometer system

encountered in the practical measurement of this difference in levels, which is extremely small if the suspension is sufficiently dilute to avoid excessive particle interference; further, both liquid levels fall, although only the difference in levels is required. Many ingenious designs of differential manometer have been described,[5] but these suffer from inertia effects or errors due to temperature variations.

A very simple form of equipment, consisting of two open manometer tubes, shown in Fig. 2, was tested. The tubes were filled with the pure dispersing liquid, and the difference in liquid levels was measured by means of a travelling microscope, using the optical system shown in Fig. 2. This equipment proved to be inaccurate, one of the reasons being the difficulty of reading the difference between two rapidly falling menisci. A new form of manometric equipment was developed, the "closed manometer," and is shown diagrammatically in Fig. 3. By enclosing the correct volume of air

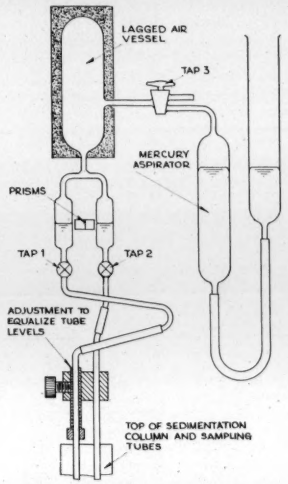

Fig. 3. Closed manometer system

above the two tubes, the common fall of both tubes can be almost entirely prevented, without affecting the differential fall. Further, by reducing the pressure in this air volume, the common level of the menisci is raised to a convenient viewing height above the sedimentation tube. The diameter of the manometer tubes at the meniscus level was 11 mm, to reduce the surface tension effects and flatten the menisci. The tubes were reduced to $2\frac{1}{2}$ mm below the reading level. They should not be smaller, as a slight uprising of suspension may occur in the tubes during an analysis, the effect of which increases with decreasing tube diameter. The sampling tubes were shown to have negligible interference effects on the suspension, provided they were vertical.

The common level of the menisci is affected by the changes in atmospheric pressure and temperature, and the air vessel is lagged. Any slight uprise of particles in the sampling tubes due to contraction of the air volume affects both readings almost equally, and can be neglected. The optical system must be mounted on a vertical slide, to follow movement of the menisci.

The two menisci were illuminated to show as bright lines on a dark ground and observed simultaneously through a microscope by means of a prism system which was the same

as shown in Fig. 2. A graticule scale in the eyepiece enabled the distance apart to be measured. The smallest trace of grease near the menisci caused the water to "stick," making readings inaccurate. Provision was made for flushing the tubes between analyses, though this has not been shown in Fig. 3. A check on any meniscus error is necessary, however, and was carried out as follows. The total change in level between the menisci from the commencement of settlement to the time when all the particles have fallen out of suspension could be calculated. The lower sampling tube was adjustable for height so that its outlet end could be brought level with the upper sampling tube. Both tubes read the same pressure under these conditions, and since they contained the pure dispersing medium, the difference between this reading and that obtained before the dust started settling out at the sampling level should equal the calculated value. If the values were not equal, the analysis was abandoned and the tubes flushed out before recommencing. In practice, routine flushing avoided this difficulty. Distilled water used in the tubes must be grease free, i.e. there must be no greased taps on the water vessels used for storage, water being removed by siphoning. Grease must not be used on the manometer taps.

The change in readings when the dust falls out of suspension is given by

$$\frac{W(D_d - D_f)(h_2 - h_1)}{(D_d \cdot V + W)Df}$$

where h_1 and h_2 are the sampling depths, D_d and D_f are the densities of the dust and dispersing medium, W is the weight of dust in the suspension, and V is the volume of the dispersing medium.

Operation of the equipment was simple. The manometer was flushed with cleaning fluid, the sampling tubes inserted into a tube of distilled water, and then filled to the required level by means of a mercury aspirator. Taps 1 and 2 were closed and tap 3 turned to isolate the air vessel from the aspirator. The tube containing the dust suspension was then placed in position and taps 1 and 2 opened. The microscope was adjusted and readings taken at suitable intervals; after the initial readings the zero was checked as described above. If the analysis was extended beyond about 2 hours, there was a tendency for the menisci to wander owing to drying of the tube walls above them. Thus the lower limit of particle size analysed was determined by the sampling depth. The research equipment was operated at a fixed depth of about 40 cm, allowing a particle size of about 8 μ to be reached. To analyse smaller sizes, the equipment could be modified to reduce the sampling depth progressively to about 10 cm.

Photoextinction method. In this method the optical density of a dilute suspension of settling particles is measured. From this measurement a size-weight analysis can be calculated, on the assumption that the optical density of the suspension is proportional to the projected area of the particles in the light beam. The optical properties of small particles are, however, very complex, so that measurements can at the moment only be regarded as comparative, rather than absolute.[6]

Electrical resistance method. Most non-metallic dusts are insulators, and the presence of particles in the field between two electrodes immersed in an electrolyte will cause an increase in resistance, compared with the pure electrolyte. The change in resistance was found to be proportional to the dust concentration between the electrodes, for dust concentrations below 0·12% by volume. Measurement of the change in resistance at a suitable sampling depth as the dust settled therefore gave the dust concentration curve. Equipment operating on this principle was developed during the research, using rectangular platinum electrodes with a guard ring, embedded in vertical polythene pillars immersed in the suspension. The suspension represented a resistance in one arm of a Y-type split-phase alternating current bridge operating at 150 kc/s. A variable step resistance in the other arm was used to keep the bridge balanced as the dust settled, provision being made for balancing out the capacity effect of the dust. The operation of the equipment was simple, but the method was so highly sensitive to the temperature of the electrolyte that in its present form it is unsuitable for dust analysis.

ERRORS OCCURRING IN ANALYSES

Apart from the instrumental errors inherent in the particular form of equipment, the following errors may occur in size analysis processes.

Sampling from a bulk supply of dust. This was outside the scope of the work described here, but suitable methods are described in other publications.[7] Great care was taken to minimize sampling errors in the experiments described.

Errors in determining the weight and density of the dust. These comprise the normal weighing errors, and errors of volumetric measurements.

Incomplete dust dispersion. The tendency for dusts to flocculate is greatly increased when a large percentage of fine particles is present. All particles below 0·5 μ were removed from the test dust by decanting in order to minimize this effect.

Calculation of particle size. Diameters of particles were normally calculated from Stokes' equation. In practical operation the following departures are made from the assumptions on which this law is based:

(*a*) *Non-spherical particle shape.* Although shape affects velocity, Stokes' law gives the diameter of a sphere of equivalent terminal velocity, and this is a unique description of the particle. For a particular test dust, the comparative results should not be affected by particle shape.

(*b*) *Interference between particles.* It is generally agreed that such interference is negligible for dust concentrations not greater than 1% by volume, and careful tests have confirmed this opinion.

(*c*) *The suspension is not infinite in extent.* This error becomes negligible with a vessel exceeding 5 cm diameter.

(*d*) *Time of settling.* Owing to the initial turbulence of the suspension the time when settlement commences cannot be measured within 5 sec. This error can affect larger particle sizes by as much as 2%, but becomes negligible for settling times exceeding 10 min.

PROPERTIES OF THE TEST DUST

The following properties of a test dust were considered desirable:

(1) Certain points on the size-concentration curve should be known accurately and be independent of the calculation of particle size.

(2) The cumulative grading curve should not be a smooth continuous curve, but should have steps, denoting the absence of certain small ranges of particle size. Thus defects such as inertia, or a large discrimination factor, would be indicated by a smoothing out of these steps.

(3) Effective dispersion was improved by the elimination of very small particles, and by the use of a dispersing agent (0·1% sodium hexa-metaphosphate).

PREPARATION OF THE TEST DUST

A silica dust was compounded of three fractions, each fraction having a restricted particle size range. The fractions were produced by repeated decanting under constant temperature conditions.

Particles in the size ranges 0–0·5 μ, 15·5–17·5 μ and 28–29 μ were absent, forming two steps in the size-distribution curve. The three fractions were mixed in known proportions by weight, and consequently the mid-points of the steps were defined accurately in terms of size and weight percentage. Instrumental errors in concentration determination would thus be shown up quite definitely. The dust was composed of the fractions 0·5–15·5 μ, 17·5–28 μ and 29 μ to minus 300 mesh, in proportions 40·5; 29·5; 30·0 by weight respectively.

COMPARATIVE TESTS ON THE EQUIPMENTS

Three size analyses from one sample of dust were made with each intrument (except the pipette, with which separate samples must be used, and the decanting equipment, with which only one analysis was made). Use of the same sample made any sampling error constant for the three analyses, so that random errors occurring at the steps in the dust curve were caused only by concentration measurement errors. Distilled water containing the dispersing agent was used throughout as the sedimentation liquid. Figs. 4 and 5 show the results obtained compared with the "standard curve" which was taken as the mean of the pipette analyses, since this equipment was found to be the most accurate. The percentage undersize at the steps was known, independent of any instrument errors, to be 40·5% and 70%, since the test dust was made up in these proportions.

The following summary of the conclusions is based on the comparative tests, but also takes into account many special tests that have not been described in the paper.

1. *Pipette method (Andreasen)*

Suitable particle size range: 0–45 μ.
Initial dust concentration: 1% by weight.
Accuracy of concentration determination: ±0·5%.

Remarks: Simple to operate, though many weighings are involved if a number of points on the size-concentration curve are required. Is the most accurate method tested, and is very suitable for occasional analyses.

2. *Hydrometer method*

Suitable particle size range: 0–25 μ. (The upper limit can be increased to 35 μ, but observations are difficult.)
Initial dust concentration: 0·01 suspension (1·6% by weight for silica).
Accuracy of concentration: 0–25 μ, ±1·5%.
25–35 μ, ±2·5%.

Remarks: Very simple to operate, but requires practice in making rapid readings before settlement of particles on the hydrometer bulb affects the density reading. This applies especially where comparatively large particles are present, and the upper size to which the method is applicable is limited by this effect.

3. "*Diver*" *method*

Suitable size range: 0–30 μ.
Initial dust concentration: 0·01 suspension.
Accuracy of concentration determination: ±1%.

Remarks: Very simple to operate. On larger particle sizes rapid readings must be made, before dust deposition on the diver affects the accuracy. Use of a large diver (about 10 cm^3 volume) facilitates readings for larger particle sizes. Especially suitable for particle size analysis below 20 μ.

3(*a*) *Roof "diver"*

Suitable particle size range: 10–53 μ.
Initial dust concentration: 0·01 suspension.
Accuracy of concentration determination: 0 to − 1·5%.

Remarks: Very simple to operate. Upper size limit determined only by sampling depth, which should be sufficient to allow at least two minutes to elapse before the largest particle has settled from the surface to the level of the roof diver.

4. *Decanting method*

Suitable particle size range: 0–53 μ. Larger particles settle very rapidly, but could be separated if the sedimentation column length were increased to 60 cm.
Initial dust concentration: 0·01 suspension.
Accuracy of concentration determination: 0 to − 2%.

Remarks: Is simple but very slow, as at least eight decantings must be made for every point on the curve. This method is not recommended for analyses.

5. *Open manometer*

Suitable size range: Tested over range 12–53 μ, but unsatisfactory.
Initial dust concentration: 0·01 suspension.
Accuracy of concentration determination: Up to ±15% error.

Remarks: Equipment is difficult to use, and very inaccurate. Unsuitable for analysis work.

5(*a*). *Closed manometer*

Suitable particle size range: 8–53 μ.
Initial dust concentration: 0·01 suspension.
Accuracy of concentration determination: ±1·5%.

Remarks: Very simple to operate. Upper limit depends only on sampling depth and could be increased. Routine flushing of meniscus tubes and checking of zero reading is important. The length of test is limited to 1½–2 h, because of drying on the tube surface above the meniscus level.

6. *Photoextinction equipment*

Suitable particle size range: 0–25 μ (can be increased to 53 μ but observations difficult).
Initial dust concentration: 0·01% by volume.
Accuracy of concentration determination: ±3%, 0–25 μ.
±6%, 0–53 μ.
These figures apply if diffraction effects are ignored.

Remarks: Equipment is very simple to operate. It is the

only method which can be used if only a very small dust sample is available. The method is suitable for comparative tests, such as are required for industrial control purposes, but the theory is complex when absolute size measurements are required. Coarse particles have relatively small surfaces and are difficult to detect; slight errors in reading the photocell output can cause large divergencies in the calculated size-distribution curves in this region.

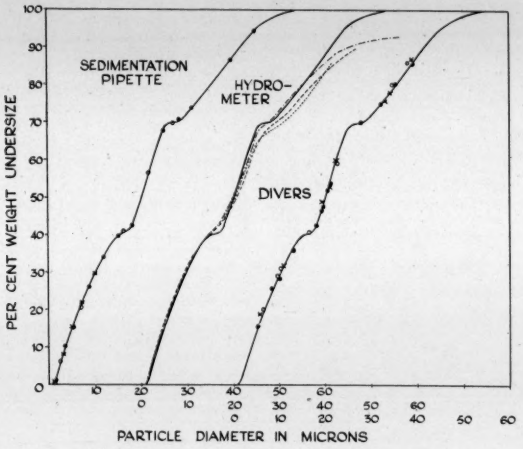

Fig. 4. Size-distribution curves. Full lines show standard curve for test dust, points or dotted lines show test results by method indicated

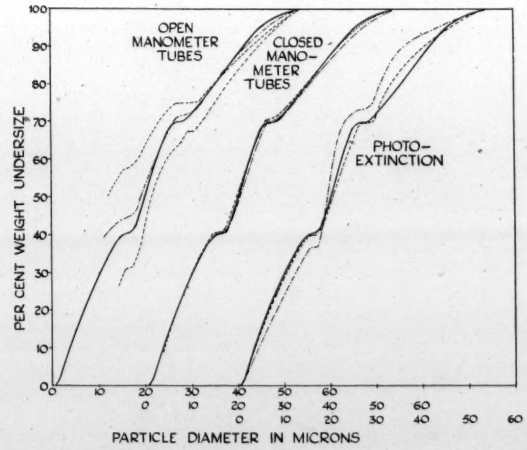

Fig. 5. Size-distribution curves. Full lines show standard curve for test dust, dotted lines show test results by method indicated

7. Electrical resistance equipment

Suitable particle size range:	15–40 μ in present form.
Initial dust concentration:	0·12% by volume.
Accuracy of concentration determination:	±3% over this limited particle size range.

Remarks: The equipment requires very accurate control of the suspension temperature. Is unsuitable for analyses in its present form.

GENERAL RECOMMENDATIONS FOR SUB-SIEVE ANALYSES

The authors make the following recommendations based on the work described above.

1. *Suspension density.* Use of a 0·01 suspension is recommended for analyses. This corresponds to approximately 0·6% by volume, or 1·6% by weight for silica dusts.

2. *Upper particle size limit.* The test dust for most of the investigations was limited to particles passing a 300 mesh sieve (aperture 53 μ). Sedimentation of the under 200 mesh (76 μ aperture) fraction of dusts would be advantageous. It is considered that the roof diver and closed manometer methods could be used up to this size, if the sampling depth were increased to 60 cm.

3. *Sampling depth in the suspension.* Tests have shown that a minimum of 1½ to 2 min must elapse between commencement of sedimentation and the first reading, otherwise the first readings will be liable to considerable error due to initial turbulence effects. Thus the sampling depth for 200 mesh size particles settling in water will be 60 cm, and for 300 mesh, 40 cm. The depth can be decreased as the particle size of the sample decreases.

4. *Calculation of particle size.* Calculation of particle sizes below 45 μ should be made by means of Stokes' equation. For the range 45–76 μ, the formulae applicable to the transitional region of velocity should be used.[8] The calculation is simplified if tables of terminal velocity at 0·5° C temperature intervals are constructed.

5. *Dimensions of the suspension vessel.* The rate of fall of particles close to the wall and the bottom of the vessel is reduced by interference. The effect will be negligible if a vessel in the form of a round-bottomed glass cylinder of 4–5 cm diameter is used. The sampling region should be not less than 10 cm from the bottom of the tube.

6. *Verticality of the vessel.* A small deviation of the vessel from the vertical causes circulation currents in the suspension and produces turbulence. A plumb bob should be used to ensure that the tube is vertical.

7. *Temperature control of suspension.* Tests should be carried out in a room where the temperature variation does not exceed 1° C in 24 h. This slow variation will not affect the settling of the suspension. Where thermostatic control of a cabinet containing the equipment is used, the temperature should be constant to ±0·05° C, since small continuous plus and minus changes tend to cause circulation effects in the suspension.[4]

8. *Discrimination factor.* The discrimination factor should not exceed 0·2 for larger particle sizes, but can be as high as 0·5 for particle sizes below 10 μ, since sudden changes in the size-concentration curve below 10 μ rarely occur in practice. With a discrimination factor of 0·2 the error at the steps on the test dust was only 0·6%.

9. *Relation between a suspension and a true fluid.* It has been established that where the dimensions of a pressure or density measuring device are large compared with the distance between individual particles in the suspension, then the suspension behaves as a true fluid with respect to the equipment (provided that particles are prevented from settling out of the suspension on to the measuring device). Thus in all calculations involved in the equipments used, the suspension may be treated as a true fluid.

10. *Mutual interference between particles.* This has been found to be negligible for concentrations below 1% by volume.

11. *Effect of physical disturbances.* Small disturbances, such as the introduction and removal of a diver or hydrometer, are found to have a negligible effect on the suspension, provided care is exercised. Disturbed portions of the suspension tend to flow back to their original positions owing to the density gradient.

REFERENCES

(1) HEYWOOD, H. Symposium on Recent Developments in Mineral Dressing, *Inst. Min. Met.*, p. 31 (1952).
(2) HEYWOOD, H. *Proc. Instn Mech. Engrs*, **140,** p. 27 (1938).
(3) B.S. 1377: 1948. Methods of Test for Soil Classification and Compaction (London: British Standards Institution).
(4) BERG, S. *IngenVidensk. Skr.* No. 2 (1940).
(5) See ref. (2) above for bibliography.
(6) See other papers at this Conference.
(7) B.S. 735: 1944, Sampling and Analysis of Coal and Coke, or B.S. 1796: 1952, Methods for the Use of British Standard Fine-Mesh Sieves (London: British Standards Institution).
(8) HEYWOOD, H. *Imp. Coll. Chem. Eng. Soc.*, **4,** p. 17 (1948).

DISCUSSION

Mr. R. Johnson: I have been very interested in Paper A.4, in view of some work I did on some of the methods in connexion with size comparisons in the pottery industry.

Initially the sedimentation pipette was used as a reference method, but was abandoned as such, because it was found that the results depended on: (*a*) rate of sampling, (*b*) type of sampling orifice, and (*c*) size of sampling tube. Quicker withdrawal of the samples gave finer results. A vertically downward orifice gave finer results than a horizontally directed one and narrower sampling tubes also gave finer results. Tables 1 and 2 summarize some results.

I am very pleased to see that very good agreement is obtained between diver results and the standard curve. I had more faith in results by the diver method than any other, and managed to get good agreement between diver and hydrometer results. Theoretical considerations with the hydrometer test showed that the effective depth is always less than that based on B.S. 1377 (*Method of Test for Soil Classification*). The additional correction depends on the size distribution of the material and the settling time; to be more precise, on the shape of the density-depth curve. For a hydrometer with a symmetrical bulb the correction to the "B.S. 1377" effective depth decreases as the density-depth curve straightens out, i.e. as sedimentation proceeds. The differences between the hydrometer results of the authors and the standard curve can at least be diminished by applying such a correction.

Table 1. *Percentage finer than stated sizes for different sampling speeds (for flint A)*

Settling time (min)	*Stokes' radius (μ)*	*Jet vertical Sampling period (sec)* 140	85	59	12	*Jet horizontal Sampling period (sec)* 140	85	59	12
15	8·2	54·3	58·5	57·3	60·2	51·0	53·6	56·7	62·8
30	5·75	47·8	49·0	48·5	—	44·4	45·1	46·6	48·3
45	4·65	39·4	42·7	42·8	45·0	40·2	40·8	41·1	43·6
60	4·0	38·8	40·0	39·9	40·0	37·5	37·3	36·2	38·4

Table 2. *Comparison of results on flint B using different sampling tubes and jets (sampling speed constant)*

Settling time (min)	*Stokes' radius (μ)*	*Wide horizoncal tube*	*Wide vertical tube*	*Medium vertical capillary*	*Narrow vertical capillary*
20	7·15	59·6	62·6	66·7	67·0

Using open manometer tubes, vertical ones and also slightly inclined to the horizontal, our spreads of results have been similar to that shown in Fig. 5 of Paper A.4.

Dr. J. R. H. Coutts: The modified form of sampling apparatus shown in Fig. 1 has been found convenient for the pipette method of mechanical analysis. The pipette is

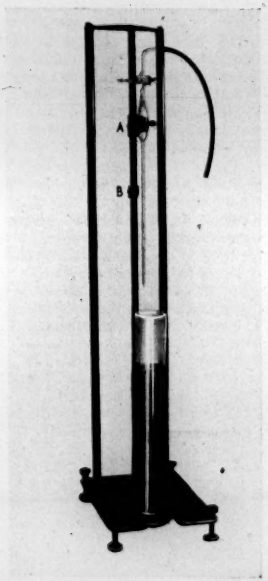

Fig. 1. Modified form of sampling apparatus

supported on a holder *A* which can be clamped in any position on a vertical pillar of square cross-section which has a scale engraved along one side. A boss *B* with levelled upper face and bevelled lower edge can also slide on the pillar; its position is defined by the scale reading opposite the bevelled edge. When the pipette has been adjusted with its tip at the surface of the suspension the boss is first raised until its upper face is in contact with the pipette holder; it is then lowered by a distance equal to the required depth of sampling and clamped in position. By lowering the pipette support until it rests again on the boss the sampling position is attained without lateral motion or risk of overshooting the depth.

Mr. W. M. T. Perkins: Would the authors say something about the use of liquids of higher viscosity than water for use with the coarser particles and also about the validity of the light extinction method for powders of limited range?

Dr. J. F. Brown and **Dr. J. K. Skrebowski** (*written contribution*): The concentration of suspension recommended by Drs. Jarrett and Heywood is 0·6% by volume or 1·6% by weight for silica dusts. Whilst this figure may well be satisfactory for silica or sand it cannot be considered as a generally recommended figure for other materials. Previous work by Stairmand* has indicated that the concentration should not exceed 0·2% by volume. This value has been confirmed on subsequent occasions and is supported by Messrs. Bessey and Soul in Paper H.1. The photo-extinction method of size analysis has considerable advantages over other methods. It measures the concentrations of the suspension directly without disturbance and works at low concentrations (0·2% by volume or less). Unfortunately it can only be used with any degree of accuracy for a comparatively narrow range of particle size.

We have recently developed a method for measuring the concentration of a settling powder using X-rays. The absorption of an X-ray beam in passing through a medium depends only on the weight of material present in the beam and the chemical composition of the material, and is independent of the physical state of the material. It can be shown that if I_0 is the intensity of the X-ray beam when passing through a cell containing pure liquid and I the intensity of the X-ray beam when passing through the same cell containing the liquid with A grammes of material in suspension, then $\log (I_0/I) = KA$, where K is a constant depending on the chemical composition of the material. Thus by measuring the transmitted intensity of an X-ray beam it is possible to follow the variations in the weight of material suspended in the beam path as the material settles out. From this a graph of weight against time can be obtained and hence the particle size distribution can be determined. The apparatus used is shown diagrammatically in Fig. 2. The X-ray beam is split into two parts, one being the reference beam falling on to a fluorescent screen, the second beam passing through the sedimentation cell on to a second fluorescent screen. The light output from each fluorescent screen, as measured by a photocell, gives a direct measure of the X-ray intensity.

Several substances have been examined by the X-ray absorption method, e.g. fly-ash, iron-oxide, bismuth oxide, at a concentration of between 0·2%-0·3% by weight (or 0·15%, 0·08% and 0·04% by volume) and the results were compared with the results from a rapid sedimentation method. The agreement between the methods is very good and within

* STAIRMAND, C. J. *Symposium on Particle Size Analysis, Suppl. to Trans Instn Chem. Engrs*, **25**, pp. 77 and 128 (1947).

the reproducibility of the normal sedimentation method. Using the X-ray method it is possible to complete a particle size analysis of a material such as fly-ash, with a range of from 76–7 μ, in about 30 min, which compares with about 3 to 4 hours for the normal sedimentation method. Furthermore,

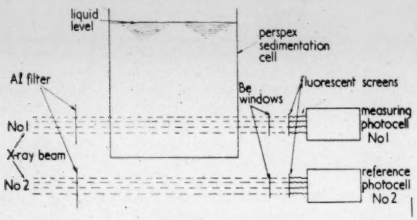

Fig. 2. X-ray absorption apparatus for particle size analysis

it gives a direct, continuous measure of the concentration of the settling powder with no disturbance of the suspension. The method is at present only suitable for material which is chemically homogeneous since the absorption coefficient K in the above equation is dependent on the chemical composition of the material. A full account of the method is being prepared for publication.

Authors' reply: In reply to Mr. Perkins, the sedimentation methods described in the paper had been investigated at the request of the Ministry of Supply with the object of providing a rapid method of analysis capable of dealing with hundreds of samples. It was therefore almost essential that the suspending liquid should be water with a suitable dispersing agent, so as to avoid the expense of a viscous liquid or the trouble of recovering such a liquid for repeated use. Viscous liquids would slow down the motion of large particles, but they would also increase the effective inertia of the measuring process, and the dispersion of fine particles in these liquids was not always as satisfactory as in water. The light-extinction method of size analysis could be applied with accuracy to powders having a size range of the order of 3 to 1, since the extinction coefficient would vary little over this range provided that the minimum particle size was not less than 10 μ.

The experiments described by Mr. Johnson are interesting, but in operating the Andreasen pipette apparatus the sampling time was maintained constant at between 30 and 45 sec with a vertical jet; a horizontal jet could introduce difficulties due to "shadowing" as shown by Davies in Paper A.3. Table 1 showed that at the smaller particle sizes the effect of sampling rate with vertical tubes was negligible. The sizes of vertical capillary tubes for which results were given in Table 2 were not stated, but probably the standard Andreasen tube would be within the range "medium" to "narrow," for which the divergence in results was slight. Although variations of the Andreasen technique were not investigated, it was found that the analyses obtained agreed precisely with the known composition of the test dust. We agree with Mr. Johnson's remarks concerning hydrometer and other tests.

The pipette apparatus described by Dr. Coutts is simple and could easily be constructed in the laboratory. It was similar to equipment used at the Road Research Laboratory, and only a detailed investigation would show whether it possessed any advantages over the standard Andreasen pipette.

In reply to Drs. Brown and Skrebowski we have to say that the permissible concentration of solids in a suspension was closely linked with the physical and chemical nature of the particles. Silica was fairly free from flocculation effects and was therefore used for the tests, but whiting was very prone to flocculation, and this could account for the results found by Stairmand and by Bessey and Soul. No general value for the higher limit of concentration could therefore be stated, the permissible value would depend upon the powdered material and the suspension liquid used. In all cases the concentration should be a minimum consistent with the method of measurement.

The X-ray method of measuring particle concentration in suspensions is a new development in particle size analysis techniques, and would seem to have considerable scope for this purpose. Publication of a full description with calibration experiments will be anticipated with interest.

Paper A.5

Theory of size classification of airborne dust clouds by elutriation

By W. H. WALTON, B.Sc., F.Inst.P., Scientific Department, National Coal Board

Particle size classification systems are considered of the type in which an airborne dust cloud is drawn at a low velocity (so that inertial forces are negligible) through a vertical or horizontal duct (elutriator) in which the larger particles are removed by gravitational settlement. It is shown that within such a system the concentration of particles of given falling speed f remains constant along any (particle) flow tube; tubes coming from the open cloud contain particles at the original cloud concentration, whereas those originating from the underside of an impervious surface are empty. It follows that if particles are drawn upwards on to a horizontal inverted filter immersed in the cloud, there being a uniform vertical air velocity v immediately beneath the filter surface, then the number of particles collected will be a fraction $1 - (f/v)$ of those originally contained in the sampled air. The addition of a vertical elutriator tube beneath the filter has no effect on the selectivity, in particular the velocity profile within the tube is of no consequence and it is not possible to obtain a sharper cut than that indicated by the above formula. If the elutriator is fitted with a convergent upper section before the filter, the sharpness of the classification will be diminished.

A similar classification of particles can be obtained by drawing the cloud through a horizontal channel. In this case the fraction passing, of falling speed f, is $1 - (fA/Q)$ where Q is the volume flow rate and A is the horizontally projected floor area of the duct. The shape of the duct and the vertical air velocity profile within it are immaterial provided that Q/A is constant for all air streams. Horizontal elutriation systems of this type are more convenient to use in practice than vertical systems since the dimensions can be much smaller for a given throughput and the penetrating cloud can be collected on a filter or other device of a small area. They provide a standard means of classifying airborne dust in sampling, which is suitable for a wide range of requirements.

In the investigation of airborne particulates it is often convenient to classify the particles during the sampling process so that subsequent measurements of quantity or composition relate to defined fractions of the cloud. This paper discusses theoretically methods of selective sampling by elutriation, in which the cloud is drawn at a low velocity through a vertical or horizontal duct so that the larger particles fall out of the airstream while the residual sample of smaller particles passes through and is collected on a filter. The main object of the work was the development of means of sampling only the respirable content of industrial dust clouds. The results are, however, of more general interest and it is believed that they form a basis for the design of a range of standard selective sampling devices suited to a variety of requirements. The parameter by which particles are classified is their falling speed, which is not uniquely related to size, but which is of greater significance than size in many applications, e.g. in determining the respirability of a dust, or the point of deposition of particulate matter emitted from a chimney stack.

The principle of size classification by elutriation is well known, but in applications that differ in important respects from the present one of sampling a continuous cloud. In the ordinary classifier a finite sample of dust is introduced into the bottom of a vertical tube and a stream of air or other fluid is passed upwards through it until all particles of less than a critical falling speed have been carried over. Two points of difference from cloud sampling are to be noted, (i) the smaller particles are removed more rapidly than the larger ones, but the process is continued until the transport of the larger ones is also complete, (ii) the dust remaining in the tube is agitated mechanically so that in the course of time all particles are brought into the air stream of highest velocity at the centre of the tube, which lifts particles that would not be carried over by the slower air near the walls. As a result of these two factors a sharp classification into two size-fractions is achieved.

Familiarity with the above system has led to various attempts to achieve a similar result in sampling a cloud by drawing it upwards through a vertical tube and collecting on a filter those particles which reach the top, but certain difficulties have been recognized. For example, to obtain a sharp separation it would be necessary to have a uniform distribution of air velocity over the cross-section of the tube, which is almost impossible to obtain in practice; also, below the tube the velocity will be less than it is within so the question arises whether particles near the limiting falling speed will ever enter the elutriator. Such considerations have led to experiments with annular systems, and with elutriators tapering to a small cross-section (giving a high air velocity) at the lower, inlet, end. It will be shown that such methods do not give a sharp size division, but that a standard form of graded cut-off can be obtained.

GENERAL THEOREMS

The discussion is confined to systems in which the air flow is streamline and inertial forces on the particles are negligible so that the velocity V of a particle at any point is the vector sum of its settlement speed f, and the air velocity v (which are both vectors) at that point. This latter condition requires that centrifugal forces in the air stream shall be small compared with those of gravity.

Two theorems relating to sedimenting inertia-less clouds which are applicable to the present problem, have previously been demonstrated by the author.[1] These state that (*a*) a change in air movement (due, for example, to the introduction of a sampling flow) within a cloud of sedimenting inertia-less particles whose concentration is initially uniform will not give rise to a change in particle concentration at any point within the cloud; and (*b*) the number of particles passing per unit time through any given area within a cloud of sedimenting inertia-less particles is equal to the number that would fall through if the air were stationary plus the product of the particle concentration and the flux of air through the area. These results relate to the unobstructed open cloud external to the sampling orifice. Theorem (*a*) may be extended to an elutriation system of the type we are now considering as follows.

The air flowing into and through the elutriator may be imagined to be divided into a number of "flow-tubes,"

bounded by stream lines, such that no air passes through the walls of the tubes. Dust particles of any given terminal velocity follow similar, but not the same, tubes of flow, the particle velocity at any point being the vector sum of the air velocity and the sedimentation velocity. The dust flow-tubes differ for particles of different terminal velocity. Now consider a group of particles of the same terminal velocity f passing along such a dust flow tube. If the group at any time occupies a small volume s, this volume will expand at the rate $ds/dt = s \operatorname{div} V$, where V the particle velocity, is equal to $f + v$; since f is constant and $\operatorname{div} v = 0$ (by continuity), we have $\operatorname{div} V = 0$ and so s is invariant with time. In other words, the concentration (number or mass per unit volume) of particles passing along any flow tube is constant. From this we draw the important conclusion that wherever within the elutriator particles of a given terminal velocity, drawn from the outside air, are to be found, their concentration will be identical with that in the outside air. Otherwise, the concentration will be zero; it is "all or none." Tubes of flow which do not come from the open cloud but which originate from an impervious surface will be "empty" in this way. Theorem (*b*) follows immediately from the fact that the scalar product $V.dA$ is equal to $v.dA + f.dA$, where dA denotes an element of area, which in this instance is a vector.

Now consider the rate of collection of particles, whether on the walls of the elutriator duct or on a filter paper after passage through the system; it is clearly, per unit area, equal to the concentration C multiplied by the particle (not air) velocity perpendicular to the surface. To take specific examples, there is no deposition on a vertical impervious wall; on any horizontal surface the rate of deposition is Cf, and on a surface making angle θ with the horizontal, it is $Cf\cos\theta$, since the air velocity v can have no component perpendicular to the surface. As shown in the preceding paragraph, C is either equal to the original cloud concentration C_0 or is zero. In the case of collection on a filter paper through which air is drawn there is an air flow perpendicular to the surface. If the filter is facing vertically downwards the rate of collection will be $C(v - f)$ per unit area so that the sample will appear to be deficient in relation to the concentration and the volume drawn through the filter in the ratio $1 - (f/v)$. It will be noted that tubes of flow cannot terminate on any downwards facing impervious surface, or originate from any upwards facing one.

VERTICAL ELUTRIATORS

Inverted filter. Consider first the simple system depicted in Fig. 1. This is an inverted filter, without elutriator tube, through which air is drawn vertically upwards at velocity v from an otherwise stationary cloud. If the paper is of uniform texture, v will be constant over the collecting surface and the direction of flow immediately below the paper will be vertically upwards.

The air flow pattern will be as indicated schematically in Fig. 1 by the continuous lines. Particle trajectories at the paper surface will be upwards whenever v is greater than f, i.e. such particles will be collected; but no particles for which f is greater than v can reach the paper surface. Since the trajectories of particles of the same settlement velocity cannot cross, all such trajectories traced backwards from the filter will lead to the free space of the cloud, or, conversely, there will be particle flow-tubes from the cloud to all areas of the paper. The general form of the trajectories will be as indicated by the dotted lines in Fig. 1, but it is unnecessary for our present purpose to enquire into their exact shape. It is of interest, however, to note that all particles sampled will be drawn from a vertical cylindrical zone above the filter of cross-sectional area v/f times the area A of the filter; particles sedimenting on the upper surface of the filter come from the inner zone of this cylinder. This follows from a consideration of the flux of particles through the two areas, which must be equal.

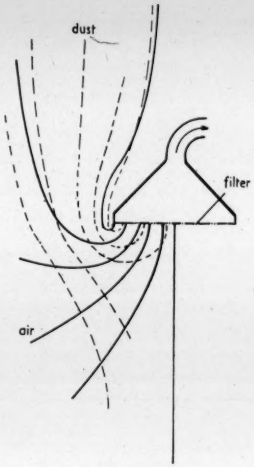

Fig. 1. Inverted filter

As shown in the previous section, the concentration of particles in each flow tube reaching the filter paper is equal to the original cloud concentration C_0 for particles of given f, and the number sampled per unit area is $C(v - f)$ in unit time. Since similar conditions prevail over the whole of the filter area, the total quantity collected per unit time will be $QC_0[1 - (f/v)]$, compared with the "ideal" quantity QC_0, where Q is the air sampling rate.

$$\text{The fractional collection efficiency} = 1 - (f/v) \qquad (1)$$

Its value is given in the table for various values of f/v and of particle diameter, d, assuming d to be "10" when $f = v$, and f to be proportional to d^2.

Percentage collection efficiency of inverted filter

f/v	0	0·1	0·2	0·3	0·4	0·5	0·6	0·7	0·8	0·9	1·0
particle diameter	0	3·2	4·5	5·5	6·3	7·1	7·7	8·4	8·9	9·5	10
% collection	100	90	80	70	60	50	40	30	20	10	0

With such a system there is a critical size of particle above which none is collected. Below this size the collection efficiency rises rapidly, being 50% at $1/\sqrt{2}$ times the critical size and 75% at half this value. It will be seen later that the form of sampling cut-off indicated in the table applies to a wide variety of elutriation devices and represents the sharpest size-cut that can be obtained by simple gravity-separation means.

If the sampling device described in the previous paragraph be placed in moving air, the air and particle flow lines will be distorted, but we shall still have the same conditions at the surface of the filter paper and similar reasoning will apply. The sampling efficiency of the device will be unchanged. The assumption is made that the wind speed is not sufficiently high to introduce serious inertial effects or to break down the uniform boundary-layer flow at the surface of the filter.

One simple conclusion that can be drawn from the foregoing is that dust will be collected uniformly over the whole surface of the inverted filter; there will not be a lighter deposit in the centre due to the screening of this area from falling commences. The effective "sweeping out" velocity for particles of any given settlement velocity is $v - f$, not v, so that the volume of air sampled before particles reach the paper will be many times the volume of the tube when f is nearly equal to v. This may impose an appreciable error if the time of sampling is short.

In practice the air flow in the elutriator tube will not be uniformly distributed at distances below the filter comparable with the tube diameter, and if the tube is long enough it may approximate, for a circular tube, to the well-known parabolic distribution characteristic of viscous flow. The picture in this case is not so simple: the higher speed air stream near the

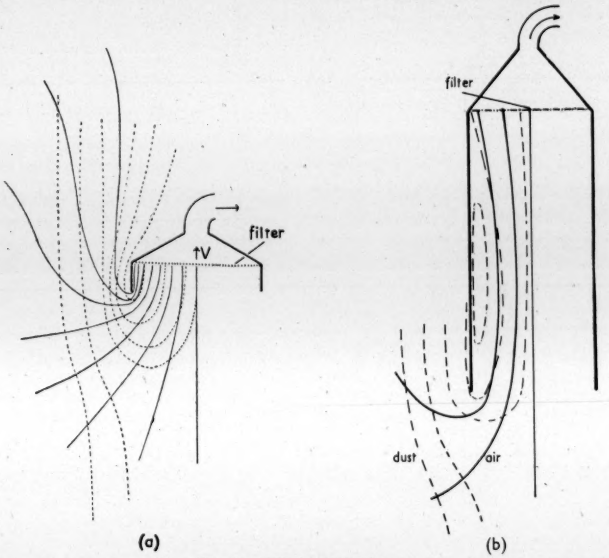

Fig. 2. Cylindrical elutriators

particles by the outer zones as might perhaps appear probable at first sight. This forms one simple means of testing the theory experimentally. The above results will not apply if the filter is surrounded by an impervious rim of appreciable width. This would provide a source of empty flow-tubes leading to the filter and result in loss of sample.

Cylindrical elutriator. Consider next an elutriation system in which an open-ended vertical cylinder is fixed below an inverted filter, the filter area being equal to the cross-section of the cylinder (Fig. 2*a*). This is a system which has frequently been used in practice. If we can assume that the air flow lines in the cylinder remain parallel and that the velocity is uniform over the cross-section as it is at the paper surface, then clearly the flow conditions at the bottom of the cylinder will be the same as those beneath the paper (with no cylinder) in the example previously considered and the sampling characteristics will be identical. There is one important difference between the two systems, however. If the cylinder is initially empty of particles, some air will have to be drawn through the system before it is "swept out" and sampling axis can carry upwards particles of correspondingly greater terminal velocity whereas the slower air near the wall can only lift small particles. The question therefore arises whether the sampling cut will be correspondingly disturbed. The answer can be given at once on general grounds. Uniform flow conditions as before prevail at the surface of the paper; no particle flow-tubes reaching the paper can originate from the vertical walls of the elutriator, so all must come from the free cloud at the open, lower end and be full of particles at the true cloud concentration. The number of particles sampled after the system has been "swept out" is therefore again $QC_0[1 - (v/f)]$. The particle flow pattern within the tube is shown diagrammatically in Fig. 2(*b*). If the elutriator is initially full of cloud there will be an internal circulation of particles as indicated in the figure. If it is initially empty, the zone of circulation will remain devoid of particles. The above result for the sampling efficiency is independent of the flow pattern within the vertical duct provided that there are no significant centrifugal and inertial effects. Similarly, an external wind of low velocity will have no effect. The previous

remarks regarding the uniformity of distribution of the sample over the filter surface again apply, and have been verified experimentally.

It appears from the foregoing that the practice of attaching a vertical cylindrical elutriator tube below a filter as a means of selective sampling serves no useful purpose except perhaps the mechanical protection of the filter. It cannot give a sharp "cut" at a critical falling speed. It has the disadvantage of causing an initial error during the sweeping-out period. If such a tube is used, the flow profile within it is of no consequence.

Conical elutriator. Another type of elutriator which has been used consists of a vertical truncated cone of small angle with a horizontal filter at the top of the cone. (See Fig. 3*a*.)

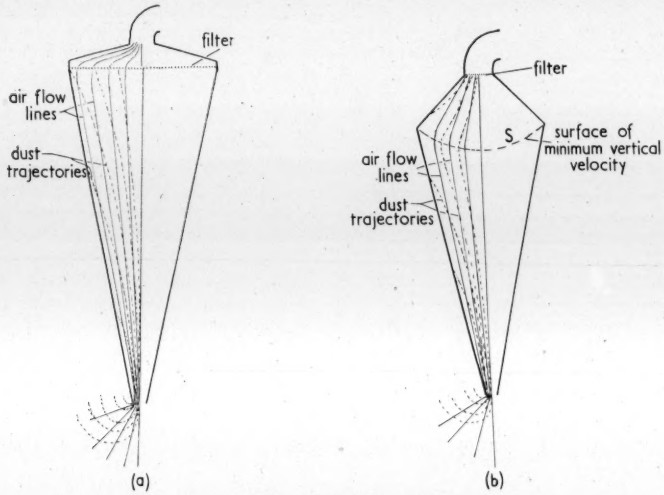

Fig. 3. Conical elutriator

(*a*) vertical truncated cone type; (*b*) convergent head type.

The sampled cloud enters the system through the small hole at the bottom (apex) of the cone. The idea behind the device is that the high velocity of entry carries a representative sample of large particles into the cone and that undisturbed flow conditions, favouring accurate segregation of different particle sizes, will prevail in the interior. The performance of the conical elutriator can be derived by an identical argument to that employed in the case of the cylindrical system. No particle flow-tubes can originate from the upwards facing inner surface of the cone; there is no source of (empty) flow-tubes within the cone so all tubes terminating on the filter must come from outside and will contain particles of concentration C_0. The total quantity of particles sampled is therefore $QC_0[1 - (f/v)]$ as before. There is no need to enquire into the detailed air flow pattern within the cone, and in particular the result is independent of the angle of the cone and of the size of the entrance orifice. Indeed the cone serves no more useful purpose than did the cylindrical elutriator. Rather there is a danger that errors may arise from (*a*) the shadowing effect of the overhanging external wall of the cone above the entrance orifice, and (*b*) the generation of appreciable centrifugal forces by the fast moving air stream at the restricted entrance.

Conical elutriator with convergent head. In all the devices so far discussed the constant form of the sampling cut [fraction sampled $= 1 - (f/v)$] has depended on the uniform vertical velocity distribution beneath the filter. The use of a large filter covering the whole area of the elutriator may, however, present practical difficulties. For example, if it is desired to measure the mass of sample collected it may be necessary to use a filter of minimum size. Alternatively it may be necessary to lead the selected sample to some other form of collector such as a thermal precipitator, which will deposit the particles in a form suitable for microscopic examination. In such cases it is usual to attach a convergent head to the elutriator, as shown in Fig. 3(*b*), so that the penetrating cloud can be collected on a filter, say, of small diameter. Davies[2] has calculated the trajectories of particles within a conical elutriator of this type. In order to make the problem tractable he assumes that the air flow lines in the lower cone diverge symmetrically and radially from a point source at the apex and that all particles that reach the height of the upper rim of the cone are swept away by the higher air velocity in the narrowing upper section. This is equivalent to their removal by a filter at this plane as we have previously considered, except that on Davies's assumed flow pattern the vertical air velocity in the plane of collection is not constant but diminishes with increase in distance from the axis. In consequence Davies finds that the fraction of particles carried through the elutriator is $1 - (f/v)$ only for cones of vanishingly small angle, with a less-sharp cut for larger angles. Only a rough approximation to the flow pattern assumed by Davies would be obtainable in a real convergent head elutriator since he neglects the influence of viscosity and other factors. The

actual flow pattern would vary with the detailed design of the instrument and with its conditions of use, and the performance would be unpredictable. Davies himself points out that the flow may break up into a vortex. This difficulty may be overcome by providing a positive control of the flow, such as that given by a filter, in the zone of greatest cross-section where the vertical air velocity is lowest, but then the lower cone becomes redundant as we have already seen. If no such control is provided, the total penetration of particles through the elutriator will be the sum of components of the form $[1 - (f/v)]$ taken over the surface S (Fig. 3*b*) containing all points at which the air flow is vertical and of minimum velocity as the flow passes from a divergent to convergent pattern. It is thus a simple matter to calculate the performance for any known or assumed flow pattern.

In the consideration of vertical elutriation systems it has so far been assumed that the selected particles are collected on a filter which also gives the required uniform vertical air flow, and the disadvantages of this have been pointed out. A similar control of the air flow could be obtained by a close array of small parallel air channels which would permit the particles to pass through to a convergent head and be collected by other means. The viscous drag between adjacent air streams of differing velocity would ensure a smoothing-out of the flow to a uniform value at a short distance below such a flow-straightener provided that the structure was sufficiently fine; indeed it is exactly a mechanism of this type that operates beneath a fibrous filter. Care would be needed in practice to ensure sufficient control of the flow without causing loss of particles in the channels.

HORIZONTAL ELUTRIATORS

An alternative method of selective sampling is to draw the cloud through a horizontal channel so that particles of large settlement velocity fall to the floor while the majority of those that fall slowly remain airborne and are carried on to the collecting filter. The principle will be understood by first considering the simple system illustrated in Fig. 4(*a*). This shows a vertical longitudinal section through a horizontal duct of uniform rectangular cross-section. The left-hand end of the duct is immersed in a cloud of constant concentration C_0 and a sample of the cloud is drawn at uniform velocity v through the system. It will be assumed in the first instance that the air velocity is uniform over the section so that the flow lines are parallel and equally spaced as indicated in the diagram. Let the height of the duct be h, and let l be the length measured from the end at which the cloud enters. Particles of concentration C_0 and settlement velocity f entering the duct will follow trajectories which are sloping downwards at an angle whose tangent is f/v so that at l there will be a layer of particle-free air of depth fl/v and below this a layer of cloud containing particles in the original concentration. The ratio of the number of particles leaving the duct (or collected on a filter at l) to the number entering is therefore

$$h - (fl/v) = 1 - (fl/vh) \qquad (2)$$

When $fl/vh > 1$, all particles reach the floor of the duct before traversing the full length and so none is sampled.

It will be seen that equation (2), giving the fractional number of particles sampled of terminal velocity f, is of similar form to equation (1), $[1 - (f/v)]$, for the selectivity of a vertical elutriator, but that the cut-off size is now given by $f = vh/l$ instead of by $f = v$ for the vertical system.

The above result is not confined to the simple ideal system we have so far considered, but is of much wider application. For example, suppose that we have a duct of uniform rectangular section as before, but that the velocity is not uniform in the vertical plane, as shown in Fig. 4(*b*). The air flow-lines and the particle trajectories no longer form straight parallel systems. For particles of given settlement velocity f there will be a bounding trajectory A, Fig. 4(*b*), which is that of a particle which just enters the duct below the upper edge at the open end, and above which no particles are to be found

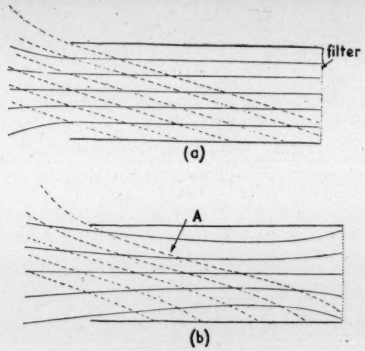

Fig. 4. Horizontal elutriators

(*a*) simple horizontal duct;
(*b*) rectangular duct having non-uniform air-velocity in the vertical plane.

within the duct. Below this bounding trajectory we have particle flow-tubes leading from the open cloud which must therefore contain particles of the original cloud concentration C_0. If f is such that the bounding trajectory A does not reach the floor in the length l of the duct, then the whole of the floor area of the duct will be covered with particle-laden air and particles will be deposited on to the floor at a rate $C_0 fl$ per unit time per unit depth of duct perpendicular to the plane of the diagram. This represents the former dust burden of volume fl of clean air reaching the filter at l per unit time. If $\bar{v}$ is the mean velocity of air flow along the duct (the air flow-lines are assumed to be parallel to the plane of the diagram), then $\bar{v}h$ is the volume of cloud sampled per unit time in the section of unit width, and $\bar{v}h - fl$ is the volume of dust-laden air (of original concentration C_0) penetrating the duct.

The amount of sampled dust collected on the filter

$$= (\bar{v}h - fl)/\bar{v}h = 1 - fl/\bar{v}h \qquad (3)$$

which is identical with equation (2), except that the mean air velocity $\bar{v}$ is now substituted for the previously assumed uniform velocity v.

The above theory will apply to a real duct of uniform rectangular cross-section whose height is small compared with the width and length. Under these conditions the flow pattern will be the same in all vertical sections parallel to the axis, except immediately adjacent to the side walls. The size selector as a whole can conveniently consist of a large duct divided by horizontal partitions into a series of elements each of the type described above, as illustrated in Fig. 5. The advantages of such a system, compared with a vertical elutriator of equivalent performance, are readily seen.

Suppose, for example, it is required to design an elutriator with a throughput of 100 litres of cloud per minute which will pass no particles of terminal velocity greater than 1 mm/sec. With a vertical system we require an upwards air velocity equal to the particle settlement speed, i.e. 1 mm/sec or 6 cm/min. Hence the cross-sectional area of the device must be 100 000/6 cm^2, corresponding to a diameter (for a circular elutriator) of about 146 cm. In a horizontal elutriator the

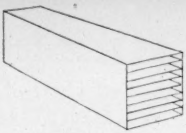

Fig. 5. Multiple horizontal elutriator

required condition is $f = \bar{v}h/l$, so that, if we use the multiple arrangement shown in Fig. 5 and make $l = 60$ cm, and the height of each section $h = 0{\cdot}5$ cm, we have $l/h = 120$ and $\bar{v} = 120f = 720$ cm/min. The required overall cross-sectional area is therefore 100 000/720 cm^2, which is given by a duct of approximately 12 cm square section. The separating device can therefore consist of a 12 cm square duct, 60 cm long, divided into 24 equal sections by thin horizontal partitions. Moreover, the sample can be collected on to a small filter at the end of the duct, whereas, with the vertical elutriator, a filter nearly 1½ m in diameter would be required.

We have so far discussed only horizontal elutriators of uniform rectangular cross-section, but they are not restricted to this form. Consider any elementary tube of air flow XY, such as that shown in Fig. 6, which is bounded by upper and lower walls and whose sides are vertical. The width of the

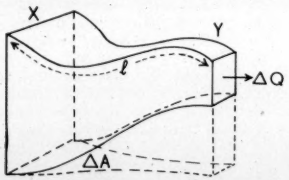

Fig. 6. Flow-tube of varying cross-section

tube is small but not necessarily constant. The height of the tube may be of any value and need not be constant along the length. The air velocity v is a function of the vertical and longitudinal position, subject only to the conditions that the sides of the tube must remain vertical and, of course, that the volume ΔQ flowing along the tube is constant. A cloud of particles of concentration C_0 and settlement velocity f enters the tube at the end X and fills the vertical cross-section at this point. The number entering per unit time is therefore $\Delta N = C_0\Delta Q$. At any distance l along the tube, provided the particles travel this distance, the number removed from the stream per unit time will be $C_0 f\Delta A$, where ΔA is the horizontally projected floor area up to this point. The fractional loss of particles from the stream is thus

$$C_0 f\Delta A/C_0\Delta Q = \Delta A/\Delta Q$$

and the fractional penetration through the flow-tube is

$$1 - f\Delta A/\Delta Q \qquad (4)$$

If the flow pattern within the duct is constant in the transverse direction so that all flow tubes of the above type are similar the overall penetration of particles through the duct will be

$$P = 1 - fA/Q \qquad (5)$$

where A is the total floor area and Q is the total flow rate. This is a more general form of equations (2) and (3), which applied only to ducts of uniform rectangular cross-section. It is now seen that the standard form of size selection can be obtained by a horizontal duct of varying, unspecified cross-section, its performance being determined only by the ratio of flow rate to floor area, subject to the condition that this is constant for all flow tubes.

If a horizontal elutriator is empty at the commencement of sampling, evidently a correct sample will begin to be collected once the original air has been replaced, the volume required depending on the velocity profile. This gives the horizontal system an advantage over the vertical cylindrical or conical elutriator, for not only can the volume of the apparatus be much less, but the number of volume changes required before near-limit particles come through is greatly reduced and the delay time is the same for all particles.

So far we have considered only systems which have an equal flow density $F(= \Delta Q/\Delta A)$ in all flow tubes.

If this is not the case, let $A(F)dF$ be the total floor area of tubes having a flow density in the range F to $F + dF$. The total flow through these is $FA(F)dF$.

In flow tubes for which f is greater than F all particles sediment on to the floor and none will penetrate the duct. In those for which f is less than F the number removed by sedimentation is $C_0 f$ per unit floor area. For the whole duct, therefore, the total number falling on the floor is

$$\int_{F=0}^{F=f} C_0 FA(F)dF + \int_{F=f}^{F=\infty} C_0 fA(F)dF$$

out of the total

$$\int_{F=0}^{F=\infty} C_0 FA(F)dF$$

which enters the system.

The fractional number of particles removed by the duct is therefore

$$R = \frac{\int_0^f FA(F)dF + \int_f^\infty fA(F)dF}{\int_0^\infty FA(F)dF} \qquad (6)$$

and the fractional penetration, P, is $1 - R$.

It will be noted that in equation (6), the denominator represents the total air flow through the duct; and the first term of the numerator represents the total flow for which the flow density is less than f.

The above results can conveniently be represented graphically as shown in Fig. 7. Here the total floor area with flow density less than a given value F, i.e.

$$\int_0^F A(F)dF$$

is plotted against F.

It will readily be seen that the total area between the ordinate axis and the curve is equal to the denominator of equation (6). The two terms of the numerator correspond

respectively to areas (1) and (2) in Fig. 7, lying under the curve between the ordinate axis and the line $F = f$. By difference the remaining area (3) represents the volume of air which still contains particles of falling speed f after passing through the duct. The penetration function of the duct for particles of different falling speeds is therefore readily found by determining the areas (3) for various values of $F = f$. This may be done either analytically or graphically.

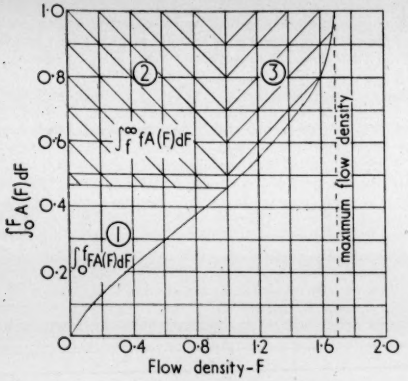

Fig. 7. Flow density for a circular duct

The actual curve shown in Fig. 7 is the flow density diagram for a horizontal circular cylindrical duct with the parabolic flow distribution characteristic of viscous flow. The plotted data relate to unit total flow rate through a duct of unit horizontally projected area, i.e. unit mean flow density. The flow density at fractional radial distance r from the axis is $F = 16(1 - r^2)^{\frac{1}{2}}/3\pi$, and

$$\int_0^F A(F)dF = 1 - r$$

Fig. 8 gives the percentage penetration versus falling speed curve for this duct derived graphically from Fig. 7 in the manner described above. The corresponding curve for a rectangular duct of constant (unit) flow density is shown for comparison. The circular duct passes particles of wider size range. If the flow density of the circular duct is reduced by a factor 0·83 the penetration curve shown by the broken line in Fig. 8 is obtained, which coincides with the curve for the rectangular duct at 50% penetration. It diverges from this latter mainly in having a "tail" of larger penetrating particles.

Intermittent flow through horizontal elutriator. In some instances it is convenient to draw air intermittently through the sampling device. It is therefore necessary to examine the behaviour of a size selector under these conditions.

Consider an intermittent sampling system in which a volume S of air is drawn into the instrument at periodic intervals of time, t. The mean sampling rate Q is thus S/t. If this flow passes through a horizontal elutriator of uniform rectangular section of height h, floor area A and total internal volume equal to $S(= Ah)$, and if there is a uniform "plug" flow of air, then the air within the elutriator is just completely replaced at each cycle and all the sampled air spends the same time t within the elutriator. During this time all particles of falling speed greater than $f_0 = h/t$ fall out of suspension. Of the remainder a fraction $1 - ft/h$, or $1 - fA/Q$, remains in suspension and is swept through on the next cycle. The properties of the elutriator are thus identical with those for continuous flow provided that the internal volume is equal to (or an exact multiple of) the volume drawn in each cycle; and that the air flows with a constant velocity front. The variation of flow with time during the periodic intervals is not significant.

In practice there is some departure from the above because the condition of uniform velocity front cannot be satisfied, although a reasonably close approximation to it can be achieved for predominantly potential flow conditions.

For the conditions of viscous flow between parallel plates the air velocity front is parabolic. If a volume S of cloud is suddenly drawn into the elutriator this will initially occupy a volume behind the parabolic front as illustrated in Fig. 9(*a*). The total volume of the elutriator up to the point of furthest advance of the cloud is 3/2 times the volume of indrawn air.

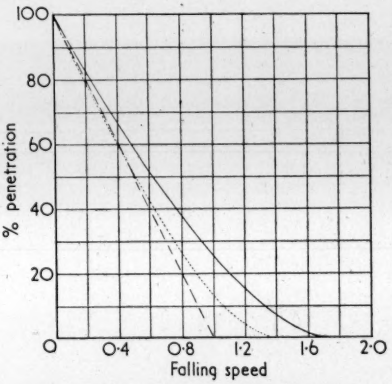

Fig. 8. Penetration curve for a circular duct

mean flow density = 1 ——— circular duct
- - - - - - - rectangular duct
mean flow density = 0·83 · · · · · · · · · circular duct
(flow density and falling speed in same units)

This is clearly the minimum size of a size-selecting elutriator under these conditions, for one smaller than this would be immediately penetrated by some particles of all sizes on each intake. While the air within the elutriator is at rest for time t between intakes, particles of falling speed f fall a distance ft, but their concentration within the space they occupy remains constant. The distribution of cloud immediately before the second intake is therefore as shown in Fig. 9(*b*) for various values of ft. At the second intake the residual clouds shown in Fig. 9(*b*) are swept forward into the positions shown in Fig. 9(*c*). None of the larger particles remaining in suspension is carried as far as the end of the duct (see curve for $ft = 0{\cdot}8h$). They are lost by sedimentation before the next (third) intake of air and so never reach the collecting filter. The maximum falling speed of particles which just penetrate to the filter is given by $ft = h/\sqrt{2}$, as may be shown analytically. This, then, gives the critical falling speed

above which no particles penetrate the system; below this value the penetration progressively increases. For all particles for which $f < h/2t$, or $f < 3Q/4A$ the whole floor area A of the duct is continuously covered by airborne cloud (after the first few intake cycles) and so the fractional number deposited

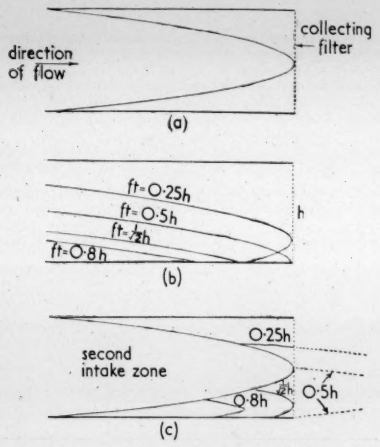

Fig. 9. Cloud profiles in conditions of intermittent viscous flow between parallel plates

(*a*) position of sampled cloud immediately after first intake
(*b*) cloud profiles immediately before second intake
(*c*) cloud profiles immediately after second intake

is Aft/S or fA/Q and the fractional penetration is $1 - fA/Q$ which is identical with equations (5) and (7). At values of f in the range $h/2t < f < h/\sqrt{2}t$, or $3Q/4A < f < 3Q/2\sqrt{2}A$ more particles penetrate than is indicated by the above equation because deposition of these sizes does not continue over the whole area of the floor for the whole of the cyclic sampling period. The resulting penetration curve is shown in Fig. 10 in comparison with that for a continuous flow of

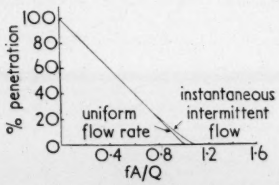

Fig. 10.—Penetration curves for continuous and intermittent (viscous) flow

the same mean value. The two curves are identical for values of fA/Q up to 0·75, i.e. for all penetrations greater than 25% but for intermittent flow zero penetration is not reached until $fA/Q = 1{\cdot}06$ instead of at 1·0. In practice the difference between the two curves is generally insignificant.

Diffusion of particles in horizontal elutriators. In addition to the particles lost by settlement between the plates of a horizontal elutriator, some will diffuse to the walls by Brownian movement and may give rise to error in the selected sample. It is therefore necessary to consider the conditions under which appreciable error may arise.

The problem approximates to that of diffusion from an infinite plane slab of thickness h, of initial concentration C_0 and zero concentration at the faces from time $t = 0$. The solution for the average concentration of particles remaining in the slab at time t is given by Carslaw and Jaeger[3] (as a problem in heat conduction). It is a function of the parameter Kt/h^2, where the diffusion coefficient K is given by Einstein's equation $K = kT/R$, k being Boltzmann's constant, T the absolute temperature and R the fluid drag on the particle at unit velocity. The number of particles lost to the walls by diffusion will be less than 10% of the total for values of Kt/h^2 less than about 0·002.

Since the loss by diffusion is greater the smaller the particle size, we will consider the case of particles which are near the limit of visibility under the light microscope, say of diameter about 0·15 μ and falling speed 10^{-4} cm/sec. For such particles K is $1{\cdot}65 \times 10^{-6}$ cm^2/sec. Taking $h = 5$ mm, say, 10% of the 0·15 μ particles would be lost by diffusion if the cloud remained in the elutriator for 300 sec, but in this time 6% of the 0·15 μ particles, and all particles greater than about 0·65 μ (falling speed $1{\cdot}7 \times 10^{-3}$ cm/sec), would be lost by settlement. In any horizontal elutriator designed to pass particles larger than about 1 μ, the loss by diffusion of any particles visible under an optical microscope is likely to be quite negligible.

DISCUSSION AND CONCLUSIONS

It has been shown that simple gravity separation methods of continuous selective sampling cannot give a sharp cut but only a fraction $1 - (f/f_c)$ of the particles of falling speed f originally contained in the sampled air, f_c being the critical value of f above which no particles are sampled. This form of separation is given by both vertical and horizontal elutriation systems, but the latter offer much greater flexibility in design. Theoretically the only essential condition is that, for each filament of air passing through the system, dQ/dA shall be constant, where dQ is the volume rate of flow of the filament and dA is the settlement area over which it passes. This condition may easily be satisfied and so practical instruments can be designed to suit a wide range of flow requirements and give a near-theoretical performance. The practical design and performance of a range of such devices, operating at various flow rates between 4 cm^3/min at 75 l./min and passing only particles of respirable sizes, have been investigated by R. J. Hamilton and the present author and will be described in a separate publication.

ACKNOWLEDGEMENTS

The substance of this paper was communicated to members of Panel 1 of the Medical Research Council Industrial Pulmonary Diseases Committee in July 1950 and January 1951, and has provided a basis for the design of selective dust sampling instruments at a number of laboratories. It also appeared in National Coal Board, C.R.E. Report No. 139, March 1952. The paper is published by permission of Dr. W. Idris Jones, Director-General of Research in the Scientific Department of the National Coal Board. The views expressed are those of the author and not necessarily those of the Board.

REFERENCES

(1) WALTON, W. H. *Symposium on Particle Size Analysis*: Discussion. Suppl. to *Trans Instn Chem. Engrs*, **25** (1947).

(2) DAVIES, C. N. *Proc. Instn Mech. Engrs*, **1B, 5**, p. 185 (1952).

(3) CARSLAW, H. S., and JAEGER, J. C. *Conduction of Heat in Solids* (London: Oxford University Press, 1947).

DISCUSSION

Dr. C. N. Davies: It is stated by Mr. Walton that when the air velocity at the face of an inverted filter is v, then particles for which the settling velocity, f, is less than v will be collected. Since the streamlines of air flow converge on the filter, the vertical component of upwards air velocity will be less than v over a certain region below the filter so that particles will be unable to reach the filter, even when f is somewhat less than v.

The critical face velocity, v, above which particles can be collected is therefore not equal to f but is greater; it is not clear that the fractional collection efficiency will, in fact, be equal to $1 - (f/v)$ as claimed.

Mr. H. H. Watson: The analysis given by Mr. Walton is elegant in its simplicity, and I hope that publication of the practical results will not be long delayed.

I am thinking of an application of the horizontal elutriator principle for obtaining a quantitative measure of particulate matter deposited from the atmosphere on to a horizontal surface. The horizontal elutriator deposit should be, up to the cut-off size, related directly to that obtained on an exposed plate, and it is protected from rain. In this application, the orifice should be kept facing into the wind and isokinetic sampling conditions approximately maintained. But often, the deposit on the floor of the elutriator is not as uniform as it should be. Could Mr. Walton give me an indication of precautions to be taken in this application? It appears possible to use such a device under certain conditions without any sampling suction, allowing the wind to blow through the elutriator, which must of course be held into the wind with a vane.

Dr. J. G. Dawes: Mr. Watson has requested information on inlet difficulties when using horizontal elutriators. Barker, O'Connor and Winder* have tested a horizontal elutriator in a dust cloud in a coal mine. In this cloud, particles of size up to 50 μ were airborne. The elutriator was designed to pass 50% of 5 μ spheres of unit density and the air flow was 0·1 ft^3/min. The size selection characteristic was obtained by comparing a sample taken by an instrument fitted with the elutriator and a sample from an exactly similar instrument to which a size selector was not fitted. The samples were evaluated by using a microscope method. The characteristic obtained was not, of course, of the parabolic form expected with spheres (cf. Walton's Paper A.5), since the shape factor relating microscope size to terminal velocity size is not single valued, but is distributed, as has been demonstrated by Timbrell in Paper A.2 and Hamilton in Paper D.4.

It was found that the size selection characteristic of the horizontal elutriator was not stable with time in the conditions of test. When a very short period (30 min) sample was taken, the 50% collecting point was at 7 μ. If sampling proceeds continuously for 8 h, the 50% point occurs at 10 μ. If, however, the elutriator is slightly tilted, inlet downwards at about 10°, and the elutriator plates are cleaned at 30 min intervals over a period of 8 h, the 50% point is again 7 μ. This effect has been established by repeated experiments and may be due to the redispersion of dust collected on the elutriator plates caused by the entrance of large particles when the elutriator faces the air stream.

The same phenomenon has been noted in experiments in the same conditions underground with a larger horizontal elutriator designed to accept 5 ft^3/min.

Dr. W. D. E. Thomas: A simple laboratory method was required for assessing the stability of D.D.T. wettable powder dispersions in water. Such powders consist of D.D.T., an insoluble carrier (e.g. silica) and a wetter, and are used in the field as aqueous dispersions. The suspension is sprayed, but continuous agitation is often not available, and settling out of the active ingredient occurs with consequent variability in insect control. The method adopted was a modified Andreasen procedure, in which a 1% suspension (by weight) of the powder was prepared in 2½ litres of water in a Winchester bottle. During the settling period, four 50 ml samples were taken after varying times from a fixed point in the suspension by means of a 50 ml pipette allowed to rest on the neck of the Winchester during sampling. Each sample was centrifuged, filtered through a sintered glass crucible which was dried and weighed, and the D.D.T. content of each determined either by loss in weight following benzene extraction, or more accurately by a modified Schechter technique. From these data and assuming the validity of Stokes' law and its extension, a curve recording percentage undersize d_s against the Stokes' diameter d_s for each powder, could be drawn for values of d_s between 2 and 120 μ. This procedure almost certainly cannot give data on the precise size distribution of the D.D.T. particles as such, since the D.D.T. is usually present as a surface coating on the carrier particles, but it does give the apparent or effective particle size distribution of the D.D.T. and reflects closely the behaviour which would be observed in the field. The method is applicable to assess the performance of other wettable insecticide powders.

Mr. J. R. D. Walker: Could the systems surveyed by Mr. Hawksley, assumed by Professor Kynch and illustrated by Drs. Timbrell and Heywood really exist? A cloud of dense particles in a lighter fluid ought to be unstable and I would expect it to behave like a layer of dense fluid lying on top of one less dense; in which case it is not possible to calculate particle velocities, and it ought not to be possible to get consistently measurable suspensions. Did the clouds of dust particles behave like this or was there some undisclosed mechanism by which they became stable?

Professor Sir Geoffrey Taylor: There might be an analogy with a column of fluid heated from the bottom, which was stable if it was not heated too quickly.

Author's reply: Mr. Walker has enquired why the higher bulk density of particulate clouds does not cause the cloud as a whole to fall in the manner of a liquid of high density.

This effect does, in fact, exist exactly as Mr. Walker suggests. It is not normally noticeable for airborne clouds because the bulk density of these is not usually appreciably greater than that of the pure gaseous medium, e.g. an airborne suspension containing 1 g/m^3 of particulate matter is a very dense cloud indeed, but the particles only increase the bulk density of the air by less than 0·1%. An equal density change would result from a small decrease in humidity or from a fraction of a

* BARKER, O'CONNOR and WINDER. *Safety in Mines Research Establishment, Res. Rep.* No. 93 (1954) (London: H.M. Stationery Office).

degree change in temperature. Such density difference will nor normally affect the stability of, say, a cloud of hot gas emitted from a chimney stack. The bulk density effect is very noticeable in the case of suspensions in liquids. Concentrations of 1 % w/v are commonly employed in sedimentation analysis. If an attempt is made to float a layer of such a suspension on the top of a column of the pure liquid, it will be found that the suspension is unstable and flows to the bottom in the manner of a heavy liquid. Indeed it is probably this which has led to the development of sedimentation analysis methods using a column of suspension, which only give an undersize distribution. With this method a vertical density gradient is established as the settlement proceeds and this is a potent factor in stabilizing the system and reducing the disturbing effect of convection currents. Sedimentation analysis would be much simplified if the method of placing a layer of suspension on the top of a column of clear solvent could be used, for then the process would give a complete separation of the particles of different sizes. It is possible to use the layer method by having a column of liquid of greater density than that in which the particles are dispersed. If the column is also graded in density from top to bottom complete stability can be obtained and convection eliminated. I have successfully used such a graded column of water and alcohol, formed by filling the lower half of the vessel with water and the upper half with alcohol and then partially mixing them so that intermediate densities were found in the middle zones. On the top of this column a suspension of particles in alcohol was floated.

Mr. Watson enquires about the difficulties that arise in the practical application of horizontal elutriation to selective sampling. Some aspects of this will be dealt with in a paper by R. J. Hamilton and myself (to be published later), which describes instruments for the selective sampling of respirable dust. The main points to bear in mind are that the flow in the elutriator must be streamline and that the ratio of flow rate to floor area must be the same for all airstreams. It is also necessary to ensure that an external wind across the entrance will not disturb the flow for an appreciable distance into the elutriator. These conditions are best satisfied by a horizontal duct whose length is large compared with the width, which in turn is large compared with the height. The arrangement shown in Fig. 5 of my paper (A.5) is convenient. A symmetrical two-sided elutriator having two entrance channels, or even a circular system, can be used, but such a system is particularly liable to be disturbed by external air movement. Particle inertia effects at the entrance, which would alter the distribution of the larger particles across the airstream, must be avoided. The condition for this is that the "stopping distance" of the particles ($mv/6\pi a\eta$) at the velocity of entry should be small compared with the dimensions of the entrance channel. It is considered that much of the attractiveness of horizontal elutriators lies in the ease with which the simple theoretical conditions can be satisfied, and the design adjusted to suit practical requirements.

I am at a loss to understand the phenomenon described by Dr. Dawes. No such effect has been noted in my laboratory, and Dr. B. M. Wright of the M.R.C. Pneumoconiosis Research Unit (private communication) has found no apparent change in the cut-off of a horizontal elutriator after the plates had become covered with dust. I agree with Dr. Dawes that it appears to be due to redispersion, and clearly further investigation is needed of the circumstances under which this may occur. Possibly redispersion could be prevented by oiling the plates of the elutriator.

Dr. Davies enquires about the dust flow pattern immediately beneath the inverted filter illustrated in Fig. 1 of the paper, and queries whether particles which would only just be lifted by the upwards air velocity at the surface of the filter can in fact approach the filter through the zone of air flow beneath where the upward velocity component is less than it is at the filter surface. This uncertainty is typical of that felt by a number of workers who have considered the use of vertical elutriation systems and, indeed, led to the development of the conical elutriator illustrated in Fig. 3(*a*) of my paper. It was thought that the high air velocity at the restricted entrance at the bottom of the cone would ensure that a representative sample of the larger particles was swept into the system. A detailed analysis of the trajectories of individual particles into a sampling system is difficult and in most practical cases impossible. Dr. Davies has himself made a notable contribution to the subject by calculating the trajectories for a number of systems involving point and line sinks. A different approach to the problem is followed in my paper, which enables the performance (in the steady state condition) of many devices to be deduced from a knowledge of the boundary conditions only. In the cases of the inverted filter and the vertical cylindrical elutriator these conditions are particularly simple. There are *no* overhanging surfaces which can create dust shadows within the cloud. In consequence all possible tubes of flow by which dust particles can reach the surface of the paper must have their origin in the open dust cloud and so represent a real flow of particles on to the paper. The result for the collection efficiency of the devices follows at once from this. It is quite unnecessary to enquire into the detailed pattern of dust flow. However, it

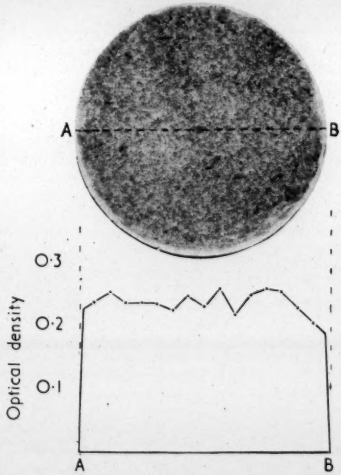

Showing uniform distribution of coal dust collected on an inverted paper filter

is easy to see qualitatively that the larger particles just reaching the filter will follow a trajectory which descends downwards close by the edge of the filter and then passes along the underside of the paper in a zone where the net upward velocity of

the particles is very small. The horizontal component of particle velocity directed towards the axis of the system arises from the horizontal velocity component of the air as it converges towards the filter. The trajectories are shown schematically in Fig. 1 of the paper. As pointed out in the paper, a consequence of these general principles is that dust will be deposited uniformly over the whole area of the filter if there is no appreciable rim to the filter holder. If there were a shadow zone under the filter as Dr. Davies suggests, this would result in a reduction in the number of particles collected in the central zone of the filter. The results of a practical experiment on these lines are given below.

A circle of filter paper was gummed to the rim of a 4 in. diameter glass funnel which was suspended in an inverted position in a chamber containing a cloud of coal dust and air was sucked through the filter at a rate of 3 litres/min. The accompanying figure is a photograph of the resulting dust deposit and with a plot of the optical density of the deposit across a diameter. It will be seen that the density is quite uniform as predicted.

GENERAL DISCUSSION ON SESSION A

Prof. F. R. Eirich: I would like to draw attention to what I feel to be missing in the range of methods of particle size analysis which is being discussed at this Conference. I refer to measurements of flow birefringence and to analyses of sedimentation velocities which, although less direct than most of the methods discussed, are of great help if the particles in question are either too small, or have such refractive index, that they are not readily visible.

It will be remembered that particles suspended in a liquid rotate in a velocity gradient. Asymmetric particles, in particular, rotate with periodic velocities and, as a consequence, exhibit preferred orientations of their long axes towards the streamlines. This tendency of hydrodynamic orientation is being counteracted by rotational Brownian movement, and there results a partial orientation which is a function of particle symmetry, particle size, and rate of shear and viscosity of the liquid (see, for instance, Edsall,[1] Sadron,[2] Cerf and Sheraga[3]). This particle orientation creates an optical anisotropy which is observable either as the occurrence of an optical axis in the streaming solution, that is of an extinction angle, or by measurement of birefringence as a function of the gradient.

Omitting here the discussion of the nature of the measurements, the data obtained permit the calculation of the rotary diffusion constant, provided the particle geometry can be approximated by rods, plates, random coils, elastic spheres or ellipsoids of revolution. It is further necessary that the particles be either small compared to the wavelength of light, say of the order of 0·1 μ or less, or that they are self-birefringent. Under these conditions one can derive from the calculated diffusion constant an effective volume, the axis ratio, and often the magnitude of the longest axis.

If the particles are rigid but spherical, or nearly so, no orientation and therefore no flow birefringence will occur. However, if the particle outlines are irregular or the particles show much Brownian movement, it may sometimes be of advantage to use visual observation to obtain the rotary diffusion constants rather than to count, or to try to measure particle dimensions. In such cases it should further be remembered that relative viscosities due to isodiametric particles, too, offer a means of determining an effective particle volume by way of Einstein's equation and counting particles. Furthermore, the same function of particle dimensions and resistance determines both rotatory diffusion and relative viscosity, and can be eliminated between these two quantities; in other words, the rotatory diffusion constant can be calculated from a knowledge of the extrapolated specific viscosity and of particle mass, or the latter from viscosity and diffusion.

The observation of flow birefringence, or even better of the extinction angle, provides also a means of ascertaining polydispersity where other methods may be difficult to apply. Again, the particles have either to be self-birefringent or to be smaller than the wavelength of light, and of course to be anisodiametric. Then, the more asymmetric particles will orient first, that is at lower gradients. As a consequence, the extinction angle will move from 45° (in the absence of orientation) towards smaller angles to the streamlines as the gradient is raised (the effect being proportional to a characteristic length of the particles to the cube), but the amount of birefringence will remain small. As the gradient is further increased, the orientation of the longer particles will tend towards saturation, whereas the orientation of the smaller particles begins to increase. Consequently, plots of extinction angles against gradient will exhibit peculiar minima and maxima if there are several distinct particle sizes, or will tend to run parallel to the ordinate of the gradient at extinction angles much larger than zero.

The theoretical analysis of such systems has been carried out by Sadron,[2] Wales,[4] Cerf and Sheraga,[3] Goldstein,[5] and others. Especially striking results have been obtained in the polymer field, and for larger particles during work on blood clotting, on gelatin gelation, on viscose ripening, and on tobacco mosaic virus degradation. The same method could probably be used to advantage in the case of many pigments, metal ores, silicates and other suspensions.

As for the widespread use of methods based on measurements of sedimentation velocities, simple and exact relations obtain only within the limits of the validity of Stokes' law. If the particles are non-spherical, charged, non-uniform in size, or if the suspension is not sufficiently dilute, quantitative conclusions are, as a rule, not possible.

Sedimentation methods, however, possess the great advantage of remaining applicable for very small and invisible particles. Furthermore, if the particles exhibit Brownian motion, combination of sedimentation velocity with translational diffusion can be used to eliminate the translational resistance function, just as viscosity and rotatory diffusion can be combined to eliminate the rotatory resistance function. The unknown factor of shape thus cancels, and particle volumes, effective axis ratios, and axes dimensions can be calculated.

Of the other complications, polydispersity and concentration effects are very relevant for the topics under discussion at this Conference. In this respect, I wish to draw attention to a recent development in centrifuge cell design by Hamington and Schachman[6] and their group which opens new possibilities in the field of ultracentrifugation and, beyond that, applies principles useful for all sedimentation methods. Schachman's cell permits the overlayering of a sedimenting suspension with another one of slightly smaller density or concentration, and thus to create artificial boundaries after the run has started. It therefore becomes possible to study the sedimentation velocities of given components in the

presence of well-defined concentrations of others. Reliable extrapolations to zero concentration, and with it determinations of true sedimentation constants, in mixtures therefore become possible for the first time. The method has so far been applied to suspensions of viruses and proved strikingly how elongated particles create much greater concentration effects than are due to more spherical particles at the same concentration.

The method of overlayering, of course, is not limited to centrifugation where it required special ingenuity to overcome the difficulties of forming boundaries during the run, but can be easily applied to stationary sedimentation in the gravity field. It is altogether surprising how little use has been made of arrangements where particles in suspension are allowed to fall into particle-free liquid, although this not only permits determination of uninterfered sedimentation rates but, because the particles can sort themselves out freely according to their velocities, gives excellent pictures of the particle size distribution. In order to avoid convection, the bottom layer has obviously to have a greater density than the thin layer of the suspension placed on top, but this is easily achieved by the addition to the lower layer of heavy miscible liquids like glycerine or mercury salts in the case of water, or of bromoform to organic liquids. The only precautions necessary are those to avoid flocculation or the development of electrical charges on the particles.

REFERENCES

(1) EDSALL. *Adv. Coll. Sci.*, **1**, p. 269 (1942).
(2) SADRON. *J. Phys. Radium*, **9**, p. 381 (1938).
(3) CERF and SHERAGA. *Chem. Rev.*, **51**, p. 185 (1952).
(4) WALES. *J. Phys. Coll. Chem.*, **52**, p. 976 (1948).
(5) GOLDSTEIN. *J. Chem. Phys.*, **20**, p. 677 (1952).
(6) HAMINGTON and SCHACHMAN. *J. Amer. Chem. Soc.*, **75**, p. 3533 (1953).

SESSION B. RELATIVE MOTION OF PARTICLES AND FLUIDS: MOLECULAR PHENOMENA

Chairman: Prof. R. M. Barrer, D.Sc., Sc.D., F.R.I.C., F.R.S.E.

Paper B.1

The measurement of surface area of finely divided solids by the flow of gases through them

By Prof. R. M. Barrer, D.Sc., Sc.D., F.R.I.C., F.R.S.E., The University, Aberdeen

An account is given of the theory and application of several procedures which have been used for determining the surface areas of finely divided solids, and which depend upon either the steady or the transient state of flow. Characteristic differences can arise between pore properties of microporous media determined by steady and by transient state methods which have at least in part received an explanation in terms of the heterogeneity of pore sizes and in the presence of some blind pores.

Attention has been directed to several additional possible procedures for measuring surface areas. These refer to flow systems in which a saturated immobile monolayer is formed at all points reached by the flowing gas. One of the latter methods covers the case where a mobile, dilute second layer forms on the immobile saturated first layer and where transport of sorbate may occur by combinations of one or more of Poiseuille, Knudsen and surface flow.

LIST OF SYMBOLS

A = internal area of 1 cm^3 of the porous bed in cm^2.
A_C = geometrical cross-section of the bed.
A_p = cross-sectional area of a pore or capillary.
A_1 = internal area of all the capillaries traversing unit cross-section of the bed.
α, β, E_0 and F_0 = constants in Adzumi's equation.
b, h = breadth and height respectively of a rectangular capillary.
C, C^0 and C^l = concentrations in molecules per cm^3 of the gas phase respectively at any point within, and at ingoing and outgoing faces of the porous medium.
C_s' and C_{s2}' = concentrations in molecules per cm^2 of the surface in first and second adsorbed layer respectively.
d = diameter of a capillary.
δ = a coefficient dependent on slip and so on the ratio d/λ.
D = diffusion coefficient of a non-sorbed gas in the capillaries of a porous medium = $k_2^2 l^2/6L$.
$D' = D/k_2^2 = l^2/6L$.
D_2 = diffusion coefficient in the capillaries of a porous medium modified by adsorption and surface diffusion.
D_s, D_{s2} = surface diffusion coefficients in first and second adsorbed layers respectively.
D_p = coefficient in Poiseuille flow defined by

$$\frac{\partial C}{\partial t} = D_p \frac{\partial^2 C^2}{\partial x^2}$$

ϵ = porosity in cm^3 per cm^3 of porous medium.
f = fractional number of molecules striking a surface that are reflected at random.
k_2 = tortuosity.
k_0, k_1 = capillary shape factors for Poiseuille and Knudsen flow respectively.
k_s, k_{s2} = Henry's law adsorption constants in first and second adsorbed layers respectively.
K = permeability.
K_k = Knudsen permeability.
L = time lag for a non-sorbed gas diffusing through a porous medium.
L_2 = time lag modified by adsorption and surface diffusion.
l = length of porous medium.
λ = mean free path of gas in the gas phase.
N = number of capillaries traversing unit cross-section of a porous medium.
M = molecular weight of a gas.
P_g, P_s = permeation rates in the gas phase and on the surface respectively.
$P_T = P_g + P_s$ = total permeation rate.
$p = \frac{1}{2}(p_1 + p_2)$ = the mean pressure across the porous medium, p_1 and p_2 being respectively the pressures at the ingoing and outgoing surfaces of the porous medium.
η = viscosity coefficient.
r = radius of a cylindrical capillary.
r_h = hydraulic radius = $\dfrac{\text{area of cross-section of pore}}{\text{perimeter of pore}}$ = $\dfrac{\epsilon}{A}$ for the porous medium.
R = the gas constant.
T = the absolute temperature.

The steady state of flow of gases and liquids in microporous media has for some time been a means of determining their surface area, whether they are composed of unconsolidated or of consolidated masses of particles (e.g. Arnell,[1] Rigden,[2] Adzumi,[3] Carman,[4] Barrer and Grove,[5] Kraus, Ross and Girifalco[6]). For swarms of unconsolidated particles, if the mass of the bed and density of the material of the particles is known, an estimate of mean particle size may be made, provided a reliable measure of surface area is obtained. More recently the transient state of flow embodied in the time-lag method suggested by Barrer[7] has been used to determine surface areas by Barrer and Grove,[8] and by Kraus and Ross.[9] These methods can be tested and compared by making use of adsorption procedures such as those of Brunauer,[10] of Huttig,[11] of Harkins and Jura,[12] or of Barrer, Mackenzie and MacLeod,[13] in which adsorption isotherms are obtained for gases such as nitrogen or argon

at 90° or 78° K, and interpreted in terms of isotherms based on various theoretical isotherm models to give the "saturated monolayer" value for the surface.

This paper will be concerned with flow methods of determining surface areas, and with some relevant fundamental information concerning gas flow which has been obtained using single capillaries.

SOME EQUATIONS OF FLOW IN CAPILLARIES AND MICROPOROUS MEDIA

A microporous mass may offer a complex system of pores of varied dimensions, shapes and tortuosities, some "blind" and some continuous through the medium. It is usual to consider the actual medium in terms of a model pore system. Following, among others, the work of Knudsen,[14] Smoluchowski,[15] Warburg,[16] Gaede,[17] Klose[18] and Clausing[19] on flow in single capillaries the actual medium is sometimes replaced by a model of the same porosity and permeability having cylindrical capillaries in parallel all of the same radius and of length $k_2 l$ running from the ingoing to the outgoing surface. The constant k_2 is designated the tortuosity, and is the ratio of the actual length of the kinked capillaries to the geometrical length of the porous bed. Limitations of this very simple model are inevitable and several of these will be referred to later. Other model pore systems have been considered by Adzumi[3] (capillaries of various diameters in series and groups of such composite capillaries in parallel) and by Flood, Tomlinson and Leger[20] (cubic cells joined into a network by narrower rectangular connecting pores).

(*a*) *Molecular streaming.* Transport of gas in a capillary may occur by various mechanisms: molecular streaming (Knudsen flow); streamline (or Poiseuille) flow, with slip; turbulent flow; and orifice flow. At the lowest pressures when the mean free path λ is much greater than the capillary diameter d and λ is much greater than half the capillary length l (Pollard and Present,[21]) the flow becomes pure molecular streaming which obeys Fick's law, e.g.

$$\frac{\partial c}{\partial t} = \frac{D\partial^2 c}{\partial x^2} \tag{1}$$

In equation (1), C denotes the concentration of streaming gas at the point x and the time t and D is the diffusion coefficient. Knudsen[14] gave for D in a cylindrical tube of radius r

$$D = \frac{4r}{3}\left(\frac{2RT}{\pi M}\right)^{\frac{1}{2}} \cdot \frac{(2-f)}{f} = \frac{8r_h}{3}\left(\frac{2RT}{\pi M}\right)^{\frac{1}{2}} \cdot \frac{(2-f)}{f} \tag{2}$$

Pollard and Present[21] have outlined a derivation of equation (2) in which the numerical constant is altered to give:

$$D = \frac{\pi r}{2}\left(\frac{2RT}{\pi M}\right)^{\frac{1}{2}} \cdot \frac{(2-f)}{f} = \pi r_h\left(\frac{2RT}{\pi M}\right)^{\frac{1}{2}} \cdot \frac{(2-f)}{f} \tag{3}$$

These authors have also offered an explanation of the minima which have been observed when the permeability K is plotted against the mean pressure p. An extreme instance of flow showing a minimum in K is given in Fig. 1 due to Carman[22] based on data of Gaede[17] for flow of hydrogen between parallel plates. As the pressure increases there is an increasing number of gas phase collisions among molecules directed more or less along the direction of flow, because although λ is much greater than d, it is still less than $\frac{1}{2}l$. One is in fact no longer concerned only with molecule-wall collisions as in pure Knudsen flow, and the permeability is diminished accordingly. When λ is much greater than $\frac{1}{2}l$ on the other hand permeability increases to a limit corresponding to molecule-wall collisions only, but this limit is lower for small than for large values of l. The capillaries in a porous bed correspond to a kinked tube in which no straight part can be much longer than its diameter d, and so in porous media there is no significant increase in K at very low pressures. Rather the relation between K and p tends to be linear or nearly linear until $p = 0$, as is observed experimentally.

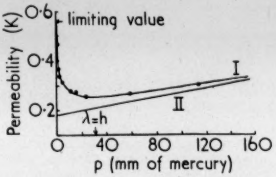

Fig. 1. Transition region for a slit, using Gaede's data[17] (after Carman[22]). Curve I, observed data; Curve II, extrapolation from high pressure

(*b*) *Streamline flow.* The effect discussed by Pollard and Present[21] depends on the relative magnitudes of λ and l rather than on those of λ and d, provided only that λ is much greater than d. However, as λ approaches and eventually becomes much less than d, molecular streaming becomes increasingly replaced by streamline flow with slip. One now has for the permeability K of a single capillary of length l and cross-section πr^2:

$$\frac{Kl}{\pi r^2} = \frac{r^2 p}{8\eta} + \frac{\pi r}{4}\left(\frac{2RT}{\pi M}\right)^{\frac{1}{2}} \cdot \frac{(2-f)}{f} \tag{4}$$

The last term in equation (4) represents the contribution of slip-flow to the transport, as derived by Millikan.[23] It differs from equation (2) or (3) only in that the numerical term 4/3 [equation (2)] or $\pi/2$ [equation (3)] is replaced by $\pi/4$. It is clear that as the pressure falls slip-flow and streamline flow must be replaced eventually by molecular streaming, so that equation (4) can be re-written as:

$$\frac{Kl}{\pi r^2} = \frac{r^2 p}{8\eta} + \frac{4r}{3}\delta\left(\frac{2RT}{\pi M}\right)^{\frac{1}{2}} \tag{5}$$

where δ is a coefficient which must change with pressure according to the ratio d/λ. The precise correlation between δ and pressure is not clear; but on the basis of equations (2) and (4) δ must approach the two limits:

$$\left.\begin{aligned} \delta = \delta_0 &= \frac{2-f_0}{f_0} \quad \text{for } d \ll \lambda \\ \delta = \delta_1 &= \frac{3\pi}{16}\frac{(2-f_1)}{f_1} \text{ for } d \gg \lambda \end{aligned}\right\} \tag{6}$$

On the other hand if we adopt equations (3) and (4) as a basis so that the coefficient 4/3 in equation (5) is replaced by $\pi/2$ the two limits are

$$\left.\begin{aligned} \delta = \delta_0 &= \frac{2-f_0}{f_0} \text{ for } d \ll \lambda \\ \delta = \delta_1 &= \frac{2-f_1}{2f_1} \text{ for } d \gg \lambda \end{aligned}\right\} \tag{7}$$

In molecular streaming $f_0 \simeq 1$, according to Knudsen and later workers, and so $\delta_0 \simeq 1$. Thus, if $f_1 \simeq 1$, δ_1 should take values of 0·59 or 0·50 according to equations (6) and (7) respectively. However, δ_1 is usually above either of these values, so that f_1 would require to be less than unity. Three

kinds of experiment have been used to determine δ_1 and f_1: flow of gases through tubes for δ_1 (cf. Adzumi's papers[3]), and the fall of droplets through gases or the use of concentric cylinder viscometers for f_1 (cf. Millikan's paper,[23] and Blankenstein's[24]).

The values of δ_1 for different gases and tubes of various kinds ranged between 0·73 and 0·90; the values of f_1 similarly ranged between 1·0 and 0·79 (cf. Carman,[22] Table 1).

Equation (5) can be generalized for a capillary of any cross-sectional shape by introducing shape factors k_0 and k_1 and replacing r by the hydraulic radius r_h. Then

$$\frac{Kl}{A_p} = r_h^2 \frac{p}{\eta k_0} + \frac{8 r_h}{3} \frac{\delta}{k_1} \left(\frac{2RT}{\pi M}\right)^{\frac{1}{2}} \tag{8}$$

These shape factors have been considered among others by Smoluchowski,[15] and some derived for infinitely long capillaries are summarized in Table 1 (after Carman[22]).

Table 1. *Values of k_0 and k_1 in equation (8) for capillaries of infinite length*

Shape of cross-section	k_0	k_1
Circle	2·00	1·00
Square	1·78	0·90
Rectangle: breadth = 2 × height	1·94	0·87
breadth = 5 × height	2·38	0·78
breadth = 10 × height	2·65	0·68
Parallel plates	3·00	(0)

One may take as an example of the use of equation (8) the flow of gas between parallel plates having breadth b much greater than height h. Equation (8) then reduces to

$$K = \frac{bh^3 p}{4k_0 \eta l} + \frac{4bh^2}{3l} \cdot \frac{\delta}{k_1} \left(\frac{2RT}{\pi M}\right)^{\frac{1}{2}} \tag{9}$$

Carman's analysis[22] of Gaede's data[17] for flow of hydrogen between parallel plates gave $\delta = 0{\cdot}66$ and $k_1 = 0{\cdot}49$. Table 1 gives $k_1 = 0$, but this is for an infinitely long slit of infinite breadth. When b is much greater than l, which is much greater than h, Clausing[19] calculated that $k_1 = \frac{8}{3} \frac{1}{\ln(l/h)}$, which for Gaede's slit capillary gave $k_1 = 0{\cdot}44$, quite close to the value obtained by Carman.

(*c*) *Equations of flow in microporous media.* The foregoing summary of observations, made primarily for single capillaries, indicates a way to approach flow in actual porous media. Using the symbols at the head of this paper we may set $\epsilon = A_1 k_2$. Accordingly $\frac{Kk_2^2 l}{\epsilon}$ will replace $\frac{Kl}{A_1}$ in equation (8) while the hydraulic radius may similarly be replaced by the ratio ϵ/A, so that for the set of tortuous capillaries traversing the porous medium we now obtain

$$K = \frac{1}{k_2^2 k_0} \cdot \frac{\epsilon^3 p}{A^2 \eta l} + \left(\frac{8\delta}{3k_1 k_2^2}\right) \frac{\epsilon^2}{Al} \left(\frac{2RT}{\pi M}\right)^{\frac{1}{2}} \tag{10}$$

The quantity $(k_2^2 k_0)$ has been found for a number of substances to be near to the value 5·0 (the Kozeny constant); while for d much greater than λ we may take δ and $k_1 \simeq 1$. For larger pressures δ has a lower limit of 0·59 [equation (2)] to 0·50 [equation (3)] but is usually about 0·9. The quotient $\delta/k_1 k_2^2$ fell in the range 0·4 to 0·6 for a number of porous media according to Carman and Arnell.[25] Nevertheless the tortuosity factor (*q.v.*) may vary within wide limits, so that too rigid a choice of the constants in equation (10) could lead to erroneous values of A.

An earlier modification of equation (10) is based on the cylindrical capillary model. In this version

$$K = \frac{\alpha_1 r^4 p}{l} + \frac{\delta \beta_1 r^3}{l} \tag{11}$$

where $\alpha_1 = \frac{\pi}{8\eta}$ and $\beta_1 = \frac{3\pi}{4} \left(\frac{\pi RT}{2M}\right)^{\frac{1}{2}}$ are constants. r^4 and r^3 in equation (11) must be weighted averages for the set of uniform parallel cylindrical capillaries having the same permeability as the actual porous medium. According to equations (10) and (11), K should be a linear function of p, the mean pressure, a behaviour which has been well established by experiment. Sometimes a flattening is observed in the curve of K against p for very small pressures, but this is seldom a major effect for the reasons given by Pollard and Present.[21] This is an important point in the use of equations (10) and (11) for the determination of surface areas.

SURFACE AREA DETERMINATIONS FROM STEADY STATE FLOW DATA

Adzumi[3] (p. 304) considered unit cube of the porous medium, and wrote equation (11) in the form

$$K = \alpha_1 E_0 p + \delta \beta_1 F_0 \tag{12}$$

Here $E_0 = Nr^4$; $F_0 = Nr^3$. The slope of K against p then gives $\alpha_1 E_0$ and the intercept is $\delta \beta_1 F_0$. The values of α_1 and $\delta \beta_1$ may be derived from independent data (assuming that $f = 1$ in the expression for $\delta \beta_1$). Accordingly, E_0 and F_0 are obtained and then $N = F_0^4/E_0^3$ and $r = E_0/F_0$. In this evaluation of N, the number of capillaries traversing unit area, and of r, the radius of each of these capillaries, Adzumi[3] was assuming the uniform cylindrical capillary model.

Some of the results obtained by Barrer and Grove,[5] when applying the Adzumi method to study the pore properties of beds of small spheroidal analcite crystals, are given in Table 2. Once N and r are obtained the porosity ϵ in cm^3/cm^3 and the value of A in cm^2/cm^3 are in terms of the model given by $\epsilon = N\pi r^2 k_2$; $A = 2N\pi r k_2$. The value taken for k_2 by Barrer and Grove was $\sqrt{2}$. Results obtained by the Adzumi procedure using sorbable vapours of carbon tetrachloride, sulphur dioxide and ammonia were poorly consistent with those obtained for gases, especially as regards N.

Table 2. *Pore properties by Adzumi's method*

Gas	$\alpha_1 \times 10^{-3}$	$\delta\beta_1 \times 10^{-4}$	$E_0 \times 10^{-8}$	$F_0 \times 10^3$	$r \times 10^4$ *(cm)*	$N \times 10^{-5}$
Helium	1·95	23·2	4·77	4·95	9·64	0·55
Neon	1·25	10·4	3·53	5·79	6·08	2·56
Argon	1·74	7·34	3·56	5·04	7·09	1·42
Krypton	1·56	5·07	3·72	5·74	6·49	2·10
Hydrogen	4·29	32·7	3·38	4·77	7·10	1·33
Nitrogen	2·20	8·78	3·18	5·29	6·02	2·43
Oxygen	1·91	8·23	2·94	5·41	5·43	3·38

It has been pointed out by Flood, Tomlinson and Leger[26] that r^4, r^3 and r are averages for which it is not generally true that $\frac{\bar{r}^4}{\bar{r}^3} = \bar{r}$. The average $\bar{r}^n = \frac{1}{N} \cdot \int_0^\infty r^n f(r) dr$, where dN the number of capillaries having radii between r and $r + dr$ is given by $dN = f(r)dr$.

Equation (10) has been used by Carman and Arnell[25] in various measurements of A, with $k_2^2 k_0 \simeq 5{\cdot}0$ and $8\delta/(3k_1 k_2^2) \simeq 4/3$ as already discussed. When K is plotted against p, the

ratio of slope to intercept of the line serves to give ϵ/A and thence A. It should be noted that the tortuosity occurs in both adjustable constants $1/k_2^2k_0$ and $\delta/k_2^2k_1$, so that the *ratio* of slope and intercept may not be affected appreciably by tortuosities varying substantially from one medium to another.

Another method of using Arnell's equation to obtain A has been employed by Kraus, Ross and Girifalco.[6] They considered the Poiseuille and the slip-flow terms of equation (10) separately. However, they gave to the latter term the value $\frac{24\epsilon^2}{13A}\left(\frac{2RT}{\pi M}\right)^{\frac{1}{2}}$, the choice of the numerical constant being based upon a treatment by Derjaguin.[27] They concluded that surface areas derived from the slip-flow term exceeded those obtained from the Poiseuille term (Table 3). The "slip-flow" areas did indeed approach closely the areas determined by the gas adsorption methods of BET and of Harkins and Jura.

Table 3. *Surface areas based on Poiseuille and slip-flow terms of equation* (10)

				Area in $m2g^{-1}$	
Powder	*Gas*	*Poiseuille flow*	*Slip flow*	*BET method* (N_2)	*Harkins Jura method* (N_2)
Cupric oxide	Hydrogen	0·073	0·17	0·30	0·31
	Helium	0·067	0·19		
Glass spheres IV	Hydrogen	0·17	0·29	0·37	0·38
	Helium	0·17	0·28		
Lead chromate	Hydrogen	2·1	3·73	3·75	4·01
	Helium	1·9	3·63		
Barium sulphate	Hydrogen	1·9	4·46	4·68	4·97
	Helium	1·9	4·04		
Titanium oxide	Hydrogen	6·0	8·37	7·97	8·26
	Helium	4·8	8·02		

Steady state flow methods of measuring A should not take count of blind pores and cracks and fine scale roughnesses of the surface in the way in which adsorption data must. The steady state procedures would therefore be expected to give areas which are less than those evaluated by adsorption. Agreement between "slip-flow" and adsorption areas may then reflect only the choice of too high a numerical constant, 24/13, in the slip-flow term. Indeed, with $\delta/k_1k_2^2 \simeq 0{\cdot}5$ as found by Carman and Arnell[25] the numerical factor of equation (10) becomes 4/3, and would bring Poiseuille and slip-flow areas about as closely in agreement as slip-flow and adsorption areas. Because of variable tortuosity among different porous media there must always be uncertainty over the separate numerical factors of equation (10). Their *ratios* however may, as already pointed out, remain more nearly constant for different media, so that the original method of deriving surface areas from equation (10) seems preferable to that of Kraus, Ross and Girifalco.[6]

THE TIME LAG METHOD OF STUDYING PORE PROPERTIES

Transient flow at first sight may seem to be more complicated to study and interpret than steady state flow. However, the time-lag procedure, while involving the transient state, requires only measurements as simple and as accurate as those of the steady state. The porous medium is bounded by planes at $x = 0$ and $x = l$, and flow begins at $t = 0$ in the x-direction. For a while little or no gas appears on the outgoing side of the membrane but then the rate of efflux builds up to its steady state value. If p_1 and p_2 are the pressures on ingoing and outgoing sides respectively, then provided p_1 is much greater than p_2 for the duration of the experiment, the curve of p_2 against time has the form shown in Fig. 2. Extrapolating the linear part of the curve back to cut the axis of t gives an intercept L, the "time-lag" of Barrer.[7] Then this intercept is given by

$$L = l^2/6D' = k_2^2l^2/6D \qquad (13)$$

where $D' = D/k^2$, and D is the diffusion coefficient of the gas in the porous medium appropriate to the cylindrical capillary model, while D' refers to the actual medium, k_2 is as before the tortuosity. It is assumed in deriving L that

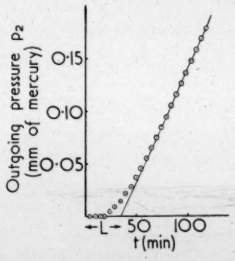

Fig. 2. Showing the time-lag L and steady flow of sulphur dioxide at 5° C, through a bed of unconsolidated analcite spheroids. Ingoing pressure $p_1 = 3{\cdot}74$ mm of mercury (after Barrer and Grove[5])

flow occurs by molecular streaming and that there is no adsorption of the flowing gas. This may easily be realized by a suitable choice of p_1 and of gas. D is, according to Knudsen's treatment, given by equation (2), and r may then be calculated. As with Adzumi's procedure one then has

$$\epsilon = N\pi r^2k_2; \quad A = 2N\pi rk_2$$

and the relation for the known porosity ϵ serves to give N while the second relation then gives A.

The foregoing procedure involves a knowledge of the tortuosity factor k_2. Wyllie and Rose[28] have suggested that k_2 may be derived from the ratio R between the specific conductivity of a porous medium saturated with a conducting liquid to the specific conductivity of the fluid itself. Provided no appreciable surface conductivity arises, or conduction by the material of the medium, they consider that $R = \epsilon/k_2$.* Wyllie and Rose obtained values of k_2 between 3·53 and 1·65 for various media, the majority giving values around 2·5. Hitchcock and also Carman have suggested for a bed of spheres a somewhat smaller value for k_2. Following Carman a value of $\sqrt{2}$ was used by Barrer and Grove[8] in their study of flow through beds of very small spheroidal crystals of analcite. In a study of porous glass, by determining r from sorption data and D by flow of helium and neon, Barrer and Barrie[29] were able to combine equations (13) and (2) to give k_2. They obtained 2·56 (helium) and 2·51 (neon). On the other hand much smaller values of k_2 have recently been found for compressed Carbolac carbon plugs by Barrer and Strachan (unpublished result).

* In the writer's opinion R may be more complex than this.

SURFACE AREAS BY THE TIME LAG METHOD

Barrer and Grove[8] determined the pore properties (r and N) and surface areas of beds of analcite spheroids by the methods of Adzumi [equation (11)] and Arnell [equation (10)] and by the time-lag procedure. The values obtained for r are notably smaller by the time-lag method (Table 3) than are these same values obtained by Adzumi's procedure (cf. Tables 2 and 4). The near constancy of $D\sqrt{M}$ in column 4 may be taken as showing the absence of adsorption effects (*q.v.*) for the several gases at 25° C. The surface area by the time-lag method was 7100 cm^2/cm^3 of the porous medium, while the Adzumi and Arnell procedures gave respectively 1500 and 1260 cm^2/cm^3. The difference is at least in part related to the limitations of the uniform capillary model.

Table 4. *Transient flow in analcite beds at 25° C*

Gas	*Time-lag, L, in min**	*D† cm^2 sec^{-1}*	*$D\sqrt{M}$*	*$r \times 10^4$ cm*
Helium	4·9	10·9	21·8	1·30
Neon	9·8	5·46	24·5	1·46
Argon	14·7	3·64	23·0	1·37
Krypton	21·7	2·46	22·6	1·34
Hydrogen	3·0	17·7	25·2	1·51
Nitrogen	11·0	4·84	25·6	1·53
Oxygen	12·5	4·26	24·2	1·44

* Length of column was 98 cm.
† Tortuosity factor k_2 assumed $= \sqrt{2}$.

Thus during the time-lag period and so before the steady state of flow is established the flowing gas must penetrate into every part of the pore structure. Once the steady state has been established, pockets, crevices and cul-de-sac pores will contribute little to the rate of flow. Accordingly the surface area derived from the steady state experiments will be too small by a factor depending on the relative surface areas of the blind pores and of pores which transmit gas right through the medium. Moreover, in the steady state, the gas will be transmitted in the main through what may be a relatively small number of pores of the largest dimensions, and the results of measurements of r will be weighted accordingly. For true surface area measurements by flow the time-lag method seems preferable to those depending on the steady state of flow.

Kraus and Ross[9] made use of the relations $D' = \frac{l^2}{6L}$ and $D' = \frac{24}{13}\frac{\epsilon}{A}\left(\frac{2RT}{\pi M}\right)^{\frac{1}{2}}$ to measure A by the time-lag procedure. They here follow Derjaguin[27] in replacing the factor 8/3 of equation (4) by 24/13. The areas obtained for several porous beds are then given below (Table 5), and the agreement between areas based on the time-lag method and those derived by adsorption measurements (in columns 4 and 5) is good. At the same time it must be remembered that there is some latitude in the choice of the numerical constant.

Table 5. *Areas of porous media by transient Knudsen flow*

Medium	*Gas*	*Area in m^2/g: Transient Knudsen flow*	*BET (N_2)*	*Harkins Jura (N_2)*
Cupric oxide	Helium	0·37	0·30	0·31
	Nitrogen	0·31		
Glass	Helium	0·64	0·55	0·59
Spheres II	Nitrogen	0·55		
Lead chromate	Helium	4·60	3·75	4·01
	Nitrogen	3·89		
Barium sulphate	Helium	5·45	4·68	4·97
	Nitrogen	4·75		
Titanium oxide	Helium	8·85	7·97	8·26
	Nitrogen	7·90		

BASIS OF FURTHER METHODS OF MEASURING SURFACE AREAS BY FLOW

Two limiting cases of gas flow with simultaneous adsorption may be dealt with relatively easily. In the first, molecules are adsorbed according to Henry's law (Barrer and Grove[8]); in the second, an immobile saturated monolayer of adsorbed gas is laid down at all points reached by the diffusing gas. This condition is represented graphically in Fig. 3(*a*). The gas diffuses into a porous substance by molecular streaming. Using the symbols given at the head of this paper, ϵC is the amount of gas in the gas phase per unit volume of the porous medium at the point x. Similarly, AC'_s is the amount of adsorbed gas per cm^3 of the porous medium at x.

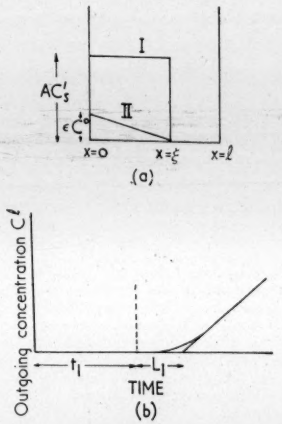

Fig. 3. Limiting cases of gas flow with simultaneous adsorption

(*a*) At point x and as a function of x Curve I shows amount adsorbed per cm^3 of medium and Curve II the amount in gas phase per cm^3 of medium.
(*b*) Concentration C^l at outgoing surface of bed, as a function of time. The break-through time t_1 and additional time-lag L are indicated.

Ignoring the tortuosity factor for the moment, the equation of flow is $D\partial^2 C/\partial x^2 = \partial C/\partial t$, which is to be solved for the boundary conditions

AC'_s is constant for $0 < x < \xi$.
$C = C^0$ at $x = l$ for all values of t.
$C = 0$ for $0 < x < l$ at $t = 0$.
$C = 0$ at $x = \xi$ for $0 < x < l$ and corresponding time.

The equation of flow is satisfied by

$$C = C^0\left[1 - A \operatorname{erf} \frac{x}{2\sqrt{(Dt)}}\right] \qquad (14)$$

This relation in which A is a constant, satisfies the boundary conditions for $x = \xi$ if $A \operatorname{erf} Z = 1$ at $x = \xi$ where $Z = \frac{\xi}{2\sqrt{(Dt)}}$. Accordingly, $Z = \frac{\xi}{2\sqrt{(Dt)}}$ is itself constant, and the required solution for C is

$$C = C^0\left[1 - \frac{\operatorname{erf}\frac{x}{2\sqrt{(Dt)}}}{\operatorname{erf} Z}\right] \tag{15}$$

We next find the flux at $x = \xi$ per unit cross-sectional area of the bed. This is

$$\frac{\alpha}{\sqrt{t}} = \frac{\epsilon C^0 D}{\sqrt{(\pi D)} \operatorname{erf} Z \exp Z^2}\frac{1}{\sqrt{t}} \tag{16}$$

At the boundary $x = \xi$ conservation of mass gives

$$\frac{\alpha}{\sqrt{t}} = AC'_s\frac{d\xi}{dt}; \quad \text{or} \quad \frac{2\alpha\sqrt{t}}{AC'_s} = \xi \tag{17}$$

Since however $\xi = 2Z\sqrt{(Dt)}$ we may rearrange the above relation to give

$$Z \operatorname{erf} Z \exp Z^2 = \frac{\epsilon C^0}{AC'_s\sqrt{\pi}} \tag{18}$$

At the break through time $t = t_1$ we know that $\xi = l$ (or $k_2 l$ if one introduces the tortuosity factor). Accordingly

$$Z^2 = \frac{k_2^2 l^2}{4Dt_1}$$

Now according to equation (13) ($L = k_2^2 l^2/6D$) we may eliminate the tortuosity factor and D and obtain

$$Z^2 = 3L/2t_1 \tag{19}$$

At the break-through time the distribution of gas in the gas phase is given by equation (15) with $x = l$. Thereafter, the problem is one of pure volume diffusion uncomplicated by adsorption, with the above initial distribution. Barrer (unpublished work) obtained an expression for the additional time lag L_1, as defined in Fig. 3(*b*), before the steady state of efflux from the medium is finally obtained. The total time-lag L_T is then given by

$$L_T = t_1 + L_1 \tag{20}$$

The expression for L_1 is rather complicated. However it was found that when ϵC^0 was much less than AC'_s then L_1 was much less than t_1, and so L_T approximately equals t_1. Accordingly the measured time-lag L_T gives t_1 to a sufficient degree of accuracy. L, the time-lag of equation (13), may be obtained from the measured time-lag of a non-sorbed gas such as neon since $L = L_{Ne}\sqrt{\left(\frac{M}{M_{Ne}}\right)}$. Hence Z is found. Next, equation (18) is used to assess $\frac{\epsilon C^0}{AC'_s\sqrt{\pi}}$. C'_s can be obtained from the known dimensions of a molecule, assuming at saturation a close-packed monolayer in the way familiar in adsorption measurements of A. Since ϵ and C^0 are also readily obtained, the value of A follows.

The procedure above may also be further simplified for L_1 is much less than t_1, because in this case the steady-state distribution in the gas phase is nearly maintained, so that equation (15) can be replaced without serious error by

$$C = C^0\left(1 - \frac{x}{\xi}\right) \tag{15a}$$

Correspondingly, equation (19) is replaced by

$$\frac{D}{\xi} = \frac{AC'_s}{\epsilon C^0}\frac{d\xi}{dt} \tag{17a}$$

whence the break-through time t_1 becomes

$$t_1 = \frac{AC'_s}{\epsilon C^0}\cdot\frac{k_2^2 l^2}{2D} \tag{21}$$

and

$$\frac{t_1}{L} = \frac{3AC'_s}{\epsilon C^0} \tag{22}$$

Barrer and Barrie (unpublished work) made a preliminary study of the above break-through method of measuring surface areas, using sulphur dioxide flowing through Vycor porous glass. They found, however, that the adsorption isotherms of sulphur dioxide were hardly rectangular enough in the range investigated and also that this sorbate showed surface diffusion in porous glass. They concluded that the experimental conditions required for the method would be best achieved for chemisorbed layers; or in some charcoal-organic sorbate systems where with suitable carbons very rectangular isotherms occur (such as in McBain,[30] Figs. 44, 45, 46, 47). Attention may still, however, need to be paid to surface diffusion.

The problem of surface diffusion may be approached by considering the adsorbed film to comprise an immobile saturated monolayer with a weakly-adsorbed mobile second layer in which the adsorbate concentration C'_{s2} is proportional to the gas phase concentration. The diffusion coefficient in this layer is then D_{s2}. One now finds that equation (15) becomes

$$C = C^0\left[1 - \frac{\operatorname{erf}\frac{x}{2\sqrt{(D'_1 t)}}}{\operatorname{erf}\frac{\xi}{2\sqrt{(D'_1 t)}}}\right] \tag{15b}$$

and that $Z = \frac{\xi}{2\sqrt{(D'_1 t)}}$, where $D'_1 = \frac{D\left(1 + \frac{D_{s2}Ak_{s2}}{D\epsilon}\right)}{1 + \frac{A}{\epsilon}k_{s2}}$

In the expression for D'_1, k_{s2} is the Henry's law constant ($k_{s2} = C'_{s2}/C$).

Similarly equation (18) becomes

$$Z \operatorname{erf} Z \exp Z^2 = \frac{\epsilon C^0\left(1 + \frac{A}{\epsilon}\cdot k_{s2}\right)}{AC'_s\sqrt{\pi}} \tag{18a}$$

with $Z^2 = \frac{k_2^2 l^2}{4D'_1 t_1}$ if we again introduce the tortuosity k_2. Now provided

$$\epsilon C^0\left(1 + \frac{A}{\epsilon}k_{s2}\right) \ll AC'_s$$

the steady state in the mobile adsorbed film and in the gas phase is approximated, and the simplified procedure then gives the relation, corresponding to equation (22),

$$\frac{t_1}{L} = \frac{3AC'_s}{\epsilon C^0\left(1 + \frac{D_{s2}Ak_{s2}}{D\epsilon}\right)} \tag{22a}$$

Finally, one may give the break-through time assuming combined Poiseuille and Knudsen flow in the gas phase together with a mobile weakly-adsorbed second layer, and a

saturated immobile monolayer. It is assumed that the quantity $\epsilon C^0(1 + Ak_{s2}/\epsilon)$ is much less than AC'_s so that the steady state is nearly maintained in the gas phase and in the mobile second layer. Then for the break-through time t_1 one finds

$$\frac{t_1}{L} = \frac{3AC'_s}{\epsilon C^0}\left(1 + \frac{D_p 4\pi\epsilon^2 C^0}{DA^2} + \frac{D_{s2}Ak_{s2}}{D\epsilon}\right)^{-1} \qquad (22b)$$

where D_p is defined by the differential equation for Poiseuille flow $D_p \frac{\partial^2 c^2}{\partial x^2} = \frac{\partial c}{\partial t}$. The constant, 4π, depends upon the cylindrical capillary pore model; other factors would be required for other forms of capillary.

A further observation may be made regarding equations (22), (22*a*) and (22*b*). The denominator of the right-hand side of each of these equations is $P_T \times (k_2^2 l)/D$ where P_T is as before the total steady state flux, per unit of cross-section of the medium. It follows that each of these equations may be rearranged to give

$$2P_T t_1 = lAC'_s \qquad (23)$$

from which A can in principle easily be derived. No test of the relationship (23) exists as yet.

REFERENCES

(1) ARNELL, J. C. *Canad. J. Res. A*, **24**, p. 103 (1946); *A*, **25**, p. 191 (1947); *A*, **26**, p. 29 (1948).
(2) RIGDEN, P. J. *J. Soc. Chem. Ind.* [*London*], **62**, p. 1 (1943); **66**, p. 130 (1947).
(3) ADZUMI, H. *Bull. Chem. Soc. Japan*, **12**, pp. 292, 304 (1937); **14**, p. 343 (1939).
(4) CARMAN, P. C. *Trans Instn Chem. Engrs*, **15**, p. 150 (1937). *J. Soc. Chem. Ind.* [*London*], **57**, p. 225 (1938); **58**, p. 1 (1939). *Disc. Faraday Soc.*, No. 3, p. 72 (1948).
(5) BARRER, R. M., and GROVE, D. M. *Trans Faraday Soc.*, **47**, p. 826 (1951).
(6) KRAUS, G., ROSS, J. W., and GIRIFALCO, L. A. *J. Phys. Chem.*, **57**, p. 330 (1953).
(7) BARRER, R. M. *Disc. Faraday Soc.*, No. 3, p. 61 (1948).
(8) BARRER, R. M., and GROVE, D. M. *Trans Faraday Soc.*, **47**, p. 837 (1951).
(9) KRAUS, G., and ROSS, J. W. *J. Phys. Chem.*, **57**, p. 334 (1953).
(10) BRUNAUER, S. *Physical Adsorption of Gases and Vapours*, ch. 6 (London: Oxford University Press, 1944).
(11) HUTTIG, G. *Monatsh. Math.*, **78**, p. 77 (1948).
(12) HARKINS, W. D., and JURA, G. *J. Chem. Phys.*, **12**, p. 112 (1944).
(13) BARRER, R. M., MACKENZIE, N., and MACLEOD, D. *J. Chem. Soc.*, p. 1736 (1952).
(14) KNUDSEN, M. *Ann. Phys.* [*Leipzig*], **28**, p. 73 (1909).
(15) SMOLUCHOWSKI, VON M. *Ann. Phys.* [*Leipzig*], **35**, p. 983 (1911).
(16) WARBURG, G. *Ann. Phys.* [*Leipzig*], **159**, p. 399 (1876).
(17) GAEDE, W. *Ann. Phys.* [*Leipzig*], **41**, p. 289 (1913).
(18) KLOSE, W. *Ann. Phys.* [*Leipzig*], **11**, p. 73 (1931).
(19) CLAUSING, P. *Physica*, **9**, p. 65 (1929).
(20) FLOOD, E. A., TOMLINSON, R. H., and LEGER, A. E. *Canad. J. Res. A*, **30**, p. 372 (1952).
(21) POLLARD, W. G., and PRESENT, R. D. *Phys. Rev.*, **73**, p. 752 (1948).
(22) CARMAN, P. C. *Proc. Roy. Soc. A*, **203**, p. 55 (1950).
(23) MILLIKAN, R. *Phys. Rev.*, **21**, p. 224 (1923).
(24) BLANKENSTEIN, E. *Phys. Rev.*, **22**, p. 582 (1923).
(25) CARMAN, P. C., and ARNELL, J. C. *Canad. J. Res. A*, **26**, p. 129 (1948).
(26) FLOOD, E. A., TOMLINSON, R. H., and LEGER, A. E. *Canad. J. Res. A*, **30**, p. 348 (1952).
(27) DERJAGUIN, B. *Comp. Rend. Acad. U.R.S.S.*, **53**, p. 623 (1946).
(28) WYLLIE, M., and ROSE, W. *Nature* [*London*], **165**, p. 972 (1950).
(29) BARRER, R. M., and BARRIE, J. A. *Proc. Roy. Soc. A*, **213**, p. 250 (1952).
(30) MCBAIN, J. W. *Sorption of gases by solids* (London: Routledge and Kegan Paul, Ltd., 1932).

DISCUSSION

Dr. J. Birks: I should like to comment on Paper B.1 as a member of the oil industry and one principally concerned with the flow of fluids through unconsolidated and consolidated formations.

The character of the pores of natural sedimentary rocks is that they exhibit a wide range of pore radii; in sandstones 0·01 to 20 μ, and in limestones 0·01 to 5 μ. Steady state permeability measurements can be used to establish relations between permeability, porosity, mean pressure and mean pore radius, such as are predicted by the theories of flow in a system of parallel capillaries, e.g. as (say) by Adzumi, or Klinkenberg. Indeed, the parallel capillary model of a porous system can be used to calculate the relative permeabilities of each of the fluids in two phase flow.

However, calculations of surface area of the pores from permeability measurements give false results except in the ideal case of a packed system of uniform spheres. For example, Brooks and Purcell[1] show that the surface areas of consolidated sandstones determined by nitrogen adsorption are from 5 to 100 times greater than those calculated from steady state permeability measurements, whereas for unconsolidated packs of uniform particle and pore size the surface areas calculated by the Kozeny equation and geometrical measurement were in good agreement.

The reason for the disagreement is that the mean radius calculated from permeability is the root mean square value, and is dominated by the larger pore radii; whereas the surface area should be calculated from the mean of the reciprocals of the radii, that is, using the nomenclature of Prof. Barrer

$$\bar{r} = \frac{\epsilon}{\Sigma(d\epsilon/r)}$$

Does not this criticism apply to all permeability methods, including the time lag method?

The ratio of the permeability calculated from pore size distribution data assuming straight parallel capillaries, and that measured by steady state flow gives a textural constant ($k_2^2 k_0$) or a tortuosity factor (k_2), depending on the form of the equations used. As pointed out by Prof. Barrer, the electrical properties of the saturated pores of the medium can give an expression for the factor k_2. Wyllie and Rose proposed $F\epsilon = k_2$ (where F is the ratio of the specific resistance of the saturated porous medium to the specific resistance of the saturating fluid; F is generally known as the formation factor), whereas I consider $F\epsilon = k_2^2$ a better equation. I get better agreement between values of k_2 using the latter equation when comparing them with values of k_2 from permeability and pore-size distribution measurements. For consolidated

rocks the average value of k_2 is 2. The real solution probably lies between the two, that is

$$\sqrt{(F\epsilon)} < k < F\epsilon$$

I should appreciate Professor Barrer's comments on the applicability of permeability methods to the measurement of the surface areas of the pores of natural sediments, and on the nature of the tortuosity factor.

Mr. R. H. Essenhigh: In connexion with the question raised by several speakers of a size distribution of pores in a permeable packing, a possible solution is to postulate a size distribution in the equivalent capillaries which are assumed to represent the permeable packing.

Experimentally, the Kozeny constant K_0 has been found to be $5{\cdot}0 \pm 10\%$ when there is only a small particle size distribution in the dust, but with a wide distribution K_0 drops to about 2.(2) To calculate K_0 for a packing of dust with a uniform particle size, the packing may be represented by a uniform set of equivalent straight capillaries, and neglecting tortuosity, slip and other corrections the value obtained is 4. With a particle size distribution in the dust, a similar distribution in the radii of the equivalent capillaries may be assumed. With an exponential distribution such as $dn = ke^{-r/r_0}dr$, where k and r_0 are constants and dn is the number of capillaries with radii between r and $r + dr$, then the calculated value of k_0 drops to 4/3, which is a change of the right order.

The point appears to be implied in Paper B.1, but it is not specifically stated that the calculated value of the Kozeny constant is affected by the introduction of a distribution in the capillary radii.

Mr. V. T. Morgan: In considering the porous bed of powder Professor Barrer has pointed out the limitations of applying the simplified model of tortuous capillaries. In this case the mean hydraulic depth (r_h) is used as the parameter of length, characteristic of the size of the capillaries. It is equated, without qualification, to the function ϵ/A, which is the ratio of pore volume to wetted surface. Clearly this is only equal to r_h, the ratio of cross-sectional area to wetted perimeter, if the cross-section is unchanging. For example, in the simple case of a hollow spherical pore, the function ϵ/A is less than r_h by $33\frac{1}{3}\%$, and for other pore shapes will vary accordingly.

In Reynolds' numbers calculation for coarse filter beds of spherical particles, I prefer the "three dimensional" parameter ϵ/A as more characteristic of the length dimension of the porous system than the "two dimensional" parameter r_h. If this is justified the capillary model may not be quite so limited as Professor Barrer has suggested, for in this respect the use of ϵ/A compensates in some measure for pore shape.

Author's reply: I refer in my paper to the tortuosity

$$k_2 = \frac{\text{the actual length of a sinuous capillary traversing the bed}}{\text{the geometrical length of the bed}}$$

and noted that Rose and Wyllie proposed a simple conductivity method of measuring k_2, in which they set the ratio of the conductivity of unit cube of porous medium impregnated by an electrolyte (K_2) to the conductivity of unit cube of the electrolyte (K_1) equal to ϵ/k_2. With the above definition of tortuosity, in my view the ratio of conductivities, K_2/K_1, should come nearer to ϵ/k_2^2, for the following reasons.

If A_1 denotes the cross-section of all the capillaries traversing unit face of the cube, each capillary being sinuous and of tortuosity k_2, then $A_1 = \epsilon/k_2$. If in addition ΔV denotes the voltage drop across the cube, then this drop is applied along the length k_2 of these capillaries. Idealizing the medium in terms of the parallel capillary model the potential gradient along the capillaries is $\Delta V/k_2$, not $\Delta V/l$. The current i is then

$$i = K_2' \text{ grad } V = \left(K_1 \frac{\epsilon}{k_2}\right)\frac{\Delta V}{k_2} = \frac{K_1\epsilon}{k_2^2}V$$

giving $K_2/K_1 = \epsilon/k_2^2$. It is of interest that while Klinkenberg[4] appears to follow Wyllie and Rose,[3] in using $K_2/K_1 = \epsilon/k_2$, Cornell and Katz[5] use $K_2/K_1 = \epsilon/k_2^2$.

The parallel capillary model has various defects, some of which have been noted in my paper. We may, for example, enquire what happens to the potential gradient along a capillary when this capillary follows the course *ABCD*, across a medium bounded by planes $x = 0$ and $x = l$ and when a voltage drop ΔV is impressed in the x direction across the medium. Before any current is drawn, we might expect the potential drop to follow the path *ABCD* (Fig. 1) the different sections *AB*, *BC*, *CD* corresponding to the same sections of path along the capillary *ABCD* in Fig. 2. However, current

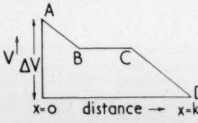

Fig. 1. Potential drop before current is drawn

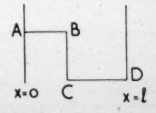

Fig. 2. Path along capillary corresponding to sections in Fig. 1

flows on impressing the voltage difference, and even if the instantaneous voltage drop was as in Fig. 1, negative ions would tend to concentrate at point *C* and positive ions at *B*. A concentration cell is thus built up, which causes a potential gradient across *BC*, and so smooths out the fluctuations in gradient along *ABCD*. It is also possible, since the aqueous phase has a high dielectric constant and the inert solid a low one, that lines of force tend to follow along the sinuous length of a capillary much as magnetic lines of force are concentrated along a ferromagnetic medium. This would also tend to give a smoothed voltage gradient $\Delta V/k_2 l$ along the length of the sinuous capillary, no matter how tortuous the actual conducting channel.

Re-interpreting data of Wyllie and Rose[3] and of Klinkenberg[4] in terms of the equation $K_2/K_1 = \epsilon/k_2^2$, we then have the following typical values for k_2^2, the tortuosity factor:

Nature of medium	k_2^2
Swarms of unconsolidated particles (sands, soils, etc.)	1·43–1·96 (sands) 1·50–3·97 (soils)
Porous consolidated media	1·85–10·6 (sandstones, limestones, dolomite) .6·55 (porous glass)

The above figures cover the data of Wyllie and Rose,[3] Klinkenberg,[4] Cornell and Katz,[5] and Barrer and Barrie.[6] In general k_2^2 tends to be less for unconsolidated than for consolidated media.

Some of the points discussed by Dr. Birks are already referred to in my paper (B.1), for example the domination of the steady state of flow by larger pores, if these are continuous through the medium. This is less true of the transient state of flow involved in the time lag method, for the flowing gas must penetrate every pore and have access to the total area of the solid before the steady state can be established. Indeed

when the flowing gas is adsorbed on this surface area, then the fine pores may in the transient state dominate the large pores, because though their pore volume may be small the total area associated with them may be very great, and much gas enters them to be retained as an adsorbed film.

Mr. Essenhigh's comment on the variability of the so-called Kozeny "constant" is, of course, correct. This "constant" is bound to be influenced significantly by the complexities of the pore geometry; perhaps it is only surprising that it varies as little as it does. Mr. Morgan's comment regarding fluctuations in cross-section along the pore lengths is also associated with pore geometry. It is important that any user of flow methods should realize these and other points, and not uncritically assume that the "area" obtained is always to be taken as quantitatively correct. In spite of all these difficulties, however, the importance of area measurements in fine powders and in microporous media is such that we must continue to employ and try to develop the methods at our disposal.

REFERENCES

(1) Brooks and Purcell. *Petroleum Trans Amer. Instn Mech. Engrs*, **195**, p. 289 (1952) T.P. 3458.
(2) Carman. *Trans Instn Chem. Engrs*, **15**, p. 150 (1937).
(3) Wyllie and Rose. *Nature* [*London*], **165**, p. 972 (1950).
(4) Klinkenberg. *Bull. Geol. Soc. Amer.*, **62**, p. 559 (1951).
(5) Cornell and Katz. *Ind. Engng Chem.*, **45**, p. 2145 (1953).
(6) Barrer and Barrie. *Proc. Roy. Soc. A*, **213**, p. 250 (1952).

Paper B.2

An examination of the behaviour of adsorbed molecules by the flow of gases through microporous media

By Prof. R. M. Barrer, D.Sc., Sc.D., F.R.I.C., F.R.S.E., The University, Aberdeen

Considerable information can be obtained by flow methods concerning the properties of gases adsorbed in microporous media. Of particular interest is the measurement of surface migration and of surface diffusion coefficients, D_s; this may be measured by a steady state method in more concentrated films. It may also be found by the transient state time-lag procedure in adsorbed films dilute enough to obey Henry's law. The ratios of the energies, E, required to render adsorbed molecules mobile to the heats of desorption (ΔH) from the surface are from 0·5 to 0·6 for simple molecules in porous glass up to 0·8 to 0·9 for complex molecules like *n*-heptane, or toluene on silica gel or carbon. The surface diffusion coefficients, D_s, depend upon the concentration in the adsorbed films. If $D_s = D_0^s(1 + f(C_s'))$ denotes the relation between D_s and surface concentration C_s' in molecules per cm^2, then a general relationship exists between $f(C_s')$ and the curvature of the adsorption isotherm. This may permit the value of D_s and its concentration dependence to be measured over the range of C_s' within which surface migration may be described by the generalized Fick law $\frac{\partial C_s'}{\partial t} = \frac{\partial}{\partial x}\left(D_s \frac{\partial C_s'}{\partial x}\right)$, while molecular streaming occurs in the gas phase.

LIST OF SYMBOLS

α, β, n = coefficients in the equation of Flood and others for surface flow.
A, A_g = internal surface areas per cm^3 and per gramme respectively of the porous medium.
A_1 = cross-section of all capillaries traversing unit cross-section of the porous plug.
C_g, C_s = numbers of molecules per unit length of a capillary in gas phase and on surface respectively.
C, C^0, C^l = numbers of molecules per cm^3 of gas phase at any point within, and at ingoing and outgoing faces respectively of the porous medium.
C_s', $(C_s')^0$, $(C_s')^l$ = numbers of molecules per cm^2 of surface at any point within, and at ingoing and outgoing faces respectively of the porous medium.
D = diffusion coefficient of gas in the capillaries in the porous medium.
$D_s = k_2^2 D_s'$ = surface diffusion coefficient in porous medium allowing for tortuosity factor.
$D_2 = k_2^2 D_2'$ = effective gas phase diffusion coefficient in presence of adsorption and surface mobility.
E = Arrhenius energy of activation for surface diffusion.
ϵ = porosity in cm^3 per cm^3 of porous plug.
G_s = surface flow in pV units (ergs per sec) per unit cross-section of porous medium.
ΔH = heat of sorption.
K_k = Knudsen permeability.
K_s = surface permeability = $G_s l/\Delta p$.
$k_s = C_s'/C$ = Henry's law adsorption constant.
k_2 = tortuosity.
L = time-lag for a non-sorbed gas.
L_2 = time-lag for a sorbed gas.
M = molecular weight.
$\bar{m}$ = mean value of the amount sorbed in grammes per gramme in the porous plug.
m_1, m_2 = amounts sorbed in grammes per gramme at ingoing and outgoing faces respectively of the porous medium.
N = number of capillaries traversing unit cross-section of the medium.
N_0 = Avogadro's number.
p = pressure.
P, P_T = total flux through a single capillary and through unit cross-section of the porous medium respectively.
P_g, P_s = flux in gas phase and on surface respectively.
R = gas constant.
ρ = true density of material of porous medium.
T = absolute temperature.
τ = lifetime of molecules in the adsorbed state.
v = amount sorbed in cm^3 at N.T.P. per gramme.

Both steady and transient states of flow may lead to interesting information regarding surface diffusion or flow and the lifetimes of adsorbed molecules. Surface migration has been

studied in the steady state of flow on carbons and on Linde silica (e.g. Flood, Tomlinson and Leger[1]; Carman and Malherbe[2]; Carman and Raal[3]). It has also been investigated in the transient state in Vycor porous glass by Barrer and Barrie,[4] and in silica gel and carbon by Haul,[5] and by Wicke and Kallenbach[6]. Where surface diffusion cannot be detected the time-lag method may still give information regarding the adsorbed state in very dilute surface films (Barrer and Grove[7]). One may also study the way in which the surface mobility of adsorbed molecules varies with the amount of adsorbed material. This can be done for more concentrated films by a somewhat approximate steady state method (Carman and Malherbe[2]; Carman and Raal[3]). It may also be done for the most dilute films through to dense films by an extension of the time-lag method now under investigation in this laboratory (Barrer and Strachan, unpublished work). The matters referred to above will be discussed in this paper.

PROPERTIES OF ADSORBED MOLECULES BY THE TIME-LAG METHOD

We are concerned here with the flow of gases through microporous media in the range of molecular streaming and under conditions when adsorption is no longer negligible. As the pore surface to pore volume ratio increases, or the gas becomes more condensible, the flowing gas may be increasingly delayed by adsorption, and the time-lag rises accordingly. The problem may be quantitatively treated provided the adsorption follows Henry's law. If the adsorbed film contributes appreciably to flow by surface diffusion the equation for molecular streaming with surface migration becomes:

$$\frac{\partial C_g}{\partial t} + \frac{\partial C_s}{\partial t} = D\frac{\partial^2 C_g}{\partial x^2} + D_s\frac{\partial^2 C_s}{\partial x^2} \qquad (1)$$

In equation (1), C_g and C_s are the numbers of molecules in the gas phase and on the surface per cm length of a capillary at the point x and time t. If C is the number of molecules per cm^3 of gas phase and C_s' the number of adsorbed molecules per cm^2 of surface then $C_g = \pi r^2 C$ and $C_s = 2\pi r C_s'$ for the capillary of radius r. If adsorption equilibrium is established and Henry's law is valid $\frac{C_s}{C_g} = \frac{C_s'}{C}\frac{2}{r} = \frac{2k_s}{r} = \frac{A}{\epsilon}k_s$, where k_s denotes the Henry's law adsorption constant. Accordingly, by substituting in equation (1), one obtains

$$\frac{\partial C_g}{\partial t} = D\left[\left(1 + \frac{D_s A k_s}{D\epsilon}\right)\Big/\left(1 + \frac{Ak_s}{\epsilon}\right)\right]\frac{\partial^2 C_g}{\partial x^2} \qquad (2)$$

The time-lag now becomes:

$$L_2 = \frac{k_2^2 l^2}{6D_2} = \frac{l^2}{6D_2'} \qquad (3)$$

where

$$D_2 = D\left[\left(1 + \frac{D_s A k_s}{D\epsilon}\right)\Big/\left(1 + \frac{Ak}{\epsilon}\right)\right] \text{ and } D_2' = \frac{D_2}{k_2^2}$$

In equation (3), k_2 denotes the tortuosity coefficient. It should be noted also that $D_s' = D_s/k_2^2$, so that $D_s/D = D_s'/D'$, and this ratio is independent of the tortuosity coefficient. Clearly when $\frac{D_s}{D}\cdot\frac{A}{\epsilon}k_s$ is much less than unity, then surface diffusion may be neglected, but only when $\frac{A}{\epsilon}k_s$ is much less than unity can adsorption be neglected.

In the steady state of flow we may set $\frac{\partial C_g}{\partial t} + \frac{\partial C_s}{\partial t} = 0$ in equation (1), and obtain for the steady state flux in a single capillary of length $k_2 l$ and radius r:

$$P = P_g + P_s = -\left(D\frac{\partial C_g}{\partial x} + D_s\frac{\partial C_s}{\partial x}\right) = -D\left(1 + \frac{D_s A k_s}{D\epsilon}\right)\frac{\partial C_g}{\partial x} \qquad (4)$$

Accordingly for all the N capillaries traversing unit area of the porous medium the flux is:

$$P_T = N(P_g + P_s) = -N\pi r^2 D\left(1 + \frac{D_s}{D}\cdot\frac{Ak_s}{\epsilon}\right)\cdot\frac{\partial C}{\partial x} = A_1 D\left(1 + \frac{D_s}{D}\frac{Ak_s}{\epsilon}\right)\frac{\partial C}{\partial x} \qquad (5)$$

where A_1 denotes the cross-section of the actual void volume per unit area of the plug normal to the direction of flow.

LIFETIME OF MOLECULES IN DILUTE ADSORBED FILMS

The adsorbable gases ammonia and sulphur dioxide flowing through beds of analcite spheroids showed much enhanced time-lags when compared with the permanent and inert gases, for which adsorption was inappreciable under the experimental conditions used (Barrer and Grove[7]). Moreover, no evidence was obtained of surface migration for

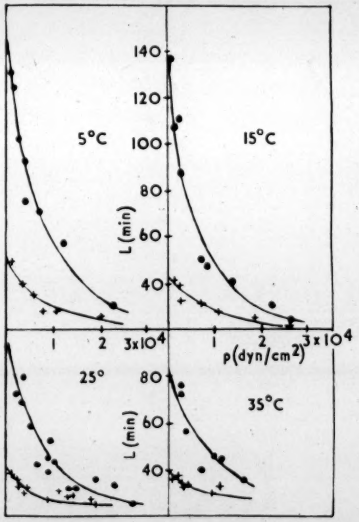

Fig. 1. Time-lags for ammonia and sulphur dioxide as functions of pressure and temperature. Porous medium was a column of analcite spheroids (after Barrer and Grove[7])

• ammonia + sulphur dioxide

dilute adsorbed films of ammonia and sulphur dioxide. It seemed likely therefore that the term $\frac{D_s}{D}\frac{A}{\epsilon}k_s$ in equation (2) could be omitted because it was much less than unity, but that this was not true of the term $(A/\epsilon)k_s$. Accordingly, using the time-lags for the non-sorbed permanent gases or inert gases, e.g. neon, one may find D for ammonia and sulphur dioxide because as shown by Barrer and Grove

$$\frac{L}{L_{Ne}} = \sqrt{\left(\frac{M_{Ne}}{M}\right)} = \frac{D_{Ne}}{D} \tag{6}$$

Also, the time-lags for the non-sorbed gases served to give $\frac{A}{\epsilon} = \frac{2}{r}$ since according to Knudsen[8]

$$D = \frac{4}{3}r\sqrt{\left(\frac{2RT}{\pi M}\right)} \tag{7}$$

With this information it is now possible to use equation (3) to calculate k_s, the Henry's law adsorption constant. Accordingly, the value of L_2 was plotted as a function of pressure (Fig. 1) and extrapolated back to zero pressure to give L_2 in the Henry's law range of sorption and in the pure molecular streaming range of flow. These values of L_2 then gave k_s as recorded in Table 1, together with the lifetimes τ of ammonia and of sulphur dioxide in the adsorbed state $\left[\tau = k_s\sqrt{\left(\frac{2\pi M}{RT}\right)}\right]$. These lifetimes decrease with rising temperature and conform to the equations

$$\text{Lifetime of ammonia} = 3{\cdot}1 \times 10^{-11} \exp\left(\frac{4300}{RT}\right) \text{sec.}$$

$$\text{Lifetime of sulphur dioxide} = 6{\cdot}6 \times 10^{-11} \exp\left(\frac{3010}{RT}\right) \text{sec.}$$

Table 1. *Properties of sulphur dioxide and ammonia adsorbed on spherulites of analcite*

Gas	$T(^\circ K)$	$k_s \times 10^4$	$\tau \times 10^8$ *(sec)*
Sulphur dioxide	278	1·19	1·58
	288	1·00	1·30
	298	0·88	1·07
	308	0·77	0·96
Ammonia	278	10·8	7·4
	288	8·8	5·9
	298	6·7	4·4
	308	5·3	3·5

MEASUREMENT OF THE AMOUNT SORBED BY FLOW EXPERIMENTS

When the gas is adsorbed according to Henry's law to give a mobile dilute film then the time-lag is given by equation (3)

$$L_2 = \frac{k_2^2 l^2}{6D_2} \text{ with } D_2 = D\left[\left(1 + \frac{D_s A k_s}{D\epsilon}\right)\Big/\left(1 + \frac{Ak_s}{\epsilon}\right)\right]$$

The steady state flux per unit cross-section of the porous medium can be written as:

$$P_T = \frac{\epsilon C^0}{k_2^2 l} D\left(1 + \frac{D_s A k_s}{D\epsilon}\right) \tag{5a}$$

as follows from equation (5) by substituting $\epsilon/k_2 = A_1$; $\frac{C^0}{k_2 l} = \frac{\partial C}{\partial x}$. Substitution of equation (5*a*) in equation (3) now leads to:

$$\frac{6L_2P_T}{lC^0} = \frac{6L_2K_k}{l^2} = \epsilon + Ak_s = \epsilon\left(1 + \frac{AC_s'}{\epsilon C}\right) \tag{8}$$

Here $K_k = P_T l/C^0$ is the Knudsen permeability of Barrer and Barrie.[4] It is thus seen that the product L_2K_k should for a group of gases be a linear function of k_s, or of

$$\frac{AC_s'}{\epsilon C} = \frac{\text{No. of molecules adsorbed per cm}^3 \text{ of porous medium at } x}{\text{No. of gaseous molecules per cm}^3 \text{ of porous medium at } x}$$

When $x = 0$, $AC_s'/\epsilon C = A(C_s')^0/\epsilon C^0$. Equation (8) might thus be used to determine $A(C_s')^0$ for various weakly sorbed gases, or, using a surface of known area, to measure k_s for the gases.

The relationship may be tested for Vycor porous glass by using the data of Barrer and Barrie.[4] The constancy of the ratio $\frac{L_2K_k}{1 + (k_sA)/\epsilon}$ as required by equation (8) is certainly promising (Table 2) when one uses for the area A its value according to the adsorption method. The ratio A/ϵ for the porous glass was $6{\cdot}7 \times 10^6$.

Table 2. *Test of equation for porous glass*

Gas	$\frac{L_2K_k(cm^2)}{(292\ ^\circ K)}$	$k_s \times 10^7$ $(290^\circ K)$	$\frac{L_2K_k}{\left(1 + k_s\frac{A}{\epsilon}\right)}$
Argon	1·07	4·9	$0{\cdot}25_0$
Nitrogen	1·13	5·1	$0{\cdot}25_7$
Oxygen	1·14	5·3	$0{\cdot}25_2$
Krypton	1·92	9·7	$0{\cdot}25_7$
Methane	1·58	7·2 (294° K)	$0{\cdot}24_7$
Ethane	8·00	52·7 (294° K)	$0{\cdot}22_2$

SURFACE DIFFUSION

When the surface to volume ratio of the particles of the porous medium is substantially increased, and the polarity of the gases sorbed on the polar sorbent decreased, surface diffusion may become important. This situation was in fact discovered in experiments using a plug of Vycor porous glass as diffusion medium, with some permanent and inert gases as sorbates and diffusates (Barrer and Barrie[4]). Values of k_s (Table 2) determined by adsorption measurements were smaller than those in Table 1. Surface mobility should be correspondingly enhanced because the more easily molecules evaporate the more readily also they should diffuse along the surface. In order to determine D_s (or D_s') equation (3) can be re-arranged with the aid of equation (6) to give:

$$\frac{D_s'}{D_2'} = \frac{D_s}{D_2} = 1 - \frac{\epsilon}{Ak_s}\left[\frac{L_2}{L_{Ne}}\sqrt{\left(\frac{M_{Ne}}{M}\right)} - 1\right] \tag{9}$$

For the determination of D_2 (and hence of D_s) the tortuosity constant k_2 is required, whereas for measurements of D_2' (and so of D_s') this constant is not involved [equation (3)]. The tortuosity factor was found by Barrer and Barrie to be 2·56 by combined sorption and flow measurements, and hence D_2 was determined. Similarly, because all the quantities on the right-hand side of equation (9) were known or measured, D_s was evaluated (Table 3). To obtain D_s' from D_s all values of the latter must be divided by $(2{\cdot}56)^2$.

In columns (4) and (7) of Table 3 are given heats of sorption, ΔH, evaluated from the temperature coefficient of k_s, $\left(\frac{\partial \ln k_s}{\partial T} = \frac{\Delta E}{RT^2} = \frac{\Delta H + RT}{RT^2}\right)$ and energies of activation for diffusion derived from the temperature coefficient of D_s $\left(\frac{\partial \ln D_s}{\partial T} = \frac{E}{RT^2}\right)$. The extreme range in the ratio $E/\Delta H$ is

from 0·5 to 0·6, so that in very dilute adsorbed films on porous glass the sorbed molecules are excited into the mobile state by an input of energy which is little more than half the heat of sorption.

Table 3. *Surface diffusion on porous glass in the Henry's law adsorption range*

Gas	*Temp.* °K	$10^7 \times k_2$	$-\Delta H$ cal/mol	*Temp.* °K	$10^3 \times D_s$ cm² sec⁻¹	*E* cal/mol
Nitrogen	273	6·8	3 200	292	1·53	1 600
	290	5·1		323	2·00	
	323	3·35		343	2·26	
	343	2·61				
Oxygen	273	6·8	3 000	292	1·30	1 800
	290	5·3		323	1·73	
	323	3·45		343	2·05	
	343	2·78				
Argon	273	6·2	2 600	292	1·31	1 400
	290	4·9		323	1·65	
	323	3·43		343	1·91	
	343	2·88				
Krypton	273	14·4	3 300	294	0·50	1 800
	290	9·7		323	0·63	
	323	6·6		343	0·78	
	343	5·3				
Methane	273	10·93	3 000	294	1·24	1 500
	294	7·9		323	1·57	
	323	5·6		343	1·73	
	343	4·4				
Ethane	294	52·7	5 300	292	0·262	3 200
	323	24·1		323	0·466	
	343	16·0		343	0·596	

Barrer and Barrie found that for very dilute films surface migration was obscured in the steady state even where it was important for the transient state. Their explanation of this was as follows. The process of penetration that precedes the steady state of flow involves creep of gas molecules into every accessible crevice. Much of the area on which adsorption occurs will be concerned with very fine pores all of which must obtain their equilibrium quota of adsorbed gas before the steady state of flow can be attained. It is this process of penetration which in the transient state reveals surface diffusion. On the other hand, when the steady state is established, larger pores will contribute relatively more to the permeability than will small pores. But larger pores have a smaller surface to volume ratio, and will so contribute relatively less to surface diffusion and more to gas phase flow. Accordingly, in the steady state, surface flow tends to be obscured while in the transient state it is most apparent.

However, as the amount sorbed increases, until dense, even multilayer, films have formed, surface migration becomes increasingly large, and even in the steady state of flow has been readily measured. The most detailed measurements of surface migration in the steady state are those of Carman and his collaborators (Carman and Malherbe[2]; Carman and Raal[3]). Under conditions when transport in the gas phase within the microporous medium is by molecular streaming, one may measure the permeability for a sorbed gas and also for a non-sorbed reference gas, such as helium. From the permeability K_{He} for helium one may calculate the gas phase permeability K for the sorbed gas $\left(\frac{K}{K_{He}} = \sqrt{\frac{M_{He}T_1}{MT}}\right.$ where T_1 and T are temperatures at which flow of the sorbed gas and of helium occurred$\left.\right)$. By subtracting K so calculated from the measured total permeability, one may then find the permeability contribution K_s which is due to surface flow. Then using the symbols indicated at the head of this paper the surface diffusion coefficients D_s and D_s' are given by

$$\frac{D_s}{k_2^2} = D_s' \simeq \frac{K_s}{\rho(1-\epsilon)} \cdot \frac{\Delta p}{\Delta v} \cdot \frac{RT}{22\,400} \tag{10}$$

Equation (10) can be derived as follows. The effective perimeter per cm² of cross-section of the plug is $2\pi Nr$, in terms of the cylindrical capillary model. If, however, A_g is the area per gramme of the porous material, then for the above plug of unit cross-section and length l

$$2\pi Nrk_2 l = A_g\rho(1-\epsilon)l \tag{11}$$

It follows from equation (11) that

$$\frac{\text{internal area of plug}}{k_2 l} = \text{perimeter} = \frac{A_g\rho(1-\epsilon)}{k_2} \tag{12}$$

We also have for the total surface flux P_s through the N capillaries traversing unit cross-section of the medium

$$P_s = 2\pi NrD_s\frac{(C_s')^0 - (C_s')l}{k_2 l} = 2\pi NrD_s\frac{\Delta C_s'}{k_2 l} \tag{13}$$

To convert C_s' (molecules per cm² of surface) to v one has

$$C_s' = \frac{N_0 v}{22\,400\,A_g} \tag{14}$$

The surface flux P_s expressed as in equation (13) is, however, related to the same surface flow rate G_s expressed in pV units (ergs per sec) by

$$P_s = G_s N_0/RT \tag{15}$$

where N_0 is Avogadro's number. The surface permeability K_s through a bed of unit cross-section is, however, by definition

$$K_s = \frac{G_s l}{\Delta p} = P_s\frac{RT}{N_0}\frac{l}{\Delta p} \tag{16}$$

where this permeability is given in ergs per second for a medium of unit cross-section and unit length with unit pressure head across it. Substitution from equations (16), (14) and (12) in equation (13) then gives equation (10).

Equation (10) is an approximation in so far as $\Delta v/\Delta p$ denotes an average concentration gradient over a finite concentration interval. The surface diffusion coefficient is a function of the amount adsorbed as the data of Carman and

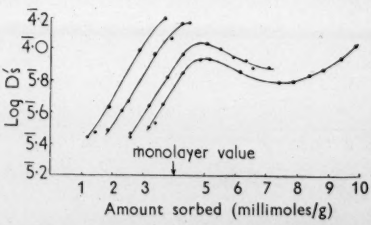

Fig. 2. Concentration dependence of surface diffusion coefficient D_s' (in cm² sec⁻¹) of Freon (CF_2Cl_2) on a Carbolac plug $\epsilon = 0{\cdot}63$ (after Carman and Raal[3])

Malherbe[2] and Carman and Raal[3] have shown. Therefore only an average D_s or D_s' is derivable from equation (10) in the surface concentration interval involved. However, by varying v^0 and v^l the volumes adsorbed per gramme at $x = 0$ and $x = l$ respectively, while keeping $\Delta v = (v^0 - v^l)$ small, one may find how these average values of D_s vary with $\frac{1}{2}(v^0 + v^e)$. Fig. 2 shows some of the data of Carman and Raal[3] on the concentration dependence of this average D_s' using Freon (CF_2Cl_2) as sorbate and diffusate in carbon and silica plugs. Fig. 3 shows how the Arrhenius energy of

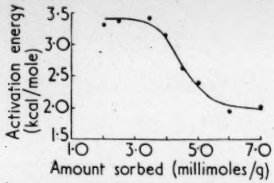

Fig. 3. Activation energy for D_s' as a function of amount sorbed, for Freon (CF_2Cl_2) on a Carbolac plug (after Carman and Raal[3])

activation for this average D_s' varied with the amount sorbed for the Freon-carbon system investigated by Carman and Raal. Table 4 shows some approximate surface diffusion

Table 4. *Surface diffusion at −50° C by the steady state method (Carman and Raal[3])*

System	*Approximate surface coverage as fraction of monolayer*	$10^8 \times D_s'$ ($cm^2\ sec^{-1}$)	*Arrhenius energy of activation for* D_s' (*cal/mol*)	*Heat of adsorption* ΔH (*cal/mol*)
n-C_7H_{16}–charcoal	0·1	1·9	10	13
n-C_7H_{16}–silica gel	0·1	1·1	10·5	13
CH_3OH–silica gel	0·1	2·4	9	16
$C_6H_5CH_3$–silica gel	0·1	0·3	13	15
CF_2Cl_2–silica	0·3	9·0	3·5	6·7
SO_2–silica	0·3	9·6	2	7·5
CF_2Cl_2–carbon black	0·3	4·2	3·4	8·3
CO_2–carbon black	0·3	4·3	3·35	5·8
CO_2–carbon black	0·1	18·6	3·5	6·5

coefficients D_s' at lower film densities (column 3). The Table 4 also gives Arrhenius activation energies E for surface diffusion, and heats of adsorption ΔH. The results of Table 4 may be compared with those of Table 3, obtained by the time-lag method. In this comparison it must be remembered:

(1) That Table 3 gives values of D_s which must be divided by $k_2^2 = (2 \cdot 56)^2$ to convert them into corresponding values of D_s'.

(2) That the diffusates of Table 3 are much less strongly sorbed than are those of Table 4 and may be expected to have on this account greater intrinsic mobility as well as volatility from the adsorbed film.

(3) That the film density in Table 3 is much less than that of Table 4. In the Henry's law region of sorption D_s (or D_s') is independent of surface concentration (Table 3); whereas for the film densities of Table 4 D_s would tend to decrease as the film became more dilute (cf. Fig. 2).

(4) That in the steady state of flow surface diffusion tends to be obscured relative to surface flow observed in the transient state.

There are thus several differences and variables which make close comparison of all the data difficult. However, it does seem clear that the larger the molecule the greater tends to be the ratio of $E/\Delta H$; and also that small energies of activation for surface diffusion are associated with small heats of sorption.

Other measurements in the steady state of flow, in which surface transport occurred, were made by Flood, Tomlinson and Leger.[1] They found that the excess transport over a theoretical value in absence of sorption effects following the Adzumi type of equation was, for C_6H_6, C_2H_5Cl, $(C_2H_5)_2O$, CH_3OH and water, represented by an empirical function of the amount sorbed:

$$K_s = \alpha\bar{m} + \beta\frac{(m_1^n - m_2^n)}{\Delta p} \qquad (17)$$

where the symbols have the meanings set out at the head of this paper. These authors made no attempt to interpret the surface flux as a diffusion. It has indeed to be recalled that with the onset of capillary condensation transport of the capillary condensate by hydrodynamic flow begins. This flow as measured by Carman[9] increases rapidly in amount as the extent of capillary condensation increases and follows qualitatively the path of the sorption isotherm. Just as the sorption isotherm often shows hysteresis so does the flow of capillary condensed liquid (Fig. 4). There should in this

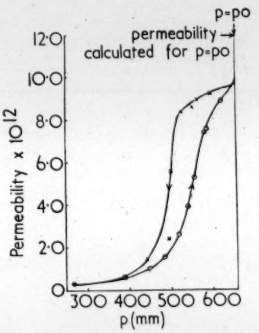

Fig. 4. Permeability corresponding to the sorption and desorption branches of the sorption isotherms. Hysteresis in permeability follows hysteresis in sorption. Freon (CF_2Cl_2) at −33·1° C on a Linde silica plug, $\epsilon = 0 \cdot 056$ (after Carman[9])

case be no difficulty in distinguishing between this kind of hydrodynamic flow and surface migration in absence of capillary condensation. It remains to find whether, in the multilayer region of sorption before capillary condensation is important, the surface migration is best described in terms of the generalized Fick law

$$\frac{\partial C_s'}{\partial t} = \frac{\partial}{\partial x}\left(D_s\frac{\partial C_s'}{\partial x}\right)$$

CONCENTRATION DEPENDENCE OF D_s IN ADSORBED FILMS

Provided surface diffusion follows the above equation there should be a relation between the curvature of an

adsorption isotherm and the concentration dependence of D_s (or D_s'), not hitherto noted. If the relation between D_s and concentration C_s' is represented quite generally by $D_s = D_0^s[1 + f(C_s')]$, then the value of D_0^s is measured for suitable media by the time-lag method (see Table 2). The function $f(C_s')$ can be found from the isotherm curvature as follows:

The equation of flow in a capillary in the steady state is

$$D\frac{\partial^2 C_g}{\partial x^2} + \frac{\partial}{\partial x}\left(D_s\frac{\partial C_s}{\partial x}\right) = 0 \qquad (18)$$

where C_g and C_s are as before the numbers of molecules per unit length of the capillary in the gas phase and on the surface respectively at the point x. Now $\pi r^2 C = C_g$ and $2\pi r C_s' = C_s$ where C and C_s' are the numbers of molecules per cm^3 of the gas phase, and per cm^2 of surface of the capillary at the point x. Accordingly, for unit cross-section of the medium traversed by N capillaries of tortuosity k_2, $N\pi r^2 k_2 = \epsilon$ and $2N\pi r k_2 = A$. Thus equation (18) may be transformed to:

$$\frac{\epsilon}{k_2}D\frac{\partial^2 C}{\partial x^2} + \frac{A}{k_2}\frac{\partial}{\partial x}\left(D_s\frac{\partial C_s'}{\partial x}\right) = 0 \qquad (19)$$

Equation (19) may now be integrated, as in a rather similar case considered by Barrer[10] to obtain:

$$\frac{x}{k_2 l} = \frac{\epsilon D(C^0 - C) + AD_0^s\{(C_s')^0 + F(C_s')^0 - [C_s' + F(C_s')]\}}{\epsilon D(C_0 - C^l) + AD_0^s\{(C_s')^0 + F(C_s')^0 - [(C_s')^l + F(C_s')^l]\}} \qquad (20)$$

where $F(C_s') = \int_0^{C_s'} f(C_s')dC_s'$. However, under the experimental conditions employed, $C^0 \gg C^l$, $(C_s')^0 \gg (C_s')^l$, and both C^l and $(C_s')^l$ are small enough at $x = k_2 l$ for Henry's law to be obeyed: $k_s = C_s'/C$. Also, as C_s' tends to zero, $f(C_s')$ tends to zero. Since integration of $f(C_s')$ is between the limits 0 and C_s' it then follows that as C_s' tends to zero so does $F(C_s')$. We may therefore re-write equation (20) introducing these conditions, and then differentiate with respect to x, and re-arrange to obtain:

$$\frac{\epsilon DC^0}{k_2^2 l} + \frac{AD_0^s}{k_2^2 l}\{(C_s')^0 + F(C_s')^0\} = -\frac{\epsilon D}{k_2}\frac{\partial C}{\partial x} - \frac{AD_0^s}{k_2}[1 + f(C_s')]\frac{\partial C_s}{\partial x} \qquad (21)$$

The right-hand side of this relation is the steady state flux through unit area of the porous medium. This flux is constant for all values of x. In particular its value at the outgoing surface is:

$$-\frac{\epsilon D}{k_2}\left(\frac{\partial C}{\partial x}\right)_{x=k_2 l} - \frac{A}{k_2}\left(D_s\frac{\partial C_s'}{\partial x}\right)_{x=k_2} = \frac{\epsilon DC^0}{k_2^2 l} + \frac{AD_0^s k_s C^0}{k_2^2 l} \qquad (22)$$

By equating the left-hand side of equation (21) and the right-hand side of equation (22) we then have:

$$k_s C^0 - (C_s')^0 = F(C_s')^0 \qquad (23)$$

The significance of this is shown in Fig. 5 where the adsorption isotherm ODA is given as a plot of C_s' against C. From the point C^0 we may read off $(C_s')^0$. We may also extrapolate the

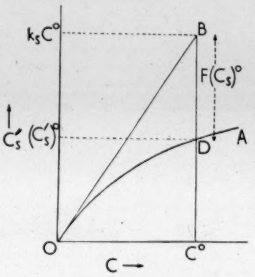

Fig. 5. Isotherm ODA and extrapolation OB of Henry's low sorption region used in derivation of the concentration dependence of D_s

Henry's law region along OB to give $k_s C^0$, and then relation (23) shows that BD is $F(C_s')^0$. For different values of C one may from the isotherm construct a graph of $F(C_s')$ against C_s', and thence by drawing tangents to the curve find $f(C_s')$ as a function of C_s'. Since, however, D_0^s can be found in the Henry's law region by the time-lag method, it is simple by combining adsorption data with time-lag data to evaluate the whole equation $D_s = D_0^s[1 + f(C_s')]$ for that interval of surface and gas phase concentrations over which the flow equation is:

$$\frac{\partial C_g}{\partial t} + \frac{\partial C_s}{\partial t} = D\frac{\partial^2 C_g}{\partial x^2} + \frac{\partial}{\partial x}\left(D_s\frac{\partial C_s}{\partial x}\right)$$

This equation should be valid until hydrodynamic flow of capillary condensed liquid and Poiseuille flow in the gas phase begin.

REFERENCES

(1) Flood, A. E., Tomlinson, R. H., and Leger, A. E. *Canad. J. Res. A*, **30,** pp. 348, 389 (1952).
(2) Carman, P. C., and Malherbe, P. le R. *Proc. Roy. Soc. A*, **203,** p. 165 (1950).
(3) Carman, P. C., and Raal, F. A. *Proc. Roy. Soc. A*, **209,** p. 38 (1951).
(4) Barrer, R. M., and Barrie, J. *Proc. Roy. Soc. A*, **213,** p. 250 (1952).
(5) Haul, R. *Angew. Chem.*, **62,** p. 10 (1950); *Nature* [*London*], **171,** p. 519 (1953).
(6) Wicke, E., and Kallenbach, R. *Kolloid Z.*, **97,** p. 135 (1941).
(7) Barrer, R. M., and Grove, D. M. *Trans Faraday Soc.*, **47,** p. 837 (1951).
(8) Knudsen, M. *Ann. Phys.* [*Leipzig*], **28,** p. 73 (1909).
(9) Carman, P. C. *Proc. Roy. Soc. A*, **211,** p. 526 (1952).
(10) Barrer, R. M. *Proc. Phys. Soc.* [*London*], **48,** p. 321 (1946).

DISCUSSION

Dr. W. W. Barkas: Would Prof. Barrer tell us what he means by the "surface" he proposes to measure. If adsorption methods and transient permeability measurements give a result nearer the true surface than constant flow experiments, why stop there? The result obtained depends on the method used because a "surface" is a geometrical abstraction, not a molecular reality. I suggest therefore that surfaces should be defined in terms of an "equivalent area" applicable to the method used.

Mr. G. L. Fairs: I would be interested to know if the author has been able to derive any relationship between adsorption and permeability surfaces in the case of any given substance.

In the course of some recent research on grinding I have been able to establish a linear relationship between the net energy input and the new (permeability) surface produced for various brittle materials in a number of different units.

Since the permeability technique measures the external surface only, whereas the adsorption technique also measures the blind pores and cracks in the particles to be ground, it would seem preferable to use the latter technique when measuring the surfaces of the ground products since the crack pattern presumably has a profound effect upon the ease of grinding. Unfortunately it has only been possible to find a constant ratio between permeability and adsorption surfaces for permeability surfaces above about 1500 cm^2/g and it would therefore be of considerable interest if Professor Barrer would give his views on this point.

Author's reply: Dr. Barkas's difficulty over the meaning of the word "surface" can be lessened by a suitable choice of the flowing gas or liquid. In using the Kozeny or Arnell equations to measure the area of a mass of tiny rubber particles, for instance, one would not choose benzene as flowing liquid or vapour; but helium or some other gas which does not dissolve appreciably in the rubber would give a satisfactory result. The use of water to find the area of a clay which swells and shrinks with interlamellar imbibition of water (e.g. montmorillonite) would also be unsatisfactory; but here again air or benzene, neither of which fluids penetrates between the lamellae, should prove satisfactory.

As far as Mr. Fairs' problem is concerned, I do not know of any *a priori* reason why among solids of differing pore geometry, exhibiting in different degrees blind pores which contribute little to the steady state of flow, there should be any regular relation between adsorption areas and areas based on measurements of the steady state of flow. As regards the transient state of flow (i.e. the time lag method) some such relation may however emerge, and one hopes it may be that the ratios of adsorption and time lag areas are near to unity.

[*See also author's reply to discussion on Paper B.1 on p.* 47.]

Paper B.3

The flow of gases through packed beds of colloidal carbon blacks

By H. W. Davidson, B.Sc., and B. M. Turk, Research Laboratories, The General Electric Co. Ltd., Wembley

The flow of hydrogen, nitrogen and argon through packed beds of lamp- and carbon-blacks has been studied at atmospheric pressure and very low gas velocities. These materials can be packed to cover an appreciable range of porosities and so permit examination of the relationship between porosity and permeability over a wide range.

It is found that: (*a*) the porosity functions suggested by Kozeny, Carman and Arnell are not applicable to such beds; (*b*) the permeability of the bed is related to the fourth power of the bed density; (*c*) in the case of undensed blacks the permeability is related to the particle size; while for densed blacks the flow is governed by the width of channels between aggregates.

There is reason to hope that this investigation provides the basis of a method for the estimation of the surface area of colloidal carbons.

NOTATION

The units are C.G.S. throughout

ρ_x = the density of the particles constituting the bed;
ρ_a = the bulk density of the bed, i.e. the weight per unit gross volume of powder;
ϵ = the porosity of the packed bed, i.e. the fraction of the volume of the bed occupied by voids;
ρ_p = the "particle density," i.e. the density of a particle with blind pores contributing to the volume of the particle;
S_v = the surface area of the particles per cubic centimetre of solid material;
A = the cross-sectional area of the packed bed;
L = the depth of the packed bed;
Δp = the pressure difference causing fluid to flow through the bed;
p = the mean gas pressure in a bed;
Q = the volume rate of flow of fluid through the bed measured at the mean pressure of fluid in the bed;
G = the mass rate of flow of fluid through the bed;
ρ_1 = density of the gas at unit pressure;
η = viscosity of the fluid;
M = the molecular weight of the gas;
T = the temperature of the gas (degrees absolute);
R = the gas constant;
k = a dimensionless quantity: Kozeny's constant (=5);
k_0 = a dimensionless quantity (2·5 ± 0·5) [Ref. (12)];
R_e = Reynolds' number.

The fundamental treatment of the flow of fluids through beds of packed powders is due to Kozeny.[1] On hydrodynamical grounds he showed that:

$$Q = \frac{\Delta p A}{k\eta L}\left[\frac{\epsilon^3}{(1-\epsilon)^2}\frac{1}{S_r^2}\right] \qquad (1)$$

Fair and Hatch[2] independently arrived at the same result by appealing to a dimensional analysis. Kozeny was able to demonstrate the validity of the porosity function

$$F_1(\epsilon) \equiv \frac{\epsilon^3}{(1-\epsilon)^2} \qquad (2)$$

by using the results of Donat's experiments[3] on the drainage of water through sand. Kozeny's equation has now been well tested under a variety of conditions and is generally accepted as the basic law governing the viscous flow of fluids through porous beds of powders. The experimental evidence for equation (1) has been reviewed by Carman[4] and Rose.[5] Arthur and co-workers[6] applied equation (1) to beds of porous particles by introducing the concept of "particle density" ρ_p and assuming that S_v represents the external surface of the particles. By putting $\epsilon = 1 - \rho_a/\rho_p$ equation (1) can be transformed to yield

$$\rho_p - \rho_a = \left(\frac{QLk\eta}{\Delta p A} S_r^2 \rho_a^2 \rho_p\right)^{\frac{1}{3}} \qquad (3)$$

The results of permeability measurements on a series of beds of different porosities can be used to plot ρ_a against

$\left(\frac{QL\eta}{\Delta pA}\rho_a^2\right)^{\frac{1}{2}}$ and this results in a straight line if equation (3) holds.

This constitutes a good test for the form of the porosity function (2) more especially as the intercept of the straight line on the ρ_a axis should yield ρ_p.

It is generally appreciated that Kozeny's equation requires modification when the particle size of the powder approaches the mean free path of the percolating gas. Rigden[7] has adjusted equation (1) by correcting the pore diameter for "slip," as it is known that the gas flow through very fine capillaries is larger than predicted by Poiseuille's relation. Arnell,[8] on the other hand, has added a variable second term to Kozeny's original equation. This accounts for gas flow of the Knudsen type and becomes dominant when the particle size is very small. Carman and Arnell[9] reviewed both modifications and concluded that they are equivalent to

$$Q = \frac{A\epsilon \,.\, \Delta p}{k\eta L}\left\{\left[\frac{\epsilon}{S_v(1-\epsilon)}\right]^2 + \frac{8}{3}\left(\frac{2RT}{\pi M}\right)^{\frac{1}{2}}\frac{\delta k_0 \eta \epsilon}{S_v(1-\epsilon)p}\right\} \quad (4)$$

According to Arnell[8] "taking δ as a constant having a value of 0·9 appears satisfactory for most flow studies." On this assumption it is easy to show that for a carbon black with a particle radius of say 20 $\mu\mu$ the ratio of the first (Poiseuille) to the second (Knudsen) term in equation (4) comes to 1 : 100. In such cases it is therefore reasonable to neglect the Poiseuille term and rewrite equation (4) as

$$Q = \frac{A\Delta p}{kL} \cdot \frac{8}{3}\left(\frac{2RT}{\pi M}\right)^{\frac{1}{2}}\frac{0{\cdot}9k_0\epsilon^2}{S_v(1-\epsilon)p} \quad (5)$$

It is now possible to examine the validity of the porosity function

$$F_2(\epsilon) \equiv \epsilon^2/(1-\epsilon) \quad (6)$$

Colloidal carbons such as lamp and carbon blacks were thought ideal for this purpose as it is possible to pack them into beds of very widely varying densities. For this reason, too, it is vital that the true form of $F_2(\epsilon)$ be established if gas flow methods are to be used for the measurement of the surface area of such materials.

EXPERIMENTAL

The permeability cell. The design was a modified version of Lea and Nurse's[10] apparatus.

The packing of the beds. An analytical balance was used to weigh the powder sample to the nearest $\frac{1}{2}$ mg. The sample was carefully poured into the cell, which was tapped to cause some settling. The plunger was then slowly pushed in while the cell was being tapped. The travel of the plunger was limited by two locking knurled rings. This ensured that the different powder samples occupied the same volume after the compression. However, it was found that the bed volume usually increased on removing the plunger, even if the compression was maintained for as long as 10 min. The plunger was therefore carefully replaced after the pressure and flow readings had been recorded, and the volume change measured by the insertion of feeler gauges between the lower knurled ring and the upper rim of the cell. Considerable practice was necessary in withdrawing the plunger so that the bed remained undisturbed by the air drawn in. The bed height was about 75% of the bed diameter. No attempt was made to pack the beds in small increments, as the surfaces of those that had increased in volume were found to be slightly domed. As this "spring-back" at the centre was greater than at the circumference there was some small radial density gradient in these beds. The elimination of these gradients by packing the beds in steps would therefore have been justified only if final bed depths of greater than one diameter had been used.

Procedure. Gas was passed in a downward direction through the cell for at least 7 min before pressure and flow measurements were made. Preliminary experiments showed that the readings were steady after the first 5 min or less and remained so; also that the plot of pressure against flow resulted in a straight line passing through the origin. Each bed was therefore tested at only one flow rate. It was found impracticable to test any one bed with more than one gas. The bed was discarded after each test. To examine the contribution of the filter paper disk (No. 541 Whatman), the latter was removed from the bed after a test and gas passed through it at the rate used for the bed. No measurable pressure drop was observed. However, a new disk was used for each bed.

Variables influencing the measurements. The flow and pressure gauges consisted of U-tubes manometers, 80 cm long and filled with coloured light mineral oil. The flow manometer was joined in parallel with 100 cm of a $\frac{1}{2}$ mm bore capillary tube; and the gauge calibrated by drawing air through it using a Marriotte bottle charged with de-aerated water. The volume flow was corrected to cubic centimetres of air at S.T.P. The flow readings were corrected for the effect of temperature on gas viscosity, but this was not found to be significant.

THE MATERIALS

The argon, nitrogen and hydrogen were of the best quality commercially available in cylinders. The samples of lampblack had been manufactured from creosote on a Wegelin plant. The samples were collected in the settling chambers in which the lampblack is deposited. A sample of this black was calcined at a temperature of about 1000° C and this treatment resulted in an increase in bulk density. Another sample was densed by passing through a triple roll mill. The acetylene-black was obtained in the "100% compressed" form. The furnace-black was manufactured from oil and obtained in unpelleted form. It had probably undergone very little compression. The channel-black was obtained in pelleted form and was lightly crushed and passed through a 100 mesh B.S. screen.

RESULTS

Equation (5) was transformed by means of the same substitution which Arthur and co-workers[6] applied to Kozeny's equation (1). Thus equation (5) becomes

$$\rho_p - \rho_a = \left(\frac{QpLS_v\rho_p\rho_a}{\Delta pA}\sqrt{\frac{M}{T}}\right)^{\frac{1}{2}}\left(\frac{3k}{8\delta k_0}\sqrt{\frac{\pi}{2R}}\right)^{\frac{1}{2}} \quad (7)$$

Therefore, if as a result of measurements on beds of varying porosity, ρ_a is plotted against $\left(\frac{QpL\rho_a}{\Delta pA}\sqrt{\frac{M}{RT}}\right)^{\frac{1}{2}}$ a straight line should result since ρ_p and the second factor in equation (7) are constant. Fig. 1 includes the results for two lampblacks and the furnace-black. The points for calcined lampblack follow a common line, which could only be true if Poiseuille flow made a negligible contribution and the square root of the molecular weight of the gas played the part characteristic of Knudsen flow. The curvature of the plot is therefore not attributable to a contribution from the Poiseuille term. It seemed difficult to adjust the Carman–Arnell equation (4) so

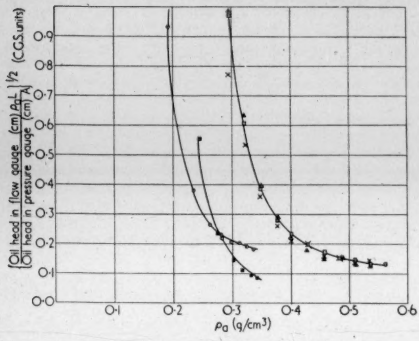

Fig. 1. The application of equation (7) to permeabilities of carbon-black beds

⊡ calcined lampblack (nitrogen).
○ "undensed" lampblack (argon)
⊠ furnace-black (nitrogen).
× calcined lampblack (hydrogen) } with molecular weight
△ calcined lampblack (argon) } and gauge constant accounted for.

Cell diameter 2·54 cm, bed height 1·9 cm, mean pressure about 20 cm w.g. above atmospheric and assumed to be approximately constant.

as to accommodate these curves and an empirical relationship was therefore sought to replace $\epsilon^2/(1-\epsilon)$ in equation (6).

It was found that the present measurements were best summarized by relating the permeability to the fourth power of the bed density ρ_a. Thus ρ_a^4 was plotted against $\frac{\Delta pA}{QLp}\left(\frac{RT}{M}\right)^{\frac{1}{2}}$ and the results for the three lampblacks, the acetylene and the furnace black are shown in Fig. 2. Apart from an initial curved portion in the low bed density region, the experimental points fall on lines which are straight within the limits of experimental error. The results for argon, nitrogen and hydrogen can be seen to fall on common lines as illustrated in the case of the acetylene- and furnace-blacks. The fact that the wide differences in molecular weight are accounted for by the factor $\sqrt{M}$ which occurs in the function plotted as abscissa supports the view that the gases flow in accordance with Knudsen's equation. This is the justification for neglecting the first term in equation (4). Fig. 2 also includes results for a very finely ground crystalline haematite and this suggests that this ρ_a^4 relationship is not peculiar to colloidal carbons. Although the slopes of the lines in Fig. 2 do classify the materials in order of their mean particle sizes (as determined by the electron microscope) there are insufficient data to establish a quantitative relation. To do so the ordinate ρ_a^4 would have to be plotted in a dimensionless form so that the slope has the required dimension of length. By analogy with the Carman–Arnell equation (4), $(\rho_a/\rho_x)^4$ would be a suitable choice of ordinate. However, density measurements of sufficient accuracy are not yet complete. Moreover, it would be necessary to take more account of the degree to

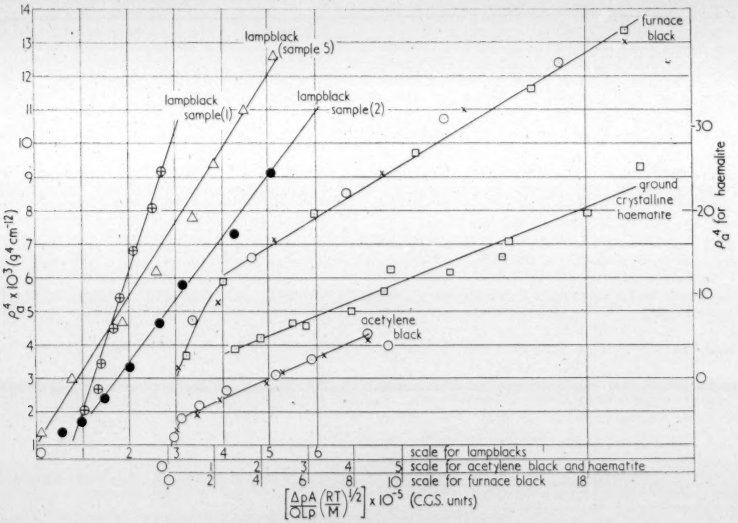

Fig. 2. Experimental evidence for the porosity function

$$F_3(\epsilon) \equiv (1-\epsilon)^{-4}$$

Key to gases used: × hydrogen, ⊡ nitrogen, ○ argon.

Mean particle diameter determined from electron micrographs: furnace-black, 34 $\mu\mu$; lampblack (sample 5), 129 $\mu\mu$; lampblack (sample 1), 114 $\mu\mu$; acetylene, 79 $\mu\mu$.

which the black samples had been agglomerated before the tests. Thus it is well known that colloidal carbons can be readily "densed" and pelleted. A newly made black may have a bulk density as low as 0·05 g/cm³ and this may rise (by a factor of 3) on handling. Subsequent processing for the market may raise the bulk density to as much as 0·5 g/cm³. Clearly this is an important factor, for it is quite conceivable that tightly packed agglomerates would be present even in undensed samples and could then survive the process of building up the beds. The gas might then flow round these agglomerates with the result that the effective surface and particle density would be lowered. Blacks which were known to have undergone a densing process were therefore examined and the results are shown in Fig. 3. It is clear that though densification has altered the permeability by a factor of 10, the ρ_a^4 relationship still holds. It is also evident from the graphs that a bed as uniformly compacted as that from undensed lampblack but compressed to a bulk density corresponding to that of the densed blacks would have negligible permeability. To explain the relatively large permeability of the densed black beds it is necessary to assume that the gas streams through channels between aggregates. This occurs over the major part of the porosity range. Moreover the slopes of the lampblack lines suggest that for these the channel diameters are comparable with the individual particle diameters. It is known that some carbon-black beads will easily survive pressures such as those employed in packing the test beds. On account of this high power of cohesion, aggregates of bead fragments would not be expected to distort, and on compressing would therefore form channels larger than the individual particles. This is the explanation of the relatively large slope of the line for the crushed channel black beads.

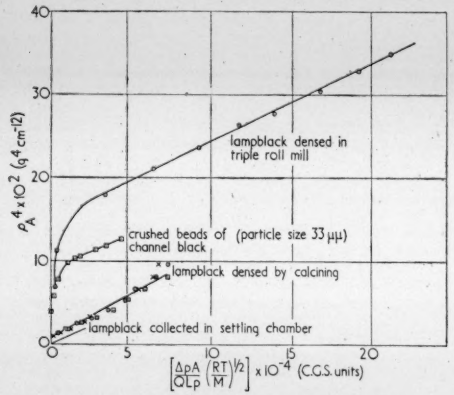

Fig. 3. The effect of "densing" on the permeability of blacks

Key to gases used: × hydrogen, ⊡ nitrogen, ○ argon.
Cell diameter 2·54 cm, bed height about 1·9 cm.
Mean pressure: atmospheric (approx.)

DISCUSSION

As the present investigation is mainly concerned with the validity of the porosity functions in equation (4) it is relevant to add to the reviews of Carman[4] and Rose.[5] Ergun[11] experimented with coarse non-porous particles (glass and sand) and gas flows corresponding to $R_e \simeq 50$. He verified Kozeny's porosity function $F_1(\epsilon)$ by using an equation similar to equation (3). Moreover, he was able to confirm that the particle density ρ_p obtained from the permeability measurements agreed with the pycnometric density of these non-porous particles. Arthur and co-workers[6] working in the region corresponding to $R_e \simeq 10$ confirmed the form of function $F_1(\epsilon)$ by means of equation (3). However, they did not verify their method by checking the particle density of non-porous particles. The present investigators working with strictly laminar gas flows ($R_e \simeq 10^{-3}$) have used equation (3) and confirmed the form of $F_1(\epsilon)$. The particle density ρ_p measured by the intercept method was, however, found to be consistently lower than the pycnometric density. This is illustrated in Fig. 4 which includes results for tungsten, natural graphite, zinc, crystalline alumina powders and a porous pitch coke powder. In view of the low values obtained for the particle density it is assumed that there is a stationary layer of gas about each particle. Moreover, it is clear that Kozeny's equation will under these conditions yield low values for the surface area S_v.

Carman and Malherbe[12] were the first to examine critically $F_2(\epsilon)$ and their work "shows clearly that it is inadequate." Other workers who have used this function, notably Arnell and Henneberry,[13] Kraus, Ross and Girifalco,[14] Barrer and Grove,[15] Rigden,[7] and Schwertz[16] were mainly concerned with the measurement of surface areas. Their work supports the form of $F_2(\epsilon)$ only inasmuch as the surface areas calculated on this assumption agreed with area measurements by other methods. As numerical values for constants such as δ, k_0 and k had to be assumed this is not conclusive.

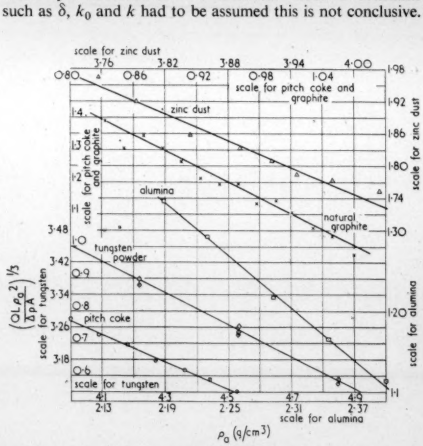

Fig. 4. Deviations from Kozeny's equation at very low rates of flow

		density	
		by xylene displacement	*by gas flow*
⊡	fused alumina	3·74	3·62
×	natural graphite	2·29	1·64
◈	tungsten powder	19·1	12·9
△	zinc dust	7·05	6·12
○	pitch coke	1·45	1·36

Arnell and Henneberry[13] have quoted results of permeability measurements on carbon blacks and it is possible to use these to test the validity of the proposed function:

$$F_3(\epsilon) \equiv (1-\epsilon)^{-4} \tag{8}$$

These authors plotted the mass rate of flow G against the mean pressure p and calculated the surface area from the equation

$$S_v = \frac{8}{3}\sqrt{\frac{2RT}{\pi M}} \cdot \frac{\delta \alpha \rho_1}{c}\left(\frac{\epsilon}{1-\epsilon}\right) \tag{9}$$

where $\log \alpha = 1{\cdot}41\epsilon - 1{\cdot}40$ and c is the intercept of the straight line plot of the mass flow rate G against the mean pressure p. (Carman and Arnell[9] later found it possible to dispense with α, with the result shown in equation (4).) Arnell and Henneberry's values for S_v have therefore been multiplied by $(1-\epsilon)/\alpha\epsilon$ and then plotted against $(1-\epsilon)^4$. The results shown in Fig. 5 are at least as consistent with straight lines as Arnell's values for the surface areas S_v are independent of ϵ.

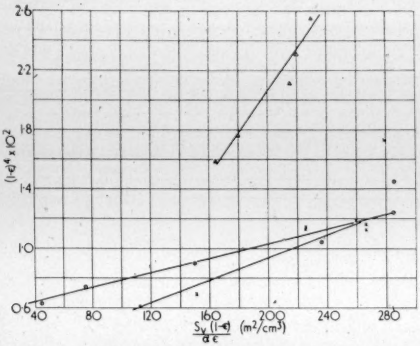

Fig. 5. Application of fourth power law to the data of Arnell and Henneberry[13]

		S_v (*determined from electron micrographs*)
○	Kosmobile S	162 m²/cm³
×	Kosmobile 77	161 m²/cm³
△	Statex B	72 m²/cm³

Carman and Malherbe[12] are opposed to substituting an empirical function for $F_2(\epsilon)$ as they believe that an individual porosity function would be required for every powder. However, an attempt has been made to test the proposed function $F_3(\epsilon)$ with the aid of their results. It is first assumed that the Poiseuille term in equation (4) makes a negligible contribution to the permeability of their powders. On this basis $S_v/F_2(\epsilon)$ was plotted against $(1-\epsilon)^4$ and the results are shown in Fig. 6. It is fair to say that the proposed function $F_3(\epsilon)$ applies. Moreover, it can be seen that the slopes of the lines correspond to the surface areas as measured by the nitrogen adsorption technique. This confirms the trends of the present investigation as reported above. Moreover, it is now possible to avoid the necessity for Carman and Malherbe's assumption that only the porosity range $\epsilon = 0{\cdot}4$–$0{\cdot}5$ is suitable for surface area measurements. Thus it is clear from Figs. 2–6 that this range is in no way distinguished from the remainder. There is, therefore, no reason to suppose that measurements obtained in their restricted range of porosities are less liable to errors arising from aggregation and channelling.

It is felt that the present results provide the framework of a simple method of measuring the surface areas of very fine

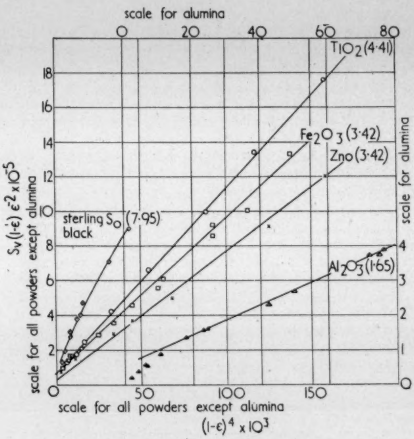

Fig. 6. The application of the fourth power law to the results of Carman and Malherbe[12]

(The figures in brackets are the values of $S_v \times 10^{-5}$.)

powders such as carbon blacks. Thus gas permeability measurements for beds of varying porosities could be plotted in accordance with the proposed porosity function. The slope of the resulting line should be a measure of the surface area, provided the bed is uniformly packed and there is no aggregation and "channelling." However, more work is necessary to establish an exact relationship between the slope of the line and the surface area as measured by, say, the electron microscope.

REFERENCES

(1) Kozeny, J. *Sitzb. Akad. Wiss., Wien*, **136**, p. 271 (1927).

(2) Fair, G. M., and Hatch, L. P. *J. Amer. Water Works Assoc.*, **25**, p. 1551 (1933).

(3) Donat. *Wasserkraft u. Wasserwirtsch.*, **24**, p. 228 (1929).

(4) Carman, P. C. *Trans Inst. Chem. Engrs [London]*, **15**, p. 150 (1937).

(5) Rose, H. E. *The measurement of particle size* (London: Constable and Co., 1953).

(6) Arthur, J. R., Linnett, J. W., Raynor, E. J., and Sington, E. P. C. *Trans Faraday Soc.*, **46**, p. 270 (1950).

(7) Rigden, P. J. *J. Soc. Chem. Ind.*, **66**, p. 130 (1947).

(8) Arnell, J. C. *Canad. J. Research A*, **24**, 103 (1946).

(9) Carman, P. C., and Arnell, J. C. *Canad. J. Research A*, **26**, p. 128 (1948).

(10) Lea, F. M., and Nurse, R. W. *J. Soc. Chem. Ind.*, **58**, p. 277 (1939).

(11) ERGUN, S. *Analyt. Chem.*, **23**, p. 151 (1951).
(12) CARMAN, P. C., and MALHERBE, P. LE R. *J. Soc. Chem. Ind.*, **69**, p. 134 (1950).
(13) ARNELL, J. C., and HENNEBERRY, G. O. *Canad J. Research A*, **26**, p. 29 (1948).
(14) KRAUS, G., ROSS, J. W., and GIRIFALCO, L. A. *J. Phys. Chem.*, **57**, p. 330 (1953).
(15) BARRER, R. M., and GROVE, D. M. *Trans Faraday Soc.*, **47**, p. 826 (1951).
(16) SCHWERTZ, F. A. *J. Appl. Phys.*, **20**, p. 1070 (1949).

DISCUSSION

Professor R. M. Barrer: The specific surface, S_V, as used by Davidson and Turk gives the area in cm^2 per cm^3 of the material of which the porous bed is composed. The specific surface, A, in my papers refers to the area in cm^2 per cm^3 of the porous bed. Thus $A = S_V(1 - \epsilon)$, and this substitution must be made in comparing their version of the flow equation with mine.

In general one must, for finely divided particles such as colloidal carbon blacks, keep in mind not only Poiseuille and Knudsen flow but also surface flow as shown in my Paper B.2. It is possible that surface flow may be a contributory factor to the curvature shown in Fig. 1 of that paper, and that deviations from the theoretical porosity function $\epsilon^2/(1 - \epsilon)$ are in part due to this. Also, accepting Davidson and Turk's porosity function as $F_3(\epsilon) = 1/(1 - \epsilon)^4$, then the linear parts of all curves of p_a^4 *versus* $A\Delta p/QLp(RT/M)^{\frac{1}{2}}$ should extrapolate back through the origin. In fact, however, inspection of Figs. 2 and 3 shows that the linear parts of the plots often fail to do this, sometimes by a substantial margin. The equation of this linear part is thus really:

$$p_a^4 = \text{const.} \times \frac{A\Delta p}{QLp}\left(\frac{RT}{M}\right)^{\frac{1}{2}} + \text{const.}$$

which gives for the empirical porosity function

$$F_3(\epsilon) = 1/[(1 - \epsilon)^4 - K]$$

where K is a constant. Thus any simplicity is lost, due to the adjustable parameter K, and one feels that no improvement has been achieved over the theoretical function $F_2(\epsilon) = \epsilon^2/(1 - \epsilon)$. One would in general question whether it is wise to try to replace the theoretical function by any empirical one, for even if the theoretical function $F_2(\epsilon)$ were less exact than an empirical one, it has the great advantage of having a physical interpretation.

Authors' reply: On consideration we think that the curvature found in our Fig. 1 is not primarily due to surface flow. According to Prof. Barrer, such flow is independent of the molecular weight of the permeating gas (equation 10, Paper B.2). However, our curves for different gases show close dependence on $\sqrt{M}$.

If, then, negligible surface flow is assumed, one is faced with two alternatives. Either one accepts an arbitrary "normal porosity" range in which deviations from the Carman–Arnell equation cannot be detected, or one must proceed from an empirical function such as ours. The disadvantage in our approach, as Prof. Barrer observes, is that anomalies arise on attempting to extrapolate our lines to the origin. Further, results such as presented in our Figs. 2, 3 and 6 extrapolate to finite flow-rates for $l_a \geqslant l_x$. This is disappointing as we had hoped to use the method for the measurement of the "particle density" of agglomerated carbon blacks.

Paper B.4

Electroviscosity in dilute heterodisperse suspensions

By G. A. H. ELTON, Ph.D., F.R.I.C., Battersea Polytechnic, London, and F. G. HIRSCHLER, Ph.D., Deering Products Ltd., London

It is shown that the ionic content of the suspending medium is of importance in determining the velocity of sedimentation of particles in the micron size range.

Calculations are made for the effect of electroviscosity on the rate of separation of particles by the sedimentation method, and it is concluded that in extreme cases it may not be possible to separate particles differing in size by up to 25%.

The elimination of the electroviscous effect in sedimentation analysis is discussed, and it is shown that the effect can generally be eliminated by carrying out the sedimentation in a moderately concentrated electrolyte solution.

Most solid particles when suspended in an electrolyte solution carry a charge produced either by surface ionization or by preferential ion adsorption. As a result of this, a potential gradient is set up when the particles fall through the solution, in such a direction as to resist the motion of the particles. This electroviscous resistance may, in suitable circumstances, represent an appreciable fraction of the total resistance to motion.[1,2,3] In a heterodisperse suspension of a given solid, the larger particles (which carry a bigger total surface charge than the smaller particles) experience a greater electroviscous retarding force, so that the rate of separation by sedimentation is decreased. In this paper, calculations are made for some simple cases to illustrate the possible importance of the electroviscous effect in sedimentation analysis.

FORMATION OF A SHARP SEDIMENTATION MENISCUS

It is found experimentally[4,5] that a specimen of particles of fairly narrow size range (of order $\pm 10\%$ about a mean size in the micron range) forms, in dilute suspension in water or dilute aqueous electrolyte solution, a sharp settling "meniscus" (between the clear liquid and the suspension) which moves at a constant rate. In non-aqueous dispersion media, or in concentrated aqueous electrolyte solutions, where electroviscosity is small,[3,4,6] or when particles are conducting, no such sharp meniscus is obtained.[5,6] If we arbitrarily take as a criterion of sharpness that all the particles should have the same velocity $\pm 1\%$, then we find from Stokes' equation that in the absence of electroviscosity the particles (if spherical) would have to be of the same radius

within $\pm 0{\cdot}5\%$, so that, for example, for particles of radius about 1 μ, a difference of only $\pm 5 \times 10^{-7}$ cm is permissible. Such constancy is virtually impossible to obtain and, as shown below, the formation of a sharp meniscus in a dilute suspension is largely due to the operation of the electroviscous effect.

HOMODISPERSE SUSPENSION CONTAINING A FEW SMALLER PARTICLES

Consider a dilute homodisperse suspension containing N_1 spherical particles of radius a_1 per unit volume of suspension. The particles will settle under gravity with a velocity u_1, given[2] by

$$u_1 = \frac{2}{9\eta} a_1^2(\rho_2 - \rho_1)g - \frac{2}{3\eta} Ea_1\sigma \tag{1}$$

where ρ_1, ρ_2 are the densities of dispersion medium and particles respectively, η is the viscosity of the dispersion medium, g is the gravitational constant, and E is the sedimentation potential gradient, given by

$$E = 4\pi a_1^2 \sigma u_1 N_1/\kappa \tag{2}$$

where κ is the specific conductivity of the suspension, and σ is the electrokinetic charge per unit area on the particles. Equations (1) and (2) are derived on the assumption that a_1 is sufficiently large to render diffusion under Brownian forces negligible, and also that the suspension is so dilute that negligible viscous interaction occurs between the particles. For accurate work they are usually only applied for volume fractions (ϕ) of solid up to about 1×10^{-3}. Contribution of the volume effect of the spheres to the viscosity (cf. the Einstein equation) is negligible in this range.

The sedimentation potential gradient in terms of the volume fraction is thus

$$E = \frac{3\sigma u_1}{a_1\kappa}\phi \tag{3}$$

Hence from equations (1) and (3)

$$\frac{u_1^0}{u_1} = 1 + \frac{2\sigma^2\phi}{\eta\kappa} \tag{4}$$

where u_1^0 is the velocity of sedimentation in the absence of electroviscosity, given by

$$u_1^0 = \frac{2a_1^2(\rho_2 - \rho_1)g}{9\eta} \tag{5}$$

If a few particles of radius a_2 (less than a_1) are present, they will tend to be left behind as the suspension settles. They will thus pass out of the sedimentation field, and settle with velocity u_2^0, given by

$$u_2^0 = \frac{2a_2^2(\rho_2 - \rho_1)g}{9\eta} \tag{6}$$

If this velocity is less than u_1, the smaller particles will be permanently left behind, but if not they will return to the suspension, and tend to congregate at the meniscus. If this is to occur, and a sharp meniscus is to be formed, we require that

$$u_2^0 \geqslant u_1 \tag{7}$$

Hence, from equations (4), (5), (6) and (7), we have

$$\frac{a_2}{a_1} \geqslant \left(1 + \frac{2\sigma^2\phi}{\eta\kappa}\right)^{-\frac{1}{2}} \tag{8}$$

Table 1 shows minimum permissible values of a_2/a_1 calculated from equation (8) for a suspension of Pyrex spheres[2,4] of volume fraction 1×10^{-3} in some dilute aqueous potassium chloride solutions at 25° C. It is seen that the electroviscous sharpening effect is greatest in the most dilute electrolyte solutions, and decreases fairly rapidly as the concentration rises. Good quality distilled water (having conductivity of about $4 \times 10^{-6}\ \Omega^{-1}\ \text{cm}^{-1}$) is roughly equivalent to $2 \times 10^{-5}\ N$ potassium chloride solution, and it is seen that in this case particles up to about 25% smaller than the majority will settle at the same rate.

Table 1. *Minimum permissible values of a_2/a_1*

KCl normality	$(a_2/a_1)_{min}$
1×10^{-5}	0·716
2×10^{-5}	0·745
5×10^{-5}	0·783
1×10^{-4}	0·820
2×10^{-4}	0·853
5×10^{-4}	0·890
1×10^{-3}	0·913
2×10^{-3}	0·940

HOMODISPERSE SUSPENSION CONTAINING A FEW LARGER PARTICLES

If the suspension considered in the previous section contains a few larger particles of radius a_3, these will fall away from the meniscus, the rate of separation being $(u_3 - u_1)$, where

$$u_3 = u_3^0 - \frac{2a_3u_1\sigma^2\phi}{\eta\kappa a_1} \tag{9}$$

$(u_3 - u_1)$ will be less than $(u_3^0 - u_1^0)$, the rate of separation in the absence of electroviscosity, and

$$\frac{u_3 - u_1}{u_3^0 - u_1^0} = 1 - \frac{9u_1\sigma^2\phi}{a_1g\kappa(\rho_2 - \rho_1)(a_1 + a_3)} \tag{10}$$

Table 2 gives values of the ratio $(u_3 - u_1)/(u_3^0 - u_1^0)$ calculated from equation (10) for larger particles of various radii in a suspension of Pyrex spheres (radius 1 μ, volume fraction 1×10^{-3}), in dilute aqueous potassium chloride solutions at 25° C.

Table 2. *Values of $(u_3 - u_1)/(u_3^0 - u_1^0)$ calculated from equation (10)*

KCl normality	$a_3 = 2\ \mu$	$a_3 = 5\ \mu$	$a_3 = 10\ \mu$
1×10^{-5}	0·838	0·919	0·956
2×10^{-5}	0·852	0·926	0·959
5×10^{-5}	0·871	0·935	0·965
1×10^{-4}	0·891	0·945	0·970
2×10^{-4}	0·909	0·955	0·975
5×10^{-4}	0·931	0·965	0·981
1×10^{-3}	0·944	0·972	0·985
2×10^{-3}	0·961	0·981	0·989

It is seen that the relative rate of separation is decreased markedly in dilute solutions, the effect decreasing with increasing concentration. Taking distilled water as roughly equivalent to $2 \times 10^{-5}\ N$ potassium chloride solution, we see, for example, that in distilled water the rate of separation of a few 2 μ particles from the 1 μ particles is about 15% less than in the absence of electroviscosity. The effect is of smaller significance for larger particles.

HETERODISPERSE SUSPENSION

It has been shown above that in an otherwise homodisperse suspension, a few particles smaller than the majority

may not be separated at all by a sedimentation process in the presence of electroviscosity; if a few larger particles are present, they may be separated, but the rate of separation will be decreased. In the case of a heterodisperse suspension, the problem of evaluating the rates of sedimentation is a complex one, and only a qualitative discussion will be given here. If a heterodisperse suspension, initially uniformly distributed in the dispersion medium, is allowed to settle, it will remain uniform below the level of the "meniscus" of the largest particles present in the suspension. All particles within the uniform zone will settle at a velocity which is characteristic of their particle size, and which does not change with time while the particles are within the field of the uniform suspension. As the largest particles settle out, the field in which any given particle of other size is falling will decrease with increasing time, so that the velocity of the particle will increase with time. Furthermore, particles of identical size which are at different heights will, in general, be in different potential fields, so that the velocity of a particle of radius a will, in the presence of electroviscosity, be a function not only of a, but also of height h, time t, and particle size distribution D, that is,

$$u_a = F(a, h, t, D) \qquad (11)$$

Solution of this equation is not possible unless D is known, i.e. unless we can solve the equation

$$N_a = f(a) \qquad (12)$$

where N_a is the number of particles per unit radius range at radius a. However, we may conclude by analogy from above that the effect of electroviscosity will be to decrease the rate of separation by sedimentation of particles of different size. Since the usual object of sedimentation experiments on heterodisperse suspensions is to effect separation, or to determine the relation expressed in equation (12), it is better to eliminate the effect of electroviscosity, when equation (11) reduces to

$$u_a = \text{constant} \times a^2 \qquad (13)$$

This may be done by carrying out the experiment either in a non-electrolyte dispersion medium, or in moderately concentrated electrolyte solutions, where as seen from Tables 1 and 2, the effects of electroviscosity are small. Usually no observable electroviscous effect is obtained in electrolyte solutions of ionic strength greater than 0·1 *N*. The usual equations used in sedimentation analysis are then adequate.

REFERENCES

(1) Elton, G. A. H. *Proc. Roy. Soc. A*, **197**, p. 568 (1949).
(2) Hirschler, F. G. *Ph.D. thesis*, University of London (1951).
(3) Dulin, C. I., and Elton, G. A. H. *J. Chem. Soc.*, p. 286 (1952).
(4) Elton, G. A. H., and Hirschler, F. G. *J. Chem. Soc.*, p. 2953 (1952).
(5) Dulin, C. I., and Elton, G. A. H. Unpublished work.
(6) Dulin, C. I., and Elton, G. A. H. *J. Chem. Soc.*, p. 1168 (1953).

DISCUSSION

Mr. J. B. J. Zaba: Have the sedimentation volume and microscopic particle size of the sediment been measured in systems where electroviscosity was observed? These two measurements may help to find whether there was a coagulation (flocculation) of the particles caused by the addition of electrolytes.

Mr. R. Johnson: A year or so ago I was perturbed when I read that variation in speed of sedimentation was due to the effects of electroviscosity. I had been led to believe that for dilute suspensions decreases in settling rates with additions of appropriate electrolyte were due to dispersion or deflocculation of the suspended material. A test we use for determining the amount of deflocculant needed for a sedimentation size analysis is to find the amount of deflocculant which gives minimum sedimentation. We seem to have ignored electroviscosity. I would like to ask if Dr. Elton has considered coagulation, because I carried out some tests on 600's carborundum suspended in distilled water and *N*/100 potassium chloride and obtained the following evidence that coagulation was responsible for the increased settling rate in that instance.

(1) The appearance of the "potassium chloride sediment" was typical of that from a coagulated suspension. The "water sediment" was not.
(2) For the same concentrations the optical density of the water suspension was slightly greater than that of the potassium chloride suspension.
(3) Microscopic examination of five comparisons by five people gave universal agreement that the material in N/100 potassium chloride was coarser than in distilled water.
(4) The permeability of the "potassium chloride sediment" was greater than the "water sediment."

It could have been convenient for me in connexion with a problem on centrifugal sedimentation to accept this idea of electroviscosity, but my experimental evidence compels me to attribute increases in rate of gravitational sedimentation to coagulation.

Prof. F. R. Eirich: In view of the confusion in the colloid chemical nomenclature already existing, I want to appeal to the authors not to add to it by applying the term "electroviscous effect" to other than the by now well investigated phenomenon of viscosity increase due to charges on particles. The classical electroviscous effect has been studied, calculated and named by v. Smoluchowski[1] forty years ago, and has further been treated by Krasny-Ergen,[2] and Guth.[3] Additional charge effects on viscosities have more recently been established and analysed by Fuoss and Strauss[4] and Onsager,[5] by Kuhn, Kuenzle and Katchalsky,[6] Hermans and Overbeck[7] and others.

To call the delayed sedimentation of charged particles or polyelectrolytes, described by the authors, an electroviscous effect is further, in my opinion, a misnomer. This retardation has very little to do with an increase in viscosity but, as the authors describe it themselves, is a preponderantly electrophoretic effect. As such, it was first described by Tolman[8] and was then studied and the theory further developed by Svedberg's school, in particular by Tiselius[9] and Pedersen[10] in 1932. The rest of the literature on the subject is too extensive to be quoted here and includes investigations on how to eliminate the effect by the addition of electrolytes. Other theories have dealt with the sharpening of boundaries in regular electrophoresis, as, for instance, in recent work by Svensson.[11]

Authors' reply: In reply to Mr. Johnson, coagulation occurs, especially on standing, in solutions where the electro-

kinetic potential is low (especially when it is less than 30 mV; see Dulin and Elton[12]). When a sediment of coagulated particles is shaken to form a suspension, the usual sharp meniscus is not obtained, and the sedimentation velocity depends on the degree of agitation. Microscopic observation of samples from such suspensions indicates that agglomerates of various sizes are present. In all cases that we have studied (using a volume fraction of particles up to 10^{-3}) vigorous shaking for about I hour on a mechanical shaker is sufficient to break up the aggregates and produce a sharp meniscus and a reproducible sedimentation velocity. If the suspension is allowed to settle out and stand for a short while, coagulation again occurs.

Mr. Johnson used suspensions of carborundum in 10^{-2} *N* potassium chloride solution, where the electrokinetic potential (estimated by extrapolation of the results of Elton and Mitchell,[13] and Fairbrother and Mastin[14]) is probably 30–50 mV, and coagulation, especially on standing, is likely in this case. In very dilute solutions (less than 10^{-3} *N*), where the electrokinetic potential is fairly high, appreciable coagulation does not occur.

It must be emphasized that in work of this kind, the greatest care must be taken to exclude contamination, especially grease, small traces of which can greatly influence the electrokinetic potential. For this reason, the use of ordinary distilled water, which is often contaminated with grease, is not to be recommended for accurate work. Conductivity water should be used, and the solid must be carefully cleared before use. As illustration of this, some experimental results of Elton[15] on electroviscous effects in narrow channels were criticized by Derjaguin and Kusakov,[16] who obtained results of an entirely different order. However, Evans and Ewers,[17] and Evans[18] showed that when extreme care was taken to exclude impurities, Elton's results were duplicated, but when solutions containing 3×10^{-6} *M* surface active impurity were used results were obtained which were in agreement with those obtained by Derjaguin and Kusakov in nominally "pure" water.

In reply to Mr. Zaba, a few experimental results and some theoretical calculations on sediment volumes of carborundum particles in potassium chloride solutions have been given by Dulin.[19]

In reply to Dr. Eirich, I think that we are justified in using the term "electroviscous effect" to describe this phenomenon, since here, as in the cases considered by v. Smoluchowski and others cited by Dr. Eirich, a decrease in the rate of shear is produced in the system as a result of a process occurring in the electrical double layer at the particle/liquid interface.

REFERENCES

(1) Smoluchowski. *Kolloid. Z.*, **18**, p. 194 (1916).
(2) Krasny-Ergen. *Kolloid. Z.*, **74**, p. 172 (1936).
(3) Guth. *Kolloid. Z.*, **74**, p. 152 (1936).
(4) Fuoss and Strauss. *J. Polym. Sci.*, **3**, p. 246 (1948).
(5) Onsager. *Ann. N.Y. Acad. Sci.*, **51**, p. 627 (1949).
(6) Kuhn, Kuenzle and Katchalsky. *Helv. Chim. Acta.*, **31**, p. 1994 (1948).
(7) Hermans and Overbeck. *Rec. Trav. Chim.*, **67**, p. 761 (1948).
(8) Tolman. *J. Amer. Chem. Soc.*, **33**, p. 121 (1911).
(9) Tiselius. *Kolloid. Z.*, **59**, p. 306 (1932).
(10) Pedersen. *Forhand Nord. Kjemikermate* [*Oslo*], **4**, p. 250 (1932).
(11) Svensson. *Arch. f. Kemie A*, **22**, p. 1 (1946).
(12) Dulin and Elton. *J. Chem. Soc.*, p. 1168 (1953).
(13) Elton and Mitchell. *J. Chem. Soc.*, p. 3690 (1953).
(14) Fairbrother and Mastin. *J. Chem. Soc.*, **125**, p. 2319 (1924); **127**, p. 332 (1925).
(15) Elton. *Proc. Roy. Soc. A*, **194**, p. 275 (1948).
(16) Derjaguin and Kusakov. *J. Phys. Chim. U.S.S.R.*, **26**, p. 1536 (1952).
(17) Evans and Ewers. *Symposium on Recent Developments in Mineral Dressing*, Institution of Mining and Metallurgy, p. 457 (1953).
(18) Evans. *Nature*, **172**, p. 776 (1953).
(19) Dulin. *Ph.D. thesis*, University of London, pp. 178–198 (1953).

SESSION C. SCATTERING AND ABSORPTION OF LIGHT BY PARTICLES

Chairman: Prof. F. T. GUCKER, JR., Ph.D.

Survey of scattering and absorption of light by particles

By C. N. DAVIES, D.Sc., F.Inst.P., Medical Research Council

The diffraction approximation and exact Mie theory, for treating light scattering by particles, are briefly compared for different sizes. Attention is drawn to the simplification of the screening function which occurs if the particles are opaque. Methods of measuring small particles in the presence of large ones are discussed and reference is made to new techniques for measuring particle concentration.

It is a common experience that a mathematical boundary value problem may possess more than one type of solution. Under certain conditions one of these will be relatively easy to compute but, as the range is extended, difficulties increase, series oscillate for many terms and the results become uncertain. When this happens another solution may yield an amenable formula which becomes easier to handle the farther one proceeds in the direction which led to trouble in the former case.

The Mie theory of light scattering by particles provides an example. This solution of Clerk Maxwell's electromagnetic equations gets tiresome when the ratio of the particle circumference to the wavelength of light exceeds about 10. It has been shown by Vouk[1] that when this ratio is large the theory tends, under suitable conditions, to the classical theory of diffraction by opaque disks. An independent, exact solution of the electromagnetic equations which gives the diffraction equations directly is lacking, however, and, if found, might well prove of great value in dealing with large particles in general.

There has been a significant difference in the approaches to this problem which have been adopted in Europe and in the United States. The theory came from Germany, set upon British foundations. Quite a lot of experimental work and computation was carried out in Europe before the war and has never been adequately reviewed. The war led to great activity in the United States, where the system of allocating large government contracts to universities has enabled remarkable computing programmes to be put in hand using the most modern automatic equipment and extending up to high values of the circumference-wavelength ratio.

Recourse to mechanical computing was not possible in Europe and the approach through the diffraction approximation was fully exploited, notably by Bricard.[2]

It was Frenchmen, too, who first demonstrated that the intensity of light in the bright spot in the centre of the shadow behind a particle is equal to that of the incident beam (Fresnel, Poisson, Arago). For large particles, most of the diffracted light goes into this central spot and since the total amount of light diffracted is equal to that which is incident on the particle, according to Babinet's principle, measurements of the extinction of light by particles are very sensitive to the angle of acceptance of the light recording device, when this is small.

Sinclair[3] showed how the apparent area of particles could be doubled by simply moving his photocell farther away from the suspension; failure to appreciate this point has caused many experimental results to have little value.

When the particles are transparent, the diffraction effect is supplemented by light which has been reflected from the outer surface of the particle, without penetration, and by light which has entered and been internally reflected and refracted. The theory of these geometrical processes is due to Wiener.[4] Such phenomena are of interest in meteorology. Bricard's work shows that diffraction makes the major contribution to forward scattering so that transparent and opaque particles have quite similar screening effects and cannot easily be distinguished when looked at against the light.

Gumprecht and Sliepcevich[5] have compared the results of diffraction calculations with machine computed data from the Mie theory for particles up to 400 wavelengths in circumference. They show that the forward scattered intensities differ appreciably, but that the ratios of forward to total scattering are in better agreement. They did not take account of reflected and transmitted light, in the manner of Bricard, and it would be interesting to know if the agreement between the approximate and the exact theories might not be better if this were done.

Their results confirm what has been the basis of experiments by Vouk and Ellison in my own laboratory, however; namely that, for practical purposes, the extinction of light by particles, whether opaque or transparent, can often be treated by diffraction theory alone provided that they are not too small and that suitable precautions are taken in designing the measuring apparatus.

The work referred to so far has been concerned with particles whose circumference is at least five or ten times the wavelength of light; this corresponds, roughly, to particles over one micron in diameter. Practically all the scattered light is then confined within 10° or less of the original direction of propagation.

In principle, of course, the Mie theory covers all sizes of particles but what continental physicists call the "Mie Effect" is associated with particles between the large ones, discussed above, and the very small ones—less than about a quarter of a wavelength in circumference, say 0·04 μ in diameter, which exhibit Rayleigh scattering. This is symmetrical fore and aft; the Mie effect is the growing tendency towards forwards scattering with increasing particle size.

Through the Mie region the total scattering coefficient fluctuates with an amplitude which decreases and dies away in the diffraction region. Lewis and Lothian in Paper C.2 show in their paper how the peaks of these fluctuations for particles having different refractive indices can be made to coincide on a graph, following a suggestion of van de Hulst[6] which now seems well established both theoretically and

experimentally. Mr. Lothian has been very careful to define angles of illumination and acceptance of his optical system.

These fluctuations are due to interference between light transmitted through the particle and the undisturbed beam. There are fluctuations of intensity with angle of observation as well as fluctuations of the total scattering. The maxima can be located if the particles in suspension are fairly uniform in size and have been used as a means of measuring size. As Mr. Ellison points out in Paper C.1, the principle involved is the same whether the angle of scattering or the wavelength is varied when searching for intensity maxima.

If the particles absorb light the maxima are suppressed, clearly because the transmitted beam is absorbed and cannot interfere with the undisturbed beam. This is shown very well in the results of recent computations by J. C. Johnson[7]. It means that calibration of an instrument measuring the cross-sectional areas of particles by axial light extinction is much simpler for opaque particles than it is for transparent.

The total screening coefficient for most opaque particles does not seem to fluctuate far from the value 2 as long as they are over about half a micron in diameter. Transparent particles increasing from this size upwards may have screening coefficients varying over a ten-fold range.

Another practical point, which might be taken advantage of, is that a rising sensitivity with decreasing particle size can be achieved by accepting light over an angle of, say 5°, thus diminishing the screening caused by particles which are greater than about 5 microns diameter. This will not balance out the inherent area screening which biases all photometric measurements towards the larger sizes present in a non-uniform cloud of particles, referred to by Mr. Ellison, but it is a step in that direction.

Sensitivity to small particles in the presence of large ones is best achieved by varying wavelength. Variation of the screening coefficient with wavelength is very much more rapid in the Rayleigh region than elsewhere.

Use of this principle has recently enabled the presence of very small water droplets to be demonstrated in clouds which had been thought to contain only large ones. The apparatus, due to Keily,[8] used a beam of infra-red and scanned wavelengths between 1 and 10 μ with a Perkin–Elmer spectrograph provided with automatic slit adjustment to allow for the varying absorption coefficient of water.

An interesting method of measurement using wavelengths very long compared with the particle has recently been developed by Thatcher and Dorain.[9] Smoke particles are passed into a cavity resonator in a microwave refractometer operating at 9400 Mc/s and the change in dielectric constant due to the particles is measured. The great sensitivity required is obtainable with microwave technique. The instrument measures the volume of the particles and is not very sensitive to their physical properties.

Another novel suggestion has been made by Cassell[10] who proposes to use a thin thread of light traversing a dust cloud in place of the usual, more substantial beam. Particles drift in and out of the beam and cause the transmitted intensity to fluctuate. Application of Smoluchowski's[11] theory of fluctuations of density, as in critical phenomena, enables the number concentration of particles to be deduced.

The size distribution in a non-homogeneous cloud of particles can be determined, if they are large enough in comparison with the wavelength for the scattering to be due to diffraction. If the particles are below about 1 μ in size it is necessary to use X-rays instead of light. The method consists of measuring the intensity distribution across the central bright spot of transmitted light and converting it into the particle size distribution, on a diameter squared basis, by means of a Mellin transformation. The theory has been given by Riseman[12].

REFERENCES

(1) Vouk, V. B. *Ph.D. thesis*, University of London (1948).
(2) Bricard, J. *J. Phys. Radium*, **4**, p. 57 (1943); *Ann. Géophys.*, **2**, p. 231 (1946).
(3) Sinclair, D. *J. Opt. Soc. Amer.*, **37**, p. 475 (1947).
(4) Wiener, C. *Nova Acta K. Leopold. Dtsch. Akad. Naturforschung, Halle*, **73**, p. 3 (1907); **91**, p. 81 (1910).
(5) Gumprecht, R. O., and Sliepcevich, C. M. *J. Phys. Chem.*, **57**, p. 90 (1953).
(6) van de Hulst, H. C. *Ph.D. thesis*, University of Utrecht (1946).
(7) Johnson, J. C. *Mass. Inst. Tech., Dept. of Meteorology Report*, AF 19 (122)–245 (1953).
(8) Keily, D. P. *Mass. Inst. Tech. Dept. of Meteorology Report*, AF 19 (122)–245 (1953).
(9) Thatcher, H. C. *J. Phys. Chem.*, **56**, p. 795 (1952). Thatcher, H. C., and Dorain, P. In course of publication.
(10) Cassell, H. M. Private communication from Bureau of Mines, Pittsburgh, Pa., U.S.A. (1954).
(11) Smoluchowski, M. von. *Ann. Phys.* [*Leipzig*], **25**, p. 205 (1908).
(12) Riseman, J. *Acta. Cryst.*, **5**, p. 193 (1952).

Paper C.1

Light scattering by polydisperse dust clouds*

By J. McK. Ellison, B.A., Ph.D., Medical Research Council's Environmental Hygiene Research Unit, London School of Hygiene and Tropical Medicine, London, W.C.1

When light is scattered by a cloud of particles of a wide range of sizes, the intensity scattered in any direction is built up from the contributions of particles of all dimensions. For forwards scattering the relative values of these contributions have been calculated as a function of diameter, by two different approximate formulae for the angular distribution of the light scattered by spheres. The approximations used are: (1) that of Rayleigh and Gans, and (2) Kirchhoff diffraction by opaque circular disks. For the latter, the scattering by a cloud of disks whose diameters are log-normally distributed with a standard geometric deviation of 2·03 has also been computed. It is concluded that the predominance of the light scattered by larger particles limits the usefulness of light scattering as a means of obtaining a mean particle size to suspensions containing a comparatively narrow range of particle sizes.

The general nature of the dependence of light scattering on particle size is well known. The scattering by coarse suspensions is concentrated forwards, whereas with finer suspensions this concentration is less marked. The finest suspensions look slightly blue by scattered light and markedly yellow by transmitted light. Phenomena so noticeably size-dependent merit investigation as potential means of particle size analysis. It is the purpose of this paper to investigate the scattering of light by polydisperse suspensions of particles of diameters in the range 0·5 to 10 μ.

LIGHT SCATTERING BY SPHERES

The exact calculation of the angular distribution of the intensity of light scattered by a particle illuminated by a parallel beam is extremely complex. For spheres, this calculation has been carried out by Mie; using van de Hulst's formulation of Mie's equations,[1] the intensity scattered per unit of solid angle and per unit area of cross-section of particle may be expressed in terms of $x = 2\pi r/\lambda$ (where r is the radius of the sphere and λ the wavelength of the incident light in the medium surrounding it), the relative refractive index m, and the angle θ between the directions of propagation of the incident and scattered beams.

For particles of diameter greater than the wavelength of the incident light, however, Mie's equations are too cumbersome to apply in the present instance. For these particles one or other of two approximations can often be used. The approximations available are those of: (*a*) Rayleigh and Gans (applicable to transparent particles if $2x(m-1) \ll 1$), and (*b*) Mecke ($2x(m-1) \gg 1$ and $x > 10$, approximately).

(*a*) *The Rayleigh–Gans approximation.* According to this approximation, each element of the particle is regarded as scattering independently, in accordance with Rayleigh's equation. The scattered amplitudes recombine with one another and in the case of the spheres give rise to an intense central spot surrounded by a series of bright and dark rings. The intensity scattered by a single particle at angle θ is:

$$P(x, z) = \frac{\lambda^2}{8\pi^2} x^6 \left(\frac{m^2-1}{m^2+2}\right)^2 G^2(z)(1+\cos^2\theta) \qquad (1)$$

where $z = 2x \sin\theta/2$, $G(z) = \sqrt{(9\pi/2z^3)}J_{3/2}(z)$, and $J_{3/2}(z) = \left(\frac{\sin z}{z} - \cos z\right)\sqrt{\frac{2}{\pi z}}$ = Bessel function of first kind of order 3/2.

(*b*) *Mecke's approximation.* This approximation regards the scattered light as being divisible into two components, each involving a light flux equal to that incident on the geometrical cross-section of the particle. One of these components is treated in accordance with geometrical optics, and its angular distribution is therefore independent of particle size. The other is supposed to be scattered near the forwards direction according to Kirchhoff's theory of diffraction, applied to an opaque circular disk of the same radius. Kirchhoff's theory is valid if $\cos\theta \simeq 1$ and if x is large. The intensity diffracted by a single particle is then:

$$P(x, z) = \frac{\lambda^2}{4\pi} x^4 \left[\frac{J_1(z)}{z}\right]^2 \qquad (2)$$

where $z = x \sin\theta$ and $J_1(z)$ is the Bessel function of the first kind of order 1. As long as θ is small, the parameters z used in the two approximations are equal.

THE LIMITATIONS ON THE RANGE OF APPLICATION OF THE APPROXIMATIONS USED

The limitations on the range of application of the two approximations arise from the nature of the simplifications on which they are based.

The Rayleigh–Gans approximation depends on the assumption that all parts of the particle are electrically polarized by an incident beam whose intensity is the same at all parts of the particle and whose phase is not appreciably affected as it passes through it. Both of these are equivalent to the condition that $2x(m-1) \ll 1$. If m is so large that, in order to satisfy this condition, $x < 0{\cdot}5$, the scattering may be regarded as being in accordance with Rayleigh's equation and the Rayleigh–Gans approximation is unnecessary.

The Mecke approximation in the form used here assumes that the diffracted and geometrical components can be treated separately, which depends on the former being scattered through small angles and the latter through wider angles. The angular dimensions of the diffraction pattern are proportional to $1/x$ and those of the central part of the geometrical pattern are proportional to $(m-1)$, so that the product $x(m-1)$ must be large if they are not to overlap. x must also be large if Kirchhoff diffraction is to be applicable.

Table 1 shows the ranges of particle size appropriate to the two types of scattering for various representative values of the relative refractive index. The diameters are calculated on the basis of a wavelength of 0·546 μ in air (mercury green).

Quoted in these forms, these two approximations are valid for scattering by spheres only, but it is clear that the same general methods of treatment can be applied to particles of other shapes. The Rayleigh–Gans scattering by randomly orientated non-spherical particles of various shapes has been calculated in connection with the scattering of light by

* This work formed part of a thesis submitted to the University of London for the Ph.D. degree.

polymer solutions (see, for example, Oster[2]). These calculations show that particle shape substantially modifies the scattering diagram, but they refer to extremes of shape (rods and coils) which it is not intended to consider here.

Table. 1. *Ranges of particle size corresponding to different types of scattering*

Suspension	*Relative refractive index*	*Upper limit of Rayleigh–Gans scattering,* $2x(m-1)=\frac{1}{2}$ *(d in microns)* x	d	*Lower limit of Mecke scattering,* $2x(m-1)=2$ *or* $x=10$ *(d in microns)* x	d
Lead monoxide in air	8/3	*0·15	0·026	10	1·74
Quartz in air	14/9	0·45	0·078	10	1·74
Water in air	4/3	0·75	0·13	10	1·74
Quartz in water	7/6	1·5	0·20	10	1·30
Quartz in paraffin	21/20	5·0	0·59	20	2·35
†PTFE in water	21/20	5·0	0·65	20	2·60

* Size corresponds to Rayleigh scattering.
† PTFE = Poly-tetra-fluoro-ethylene, $m = 1{\cdot}40$.

For "compact" particles it seems probable that the scattering diagram will not be very different from that of spheres of the same volume. With Kirchhoff diffraction, Vouk[3] shows that the distribution of intensity of light diffracted by opaque non-circular screens is very similar to that diffracted by circular screens as long as only the light near the central maximum of intensity is considered, and as long as the screens are not too extreme in shape. In both cases, therefore, the calculations which follow have been based on the assumption of spherical particles.

THE TYPES OF SCATTERING MEASUREMENTS WHICH ARE SENSITIVE TO PARTICLE SIZE

(*a*) *Polarization of scattered light.* In general, the light scattered by fine particles is polarized, and in some circumstances the polarization has been used as an indication of particle size. Incident unpolarized light may be regarded as consisting of two components, one polarized in and one normal to the plane of scattering, and with particles possessing spherical symmetry these can be treated independently. In the Rayleigh and the Rayleigh–Gans regions the ratio of the two scattered components is, however, $\cos^2\theta$, and the light scattered in accordance with Kirchhoff's theory of diffraction is unpolarized. In neither case, therefore, does the polarization of the scattered light depend on size.

(*b*) *Relative refractive index of particles and medium.* If the wavelength of the incident light in the suspending medium is fixed, the intensity of Rayleigh and Rayleigh–Gans scattering is proportional to $(m^2-1)^2/(m^2+2)^2$, but its angular distribution is independent of the relative refractive index m. Under the same conditions scattering according to Kirchhoff's theory of diffraction is independent of m without reservation. Consequently, any changes brought about by varying the relative refractive index of the incident light arise from the change of the effective wavelength λ.

(*c*) *Wavelength of incident light* λ. The wavelength appears in $P(x, z)$ both as a multiplier contained in λ^2x^6 [equation (1)] and λ^2x^4 [equation (2)], and also in the argument z of the functions $G^2(z)$ and $J_1^2(z)/z^2$. λ^2x^6 and λ^2x^4 are respectively equal to $64\pi^6r^6/\lambda^4$ and $16\pi^4r^4/\lambda^2$, and in each case the terms $1/\lambda^4$ and $1/\lambda^2$ affect by the same factor the scattering by particles of all sizes and the scattering in all directions. On the other hand, in the terms involving z the change in λ is equivalent to a change in $1/\sin\theta$. It can therefore be assumed that any set of scattering measurements intended to throw light on the particle size of the scattering material is equivalent to a corresponding set of measurements of the intensity scattered at different angles.

LIGHT SCATTERING BY POLYDISPERSE CLOUDS

Any measurement of the light scattered by a polydisperse cloud measures an integral of the product of the size distribution function $F(x)$ and the scattering function $P(x, z)$

$$I(\theta) = \int_{x=0}^{\infty} F(x)P(x, z)dx \qquad (3)$$

For the approximations under consideration, Rayleigh–Gans scattering and Kirchhoff diffraction, $P(x, z)$ takes the forms given by equations (1) and (2) respectively.

The function P contains a factor x^6 in the Rayleigh–Gans case and x^4 in the case of Kirchhoff diffraction. It is clear therefore that, unless the other factors $G^2(z)$ and $[J_1(z)/z]^2$ decrease more rapidly than do x^{-6} or x^{-4}, respectively, the particles giving the greatest contribution to this integral will be larger than those corresponding to the peak of the distribution function F. $G^2(z)$ and $[J_1(z)/z]^2$ are both oscillating functions. Each has a peak at $z = 0$, and subsequently a series of maxima and minima. At their minima both functions are zero, and at their maxima they have values which fall off approximately as z^{-4} and z^{-3}, respectively. Consequently, the maxima of the products $x^6G^2(z)$ and $x^4[J_1(z)/z]^2$ increase with x^2 and with x respectively, and unless the particle size distribution function F falls off with increasing x more rapidly than does x^{-2} or x^{-1} respectively, the larger particles will

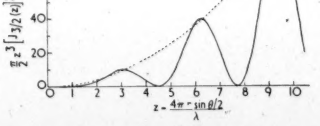

Fig. 1. Rayleigh–Gans scattering $\frac{1}{9}z^6G^2(z)$ plotted against z

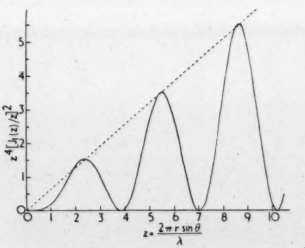

Fig. 2. Kirchhoff diffraction $z^4[J_1(z)/z]^2$ plotted against z

make progressively larger contributions to the total scattering at any angle.

It is not immediately apparent that the first peak value of $P(x, z)$ (i.e. that lying between $z = 0$ and the lowest value of z for which $G(z) = 0$ or $J_1(z)/z = 0$) will not be higher than that corresponding to higher orders of interference, since the peaks of $G(z)$ and $J_1(z)/z = 0$ are so very much higher than those at higher values of z. If, however, $z^6G^2(z)$ and $z^4[J_1(z)/z]^2$ are plotted against z, it is clear that in both cases the innermost peak conforms very closely to the trend followed by the outer ones. This is illustrated in Figs. 1 and 2. The two curves give the relative contributions by particles of different sizes to the total scattered intensity at a given angle $\theta(\theta \neq 0)$, if the particle size distribution is uniform and all particle sizes are equally probable.

It was pointed out earlier, however, that with non-spherical particles only the light within the first diffraction minimum could be approximated to the corresponding diffraction of scattering by spheres. Consequently, if measurements of scattering are to be readily interpreted, each intensity measurement made at a particular angle must contain the zero-order component as its principal contributor. This zero-order contribution will arise only from particles below a certain size. Therefore, only if on the average the size distribution function $F(x)$ falls off with increasing x more rapidly than does $1/x^2$ (in the case of Rayleigh–Gans scattering) or than $1/x$ (in the case of Kirchhoff diffraction) for all values of x greater than x_0 will the zero-order scattering by particles of size $x = x_0$ exceed that of each of the higher orders.

In the measurement of the light scattered at any particular angle, however, it is the sum of the contributions by particles of all sizes which is recorded. In equation (3) this is reflected in the fact that the integral of $F(x)P(x, z)$ is taken over all values of x from zero to infinity. This range embraces diffracted light of all orders. The main interest lies, therefore, in whether the sum of the higher-order contributions to the scattered intensity exceeds the zero-order. Since the analogy between Rayleigh–Gans scattering and Kirchhoff diffraction is very close, the former will be used to demonstrate the conditions under which zero-order scattering will predominate.

THE EFFECT OF PARTICLE SIZE DISTRIBUTION ON THE ANGULAR DISTRIBUTION OF RAYLEIGH–GANS SCATTERING

The maxima of $z^6 \times G^2(z)$ occur at $z = \pi,\ 2\pi,\ \ldots\ (n+1)\pi,\ \ldots$ (where n is the corresponding order of interference), and the minima at $z = (n + 3/2)\pi$. The intensity scattered at any angle by a cloud containing equal numbers of particles in equal ranges of particle diameter (i.e. $F =$ const.) is proportional to the area under the curve in Fig. 1. For each order of scattering this area is roughly proportional to the height of the corresponding peak, since the curves are similar in form and have bases of equal length π. These heights are proportional to $z^2 \propto (n+1)^2$. If, however, $F(x)$ falls off as $1/x^r$, then since $P_{max}(x, z)$ increases as x^2, $[FP]_{max}$ decreases as $1/(n+1)^{r-2} = 1/(n+1)^s$ say. The contribution to the light scattered at any angle by the part of the curve corresponding to the nth order interference is then proportional to $1/(n+1)^s$, and the total contribution by all orders is $\sum_{n=1}^{\infty} 1/(n+1)^s$. The sum of $1/(n+1)^s$ is only convergent if s is greater than 1. Consequently, the total light scattered by higher-order interference will be infinitely greater than that scattered by zero-order unless $F(x)$ falls off

Table 2. *Rayleigh–Gans scattering by polydisperse clouds of spheres*

The effect of particle size distribution on the sizes of particle whose scattering predominates in the scattered light $F(x)$ represents the particle size distribution by number

Type of distribution	F	x_m = *model value of x, at which* $\frac{dF}{dx} = 0$	x_c = *value of x beyond which* $\frac{d}{dx}(x^4F) < 0$	x_c/x_m	*Numerical examples*
Normal	$\frac{1}{\sigma\sqrt{(2\pi)}} e^{-(x-\bar{x})^2/2\sigma^2}$	$\bar{x}$	$\frac{\bar{x} + \sqrt{(\bar{x}^2 + 16\sigma^2)}}{2}$	$\frac{1 + \sqrt{(1 + 16\sigma^2/\bar{x}^2)}}{2}$	If $\sigma = \bar{x}/4$, $x_c = \bar{x} + 0{\cdot}82\sigma$ If $\sigma = \bar{x}/3$, $x_c = \bar{x} + \sigma$
Log-normal	$\frac{1}{x_g\sqrt{(2\pi)}\ln\sigma_g} \cdot e^{-\frac{1}{2}\left(\frac{\ln x/x_g}{\ln\sigma_g}\right)^2}$	$x_g \times e^{-(\ln\sigma_g)^2}$	$x_g \times e^{3(\ln\sigma_g)^2}$	$e^{4(\ln\sigma_g)^2}$	If $\sigma_g = 1{\cdot}5$, $x_c = x_g \times 1{\cdot}64$ If $\sigma_g = 2{\cdot}0$, $x_c = x_g \times 4{\cdot}22$
Negative exponential	e^{-x/x_0}	—	$4x_0$	—	—

Table 3. *Kirchhoff diffraction by polydisperse clouds of opaque circular disks*

The effect of particle size distribution on the sizes of particle whose scattering predominates in the scattered light $F(x)$ represents the particle size distribution by number

Type of distribution	F	x_m = *modal value of x, at which* $\frac{dF}{dx} = 0$	x_c = *value of x beyond which* $\frac{d}{dx}(x^3F) < 0$	x_c/x_m	*Numerical examples*
Normal	$\frac{1}{\sigma\sqrt{(2\pi)}} e^{-(x-\bar{x})^2/2\sigma^2}$	$\bar{x}$	$\frac{\bar{x} + \sqrt{(\bar{x}^2 + 12\sigma^2)}}{2}$	$\frac{1 + \sqrt{\left(1 + \frac{12\sigma^2}{\bar{x}^2}\right)}}{2}$	If $\sigma = \bar{x}/4$, $x_c = \bar{x} + 0{\cdot}64\sigma$ If $\sigma = \bar{x}/3$, $x_c = \bar{x} + 0{\cdot}78\sigma$
Log-normal	$\frac{1}{x_g\sqrt{(2\pi)}\ln\sigma_g} \cdot e^{-\frac{1}{2}\left(\frac{\ln x/x_g}{\ln\sigma_g}\right)^2}$	$x_g \times e^{-(\ln\sigma_g)^2}$	$x_g \times e^{2(\ln\sigma_g)^2}$	$e^{3(\ln\sigma_g)^2}$	If $\sigma_g = 1{\cdot}5$, $x_c = 1{\cdot}39x_g$ If $\sigma_g = 2{\cdot}0$, $x_c = 2{\cdot}62x_g$
Negative exponential	e^{-x/x_0}	—	$3x_0$	—	—

more rapidly than $1/x^3$. If the zero-order term is to exceed the sum of all others, then $1/2^s + 1/3^s + \ldots + 1/(n+1)^s + \ldots$ must be less than unity. But $\sum_{n=1}^{\infty} (1/n)^s < s/(s-1)$ (see Hardy[4]), so that $\sum_{n=1}^{\infty} 1/(n+1)^s$ must be less than $1/(s-1)$, and this must be less than unity. Hence s must exceed 2. If, therefore, the zero-order scattering is to predominate, then the distribution function $F(x)$ must fall off at least as rapidly as $1/x^4$. This condition has been calculated on the basis of approximations and is itself clearly only approximate, but it will give some indication of the region of the size distribution $F(x)$ concerning which the Rayleigh–Gans scattering will give readily interpretable information.

In order to determine the practical implications of this conclusion, the value of x corresponding to the maximum of $x^4 \times F(x)$ has been calculated for each of three different distribution functions, namely, the normal, log-normal, and negative exponential distributions. This value is denoted by x_c. (In no instance has $x^4 \times F(x)$ more than one maximum, nor any minimum except at $x = 0$). If $x > x_c$, then the zero-order scattering will predominate over the sum of all the higher-order effects. With most distributions this is in fact an unnecessarily stringent condition as $F(x)$ falls off more and more rapidly with increasing x, so that the very high order terms which contribute so largely to $z^6 \times G^2(z)$ can in fact be neglected. Nevertheless, this seems the simplest way in which to put the various forms of distribution function on a common basis with respect to this feature. The results of these calculations are summarized in Table 2. (The corresponding results for Kirchhoff diffraction are shown in Table 3.)

It must be stressed that the actual values of m, λ, and the parameters appearing in F will determine the scattering angle at which the higher-order effects begin to take charge of the total scattering at that angle, but they will not affect the relative positions of the size parameters and the radius x_c. Owing to the presence of the terms in x^4 and x^3, the radius x_c is necessarily greater than the mode of the distribution $F(x)$, and it is clear that only the particles which are considerably larger than the mode can be profitably studied.

In all of the above expressions the power of z appearing in the expansion appropriate to Kirchhoff diffraction is lower by one than the corresponding power in the expansion of the term $z^6G^2(z)$ appearing in Rayleigh–Gans scattering. In a polydisperse cloud this increases the contribution of the smaller particles relative to that of the larger ones. Moreover, there is no upper limit to the range of sizes to which Kirchhoff's theory of diffraction can be applied. By contrast, the Rayleigh–Gans approximation cannot be applied unless $2x(m-1) \ll 1$, and unless $m \simeq 1$ the available range of values of x is small. The region of diffraction, reflexion and refraction embraces the ranges of size and refractive index found in a large number of dusts, and the remaining calculations have been based on its size-dependent component, Kirchhoff diffraction.

KIRCHHOFF DIFFRACTION BY A CLOUD OF OPAQUE CIRCULAR DISKS WHOSE DIAMETERS ARE LOG-NORMALLY DISTRIBUTED

In samples of industrial dusts the central portion of the particle size distribution not infrequently resembles the log-normal (Drinker and Hatch[5]) at any rate for particles large enough to be in the region in which the separation into geometrical and diffracted components is justifiable. For this distribution, therefore, more detailed calculations have been carried out.

The log-normal distribution contains two parameters, a geometrical mean diameter M_g and a geometrical standard deviation σ_g. Once σ_g is determined, the proportion in any size range $d \to d + \delta(d)$ depends only on d/M_g and on $\delta(d)/d$. For example, if $M_g = 1\ \mu$ the proportion of particles lying in the size-range 1–1·1 μ will be the same as that in the size range 2–2·2 μ if $M_g = 2\ \mu$.

Since diffraction phenomena are characterized by the parameter z (see above), any change in r/λ can be compensated by a corresponding change in $\sin\theta$ in the opposite direction. Reduction of M_g reduces the value of x at corresponding points in the size distribution by the same factor, and this can therefore be compensated by increasing all the corresponding values of $\sin\theta$ by this factor.

The feature of interest is the contribution of the different size ranges to the total diffracted scattering at particular angles, and for a given value of σ_g this can be calculated in terms of $x_g = \pi M_g/\lambda$ and $z_g = x_g \sin\theta$: in interpreting the results the value of θ which is appropriate can then be determined from that of M_g/λ. Although both M_g and λ can vary over wide ranges of values, the range of variation of σ_g for samples of industrial dust is comparatively narrow. $\sigma_g = 1{\cdot}3$ corresponds to an unusually homogeneous cloud, and $\sigma_g = 3{\cdot}0$ to one which is comparatively heterogeneous. Consequently, calculations have been carried out in terms of $\sigma_g = 2{\cdot}03$. This particular value was chosen because $\ln 2{\cdot}03 = \sqrt{\frac{1}{2}}$, so that the distribution was very easily calculated.

Fig. 3 shows the contributions by particles of different sizes to the integral $I(\theta)$ [equation (3)] at various angles. In other words, at each of these angles the intensity scattered is a weighted mean of the particle size distribution, the distribution so weighted being given by the corresponding curve in this figure. The parameter x giving particle size has been plotted logarithmically, and the ordinate, giving the relative contribution to the total scattering, has therefore been increased so that equal areas correspond to equal total contributions to the light scattered. The abscissae are graduated in terms of a cloud of disks of geometric mean diameter $M_g = 2{\cdot}12\ \mu$ and of incident light of wavelength $\lambda = 0{\cdot}41\ \mu$ (mercury green light in water). For this case $x_g = 16{\cdot}2$.

These graphs illustrate very clearly the way in which the forward scattering quite predominantly arises from zero-order diffraction. As the angle of scattering is reduced, this approximates more and more closely to a mean of $F(x)$ weighted by a factor of x^4. As the angle of scattering increases, the higher-order diffraction becomes more and more important until it finally dominates the zero-order.

In general terms, this is easily enough understood. At small angles of scattering, higher-order diffraction can only arise from the very largest particles, so large that despite the "weighting" they contribute comparatively little to $x^4F(x)$. As the scattering angle increases, however, the corresponding particle sizes move inwards towards the peak of $x^4F(x)$. The particles contributing to the zero-order diffraction likewise shrink towards smaller particles, but in this case the shrinkage is away from the peak towards the low values of $x^4F(x)$. This effect will be more marked as σ_g increases, since the mean value of the distribution of $x^4F(x)$ will then move further away from the mean of $F(x)$ and the weighting accorded to the larger particles will increase.

It should be borne in mind that if $x(m-1) \simeq 1$, or $x(m-1) < 1$, the scattering can no longer be regarded as

being of Kirchhoff type. If $x(m-1) < 1$, the total light scattered falls away rapidly as x diminishes, and the contribution by particles in this range of sizes at all angles will be negligible.

Hitherto, only the intensity of scattering at a particular angle has been considered. The variation of the scattered intensity with scattering angle $dI(\theta)/d\theta$ is also dependent on particle size distribution. The total light scattered by higher-order diffraction I_{h0} varies less rapidly with angle than does the light scattered by zero-order diffraction I_{z0}. For small angles of scattering the error in assuming that the observed gradient $dI(\theta)/d\theta$ arises solely from changes in I_{z0} is small. Consequently, the range of particle sizes effectively contributing to $dI(\theta)/d\theta$ is considerably narrower than that contributing to $I(\theta)$. This is illustrated in the bottom curve of Fig. 3 which represents the difference between the values of I_{z0} for $z_g = (\pi M_g \sin\theta)/\lambda = 1{\cdot}62$ and $z_g = 2{\cdot}16$. This difference is an average value for $dI/d\theta$ over a range of angles. It has a sharp peak near $x = 3x_g/2$ but a considerable part of the area under the curve comes from values of x which differ from $3x_g/2$ by more than 25%. Reducing the difference in $\sin\theta$ will not greatly reduce this spread, which arises mainly from the fact that $[J_1(z)]/z$ varies rapidly throughout the range $0{\cdot}5 < z < 3{\cdot}5$, and considerable contributions to $dI(\theta)/d\theta$ will arise from the corresponding range of values of x. As the angle of scattering increases, the higher-order contribution to $dI(\theta)/d\theta$ increases with it and can no longer be neglected. In that case this method seems likely to involve more complication and arbitrary assumption than is justified. It may be mentioned that the sum of the contributions of the first, second, third and fourth orders to the difference $I(z_g = 1{\cdot}62) - I(z_g = 2{\cdot}16)$ is 13% of the total.

In conclusion, therefore, we may say that, even with moderately heterogeneous dust clouds, the variation of the scattered intensity with scattering angle will be due almost entirely to particles larger than the geometrical mean diameter if this is determined on the basis of number. For more uniform clouds the smaller particles will contribute a greater proportion of the scattered light, but the weighting will still tend to be against them.

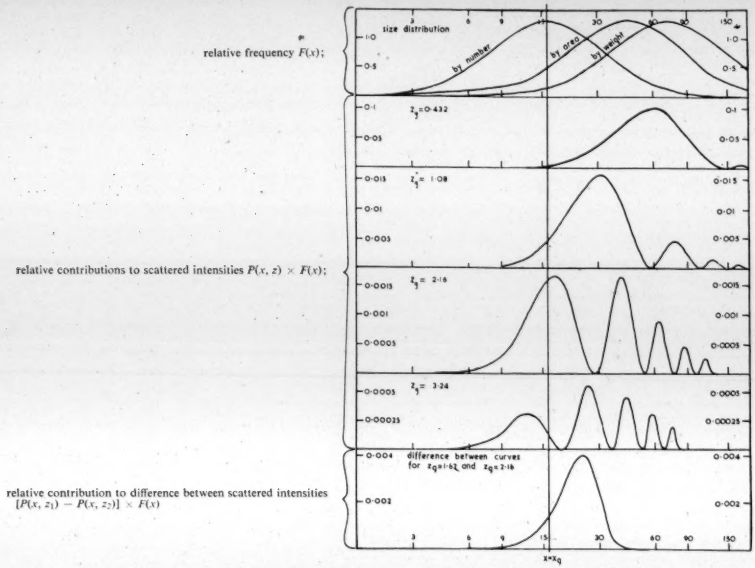

Fig. 3. Contribution by particles of different sizes to total scattering: Kirchhoff diffraction by circular disks of diameters distributed log-normally: $\sigma_g = 2{\cdot}03$

If the range of particle sizes extends into the Rayleigh and Rayleigh–Gans regions, but a considerable proportion of the total area of cross-section of the particles is in the Mecke region, then one other method of differentiating between the smaller and larger particles offers itself. Under these conditions, a large part of the wide-angle scattering arises from the geometrical component of the Mecke scattering. This is, however, largely independent of wavelength, and the dependence is calculable from the optical dispersion of the material of the particles. The scattering by the smallest particles is, however, highly dependent on wavelength, and consequently the dependence of this wide-angle scattering on wavelength will indicate the presence of particles in or near the Rayleigh region. This requires the measurement of the ratio of the absolute scattering coefficients at different wavelengths.

CONCLUSIONS

All the methods of using light scattering for estimating the particle size are characterized by intensity distributions

weighted by volume (Rayleigh and Rayleigh–Gans regions) or by surface area (other regions). These weightings are constant multiplying factors superimposed on all other effects, and the size-effects produced by the smaller particles tend therefore to be masked by the scattering of the larger ones, in particular when the weighting is by the volume. This limits the range of usefulness of light-scattering methods to dispersions which do not contain too wide a range of particle sizes. Such dispersions are unlikely to occur naturally, but might result from a process of preliminary size selection. With particles in the Rayleigh–Gans region, this limitation is very severe, but with particles which can be treated as equivalent to Kirchhoff's opaque disks a rather wider range of sizes can be studied.

ACKNOWLEDGEMENTS

The author is very grateful to Dr. T. Bedford and Dr. C. N. Davies for advice and encouragement in the course of this work. Miss J. A. Stevenson kindly prepared the diagrams.

REFERENCES

(1) VAN DE HULST. *Recherches Astronomiques de l'Observatoire d'Utrecht*, **11**, Pt 1 (1946).
(2) OSTER, G. *Chem. Rev.*, **43**, p. 319 (1948).
(3) VOUK, V. *Ph.D. thesis*, University of London (1948).
(4) HARDY, G. H. *Pure Mathematics*, p. 319 (London: Cambridge University Press, 1933).
(5) DRINKER, P., and HATCH, T. F. *Industrial Dust* (London: McGraw-Hill Book Co. Ltd., 1936).

Paper C.2

Photoextinction measurements on spherical particles

By P. C. LEWIS, B.Sc., and G. F. LOTHIAN, M.A., F.Inst.P., Physics Department, University College, Exeter

Experimental determinations, in the wavelength range 0·4–2·0 μ, of the transmissions of suspensions of spherical particles (barium sulphate and spores of *Lycoperdon pyriforme*) are used to calculate values of the total scattering coefficient K. The results are in approximate agreement with theoretical expectations. The measurements can also be used to determine the refractive indices and in certain cases the water content of the spheres.

Suppose a parallel beam of light be passed through a suspension of thickness l, containing N spherical particles per unit volume of radius r. If the particles behave as opaque disks and if the laws of geometrical optics are applicable, then it is easily shown[1] that the optical density $\log_{10} I_0/I$, where I_0 and I are the intensities of the incident and transmitted beams respectively, is given by $\log_{10} e \,.\, N\pi r^2 l$. In general, however, some at least of the incident radiation is transmitted through the particles, emerging with a phase change and so producing interference effects with the radiation passing through the adjacent medium; diffraction effects also occur. The result is that the above expression must be multiplied by a factor K, sometimes known as the total scattering coefficient, to give

$$\text{optical density} = K \log_{10} e \,.\, N\pi r^2 l \qquad (1)$$

Expressions for K have been deduced from electromagnetic theory by Mie[2] assuming uniform spherical particles, a plane incident wave and observation at an infinite distance. It is found that K depends on (i) the ratio of particle radius r to the wavelength λ of the radiation measured in the surrounding medium; the parameter $x = 2\pi r/\lambda$ is commonly used; (ii) the refractive index m of the particle relative to the surrounding medium, $m = n_s/n_m$ where n_s and n_m are the absolute refractive indices of the particle and the surrounding medium respectively; (iii) the amount of absorption in the case of absorbing particles, and so on the complex refractive index $m = m_{real}(1 - ik)$, where k is the absorption index (defined by $I = I_0 \exp(-4\pi k l/\lambda)$ for transmission through a parallel slab). In practice K also depends on (iv) the semi-angles θ_s, θ_d subtended by the source of radiation and the detecting device respectively at the suspension (Fig. 1). In the measurements reported here θ_s and θ_d have been kept small (see legend to Fig. 1) so that the results should correspond to the theoretical values for which $\theta_s = \theta_d = 0$.

Although in principle K values may be calculated from the Mie theory the calculation is extremely laborious, except in special cases, and only a few numerical values are available.[3–5] van de Hulst[6] has deduced an expression for K using the principles of physical optics, which is applicable when r/λ is much greater than unity and when m_{real} approaches unity; this will be discussed more fully below.

Several workers have made transmission measurements on spherical particles of sulphur,[7] barium sulphate[8] and glass[9] which confirm in a general way the calculated values of K. The experimental data is, however, somewhat meagre and the results presented here are the beginning of an attempt to extend the experimental information. The use of a 5 : 1 range in wavelengths (0·4–2·0 μ) has permitted a large range of x values to be covered with a single size of specimen.

EXPERIMENTAL ARRANGEMENT

The experimental arrangement is shown in Fig. 1. A filament lamp F illuminates an aperture S, 1·2 mm square, which is at the focus of the lens L_1. After passing through the cell C containing the specimen or the suspending medium, an image of S is formed on S_1, the entrance slit of a prism monochromator M, behind the exit slit of which is a photocell

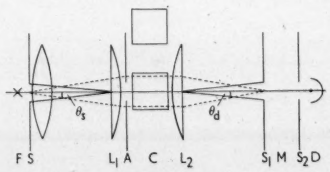

Fig. 1

F, filament lamp; S, aperture, 1·2 mm square; C, cells for specimen and blank solvent; A, limiting aperture; L_1 L_2, lenses of focal length 30 cm; S_1, S_2, slits of prism monochromator M; D, photocell detector. Height of entrance slit 2·8 mm; width up to 0·5 mm. Semi-angle $\theta_s = 0{\cdot}6/300 = 0{\cdot}11°$ square (for the measurements on *Lycoperdon pyriforme* in air it was necessary to increase θ_s to $0{\cdot}22° \times 0{\cdot}11°$). Semi-angle $\theta_d = 0{\cdot}27°$ vertically and up to $0{\cdot}05°$ horizontally.

D. The wavelength range 0·4–2·0 μ has been covered in three stages by using (i) a photomultiplier cell (R.C.A. type 931), (ii) a vacuum photocell with caesium cathode used in conjunction with a d.c. bridge amplifier, and (iii) a lead sulphide cell used with a chopped beam and tuned a.c. amplifier. In all cases, measurements consist in reading in turn the deflexions of a mirror galvanometer for two cells containing the suspension and blank medium respectively. Linearity of deflexion and radiation intensity has been tested and found satisfactory except for small signal levels with the lead sulphide cell; measurements in these last conditions have been avoided. At optical densities near 0·5, the equipment gives measurements reproducible to within 0·01.

PREPARATION OF UNIFORM SUSPENSIONS

Uniform suspensions of barium sulphate have been prepared by precipitation from barium chloride and sulphuric acid in presence of hydrochloric acid—following Andreasen.[10] The particles are fairly uniform in size and may be obtained from about $\frac{1}{2}$ to 6 μ in radius by modifying the precipitating conditions. The suspension on which measurements are reported below had particles with a mean radius of 4·6 μ; all the particles were within $\pm 6\%$ of the mean size and two-thirds were within $\pm 3\%$. They tend to agglommerate into groups, but by dispersing in 0·2% Teepol and separating by sedimentation, suspensions in which most of the particles are single may be obtained.

Reasonably uniform spheres are more readily obtained from natural sources; measurements have been made on spores, of radius 1·8 μ, of *Lycoperdon pyriforme* (a species of puff-ball) suspended in water containing 0·2% Teepol as a dispersing agent and 5% formalin as a preservative. These spores were also measured in air by allowing a cloud to settle on microscope slides; 12 such surfaces on 6 slides give a useful density. The size distribution is such that 90% of the particles are within $\pm 10\%$ and 40% are within $\pm 5\%$ of the mean size. Although this degree of uniformity is not so good as for the barium sulphate used, the suspensions are more readily prepared and are very stable, whereas the barium sulphate suspensions break down within hours.

MEASUREMENT OF n

The suspensions were allowed to settle in a counting chamber of known depth and the number in a given area counted in a microscope. Since the standard error if n particles are counted is $\sqrt{n}$, it is necessary to count 1000 particles to keep the standard error about $\pm 3\%$; in practice, several thousand particles have been counted. Since the spores mounted on glass slides were very irregularly spaced, no attempt was made to count them and therefore no absolute values of K were determined in this case.

RESULTS AND DISCUSSION

Values of K were calculated from equation (1) and are shown tabulated against reciprocal wavelengths in Tables 1 and 2. Table 3 shows for *Lycoperdon pyriforme* in air the measured values of optical density and wave-number.

The experimental results may usefully be compared with the expression for K deduced by van de Hulst who showed that K is a function of ρ where

$$\rho = 2x[(n_s/n_m) - 1] = 4\pi(r/\lambda_0) \cdot (n_s - n_m) \qquad (2)$$

where λ is the wavelength of the radiation in the suspending medium and λ_0 the corresponding wavelength in vacuum. Curve *A* of Fig. 2 shows K values, calculated by this method for non-absorbing spheres, plotted against ρ. The maximum and minimum values of K occur at the following ρ values:

1st max.	*1st min.*	*2nd max.*	*2nd min.*	*3rd max.*	*3rd min.*	*4th max.*	*4th min.*
4·09	7·63	10·79	14·00	17·16	20·33	23·52	26·63

Experimental and theoretical curves were therefore plotted with the abscissae on a logarithmic scale and it was possible to shift the curves horizontally to obtain at least horizontal correspondence of the maxima and minima.

Table 1. *Barium sulphate in water*

Wave No. (μ^{-1})	1·00	1·10	1·20	1·30	1·40	1·50	1·60	1·70	1·80
K	2·55	2·30	2·01	1·94	2·08	2·23	2·24	2·05	1·83
Wave No. (μ^{-1})	1·90	1·95	2·00	2·10	2·20	2·30	2·40	2·50	
K	1·86	1·92	2·06	2·02	2·06	1·96	1·89	1·91	

Table 2. *Lycoperdon pyriforme in water*

Wave No. (μ^{-1})	1·05	1·11	1·18	1·25	1·33	1·43	1·54	1·60	1·67
K	2·64	2·80	2·95	3·09	3·21	3·29	3·27	3·22	3·14
Wave No. (μ^{-1})	1·74	1·82	1·91	2·00	2·11	2·22	2·35	2·50	
K	3·11	3·02	2·83	2·78	2·49	2·34	2·24	2·17	

Table 3. *Lycoperdon pyriforme in air*

Wave No. (μ^{-1})	0·50	0·55	0·60	0·70	0·80	0·90	0·95	1·00	1·10	1·20	1·30	1·40
Optical density	0·58	0·61	0·61	0·56	0·50	0·45	0·42	0·42	0·42	0·43	0·42	0·40
Wave No. (μ^{-1})	1·50	1·60	1·70	1·80	1·90	2·00	2·10	2·20	2·30	2·40	2·50	
Optical density	0·37	0·35	0·34	0·35	0·37	0·38	0·40	0·40	0·39	0·38	0·38	

If this is done, for example for the barium sulphate curve of Fig. 3, it is seen that its two maxima at 1·56 and 2·12 μ^{-1} can be made to coincide well with the 3rd and 4th maxima of Fig. 2 at $\rho = 17{\cdot}16$ and 23·52 respectively. Hence by substitution in equation (2) the product $r(n_{bar.sulph.} - n_{water})$ may be calculated; the values for the 3rd and 4th maxima are 0·875 and 0·883 respectively. This gives an interesting method of measuring particle radius when the refractive indices are known, as was pointed out by Hawksley.[11] (In a more limited sense location of the maximum to determine particle size was used earlier by Caspersson[12] and by LaMer and Barnes.[13]) Conversely, if the radius be measured microscopically, the refractive index of the particle may be

calculated; this latter calculation has been made from our measurements giving $n_{bar.\,sulph.}$ 1·520 and 1·522 respectively for the 3rd and 4th maxima. These results, together with similar calculations for the minima of the barium sulphate curve are summarized in Table 4. Similar values for the of Fig. 2 plotted for $\beta = 25°$. Nevertheless the maxima and minima occur at approximately the same ρ values as for non-absorbing specimens. Thus in so far as a specimen absorbs uniformly throughout the wavelength range studied, superposition of an experimental curve on Curve *A* of Fig. 2

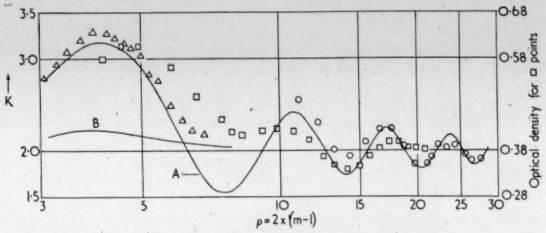

Fig. 2. Theoretical values of total scattering coefficient K plotted against $\rho = 4\pi(r/\lambda)(m-1)$

Curve *A* transparent spheres. Curve *B* absorbing spheres for $\beta = 25°$. (Calculated after van de Hulst for spheres where $r \gg \lambda$ and $m \to 1$.) Experimental values of K are plotted choosing the value of refractive index which gives the best correspondence of maxima and minima for barium sulphate ○ and *Lycoperdon pyriforme* in water △. Measurements on *Lycoperdon pyriforme* in air □ are plotted as optical densities (right-hand ordinate scale) which are proportional to K values.

refractive index have been found for barium sulphate prepared in other sizes. This value is intermediate between the indices for water and crystalline barium sulphate (1·64) and it is concluded that the spheres contain about 60% by volume of water. This is confirmed quantitatively by the specific gravity determined from sedimentation velocity; and such an effect is to be expected if the particles are formed by condensation of submicroscopic units.

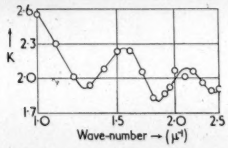

Fig. 3. Experimental total scattering coefficients K plotted against $1/\lambda$ in μ^{-1} for barium sulphate (radius = 4·6 μ) in water

In the case of absorbing specimens, van de Hulst's treatment shows that K is also a function of β where $\tan\beta = m_{real}k/(m_{real}-1)$. For finite absorption ($\beta \neq 0$) the magnitude of the fluctuations of K is reduced and K approaches its limiting value of 2 at smaller values of ρ, as seen in Curve *B* will still be possible so far as concerns positions of maxima and minima in the direction of abscissae; although absolute values of K should not be expected to correspond. But if the absorption varies with wavelength (i.e. with ρ) an experimental curve will correspond with a composite theoretical curve made by adding portions of a family of curves of the type of Curve *B* (Fig. 2), and the peaks of such a curve may well be displaced along the ρ axis from those of Curve *A* (Fig. 2).

The spores measured are selectively absorbing, being brownish in colour; since at present the values of absorption index are not known, the best that can be done is to compare the experimental curves with the theoretical curve for transparent materials. The experimental results have therefore been plotted on Fig. 2 to give the best correspondence of peaks. For the spores in air the correspondence is not very good; for example, the 1st minimum and 2nd maximum are almost nonexistent. Nevertheless calculations of refractive index made from equation (2) and summarized in Table 4 show some degree of consistency. The mean values of $1{\cdot}3_4$ and $1{\cdot}4_6$ for dry and wet spores respectively show that the wet spores have absorbed water, as would be expected.

It is hoped to extend these measurements to other sizes and types of particle. The results to date suggest the desirability of determining K in any particular case in which it is required.

Table 4. *Summary of results*

Particle	*Radius in μ*	*Suspending medium*	n_m	*Max. or Min. in μ⁻¹*		*Corresponding value of ρ*	n_s
Barium sulphate	4·6	Water	1·33	1·27	2nd min.	14·00	1·52
				1·56	3rd max.	17·16	1·52
				1·84	3rd min.	20·33	1·52
				2·12	4th max.	23·52	1·52
				2·42	4th min.	26·63	1·52
Lycoperdon pyriforme	$1{\cdot}8_2$	Air	1·00	0·56	1st max.	4·09	1·32
				1·70	2nd min.	14·00	1·36
		Water/formalin	$1{\cdot}33_6$	1·46	1st max.	4·09	1·46

n_m = refractive index of suspending medium.
n_s = particle refractive index calculated from equation 2.

ACKNOWLEDGEMENTS

We are indebted to Dr. G. C. Ainsworth for supplying specimens of plant spores and for the value of discussions about their properties. Mr. F. P. Chappel assisted in the design of the apparatus and with some preliminary measurements. One of us (P. C. L.) is being assisted in this work by a grant from the Department of Scientific and Industrial Research.

REFERENCES

(1) LOTHIAN, G. F., and CHAPPEL, F. P. *J. Appl. Chem.*, **1**, p. 475 (1951).
(2) MIE, G. *Ann. Phys.*, **25**, p. 377 (1908).
(3) LOWAN, A. N. *Nat. Bur. Stand., Appl. Math. Ser.*, No. 4 (1949).
(4) HOUGHTON, H. G., and CHALKER, W. R. *J. Opt. Soc. Amer.*, **39**, p. 955 (1949).
(5) HOLL, H. *Optik*, **4**, p. 173 (1948).
(6) VAN DE HULST, H. C. *Recherches astronomiques de l'Observatoire d'Utrecht*, **11**, Part I (1946) and Part 2 (1949).
(7) LA MER and co-workers; several papers, e.g. Barnes and La Mer. *J. Coll. Sci.*, **1**, p. 79 (1946).
(8) ANDREASEN, A. H. M., and co-workers. *J. Soc. Chem. Ind.*, **69**, p. 312 (1950).
(9) PAUL, W., and JONES, R. V. *Nature* [*London*], **168**, p. 554 (1951).
(10) ANDREASEN, A. H. M. *Koll. Z.*, **104**, p. 181 (1943).
(11) HAWKSLEY, P. G. W. *B.C.U.R.A. Bull.*, **16**, p. 200 (1952).
(12) CASPERSSON, T. O. *Koll. Z.*, **60**, p. 151 (1932).
(13) LA MER, V. K., and BARNES, M. D. *J. Coll. Sci.*, **2**, p. 361 (1947).

GENERAL DISCUSSION ON SESSION C

Mr. W. H. Walton: Can any of the authors suggest an optical means of assessing the quantity of dust on a glass slide, in units which will correlate with one of the standard measures such as number of particles, surface area or mass? I am thinking of mine dust samples containing particles of coal and/or stone of sizes from below the limit of visibility up to a maximum of about 10 μ. A difficulty of the problem is that, on the one hand, if an optical measuring system of small aperture is used, the extent to which diffracted light is accepted becomes very uncertain because of the wide size-range and angularity of the particles. On the other hand, if a large aperture system is used, uncertainty arises from the quantity of light refracted through the stone dust particles, which in some cases may be quite transparent.

Dr. E. G. Richardson: The possibility of using the attenuation of ultrasonic pulses in place of light to determine particle diameter has not heretofore been suggested. It is true that sound waves cannot be polarized when they are scattered as light waves are, but as far as extinction, or—as it is more often called in sound—attenuation, is concerned, a similar law should apply to the ultrasonic case.

Rayleigh's theory for the scattering of sound by immobile particles small compared to the wavelength of sound leads to an extinction coefficient involving the particle volume and the fourth power of the wavelength. Sewell extended this by allowing for friction and later for the mobility of the particles.

For the range of frequencies over which we are interested, Sewell's expression for the (amplitude) coefficient has three effective terms, viz.:

$$\alpha = N\pi a^2\left(\frac{6\nu}{ca} + \frac{6\omega^{\frac{1}{2}}\nu^{\frac{1}{2}}}{c} + \frac{2}{9}\frac{\omega^4 a^4}{c^4}\right)$$

where N = number of particles per cm^3;
a = their radius;

(so that $N\pi a^2$ is the specific surface);

ν = kinematic viscosity of the medium;
c = velocity of sound in the medium;
ω = pulsatance ($= 2\pi \times$ frequency).

The first two are frictional terms and the third the scattering term.

Calculations of the relative values of the three coefficients in the attenuation formula have been carried out by Laidler and Richardson in reference to their experiments on the attenuation (at kilocycle per second frequencies) by lycoperdon spores *in air*, when the frictional terms predominate, but in the recent experiments of J. Busby at Newcastle upon Tyne frequencies of megacycles per second and suspensions of glass spheres ($a > 40\ \mu$) in water have been used, in which case the scattering term is more important. The figure shows how the viscous and scattering coefficients (for a density ratio of 2·5 and concentration 1%) vary with particle size.

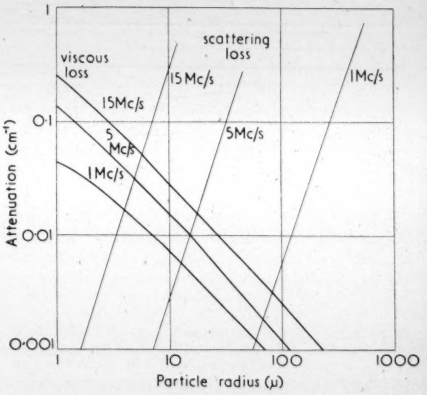

Variation of viscous and scattering loss with particle size

Even with frequencies of megacycles per second the wavelength of ultrasonics in liquids much exceeds the likely diameters of solid particles in suspension therein, so that the Rayleigh scattering law is relevant. A test of this has been made by Busby using sized glass spheres in the range 40–70 μ, kept in suspension in water by stirring. As far as variation with concentration is concerned, there appears to be direct proportionality between attenuation and the number of spheres in unit volume up to 15% concentration. It should be pointed out, however, that smaller particles in low-frequency fields would experience a viscous traction which would increase the attenuation. The experiment requires a quartz or barium titanate disk pulsed for periods of about

15 μsec and a similar disk as detector of the transmitted radiation with its associated amplifier.

It appears that this method could be used in conjunction with a sedimentation cell, without more experimental difficulty than is involved in an optical measurement.

A comparison is now being carried out between the results of a size analysis in sedimentation of a polydisperse system (*a*) by the more usual optical technique, (*b*) by the ultrasonic technique. Results of this comparison and more experimental details of the ultrasonic technique will be published[b] later. The main experimental advantage of method (*b*) appears to lie in the pulsing operation, whereby mechanical analogues of photophoresis and convection are avoided since the radiation is not continuously operated. The apparatus would, however, be somewhat larger than that of (*a*), requiring a larger sample of powder for analysis. Mr. Busby is using about 1% by volume.

On the other hand, the specific acoustic impedance of the particles is usually so ill-matched to that of the liquid that little radiation penetrates the solid and variations in scattering with complex refractive index need not trouble the calculations as they may do when light is being used. Furthermore, the mean value of $2\pi a/\lambda$ can, by suitable choosing of the wavelength, be set squarely in the Rayleigh region and not overlap the difficult Mie region. This suggests that the ultrasonic method may be most useful for (1) particles that would overlap this region if light were used, (2) large particles greater than 40 μ for which other methods may not be suitable.

SESSION D. PARTICLE SHAPE FACTORS

Chairman: H. L. GREEN, M.A., F.Inst.P.

Paper D.1

The shape of ground petroleum coke particles

By T. BEIRNE and J. M. HUTCHEON, B.Sc., Atomic Energy Research Establishment, Harwell

The variation with size of particle shape and other particle characteristics has been determined for a petroleum coke ground in standard equipment. Novel methods have been developed for particle counting and projected area measurement. Existing methods for particle density measurement have been examined and modified.

The work to be described derives partly from studies of close packing of ground coke particles and partly from an interest in the extent to which such particles would be oriented in a fluid stream.

It appeared that such work would be assisted by quantitative measurements of the shape of the particles. The first requirement was to define shape in a quantitative manner. Hawksley[1] has given a summary of the many shape factors which have been described in the literature and are obtained as dimensionless combinations of pairs of different linear parameters of the particle. The parameter selected for the present work is the ratio of two diameters. The numerator is the diameter δ of the sphere having the same volume as the particle, and the denominator d_{as} is the diameter of the circle having an area equal to the projected area of the particle in its most stable position. This ratio σ is related to Heywood's[2] volume constant k by the relation

$$\sigma = \frac{\delta}{d_{as}} = \left(\frac{6k}{\pi}\right)^{\frac{1}{3}}$$

Certain features concerning this definition may be noted. It has the value of unity for spheres and smaller values for any other shape. The use of projected area rather than surface area permits of its use for porous particles with minimum complications due to internal surface. Lastly, it is a quantity which appears significant from the point of view of orientation.

Experimentally, the measurement of σ requires the determination of three quantities.

(i) *Specific projected area* (A cm^2/g). This is the integrated area of the orthogonal projections of particles of the powder having a total mass of 1 g when they are settled in their most stable positions without overlap.

(ii) *Specific particle volume* (V cm^3/g). This is the integrated volume of particles, including internal pores (i.e. the envelope volume), of the powder having a total mass of 1 g. This quantity is thus the reciprocal of the "particle density."

(iii) *The number of particles per gramme* (N) is the reciprocal of the mean particle mass.

From these experimental quantities are derived:

(i) The "volume diameter" δ defined by $V = \frac{\pi}{6}\delta^3 N$.

(ii) The "stable area diameter" d_{as} defined by $A = \frac{\pi}{4}d_{as}^2 N$.

(iii) The "shape constant" $\sigma = \frac{\delta}{d_{as}} = \frac{(6V/\pi N)^{\frac{1}{3}}}{(4A/\pi N)^{\frac{1}{2}}} = \frac{1{\cdot}1\,V^{\frac{1}{3}}N^{\frac{1}{6}}}{A^{\frac{1}{2}}}$

MATERIALS AND PREPARATION OF SAMPLES

For all the determinations described in this paper, the coke used was a shale oil coke manufactured by Scottish Oils and Shell Mex, Ltd., and supplied to us through the courtesy of British Aluminium Co., Kinlochleven, Argyll, after calcining in their equipment. As received at Harwell, the coke was in approximately 4 in. lumps. Determination of the moisture content and volatile matter contents by standard methods[3] gave values of 0·67% and 2·55% respectively.

For these tests, the coke was crushed in a vertical-shaft rotary crusher to pass a $\frac{1}{4}$ in. sieve and the resulting material pulverized in a laboratory sample grinder. In this equipment the material to be crushed passed between two hardened manganese-steel disks, one fixed and the other rotating at high speed, the clearance being adjustable by a hand-wheel. The finely-ground product from this machine was then classified into fractions using British Standard test sieves. These fractions were used for the various determinations.

DETERMINATION OF THE SPECIFIC PROJECTED AREA

The specific projected area was measured on an instrument developed for this work. The essential principle of the instrument is shown in Fig. 1. A simple optical system produces an even collimated light beam which is directed on

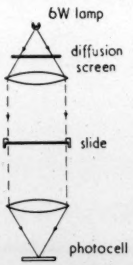

Fig. 1. Principle of instrument for determination of specific projected area

to the slide and the transmitted light is then refocused on to a selenium barrier-layer photocell. A simple electrical circuit (Fig. 2) enables the illumination to be stabilized and controlled with sufficient accuracy for measurement of the voltage output of the photocell to be made on a vernier potentiometer which has a sensitivity of 1 μV. This permits measurement of the light falling on the photocell to be made with 0·25–0·5% precision.

Slides were prepared with the dry powder well dispersed on them and inserted in the sockets of the turret arrangement on

the measuring unit. These slides had all been previously calibrated with accurately-cut sectored disks so that the obscured area corresponding to any photocell voltage could be read off a graph. This allowed for the non-linear response of the photocell. The potentiometer was then standardized

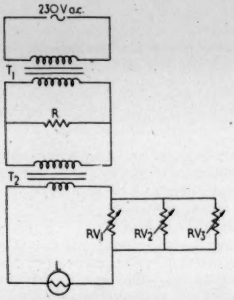

Fig. 2. Circuit for stabilizing and controlling lamp voltage

R = load resistor
$RV_1 = 10\ \Omega$
$RV_2 = 250\ \Omega$
$RV_3 = 5000\ \Omega$
T_1 = constant voltage transformer
T_2 = 230–6 V transformer
L = 6 W lamp

using a Weston cadmium cell and the illumination adjusted to give a photocell output of 500 μV with a blank "control" slide in place. Measurements were made on at least six slides for each grade of coke and the mean value calculated. Typical examples of the scatter for a coarse and a fine fraction are shown in Table 1.

Table 1. *Example of results of projected area measurements showing repeatability*

−16 +22 B.S.S.		−240 B.S.S.	
Slide No.	*Specific projected area*	*Slide No.*	*Specific projected area*
2	25·3	2	434·1
3	26·0	3	416·0
4	27·9	4	453·3
5	26·9	5	417·7
6	25·8	6	430·3
Mean = 26·4		Mean = 430·3	

The main practical difficulties in making these measurements arose in the preparation of slides. These were thin, optically flat glass disks mounted in rings of anodized aluminium. Approximately 1 ml of a suspension of the powder in absolute alcohol was transferred to the slide by a 5 ml safety pipette, from which the capillary tip had been removed, the suspension being stirred during withdrawal of the samples. The alcohol was then evaporated by overhead infra-red lamps at the minimum practicable rate, other methods of evaporation having been found to aggregate the particles. Aggregation also resulted from changes in surface tension as the last traces of alcohol were dried off unless the slides had been thoroughly degreased beforehand. It was found also to be advantageous to wash the coke well with alcohol prior to making up the suspension.

The obscured area was generally about 25% of the total slide area and in no circumstances was it allowed to increase beyond 50%. This prevented any serious error due to overlapping of particles. The greatest source of error was found to be in sampling the powder. This was reduced by using a sample-splitter and by taking at least six samples from the suspension. It can be seen from Table 1 that the r.m.s. deviations lie between 3% and 4%. In calculating the shape factors, the projected area enters as $A^{\frac{1}{2}}$, so that the error introduced in this way is less than 2%.

DETERMINATION OF THE SPECIFIC PARTICLE VOLUME

The porous nature of coke particles makes this determination difficult and the results at best somewhat arbitrary. Gilchrist and Taylor,[4] after critically reviewing the applicability of other methods, based their own results on the assumption that the shape of the particle does not change with size. Since one purpose of the present work was to test Gilchrist and Taylor's assumption (which is not confirmed) it was necessary to choose an independent method.

A method was examined in which the pores of the particles are first filled with a liquid which is immiscible with the one used for the density determination by the usual pyknometric method. The liquids chosen were water and a benzene-carbon tetra-chloride mixture but the method was rejected when, as in Gilchrist and Taylor's work, the liquid interface was found unstable so that water was lost from the pores. The air permeability method used by Arthur and his co-workers[5] for charcoals, Davidson[6] for soot blacks and Ergun and Orning[7] and Ergun[8] for cokes was also explored, but it was found that, because of the rather elaborate mathematical transformations required, it gave insufficiently precise results. This difficulty was accentuated by the fact that, although the directions given by Ergun were followed, a range of packing density of only about 8% could be obtained, compared with the 25% reported by Ergun.

The mercury density method which was finally adopted was that described in principle by Washburn[9] and used for petroleum cracking catalysts,[10,11] charcoal[12], ceramic materials[13] and coke.[14] Drake[10,11] used this method both at normal and elevated pressures. Provided that the pores within the particles are significantly smaller than the particles themselves, then, if the particles are confined in mercury in a closed, evacuated system and the pressure over the mercury varied, a plot of volume of mercury in the system against applied pressure should show a plateau. This will occur over a range of pressure which is adequate to outline the particles but insufficient to force mercury into the pores. The method is particularly suitable for coarse particles which can be readily retained on a filter permeable to mercury, thus facilitating the outlining process. Fine particles tend to pack together and resist penetration of mercury unless the apparatus is arranged to prevent this. Satisfactory results were obtained, however, using the Dutch State Mines design[15] of glass apparatus for coarser particles and a similar apparatus in stainless steel, adapted for use up to 100 lb/in.^{2} pressure, for the finer particles. The plateaux obtained were sometimes very short or, in some experiments with the finer grades, were no more than points of inflexion, but it was generally possible to interpolate the required density value easily to within $\pm 0{\cdot}01$, i.e. to about 0·5%.

The glass apparatus is shown in Fig. 3. The glass bottle (25 ml capacity) was evacuated through the capillary (2 mm internal diameter, 40 cm long) and a weighed amount of mercury allowed to be drawn through tap B to lower mark A. The vacuum was then released and the weighed coke sample

put into the bottle. The bottle was then evacuated a second time and more mercury introduced from a weighed container so that the amount could be determined at various levels of the mercury meniscus in the capillary. After the meniscus

Fig. 3. Glass apparatus for determining density of coke immersed in mercury

had reached mark *C* at the top of the capillary, its fall was noted as the pressure was increased in increments. The volume of the bottle and capillary had been previously calibrated by filling with mercury and weighing. The volume occupied by the coke at various pressures was calculated from these measurements and the results plotted, to give a curve of the type shown in Fig. 4. With this design the coke particles are forced to the wall of the bottle because of the curvature of the meniscus. Thus, as the mercury rises the coke is spread

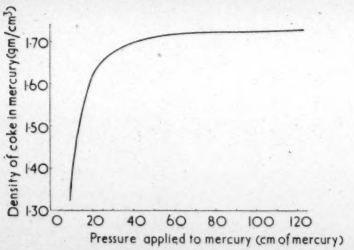

Fig. 4. A typical plot showing the change in density of a coke fraction immersed in mercury as pressure is applied. The density corresponding to the plateau gives the particle density

in a relatively thin layer around the wall of the bottle and readily outlined by the mercury.

The all-glass type of apparatus was found to be suitable only for sieve fractions coarser than 60 mesh, this being the finest size which could be outlined at 2 atmospheres pressure. A similar piece of equipment was manufactured of stainless steel thus permitting the use of pressures up to 100 lb/in.^{2} above atmospheric. Fractions down to 240 mesh size were measured with this, the mercury level being observed in a glass capillary which was sealed and sheathed in a steel tube.

DETERMINATION OF NUMBER OF PARTICLES PER GRAMME

The normal method of determining this number by counting a known weight on a microscope slide was found to be very tedious and inaccurate with the finer fractions because of the small weight and large sampling errors.

These drawbacks were overcome[16] by the development of automatic counting equipment which enabled $10^5 - 10^6$ particles to be counted rapidly and thus provided a reasonable amount of powder for weighing. The apparatus was based on the principle of drawing the particles in suspension through a capillary so that they passed successively under the objective of a microscope and intercepted light falling on a photomultiplier mounted in the eyepiece. The general arrangement is shown in Fig. 5.

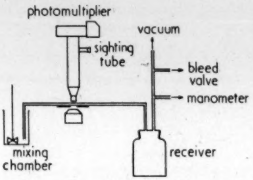

Fig. 5. Automatic counting equipment

For each coke fraction about 10^5 particles were counted and then weighed after they had been filtered, washed and dried. A set of these results can be seen in Table 2. An individual determination could be reproduced to within $\pm 0{\cdot}25\%$.

RESULTS

The values for particle density, projected area, number of particles per gramme and shape constant σ, are tabulated for different fractions in Table 2 and the results are plotted in Figs. 6–9.

Table 2. *Measured and derived quantities for sized fractions*

Size of fraction B.S. test sieves	*Mean size, D_m (μ)*	*Particle density, $\left(\frac{1}{V}\right)$ g/ml.*	*Projected area, A cm²/g*	*No. of particles per gramme, N*	*Projected area diameter, d_m (μ)*	$\frac{d_m}{D_m}$	*Elongation n*	*Shape constant σ*
− 22 + 36	560	1·69	45·1	$0{\cdot}34 \times 10^4$	1 030	1·84	1·8	0·575
− 36 + 52	358	1·73	72·0	$1{\cdot}90 \times 10^4$	695	1·94	1·8	0·558
− 60 + 72	231	1·72	121·0	$7{\cdot}23 \times 10^4$	461	2·00	—	0·539
− 52 + 72	253	1·77	96·8	$4{\cdot}7 \times 10^4$	511	2·02	1·9	0·556
− 72 + 100	182	1·73[5]	153·5	$8{\cdot}39 \times 10^4$	483	2·65	1·9	0·489
−100 + 120	138	1·79	212·7	$2{\cdot}98 \times 10^5$	301	2·18	2·5	0·507
−120 + 150	114	1·81	225·8	$4{\cdot}78 \times 10^5$	245	2·15	—	0·531
−120 + 200	100	1·79	245·5	$8{\cdot}88 \times 10^5$	187	1·87	2·3	0·566
−200 + 240	71	1·82	383·7	$2{\cdot}20 \times 10^6$	149	1·84	1·9	0·524

Particle density. The results for particle density are shown in Fig. 6. The general tendency is for the particle density to rise as the particles become finer. However, a fairly smooth variation is interrupted by a fall to a minimum and a sub-

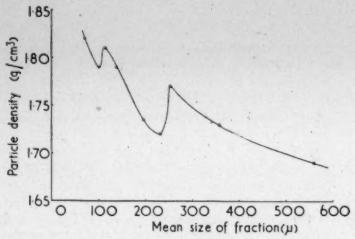

Fig. 6. Variation of particle density with the mean size of fraction

sequent rise in the range 100–250 μ, with possibly another minimum at just under 100 μ. The form of the curve broadly resembles that of similar curves for coal cokes recently published by Ergun and Owen[17] except that these authors find plateaux rather than minima.

Specific projected area and number of particles per gramme. These values are plotted on logarithmic scales against mean particle size in Figs. 7 and 8. The curves approximate to straight lines of slopes -1 and -3 respectively as required by simple theory for spheres. The specific projected area values show a departure from the smooth curve in the critical region 100–250 μ and there is some suggestion of a similar tendency in the values of N. The projected area diameter d_{as} can be obtained from the values of A and N, since by definition

$$A = N\frac{\pi}{4}(d_{as})^2$$

and the values are given in Table 2, column 6.

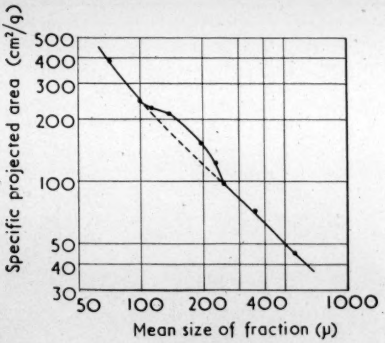

Fig. 7. Variation of specific projected area with mean particle size (logarithmic scales)

Microscopic examination. By direct measurement on photomicrographs of the individual sieve fractions, values of Heywood's elongation ratio[18] n (i.e. ratio length/breadth) were obtained for each particle. These were then averaged over all the particles (approximately 50) in a photograph. The resulting mean values are shown in column 8 of Table 2.

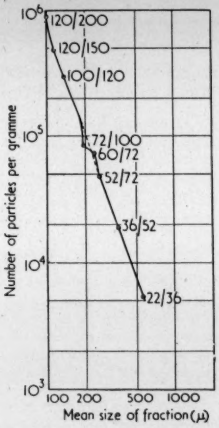

Fig. 8. Variation of number of particles per gramme with mean particle size (logarithmic scales)

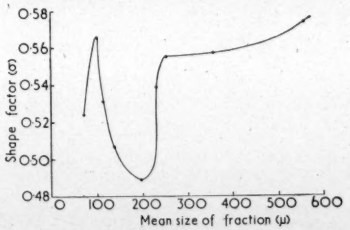

Fig. 9. Variation of shape constant with mean size of fraction

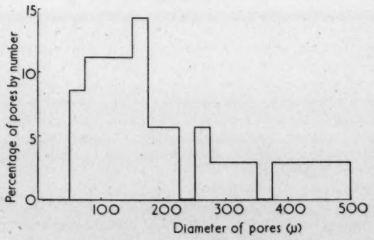

Fig. 10. Histogram showing frequency distribution by number of pores in a Scottish shale oil coke

A photograph was also made of the polished plane surface of a lump of unground coke. The diameters of 35 pores shown in this photograph were then measured according to Martin's convention[19] for particles. A histogram plot of frequency against diameter, using 25 μ intervals, shows most of the pores to lie between 50 and 280 μ, with a peak at about 150 μ. The histogram is shown in Fig. 10.

DISCUSSION

General shape of the particles. The numerical value of the shape constant is seen to vary from about 0·49 to 0·58, corresponding to particles which are very far from spherical. Therefore the possibilities are that the particles are flaky (length approximately equal to breadth and both much greater than thickness), rod-like (breadth approximately equal to thickness and both much less than length) or splint-like (length much greater than breadth, breadth much greater than thickness). The values for n of 1·8 to 2·5, however, obtained microscopically and shown in Table 2, suggest that in fact the particles are flakes.

Another shape constant may be defined as the ratio of the projected area to the aperture of the sieve which the particle will just pass. Heywood[18] has calculated the values of this constant (d_p/A in his notation) for various geometrical shapes and tabulated them against n, as defined above, and m, the "flakiness" ratio of breadth/thickness (Table 7 of Reference 18). Approximate values of this shape constant may be obtained from the present results by substituting the mean sieve size of the grade D_m for Heywood's A, the size of the sieve which the particle will just pass, and the mean projected area diameter over the grade, d_{as}, for Heywood's d_p. The values so derived are shown in column 7 of Table 2. Use of these values together with the corresponding value of n (column 8 of Table 2) makes it possible to estimate m from Heywood's table. This in fact involves extensive extrapolation for the coarser grades. The values for these grades are therefore very approximate and are shown in brackets in Table 3 below. The general tendency, however, is clearly for the particles to be "flaky."

Table 3. *Variation of* n *and* m *with mean sieve aperture*

Size of fraction	$\frac{\text{length}}{\text{breadth}}$ n	$\frac{d_{as}}{A_m}$	$\frac{\text{breadth}}{\text{thickness}}$ m
− 36 + 52	1·77	1·94	(8)
− 52 + 72	1·89	2·02	(8)
− 72 + 100	1·90	2·65	(35)
−100 + 120	2·46	2·18	4
−120 + 200	2·31	1·87	2·1
−200 + 240	1·9	1·84	3·2

The range of values obtained for σ corresponds to a range of 0·06 to 0·11 for Heywood's k. Table 1 of Heywood's earlier paper[2] shows how k varies with m and n for different regular solids and from his table it may be seen that flat plates ($m = 10$) give k values of the right order but that for rod-like particles no reasonable value of n can give this result.

This evidence therefore all indicates that the general shape of the particles is flaky.

General pattern of variations. As noted above, the curves for particle density and specific projected area show sharp changes of slope at about 250 μ and pronounced minima at rather smaller sizes. These experimental quantities are determined by completely independent methods and the results must therefore be taken as an index of marked variations in the shape of the particles. In fact the derived shape factor does show similar variations, falling steeply from a value of 0·56 at 250 μ to a minimum of 0·49 at 200 μ and then increasing again to 0·57 at 100 μ. As noted above, microscopical measurements, combined with Heywood's table, supplement these results and enable the conclusion to be drawn that from 250 μ down to 200 μ the particles become rapidly more flaky, indicating a lamellar type of fracture in this range. Thereafter the particles become more nearly equiaxial, indicating a tendency to fracture across the plates.

It is known[20,21] that some petroleum cokes show significant crystallite orientation, the lamellar planes of the carbon crystallites being preferentially oriented at right angles to the shortest dimensions of the particles, and this might explain the tendency of the coke grains to undergo lamellar fracture. At some limiting m value, dependent on the mechanical strength of the grain, however, one might expect fracture across the planes, with consequent increase in the value of σ and decrease in m.

The sharp changes at 250 μ indicate that some critical significance attaches to this dimension and it is natural to suppose that it may be connected with the pore structure of the coke. In fact, the pore distribution histogram (Fig. 10) shows that the great majority of the pores have diameters in the size range in which sharp changes in particle characteristics have been noted. Perhaps the "distance between adjacent pores" may be a better measure of particle diameter than the pore diameter. The latter, however, is a relatively simple and definite quantity to measure and with this coke the two quantities seem to be roughly of the same order of magnitude.

One can readily imagine a shell type of structure around the pores in the coke, causing particles of the appropriate size to have a plane lamellar structure which would then undergo fracture as suggested above. This structure can in fact be seen in Fig. 11, which is a photograph of a small area of a plane polished section of a lump of this coke.

Relation between shape constant and packing characteristics. A correlation between a particle shape constant and a packing

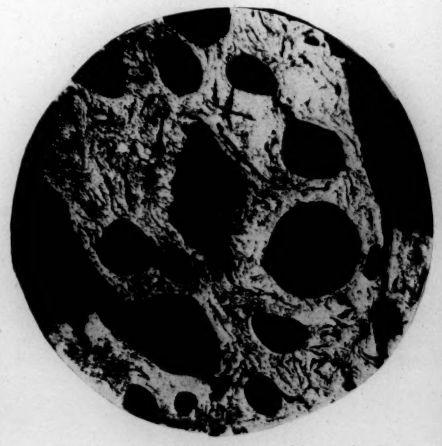

Fig. 11. Plane polished section of lump of coke. (Magnification ×46)

characteristic such as fractional voidage would be useful technically. Measurements of bulk density have been made on all the sieve fractions described in this work, and, with the aid of the measured particle densities, these have been converted to fractional voidages. The results showed the expected general trend towards higher voidages with more irregular particles but a quantitative correlation did not emerge. The variation in "bandwidth" of the sieve fractions used might well have an effect, but orientation in packing, which is to be expected with these markedly flaky particles, is probably even more important.

ACKNOWLEDGEMENTS

The authors are grateful to the Director, Atomic Energy Research Establishment, for permission to publish this work. Acknowledgement is also due to Mr. J. Hawkins for much help with the experimental work during the later stages of this investigation.

REFERENCES

(1) HAWKSLEY, P. G. W. *B.C.U.R.A. Monthly Bulletin*, **15**, p. 105 (1951).
(2) HEYWOOD, H. *Trans Inst. Mech. Engrs*, **125**, p. 383 (1933).
(3) *Sampling and Analysis of Coals and Cokes*. B.S. 725: 1944.
(4) GILCHRIST, J. D., and TAYLOR, J. *J. Inst. Fuel*, **24**, p. 207 (1951).
(5) ARTHUR, J. R., LINNETT, J. W., RAYNOR, E. J., and SINGTON, E. P. C. *Trans Faraday Soc.*, **46**, p. 270 (1950).
(6) DAVIDSON, H. W. (Private communication.)
(7) ERGUN, S., and ORNING, E. G. *Ind. Eng. Chem.*, **41**, p. 179 (1949).
(8) ERGUN, S. *Anal. Chem.*, **23**, p. 151 (1951).
(9) WASHBURN, E. W. *Proc. Nat. Acad. Sci. U.S.A.*, **7**, p. 115 (1921).
(10) DRAKE, L. C. *Ind. Eng. Chem.*, **41**, p. 780 (1949).
(11) RITTER, H. L., and DRAKE, L. C. *Ind. Eng. Chem.* (Anal. Edit.), **17**, p. 782 (1945).
(12) JUHOLA, A. J., and WIIG, E. O. *J. Amer. Chem. Soc.*, **71**, p. 2078 (1949).
(13) BUSBY, T. S. *J. Soc. Glass Tech.*, **34**, p. 10 (1950).
(14) VAN HEERDEN, C., NOBEL, A. P. P., and VAN KREVELEN, D. W. *Chem. Eng. Sci.*, **1**, p. 47 (1951).
(15) VAN KREVELEN, D. W. (Private communication.)
(16) BEIRNE, T., and HUTCHEON, J. M. *A.E.R.E. Report CE/R.* 1206.
(17) ERGUN, S., and OWEN, J. *Anal. Chem.*, **25**, p. 1222 (1953).
(18) HEYWOOD, H. *Symposium on Particle Size Analysis, Suppl. to Trans Instn Chem. Engrs*, **25**, p. 14 (1947).
(19) MARTIN, G. *Trans Brit. Ceram. Soc.*, **23**, p. 61 (1923).
(20) FRANKLIN, R. E. *Proc. Roy. Soc. A*, **209**, p. 213 (1951).
(21) HUTCHEON, J. M. *J. Inst. Fuel*, **26**, p. 309 (1953).

DISCUSSION

Mr. H. H. Watson: The width range of *inferred* breadth to thickness ratios given in Table 3 suggests this ratio would be sensitive to measurement, using a shadow-casting technique.

Dr. S. Guruswamy: I wish to say a few words on the method we have followed to determine the shape of coal particles and on the results obtained[1] for the shape of coal particles of different sizes, produced during the breakage of coal under different conditions. Our method to determine the shape consists in determining experimentally the statistical "diameter" D, volume V, and the surface area A of the coal particle of definite sieve sizes. D was determined by using a microscope fitted with a disk micrometer, the volume calculated from the number per gramme and the density of the coal particle, and the surface area by the liquid permeability method developed by Carman.[2]

The surface area factor f and the volume shape factor k were determined from the relations

$$A = fD^2 \text{ and } V = kD^3$$

The range of sieve size of coal particles used was from 7 to 170 B.S. mesh (approximately 3 to 0·1 mm, sieve opening). Coal particles obtained from (1) a hand-operated grinder, (2) pestle and mortar and (3) shatter test apparatus, were used to determine the shape; the experimentally determined value of k was found to lie between 0·13 and 0·28 and f between 2·5 and 4·5.

It has been found possible to give a "standard" shape to the coal particle. The coal particle can generally be described as a rectangular prism in shape, of length 1·5 to 2·4 times the breadth and thickness 0·3 to 0·5 times the breadth. The actual shape of the coal particle is compared with the "standard" rectangular prism shape by calculating the value of the ratio of the calculated surface area shape factors, to the observed ratio. The value of this ratio is less than one (0·6 to 0·98). It is concluded that coal particles are more angular than the "standard" rectangular prism shape. Further, it is found that coal particles produced by fracture are more angular than the ones obtained by crushing.

Authors' reply: We wish to say in reply to Mr. Watson that the object of our work was to measure shape factors by a method which did not involve microscopic observations with the attendant risk of personal errors. We have referred to breadth/thickness ratios only in so far as such measurements by other workers reinforce our own conclusions.

REFERENCES

(1) GURUSWAMY, ROY, DAS VARMA and SRINIVASAN. *J. Sci. Industr. Res.* (India), **12B**, pp. 91–101 (1953), and in course of publication.
(2) CARMAN. *J. Soc. Chem. Ind.*, **57**, p. 226 (1938).

Paper D.2

The significance and application of shape factors in particle size analysis

By W. H. M. Robins, B.Sc., National Coal Board, Pneumoconiosis Field Research, Ystrad Mynach, Glam.

By use of a new method for measuring the thicknesses of individual sub-sieve particles with the optical microscope and being able to measure the dimensions of their projected images as well, the surface and volume shape factors of the particles can be calculated. An expression can be derived for the ratio of the particle's projected diameter to its Stokes' diameter in terms of these factors.

Results of the examination of coal dust particles revealed a large variation in the shape factors between particles, which should also be found for particles of other materials. It is shown that in the application of shape factors to the correlation of results obtained by different methods for particle size analysis, the variation of these factors should be taken into account.

The method of application has been devised for use when comparing results of the microscope method with those of sedimentation methods, both gravimetric and light extinction. This method has been compared with the normal way in which only the average shape factor is applied. Differences occurred which could account for some of the past difficulties when the correlation of the sizing methods was attempted.

The largest particles of a sub-sieve fraction of a powder seen under the microscope have shape factors different from those of the smaller sizes.

The different methods[1] available for particle size analysis should give the same results for particles of spherical shape but agreement is not expected for particles of irregular shape and correlation of the results is achieved by the use of shape factors. These shape factors are usually the ratio of two average sizes rather than the average of the ratio of two sizes[2] and variation of the shape factors is ignored owing to the lack of a convenient method for measuring the three dimensions of individual particles whose sizes lie in the sub-sieve range. In the sub-micron range this can be done by use of the shadow-casting technique of electron microscopy. This method can be adopted for light microscopy, but the high vacuum techniques associated with electron microscopy are required.[3]

A method has been devised and developed for the optical microscope for measuring the thicknesses of fine particles and also the dimensions of their projected images.[4] The volume and surface shape factors of individual particles can be calculated by the use of the empirical formulae derived by Heywood.[1]

The results of the examination of fine coal particles revealed a large variation in shape between particles, and the significance and application of shape factors taking into account this variation will be discussed.

DEFINITIONS OF PARTICLE SIZE AND SHAPE

The sizes assigned to the particles of irregular shape by the different methods are given below with their symbols.

Sieve size A: the size of the smallest square aperture through which the particle will just pass.

The projected diameter measured under the microscope d_p: the diameter of the circle which has the same area as the projected image (unmagnified) of the particle with the least dimension of the particle in the line of sight.

The Stokes' diameter, measured by sedimentation methods d_s: the diameter of the sphere which has the same falling speed in a fluid as the particle.

Definitions of the various shape factors of an irregular particle are given below.[1]

The volume shape factor k is defined in the expression:

$$V = kd_p^3$$

where V is the volume of the particle.

The surface shape factor f is defined in the expression:

$$S = fd_p^2$$

where S is the surface area of the particle.

The proportions of the particle are n, the elongation ratio, and m the flakiness ratio.

$n = L/B$ where L and B are the length and breadth of the rectangle of smallest area that encloses the particle's projected image.

$m = B/T$ where T is the thickness of the particle, the dimension in the line of sight.

Expressions giving k and f in terms of m and n have been derived by Heywood.[1]

$$k = \frac{k_e}{m\sqrt{n}}$$

$$f = 1{\cdot}57 + Ck^{\frac{4}{3}}\left(\frac{n+1}{n^{\frac{1}{3}}}\right)$$

Where k_e and C are experimentally determined constants whose values depend on the geometric shapes approximated. Values for k_e and C of 0·47 and 3·0 respectively have been taken in this paper.

The ratio d_p/A has also been derived by Heywood in terms of the proportions of the particle:

$$\frac{d_p}{A} = \sqrt{[6nm^2/\pi(m^2+1)]} \qquad (1)$$

No entirely satisfactory expression for the ratio d_p/d_s has been found, but this can be derived from the one given by Hawksley.[2] This expression related the Stokes' diameter of a particle to its nominal diameter which is the diameter of the sphere having the same volume as the particle. By substitution the ratio d_p/d_s can be given in terms of k and f, thus

$$\frac{d_p}{d_s} = \sqrt{\left[\frac{(\pi f)^{\frac{1}{2}}}{6k}\right]} \qquad (2)$$

From equations (1) and (2) the ratio d_s/A can be found:

$$\frac{d_s}{A} = \sqrt{\left[\frac{36km^2n}{(\pi f)^{\frac{1}{2}}\pi(m^2+1)}\right]}$$

In Table 1 are given the values of the ratio d_p/d_s for varying proportions.

Table 1. *Values of d_p/d_s for varying proportions*

m \ n	1	$\sqrt{2}$	2
1	1	1·17	1·27
$\sqrt{2}$	1·26	1·32	1·44
2	1·39	1·50	1·61
$2\sqrt{2}$	1·59	1·73	1·86
4	1·85	2·01	2·17

In Table 2 are given the values of the ratio d_s/A for varying proportions.

Table 2. *Values of d_s/A for varying proportions*

m \ n	1	$\sqrt{2}$	2
1	1	1·02	1·11
$\sqrt{2}$	0·89	1·02	1·11
2	0·89	0·98	1·08
$2\sqrt{2}$	0·82	0·89	0·99
4	0·72	0·79	0·87

THE VARIATION OF THE SHAPE FACTORS OF FINE COAL PARTICLES

The volume shape factors were determined for individual particles of four coal dusts. The factor was determined for particles of projected diameter in the range 76 to 3 μ and the degree of accuracy was the same throughout. No real variation in k with size was found and the shape factors of the particles are given below as a grouped frequency distribution for each dust in Table 3.

Table 3. *Distribution of k for coal dusts*

Interval for k	*No. in interval for dust* Aa	Ag	Ba	Bg	*Overall distribution by* No.	%
0·047–0·075	0	0	6	1	7	0·9
0·075–0·103	12	10	14	6	42	5·5
0·103–0·132	20	12	20	10	62	8·1
0·132–0·160	25	21	32	21	99	12·9
0·160–0·188	33	22	37	22	114	14·9
0·188–0·216	31	26	32	31	120	15·7
0·216–0·245	32	20	33	27	112	14·7
0·245–0·273	21	12	32	25	90	11·9
0·273–0·301	11	7	24	15	57	7·4
0·301–0·329	15	2	7	3	27	3·5
0·329–0·357	7	2	8	7	24	3·1
0·357–0·386	1	0	5	1	7	0·9
0·386–0·413	0	1	1	2	4	0·5
Total	208	135	251	171	765	100·0

Statistical testing of the distributions for the dusts showed no significant differences between them, and the overall distribution has been taken in the succeeding analysis.

Taking the overall average of the elongation ratio for the coal particles, the intervals for f were calculated and then the intervals for the ratio d_p/d_s. The range of this ratio extended approximately from 1 to $2\sqrt{2}$ and in Table 4 are given the percentage of values in each of three intervals, together with the average values of k and f for each interval. Each figure has been given a symbol which will be used later.

Table 4. *Distribution of ratio d_p/d_s*

d_p/d_s *interval*	*% in interval*	*mean k for interval*	*mean f for interval*
$2\sqrt{2} - 2$	6·4 (p_1)	0·085 (k_1)	1·82 (f_1)
$2 - \sqrt{2}$	66·3 (p_2)	0·181 (k_2)	2·25 (f_2)
$\sqrt{2} - 1$	27·3 (p_3)	0·295 (k_3)	2·83 (f_3)

Overall average values of f, k and d_p/d_s are given below:

$$\text{mean } f = 2{\cdot}39;$$
$$\text{mean } k = 0{\cdot}206;$$
$$\text{mean } d_p/d_s = 1{\cdot}56.$$

The above table shows that of 1000 coal particles of Stokes' diameter 20 μ, 64 will have projected diameters in the range 57–40 μ, 663 in the range 40–28 μ and 273 in the range 28–20 μ and there will be variation in the shape factors between the size groups.

METHOD OF APPLYING SHAPE FACTOR d_p/d_s TAKING INTO ACCOUNT ITS VARIATION

Suppose a microscope count is made using the size intervals of Fairs,[5] the diameters in geometric progression with a common ratio $\sqrt{2}$. In Table 5 are given the results of a count symbolically in order of decreasing diameter.

Table 5. *Results of count*

Size interval (μ)	$d_{p1}-d_{p2}$	$d_{p2}-d_{p3}$	$d_{p3}-d_{p4}$	$d_{p4}-d_{p5}$	$d_{p5}-d_{p6}$	$<d_{p6}$
Frequency (v)	v_1	v_2	v_3	v_4	v_5	v_6

If the particles of the material have the variation in shape factors given in Table 4 then to convert the number distribution by d_p to the number distribution by Stokes' diameter, the following procedure is carried out. Taking the same numerical values for d_s (i.e. $d_{p1} = d_{s1}$, etc.) it can be seen that the particles lying in the interval $d_{p1} - d_{p2}$ will possess Stokes' diameters lying in the range $d_{s1} - d_{s5}$. In Table 6 is given the number distribution by d_s of the particles in the size interval d_{p1}–d_{p2}.

It has been assumed that there is a uniform distribution of values within the intervals for d_p and d_p/d_s. This is not strictly true, but will allow the significance of the shape variation to be shown.

When the number distribution by d_s has been derived for each d_p interval, the complete distribution by d_s is obtained by summing over each d_s interval. The mass and surface area distributions are obtained by substituting $pk\bar{d}_p^3$ and $pf\bar{d}_p^2$ respectively where p occurs in the number distribution, $\bar{d}_p$ being the central value of the d_p interval, and k and f have the values associated with each value of p in Table 4.

Table 6. *Derivation of number distribution by d_s*

d_p \ d_s	*Frequency of occurrence in d_s interval* d_1-d_2	d_2-d_3	d_3-d_4	d_4-d_5	d_5-d_6	$< d_6$	*Frequency of occurrence in d_p interval*
d_1-d_2	$\frac{p_3\sqrt{2}}{(1+\sqrt{2})}v_1$	$\frac{(p_3+p_2\sqrt{2})}{(1+\sqrt{2})}v_1$	$\frac{(p_2+p_1\sqrt{2})}{(1+\sqrt{2})}v_1$	$\frac{p_1}{(1+\sqrt{2})}v_1$			v_1

A NUMERICAL EXAMPLE OF THE APPLICATION OF SHAPE FACTORS

In Table 7 a typical distribution by number found by microscopy is given. The distributions by mass and surface were calculated in the normal manner and are also given in the table.

Table 7. *Typical distributions by microscopy*

$d_p(\mu)$ / Parameter	76–38	38–19	19–9·5	9·5–4·75	4·75–2·4	<2·4
No.	0·70	4·25	15·65	29·40	29·40	20·60
Mass	39·6	36·7	18·3	4·71	0·64	0·05
Surface	18·1	31·6	30·6	15·1	3·99	0·61

Table 8 shows the distributions of surface area by Stokes' diameter derived by (i) taking into account the variation in particle shape found for coal particles, and (ii) by applying the average value for the ratio of d_s to d_p. This latter method has in the past been the normal method of applying shape factors. The distributions would be derived in order to correlate with the distributions of surface area obtained using the light extinction method.

Table 8. *Surface area distributions by Stokes' diameter*

Stokes' diameter interval (μ)	*% area in size interval by method* 1	2
76–53·8	0·9	—
–38	4·8	2·0*
–26·9	10·9	11·0
–19	14·7	16·0
–13·4	16·2	16·0
– 9·5	16·2	17·0
– 6·7	13·9	15·0
– 4·75	10·1	10·5
– 3·36	6·33	6·7
– 2·4	3·42	3·3
< 2·4	2·55	2·5

* Top size of interval = 49 μ.

Similarly the distribution of mass by Stokes' diameter is derived from the distribution by d_p by (i) taking into account the variation in shape factors, (ii) by applying the average of the ratio d_s/d_p, and (iii) the indirect method of determining mass distribution from the surface area distribution of method (i) in Table 8. The distributions are shown in Table 9.

Table 9. *Mass distributions by Stokes' diameter*

Stokes' diameter interval (μ)	*% mass in size interval by method* 1	2	3
76–53·8	2·9	—	3·6
–38	12·6	7·0*	13·5
–26·9	21·5	25·0	21·8
–19	21·0	24·0	20·6
–13·4	16·4	16·0	16·1
– 9·5	11·7	13·0	11·4
– 6·7	7·35	8·0	6·95
– 4·75	3·78	4·2	3·55
– 3·36	1·77	1·8	1·58
– 2·4	0·68	0·7	0·60
< 2·4	0·32	0·3	0·32

* Top size of interval = 49 μ.

The distributions given by methods (i) and (ii) would be derived in order to correlate the microscope method with, say, the Andreasen pipette method. The distribution given by method (iii) would be derived from the surface area distribution given by the light extinction method.

DISCUSSION

The results of the preceding analysis rest on the assumption that a unique relationship between the projected and Stokes' diameters of a particle exists. The relationship chosen in this work is thought to be the best available and is based on the assumption that there is random orientation of the particles while sedimenting. A check on the chosen relationship can be made by comparing the average value of d_p/d_s for coal dust found by Watson[6] with the average value found in this work. The value of mean d_p/d_s found by Watson was 1·33 compared with the value of 1·56 found by the writer. The writer's estimate was made from measurements on particles whose largest sectional areas were in the plane of view. The ratio was derived by Watson using the Conifuge[7] and the particles might have been randomly oriented in the plane of view so that the surface diameter Δ of the particles was being measured. This diameter is related to the projected diameter thus:

$$\pi\Delta^2 = f d_p^2$$

Taking the average value of f found for coal dusts, 2·39, and substituting in the expression $d_p/d_s = 1{\cdot}56$ we have:

$$\Delta/d_s = 1{\cdot}36$$

Therefore, with the assumption that the particles were randomly oriented in Watson's work, the relationship chosen by the writer in this work is very likely the true one.

The application of shape factors, taking into account their variation, requires a knowledge of the variation of the ratio d_p/d_s and the values of volume and surface shape factors associated with each value. A combination of a method for determining d_p/d_s directly with the method for measuring particle thickness should produce all the necessary information required.

In the computation of the distribution given in Table 4 simplifications were made in order to lessen the amount of rather tedious calculations. These simplifications would tend to give a variation smaller than the true variation but should not affect the conclusions drawn from the analysis.

Inspection of Tables 8 and 9 shows that the distributions for mass and surface area derived by method (i), which takes into account the variation of the shape factors, give larger percentages for sizes greater than 38 μ than those derived by method (ii) in which only the average of the shape factors is applied. Fair agreement is obtained for the sizes less than 38 μ. Method (i) gives 76 μ as top size whilst method (ii) gives 49 μ.

The mass distribution given by method (iii) obtained from the surface area distribution is in good agreement with that given by method (i). This justifies the assumption that, in the light extinction method, the product of the particles' projected area and their Stokes' diameter is proportional to their mass.

In this discussion imperfections in the different forms of apparatus used to determine distributions by Stokes' diameter, for example, the hindered settling in the pipette method, have been ignored. An attempt has been made to devise the best method of applying shape factors in order to improve the

correlation of the results obtained by different methods of particle size analysis.

Only a comparison between microscope and sedimentation methods has been made but a similar analysis could be made to aline microscope results with sieving results from a knowledge of the variation in the ratio d_p/A and the value of the volume shape factor associated with each value of the ratio. From an examination of Table 2, which gives the values of d_s/A for varying proportions, it is seen that the results of sieving could be alined to sedimentation results without the use of shape factors as the value of d_s/A is fairly insensitive to the particle proportions.

Another effect of the variation in particle shape that must be mentioned is the case of powders having a top size fixed by sieving or an aerodynamic method. If the particles were all those that passed through a 200 B.S. sieve (75 μ aperture), particles having projected diameters as high as 150 μ might be seen under the microscope and these particles down to 75 μ in size would possess shape factors different from those of the smaller sizes. Similarly if a cut-off is made at 20 μ Stokes' diameter, particles of projected diameter as high as 60 μ would occur in the powder and the shape of the particles in the range 60 to 20 μ would be different from those in the less than 20 μ range.

The variation in shape shown by coal particles should not be typical of this material only, and particles produced from most solid materials should display a similar variation.

ACKNOWLEDGEMENT

I am extremely grateful to Mr. J. R. Ashford of the Scientific Department, National Coal Board, for deriving Table 6 of the paper.

REFERENCES

(1) HEYWOOD, H. *Symposium on Particle Size Analysis, Suppl. to Trans Instn Chem. Engrs.*, **25,** p. 14 (1947).
(2) HAWKSLEY, P. G. W. *British Coal Utilisation Research Association*, **15,** p. 105 (1951).
(3) WALTON, W. H. *Symposium on Particle Size Analysis, Suppl. to Trans Instn Chem. Engrs* (1947).
(4) ROBINS, W. H. M. *Nature* [*London*], **170,** p. 583 (1952).
(5) FAIRS, G. L. *Chem. Ind.*, **62,** p. 374 (1943).
(6) WATSON, H. H. *Brit. J. Industr. Med.*, **10,** p. 93 (1953).
(7) SAWYER, K. F., and WALTON, W. H. *J. Sci. Instrum.*, **27,** p. 272 (1950).

DISCUSSION

Dr. H. Heywood: It was realized that the mean values for shape factors determined on groups of equal sized particles could only be applied statistically, i.e. that there was a very considerable variation in the shape factor for such particles, but Mr. Robins's paper was, he believed, the first account of measurements to show the frequency distribution of shape factors in different particle size groups.

Mr. Robins had quoted an equation that I had developed to relate the surface and volume coefficients for irregularly shaped particles. The theory by which this equation had been derived had not been published, but briefly the basis was as follows.

The values of the surface and volume coefficients f and k respectively were a maximum when the particle was equidimensional, i.e. the flatness m and the elongation n were both unity. This applied to all shapes of particles, though the numerical values would differ. If the particle were flattened, n remained unity but m increased, and the values of f and k both decreased until for a particle of negligible thickness k became zero and f became $\pi/2 = 1{\cdot}57$. This characteristic also applied to all shapes of particle when m tended to infinity. If, however, the particle were elongated, m remained unity and n increased; f and k would both decrease as before, but would not have the same relationship as for flattened particles. The graphical relationship between f and k for flattened prisms was expressed by a straight line starting from the point $f = 1{\cdot}57$, $k = 0$, but for flattened particles of tetrahedral or ellipsoidal shape the relationship was expressed by curves starting from the same origin. Within the range $m = n = 1$ to $m = n = 3$ it was possible to represent the relationship between f and k with sufficient accuracy by the equation which had been quoted, namely, $f = 1{\cdot}57 + Ck^{4/3}(n + 1)/n^{\frac{1}{3}}$, in which the coefficient C varied from 3·3 for angular tetrahedral particles to 2·1 for rounded particles. If the proportions and the geometrical shape class of the particles were estimated from microscopical observations, the surface coefficient f could be calculated with a degree of accuracy that was sufficient for many purposes.

Author's reply: The method described by Dr. Heywood to derive the relationship between the volume and surface co-efficients of an irregular particle is of great interest and it is satisfying to know that the equation is valid over wide ranges of values for the particle proportions—ranges which cover the majority of values found for coal particles.

When measuring particle proportions, I made no attempt to classify the particles by geometric shape, but took average values for the empirical constants k_e and C. The average value of k_e was found by Dr. Heywood* to be fairly constant for particles of different materials and the overall average of 0·47 was taken by the writer. The constancy was due to the particles of a material falling into, not one, but a number of geometric shape classes, and for this reason 3·0 was considered a fair average to take for C.

* HEYWOOD. *Chemistry and Industry*, **56,** p. 149, (1937).

Paper D.3

The terminal velocity and size of airborne dust particles

By V. TIMBRELL, B.Sc., A.R.C.S., D.I.C., Ph.D., Pneumoconiosis Research Unit, Llandough Hospital, Nr. Penarth, Glam.

An instrument for sampling airborne particles is briefly described, in which the particles are classified according to their terminal velocities and deposited on a glass plate in a continuously graded sample. It can be employed to determine: (i) the Stokes' diameter-frequency distribution; (ii) the variation of mean projected diameter for a constant value of Stokes' diameter, and the variation of the Stokes' diameter for a constant value of mean projected diameter; (iii) the mean weight of particles of given Stokes' diameter.

The numerous techniques that have been developed and suggested for the measurement of the concentration of airborne dust, are based on a number of different physical parameters of the particles. However, the motion of a dust particle in air and within the human respiratory system is determined by the value of the parameter, terminal velocity, and only particles of low terminal velocity are respirable and able to reach the lung alveoli where they may cause pulmonary disease.

To estimate how well the measure of dust concentration as provided by a given sampling technique is likely to correlate with the amount of dust that would be deposited in the lung, it is ideally necessary to know the relation of the parameter measured by the method to the terminal velocity of particles for typical dust clouds.

This paper deals with a method of investigating the relationships between the terminal velocity and other size parameters of particles constituting a dust cloud. After describing in outline the dust sampling instrument used in such an investigation the following will be considered:

(i) the determination of the Stokes' diameter—frequency distribution;
(ii) the determination of the variation of the (mean) projected diameter, as measured by microscope, for a constant value of Stokes' diameter;
(iii) the determination of the variation of the Stokes' diameter for a constant value of projected diameter;
(iv) a model which demonstrates the combined relationship between the Stokes' diameter, the projected diameter, and the two frequency distributions based on these parameters;
(v) the determination of the mean weight of particles of given Stokes' diameter.

THE GRAVITATIONAL TERMINAL VELOCITY DUST SAMPLER

The sampling instrument resembles the Conifuge described by Sawyer and Walton,[1] in that the particles are "winnowed" by a stream of clean air, but differs from the Conifuge by employing gravity instead of centrifugal force to deposit the particles. An exploded diagram of the instrument is shown in Fig. 1.

In operation the instrument is air-tight except for the sampling orifice. The centrifugal fan *K* driven by a constant-speed electric motor *M* circulates clean winnowing air round the instrument at a constant rate in the directions indicated by the arrows. The flow rate (of the order of 100 c.c./min) is measured by the Rotameter *R* and can be set to the desired value by means of the restricting tap *T*.

A is a right-cylinder with its axis vertical and with its ends closed by the two parallel disks *B* and *C* to form a drum. A third disk *D*, which is of slightly smaller diameter than the drum, is mounted axially within it. *EFGH* is a duct of rectangular cross-section and contains two right-angle bends. The lower limb *GH* of the duct passes through the wall of the drum and extends to the axis of the drum with the disks *B* and *D* forming the roof and floor respectively: the limb *GH* expands horizontally from the wall to the axis of the drum. Before sampling, two thin glass plates are inserted

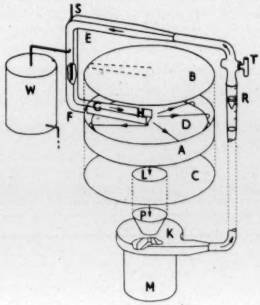

Fig. 1. The gravitational terminal velocity dust sampling instrument

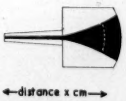

Fig. 2. Profile of the deposit on the collecting glass plates

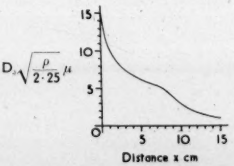

Fig. 3. A typical calibration curve

through a door in the wall of the drum; one is placed on the floor of the duct *GH* and the other is placed on the disk *D* in front of the exit of the section *GH*.

It will be seen that the circulating winnowing air after passing the point *G* in the duct, gradually loses speed in the section *GH* and after reaching the end moves radially outwards between the disks *B* and *D* at rapidly decreasing speed.

After rounding the periphery of the disk D the air passes radially inwards towards a hole L in the base of the drum and then through a filter paper P into the fan to be re-circulated. Except in the fan the motion of the air in the circuit is streamline.

The dust-laden air is drawn through the small-bore tube S which enters the system at the bend E in the duct and lies on the axis of the vertical section. The sampling rate is controlled by the rate at which clean air is withdrawn from the duct into the aspirator W *via* the small-bore bleed tube, and is nominally 1% of the winnowing rate. The sampled air leaves the sampling tube in the form of a fine filament which rapidly becomes isokinetic with the winnowing air.

All sampled dust particles, after traversing the bend at F, have a horizontal velocity equal to that of the winnowing air and fall under gravity at their individual terminal velocities. The lower the terminal velocity of a dust particle the further the particle is carried along by the winnowing air before being deposited on a glass plate. The profile of the dust deposit on the plates is shown in Fig. 2; the plates are shown vertically below their actual position in the sampling instrument in Fig. 1. On the plate on the floor of the duct GH, the particles are confined to a strip which gradually widens as the duct widens; particles of the same terminal velocity lie on a line perpendicular to the length of the strip. On the other glass plate the particles are confined to a sector of a circle; particles of the same terminal velocity lie on an arc of the sector. The filter paper prevents the very fine particles which are not deposited from being re-circulated.

The quality of the separation of particles according to terminal velocity is demonstrated by the uniformity of size of solid spherical particles. Fig. 4 shows a photomicrograph

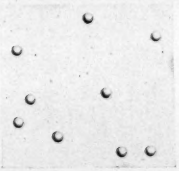

Fig. 4. Photomicrograph of Pyrex glass spheres (density 2·25) of diameter 10 μ

at a site in the deposit where the diameter of glass spheres collected is 10 μ; the separation at other diameters is of similar quality. Once the instrument has been calibrated, the Stokes' diameter of an irregular particle can be determined from the position of the particle in a deposit. Calibration consists of collecting solid spherical particles of known density in the same deposit as the irregular particles, and under the same operating conditions, and determining the average diameter of the spheres encountered when the deposit is scanned under the microscope along lines of nominally constant terminal velocity at different distances along the deposit; the diameters are measured accurately by means of the microscope attachment described elsewhere.[2] Glass spheres are particularly suitable for the purpose because of their exact sphericity and because their homogeneity can be checked by microscopic examination. The typical calibration curve shown in Fig. 3 was obtained by using Pyrex glass spheres of density 2·25 g/cm^3; its distance axis is vertically below and to the same scale as that of the deposit in Fig. 2. As the product of diameter and square root of the density is constant for spheres of different density at a given site in the deposit, the vertical axis of the calibration curve is drawn in units of $D_s\sqrt{(\rho/2{\cdot}25)}\mu$ so that the Stokes' diameter D_s of a particle of density ρ may be read directly.

The particles collected in a single sample cover a 200 : 1 range of terminal velocity; the absolute range depends on the flow rate of the winnowing air.

DETAILS OF TWO LABORATORY DUST CLOUDS EXAMINED

In the laboratory the dust clouds have been generated by dispersing the dust from a packed sample into a large cabinet by means of a dust feed mechanism.[3] The clouds formed in this way contain relatively few aggregates.

Some results on two materials, a ground glass and a coal, are quoted later. The factory-ground glass (which was the same as that used to produce the glass spheres for calibrating the instrument), although not of immediate practical importance, is of interest because any aggregates present in the deposit could be recognized during microscopic examination and discounted, and the variation of shape with size of only unitary particles studied with little chance of artefacts.

The lump of coal (bituminous) was passed through a pulverizer[4] to produce a sample for dispersion. As far as possible aggregates in the deposit were again discounted during microscopic examination.

STOKES' DIAMETER-FREQUENCY DISTRIBUTION

The Stokes' diameter-frequency distribution of irregular particles of a substance can be readily determined from the graded deposit. By scanning the deposit under the microscope along lines of constant Stokes' diameter, the numbers $N_1, N_2, N_3 \ldots$ of particles that occur within narrow zones of widths $\Delta x_1, \Delta x_2, \Delta x_3 \ldots$ situated at $x_1, x_2, x_3 \ldots$, are counted. From the calibration curve the values of the mean Stokes' diameter of the zones are $D_{s1}, D_{s2}, D_{s3} \ldots$ and the widths of the zones in terms of Stokes' diameter are

$$\Delta x_1\left|\frac{dD_s}{dx}\right|_{x_1}, \quad \Delta x_2\left|\frac{dD_s}{dx}\right|_{x_2}, \quad \Delta x_3\left|\frac{dD_s}{dx}\right|_{x_3} \ldots$$

where $\left|\frac{dD_s}{dx}\right|_{x_1}, \left|\frac{dD_s}{dx}\right|_{x_2}, \left|\frac{dD_s}{dx}\right|_{x_3} \ldots$ are the corresponding gradients of the curve. The frequencies of the particles within equal intervals of Stokes' diameter at $D_{s1}, D_{s2}, D_{s3} \ldots$ are therefore

$$\frac{N_1}{\Delta x_1\left|\frac{dD_s}{dx}\right|_{x_1}}, \quad \frac{N_2}{\Delta x_2\left|\frac{dD_s}{dx}\right|_{x_2}}, \quad \frac{N_3}{\Delta x_3\left|\frac{dD_s}{dx}\right|_{x_3}}, \ldots,$$

and are the ordinates of a histogram.

It will be noted that the area allotted within the deposit to particles of given Stokes' diameter decreases with increase of Stokes' diameter. Thus, although in general the relative frequency of particles in an airborne cloud decreases with increase of Stokes' diameter, the actual counts $N_1, N_2, N_3 \ldots$ are of the same order of magnitude and the percentage accuracy of the frequency determination is approximately the same for particles of all sizes. Counting of the particles is normally done under a 4 mm objective, and while the widths $\Delta x_1, \Delta x_2, \Delta x_3 \ldots$ of the zones are kept small the actual values are so chosen that a large number of particles is counted within each zone.

VARIATION OF THE PROJECTED DIAMETER FOR A GIVEN STOKES' DIAMETER

The method that has been used for measuring the projected area of an irregular particle, from which the projected diameter can be calculated, is similar to that used by Watson.[5]

With an opaque ink the silhouette of the image of the particle on the screen of a Vickers projection microscope is drawn on tracing paper. The silhouette and a blank piece of the tracing paper are then placed in turn on an aperture illuminated by a steady light source and backed by a selenium photocell. Once the arrangement has been calibrated with silhouettes of simple shape and known area, the area of the silhouette of the irregular particle can be determined from the fractional reduction of the photocell current which is caused by the silhouette. The projected area of the particle, and hence the value of the projected diameter, can then be evaluated from the area of its silhouette and the magnification of the microscope.

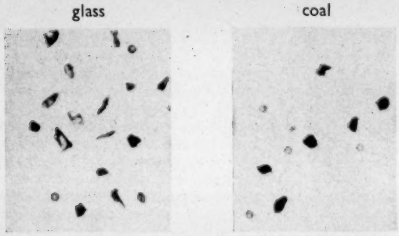

Fig. 5. Photomicrographs of glass and coal deposits each containing calibrating glass spheres of diameter 6 μ

To investigate the variation of the projected diameter for particles of a specified Stokes' diameter, the deposit is scanned along the line of constant Stokes' diameter at the position indicated by the calibration curve, and the projected diameter of each particle determined in the manner described above. Fig. 5 shows photomicrographs of small areas in the deposits of the ground glass and the coal. The results are plotted as histograms of relative frequency against the ratio, projected diameter (D_p)/Stokes' diameter (D_s).

Calculated values and standard errors of mean D_p/D_s and the standard deviations of the distributions

	D_s	Mean $\frac{D_p}{D_s}$	Standard deviation of distribution	No. of observations
Glass	2 μ	1·49 ± 0·019	0·227	145
($\rho = 2{\cdot}25$)	6 μ	1·49 ± 0·019	0·243	160
	10 μ	1·49 ± 0·020	0·295	213
Coal	2·5 μ	1·34 ± 0·022	0·267	147
($\rho = 1{\cdot}35$)	7·5 μ	1·35 ± 0·018	0·226	153
	12·5 μ	1·35 ± 0·024	0·287	146

Figs. 6 and 7 and the table show the results that have been obtained at three values of Stokes' diameter, for the glass and the coal respectively.

Neither in the glass nor the coal is there a significant difference in the value of mean D_p/D_s for the various values of the Stokes' diameter, this indicating no change in the shape of the particles with size.

The results for both the glass and the coal show particles with D_p less than D_s. In the case of the glass particles, whose densities are always very nearly equal to the bulk

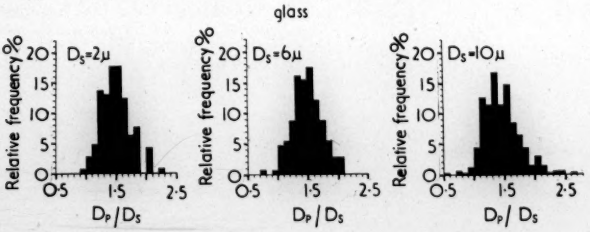

Fig. 6. Histograms showing variation of projected diameter of the glass particles for given Stokes' diameters

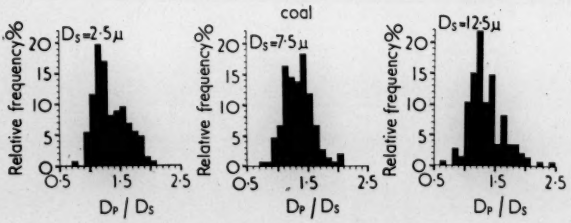

Fig. 7. Histograms showing variation of projected diameter of the coal particles for given Stokes' diameters

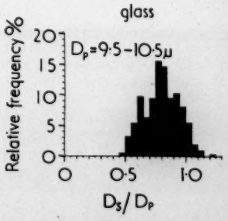

Fig. 8. Histogram showing variation of Stokes' diameter of the glass particles for a given projected diameter

density, these are elongated particles deposited in positions other than those of maximum stability and presenting a small projected diameter to the vertical view under the microscope. In the case of the coal, these particles are either elongated or contain material whose density is greater than the bulk density.

VARIATION OF STOKES' DIAMETER FOR GIVEN PROJECTED DIAMETER

The method of this determination is similar to the method of determining the Stokes' diameter-frequency distribution as described earlier, except that the only particles of interest are those with projected diameters within a narrow range. At various distances along the deposit it is scanned under the Vickers microscope along the lines of constant Stokes' diameters and, by sizing all the particles, the numbers of particles in each zone which have projected diameters within a narrow range are determined. The relative frequencies of the particles within equal intervals of Stokes' diameter, at the values of Stokes' diameter corresponding to the various positions, are calculated by dividing each number count by the known width of the zone and by the gradient of the calibration curve.

Fig. 8 shows a result obtained for the glass, plotted as a histogram of relative frequency against D_s/D_p. The value of mean D_s/D_p is 0·84 and the standard deviation of the distribution is 0·128. The spread demonstrates the appreciable effect of shape on the Stokes' diameter of a particle of given projected diameter.

MODEL OF THE RELATIONSHIP BETWEEN STOKES' DIAMETER AND PROJECTED DIAMETER

The relationship between the Stokes' diameter, the projected diameter and the frequency distributions according to these parameters is demonstrated by a model suggested by R. G. Carpenter. Fig. 9 shows the model constructed from results on the glass. In the model:

(i) the two horizontal axes of the mutually perpendicular system are of Stokes' diameter and projected diameter respectively, while the vertical axis is of relative frequency;

(ii) the curves of intersection of planes perpendicular to the Stokes' diameter axis with the surface of the model (one of which is indicated by the full line), show the variation of projected diameter for constant values of Stokes' diameter. The areas of the vertical sections bounded by these curves and by the horizontal plane are proportional to the relative frequencies of the particles on the basis of Stokes' diameter;

(iii) the curves of intersection of planes perpendicular to the projected diameter axis with the surface of the model (one of which is indicated by the broken line), show the variation of Stokes' diameter for constant values of projected diameter. The areas of the vertical sections bounded by these curves and the horizontal plane are proportional to the relative frequencies of the particles on the basis of projected diameter.

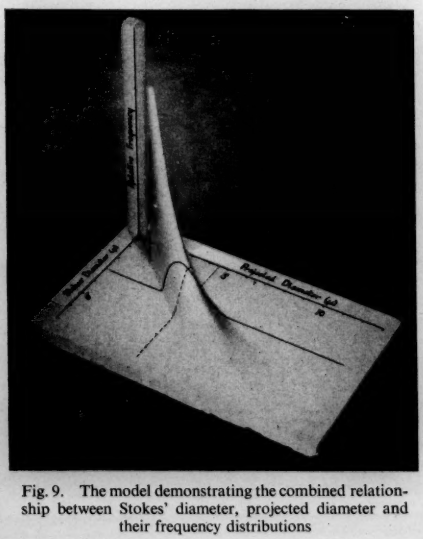

Fig. 9. The model demonstrating the combined relationship between Stokes' diameter, projected diameter and their frequency distributions

MEAN WEIGHT OF PARTICLES OF GIVEN STOKES' DIAMETER

For this determination the sampling instrument after being calibrated is operated in the cloud of irregular particles, two pairs of glass collecting plates being enclosed alternately in the instrument, the first pair for long periods to collect a deposit heavy enough for weighing and the second pair for short periods to collect a thin countable sample; the total volume of air sampled during the collection of each deposit is noted.

The weights of particles within narrow intervals of Stokes' diameter are determined by weighing the first pair of plates before and after the successive removals of zones of the deposit; the values of Stokes' diameter corresponding to these zones are read from the calibration curve. The number distribution by Stokes' diameter of the particles in the countable deposit is determined in the manner described previously, and by multiplying the number scale by a factor equal to the ratio of the volumes of air sampled during the collection of the two deposits, the number distribution within the heavy deposit is obtained.

Both the weight and number of irregular particles in the same interval of Stokes' diameter at a given value of Stokes' diameter can therefore be determined, and the mean weight of the particles and (knowing the density) the diameter D_v of the sphere with the same mean volume as the particles can be calculated.

For the glass, D_v/D_s has been found to have an average value of 1·5 over the range of D_s of 3–15 μ and is equal, within experimental error, to the mean value of D_p/D_s which has been quoted earlier. The mean volume of the irregular particles of given Stokes' diameter can therefore be estimated for this material from the mean value of the projected diameter of the particles as measured by the microscope.

ACKNOWLEDGEMENTS

I wish to express my thanks to Mr. S. R. Morgan who carried out most of the experimental investigation; to Mr. R. G. Carpenter for suggesting and computing the model

shown in the paper, and to Mr. T. J. H. Cooke for constructing the model.

REFERENCES

(1) SAWYER, K. F., and WALTON, W. H. *J. Sci. Instrum.*, **27**, p. 272 (1950).
(2) TIMBRELL, V. *Nature [London]*, **170**, p. 318 (1952).
(3) WRIGHT, B. M. *J. Sci. Instrum.*, **27**, p. 12 (1950).
(4) WRIGHT, B. M. *Chem. Ind.*, p. 8 (1953).
(5) WATSON, H. H. Private communication.

[*Comments relating to Paper D.3 will also be found among those on Paper D.4 on p.* S 93.]

Paper D.4

The relation between free falling speed and particle size of airborne dusts

By R. J. HAMILTON, B.Sc., A.Inst.P., Scientific Department, National Coal Board.

The relation between the particle size, as measured microscopically, and the free-falling speed of some industrial dusts—coal, rock, cotton and asbestos—has been studied with the aid of the Conifuge. It was found that particles of a given falling speed cover a wide range of sizes, the relation between the two parameters differing with various dusts, and even with different types of coal. The result is significant in relation to the assessment of health hazard of industrial dusts, since these are conventionally classified by microscope sizing, whereas respirability is a function of falling speed.

Conventional methods of airborne particle sampling and classification are largely based upon microscope size analysis. It is, however, the aerodynamic properties of dust particles which determine whether or not they will penetrate into the lungs, since the protective filtration afforded by the nose and upper respiratory passage is due to the mechanisms of impingement and sedimentation.(1) Methods of selective sampling have been developed, and are described in another paper presented to this conference;(2) these methods provide classification of particles by free-falling speed, and thus allow the respirable fraction only to be collected. It is necessary to determine the relation between the parameters of microscope size and free-falling speed in order to appreciate fully the effect of using this selective sampling technique.

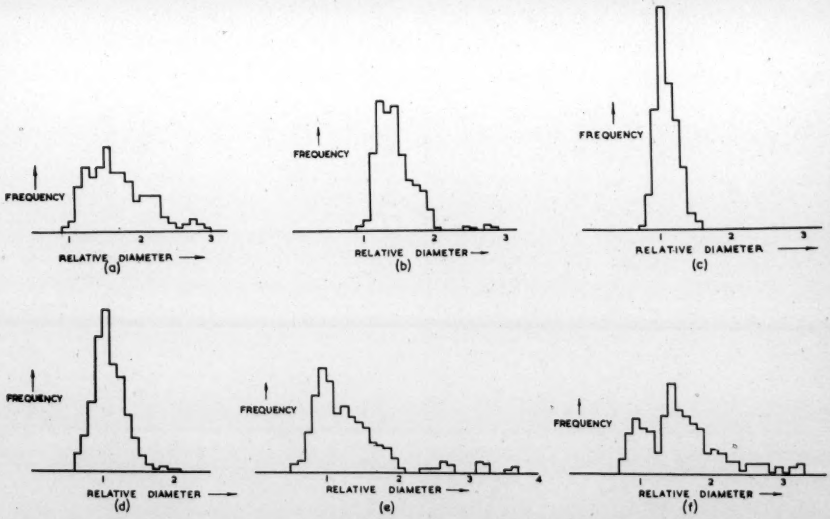

Fig 1. Frequency histograms, in which particle frequency for a given falling speed is plotted against particle diameter relative to that of unit density spheres of the same falling speed. The spheres are in the 5–6 μ size range

(*a*) Llandebie anthracite laboratory cloud; (*b*) Wattstown (coal) face (high rank); (*c*) Cannock Wood (coal) face (low rank); (*d*) Betteshanger (rock dust); (*e*) asbestos dust; (*f*) cotton dust.

EXPERIMENTAL WORK

The Conifuge[3] is an almost ideal tool for this investigation. In this instrument, the particles are segregated according to their free-falling speed. An almost pure "spectrum" of particles results, and examination of the deposits at any given position along the length of the slide reveals the shapes and sizes of all particles having the falling speed characteristics of their position. It is possible to cover a 500 : 1 range of falling speed in a single sample.

The Conifuge used in the trials described was constructed from drawings made available by the Chemical Defence Experimental Establishment. For use underground, the instrument was driven by an air turbine, arranged with the aid of a centrifugal governor and air-pressure reducing valve, to rotate at a constant speed of 3000 r.p.m. For the samples taken above ground, the instrument was driven by a 230 V electric motor. It is important that the speed of rotation be kept constant during the sampling process.

Although it is possible to relate the position of a particle on the Conifuge slide with its falling speed once the instrument has been calibrated, a different technique was employed in this work. After the "industrial" dust sample had been collected, a cloud of solid spheres was sampled, so that the relation between size of dust particle and size of sphere of equal falling speed was immediately apparent from an examination of the slide at a given point. At the same time the constancy of size of the spheres gives an indication as to whether the instrument is operating correctly. The spheres were produced by spraying an aqueous solution of Indian ink with a spinning disk-type sprayer, adjusted in such a way that, after evaporation, solid spheres varying in diameter from 1·5 to 15 μ were produced. The density of these spheres was 1·4 g/cm^3, confirmed by comparing their diameters with those of paraffin wax spheres of the same settling velocity.

In each sample, after the industrial dust and the spheres had been collected, photomicrographs of a series of traverses across the slides were obtained with a Vickers projection microscope; each traverse corresponded to a given falling speed, characterized by the diameter of the spheres. It was found convenient and economical to use bromide paper negatives for this work. The mean projected diameters of the irregular shaped particles were calculated from their projected areas determined by examination through millimetre square graph paper. Finally, the results of this particle measurement were plotted as a frequency histogram showing the number of particles as a function of the ratio: (mean projected diameter of particle)/(diameter of spheres of density 1·4 g/cm^3) for each traverse.

The following dust clouds were examined:

(1) Four types of coal dust, generated in a wind-swept "tumble mill."

(2) Three coal dusts, obtained under normal mining conditions.

(3) Two rock dusts, obtained underground during mining operations.

(4) "Cotton" dust, obtained from a carding room.

(5) "Asbestos" dust, produced in a workroom where asbestos board is trimmed by grinding on an emery wheel.

From the experimental data, various quantities have been calculated and these are set out in Table 1. Selected histograms from which these results were obtained are shown in Fig. 1. Photomicrographs of items (1), (4) and (5) are reproduced in Fig. 2.

It will be observed that for coal dust samples obtained in the laboratory there is a tendency for there to be a greater

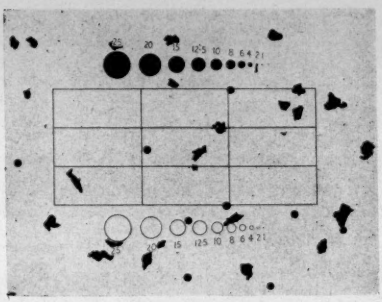

(*a*)

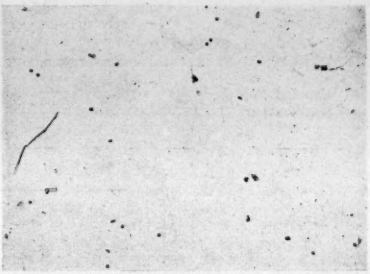

(*b*)

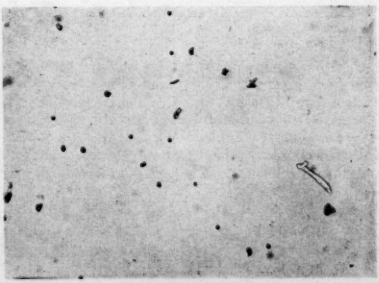

(*c*)

Fig. 2. Photomicrographs of dust samples

(*a*) Coal particles and spheres (1·4 g/cm^3) of the same falling speed (magnification ×225).

(*b*) Asbestos dust with spheres (1·4 g/cm^3) of same falling speed (magnification ×150).

(*c*) Cotton dust from a carding room with spheres (1·4 g/cm^3) of same falling speed (magnification ×150).

Table 1. *Quantities calculated from experimental data*

Dust	Method of production	Diam. (μ) of spheres (1·4 g/cm³)	Range of dust size (μ)	Median rel. diam. *	Effective density g/cm³ †
Coal					
Llandebie anthracite	Laboratory tumble mill	8	9·6–29·6	2·05	0·33
		5	5·5–17·5	1·9	0·39
		3	3·6– 9	1·65	0·51
"Unknown" anthracite	Laboratory tumble mill	8	8·8–25·6	1·9	0·39
		5	5·5–18·5	1·6	0·54
		3	3– 6·3	1·4	0·71
Cwm "Mildred"	Laboratory tumble mill	8	8–25·6	1·83	0·42
		5	5–15	1·7	0·48
		3	3·3– 6·9	1·55	0·58
Ashington "Plessey"	Laboratory tumble mill	8	10·4–26·4	1·9	0·39
		5	6–19	1·8	0·43
		3	3– 6·9	1·25	0·9
Wattstown (steam coal)	Coal face	8	8–25·6	1·55	0·58
		4	4·4–14	1·63	0·53
Cannock Wood (low rank coal)	Coal face	9	7·2–18·9	1·5	0·62
		3	2·7– 5·7	1·3	0·83
Coventry (low rank coal)	Coal face	8	8–15·2	1·12	1·1
		5	5–11·5	1·35	0·76
		3	3– 7·5	1·3	0·83
Cannock Wood (coal)	Transfer point	4	4·4–11·6	1·6	0·55
Rock					
Cannock Wood	Transfer point	4	4·4–9·6	1·5	0·62
Betteshanger	Drift	7	4·9–14	1·15	1·1
		5	3·5–12	1·25	0·9
Cotton	Carding room	5	4·5–19	1·7	0·49
		4	3·6–15·6	1·7	0·48
		3	2·4–11·1	1·57	0·57
Asbestos	Grinding	5	2·5–25·5	1·22	0·95
		4	2·4–13·2	1·45	0·67
		3	2·1–15	1·38	0·74

* From histograms, in which frequency was plotted against diameter relative to diameter of $p = 1{\cdot}4$ spheres of equal free-falling speed.

† The density of a spherical particle which is of the same projected diameter as the irregular particle and has the same free-falling speed.

difference between the size of spheres and coal particles with increase in particle size. This effect was investigated further by "shadow-casting" with tin a Conifuge slide, on which was a sample of coal dust and Indian ink spheres. This technique is similar to that used in the preparation of electron microscope samples. The length of shadow cast by the spheres indicated the angle of incidence, and from the lengths of shadows cast by the coal particles an estimate of their projected height could be obtained. Results are given in Table 2.

Table 2. *Measurements obtained from "shadowed" Conifuge slide*

	Coal dust particle dimensions		
Diam. (μ) of spheres (1·4 g/cm³)	Median width (A) (μ)	Median height ($S \sin \theta$) (μ)	$S \sin \theta / A$ %
9	19·2	7·3	37
6	10·0	4·6	46
4	5·9	3·4	58

DISCUSSION AND CONCLUSIONS

It will be seen from the results of this work that in every case the particles of a given free-falling speed cover a wide range of sizes. The extent of this size range varies with different dusts, as also does the relation between the diameter of unit density spheres and the "median" particle diameter for dust of the same falling speed.

Coal dust particles vary in size from one to three times the diameter of the sphere of the same falling speed and density, and there is also evidence that the relation between dust size and spherical diameter varies in samples from different collieries (e.g. between Wattstown, Cannock Wood and Coventry). There is an even greater difference between the coal dust samples obtained underground and in the laboratory. This appears to be due to the increased degree of aggregation present in the laboratory clouds. Results obtained from the shadow-casting technique indicate that with laboratory dust the particles tend to become more spherical in shape as they become smaller. There is no evidence that the shape of single coal particles do vary with size within the range examined (5–10 μ) and it appears that this effect is due to

the larger, flatter objects being aggregates and not single particles.

Rock dusts sampled underground show the same order of size variation at a given falling speed as coal dust, but it will be seen that in general rock particles are smaller than coal particles of the same falling speed. However, this effect is not as marked as one would expect, having regard to the large difference in "true" density between coal and rock (about 1·4 g/cm^3 and 2–2·5 g/cm^3 respectively).

The two "factory" dusts, from cotton and asbestos, show even greater ranges of particle size corresponding to a given falling speed than do the "mining" dusts. This seems to be due to the fact that both of these dusts consist of two types of particle. Cotton carding dust consists of fibres and particles far more "condensed" in appearance and which probably consist of leaf debris and earth fragments. The "asbestos" dust also comprises fibres, much finer than those of cotton, and a large number of more rounded particles. This material shows the greatest range of particle size associated with a given free-falling speed for any of the dust sampled—with a ratio between the largest and smallest particle mean projected diameters of about 10 to 1, or 60 to 1 between maximum linear dimensions.

It is clear from these results that the free-falling speeds of industrial dust particles give little indication of their size (mean projected diameter) as measured by the microscope, and conversely that conventional microscope measurements of size fail to represent the "respirability" of the particles. There are major differences between the relationship of falling speed and size for the types of dust sampled, and in addition coal dusts from different sources show unexpectedly large variations.

It is concluded that the data given here add strong support to the contention that measurements of airborne dust for medical purposes should classify particles by their free-falling speed and not by their size.

ACKNOWLEDGEMENTS

The author is indebted to the National Coal Board Divisional Scientific Control personnel and the managements of the colleries concerned for their help with the underground work, to the Director of The Shirley Institute for permission to obtain the cotton dust sample, and to Bell's Asbestos Ltd., Slough, Bucks, for permission to obtain the asbestos dust sample. The author is also indebted to Mr. W. H. Walton for his help and advice with the work described.

This paper is presented by permission of Dr. W. Idris Jones, Director-General of Research in the Scientific Department of the National Coal Board. The views expressed are those of the author and not necessarily those of the Board.

REFERENCES

(1) DAVIES, C. N. *Brit. J. Industr. Med.*, **6**, p. 245 (1949).
(2) WALTON, W. H. This Supplement: Paper A.5.
(3) SAWYER, K. F., and WALTON, W. H. *J. Sci. Instrum.*, **27**, p. 272 (1950).

DISCUSSION

Dr. H. Heywood: Dr. Timbrell and Mr. Hamilton determined the value of the ratio, mean projected diameter to equivalent Stokes' diameter for various dust samples as 1·3 to 2, according to the particle shape. I derived a ratio of 1·7 for a particle with a volume coefficient equal to 0·15 if the motion of the fluid was streamline or laminar.(1) If the fluid motion was turbulent the above ratio was increased to 4 because of the eddy formation in the wake of a flat particle. The method of calculation had been published,(2) and was based on the experimental measurement of the terminal velocities of 10 mesh size particles of various shapes falling in glycerine–water mixtures of different viscosities. Within the streamline region of flow it was believed that a falling particle had no preferred position of orientation, since the drag was a function of the surface area, but as turbulence developed the particle became orientated to the attitude of maximum drag, i.e. a disk would have the flat surface horizontal, a rod would have the axis horizontal. When turbulence was fully developed the motion became oscillatory, of the "falling leaf" type.

Particle shape was also important in the comparison of sieving and microscopical measurements. A flat particle could have a breadth 1·414 times the sieve aperture and length, say, three or four times the breadth. Consequently it appeared under the microscope to be far too large to have passed through the sieve aperture. The average ratio of mean projected diameter to sieve aperture was 1·4 for mineral particles.

Dr. A. van Kreveld: There seems to be much confusion on the position irregular particles will take while moving in an air stream. This may partly be caused by the fact that there are to be considered two fields of force acting on the particle, viz. gravity and drag. If these are parallel as in vertical sedimentation tubes the situation is relatively simple, but if the two forces are at an angle, as in Dr. Timbrell's apparatus, it is less so. In his apparatus the angle is not even constant, but depends on the Stokes' diameter. In this connexion I should like to ask Dr. Heywood what positions the particles took in his experiments on vertical sedimentation.

Mr. D. H. Lucas: I suggest that the positions of particles on a Conifuge slide or on the base of a horizontal elutriator bear no relation to their positions while falling. We may take as an analogy parachute troops landing in a high wind in a field covered with treacle. The men will clearly not be upright after landing. A few may well be upright but inverted!

Dr. C. N. Davies: In the viscous flow or "Stokes' law" size range, isolated non-spherical particles experience no orienting force if they possess three separate planes of symmetry.(3) The rate and direction of fall then depend on chance orientation.

Orientation can be caused by proximity to the container wall or by the presence of other particles.

Irregular and unsymmetrical particles orient in a way which has nothing to do with maximum or minimum drag or energy dissipation, but is governed by the distribution of weight in the particle and of viscous drag over its surface. The fall is not necessarily vertical.

Differences of speed and departure from vertical settlement must account for some of the spread in the deposit in Dr. Timbrell's and Mr. Hamilton's instruments.

Mr. A. Radcliffe: In Mr. Hamilton's paper and also others presented at this Conference it is claimed that the Conifuge and other air elutriation methods separate particles according to their Stokes' diameter which is normally taken to mean the diameter of a spherical particle of the same density falling in free air.

It may well happen that the orientation of a non-spherical

particle with respect to the gravitational or centrifugal forces will be different in still and moving air because there is sure to be a decrease in gas velocity at right angles to the gravitational direction as the collecting surface is approached.

If this is so then elutriation methods do not necessarily distribute particles in the order of the Stokes' diameter in still air.

Mr. J. K. Donoghue: Mr. Hamilton in his paper, and several speakers in the discussion, have suggested that measurements of particle size under the microscope may give a false idea of the health hazard of the dust and should be replaced by measurements of falling speed. Throughout the discussion, however, it seems to have been assumed that the particles always lie in their most stable position. If this were so, microscopic measurements would obviously give a false impression of the hazard.

Most microscope counts are, however, made on samples which have been collected with the thermal precipitator and with this instrument there certainly does not seem to be any preferred orientation of particles in the trace. During some experiments at the Shirley Institute, in which I took part, thermal precipitator traces of cotton dust were "shadow-cast" with silver and examined under the optical microscope. Quite clearly very few particles were in their most stable position. It does seem possible, therefore, that when a large number of particles are examined the mean projected diameter obtained may in fact not be very far from the true one.

Mr. H. H. Watson: The values of the ratio D_p/D_s for coal obtained by Dr. Timbrell with his sedimentation apparatus are almost equal to the values I have obtained for particles of three different coals,[4] using a Conifuge to collect the samples. This is interesting in view of the fairly large gravitational fields in the Conifuge. Not all the particles on the Conifuge samples were in positions of maximum stability, though there was a preponderance in this position. As far as I can determine (in reply to Mr. Donoghue) particles are orientated at random on a thermal precipitation deposit.

Author of Paper D.3's reply: I think Dr. Kreveld over-estimates the possible magnitude of horizontal drag on a particle in my instrument. We can consider a steady air-flow along a horizontal straight tube with uniform velocity across a section. Even if a particle is initially at rest it will in a very short time be accelerated to the air velocity by drag. Thereafter, the particle will continue at the same horizontal velocity, not because of drag (for what force would this be opposing?), but because there is no horizontal force tending to change its steady motion (Newton's First Law). The trajectory of a particle under these steady conditions will be the resultant of the vertical motion relative to the air (similar to the vertical motion in still air), and the horizontal motion of the air relative to the tube.

We must, however, consider the maximum possible value in the instrument of the acceleration of a particle relative to the air, which would result in drag. The maximum horizontal acceleration of the air relative to the instrument is of the order of 1 cm/sec^2. The maximum horizontal acceleration of a particle relative to the air will be even less, much less than the vertical acceleration of gravity (981 cm/sec^2).

These conclusions are supported by the experimental results. The table in the paper shows, for two substances, a constant value which is independent of D's for the mean ratio D_p/D_s. This result, which indicates that for each substance the average shape of the particles is independent of the size, is acceptable, and does not make one suspect that the vertical motion of particles in the instrument differs from their motion in still air in a manner dependent on the Stokes' diameter. It is unlikely that this acceptable result is due to artefact produced by the instrument, especially since the same result has been obtained with the instrument operating under different conditions of winnowing air speed, etc.

I would remind Mr. Lucas that because of their different shapes, irregular particles have different orientations while falling. Therefore, from the observation that irregular particles seem to be randomly orientated on a horizontal-elutriator slide, it cannot be concluded that the observed orientation of an individual particle bears no relation to its orientation while falling. The particles on the slide will appear to be randomly orientated whether a relation between these two orientations for a given particle exists or not.

The short-range forces of adhesion between dust particles and a slide (discussed by Mr. Jordan in Paper H.4) are usually powerful enough for a particle to retain the orientation it possesses at the instant of contact with the slide. The orientations on the slide of identical particles will not be random (unless the falling orientations are random), but will be related in a definite way to the falling orientation, as is borne out by the observations on doublets, discussed in Paper A.2; similar doublets possessed similar orientations on the slide indicating a relation to the falling orientation. The relation between the two orientations may not, of course, be the same for particles of different shape, etc.

It would be interesting to know whether an experiment on the lines of Mr. Lucas's analogy has been carried out, and the results.

As Dr. Davies has pointed out in the paper he refers to, the difficulty in investigating experimentally the rate of fall of symmetrical non-spherical particles is that of producing particles with such small deviations from the perfect form that one can be certain there will be no preferred orientation. Even if such particles could be produced, their vertical descent in my instrument would be different from that in still air because the small velocity gradients would probably upset the unstable orientation of a particle.

In reply to Mr. Radcliffe I must point out that in size separation by flow between parallel plates, as in my instrument, the horizontal drag on a particle due to horizontal acceleration of the air at right angles to the gravitational direction is very small: in any case the particles and the calibrating glass spheres are affected to very nearly the same degree.

We have to consider, however, the decrease of horizontal velocity of the air in the direction of gravity, which may result in small differences between the velocities of different parts of the particle relative to the air. This is only likely to be significant over the last part of the trajectory where the vertical gradient is high. Although I think this inclines particles in the direction of the winnowing air just before deposition (see Paper A.2 on doublets), experimental results, which show the effective Stokes' diameter of an unsymmetrical particle to be independent of the winnowing air speed, flow pattern, etc., suggest that the effect on the average velocity of descent of a particle, which determines its site of deposition, is probably very small. This requires further investigation.

In reply to Mr. Donoghue I wish to say that as in a thermal precipitator sample (mentioned by Mr. Watson), irregular particles in the deposit of the instrument I have described seem to be orientated at random. They are certainly not all in their most stable positions because of the forces of adhesion to the slide, which usually enable a particle to retain the orientation of first contact.

The constancy of the mean ratio D_p/D_s that we have found

for single particles of coal supports Mr. Donoghue's suggestion that mean projected diameter may be a satisfactory index of the respirability of such particles. It is difficult to generalize about its suitability for all substances, especially since the mean ratio D_p/D_s is dependent on the state of aggregation of particles.

Although the size parameter used in the assessment of the health hazard of the dust must be descriptive of the respirability of the particles, many other considerations must be taken into account in selecting the parameter, e.g. the magnitude of the errors due to the fluctuations of dust concentrations in space and time. The error in the assessment of the sample using any parameter must also be considered and the automatic size-separation of elutriation methods may be of benefit in reducing these errors.

Mr. Watson's remark on the close agreement between the value for the mean ratio of D_p/D_s for coal obtained in his investigation using the Conifuge (in which I understand he also discounted aggregates), and the value obtained by my instrument, is very relevant.

This close agreement between the results on similar material strongly suggests that although the gravitational fields, winnowing air speeds, flow patterns, etc., are very different in the two instruments, the particles were separated by both instruments in order of their normal Stokes' diameters. It is far less likely that, while the effective Stokes' diameters of particles in each instrument were different from those in still air, the conditions in each instrument were so related that the net effect on the Stokes' diameter was the same in both instruments.

Author of Paper D.4's reply: The points raised by Dr. Davies and Mr. Radliffe are interesting, and it does appear possible that some of the spread in the relationship between particle size and "Stokes' diameter" as indicated in the Conifuge samples is due to the effects they mention. It seems doubtful, however, that these effects are really very important—in experiments with a "horizontal elutriator" fitted to a thermal precipitator, I have found that the differences between the "cut-off" curve obtained with coal particles and spheres of the same density are in excellent agreement with those expected if the distributions obtained in the Conifuge samples apply. The fact that even particles of the same size and shape may land different ways up and so appear of different size to the microscopist merely adds to the uncertainties of microscopic measurements in cases where falling speed is the most important parameter.

REFERENCES

(1) HEYWOOD, H. *Symposium on Recent Developments in Mineral Dressing*, Instn Min. Met., p. 31 (1952).
(2) HEYWOOD, H. *J. Imperial College Chem. Engng Soc.*, **4**, p. 17 (1948).
(3) DAVIES, C. N. *Symposium on Particle Size Analysis* (p. 15), *Suppl. to Trans. Instn Chem. Engrs*, **25** (1947).
(4) WATSON, H. H. *Brit. J. Indust. Med.*, **10**, p. 93 (1953).

GENERAL DISCUSSION ON SESSION D

Mr. W. H. Walton: Several speakers have used the term "Stokes' diameter" in a sense which implies that it is uniquely related to terminal velocity; this is incorrect and should be avoided. The Stokes' diameter of a particle is the diameter of a sphere *of the same density* as the particle and having the same terminal velocity. It is thus not a unique measure of terminal velocity. As pointed out in many papers presented to the Conference, terminal velocity is frequently the most important parameter defining the behaviour of a particle and it is convenient to characterize this by the diameter of a sphere of *unit density* having the same terminal velocity as the particle. A name is required for this diameter and I hope that one will emerge from the proceedings of this Conference.

Mr. Hamilton has referred to the dangers of the use of mean projected diameter to define the sizes of dust particles that can enter the human lungs. Although it has become conventional to regard as respirable the particles that are smaller than 5 μ diameter in a dust cloud, it is well known that the behaviour of dust in the lungs is characterized by its aerodynamic properties (ratio of mass to resistance factor), or, what amounts to the same thing, by its terminal velocity. In view of the very wide divergence between terminal velocity and size, which has been demonstrated by Mr. Hamilton and Dr. Timbrell, it is clear that the diameter of particles as seen under the microscope may give a very misleading indication of respirability. I would therefore like to give the strongest possible support to the plea that the range of respirable dust should be defined in terms of the terminal velocity of the particles and not size.

Mr. H. H. Watson: Mr. Walton has raised an objection to the term "Stokes' diameter." I have used "aerodynamic diameter"* to denote the diameter of a sphere, of the same density as that of an irregularly shaped particle (or an aggregate), with falling speed equal to that of the particle.

* WATSON. *Brit. J. Indust. Med.*, **10**, p. 93 (1953).

SESSION E. VISUAL COUNTING AND SIZING OF MICROSCOPIC PARTICLES

Chairman: F. I. G. RAWLINS, M.Sc., F.R.S.E., F.Inst.P.

Paper E.1

Inter-laboratory checks on the counting of coal dust particles on thermal precipitator slides

By J. F. HOLDSWORTH, M.A., F. HENLEY PRICE and R. C. TOMLINSON, D.I.C., M.A., Scientific Department, National Coal Board

The paper describes experiments carried out by the Medical Research Council and the National Coal Board to compare the results obtained by observers in different laboratories when counting coal dust particles on thermal precipitator slides. Serious differences were discovered which have now largely been removed within the National Coal Board by the institution of regular inter-laboratory checks. These checks have also aided the development of improved methods of mounting and counting the slides.

For many years different observers have been reporting dust concentrations in terms of particles/cm^3 as a result of measurements obtained with the thermal precipitator, but little work has been carried out to discover whether the figures obtained by observers in different laboratories are directly comparable. One of the major possible sources of error lies in counting the number of particles of a given size range on the thermal precipitator record, and the present paper describes two sets of experiments to investigate these errors. First, a single preliminary experiment was carried out for the Medical Research Council by the following laboratories: Central Research Establishment of the National Coal Board, the Environmental Hygiene Research Unit, the Pneumoconiosis Research Unit, The Safety in Mines Research Establishment and the South Western Division of the National Coal Board. Secondly, a series of four checks have been carried out between the nine Divisions and the Central Research Establishment of the National Coal Board. These latter experiments were intended not only to measure the differences obtained, but also to aid the development of a standardized counting procedure and of a reliable checking system to ensure that as far as possible a constant standard is maintained. All the experiments were designed statistically so as to give unbiased efficient estimates of the parameters required.

Although the work described was carried out on samples of coal dust, the results are of interest in the wider field of counting irregularly shaped particles under a microscope.

COUNTING OF DUST RECORDS

The thermal precipitator dust deposits on the two cover slips are about 9·3 mm long, and not more than 0·8 mm wide. They are evaluated under the microscope at an overall magnification of the order of × 1700 with the aid of a graticule of the globe and circle type. If for instance the graticule of N.C.B. design (described by Hamilton at this Conference) is used, its length in the plane of the objective is 50 μ, its width 30 μ and the diameters of its reference circles are 5, 2·5, 1 and 0·5 μ.

In counting, three traverses, each the width of the graticule, are made across each dust trace, one at the centre and the other two at 2 mm distance from either end of the trace. Counting is stepwise; all particles lying within the graticule boundaries are counted at each step and the convention is adopted that of the particles lying across the boundaries only those along the top and right-hand edges are counted. The sizes of individual particles are determined by visual comparison with the graticule reference circles. The total number of particles lying in a given size range on each cover slip is then calculated from the known total length of the deposits and the known traverse width.

The density of the deposits is usually such that 100 to 150 particles are counted at each traverse, for it is considered that less than 50 or more than 200 particles per traverse would introduce serious counting errors.

Particles up to a size of approximately 30 μ are found on thermal precipitator slides, but for normal purposes counting of coal dust particles is restricted to the size range 1 to 5 μ which it is believed correlates with the greatest health hazard.

EXPERIMENTAL DESIGN

In each experiment a number of thermal precipitator coal dust slides were prepared at each laboratory and then counted. These were circulated to be counted by the operators of other laboratories and finally returned to be recounted by the parent laboratory. As one of the primary difficulties lay in the risk of particles being knocked off cover slips or crushed, laboratories were asked to handle the slides carefully and additional safeguards were incorporated in the statistical design of the experiments.

In the preliminary experiment involving two operators at each of five laboratories of different organizations, two slides were first prepared at each laboratory and then counted by all operators taking part. The order of circulation was as in Table 1.

Table 1. *Order of circulation of slides in M.R.C. check.*

Slide	*Originating laboratory*	*Order of circulation* 1	2	3	4	*Slide*	*Originating laboratory*	*Order of circulation* 1	2	3	4
1	I	V	II	IV	III	6	I	III	IV	V	II
2	II	I	III	V	IV	7	II	IV	V	I	III
3	III	II	IV	I	V	8	III	V	I	II	IV
4	IV	III	V	II	I	9	IV	I	II	III	V
5	V	IV	I	III	II	10	V	II	III	IV	I

Because of this balanced design, differences in the mean counts of observers gave a fair comparison of operator counting levels comparatively free of degradation effects. The same objective was reached in the experiments carried out within the National Coal Board by arranging that in the main part of each check each slide was counted by only one

or two laboratories other than the parent laboratory. The circulation of slides was carried out according to an incomplete randomized block design so that a fair comparison of operator counting levels was finally obtained which was independent of the basic differences in the number of particles on each slide. The design can perhaps best be appreciated from Table 7.

In all the experiments the standard statistical method of analysis had to be carried out on the logarithms of the reported variables in order to make the errors homogeneous. A consequence of this was that the mean figures obtained were geometric means. The analysis of an incomplete randomized block gives the operator's mean count in terms of an arbitrary level and it has been convenient to express this arbitrary level as a particle concentration of 500 particles/cm^3 in the size range 1–5 μ; these are the units in which the results of dust work are finally expressed. In the preliminary experiment a corresponding level of 500 particles/cm^3 in the size range 0·8–5 μ was chosen.

Since the purpose of the work was to compare the counts returned by operators in the course of their normal work each used the equipment to which he was accustomed. Consequently a number of different types of microscope and graticule design were used; subsidiary unpublished work has indicated that these would have negligible effects on an operator's counting level of particles greater than 1 μ size.

PRELIMINARY EXPERIMENTS

In the preliminary experiment organized by the Medical Research Council the Paterson–Cawood graticule was used, with which it is more convenient to count to a lower limit of 0·8 μ than 1 μ. The number of particles in the three size ranges of less than 0·8, 0·8–5, and greater than 5 μ on each of the ten slides were counted by two operators at each laboratory and were subsequently adjusted to allow for differences in graticule width. The results received in the range 0·8–5 μ are given in Table 2 and estimated mean particle concentrations for all three size ranges are tabulated in Table 3 below.

It will be seen that the counts of observers differed markedly from one laboratory to another but that within the same laboratory they were in good agreement. One laboratory (II) systematically counted almost twice as many particles in the most important size range 0·8–5 μ as the others and also returned low counts in the size range of greater than 5 μ. A second laboratory (III) also showed a tendency to return higher figures in the size range 0·8–5 μ, though to a lesser degree. There were considerable differences in the size range of less than 0·8 μ but it is not possible to draw definite conclusions from this since the results will depend to a certain extent on the resolving power of the microscope used.

Wherever possible, the slides were re-counted by the parent laboratories after the experiment had been completed, and it was found that on eight of the ten slides the number of particles in one of the two smaller size ranges had more than doubled. An examination of the individual results indicated that this increase had not occurred gradually, but that it had appeared suddenly at some stage during the experiment. This would be expected if degradation had occurred because of rough handling.

A single operator was appointed to take part in the N.C.B.'s first inter-divisional check by each of the divisional laboratories and the Central Research Establishment with the intention that, if satisfactory agreement could be obtained between these "master" counters, the rest of the divisional staff could be trained round them. Eight slides were prepared by each operator and the number of particles in the size range 1–5 μ counted; one slide was then sent to each other operator and a second count made. The results are summarized in Table 4.

It will be seen that the mean counting level varied from 310 to 840 particles/cm^3, a ratio of over two to one. Greater

Table 2. *Five laboratories of different organizations.*

Number of particles, size 0·8–5 μ, counted in six traverses of slide (uncorrected for differences in traverse widths).
(Unit = 1 particle.)

	Laboratories											
	I		*II*		*III*		*IV*		*V*		*Recount*	
Slide	*Obs. 1*	*Obs. 2*	*Obs. 1*	*Obs. 2*	*Obs. 1*	*Obs. 2*	*Obs. 1*	*Obs. 2*	*Obs. 1*	*Obs. 2*	*Obs. 1*	*Obs. 2*
1	142	111	279	292	339	345	147	129	117	131	138	122
2	208	234	349	366	303	290	267	264	213	274	550	611
3	420	296	1006	930	371	396	358	407	N.A.	637	428	555
4	122	138	320	402	190	197	128	118	152	152	203	298
5	190	168	323	389	190	203	125	145	134	141	N.A.	221
6	109	115	339	350	119	111	80	101	188	156	N.A.	N.A.
7	187	179	409	409	218	301	246	294	268	315	N.A.	798
8	421	420	781	787	410	515	476	476	370	459	528	530
9	181	145	452	486	230	225	129	149	227	208	198	157
10	450	465	1072	1047	868	1061	696	635	372	333	N.A.	879
Traverse width	22·5 μ		20 μ		22 μ		21·6 μ		22·5 μ			

N.A. = No available result.

Table 3. *Five laboratories of different organizations.*

Mean counts referred to a standard of 500 particles/cm^3 in the size range 0·8–5 μ. (Unit = 1 particle/cm^3.)

	Size range								
	Less than 0·8 μ			*0·8–5 μ*			*Greater than 5 μ*		
Laboratory	*Obs. 1*	*Obs. 2*	*Mean*	*Obs. 1*	*Obs. 2*	*Mean*	*Obs. 1*	*Obs. 2*	*Mean*
I	211	181	196	379	354	367	59	46	53
II	862	952	907	936	986	961	28	42	35
III	340	319	329	506	549	528	73	64	69
IV	161	212	187	393	412	403	62	49	56
V	657	581	619	404	434	419	87	66	76

differences than this were observed on single slides. The standard deviation of an operator's mean counting level was 160 particles/cm³.

Table 4. *First inter-divisional check (National Coal Board).*

Mean counts referred to a standard of 500 particles/cm³ in the size range 1–5 μ. (Unit = 1 particle/cm³.)

Division	A	C	D	E	F	G	H	J	K
Mean count	635	565	370	415	570	840	460	310	500

From the results of the two preliminary trials it was apparent that there were large systematic differences in the counting levels of laboratories whether they belonged to the same or to different organizations. Furthermore the risk of degradation of dust records was very real. Consequently the National Coal Board was prompted to undertake further checks similar in design to the first but with each slide counted by operators from two laboratories other than the parent laboratory.

RE-DEFINITION OF AGGREGATES

One of the most likely causes of the discrepancies was considered to be the treatment of aggregates or clusters of small particles, for the count would depend on whether such clusters were counted as one or a number of particles. In an attempt to eliminate this source of error the method of treatment of aggregates was re-defined so that every particle was to be counted if "at some stage of the focusing a clear margin of separation is visible between the particle and its neighbours."

A test of the effectiveness of the new treatment of aggregates was included in the second National Coal Board inter-divisional check. This was in two parts with the ten operators together in one laboratory. In the first, operators were asked to count a group of slides following their customary practice in dealing with aggregates, and then to count the same slides using the new procedure. The results were then discussed with the aid of a projection microscope and the second part of the experiment, a repeat of the first with other slides, carried out. The standard deviation of the counting levels of operators in each section of the experiment is shown in Table 5 below.

Table 5. *Second inter-divisional check (National Coal Board).*

Standard deviation of an operator's counting level referred to a standard of 500 particles/cm³ in the size range 1–5 μ. (Unit = 1 particle/cm³.)

	Old aggregate treatment	*New aggregate treatment*
Before discussion	42	29
After discussion	54	41

Upon comparing the results with the standard deviation of 160 particles/cm³ obtained in the first inter-divisional check it was evident that a considerable improvement had taken place which was not attributable to the change in the treatment of aggregates. Some other factor, possibly the psychological effect of working together, might be the reason for the improvement. There was little apparent improvement in results which could be directly attributed to the change in aggregate treatment, although it was stated by some operators that the new treatment made counting easier.

COMPARISON OF INTER-DIVISIONAL CHECKS

Using the revised procedure for treating aggregates two further checks were made. The master counters worked in their respective laboratories and slides were posted from one to another. The results of all four inter-divisional checks are compared in Table 6. In each case counting levels are referred to an arbitrary level of 500 particles/cm³. However, there is no means of comparing the counting level of an operator from one check to another as no two slides were common to any two.

Table 6. *Inter-divisional checks (National Coal Board).*

Mean counts referred to a standard of 500 particles/cm³ in the size range 1–5 μ. (Unit = 1 particle/cm³.)

Division	*Check* 1st	2nd*	3rd	4th
A	635	525	415	475
B	†	520	455	500
C	565	545	650	605
D	370	500	585	490
E	415	475	520	440
F	570	535	440	500
G	840	560	440	485
H	460	455	580	490
J	310	440	460	490
K	500	465	505	545
Standard deviation	160	41	78	44

* The figures are those obtained in the second part of the check
† Laboratory B was not in existence at the time of the first check

There was some falling off in agreement at the third check from that at the second but the general position was still markedly better than originally. Agreement was still good at the fourth check in which seven of the ten laboratories had mean counting levels within 5% of each other. Even when the one laboratory that returned very high figures in the first check is excluded from the comparison there is a marked improvement from the first to the last check (highly significant on an F test). The magnitude of the differences obtained on single slides can be seen from Table 7 which gives the detailed results of the fourth check. Results are given in terms of the estimated number of particles on the slide, as differences due to the varying traverse widths employed are then eliminated.

MOUNTING COVER SLIPS

One method by which the amount of degradation of dust records could be reduced is to insert a thin paper ring when mounting cover slips on to microscope slides in order to eliminate the possibility of crushing large particles between the cover slip and the slide. One possible source of error with this method of mounting is that large particles may fall off the cover glass on to the slide, so that there may be a reduced count if only the field of the cover glass is examined. In practice it is difficult to check this as the thickness of the paper ring usually makes it difficult or impossible to examine the field of the slide.

To compare this method with the customary practice of direct mounting using wax, one of the two cover-slips on each slide used in the third inter-divisional check was mounted by each method. On twenty-four slides the percentage increase in the recount above the original count on direct mounted cover slips exceeded that on paper ring mounted

Table 7. *4th inter-divisional check (National Coal Board).*
Total estimated number of particles on slide. (Unit = 100 particles.)

	Laboratory									
Slide	A	B	C	D	E	F	G	H	J	K
A/CE	417		603		406					
A/BJ	424	474							497	
A/KH	368							369		295
B/CD		527	763	583						
B/HE		837			585			720		
B/FA	732	796				830				
C/HJ			870					729	716	
C/AD	581		646	589						
C/BF		632	788			720				
D/JG				1136			1163		798	
D/EF				1056	795	1100				
D/HK				1096				1135		1057
E/DG				650	753		747			
E/JF					681	660			632	
E/KB		698			678					850
F/DH				504		700		555		
F/AG	610					505	642			
F/CK			885			640				962
G/EC			712		505		577			
G/FK						730	561			741
G/BH		713					680	697		
H/EA	1597				1448			1594		
H/FJ						470		481	590	
H/GC			613				489	438		
J/AD	478			577					562	
J/KE					565				638	666
J/GB		535					455		573	
K/DB		1019		878						952
K/GA	702						687			856
K/JC			763						620	841

In this table the coding A/CE indicates that the slide was prepared by laboratory A, and sent first to laboratory C and then to laboratory E.

cover slips and on six slides it was less. Clearly some reduction in the amount of degradation was to be had by the use of paper rings which were, therefore, used throughout the 4th inter-divisional check.

To determine the number of occasions a slide could be safely counted, each laboratory re-circulated one of its slides in two stages to the other laboratories which had not yet counted it. After each stage the slide was returned to be recounted at the parent laboratory. After the first recount a slide had been counted four times and after the second eight times, and after the third thirteen times. The percentage increase, at each recount, above the original count of two cover slips is shown in Table 8 below.

Table 8. *Percentage increase in particle count in size range 1–5 μ*
(Unit = 1%.)

Number of times slide counted	*Parent laboratory*									
	A	*B**	*C**	*D*	*E*	*F*	*G**	*H**	*J*	*K**
4	6	5	13	5	−5	0	5	1	−4	6
8	14	−6	9	−14	2	13	15	−11	−4	−3
13	26	20	10	−5	−7	19	−3	8	−9	−13

* One of the two cover slips was broken.

It will be seen that there was little indication of degradation although five of the cover slips broke. The breakage of cover slips is not a serious disadvantage for the purposes of these checks provided that the number does not become excessive, for there is no danger of inappropriate results being included in the analysis, such as arises when degradation occurs without breakage. It would appear, therefore, that the introduction of mounting using paper rings has made it possible to circulate slides to a number of laboratories without serious danger of invalidating the results of the check because of the possible occurrence of degradation.

It should be noted that the results also indicate that any loss of particles in the relevant size range in falling from the cover slip on to the slide is not sufficient to affect any comparison between operators.

ACCURACY OF COUNTING

The experiments described were mainly concerned with systematic errors, such as the tendency of one operator to return consistently higher or lower counts than another. When the counts of a single dust record are considered, however, it is necessary to take into account the random errors which are also present and are due to the inability of an operator to repeat his own results exactly. Such errors are not only personal in origin but are due to many other causes such as the position of the individual traverses counted. It appears that this random error was remarkably consistent from one National Coal Board experiment to another and

had a standard error of the order of 14% of the total count. This may, however, be an over-estimate as the experiments were not specifically designed to estimate it.

CONCLUSIONS

Preliminary experiments revealed gross differences in the counts of thermal precipitator dust records at a number of laboratories, whether they belonged to the same or to different organizations. Within the National Coal Board these discrepancies were much reduced in subsequent inter-divisional checks without any definite reason being shown. There had been little contact between operators prior to the preliminary experiments, and it is possible that to some extent the improvement was due to the very introduction of check trials and the opportunities this afforded of discussion between operators. It may be concluded that reasonably good agreement can be obtained between well trained operators in different laboratories provided that there is a constant interchange between them. This conclusion has been confirmed in similar work carried out within a number of divisions of the National Coal Board. It must also be concluded that close agreement between operators in the same laboratory is not necessarily a guide to the accuracy of the figures reported, and that these must be accepted with reserve unless some external checks have been carried out.

It was formerly thought that one of the predominant factors influencing discrepancies between counts might be the treatment of aggregates. Revised instructions on this were issued but there was little improvement which could be directly attributed to the change. The differences now arising between operators are of the same order as those that can occur from systematic over-estimation or under-estimation of the size of irregular particles.*

It was shown that by mounting the cover slip on a paper ring, and consequently only counting the field of particles on the cover slip, the risk of degradation was considerably reduced so that individual slides were counted at as many as thirteen laboratories without invalidating the results obtained.

ACKNOWLEDGEMENTS

The inter-divisional checks of the National Coal Board were part of a general programme concerned with the measurement of respirable air-borne dust; the second inter-divisional check was held in the South Western Division by courtesy of the Divisional Chief Scientist. Acknowledgement must be given to all the counters, too numerous to be mentioned individually, who took part in the work described. The paper is published by permission of the National Coal Board.

* PHILLIPS, J. W., *National Coal Board, C.R.E. Report No.* 158.

DISCUSSION

Mr. T. A. Eames: Paper E.1 provides interesting quantitative information on a difficulty which workers in single laboratories must be conscious of, namely, the possible inaccuracies in their counting. What is particularly disturbing is the implication that even a steady improvement in consistency between observers in one laboratory may only mean consistency with a false standard. Obviously the elaborate inter-laboratory check will only rarely be possible, and the question is what can be done to assist the single laboratory. Could a test strip technique, as described by Mr. Watson and Mr. Mulford in Paper E.3, be extended, and strips representative of various types and sizes of dust be made available for checking purposes? As to the reasons for the discrepancies, how far might these be due to the difficulty of defining the lower end of the size range, where a small change in the mental criteria adopted by the observer might lead to a fairly large change in the particles accepted or rejected?

Mr. W. H. Walton: In commenting on the Paper E.1, several speakers have pointed out that by proper training they have been able to secure good agreement between different microscopists in the same laboratory. This was also found in the work described by the authors; the real problem is the correlation between different laboratories. I have known personally of two laboratories, each well respected and in the forefront of research on industrial dust problems, who have regularly applied a substantial correction factor when comparing their microscope counts of dust samples. The problem is how to bring such laboratories to a common measure, or how to recognize such differences in the published literature. The authors of Paper E.1 have been courageous in risking criticism of their own counting procedures in order to draw attention to the serious differences that can and do arise.

Mr. J. Anrep: I have experience of microscopic counts on materials generally coarser than 1–2 μ, using a projection microscope with a line graticule similar to that shown in Fig. 2 of Paper E.2. Greater variability has been found between slides sampled from the same packet than between re-counts on the same slide. In fact by counting only 200 particles on each slide sufficient information has been gained to improve a product considerably. Good agreement has been obtained between this count and a photo-extinction measurement to which the extinction coefficient has been applied as a correction.

Mr. G. L. Fairs: Paper E.1 has demonstrated most clearly the necessity for careful checking of microscope counts if inter-departmental tests are being carried out.

The authors give no indication of the quality of microscope equipment employed and it might be that some of the discrepancies referred to in this paper could be attributed to the varying degrees of skill with which the various operators set up their microscopes. It is also important in comparative tests of this nature to ensure that the illuminant is of the same wavelength in all cases. The use of a filter in some cases and not in others might well account for a 2 : 1 difference in a count particularly in the less than 2 μ diameter range.

Mr. H. H. Watson: I cannot help but feel that variations in microscopes and microscope techniques are responsible for some of the big differences observed, particularly in the earlier trials. As I have noted in my paper (E.3), the errors in counting between 0·5 and 5 μ are small, even when sizing bias is high, when the dust is a coarse one, as is the case with those used for the trials reported.

Mr. R. J. Courshee: Human observation errors were a source of trouble to us when we were trying to establish a standard of accurate sizing with which to compare the performance of our sizing and counting machine. Therefore in order to check on the observers' performance under the most favourable circumstances I asked three people to use two sizing methods: (i) a globe and circle graticule and (ii) a linear scale, and also to measure the mean linear diameter of some 2000 black, sharply defined circles in a range of sizes. The range of the answers obtained was $\pm 3\%$ of the average mean linear diameter and it was this value which we

assumed was nearest the correct answer. The machine, incidentally, gave answers nearer this value than any of the measurements made by eye.

Mr. Rosebery: I suggest that discrepancies between operators might to some extent be due to the fact that a particle image is being matched with a circle on the edge of the graticule. When using the projection microscope a piece of celluloid or Perspex, having circles drawn on it, can be moved about on the screen and the circles fitted to the particles, and a better estimation of their sizes obtained.

Authors' reply: Mr. Fairs and Mr. Watson have both referred to the need for microscopes of good quality and for a high standard of microscope technique. In fact it has been found necessary to standardize microscopic equipment very carefully, and all the laboratories referred to now use standard equipment of the highest quality. It has also been found necessary to ensure, first by a course in microscopy attended by representatives of all laboratories and secondly by visits to the laboratories by two expert microscopists, that a really high standard of technique is attained and maintained.

In reply to Mr. Roseberry it should be said that most of the laboratories now use standard projection equipment and that some of them have for several years used the moveable, transparent graticules, particularly for training in size discrimination.

Mr. Eames's contribution re-states the fundamental difficulty from which we started. We do not feel that training to any artificial standard will be likely to help, largely because of the peculiarities of aggregation in the natural air-borne mine-dusts and because the latter are without exception heterogeneous in petrographic constitution. The difficulty of the single laboratory is a very real one; we can only suggest that such laboratories should go to considerable lengths to obtain comparison with others studying the same subject.

Paper E.2

Factors in the design of a microscope eyepiece graticule for routine dust counts

By R. J. Hamilton, B.Sc., A.Inst.P., J. F. Holdsworth, M.A., W. H. Walton, B.Sc., F.Inst.P., Scientific Department, National Coal Board

The limitations of existing microscope eyepiece graticules for use in routine dust counting work and the problems of determining the geometrical form and physical dimensions of a graticule for use with commercial microscope equipment are discussed. Comparison is made of the consistency and accuracy obtainable with three types of graticule: the Patterson–Cawood, a simplified globe and circle type and a parallel line graticule. The simple globe and circle graticule described has been taken into general use in the National Coal Board.

Limitations of existing graticules

The work described in this paper was carried out because of the lack of microscope eyepiece graticules suitable for the routine dust counting requirements of the National Coal Board. The regulations at present in force require thermal-precipitator measurements of dust concentration to be recorded as the number of particles per cubic centimetre lying in the size range 1 to 5 μ for coal and 0·5 to 5 μ for rock dust.

Normally, when thermal precipitator samples are counted,[1] a 2 mm oil immersion objective is employed and assessment is carried out with the aid of a graticule of the "globe and circle" type consisting of a rectangular grid defining the "counting field" and a series of reference circles with which particles are visually compared for the assessment of their size. That described by Patterson and Cawood[2] was the first of this type and was recommended by Watson[1] for thermal-precipitator work. It is unsuited for the present requirement, firstly because the reference circles cannot be made to correspond to the required sizes unless the microscope is used at an unfavourable tube-length, and secondly because the eye is confused by an unnecessarily large number of reference circles.

A number of other graticules have been described in recent years. Fairs[3] has described one using reference circles whose diameters increase in a $\sqrt{2}$ progression except at the smallest sizes—but again this graticule does not conform with the specified requirements. May[4] also describes a graticule with a $\sqrt{2}$ progression in circle diameter, and having, in addition, a grid containing a series of parallel lines whose distances from a centre "zero" line increase with $\sqrt{2}$ progression, and which can also be used for particle size estimation.

H. H. Watson[5] has used a simplified graticule for routine dust count work containing only three reference circles corresponding to 0·5, 2 and 5 μ diameter respectively, and particles are classified in four size groups, less than 0·5 μ, 0·5–2 μ, 2–5 μ and greater than 5 μ.

New graticule. Design considerations

Two factors are to be considered: (*a*) the geometrical form of the graticule, and (*b*) its physical dimensions. The latter are conditioned by the microscope equipment to be used; specifically by the magnification of the real image formed by the objective in the object plane of the eyepiece, where the graticule is located.

Geometrical form. Essential features of the graticule are the rectangular grid to define the counting area, and some form of particle size measuring device such as comparison circles or parallel lines of known separation as described above. Previous practice favours the use of comparison circles. This method of sizing is well established; it is rapid and since *areas* of particles and circles are compared, it measures size by "mean projected diameter." The design of graticule shown in Fig. 1 was therefore evolved. It has reference circles corresponding to diameters of 0·5, 1 and 5 μ when used with the normal 2 mm objective. These meet the specified sizing requirements. A further 2·5 μ circle has also been added. This single additional circle does not distract the eye in simple "range" counting, such as of particles between 1 and 5 μ, but it does enable the graticule to be used when desired for size-frequency determinations of sufficient accuracy for normal

requirements, giving five size ranges. 2·5 μ is chosen for the intermediate circle rather than 2 μ as in Watson's graticule, so that the essential particle sizes of 1 and 5 μ can be still measused (by the 0·5 and 2·5 μ circles) if the magnification is halved by changing from a 2 mm oil immersion objective to a 4 mm dry objective. Furthermore, an overlap of ranges can be obtained between the 0·5 and 1, and 2·5 and 5 μ circles,

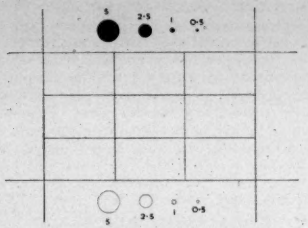

Fig. 1. "Globe and circle" graticule

if the magnification be changed five-fold in measuring a sample of wide size distribution. The length of the longer side of the rectangular grid has been made equal to 10 diameters of the largest circle, as in the Patterson–Cawood graticule, to facilitate adjustment of the microscope magnification to the correct value. Attention has been paid to the grouping of the reference circles, the line thickness (10 μ actual), and the size of the numerals, but no doubt the best form of these will remain matters of personal opinion.

The sizing of particles by visual comparison with reference circles at some distance from the particle under consideration is subject to a personal error which may be appreciable and may be systematic. Consistency between different observers is as important as absolute accuracy, and it was thought that the former might be greater with the parallel line method of measurement than when using comparison circles. The second graticule shown in Fig. 2 was therefore designed, and

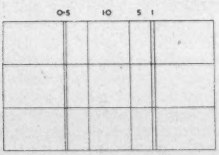

Fig. 2. Line graticule

has vertical lines of known separation similar to those used by May.[4] The lines in the left-hand half of the graticule are at distances of 0·5 and 5 μ respectively from the zero line, while those on the right-hand side are at 1 and 5 μ. The overall length of the graticule is again 50 μ. With this graticule, the thermal precipitator slide is traversed continuously and particles are sized as they cross the reference lines; Feret's diameters are, of course, obtained. Heywood[6] has criticized this technique as introducing gross errors for elongated particles, but Walton[7] has shown that Feret's diameter averaged over all particle orientations is equal to particle-perimeter/π.

Dimensions. The graticule is normally required for use with a 2 mm or $\frac{1}{12}$ in. apochromatic oil immersion objective and suitable compensating eyepiece. The graticule is placed in the plane of the primary image formed by the system illustrated in Fig. 3 and its physical dimensions must be such that the "5 μ" reference circle is equal in size to the primary image of

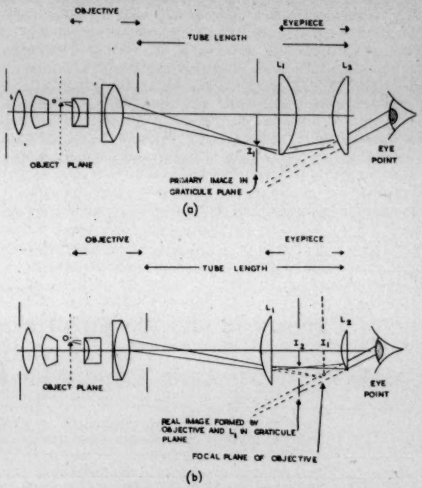

Fig. 3. Optical system of compound microscope showing reduction in primary image size by field lens: (*a*) with positive (Ramsden) eyepiece; (*b*) with negative (Huygens) eyepiece

a 5 μ object. The longer side of the graticule grid is to represent 50 μ in the object plane and it is convenient to specify the graticule size by the length of this side. This dimension is determined by the characteristics of the optical system and by the tube length (distance between objective and eyepiece). Objectives are usually designed to be used at a given tube length—in most cases 160 mm—and for high resolution work it is undesirable to vary this by more than 5–10 mm. Hence very little tolerance in the graticule dimensions is acceptable. It appears that insufficient attention has been given to this point in the past.

The influence of the eyepiece depends on the type used. Eyepieces fall into two classes, positive and negative, as exemplified by the well-known Ramsden and Huygenian types. With positive types, the primary image and graticule (which lie in the lower focal plane) are situated in front of the eyepiece as shown in Fig. 3(*a*) so that the image size and graticule dimension depend only on the objective characteristics and tube length (allowing for the effect of eyepiece working distance on tube length). For negative systems, however [Fig. 3(*b*)], the focal plane lies between the eyepiece lenses, and the initial magnification of the objective is reduced by the field lens. The required graticule size is therefore a function also of the eyepiece characteristics. Positive eyepieces are in general preferred for micrometric work with an eyepiece graticule, because negative types subject the image to some geometric distortion by the front lens. Compensating eyepieces supplied by manufacturers for use with their apochromatic objectives are found in either class.

A number of leading microscope manufacturers in this country have been asked to state the relationship between object size and primary image size for their 2 mm apochromatic oil immersion objectives and suitable compensating eyepieces. The data supplied is summarized in Table 1, which also includes figures for one achromatic type. It will be seen from this table that considerable differences exist in the primary magnifications obtainable with various equipment. This difficulty has largely been overcome by specifying the two sizes of graticule, one having a grid length of 4 mm which is suitable with a positive eyepiece, and another with a grid length of 3·5 mm which is suitable for at any rate a large proportion of negative eyepieces. It is interesting to note here that the grid length of the Patterson–Cawood graticule is 4·44 mm.

Table 1. *Object—primary image for various microscope systems*

Manufacturer	*Objective*	*Eyepiece*	*Tube length (mm)*	*Primary image size in mm for 50 μ object*
R. and J. Beck, Ltd.	Apochromatic 2 mm N.A. 130	× 11 compensating (positive)	155	3·775
			160	3·9
			165	4·02
		× 17 compensating (positive)	155	4·08
			160	4·2
			165	4·26
Cook, Troughton and Simms, Ltd.	Apochromatic 2 mm (M 1456)	× 10 compensating (negative)	155	2·89
			160	2·97
			165	3·06
		× 15 compensating (positive)	155	3·79
			160	3·90
			165	4·01
W. Watson and Sons, Ltd.	Apochromatic 2 mm N.A.1.37	× 10 Holos (negative)	140	2·15
			160	2·40
			180	2·625
			200	2·825
		× 14 Holos (negative)	140	2·875
			160	3·20
			180	3·625
			200	3·875
		× 20 Holos (negative)	140	3·025
			160	3·40
			180	3·75
			200	4·175
C. Baker of Holborn, Ltd.	Achromatic $\frac{1}{12}$ in. Oil Immersion N.A.I.30	× 7·5 micrometer Huygenian (negative)	155	3·00
			160	3·05
			165	3·15

COMPARISON OF GRATICULES

It is feasible that both the mean level and the consistency of an operator's counts of a dust record are partly affected by the design of the graticule used. An experiment was therefore carried out in the laboratory to compare the relative merits of the new "globe and circle" and "parallel line" designs of graticule and the existing Patterson–Cawood design.

One thermal precipitator coal dust slide was set up under a microscope (by R. and J. Beck, Ltd.) and the number of particles lying in the two size ranges of "1 to 5 μ" and "greater than 5 μ" counted in three traverses of the dust stain on each of the two cover slips. Two repeat counts were made at approximately the same traverse positions by four observers with each of the three graticules. It was, of course, not possible to recount exactly the same traverses, partly because of the difficulty of identifying the previous traverse positions, but mainly because of the difference in width of the graticules. As used, the width of the two new graticules was 30 μ whereas that of the Patterson–Cawood one was 27·5 μ. The counts obtained with the latter graticule were therefore corrected to allow for this difference in width.

A convenient measure of the counting consistency of an operator in the important size range of 1 to 5 μ is the standard deviation of the number of such particles counted on a single traverse, expressed as a percentage of the mean count. These values are tabulated by observer and graticule in Table 2 below, and it is clear there is no evidence to suggest that operator counting consistency differed with the design of graticule (Bartlett's homogeneity test gives $\chi^2_{(11)} = 6{\cdot}3$; $0{\cdot}90 > p > 0{\cdot}50$).

Table 2. *Count standard deviation on single traverse expressed as percentage of mean* (1 *to* 5 μ)

Unit: 1%

	Observer (each entry based on 6 degrees of freedom)				
Graticule	*S*	*G*	*W*	*H*	*Pooled value*
Patterson–Cawood	5·3	7·0	7·0	7·3	6·8
Globe and circle	5·1	8·4	9·5	7·4	7·8
Parallel line	7·0	6·5	10·6	9·6	8·7

The mean counts per traverse in the particle size range 1 to 5 μ are set out by observer and by type of graticule in Table 3. In addition, the corresponding mean counts of all observers with each graticule in the size range of greater than 1 μ are shown.

Table 3. *Mean number of particles counted per traverse*
Unit: 1 particle

Graticule	Size range 1–5 μ: Observer mean count (each mean based on 12 readings) S	G	W	H	Mean of observers (std. error 0·7)	Size > 1 μ: Mean of observers (std. error 0·8)
Patterson–Cawood	51·5	57·0	64·7	78·7	63·0	80·3
Globe and circle	53·8	56·8	63·5	78·2	63·1	81·1
Parallel line	53·7	59·9	65·2	78·8	64·4	85·9
Mean	53·0	57·9	64·5	78·6		

Inspection of the above table clearly shows that there were systematic differences in the mean counts of operators in the size range 1 to 5 μ. There is, however, no evidence that these differences were in any way altered by the type of graticule used. It is further seen that there were no real differences in the overall mean counts in this size range obtained with the different graticules although the highest was with the "parallel line" graticule. In the size range of "greater than 1 μ," however, there were real differences. The count with the "parallel line" graticule was definitely the greatest, but the mean counts with the other two graticules were virtually the same. No doubt this reflects the known tendency of the Feret diameter to overestimate particle size. The effect would, of course, be more noticeable in this size range, which is closed at one end only, than in the size range 1 to 5 μ, which is closed at both ends.

CONCLUSIONS

The routine counting requirements of the N.C.B. call for dust counts within specified size ranges. This has necessitated the design of a new graticule with provision for measuring these specified sizes and without the confusion of an unnecessarily large number of reference circles.

Two types of graticule, one with reference circles, the other with parallel lines, were designed for trial, careful note being given both to these factors and to the physical dimensions required to suit commercial microscope equipment.

Counting trials with these graticules in comparison with the Patterson–Cawood type showed that equal accuracy and consistency was obtainable with all three. All the operators expressed a definite preference for the simplified graticules over the Patterson–Cawood type on the grounds of their being less trying to use. The "line" graticule was easier to use than the globe and circle type when the density of deposit was light, with a dense deposit the globe and circle graticule was found to be more convenient. On balance there seemed to be no justification for a departure from the traditional globe and circle arrangement.

As a result of the work described, the globe and circle graticule depicted in Fig. 1 has been generally adopted for routine dust counting work in the National Coal Board. It is available in two sizes with grid lengths of 4·0 mm and 3·5 mm to suit positive and negative types of eyepiece respectively.

The extensions of the outer lines of the counting grid beyond the corners of the rectangle, as in Watson's graticule, were introduced later to serve as guides when particles are counted as they cross the boundary lines of the rectangle.

ACKNOWLEDGEMENT

This paper is presented by permission of Dr. W. Idris Jones, Director-General of Research in the Scientific Department of the National Coal Board. The views expressed are the authors', and not necessarily those of the Board.

REFERENCES

(1) WATSON, H. H. *Trans Inst. Min. Metall.*, **46**, p. 176 (1936).
(2) PATTERSON, H. S., and CAWOOD, W. *Trans Faraday Soc.*, **32**, p. 1084 (1936).
(3) FAIRS, G. L. *Chem. Ind.*, **62**, p. 374 (1943).
(4) MAY, K. R. *J. Sci. Instrum.*, **22**, p. 187 (1945).
(5) WATSON, H. H. *Brit. J. Industr. Med.*, **9**, p. 80 (1952).
(6) HEYWOOD, H. *Bull. Inst. Min. Metall.*, No. 477 (1946).
(7) WALTON, W. H. *Nature* [*London*], **162**, p. 329 (1948).

DISCUSSION

Dr. H. Heywood: Reference has been made to hand-held test cards of particle profiles for assessing the factors in estimating particle size by microscopical observation. A description of these cards and of the following test results have been published.* The profiles were viewed by the unaided eye to eliminate variation due to microscope adjustments, but in gauging the suitability of potential operators it would be preferable to view the profiles through a microscope. The tests I organized showed that the globe and circle averages were within 5% of the correct diameters, Martin's statistical intercept diameter was about 1·5% small and Feret's tangential intercept was about 13% large. These errors varied with the elongation of the particle but applied to a mean elongation ratio of 1·5.

Feret's system of measurement gave dimensions that could never be less than Martin's diameter and were often greater, therefore the error must be positive. The reason for Martin's diameter being slightly undersize was more obscure, but could be deduced theoretically. Taking an ellipse as an example, then Martin's statistical diameters could be represented by a number of diameters drawn so as to be spaced at equal angles. These diameters, or, to be more precise, the corresponding radii, would enclose unequal areas of the ellipse, i.e. radii near the major axis would enclose greater areas than those near the minor axis, and the corresponding diameters would be unequally weighted as regards the mean. To obtain the correct mean diameter, the radii should be spaced so that they enclosed equal areas (compare with Kepler's law of planetary motions), and would therefore be more closely spaced near the major axis. Since with this arrangement the mean of all the diameters would correctly represent the size of the ellipse, it followed that with the spacing at equal angles the mean would be less than the correct value.

Mr. G. L. Fairs: In the graticules developed in Imperial Chemical Industries Ltd. a $\sqrt{2}$ progression in circle diameter was chosen since under those conditions Bosanquet has shown that the error due to assigning a particle to a wrong class is only about 0·2 of the inevitable counting error. Can the authors say what is the relative error of assignment of particles to their respective classes in relation to the inevitable counting error in the case of the graticule which they have developed?

Authors' reply: In reply to Mr. Fairs, we made no attempt to assess the error of assigning particles to incorrect classes because, as stated in the paper, the graticule is intended for use in making "range" counts rather than "size distri-

* HEYWOOD, H. *Trans Instn Min. Met.*, **55**, p. 391 (1946).

bution" counts. It is perhaps relevant to state that when we designed the graticule, we were interested in the question as to whether the practice of counting particles in only one wide size range gave results of smaller accuracy than the technique of size distribution counting in which this size range lay in the centre of a longer "scale." We found that there was no significant difference in the counts obtained with the new graticule in the 1–5 μ range, and those obtained with a Patterson–Cawood graticule, in which sizing was carried out in the scale from 0·5 to 6·25 μ.

Paper E.3

A particle-profile test strip for assessing the accuracy of sizing irregularly shaped particles with a microscope

By H. H. Watson, B.Sc., F.Inst.P., and D. F. Mulford, Suffield Experimental Station, Ralston, Alberta, Canada

This paper describes a particle-profile test strip, which can be used for assessing the errors of sizing irregularly shaped particles with a microscope, using a globe and circle eyepiece graticule. The two hundred irregularly shaped profiles on the test strip were sized under a microscope by nine observers on two occasions. The results obtained and the errors revealed are discussed. It should be possible using the test strip to weed out bad dust sizing microscopists, and to correct sizing bias of others.

Hand-held test cards similar to the pattern described by Heywood[1] are useful for training microscopists to avoid or to correct for bias when making size distributions of the profiles of irregularly shaped particles, using the globe and circle graticule method. Such a test card is illustrated in Fig. 1, the actual size of the 25-circle being 1 cm. The microscopist is invited to compare the profiles with the

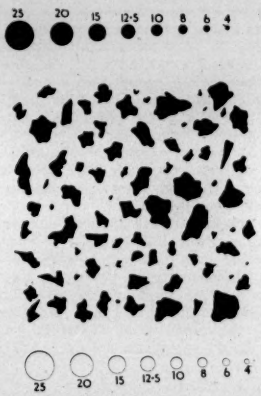

Fig. 1. Example (reduced) of hand-held test card. On the actual card the 25-circle is 1 cm in diameter

circles situated above and below the array and to assign each to a circle size group, size of profile being assessed in terms of its mean projected diameter.

The actual area of each profile is previously measured accurately, either by "counting squares," or with a photo-electric method, such as that due to Watson and Cruise.[2] There is a tendency to oversize irregularly shaped profiles in this way. If a microscopist finds he is sizing with a bias, he can attempt to correct this tendency, by making from time to time a size distribution of the profiles on a series of test cards. A sufficient number of cards should be prepared so that the correct sizes of the individual profiles are not memorized.

The particle-profile test strip

It was felt that a test card of the type described above gives a presentation sufficiently different from that seen under a microscope to limit somewhat its usefulness, and so a particle-profile test strip was produced that can be viewed under a microscope.

Two hundred single unaggregated particles of coal dust were traced, at a magnification of × 1000, and arranged in a strip similar to that of a thermal precipitator deposit. The profiles were numbered and filled in with black poster ink; their areas were measured and the corresponding mean projected diameters calculated. The test profiles covered a limited size range (4·5 to 1) and some smaller unnumbered profiles were intermingled with them to add a little more reality to the array. A 1 cm grid scale was added to serve as a size reference (Fig. 2).

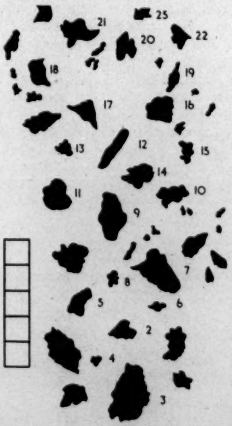

Fig. 2. Photomicrograph of portion of particle-profile test strip

The test strip was reduced photographically to a size suitable for low power microscopy. It was cemented to a

cover-glass and mounted on a 3 × 1 in slide. The array of profiles can be traversed across the field of view of a microscope and profile sizes estimated by comparison, in the usual way, with the circles of an eyepiece graticule. A realistic impression of a sample of black dust is obtained, with the advantage over the hand-held test cards that all the conditions of microscope working are fulfilled.

The size distribution of the test profiles is given in Table 1, and the distribution of their elongation ratios (ratio of length to breadth of enclosing rectangle) in Table 2.

Table 1. *Size distribution of test profiles*

The data are given in terms of the circles of a Patterson–Cawood graticule with microscope magnification adjusted to make 4% of the profiles larger than the 25-circle.

Graticule circle size-group	*Number of profiles*
6 – 8	6
8 –10	36
10 –12·5	49
12·5–15	29
15 –20	49
20 –25	23
>25	8

Table 2. *Distribution of elongation ratios of test profiles*

Elongation ratio	*Number of profiles*
1·00–1·20	33
1·21–1·40	44
1·41–1·70	67
1·71–2·00	35
2·01–2·75	18
>2·75	3

EXPERIMENTAL USE OF THE TEST STRIP

Nine observers were invited to estimate the sizes of the profiles in terms of the circles of a Patterson–Cawood eyepiece graticule. The open or the opaque circles were used by choice of the individual observer. The sizings were repeated a day later, and no results were examined until all readings had been recorded. Results are summarized in Table 3, which includes data for consistency between the two succeeding days as well as the "scores" of the observers. Times taken to complete the sizings are also given.

Details of the best and lowest scores of correct results are given in Tables 4 and 5 respectively. Size group 10–12·5 is given briefly as 12·5, and so on. With a 2 mm oil immersion objective, and a suitable microscope tube length, the 25-circle on the graticule would correspond to a diameter of 5 μ.

DISCUSSION OF RESULTS

Bias. The estimated mean size of the profiles has been calculated from

$$\bar{d} = \frac{\Sigma(nd)}{\Sigma(n)}$$

where n is the number of profiles allocated to a size group of mean size d. The estimates of mean size made by each observer are given in Table 6 as ratios of the correct mean size ($\bar{d}_0$), calculated in the same way.

All observers were consistent in the direction of their bias, whether positive or negative; five observers were underestimating and four were overestimating sizes.

Using test cards, Heywood[1] found that only two out of ten observers underestimated profile sizes. His experimental conditions were rather different and so direct quantitative comparison with the present results is not possible. He used a narrower range of profile sizes and asked observers to move the comparison circles, which were on a separate transparent surface, to the side of or over each profile. The range of $\bar{d}/\bar{d}_0$ found by Heywood was 0·97 to 1·10 using the opaque comparison circles, and 0·99 to 1·04 using the open circles. In the present studies, only when there was difficulty in estimating size did the observer attempt to rotate the eyepiece graticule to a position close to or over that of a profile.

The present finding, that more observers were undersizing than oversizing, is at variance with the usually accepted trend. This is possibly due to the fact that all five of those undersizing had done a considerable amount of sizing of dust samples and had taken note of the usual bias in the direction of oversizing. It is evident that they had overcorrected, observer 7 seriously so.

Observers 3 and 4 were expert in observational microscopy, but neither had been specifically made aware of the oversizing tendency. Observer 8 was experienced in sizing dust particles, while observer 9 was not.

Observers who biased badly in either direction tended to increase this bias with decreasing size of profile, but for average observers little effect varying with profile size was observed within the limits of the actual sizes used.

Consistency. As noted above, all nine observers were consistent in the direction of their bias. Six of them reduced this bias on the second sizing (Table 6), but only one (observer 2) by an appreciable amount. Apart from this

Table 3. *Summary of results*

Obs.	*1st reading* –	*Correct*	+	*2nd reading* –	*Correct*	+	*Consistency* (*a*)	(*b*)	(*c*)	*Times (min sec)* 1st	2nd
1	58	128	14	52	131	17	14	162	24	21·30	25·00
2	93	97	10	40	141	19	5	123	72	11·45	15·30
3	4	78	118	3	91	106	27	158	15	21·30	21·15
4	4	112	84	4	96	100	15	147	38	16·00	14·45
5	70	115	15	48	130	22	20	128	52	26·45	20·30
6	72	118	10	72	118	10	24	150	26	21·25	16·30
7	128	66	6	106	79	5	25	138	37	19·45	26·00
8	33	125	42	12	134	54	16	132	52	26·30	24·45
9	18	137	47	17	140	43	24	155	21	21·45	21·00

Notes: (i) Under 1st and 2nd readings, the symbol + means the number of profiles an observer placed in a group larger than the correct one.

(ii) Under consistency, (*a*) is the number of profiles that were judged smaller in size on the second assessment as compared with the first, (*b*) the number that were placed in the same size group, (*c*) the number that were judged to be larger on the second assessment.

Table 4. *Detailed results of best score of correct sizings*

Number placed in different size groups by observer 2, on second reading

Size group	6	8	10	12·5	15	20	25	>25	Correct no. in group
6									—
8	1	3	1	1		*No. oversized* 19			6
10	2	7	23	4					36
12·5			9	34	6				49
15				7	18	4			29
20		*No. undersized* 40		1	5	42	1		49
25						7	14	2	23
>25							1	7	8
							Total correct		141
Estimated no. in group	3	10	33	47	29	53	16	9	

Table 5. *Detailed results of worst score of correct sizings*

Number placed in different size groups by observer 7, on first reading

Size group	6	8	10	12·5	15	20	25	>25	Correct no. in group
6									—
8	4	1	1			*No. oversized* 6			6
10	2	28	6						36
12·5	1	8	28	10	2				49
15			2	15	10	2			29
20				2	25	22			49
25		*No. undersized* 128				11	11	1	23
>25							2	6	8
							Total correct		66
Estimated no. in group	7	37	37	27	37	35	13	7	

one observer, the results do not suggest a significant leaning effect.

Observer 2 made his first sizing quickly and at a time when he was occupied with other matters and was interrupted during the run. His consistency was the lowest of all, and on the second reading attained the highest score of correct sizings. On a third series of readings, this observer, ten days after his second reading, recorded in 19 min 15 sec a still higher score of 146 correct sizings.

Speed of sizing. In general, different observers made their own speed, and it is instructive to note that the score of correct estimates was not generally dependent on the time taken by any one observer. The experience of observer 2 suggests, however, that a minimum time and a steady concentration is necessary for reasonably correct results, even with an experienced microscopist. Most observers sized between 8 and 10 profiles per minute. This is at a slower rate than would often be used for routine work, but it appears important to suggest a minimum time of 5 sec for studying and estimating the size of each particle, using the globe and graticule method.

Table 6. *Values of* $\bar{d}/\bar{d}_0$

Observer	*1st reading*	*2nd reading*
1	0·952	0·963
2	0·904	0·977
3	1·129	1·120
4	1·081	1·116
5	0·942	0·973
6	0·935	0·931
7	0·826	0·834
8	1·016	1·048
9	1·027	1·026

Effect of elongation ratio. Heywood[1] found that bias was not affected by an elongation ratio of less than 2·00 when using open circle comparison and of less than 2·75 when using the opaque circles. This effect has not been investigated in the present work, as the number of profiles with elongation ratios larger than 2·00 was small (see Table 2).

Some practical considerations. When estimating, for instance, mass median diameters, from a microscope count, the errors introduced by a bias in sizing will be larger than those represented by the ratio $\bar{d}/\bar{d}_0$.

For much routine work it is customary to count a dust sample between two limits of size, omitting a size distribution. Thus, for work in connexion with the pneumoconiosis hazard of a dust, counts within size ranges of 0·5 to 5 μ or 1·0 to 5 μ are commonly used. Calculations have been made (Table 7) of the percentage of true count obtained between 0·5 and 5 μ for a number of values of $\bar{d}/\bar{d}_0$ for two size distributions:

Fine dust: 80% of particles smaller than 0·5 μ
99·9% of particles smaller than 5 μ

Coarse dust: 15% of particles smaller than 0·5 μ
85% of particles smaller than 5 μ

Table 7. *Calculated percentage of actual count to true count within size limits of 0·5 μ and 5·0 μ of two dust clouds, made with different sizing biases*

Sizing bias ($\bar{d}/\bar{d}_0$)	*Percentage*	
	Coarse cloud	*Fine cloud*
0·7	95·3	185·9
0·8	99·1	137·9
0·9	99·9	118·4
1·0	100·0	100·0
1·1	99·9	84·5
1·2	99·8	70·5
1·3	98·4	60·0

GENERAL CONCLUSIONS

The particle-profile test strip is likely to be a useful component in a laboratory where particle-profile size distributions are being made. It reveals and gives a quantitative estimate of observer bias. An attempt can be made by training to reduce or effectively to eliminate a bias, or less satisfactorily, a correction can be made for a measured bias.

A few people will never make reliable dust sizing microscopists and it should be possible to detect these with the test strip. Even under good conditions and with well-tried microscopists sizing of irregularly shaped particles is not an easy task. An occasional check up with the test strip should give continued confidence to the expert.

Although the profiles in the test strip that has been described are opaque, there should be no difficulty in producing a test strip with clear particles in order to represent rock particles such as quartz.

ACKNOWLEDGEMENT

The particle-profile test strip was made by Graticules Ltd.

REFERENCES

(1) HEYWOOD, H. *Trans Instn Min. Metall.*, **55**, p. 391 (1945–46).
(2) WATSON, H. H., and CRUISE, A. J. *Engineering*, **177**, p. 594 (1954).

DISCUSSION

Mr. E. W. Meyer: Mr. Watson's approach to the training and analysing of results of people employed for particle counting is one of value and importance. However, on reflecting on what he is actually estimating, that is the difference between the known number of particles and the size distribution of particles on his controlled slide and the result obtained by an operator, this latter difference is a complex measure and really falls in the domain of the psychologist. This applies, of course, also to the type of graticule that is employed. The use of a circle is a mathematical convention, but probably has no advantage over any other shape when one is actually estimating either diameters or areas. This is a matter of perception, the subject of which is fraught with danger.

Some of the difficulties experienced and peculiarities are shown in papers by Köhler and co-workers on "Figural After Effects,"[1,2,3] or "The Moon Illusion" as described by Boring,[4] and Thouless's work[5] on "The Phenomenal Regression to the Real Object." The latter paper, I think, is of value and it was some little while ago that I tried to persuade people to take an interest in the psychological aspect and even employ a psychologist to help in training and advising on the correct type of graticule and methods for obtaining reproducible and more tolerable conditions for the operator.

Mr. A. Radcliffe: The counting and sizing of irregularly shaped particles involves two distinct steps. In the first step the equivalent circular area has to be recognized; in the second step the size has to be estimated. In Paper E.3 there is no evidence that these steps have been separated. An essential part in the training of a microscopist in the art of recognizing particles of the same area is surely to show him many particles of different shape but equal area.

Mr. G. L. Fairs: I have been most interested to read about the test cards and test strips designed by Mr. Watson for the training of microscopists in size analysis.

For a good many years I have used a projection microscope for such training and have found it ideal for the purpose since a trained operator can size a given area on a slide which can then be sized by the trainee and the results compared and discussed. This process is extremely difficult with an ordinary bench microscope and it seems that Mr. Watson's proposal will be most useful where a projection microscope is not available.

REFERENCES

(1) KÖHLER and DINNERSTEIN. *Sonderabdruck aus Miscellanea Physicologica Albert Michotte* (Louvain: Institut Superieur de Philosophie, 1947).
(2) KÖHLER and WALLACH. *Proc. Amer. Phil. Soc.*, **88**, p. 269 (1944).
(3) KÖHLER and EMERY. *Amer. J. Psychol.*, **60**, p. 159 (1947).
(4) BORING. *Amer. J. Phys.*, **11**, p. 55 (1943); **14**, p. 99 (1946).
(5) THOULESS. *Brit. J. Psychol.*, **21**, Part 4 (1931); **22**, Part 1 (1931).

Paper E.4

The electron microscopy of airborne dusts

By J. Cartwright, Safety in Mines Research Establishment, Sheffield

A technique is described for collecting airborne dust samples on membrane coated cover glasses in a thermal precipitator. Samples thus collected can be counted with either an optical or an electron microscope and only one sample is required for the measurement of the size distribution and concentration of particles in the range from 10 to 0·01 μ. Particles of diameter between 10 and 0·23 μ are counted with an optical microscope and those with diameters between 3·0 and 0·01 μ are counted with an electron microscope.

It is shown that any differences between the assessments in the overlap range of the two instruments are due to the greater resolving power of the electron microscope.

Previous work by Walton and Wainwright[1,2] and by other investigators has shown that there is difficulty in reconciling optical and electron microscope assessments of airborne dusts. The differences between optical and electron microscope assessments could be due to experimental errors or to the limitations of the microscopes. Errors in sampling and in manipulation are more likely to arise with the electron microscope because of the greater complication of the technique used. On the other hand, size classification errors are less likely to occur with the electron microscope because particle boundaries are much more clearly resolved. This paper describes work carried out to examine the relationship between optical and electron microscope counts in the range from 0·3–3 μ.

In the experiments described the thermal precipitator was chosen as the sampling instrument for the following reasons: (i) it has a high sampling efficiency at least down to 0·01 μ;[1] (ii) it is less likely than most other instruments to shatter particles during sampling or to disperse airborne aggregates of particles; (iii) it can safely be used in atmospheres where there is a risk of explosion; (iv) in British coal mines it is the standard instrument for airborne dust assessment where the counts are made with the optical microscope, and results obtained with the electron microscope can be related to accumulated data based on optical counting.

Some electron microscopes have insufficient stage motion to scan the full width of the normal thermal precipitator deposit, and the oscillating thermal precipitator described by Walton[1] and by Drummond[3] was designed to produce a dust deposit that could be evaluated by using a limited traverse across a central region of uniform deposition. In our experiments a normal thermal precipitator was used, the type E.M.3 electron microscope by Metropolitan-Vickers Electrical Co. Ltd., having sufficient traverse motion to scan the full width of the dust trace.

Experimental Techniques

Most previous workers have obtained samples for electron microscopy by using membrane-coated specimen grids in place of cover glasses in the thermal precipitator. The electron microscope sample is not then collected under precisely the same conditions as a sample taken on a cover glass for optical counting. If the thermal precipitator is used with a cover glass at one side, and an electron microscope grid at the other side, the two samples can differ because of uneven division of the air flow past the heated wire. If separate thermal precipitators are used their results can differ even when samples are taken simultaneously.[4] If consecutive samples are taken with the same thermal precipitator the dust cloud can vary. Even if these effects can be minimized it is doubtful whether electron microscope grids should ever be used in the thermal precipitator, since dense samples, when examined with a stereoscopic microscope, show a preferential deposition of dust on the grid bars. Such an accumulation is shown in Fig. 1 but less clearly than with a stereoscopic view. Walkenhorst[5] attributes this effect to differences in thermal gradient in the region above the grid bars and in the region above the apertures.

After samples are taken, errors of evaluation may arise as follows: (i) Viewed at high magnification in the electron microscope the direction of the trace cannot always be recognized with certainty and if a scan is made obliquely

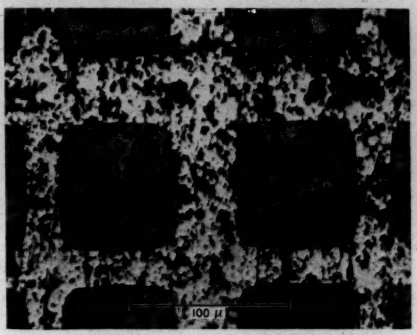

Fig. 1. Thermal precipitator dust sample collected on membrane-coated specimen grid

across the trace a spuriously high count will result. (ii) The portion of the dust trace that can be traversed in the electron microscope is restricted to a narrow band encompassed by the 2 mm diameter specimen grid. If the density of the deposit varies along the length of the trace, a count from a single narrow band may lead to an incorrect estimate of the total deposit. (iii) The magnification of the electron microscope is not easy to calibrate with accuracy and is liable to subsequent errors due to slow changes of accelerating voltage and lens current and to hysteresis effects in magnetic lenses. (iv) Particles may be lost from the samples during manipulation. This is more likely to occur in specimens for electron microscopy than with those for optical microscopy because the manipulative techniques are more complicated. The extent of loss of particles can be checked by metal shadowing the samples immediately after they are removed from the thermal precipitator. Movement or loss of particles is then shown by the appearance of shadows without corresponding particles.

We have avoided the above difficulties by careful attention

to manipulative techniques and by using a different sampling method in which samples are taken on membrane-coated cover glasses. Counts are made in the normal way with an optical microscope, and the membranes are then stripped from the glass, mounted on grids, and examined in the electron microscope.

Preparation of membrane-coated cover glasses. The membrane forming material used for covering the cover glasses is polyvinyl formal (Formvar). It is prepared as a 0·7% solution in ethylene dichloride. Before the cover glasses are coated they are first treated so as to form on their surface a hydrophilic layer to facilitate subsequent stripping of the membrane. A satisfactory way to ensure easy stripping is to dip clean cover glasses in a bath of 5% Teepol solution. They are then dried by gently wiping them with silk; a thin layer of wetting agent remains on the glass surface. The cover glass thus prepared and held by fine tweezers is dipped into the Formvar solution and then steadily withdrawn and held vertically for a few seconds to drain. It is preferable to hold the cover glass just clear of the liquid so that it is drained in the presence of the solvent vapour. This prevents too rapid drying which may otherwise produce an uneven film. The film coated cover glasses are allowed to dry in still air for about 10 min and are then mounted on the thermal precipitator plugs with esterwax.

Collection of sample. The sample is obtained in the normal way but the sampling time is rather longer than it would be for optical work alone. This is done to produce a denser deposit so that fewer electron micrographs need be taken. Usually the maximum allowable density is decided by the strain of counting the sample with the optical microscope, but in some cases the possibility of obscuration of the field by overlapping particles is a more important factor.[6]

It has been found necessary in many cases to take a pilot sample before taking the sample for complete evaluation.

Optical counting. After the sample has been taken the cover glasses are removed from the thermal precipitator and shadowed with an alloy of 60% gold and 40% palladium. They are then secured with scotch tape to microscope slides with the specimen side of the cover glass facing the glass slide. A paper ring between the cover glass and the slide prevents chafing of the membrane and disturbance of the dust deposit.

With the specimen so mounted counts are made with an optical microscope using a 2 mm oil immersion objective. If reasonable care is taken there is no risk of the immersion oil contaminating the specimen.

Preparation for the electron microscope. After optical counts are completed the cover glasses are removed from the slides and the membranes stripped off by floating on water. The cover glass is held at the edge with fine tweezers at an angle of about 40° to the horizontal and the diametrically opposite edge is allowed to touch the surface of clean distilled water for a few seconds. The cover glass is then steadily slid under the water leaving the membrane floating. Although very thin, the membrane and its dust trace can be clearly seen on the water surface. The next operation is to remove the membrane from the water and transfer it to a specimen grid which is supported on a simple jig designed for this purpose. The jig is a brass cylinder about 1 in. long and ¼ in. diameter with a hole of the same diameter as the specimen grid drilled and tapped through its axis. A set screw in the threaded hole is adjusted so that its end is flush with the face of the plug and then withdrawn slightly to leave a shallow recess. The specimen grid is held in this recess and before placing the membrane on it the grid is rotated until its bars are in line with a mark scribed across a diameter of the face of the plug.

When the grid is mounted and alined on its jig the membrane is lifted from the water surface with a wire loop of slightly larger diameter than the jig and surplus water is carefully removed with filter paper. Then the wire loop carrying the membrane and its clearly visible dust trace is lowered over the jig, with the dust trace in line with the scribed mark and therefore in precise alinement with the grid bars. When dry, the grid is raised by means of the screw and, after scoring round it with a needle, it can be removed and placed in the electron microscope. The jig just described will be seen to be similar to, but smaller than, the normal thermal precipitator plugs which had been adapted in an almost identical way to support specimen grids directly in the thermal precipitator.[3]

Manipulation of the electron microscope. The electron microscope is used with an accelerating voltage of 75 kV for this work.

The specimen is first viewed at a low magnification of about ×150 and a map of the field is drawn showing prominently shaped particles. This helps in finding the position and direction of the trace when a higher magnification of about ×3000 is used later. Viewed at this higher magnification the direction of the length of the trace is again checked and a series of micrographs taken across its width.

To avoid any selection of fields, one micrograph is taken in the same position in each grid square irrespective of the appearance of the field on the viewing screen. No bias is introduced by this because the grid is randomly placed on the sample. Enough micrographs are taken to provide a sufficient number of particles and in the work here described this usually entailed photographing fields in four or five rows of grid squares, making a total of sixty or more micrographs.

Magnification calibration. To measure the absolute magnification in the electron microscope four overlapping micrographs along the bar of a readily identifiable grid square are taken and the total length of the image of the grid bar is measured on the micrographs.

When the grid is later removed from the electron microscope and mounted on a glass slide, the length of the grid bar is measured in the light microscope. This is done using a stage micrometer as a reference standard. The length of a grid bar is about 70 μ and its image would cover a total distance of 21 cm at a magnification of ×3000. This is covered with an adequate overlap on four of the standard 8 cm square photographic plates used in the electron microscope.

While routine micrographs are being taken a check is kept on the magnification by measuring the movement of a pointer, fixed to one of the stage traverse controls, while a particle is moved across a diameter of the field. Corrections for any change in magnification can then later be applied in projecting the micrographs during evaluation.

TESTING THE MODIFIED SAMPLING TECHNIQUE

It was found that intact membranes carrying the thermal precipitator dust deposit could be obtained by floating on to a water surface, the operation being completely successful in about 75% of the trials. To test the effect of the coatings on the sampling efficiency of the thermal precipitator, samples were taken with coated cover glasses and with normal cover glasses in a cloud of ground coal dust in a wind tunnel. Counts were made on two of these samples (Tables 1 and 2). The totals for coated and uncoated cover slips differ by approximately 6%. Dawes and his co-workers[4] have shown

Table 1. *Thermal precipitator sample using normal cover glasses—optical counting*

Traverse	*Number of particles counted; Size range: μ* 0·32–0·45	0·45–0·64	0·64–0·90	0·9–1·3	1·3–1·8	1·8–2·6	2·6–3·6	3·6–5·1	5·1–7·2	7·2–10·2	
					Cover glass A						
a	168	105	167	240	225	109	49	25	3	3	
b	119	103	141	186	206	89	62	40	16	4	
centre	108	118	102	176	165	74	52	18	8	2	
d	84	81	95	186	139	73	48	15	3	3	
e	84	84	88	145	122	63	37	23	8	1	
Total	563	491	593	933	857	408	248	121	38	13	Grand total = 4265
Average	112	98	119	187	171	82	50	24	8	3	
					Cover glass B						
a	89	85	97	114	130	72	52	26	7	3	
b	89	79	93	153	134	76	43	17	5	2	
centre	80	92	91	152	141	74	33	18	2	2	
d	68	81	97	128	122	108	61	23	6	2	
e	79	81	84	152	143	84	43	32	7	2	
Total	405	418	462	699	670	414	232	116	27	11	Grand total = 3454
Average	81	84	92	140	134	83	46	23	5	2	

Total $A + B = 7719$

Table 2. *Thermal precipitator sample using coated cover glasses—optical counting*

Traverse	*Number of particles counted; Size range: μ* 0·32–0·45	0·45–0·64	0·64–0·90	0·9–1·3	1·3–1·8	1·8–2·6	2·6–3·6	3·6–5·1	5·1–7·2	7·2–10·2	
					Cover glass A						
a	56	66	76	141	126	69	40	22	6	1	
b	129	99	129	195	143	92	59	26	12	1	
centre	102	100	109	207	145	96	57	35	14	1	
d	89	88	91	187	184	96	79	31	15	0	
e	109	112	113	215	189	78	52	25	10	1	
Total	485	465	518	945	787	431	287	139	57	4	Grand total = 4118
Average	97	93	104	189	157	86	57	28	11	1	
					Cover glass B						
a	104	77	91	132	106	50	22	17	0	1	
b	112	95	68	112	117	51	34	10	5	0	
centre	120	108	82	118	105	58	30	19	3	1	
d	125	96	108	107	112	57	29	18	3	1	
e	104	119	115	125	99	49	28	20	1	0	
Total	565	495	464	594	539	265	143	84	12	3	Grand total = 3164
Average	113	99	93	119	108	53	29	17	2	1	

Total $A + B = 7282$

that the coefficient of variation of the instrumental error associated with the thermal precipitator is at least 5%. This means that if two thermal precipitators (with uncoated cover slips) sample in the same cloud, the numbers counted will lie between ±10% of the mean on 19 occasions out of 20. Thus the observed difference of 6% between the counts on the two precipitators used in the tests is within experimental error, and there is no reason to suppose that there is a significant difference between counts on the coated and uncoated cover slips. The samples were then used to determine whether a consistent estimate of dust concentrations could be made from counts of the portion of the 10 mm long trace encompassed by the 2 mm diameter field coverage available in the electron microscope; this was necessary as the thermal precipitator deposit could vary along its length with a small misalinement of the heater wire. A typical result of these tests is shown in Fig. 2, where counts of five

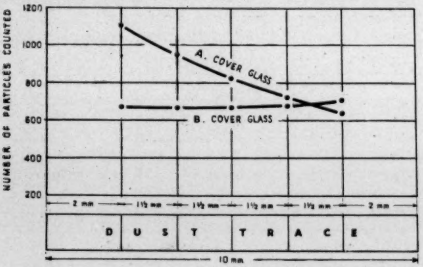

Fig. 2. Optical count of thermal precipitator sample showing variation of count along the length of the trace

Number of particles counted

	A. Cover glass	*B. Cover glass*
Centre traverse	823	685
Average of five spaced traverses	853	691

traverses spaced 1·5 mm apart are shown. Further results are given in Tables 3 and 4 and these show that in the case of the particular thermal precipitator used, the count along the centre traverse was not appreciably different from the average of the spaced traverses and could be used to provide a reliable estimate of the total deposit. The counts also showed that unequal numbers of particles were collected on the *A* and *B* pairs of cover glasses of each sample, and that the ratio between the numbers varied from sample to sample. Thus it was shown that the total dust deposit could be estimated by traversing the centre of each trace, but it would be essential to make counts on each of the pair of cover glasses of each sample.

COMPARISON OF OPTICAL- AND ELECTRON-MICROSCOPE ESTIMATES

If the modified technique is successful in appreciably reducing the sampling and manipulative errors the remaining discrepancies between optical- and electron-microscope evaluation methods are likely to be largely due to differences in resolving power. Fig. 3 shows how this can occur. The electron-microscope image when compared with the optical-microscope image shows that particles greater than 1 μ, and nominally within the optical range, can look very different when the field is properly resolved.

In order to establish that observed differences between optical- and electron-microscope counts can be due to differences in resolving power alone, it was first necessary to show that all other causes of difference had been removed.

Table 3. *Optical counts of thermal precipitator samples*

Samples 1 to 4 plain cover glasses
Samples 5 to 8 coated cover glasses

Total of all particles 0·3–10·2 μ

Sample	*Cover glass*	*Mean of 5 traverses*	*Centre traverse*	*Standard error of mean of 5 traverses*	*95% confidence limits of mean*
1	A	280	268	5·48	265–295
	B	399	409	30·30	315–483
2	A	364	352	14·46	324–404
	B	232	229	3·61	222–242
3	A	349	350	3·13	340–358
	B	305	316	4·15	293–317
4	A	354	352	4·00	343–365
	B	339	356	5·38	324–354
5	A	313	300	7·56	292–334
	B	340	337	1·69	335–345
6	A	413	408	6·94	394–432
	B	213	199	8·24	190–236
7	A	327	325	2·63	320–334
	B	334	372	12·79	298–370
8	A	424	441	10·56	395–453
	B	331	310	6·31	313–349

This could be done if it could be shown that, when the resolving powers were made equal, the counts did not differ beyond statistically acceptable limits. The only way to equalize the resolving powers was to degrade the electron-

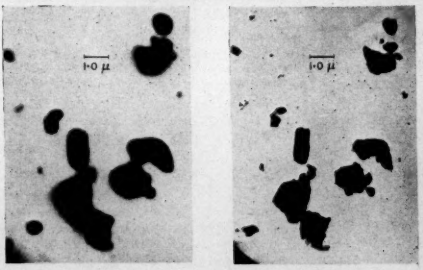

(*a*) (*b*)

Fig. 3. Identical fields of thermal precipitator sample of airborne dust

(*a*) Optical-microscope image obtained with 2 mm oil immersion objective. Twelve distinguishable particles greater than 0·25 μ

(*b*) Electron-microscope image. Eighteen distinguishable particles greater than 0·25 μ

microscope resolution to that of the optical microscope, and this was done by ignoring all particle separations less than 0·2 μ when counting from electron micrographs. Later, the counts were repeated taking advantage of the full resolution of the electron microscope and thus three series of counts were available for comparison; the optical counts; the low

resolution electron-microscope counts; and the high resolution electron-microscope counts.

The samples for these tests were from clouds of three different dusts, a ground coal dust in a wind tunnel, a coal mine dust, and a quarry dust. To improve contrast and increase the reliability of the counts the samples were metal shadowed.

Each sample was counted optically using a 2 mm oil immersion objective and then photographed in the electron microscope. For each sample about sixty electron micrographs were taken at a magnification of ×3000, and for counting, these were further enlarged to a total magnification of ×15000. Results of the counts are given in Fig. 4 and in Table 5, where optical counts are compared with electron-microscope counts at the same resolution. The actual optical counts were made over approximately four times the area of the electron-microscope counts and a correction applied so that the area-corrected optical count could be directly compared with the electron-microscope count.

All the counts match fairly well except for the 1·3–1·8 μ range in the mine sample. Here the electron-microscope count is 50% lower than the optical-microscope count.

To test the results statistically X^2 was calculated for each sample by using a $2 \times n$ contingency table, and the corresponding probability was then obtained from statistical tables. The probability that the differences are due to random sampling errors is given in Table 5.

Table 4. *Counts of two thermal precipitator samples showing the comparison between the mean size distribution of five traverses and the size distribution of the centre traverse alone*

	Size range: μ									
	0·32–0·45	0·45–0·64	0·64–0·9	0·9–1·3	1·3–1·8	1·8–2·6	2·6–3·6	3·6–5·1	5·1–7·2	7·2–10·2
Uncoated cover glass A										
Mean count of 5 traverses	112	98	119	187	171	82	50	24	8	3
Centre traverse count	108	118	102	176	165	74	52	18	8	2
Standard error of mean of 5 traverses	15·38	6·92	15·18	15·28	19·35	8·00	4·00	4·32	—	—
95% confidence limits of mean	69–155	79–117	77–161	145–229	117–225	60–104	39–61	12–36	—	—
Uncoated cover glass B										
Mean (as above)	81	84	92	140	134	83	46	23	5	2
Centre (as above)	80	92	91	152	141	74	33	18	2	2
Standard error of mean of 5 traverses	3·85	2·31	2·38	8·00	3·80	6·62	4·73	2·75	—	—
95% confidence limits of mean	70–92	78–90	85–99	118–162	123–145	65–101	33–59	15–31	—	—
Coated cover glass A										
Mean (as above)	97	93	104	189	157	86	75	28	11	1
Centre (as above)	102	100	109	207	145	96	57	35	14	1
Standard error of mean of 5 traverses	12·20	7·78	9·09	12·95	12·37	5·43	—	2·31	1·60	—
95% confidence limits of mean	63–131	71–115	79–129	153–225	123–191	71–101		22–34	7–15	
Coated cover glass B										
Mean (as above)	113	99	93	119	108	53	29	17	2	1
Centre (as above)	120	108	82	118	105	58	30	19	3	1
Standard error of mean of 5 traverses	4·22	7·03	10·48	4·55	3·09	1·87	1·92	1·77	—	—
95% confidence limits of mean	101–125	79–119	64–122	106–132	99–117	48–58	24–34	12–22	—	—

Only in the coal mine dust sample does there appear to be a serious discrepancy. This results mainly from the high optical count in the range 1·3–1·8 μ. On investigation of the micrographs, marks on the membrane suggesting dried oil or similar matter were observed, the majority of these being about 1 μ in size and their number about equal to the apparent counting error. It is probable that these oil droplets were classed as particles in the optical count. The quarry dust sample, which was shadowed before optical counting, showed similar marks on the micrographs but apparently the preshadowing eliminated this source of error in the optical

counts. The results in the case of this sample were very satisfactory. More than 1000 particles were counted in the electron microscope and almost 4000 in the optical microscope. There was no difference between these large counts at the 10% level of significance, i.e. such a difference could arise once in ten from the random fluctuations.

is taken with any other method of electron-microscope evaluation of airborne dusts so long as the electron microscope is used to study the ranges of particle sizes below about 2 μ, and the optical microscope for larger particles. In some trials almost a hundred plates per sample were exposed in order to establish a wide overlap between optical- and electron-

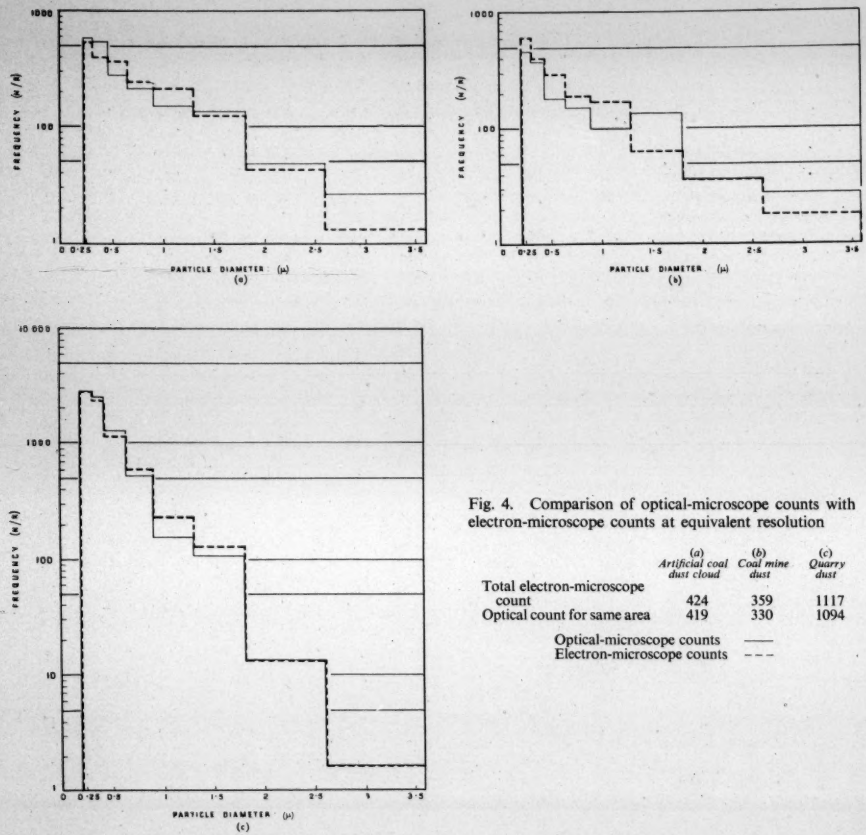

Fig. 4. Comparison of optical-microscope counts with electron-microscope counts at equivalent resolution

	(a) *Artificial coal dust cloud*	(b) *Coal mine dust*	(c) *Quarry dust*
Total electron-microscope count	424	359	1117
Optical count for same area	419	330	1094

Optical-microscope counts ——
Electron-microscope counts - - -

In all counts, no matter how carefully they are carried out or how precise the instrumentation, there will be a residue of observational error. The results of the work described show differences which are small enough to be explained by residual scatter. There is a suggestion, however, of systematic error which could be further investigated with a series of different observers should the need arise.

The procedure described need not consume more time than microscope counts. Now that the technique is shown to be satisfactory there is no need for this wide overlap and with a deposit of suitable density a maximum of twenty exposures will be sufficient.

These results show that with the method described there is agreement between electron- and optical-microscope results when the resolution of the electron-microscope images is degraded to that of the optical-microscope images. If now the electron-microscope images are evaluated, as they actually appear, the difference between these and the previous

Table 5. *Comparison between optical and electron-microscope counts of the same dust samples*

Sample	*Size range (μ)*	*Optical count*	*Area-corrected optical count*	*Electron-microscope count*	*χ^2 and degrees of freedom*	*Probability, P, that differences between the e.m. and optical microscope are due to chance alone*
Artificial coal dust in wind tunnel	0·23–0·32	165	47	48	$\chi^2 = 12·730$	$0·1 > P > 0·05$
	0·32–0·45	239	68	50	d.f. = 7	
	0·45–0·64	194	55	64		
	0·64–0·90	196	56	65		
	0·90–1·30	218	62	85		
	1·30–1·80	230	66	64		
	1·80–2·60	134	38	35		
	2·60–3·60	93	27	13		
	Totals	1469	419	424		
Coal mine dust	0·23–0·32	220	41	54	$\chi^2 = 29·508$	$0·001 > P$
	0·32–0·45	260	49	52	d.f. = 7	
	0·45–0·64	184	35	57		
	0·64–0·90	217	41	50		
	0·90–1·30	211	40	68		
	1·30–1·80	357	67	31		
	1·80–2·60	154	29	29		
	2·60–3·60	148	28	18		
	Totals	1751	330	359		
Quarry dust	0·23–0·32	850	240	239	$\chi^2 = 10·276$	$0·2 > P > 0·1$
	0·32–0·45	1160	322	314	d.f. = 7	
	0·45–0·64	914	254	226		
	0·64–0·90	517	144	160		
	0·90–1·30	222	62	95		
	1·30–1·80	182	55	66		
	1·80–2·60	38	11	11		
	2·60–3·60	21	6	6		
	Totals	3904	1094	1117		

The optical counts in Column 3 are multiplied by e.m. area/optical area to give Column 4. This makes the area-corrected optical count directly comparable with the e.m. count (Columns 4 and 5). The goodness of fit between the corrected optical and the e.m. counts was tested using a $2 \times n$ contingency table and gave the result shown in Column 6.

counts will be due to increased resolution and to no other cause.

The results of recounts of the micrographs using their full resolution are given in Fig. 5 and Table 6. These include counts of particles of smaller sizes than those previously studied but no attempt will be made to assess their significance until more work has been done.

Counts of particles less than $0·08\,\mu$ are not included because a higher initial magnification than that used in these experiments would be required in order to make full use of the resolving power of the electron microscope.

Over most of the size ranges, the high-resolution counts show a change from the previous low-resolution counts. Above $1\,\mu$ the change is small and its significance difficult to assess, but below this size the high-resolution counts are in almost all cases greater than the low-resolution counts. The most striking change is seen in the sample of coal mine dust. In this case there is a steady upward trend from optical-microscope count, to low-resolution electron-microscope count, to high-resolution electron-microscope count.

These differences between samples may be due to the varying degrees of aggregation of the dusts but this is speculative. The important consideration is that the differences between the high- and low-resolution counts are appreciable.

CONCLUSIONS AND COMMENTS

It is clear that in order to justify the use of the electron microscope for dust evaluation full advantage must be taken of its resolving power. If this is done it will probably give a

different result from that of the optical instrument for most particle sizes even if the utmost care is taken to avoid instrumental errors. The main cause of disagreement is the inability of the optical microscope to define clearly the boundaries of particles. Even when the observer is experienced in the judgment of particle sizes as they are seen in the optical microscope it is inevitable that he will class a group of particles as a single particle if the separations within the group are less than the instrumental resolving power.

It would seem, therefore, that if in the interests of economy the particles of larger size are counted with an instrument of inferior resolution there may be a discontinuity where the counts are fitted together. If the counts overlap, there may be disagreement in the overlap range. This is unfortunate because for most purposes it is impracticable to count the full ranges of particles of respirable size with the electron microscope. Even if the cost were not important the time consumed in obtaining results would be excessive if more than a few samples were to be evaluated.

It is normally desirable to use a combination of optical- and electron-microscope counting and to make a compromise

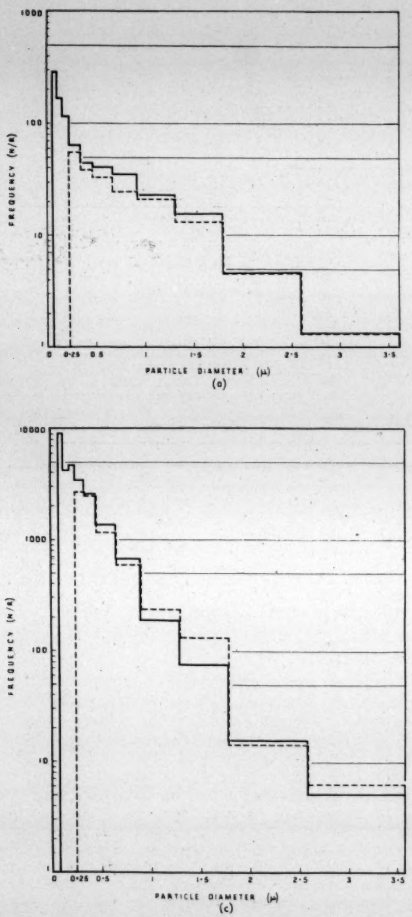

Fig. 5. Comparison of electron-microscope counts at high resolution and at 0·25 μ resolution

Total count in range 0·23 to 3·6 μ	(a) *Artificial coal dust cloud*	(b) *Coal mine dust*	(c) *Quarry dust*
at 0·01 μ resolution	497	508	1173
at 0·25 μ resolution	424	359	1117

High resolution ———
0·25 μ resolution – – – –

Table 6. *Comparison between counts using different resolving powers*

Sample	*Size range (μ)*	*Area-corrected optical count*	*Low resolution e.m. count*	*High resolution e.m. count*
Artificial coal dust in wind tunnel	0·08–0·11			84
	0·11–0·16			83
	0·16–0·23			78
	0·23–0·32	47	48	57
	0·32–0·45	68	50	57
	0·45–0·64	55	64	77
	0·64–0·90	56	65	94
	0·90–1·30	62	85	91
	1·30–1·80	66	64	75
	1·80–2·60	38	35	34
	2·60–3·60	27	13	12
Coal mine dust	0·08–0·11			48
	0·11–0·16			117
	0·16–0·23			80
	0·23–0·32	41	54	103
	0·32–0·45	49	52	74
	0·45–0·64	35	57	93
	0·64–0·90	41	50	86
	0·90–1·30	40	68	70
	1·30–1·80	67	31	40
	1·80–2·60	29	29	25
	2·60–3·60	28	18	17
Quarry dust	0·08–0·11			276
	0·11–0·16			210
	0·16–0·23			324
	0·23–0·32	240	239	312
	0·32–0·45	322	314	324
	0·45–0·64	254	226	226
	0·64–0·90	144	160	178
	0·90–1·30	62	95	77
	1·30–1·80	55	66	38
	1·80–2·60	11	11	13
	2·60–3·60	6	6	5

in fitting the results. The need for such a compromise arises from the shortcomings of the optical microscope and is in no way due to failure on the part of the electron microscope. This compromise in the overlap region prevents agreement in this range being directly used as a test of the validity of the results obtained with the two instruments. Such a test could be made, however, by adopting the method used by the author, namely to degrade the electron-microscope images to an effective resolution equal to that of the optical microscope. This check would be additional to the normal high-resolution count but need not consume a lot of time because it could be confined to a limited size range in the overlap region.

ACKNOWLEDGEMENTS

The author wishes to make acknowledgement to Mr. J. W. Skidmore who carried out the experimental work described in this paper, to Mr. B. A. Maguire for his co-operation with the statistical work and to the Ministry of Fuel and Power and the Director of the Safety in Mines Research Establishment for permission to publish this paper. All the figures are Crown copyright reserved. Figs. 1 and 3 are reproduced from Safety in Mines Research Establishment Research Report No. 79.

REFERENCES

(1) WALTON, W. H., and HARRIS, W. J. *Porton Technical Paper* No. 1 (1947).
(2) WAINWRIGHT, T., and WALTON, W. H. *National Coal Board, Central Research Establishment Report* No. 122 (1951).
(3) DRUMMOND, D. G. *J. Roy. Micr. Soc.*, **70**, p. 48 (1950).
(4) DAWES, J. G., MAGUIRE, B. A., and TYE, D. L. *Safety in Mines Research Establishment Research Report.* In course of publication.
(5) WALKENHORST, W. VON. *Beiträge zur Silikose-Forschung*, **18**, p. 29 (1952).
(6) IRWIN, J. O., ARMITAGE, P., and DAVIES, C. N. *Nature* [*London*], **163**, p. 809 (1949).

DISCUSSION

Dr. C. N. Davies: The visibility and apparent size of small particles seen under a microscope at high magnification depend on the setting of the condenser. Dust samples are usually mounted dry, without any medium around the particles, and examined with an oil immersion objective. It pays to use oil between the cover slip and objective, even though there is air surrounding the particles, because they scatter light over a wide angle (Mie region diffraction theory is inadequate) and the oil film ensures that the full working aperture of the objective is employed.

If the condenser is used at the same numerical aperture as the objective (bright field illumination with the source imaged in the object plane) all the peripheral cone of light which cannot enter the objective, owing to the interposition of an air film between the slide and cover slip, is multiple-reflected and causes loss of contrast.

It is therefore necessary to reduce the condenser aperture after centreing and focusing in order to get the best results.

Mr. P. S. Williams: In reply to Dr. Davies's suggestion that there should be a standard method of setting the microscope, I should like to draw attention to that advised by Martin and Johnson in their *Practical Microscopy* where a "routine method for correct setting-up of the microscope for general use" is given (p. 48). Using similar specimens to Dr. Davies and setting the microscope in the way mentioned, I have not met with the difficulty experienced by him when examining dust specimens mounted in air.

Mr. T. G. Callcott: The very large amount of careful experimental work that Mr. Cartwright has put into the preparation of Paper E.4 makes it important that the methods by which he draws his conclusions be quite valid. He has used in an analysis of the data of Table 5 significance tests, $2 \times n$ contingency test, in order to conclude that the numbers of particles counted by electron and optical microscopes are in the size range 0·23–3·60 μ identical. Unhappily the contingency test does not enable him to make his conclusions as this form of test is one of the independence tests, i.e. a test to establish whether or not two forms of classification are independent. It does not concern itself with a comparison of the total numbers in the columns of, for example, Table 5. This test, however, can be used to distinguish whether or not the two methods of counting at equal resolution yield the same size distribution, i.e. whether the classification of the sizes is independent of the type of microscope. For this purpose the

original data ought to be used, and calculation shows that χ^2's for each of the dusts of Table 5 are 18·3, 47·2 and 19·1 respectively. (Cartwright's χ^2's are lower because of a rounding off in the reduction of the numbers from the optical count to a "corrected" count.) These on seven degrees of freedom are undoubtedly significant. There is no simple adjustment which brings each of them into agreement with the notion that the classifications are independent. It seems most likely that we must conclude that the size analysis of the dust is not independent of the microscope used to classify the dust. That such a difference should exist between the size analyses is not surprising. There does not seem to be sufficient evidence to make any definite assertion as to the identity of the total counts.

A further analysis of Table 6 is possible by using the $2 \times n$ contingency test to establish whether or not there is a significant difference between the size distribution of the counts with the electron microscope at high and low resolution. The χ^2's, seven degrees of freedom, are 3·00, 13·59 and 19·11 for the three dusts of Table 6 and hence it seems that the evidence is not a uniform assertion in that the change of resolution has affected the distribution of the counts. It is quite evident that the groups of data contain a fairly obvious discrepancy between the counts in the range 0·23 to 0·32 μ. Omission of this range from the contingency tests results in χ^2's of 3·08, 9·61 and 7·03, six degrees of freedom for the dusts respectively. Obviously then it is reasonable to assert that the size distributions are very similar, possibly even identical, irrespective of whether the microscope is at high or low resolution. It seems, thus, that the difference between counts at high and low resolution may only be in the actual total numbers. Examination of the numbers greater than 0·32 μ suggests that there is not a significantly greater number counted by the microscope at high resolution. In fact the suggestion seems to be that the resolution of the microscope is unimportant in either the number counted or the size analysis of dusts with particles greater than about 0·3 μ.

Clearly Mr. Cartwright's conclusions are in doubt and his data tends to substantiate alternative views, namely, the electron and optical microscope at same resolution do not give the same size distributions and that there is little or no difference in the size distribution of an electron microscope at high or at low resolution, provided the particle size is greater than 0·3 μ. This implies that the problem of utilizing the electron microscope in overlap counts is still with us.

Mr. J. Anrep: I should like to support Mr. Callcott's view that Mr. Cartwright's use of the χ^2 test is incorrect. Two samples from a population may fit the population but may not show "good fit" between themselves when tested against each other.

Dr. R. G. H. Boddy: I would like to comment on three points: (i) the question of the respirable size of dust, (ii) the method of collecting a sample of dust, (iii) the method of counting.

(i) It is not sufficient to adopt as the parameter of respirable size, the settling velocity. The lung is a system of tubes of decreasing diameter the narrowest part being of the order of 150–250 μ. It is clear, therefore, that the size of the particle is of importance. A large, light lamina would tend to be deposited more readily than a small, heavy spheroid even though both were settling at the same velocity.

(ii) It seems to me an unnecessary complication to collect a sample of all the airborne dust. In the first case the lung is not primarily a dust collecting instrument. Most of the dust inhaled is rejected by the lungs' defences and an instrument like the thermal precipitator which collects all the dust in the air over-emphasizes the danger. I prefer an instrument on the lines of my own size analyser and concentration recorder. The general arrangement is as shown in Fig. 1.

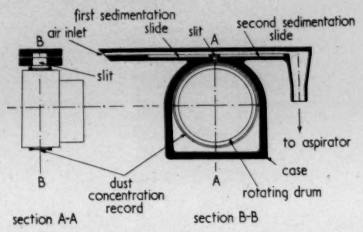

Fig. 1. Boddy's size analyser and concentration recorder

In this instrument the dusty air is drawn along a horizontal duct and the particles settle out in streamline conditions. At a convenient point in the duct there is a slit at right angles to the airstream and particles fall upon a plastic sheet fitted to a slowly moving drum. In the horizontal duct the smaller particles are spread more thinly than the larger sizes since they remain in the air longer. There are usually considerably greater numbers of small particles than large ones and thus by only collecting aliquot parts of the finer particles counting is made much simpler. If, for any reason, it is necessary to know the absolute numbers of each size of particles then factors to obtain them can readily be calculated from the characteristics of the apparatus and the airflow.

(iii) It is usual to dry mount collected airborne dusts, so as not to disturb the aggregates, and then to assess the respirable portion by counting with the microscope. Unfortunately, the counting is often done using a 2 mm oil-immersion objective and this is not good practice. The presence of an airfilm reduces the numerical aperture of the system to 1·0 and there is no valid reason for not using a 4 mm objective and high eye-piecing, or enlargement.

It must be remembered that the depth of focus of a high power objective is very small and in the case of the 2 mm objective is only $\frac{1}{2}$ μ. Attempts to focus through the whole thickness of an aggregate which may be 10–20 μ deep bring in problems of technique which ought not to be allowed to arise in routine counting. We have seen from the papers presented at this Conference that diffraction and light scatter are very important when measuring the size of small particles. Many of the difficulties of making an assessment of the amount of respirable dust in a cloud can be removed if only the dust of respirable size is collected and the particles counted after crushing; both aggregates and single particles are then brought into a thin plane, well within the depth of focus of even a 2 mm oil-immersion objective, as will be seen from Figs. 2 and 3. Since the crushing causes the particles to spread, it has the effect of an increase in magnification and there is no need to use more than a 4 mm objective. The thickness of the particles can readily be deduced from the Newton's rings set up, both in the particles and the airfilm of the mount; an example is shown in Fig. 4. An estimate of the volume of the dust can be made quite easily and simply, and from my own experience of colliery dust clouds this could be applied generally. Small particles of the harder dusts such as silica tend to break up into smaller fragments when crushed and simulate spreading.

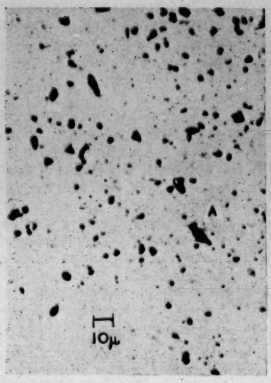

Fig. 2. Photomicrograph by transmitted light. Colliery dust collected by an upward elutriating thermal precipitator. A few white mineral particles *A* are present amongst the coal

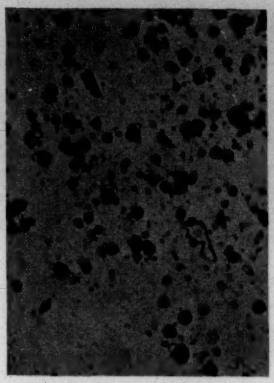

Fig. 3. Same field as Fig. 2 by transmitted light at the same magnification and after crushing, showing that the mineral particles as well as the coal have spread

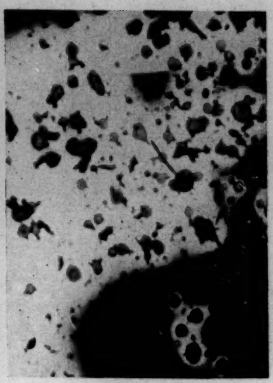

Fig. 4. Same field as Fig. 2, using vertically incident light. The reflexion from the mineral particle *A* is different from that of the coal

Mr. W. H. Walton: Some years ago I carried out experiments similar to those described by Mr. Cartwright, in which I attempted to correlate light microscope and electron microscope measurements of the same dust cloud. I fully appreciate the difficulties experienced by Mr. Cartwright and congratulate him on the excellent agreement which he has obtained. I would be interested to know whether, in the course of his work, Mr. Cartwright has obtained an indication of the smallest particle size that can be detected under the optical system conventionally used for the assessment of thermal precipitator samples, i.e. 2 mm oil-immersion apochromatic objective and light ground illumination. In the earlier work to which I have referred I estimated this to be about 0·14 μ diameter for spherical particles.

Various speakers have suggested factors which may possibly contribute to the discrepancies between the counts of different observers. Some of these have already been investigated at the National Coal Board's Central Research Establishment. Dr. Davies has pointed out that errors will inevitably arise when counting particles near the limit of resolution, and that these will depend on details of the microscope system. He suggests that projection systems may be inferior to direct visual microscopy in this range. Dr. Boddy suggests that a 2 mm apochromatic objective cannot give its best performance with thermal precipitator specimens which are dry mounted and that a 4 mm objective would give equally good results. The problem of resolution is a real one and particularly important since most dust clouds extend to sizes well below the limit of optical visibility so that counts of the concentration are indeterminate unless the lower limit is specified. It is for this reason that the N.C.B. normally counts coal particles in the size range 1–5 μ. The lower limit is set at 1 μ because at this size it is still possible to measure particles with a reasonable accuracy which is not critically dependent on the microscope system or on the visual acuity of the observer. Tests of various microscope systems by my colleagues, Mr. R. J. Hamilton and Mr. J. Gammon, showed that for counts down to 1 μ there was no difference between the results obtained with 2 mm apochromatic or achromatic objectives and that both direct vision and projection type microscopes gave substantially the same results. There was a tendency for the difference between observers to be greater with the direct microscope than with the projection system. When particles smaller than 1 μ are counted the microscope system becomes more critical (the N.C.B. counts down to $\frac{1}{2}$ μ for rock dust clouds, which tend to be much finer than coal dusts). D. G. Beadle (in a private communication) has reported that when counting down to the limit of visibility many more particles can be seen (even though dry mounted) with a 2 mm objective than with a 4 mm one, which in turn is better than an 8 mm objective. Beadle found a high-grade apochromatic objective to be essential for the best results. Dr. Timbrell asked whether, when counting in a restricted range, such as 1–5 μ, there is a tendency to include more or less particles in the range than would be done if a complete measure of size distribution extending beyond the limits of this range were made. This has been investigated by Mr. R. J. Hamilton under the normal conditions for counting thermal precipitator slides and no difference was found.

Reference has been made in the discussion to the possible use of geometrical shapes to investigate errors of particle sizing with the aid of a graticule containing reference circles. Mr. J. W. Phillips has conducted such experiments with printed test papers which were circulated to 55 different microscopists within the organization of the N.C.B. He found a very marked bias to over-estimate sizes for all but simple circular shapes amounting on average to about 10% in diameter. Different observers showed different mean biases, the standard deviation of these mean biases being about 16% in diameter. A few observers showed mean biases (for all shapes and sizes) of 40% or more.

Author's reply: In reply to Mr. Callcott, I am able to say

that my own statistical analysis gave probability values that were just within acceptable limits. Mr. Callcott's correction of my method indicates that the values I gave are too high and that the true values would be such as to indicate that there is a significant difference between the optical- and electron-microscope distributions at the same resolution.

As the totals of these counts are in all cases quite close, any differences are likely to be due to size classification errors. There is, in fact, a strong suggestion of a systematic error in the sizing of particles of the order of one micron, and as I stated in the paper such an error could be investigated with different observers should the need arise.

Regarding the comparison between high-resolution and low-resolution counts it can be seen on examination of the histograms that at least in the case of counts (*a*) and (*b*) the high-resolution counts are consistently higher for all particles below 2 μ. The χ^2 test is based on the squares of differences between counts and cannot take into account whether the signs of the differences occur randomly or whether they are all in one direction. Consequently I considered the χ^2 test an inadequate criterion and did not use it.

On the question of the limit of visibility of a microscope with a 2 mm oil immersion objective and a dry mounted specimen, raised by Mr. Walton, I have made estimates of this from the counts of one observer over a period of several months. The estimates were made with three different types of dust and were 0·17, 0·18 and 0·175 μ. During the tests the same microscope was used and room lighting was fairly constant. I have no information as to how much this estimate would have altered with different observers and microscopes.

GENERAL DISCUSSION ON SESSION E

Mr. B. J. Mason: It might, perhaps, be of some interest to mention two very simple techniques which have been used by meteorologists to collect atmospheric aerosol, in particular, salt particles produced by sea-spray. In order to ensure a high collection efficiency one may use either a large collector and draw the air past it at high speed or a very narrow collector in a slow airstream. The latter alternative can be pushed to the limit by using a mesh of very fine spiders' threads of diameter about 0·01 μ. The spider is encouraged to spin a network of threads on a rectangular wire frame which may be exposed to the particle-laden air on a wind-vane or rotated at a known constant speed on a gramophone turntable. In this way, very small droplets and solid particles of radius down to 0·1 μ can be captured; these adhere quite strongly to the threads and can be examined under the microscope. If the velocity of the frame relative to the air and the time of exposure are known, the size distribution of the particles and their concentration can be determined. The method, though laborious, is simple and direct; the most important precaution is to limit the density of the sample so that overlap and coagulation of the particles does not occur.

We have used this technique on board a weather ship in the North Atlantic to collect salt particles in the mass range 2×10^{-14} g to 10^{-8} g.

An alternative and in some respects more convenient method is to expose narrow glass ribbons coated with a hydrophobic silicone. The ribbons are then placed in a small constant-humidity chamber attached to the stage of a microscope. Condensation occurs on the salt particles to form hemispherical droplets with a contact angle of 90°. The humidity is fixed by placing a 10% solution of sodium chloride in the chamber and the mass m of a captured salt particle is determined by measuring the droplet radius r, since $m = 0{\cdot}1 \frac{4}{3}\pi r^3$.

Dr. A. van Kreveld: Even if the drops of salt water have a contact angle of 90° with the slide on which they are collected they may not be semi-spheres. Free floating drops are, of course, spheres, since this shape has minimum surface energy for a given volume. But the minimum energy criterion when a drop of liquid sticks to a plane surface is quite different and I doubt whether it really yields a half-sphere.

Mr. D. S. Beard: Even where the shape and size of particles are substantially uniform, quite large subjective errors can arise with straightforward visual counting. Such errors have been discussed by Biggs and MacMillan* in their investigations on sources of error in routine blood-counts.

Dr. H. Heywood: The answer to the question "Why was the mean projected diameter of particles measured when this had little direct application to the properties of the particles it was desired to know?" is that it is quite correct that the mean projected diameter of the particles represents neither the true surface, nor the volume of the particle, nor the free-falling velocity. It is, however, the only particle dimension that can be measured for all sizes of particle, from lumps that can be handled to the smallest particle rendered visible by the electron microscope. The complexities of surface measurements have been discussed in earlier papers at the Conference, volume measurements of small particles presented experimental difficulties, and the direct measurement of free-falling velocities required complex equipment, although such measurements were quite possible. Thus it is important to determine the numerical coefficients that would enable the above characteristics of particles to be calculated from measurements of the mean projected diameters.

Mr. A. K. Soper: When viewing an enlarged image of a geometrical edge, one sees a diffuse region, within which the true edge is presumed to lie. It is usual to take a point midway through the diffuse region as defining this true edge. Recent work suggests, however, that the true edge may not be so symmetrically placed, and it would be interesting to know if any general rules exist for its better location.

* Biggs and MacMillan. *J. Chim. Path.*, **1**, p. 288 (1948).

SESSION F. AUTOMATIZED COUNTING AND SIZING: THEORY

Chairman: F. I. G. RAWLINS, M.Sc., F.R.S.E., F.Inst.P.

Survey of the automatic counting and sizing of particles

By W. H. WALTON, B.Sc., F.Inst.P., Scientific Department, National Coal Board

A simple account is given of the basic principles employed in automatic counting and sizing devices and of some of the difficulties encountered.

1. INTRODUCTION

It frequently happens in scientific affairs that the time becomes ripe for a particular advance, and development proceeds rapidly and independently at numerous centres. This has happened in the automatic counting and sizing of particles, and is the result of increasing demand for improved means of investigating particulate systems, coupled with new techniques in other spheres which form suitable jumping-off points. The rapidity of growth of the subject in the post-war years is exemplified by the experience of a colleague of mine who, after setting out to write a paper on it, complained after a few months that he was losing ground, the subject was growing more rapidly than he could report it. This session of the conference is the first occasion on which automatized counting and sizing has been given a full discussion by a learned society and is likely to be remembered as a noteworthy event in the history of the subject.

Automatized counting and sizing embraces a wide variety of problems: mathematical and statistical, electronic and electrical, optical, and mechanical. Many particular aspects are described in detail in the papers presented to the Conference. These are specialist papers, necessarily rather condensed by restrictions of space, and consequently, as Professor Sir Geoffrey Taylor remarked in his opening address, may perhaps be found somewhat difficult by the newcomer. In this opening survey, therefore, an attempt will be made to explain some of the principles and problems of the subject quite simply, and to show how the later papers fit into the picture as a whole.

2. THE PROBLEM

In almost all particle problems we are concerned not with individual particles but only with statistical measures of a large "population": we require to know the total quantity of material and the relative proportions that possess some particular property such as a characteristic size, shape, or composition. Frequently the only way to compile this statistical information is from many individual observations, as in a Gallup poll. It is this which makes the problem so tedious when done by human agency, for example, by visual examination of particles under a microscope, and creates the demand for automatic methods. For our present purpose the normal starting-point is a sample of particles randomly distributed over a plane surface such as a microscope slide, and we wish to determine the number per unit area and their size distribution. We shall not consider the problem of ensuring that the sample on the slide is a representative one. It is the randomness of the sample that is the main source of difficulty in making measurements by machine. The eye and brain can take in a random distribution as a whole, can pick a way from one particle to another, evaluate each separately and remember which have been examined. Machine methods essentially amount to passing the particles through a light beam falling on a photocell and measuring the changes in intensity resulting from the presence of the particles. The photocell cannot detect any detail within its field of view, but only changes in total illumination. It cannot discriminate whether the changes arise from more than one particle or whether only part of a particle is protruding into the beam. Much of this paper is concerned with means of overcoming these limitations.

3. ORDERED SYSTEMS OF PARTICLES

The problem of automatic measurement is clearly simplified if the particles can be marshalled into a row and passed one by one through the light beam. This is sometimes possible for fluid-borne particles and the paper by Professor Gucker and Dr. Rose (G.1) describes such a method. A cloud of airborne particles is passed in a thin stream through a dark ground illumination system under conditions such that there is only a very small chance of more than one particle falling within the light beam at the same time. The number and size of the particles passing through the beam are determined from the number of pulses of scattered light and their intensity. An ingenious feature of the apparatus is the use of a sheath of clean air surrounding the dust stream which confines the particles to a well-defined zone and prevents deposition on the windows. Particles as small as $0{\cdot}34\ \mu$ in diameter can be detected. A rather similar system has been used by Dr. Crossland Taylor at the Middlesex Hospital, London, for the counting of red cells in blood. In this case the suspending medium is liquid and again the stream of suspension emerging from a small orifice is surrounded by a sheath of clean fluid. The composite stream is drawn out by passage through a tube of converging section until the central filament containing the blood cells is only about $10\ \mu$ diameter.

4. SCANNING BY A SPOT

Turning now to the more general problem of measuring particles of various sizes and shapes randomly distributed on a plane surface, let us first consider what happens when such a sample is traversed or scanned by a beam of light. The cross-section of the scanning beam can have any value, but since the photocell cannot see detail within the beam, increase of the size inevitably results in a loss of resolving power. In the extreme case of a very large beam we could measure the overall transmissivity of the whole slide, which would give a measure of the total cross-sectional area of all the particles but would give no information at all about the number or the size of the individual particles. At the other extreme we may scan with a very small spot which effectively draws a line

across the specimen as illustrated in Fig. 1(*a*). Signals arising from an interception of the beam by a particle are of the on/off type; a quantitative measure of the light intensity is not required. Measurements of the duration of the signals give the lengths of the intercepts of the scan line across the particles. We can measure only the number of signals and

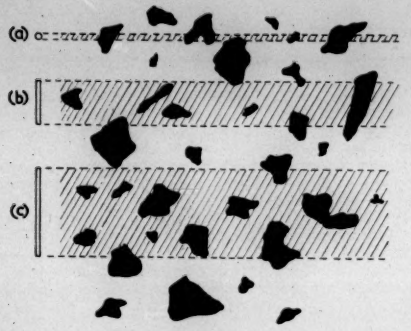

Fig. 1. Spot and slit scans
(*a*) Spot scan. (*b*) Short slit. (*c*) Long slit.

their lengths in a given distance of scan. The number of signals does not give a direct measure of the number of particles in a given area of the slide, because the chance of intercepting a large particle is greater than that of intercepting a small one, and is, in fact, proportional to the particle perimeter. Neither does the length of the intercepts give the particle size directly, because particles of given size give intercepts of various lengths according to whether they are cut near an edge or across a diameter. However, if many scans are made across the specimen, each particle of given size and shape will give rise to a characteristic group of line intercept signals, and consequently, if the particle shape is known, the signals can be analysed into groups corresponding to individual particles. Such a method of analysis is described in the paper by Mr. Courshee (G.5), who uses it to measure the stains formed by spray droplets falling on paper. The difficulty of applying the line intercept method to particles of other than circular shape is discussed by Mr. Phillips in Paper F.2. Since all lines of scan across a random sample are statistically equivalent, it is immaterial whether the lines are regularly or randomly positioned in relation to one another.

5. SCANNING BY A SLIT

Figs. 1(*b*) and (*c*) illustrate the scanning of a specimen by a slit aperture moving perpendicularly to its length. A wider aperture than a slit could be used, but would result in a further loss of resolution. In contrast to the spot scan considered above, the slit scan sweeps out a path of defined area. We can count the number of times the slit is completely or partially obscured by a particle passing before it, and we can measure the amplitude or duration of the signals. As illustrated in Fig. 1(*b*), some particles will fall wholly within the scan, in other cases they will partially overlap the edge of the track, and sometimes more than one particle will be intercepted simultaneously. If the length of the slit is increased as in Fig. 1(*c*) so that a wider track is scanned, more particles will lie within the track and the proportion of edge fractions will be reduced, but the number of coincident interceptions will increase. The apparatus described by M. Le Bouffant and M. Soulé (G.2) is of the slit scan type. They show that, depending on the density of the sample, the length of the slit can be chosen so that the errors from edge fractions and coincidences cancel and a reliable measure of the number and size of the particles lying within the area traversed by the slit can be obtained.

An alternative method of correction for particles partially intercepted at the edge of the scan track is used in the apparatus for counting blood cells described by Mr. Cooke-Yarborough and Mr. Whyard in Paper G.3. The principle is as follows. If the length of the slit is w_1 then a signal will be obtained from all particles whose centres lie in a track of width $w_1 + d$ where d is the particle diameter. This width is different for particles of different size. If the process is now repeated with a slit of length w_2, the number of particles lying in a track of width $w_2 + d$ will be determined. The difference of these two counts gives the number lying in a band of width $w_1 - w_2$ independently of the particle size d. Mr. Cooke-Yarborough and Mr. Whyard make a statistical correction to the results for coincident interceptions. This is simplified in the particular case of counting blood cells because the particles are all approximately the same size. Note that the length of the smaller slit, w_2, can be made vanishingly small so that in the limit the second scan becomes a spot scan.

Measurements such as the above, which involve the difference between two values each of which is subject to statistical error, have the disadvantage that the errors of each individual measurement must be added to give the error of the difference figure. Thus if we make a straight count of 100 particles distributed at random, we have an inevitable probable error of $\pm\sqrt{100}$ or 10%. If, however, our value of 100 is formed of the difference between separate counts of 200 and 100 respectively, the probable error of the result will be $\pm\sqrt{300}$ or 17%. To reduce this to 10% would require differencing two counts of 600 and 300 respectively, giving values of $300 \pm \sqrt{900}$. The difference method has required the counting of 900 particles instead of 100 to obtain a result of the same percentage accuracy. This statistical problem of difference methods is considered in greater detail in the Papers F.2 and G.3.

6. USE OF A GUARD SPOT

A clue to a means of avoiding the statistical difficulties of differencing counts to compensate for edge errors is afforded by the ordinary practice of counting particles under the microscope with the aid of an eyepiece graticule, see Fig. 2(*a*). Correction for particles overlapping the edge of the graticule is obtained by counting all particles which overlap the top and right-hand edges of the graticule and omitting from the count all that cut the bottom and left-hand edges. A similar procedure is followed if the specimen is continually traversed across the centre line of the graticule which then sweeps out a track of width equal to the length of the line. All particles which project into the track of the scan from the top are counted, whereas all which protrude over the bottom edge of the track are omitted. In an automatic counting device the vertical line is replaced by an illuminated slit and a second spot of light at the lower end of the slit is used to detect overlap of the lower end [Fig. 2(*b*)]. Two photocell and electronic amplifier channels are needed. We count all signals (of any magnitude) arising from interceptions of the slit except when there is a simultaneous signal from the "guard spot" at the lower end. In this manner a count is obtained of the number of particles whose lower ends lie

within the track swept out by the slit. With this system there still remains the problem of coincident interceptions of the slit and the necessity to measure interceptions of only a small fraction of its area. The method is valid for a slit of any length and in the limit may be reduced to the system shown in Fig. 2(*c*). Here the slit has been replaced by a spot corresponding to the upper end of the slit and the separation of this spot from the guard spot has been made smaller than the diameter of the smallest particles to be counted so that it is

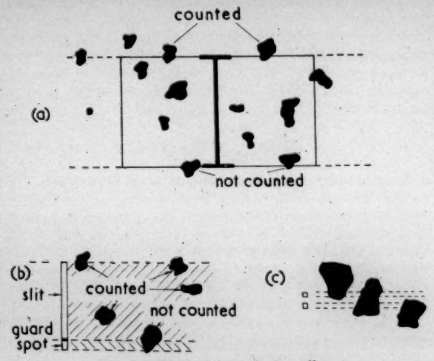

Fig. 2. Elimination of edge effects

(*a*) Only particles whose lower edges lie within the defined area are counted. (*b*) Guard spot detects overlap of lower edge of scan track. (*c*) Two spots of known separation less than the smallest particle diameter, locate and count lower edges of particles and minimize coincidences.

impossible for a particle to pass between the two spots without detection. The system counts all particles whose lower edges lie within the track traced out by the two spots. It will be noted that since the separation of the spots must be accurately known their separation should not be reduced to a value comparable with the spot size or with the limit of resolution of the optical system. This method of counting particles by scanning with two spots, one being a guard spot, was introduced by Dr. H. A. Dell and is described in his Paper G.4.

Instead of using two spots which simultaneously scan two adjacent lines we may scan two lines consecutively by a single spot and make a record of the signals obtained on the first line which is then played back synchronously with the scanning of the second line, and so achieve the same effect. If this process is continued over a large number of adjacent scan lines then the total track width in which particles are counted becomes the sum of the separations between each scan line and the one immediately preceding, that is, the total width of all the scans. This procedure avoids the difficulties of the simple guard spot method when the spot separation must be made very small in order to avoid missing small particles, for any errors in line separation now cancel instead of being accumulative. These advantages are discussed in greater detail in Papers F.2 and G4. The use of recorded signals or memory systems will be considered further in Section 8 of this paper.

7. THE MEASUREMENT OF SIZE

So far we have discussed methods of counting, not of sizing, but sizing may be effected by relatively simple extensions of these.

In a simple slit scan the length of slit intercepted by the particles can be determined from the amplitude of the signals given by the photocell. This gives a measure of size for all particles that lie completely within the track of the scan (if coincidences are neglected), but a correction must be made for edge errors as discussed in Section 5. The correction can be made in the same way as before, by taking the difference between measurements obtained with two slits of different length. If we scan with a slit of length w as shown in Fig. 3, a length greater than some given value $z(<w)$ will be obscured by all particles of diameter greater than z which lie within a track of width $w + d - 2z$, where d is the particle diameter. Hence, if all signals corresponding to interceptions greater than z are recorded for scans with slits of length w_1 and w_2 respectively, the difference between the counts gives the number of particles larger than z lying in a track of width $w_1 - w_2$. An oversize distribution curve is obtained by repeating the procedure at various values of z. The particular case when $z = 0$, i.e. all signals are recorded however small,

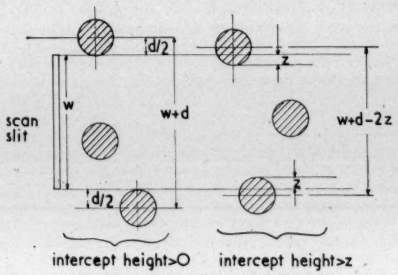

Fig. 3. Sizing by intercept height

Intercepts greater than z are given by particles of size $d(>z)$ having centres lying in track of width $w + d - 2z$. The difference between the numbers of intercepts for two track widths w_1 and w_2 gives number of particles of size greater than z lying in track of width $w_1 - w_2$.

corresponds to simple counting without size measurement as discussed in Section 5. A complete size distribution curve could be obtained from a single pair of scans by simultaneously recording signals at various levels z on a "kick sorter" instead of only above a single value of z. The above method of size measurement is that preferred by Mr. P. G. W. Hawksley in his Paper F.1 on the theory of particle sizing and counting by track scanning, and was used in the experiments described by Messrs. Hawksley, Blackett, Meyer and Fitzsimmons in Paper G.6.

The guard spot techniques for counting can also be applied to the measurement of size. We have seen that by scanning with two spots of known (small) separation, particles having their lower extremities lying within the double track can be located and counted. If one spot (say the upper) is replaced by a slit of length w and the other (guard) spot is situated at a distance Δw below the lower end of this slit, we shall obtain complete interceptions of the slit without a simultaneous signal from the guard spot from all particles of height greater than w having their lower ends lying within the track of width Δw. By repeating the process at various values of w we can obtain a complete oversize distribution curve. Alternatively, instead of using a guard spot we can difference the counts of complete obscurations of the slit in two scans of

widths w and $w + \Delta w$ respectively. This latter method of obtaining size distributions was suggested by Mr. Hawksley and is discussed by Mr. Phillips in Paper F.2. It raises awkward statistical problems as discussed previously in relation to other methods involving the difference between two counts. All methods of sizing by slit scans are subject to coincidence errors, which impose a serious limitation on the permissible density of sample.

Another procedure for size measurement after the edge of a particle has been uniquely located by the two-spot technique, is to cause one spot to explore the particle by a subsidiary transverse scan. For example, the spot might cross to the opposite boundary of the particle and thus measure its width, or a more complicated exploration could be made. If necessary the main scan can be arrested while this subsidiary exploration takes place. This is the principle of the arrested scan technique described by Dr. Dell in Paper G.4.

A further ingenious method of measuring size which also employs the guard spot technique to ensure that the measurement is only carried out once on each particle has been used by Dr. Taylor and is described in Paper G.7. Instead of recognizing all intercepts of a particle, as in the ordinary guard spot particle counter, only those greater than a given length are accepted and so a count is obtained of particles of diameter greater than this value.

8. MEMORY METHODS

So far we have considered only the scanning of specimens by spot or slit systems which trace paths in randomly chosen positions and this has limited the amount of information derivable from the signals. If, however, a small scanning spot draws a sequence of closely arranged parallel lines across the specimen, it will explore all points of it, and the signals from the photocell will contain all possible information about the specimen, for the signals can be reassembled as in a television set to recreate the complete picture. In reassembling the picture, it is necessary to bring together or associate signals arising at corresponding positions in successive lines. Thus we can recognize the identity of different interceptions of the same particle in successive lines of scan by the fact that they occur at corresponding positions in the line or at the same time interval after the beginning of each scan. The principle of identifying and associating signals from the same particle by their occurrence at corresponding times in successive lines of scan was first introduced by Dr. D. W. Gillings, who proposed to use a series of electronic counters and time switches which would bring each counting channel into the circuit at the appropriate time to receive the next signal from the same particle. A more practical form of memory device is, in effect, to record the signals from a scan line on a moving belt and to play back the record synchronously with the scanning of the next line. The recorded signal and the new signal from the same particle will then be received at the same time and are thus identified as belonging to the same particle. In practice, owing to the effects of particle shape, these successive signals may not occur at exactly identical times in the scan. Either a small tolerance must be allowed, or the association can be recognized by the fact that the two signals must overlap. These criteria of association are discussed in Papers F.2 and G.4. Memory systems which have been proposed include magnetic drums rotating in synchronism with the scan frequency, and magnetostriction delay lines.

If the memory system is used to associate signals from two adjacent scan lines we have in effect a double spot scan or a guard spot system as described in Section 6.

The system of recording scan lines and playing them back in synchronism with the scanning of a new line need not be restricted to one line in arrears. The record can extend over any number of lines and, by the use of a series of pick up heads, we can obtain simultaneously the signals from corresponding positions in these lines. The effect is that of scanning the specimen with a row of points, or a comb; the advantages of such a system are discussed by Mr. Phillips in Paper F.2. A great deal of information can be obtained about a particle from the associated signals obtained in this way. For example, the number of signals from the same particle, that is, the number of successive lines by which it is intercepted, gives its overall height; the signal of greatest length gives a measure of the particle's width in the direction of scan; the integrated length of all the signals gives the surface area of the particle.

9. SOME PRACTICAL CONSIDERATIONS

Density of specimen. An advantage of scanning with a spot as distinct from a slit is that the risk of coincident interceptions of more than one particle is eliminated. In principle, therefore, spot scan methods are capable of dealing with much more crowded specimens than are slit scan methods. This point is emphasized by Dr. Dell. It even appears that spot scan methods would be capable of analysing a specimen comprising contiguous areas of different optical densities, as for example metallurgical or petrological specimens. In theory, when preparing a particulate specimen, it is often possible to make it so sparse that there is very little risk of coincident interceptions in scanning. In practice there is a limit to this, for it is never possible to obtain a completely clean "blank" and, moreover, the area to be covered in order to obtain a statistically significant result may become unduly large. It is, however, always desirable to avoid overcrowding a specimen by unwanted particles. For example, samples of airborne dust obtained for the purpose of assessing the danger to health may contain perhaps 90% by area of particles that are too large to be dangerous. In such cases it is of great help if the oversize particles are excluded from the specimen by a selective sampling technique.

Method of scanning. So far nothing has been said about the means of scanning other than that the specimen is to be traversed by a beam of light. It matters not in principle whether the beam of light is moved relatively to a stationary specimen or whether the beam is stationary and the specimen is moved, but there are practical advantages and disadvantages attached to each method. If the specimen is moved relatively to the optical system, clearly there are limitations to the speed and frequency with which the scans can be made, and also to the accuracy with which the movement can be carried out in one plane so that a sharp focus is maintained. There is the advantage that, since the light beam is not moved in any way, the maintenance of a constant intensity is favoured. Mechanical scanning by movement of the specimen is therefore best suited to slit scan systems which require a lower frequency of scanning than do spot methods, but which may require a quantitative measure of the transmitted light intensity.

When a scan at high frequency is required, as in spot scanning, it is more convenient to move the light beam than the specimen. A suitable technique in such a case is to produce the scan by the moving spot of light on the face of a cathode-ray tube and to project this at reduced size through a microscope on to the specimen. An example of such a system is to be seen in the flying spot microscope of Roberts and

Young.* This method has the disadvantage that, as the spot crosses the field of view, the amount of light transmitted may show some variation due to the cosine effect when the beam is in an oblique position and to imperfections in the optical system. It is, therefore, not well suited to accurately quantitative measurements of the light intensity, but is quite adequate where only on/off signals are required. This, however, is usually the only requirement in spot scan systems.

Brightness. A serious practical difficulty in the design of automatic counting devices for very small particles is the small amount of light that is available for measurement at the photocell. If we require to resolve fine detail in the specimen, as small as, say, 1 μ, then clearly we have to measure the light which traverses a specimen area of only about 1 μ^2 or 10^{-8} cm^2. This is true whether we scan with a single spot of this area or whether we scan with a slit of relatively great length but look for small fractional changes in the light intensity. Now it is a law of nature that by no optical system can we concentrate more light per unit area in the image plane than is emitted per unit area from the source (assuming the source to be a diffuse radiator). Thus, if the source of illumination is a spot 1 mm in diameter on the face of a cathode-ray tube and this is reduced in size by a lens system to a spot 1 μ in diameter at the specimen, then not more than one-millionth of the light from the source can be concentrated into the specimen. The only way to increase the flux of light through a small area at the specimen is to increase the intrinsic brightness of the source. This limitation to the quantity of light that can be focused through a very small area means that very little light reaches the photocell, and in practice we have to use photomultiplier cells to obtain the requisite sensitivity. In most of the apparatus now under development the performance is limited by the signal to noise ratio in the photocell circuit, which in turn is determined by the available illumination.

Resolution and depth of focus; use of intermediate photography. In many applications of microscopic particle size analysis it is customary to extend the measurements down to the smallest sizes that can be measured with the available apparatus. Usually this is a conventional limit representing the range of practicable measurement and does not correspond to the smallest particles present in the specimen. When stating the requirements of an automatic counting machine, it is therefore natural to ask for a resolution down to the limit obtainable with the ordinary direct vision microscope. It is probably inevitable that automatic machines (using visible light) will always be inferior in resolving power to direct vision microscopy. One reason for this is the difficulty of maintaining accurate focus in a machine. For high resolution we need an objective of large numerical aperture which has of necessity a very small depth of focus, perhaps only a fraction of a micron. The visual microscopist constantly adjusts the focus of his microscope to allow for unevenness of the slide or to correct for curvature of the field in the microscope, and also to give the particles a "live" appearance which distinguishes them from fixed imperfections and specks of dirt in the optical system. In a machine such critical adjustment of the focus is not possible and it may be necessary to sacrifice resolving power in order to obtain a greater depth of focus. It seems to the writer unlikely that we shall see an automatic scanning machine within the next few years which will accurately measure the size of particles down to, say, 1 μ. One of the main requirements for an automatic machine is, however, to do just this task, and a possible way out of the difficulty is by the use of intermediate photography, as is done by M. Le Bouffant and M. Soulé. The use of enlarged photographic images would separate the optical problems of resolution, contrast and brightness from the electrical and mechanical problems of designing the machine and would, it is felt, considerably speed the practical development of the latter. Photography does not, of course, eliminate the problem of resolution; theoretically it is just as difficult to obtain a high resolution in photomicrography as in an automatic scanning machine. The benefit lies rather in the separation of the two problems so that each can be tackled separately. A further advantage of intermediate photography is that it gives a large measure of control of the contrast of the specimens presented to the machine. It is not suggested that intermediate photography should be a permanent feature of automatic counting machines, but merely that it would save time in bridging the gap between what is now practicable and what the user requires.

* Roberts and Young. *Proc. Instn Elect. Engrs*, **99**, Pt. IIIA, p. 747 (1952).

Paper F.1

Theory of particle sizing and counting by track scanning

By P. G. W. Hawksley, British Coal Utilisation Research Association, Leatherhead, Surrey

A theoretical relation is developed between the number and size distribution of particles dispersed in a plane field of view and the number of particles intercepted by a scanning track drawn across the field; it is shown that the number of oversize particles per unit area can be obtained from observations of the numbers intercepted by tracks of different widths. It is shown also that the usual methods of counting are special cases.

There are many cases where it is required to find the number and size distribution of particles dispersed in a plane field of view; for example of dust particles, spray droplets, blood cells, etc., as seen through the microscope; of star images, developed grains, or electron microscope images on photographic plates. A large number of tedious measurements are needed for a reasonably representative sample of the field and in recent years methods have been sought of applying photoelectric detecting systems combined with high speed, pulse counting devices. Although methods of varying degrees of complexity have been proposed they all broadly involve scanning the field with a light beam such that the presence of particles on the scanning line or track modulates the output of a photocell. The number, length or height of pulses may be recorded by means of suitable discriminating and counting circuits.

The theoretical problem is to translate observations derivable from the scanning into the number and size distribution of particles in the field. In line scanning, observations can be made of the number and length of intercepts on particles given by a line drawn across the field. There is an extensive literature on the relation between the frequency distribution of intercept or chord lengths and the size distribution of the particles. A complete solution is available only for circular particles; it was first obtained by Wicksell,[1] who considered the relation between the frequency distribution of a system of spheres (in three dimensions) and that of the diameters of the section circles obtained by a random sectioning plane. With changes in terminology the analysis is applicable to the present case. In an earlier paper by Hagerman,[2] F. K. G. Odquist solved the same problem for the case where the chance of the section plane intercepting a particle is assumed to be independent of its size. This assumption is possibly justified in the type of petrological problem considered by Odquist (see Krumbein and Pettijohn[3]). Willis[4] has recently derived the relation between the size distribution of spheres and the distribution of intercept lengths for a line scan across the section circles cut by a random sectioning plane. His result can be obtained also from a double application of Wicksell's solution. An approximate solution, by Wicksell,[5] for the sectioning of ellipsoids is not applicable to line scanning across elliptical particles. Certain of the moments of the distributions in the complete solution can be related by expressions independent of particle shape; the work of Crofton,[6] Williamson [7] and Czuber[8] should be consulted. The intercept length method of sizing, which has been employed by Hoare (see Walton[9]), is not further discussed here.

In track scanning the number, length and height of pulses from intercepted particles can be found; and it is shown below that the number of particles per unit area and their size distribution can be obtained from simple observations. In contrast to the determination of size distribution from line intercepts, which involves heavy computation, the calculations are simple. Moreover, the theoretical treatment is not restricted to circular particles, although the practical application is most readily made where such an assumption is justified.

The scanning method of particle counting and sizing is not limited to photoelectric applications. In fact it provides a method suitable for visual use, especially for projection microscopes and with the continuously driven mechanical stages that have been developed for petrological analysis.

1. DEFINITIONS AND NOTATION

Projected size. We define the projected size x of any particle encountered in a scan as the projection of the outline of the particle on a straight line perpendicular to the direction of scan at the particle (Fig. 1). No restrictions are placed on the shape or orientation of the particles: their outlines may be convex or have re-entrant angles; they may be randomly or systematically orientated. For all but circular outlines, the size x of any given particle depends on its orientation relative to the direction of scan. The relationship of the size x to the diameter of the particle in terms of, for example, its perimeter, is discussed in Section 5.

Centre. The centre of a particle is defined as the intersection of the line, parallel to the direction of scan, passing through the mid-point of the projection x, with the line, perpendicular to the direction of scan, passing through the mid-point of the projection of the particle on the direction of scan (Fig. 1). At this stage, no restriction is placed on the distribution or arrangement of particle centres in the field. Some particles may, for example, overlap others wholly or partially. Where this happens (as would be the case for a random distribution of particle centres) we shall assume for the present (Sections 2–5) that each particle in any group of overlapping particles, is separately distinguishable. The effect of overlapping is discussed in Section 6.1.

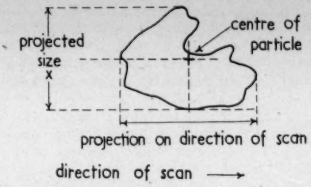

Fig. 1. Definition of projected size and centre of particle

Projection. The projection h of a particle intercepted by a scanning track of width w drawn across the field (Fig. 2), is defined as that part of its projected size x lying within the track. The magnitude of the projection h (within the ranges $w \geqslant h \geqslant 0$, $x \geqslant h \geqslant 0$) depends on the position of the centre of the particle relative to the scanning track.

Intercept length. Similarly the intercept length y of an intercepted particle is defined (Fig. 2) as the projection on a line parallel to the direction of scan, of that part of the particle lying within the scanning track.

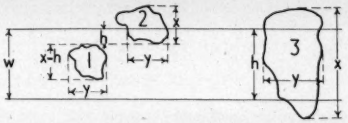

Fig. 2. Interception of particles by a track scan

(w = track width, x = projected size of particle; h = projection of particle within track; Class 1 particles ($x < w$) wholly intercepted; Class 2 particles intercepted by one edge; Class 3 particles ($x > w$) intercepted by both edges).

It is convenient also to distinguish (see Fig. 2) three classes of intercepted particle: Class 1 particles, of size x less than w and projection h equal to x, lie wholly within the track; Class 2 particles, of any size x and projection h, fall partially within the track; and Class 3 particles, of size x greater than w and projection h equal to w, lie wholly across the track.

To clarify these definitions it is helpful to consider a particular scanning system. Suppose an illuminated field of well-separated circular particles, of constant optical density, is scanned by a slit-shaped aperture of length w and negligible breadth. A photocell behind the aperture records the changes in light flux as the slit intercepts particles in the scanning track. The (peak) heights of the pulses are then proportional to the projections h, whilst their durations are proportional to the intercept lengths y. The total number of pulses is equal to the total number of particles intercepted. If the pulses are fed to a pulse amplitude discriminator that records only those pulses exceeding some preset height, the recorded number of pulses is equal to the number of projections h exceeding a value $h = z$ corresponding to the

setting of the amplitude discriminator. A multi-channel discriminator would permit the determination of the frequency distribution of pulse heights and hence of projections h.

In addition to the symbols defined above, the following notation is used. The size distribution of particles in terms of their projected size is denoted by $f(x)$, such that

$$\int_a^b f(x)dx = 1 \tag{1}$$

where a and b are the smallest and largest projected sizes present in the field. The total number of centres of particles of all sizes, $a \leqslant x \leqslant b$, present per unit area of the field is denoted by N, so that the number per unit area of any size x to $(x + dx)$ is $Nf(x)dx$. The mean size of particles is

$$\bar{x} = \int_a^b xf(x)dx \tag{2}$$

The number of projections h (pulse heights) exceeding a value z, obtained per unit length of a track of width w will be denoted by $\phi(w,z)$.

In counting we wish to find the number N of particles per unit area from observations of the number ϕ of pulses per unit length of scan; the observations, as will be shown, yield also the mean size $\bar{x}$.

In sizing we wish to find the proportion $f(x)$ of particles of size x or the number per unit area $Nf(x)$ from observations of ϕ. It is, however, easier in some cases to find the oversize distribution, that is the proportion $F(z)$ of particles of sizes greater than some specified size z,

$$F(z) = \int_z^b f(x)dx \tag{3}$$

The cumulative oversize curve is often as convenient a description of the size analysis as the size distribution curve, which can be obtained by differentiating the cumulative curve.

2. NUMBER OF PARTICLES INTERCEPTED IN A TRACK SCAN

We derive first an expression for the number of particles intercepted by a track scan in terms of the number and size distribution of particles present in the field. The resulting integral equation is then solved to give an expression for the relative number of particles per unit area of different sizes in terms of the (observable) numbers intercepted.

Instead of finding simply the total number of intercepted particles, it is more useful to obtain the number of particles giving projections h exceeding some specified value z. The total number of intercepted particles is the special case of $z = 0$.

Consider first only particles of size x to $(x + dx)$; there are $Nf(x)dx$ particles of this size per unit area. A track of width w and length L will intercept those particles of size x whose centres lie within the rectangle of width $(w + x)$ and of length L. For the particles to be intercepted and also to give projections h exceeding z, their centres must lie within the smaller rectangle of length L and width $(w - 2z + x)$. The average number of particles having centres in this rectangle will be $(w - 2z + x)LNf(x)dx$, irrespective of the arrangement of the particles in the field, provided that the track is drawn in all possible positions across the field $(L \to \infty)$. (The sampling errors arising in a finite length of scan are discussed in Section 6.2.) Thus if $m(x; w, z)$ denotes the number of particles, per unit length of scanning track, of size x, giving projections h exceeding z at a track width w, we have

$$m(x; w, z) = N(w - 2z + x)f(x), \quad L \to \infty \tag{4}$$

The number $\phi(w, z)$ of particles, per unit length of scan, of all sizes, giving projections h exceeding z at a track width w, is

$$\phi(w, z) = \int_z^b m(x; w, z)dx \tag{5}$$

The integration extends from a lower limit z because particles of size x less than z cannot give projections h exceeding z. From equations (4) and (5) we have therefore

$$\phi(w, z) = N \int_z^b (w - 2z + x)f(x)dx \tag{6}$$

as the expression for the number, per unit length of scan, of projections (pulse heights) exceeding z (discriminator setting) in a track of width w due to N particles per unit area of size distribution $f(x)$.

It is convenient to re-write equation (6) with z expressed as a fraction p of the track width;

$$\phi(w, p) = N \int_{pw}^b [w(1 - 2p) + x]f(x)dx \tag{7}$$

This form is chosen because, in practical terms, $\phi(w, p)$ is the number of pulses, per unit length of scan, that pass an amplitude discriminator set to a fraction p of the maximum pulse height given by total observation of a slit shaped scanning aperture of length w.

There are numerous special cases contained in equations (6) and (7). Some are illustrated by graphs of $\phi(w, p)$ against w for various values of p (Fig. 3). For z less than or equal to

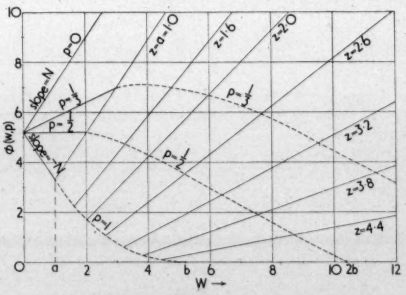

Fig. 3. Graphs of $\phi(w, p)$ against w for various values of p

Full thick lines: $z \leqslant a$. Full thin lines: z constant. Dotted curves: p constant.

a, the size of the smallest particle present in the field, $\phi(w, p)$ is linear in w and p (thick lines in Fig. 3), irrespective of the size distribution $f(x)$, and depends only on the number N per unit area and the average size $\bar{x}$. For z greater than a, the graph of $\phi(w, p)$ against w depends on the size distribution $f(x)$; and, for illustrative purposes only, the dotted

curves in Fig. 3 have been calculated for an exponential size distribution. The general case is discussed in the next section and some special cases in Section 4.

3. NUMBER AND SIZE DISTRIBUTION FROM NUMBER INTERCEPTED

The solution of the integral equations (6) or (7) gives the number and size distribution in terms of the observable function $\phi(w, z)$. There are two important cases: (i) when z is constant; and (ii) when p is constant. The first corresponds to scanning under conditions of constant discriminator setting; the second to scanning at a fixed fractional discriminator setting.

3.1 *z constant* (thin lines in Fig. 3). When z is constant, equation (6) may be written, putting $\phi(w)$ for $\phi(w, z =$ constant)

$$\phi(w) = (w + \bar{z} - 2z)N \int_z^b f(x)dx = (w + \bar{z} - 2z)NF(z) \quad (8)$$

where $\bar{z}$ stands for

$$\bar{z} = \int_z^b xf(x)dx \Big/ \int_z^b f(x)dx \quad (9)$$

and is the mean size of particles larger than z. Thus ϕ varies linearly with w (thin lines in Fig. 3) with slope equal to the number oversize z per unit area, $NF(z)$. The intercept on the abscissa is $2z - \bar{z}$.

This provides the most useful method of sizing and counting. The number oversize per unit area is found for each of a series of values of z in the range $a \leqslant z \leqslant b$ by determining the slope of ϕ against w for each value of z. It is sufficient to make counts ϕ at two different track widths for each value of z. Size classification into n size grades requires n pairs of counts.

3.2 *p constant* (dotted lines in Fig. 3). When p is constant, we start from equation (7). Putting $\phi(w, p =$ constant) and differentiating with respect to (w), gives

$$\phi'(w) = N(1 - 2p) \int_{pw}^b f(x)dx - Np(1 - p)wf(pw) \quad (10)$$

Excluding for the moment the special cases of $p = 0$ and $p = 1$, we can rearrange equation (10), since $p(1 - p) \neq 0$, in the form

$$f(z) = g(z) + \lambda \int_z^b \frac{1}{z} f(x)dx \quad (11)$$

where $z = pw$, $g(z) = -\phi'(w)/Npw(1 - p)$ and $\lambda = (1 - 2p)/(1 - p)$. This is a Volterra integral equation of the second kind, whose solution[10] can be shown to be

$$f(z) = g(z) + \frac{\lambda b^\lambda}{z^{\lambda+1}} \int_z^b g(x)dx \quad (12)$$

and on substituting for $g(z)$ and $g(x)$ we have

$$Nf(z) = \frac{-1}{p(1-p)} \left[\frac{\phi'(w)}{w} - \lambda \left(\frac{b}{z}\right)^\lambda \frac{\phi(w)}{w^2} + \lambda \left(\frac{b}{z}\right)^\lambda \frac{1}{w} \int_w^{b/p} \frac{\phi(t)}{t^2} dt \right] \quad (13)$$

where $z = pw$, $\lambda = (1 - 2p)/(1 - p)$ and the prime denotes differentiation with respect to w.

The determination by means of equation (13) of $f(x)$ from observations of the variation of ϕ with w at constant p (dotted lines of Fig. 3) involves, in general, heavy computation. The observations must, moreover, be made at a large number of values of w, since the (dotted) curve must be differentiated at w and also integrated from w to b/p.

There are, however, simple solutions of equation (10), involving a minimum of computation, in the special cases of $p = 0$, $p = 1$ and also for $p = \frac{1}{2}$. It is easily shown that for

(i) $p = 0$ $\quad N = \phi'(w, 0)$ (13*a*)

(ii) $p = \frac{1}{2}$ $\quad Nf(w/2) = -4\,\phi'(w, \frac{1}{2})/w$ (13*b*)

(iii) $p = 1$ $\quad NF(w) = -\phi'(w, 1)$ (13*c*)

or $Nf(w) = \phi''(w, 1)$ (13*d*)

The special case of $p = 0$ (thick line marked $p = 0$ in Fig. 3) gives the total number per unit area and is discussed later. The case of $p = \frac{1}{2}$ yields the size distribution from a single differentiation of the observations, as does the method discussed in Section 3.1. The case of $p = 1$, which corresponds to recording the number of particles totally obscuring a scanning slit, gives the oversize distribution from a single differentiation or the size distribution from a double differentiation. This method of total obscuration has been employed by Pigford[11] and was proposed independently by Hawksley.[12]

3.3 *p constant: moments of size distribution.* The moments about zero of the size distribution can be readily expressed in terms of the moments of the observed distribution of ϕ. They may be more easily computed than is the size distribution; and, for many purposes the first few moments provide a more convenient description of the size distribution. Denote the moments about zero by

$$M_n = \int_a^b x^n f(x)dx \quad (14)$$

and

$$m_n = \int_0^b w^n \phi(w)dw \quad (15)$$

where $\phi(w)$ stands for $\phi(w, p)$.

For the first moment we have from equation (7) with $pw = a$

$$M_1 = \bar{x} = \phi\left(\frac{a}{p}\right) \Big/ N - (1 - 2p)\left(\frac{a}{p}\right) \quad (16)$$

The second and higher moments are obtained by substituting for $\phi(w)$ from equation (7) in m_n,

$$m_n = N \int_0^b w^n dw \int_{pw}^b [w(1 - 2p) + x]f(x)dx \quad (17)$$

Put $z = pw$ and $k = (1 - 2p)$, then

$$m_n = \frac{N}{p^{(n+1)}} \int_0^b z^n dz \int_z^b (kz/p + x)f(x)dx \quad (18)$$

$$= \frac{N}{p^{n+1}} \int_0^b f(x)dx \int_0^x (kz^{n+1}/p + xz^n)dz \quad (19)$$

which, on integrating, substituting for k and re-arranging gives

$$M_n = \frac{n(n-1)p^n}{N[n(1-p) - (1-2p)]} m_{n-2} \quad (20)$$

Thus, for example, the 2nd, 3rd and 4th moments are:

$$\left.\begin{aligned} M_2 &= \frac{2p^2}{N}\int_0^b \phi(w,p)dw \\ M_3 &= \frac{6p^3}{N(2-p)}\int_0^b w\phi(w,p)dw \\ M_4 &= \frac{12\,p^4}{N(3-2p)}\int_0^b w^2\phi(w,p)dw \end{aligned}\right\} \qquad (21)$$

Note especially that, for this purpose, ϕ extends to a lower limit of zero. The observations do not have to be taken below $w = a/p$ since from this point ϕ is linear to the value $N\bar{x}$ at $w = 0$ (thick lines in Fig. 3).

4. SPECIAL CASES: NUMBERS OF PARTICLES OF DIFFERENT CLASSES

The various methods of counting that have been proposed or investigated[9] are special cases of equations (6) or (7). To obtain the total number N per unit area, the condition $z \leqslant a$ must be satisfied. Then we have

$$\phi(w) = N[w + \bar{x} - 2z], \qquad z \leqslant a \qquad (22a)$$

or

$$\phi(w) = N[w(1-2p) + \bar{x}], \quad w \leqslant a/p \qquad (22b)$$

when z is constant, ϕ varies linearly with w, the slope being N and the intercept at $w = 0$ being $(\bar{x} - 2z)$. This is the basis of the method of blood cell counting employed by Wolff,[13] Lagercrantz,[14] McFarlane and Cooke-Yarborough (see Walton).[9] The number N is given by the difference of counts per unit length at two track widths, divided by the difference in track widths. It is not necessary to know the value of z (unless $\bar{x}$ also is required) providing it is smaller than a and is kept the same for both track widths. (A minor point that has not been explicitly stated previously is that the track width may have any value relative to the size of the particles.) In the investigations cited, the scanning aperture was not slit shaped, the breadth being comparable with the length. This is permissible either if z is very small compared with a or if the particles are all the same size, as is the case for blood cell counting. When there is a range of sizes present (and this usually means also that the lower limit a is smaller than the smallest practical value of z), a rectangular scanning aperture leads to a value of z that is not independent of particle size.

When p is constant equation (22b) represents, in the plot of ϕ against w, a fan of straight lines (thick lines in Fig. 3) radiating from the point $N\bar{x}$ at $w = 0$ of slopes $N(1-2p)$. They are terminated at $w = a/p$ and then pass into the curves, discussed in Section 3.2, for z greater than a. The following special cases may be noted:

(i) Case of $p = w = z = 0$: $\phi(w = 0, p = 0) = N\bar{x}$ (23a)

(ii) Case of $p = 0, z = 0$: $\phi(w, 0) = N(w + \bar{x})$ (23b)

(iii) Case of $p = 1, z = w$: $\phi(w, 1) = N(\bar{x} - w)$ (23c)

The first case describes a line scan; the number of particles intercepted per unit length of a line drawn across the field is equal to the product of the number per unit area and the mean projected size. The second describes a track scan of infinite sensitivity and gives the number of particles intercepted per unit length by the track. The third describes a track scan in which only particles lying wholly across the track (Class 3 particles in Fig. 2) are recorded: $\phi(w, 1)$ for z greater than a is given by equation (13c).

We may now derive expressions for the numbers of particles intercepted in the three different classes shown in Fig. 2. These are useful because it is feasible to detect and record the particles of different classes or of combinations of classes. This is the basis of guard spot systems of counting and sizing (see Walton[9]). Let $\phi_1(w)$, $2\phi_2(w)$ and $\phi_3(w)$ denote the number in the three classes intercepted per unit length of track of width w. (Note that $\phi_2(w)$ is the number of Class 2 on one edge of the track, so that the total number of Class 2 particles is $2\phi_2(w)$.) Since the total number $(\phi_1 + 2\phi_2 + \phi_3)$ of all classes is given by equation (23b), and the number $\phi_2 + \phi_3$ intercepted by a line scan by equation (23a), whilst the number ϕ_3 lying wholly across the track is given by equations (13c) and (23c), it is easily shown that

$$\phi_1(w) = N\int_a^w (w - x)f(x)dx \qquad (24a)$$

$$\phi_2(w) = N\int_a^w xf(x)dx + N\int_w^b wf(x)dx \qquad (24b)$$

$$\phi_3(w) = N\int_w^b (x - w)f(x)dx \qquad (24c)$$

These are valid for all values of w and x. It is readily shown that the cumulative oversize distribution is

$$NF(w) = N\int_w^b f(x)dx = N - \phi_1'(w) = \phi_2'(w) = -\phi_3'(w) \qquad (25a)$$

and that the size distribution is

$$Nf(w) = \phi_1''(w) = -\phi_2''(w) = \phi_3''(w) \qquad (25b)$$

where the primes denote differentiation with respect to w. The size distribution can thus be obtained by determining the number intercepted in any one of the three classes.

More important is that, from equations (24a) and (24b), the sum $\phi_1(w) + \phi_2(w)$ is equal to Nw. Thus any method of selecting Class 1 and Class 2 particles provides a direct measure of the number per unit area. For example, the standard procedure in visual counting is to record the number $\phi_1(w)$ wholly within the sample area, plus the number $\phi_2(w)$ lying on half the perimeter of the sample area. In visual counting, the "track width" is usually larger than the largest particle present so that there are no Class 3 particles; but when this is not the case, the present discussion shows that any particles lying wholly across the sample area should be ignored.

Another method, also applicable whatever the width of the track relative to the particle size, is to record by a slit scan the total number of all classes, $\phi_1 + 2\phi_2 + \phi_3$, and to subtract from this the number $\phi_2 + \phi_3$ lying on one edge (a "spot" scan); the difference divided by the track width gives N. The difference can be obtained from successive counts with a slit and a spot scanning aperture, not necessarily alined together; or in one operation by a guard spot system that cancels from the slit scan particles lying on one edge of the track. This latter method has been proposed by Meyer (see Walton[9]).

A further method may be used when the track width is smaller than the smallest particle present. In that case $\phi_1(w) = 0$, and Nw is given by recording $\phi_2(w)$, which can

be done in a variety of ways. Since $\phi_1(w) = 0$, the scanning slit may be replaced by two spot apertures, spaced $w(< a)$ apart. The number recorded by such a double spot scan is $2\phi_2 + \phi_3$; a separate single spot scan gives $\phi_2 + \phi_3$. The difference ($= Nw$) can be obtained from two separate scans or by a cancelling guard spot system. This method was proposed and investigated by Dell (see Walton 1952[9]) and employed by Roberts and Young[15] in their "flying spot" microscope system of particle counting.

The conditions $p = 0$ or $w = 0$ cannot be realized in practice; z cannot be less than some finite value z_{min}. Methods based on recording all projections, however small, in a track scan, or all particles intercepted, however slightly, by a line scan, are subject to an error that is negligible only if z_{min} is very much smaller than a.

5. SIGNIFICANCE OF PROJECTED SIZE

In the preceding discussion we have considered the number of particles intercepted. Now if there are re-entrant angles in the particle outlines the number of interceptions can exceed the number of particles intercepted. Consider a line scan across the field. It is well known [e.g. references (6) and (7)] that the mean value of the number of times a straight line intersects, per unit length, any system of lines of total length P, per unit area of the field, averaged over all possible positions of the straight line, is equal to $2P/\pi$. This is true whatever the nature of the system of lines P, whether closed or open, continuous or discrete, convex or having re-entrant angles, arranged systematically or randomly in the field. Buffon's celebrated problem is a special case; the probability that a rod of length y, dropped at random on a system of parallel lines spaced a distance w apart greater than y, will fall across a line is $2y/\pi w$. In the present instance, for particles having closed outlines, the mean number of intercepts is half the mean number of intersections and is equal to P/π per unit length. If $\bar{d}_p$ denotes the mean perimeter diameter (the diameter of a circle having the same perimeter as a particle), the total perimeter per unit area is $P = N\pi\bar{d}_p$ and hence the number of intercepts in a line scan is $N\bar{d}_p$ per unit length whatever the shape of the particles.

Since for convex outlines the number of intercepts equals the number of particles intercepted, which from equation (23a) is $N\bar{x}$ per unit length, it follows that for convex particles the mean projected size $\bar{x}$ is equal to the mean perimeter diameter $\bar{d}_p$. This identity has been re-discovered many times.

Although the mean sizes are the same for convex particles, it is not obvious whether the size distribution $f(x)$ may be equated with the size distribution by perimeter diameter.

Now let $\psi(t)$ be the size distribution of particles by some specified diameter t. In general the projected size x will depend on the orientation θ and the size t of the particle. Assume that particles of all sizes have the same shape in the sense that for any given particle the ratio x/t is a function of t and θ only. Then we can define a function ζ such that $d\theta = dx\zeta(t, x)$ and it can be shown that, for particles orientated at random

$$f(x) = \frac{2}{\pi}\int_{t_1}^{t_2} \zeta(t, x)\psi(t)dt \tag{26}$$

where the limits t_1, t_2 are the extreme values of t capable of yielding a projected size x and are in general functions of both t and x. The solution of this integral equation depends on the explicit form of $\zeta(t, x)$ and of the limits.

If, as an example, we consider elliptical particles of constant eccentricity e and if t is defined as the perimeter diameter, then it can be shown that

$$\zeta(t, x) = -x/(x^2 - C^2t^2)^{\frac{1}{2}}(B^2t^2 - x^2)^{\frac{1}{2}} \tag{27}$$

$$t_1 = x/B,\ t_2 = x/C$$

where $C = (1 - e^2)^{\frac{1}{2}}B$, $B = \pi/2E$ $\sin^{-1}e$, E being the complete elliptic integral of the second kind with argument $\sin^{-1}e$. The solution of equation (26) with these substitutions may be found by inserting the resulting expression for $f(x)$ in equation (7), thus

$$\phi(w, p) = \frac{-2N}{\pi}\int_{pw}^{b}[w(1 - 2p) + x]xf(x)dx \int_{x/B}^{x/C}\frac{\psi(t)dt}{\sqrt{(x^2 - C^2t^2)}\sqrt{(B^2t^2 - x^2)}}$$

$$= \frac{-2N}{\pi}\int_{pw}^{b}\psi(t)dt \int_{Bt}^{Ct}\frac{[wx(1 - 2p) + x^2]dx}{\sqrt{(x^2 - C^2t^2)}\sqrt{(B^2t^2 - x^2)}} \tag{28}$$

The integration under the integral sign gives

$-\pi[w(1 - 2p) + t]/2$ and hence

$$\phi(w, p) = N\int_{pw}^{b}[w(1 - 2p) + t]\psi(t)dt \tag{29}$$

Thus scanning of randomly orientated elliptical particles of constant eccentricity gives the size distribution $\psi(t)$ by perimeter diameter, $t = d_p$.

6. PRACTICAL APPLICATION

The number $\phi(w, z)$ of intercepted particles can always be determined, to any desired precision, by visual scanning over a sufficiently long track. But there are many problems in measuring $\phi(w, z)$ by photoelectric scanning, which is essential for covering an adequate track length in a reasonably short scanning time. The (peak) pulse heights in photoelectric scanning correspond to the projections only for the ideal case (Section 1) of scanning a field of well-separated circular particles of constant optical density, with a slit-shaped aperture of negligible breadth. If the particles are not circular the peak pulse heights depend not on the projection, but on the largest chords, perpendicular to the direction of scan, of those parts of the particles lying within the track; moreover, if the particle outlines contain re-entrant angles, the number of pulses is not the number of intercepted particles, but the number of intercepts on particles. If the breadth of the slit is not negligible, the pulse height varies with the largest chord, particle size and slit breadth in a manner depending on the particle shape. If the particles do not have the same density, they will be classified by an effective size depending on their optical density. If the particles are not well separated, two or more particles may produce coincident pulses. These difficulties arise not only in sizing but also in counting.

Here attention is restricted to two particular questions: the effect of the arrangement of particles in the field on overlapping and coincidence of particles in the scanning aperture; and the effect of the finite length of scan on the precision of

the estimate of $\phi(w, z)$. The errors arising from other departures from the ideal case are not likely to be large in many practical applications.

6.1. *Coincidence and overlapping.* We consider now the effect on the practical application of scanning methods of sizing, of the arrangement of particles in the field. (The theoretical treatment above is applicable to any arrangement of particles, provided the scanning track is taken over all possible positions in the field—Section 6.2). If the particle centres are distributed at random, some particles will overlap others. The resulting clump will be seen by the photocell as a single particle; and the size distribution deduced from the observations will be that of the overlapped system. In addition there will occur coincidences of two or more particles or clumps in the scanning aperture at the same time so that a single pulse of larger amplitude is recorded in place of several smaller pulses. (Even when pulses are separated, the interval between them may be shorter than the recovery time of the detecting and counting circuits; or "paralysis" may be deliberately introduced.) The recorded count ϕ_R thus differs from the theoretical count ϕ on account of both overlapping and coincidence.

In many practical applications there is no overlapping of particles and a random distribution of centres cannot be assumed. Although the objective of dispersing techniques in preparing samples is to secure a uniform separation of particles, it is probably permissible to assume that a particle may occupy any position in the field not already occupied by another. The recorded count will then differ from the expected count on account of coincidence only.

The problem of correcting the recorded count ϕ_R for coincidence and overlapping is a difficult one and a complete solution has not been obtained, even for the relatively simple case of a random arrangement of particles. A solution is given below for the special case of scanning, when p and z are zero, a field of randomly distributed circular particles. This enables the number and mean size of the particles to be found in spite of overlapping and coincidence. It serves also to indicate the magnitude of the coincidence effect for the case where particles may occupy any positions not already occupied.

In the special case of counting the number $\phi(w, 0)$ of intercepted particles at $p = 0$, the effect of coincidence and overlapping is solely to produce an undercount, i.e. ϕ_R is less than ϕ. Since pulses of all heights are to be recorded, it does not matter that coincidence and overlapping may increase the pulse height. Now let Σy denote the total of the intercept lengths y (Fig. 2) occurring in a track of width w and length L. (Σy would also be the total duration of pulses if each pulse could be registered independently of the occurrence of a coincident pulse.) If n is the number of intercept lengths, the probability that a second intercept, occurring at random, will start within the length y of a previous intercept, is $1 - \exp(-ny/L)$. It follows that the ratio of the recorded number ϕ_R to the actual number ϕ of intercept lengths is $\exp(-\Sigma y/L)$.

Now for circular particles $\Sigma y/L$ is made up of two parts: the total length, per unit length of track, of particles whose centres lie within the track, which is equal to $Nw\bar{x}$; and the total length, per unit length of track, of intercepts due to particles whose centres lie outside the track, which is equivalent to a single line scan and is equal to the total area of particles per unit area of the field or the area concentration $c(= \pi N\bar{x}^2/4)$. Hence

$$\phi_R(w, 0) = N(w + \bar{x}) \exp -(Nw\bar{x} + c) \qquad (30)$$

This gives the recorded number ϕ_R of intercepted particles, per unit length of a scan, at $p = 0$, due to N circular particles per unit area of mean size $\bar{x}$ at a concentration of c, whose centres are randomly distributed so that there is both overlapping and coincidence.

The above equation may also be written in terms of the number N_0, mean size $\bar{x}_0$ and concentration c_0 of the overlapped system resulting from the N particles of mean size x at concentration c. A line scan across the overlapped system records $N_0\bar{x}_0$, which from equation (30) is equal to $N\bar{x}\exp(-c)$. It can also be shown that c_0 is equal to $1 - \exp(-c)$ and if we use also the approximation due to Armitage[16] that, for $c \ll 1$, N_0/N is equal to $(1 - 2c)$, then on substituting in equation (30)

$$\phi_R(w, 0) \simeq N_0(w' + \bar{x}_0) \exp(-N_0\bar{x}_0 w'),\ c_0 \ll 1 \qquad (31)$$

where w' stands for $w(1 + c_0)$. This enables the number N_0 and mean size x_0 of discrete clumps to be deduced from observations of ϕ_R.

In the case where particles are distributed without overlapping, we may expect the above relations to provide useful approximations (but still restricted to $p = 0$). When the concentration c is negligibly small and the track width is large, it is obviously permissible to assume a random distribution of particle centres and the effect of coincidence is, from equation (30), to reduce the true count by the factor $\exp(-Nw\bar{x})$. Since c is of the order $N\bar{x}^2$, the approximation will improve as w/x increases. At the other extreme when $w = 0$, the correction factor must be unity. This suggests that the first order correction for coincidence for particles distributed without overlapping is simply $\exp(-Nw\bar{x})$.

When p is not zero, besides an undercount, there may also be an overcount from the coincidence of particles, which individually would not give projections h exceeding z. In the important case of scanning at constant z (Section 3.1), coincidence is unlikely to produce any appreciable error at $p = 1$; an undercount or overcount can arise only if the particles are in contact and for a particular orientation of the line of centres. At smaller values of p the relative extent of over and under counting depends on the value of z relative to the mean size $\bar{x}$ of all particles present in the field. For large values of z, where there are many undersize particles capable of combining to give an overcount, the recorded count will tend to exceed to true count. At small values of z the net effect is likely to be an undercount. Any more detailed discussion must be deferred until experimental evidence is available on the nature of the arrangement of particles in the field.

6.2. *Sampling errors.* The expressions derived in Section 1 refer to the limiting case of an infinitely long scanning track. The observed counts ϕ for a finite track length will be distributed about a mean value given by the expressions. The reliability of a single observation will depend on the length of the track and thus on the magnitude of the recorded count. The sampling error is best determined experimentally but its magnitude can be predicted if the particle centres are assumed to be randomly distributed. Since the uniform distribution of field concentration or density implied by a random arrangement is rarely achieved in preparing samples for size analysis, the predicted sampling error will be an underestimate.

For a random distribution of point events in a field the numbers of points in sample areas are normally distributed, for large numbers, about their mean value with a variance equal to the mean. In scanning methods of counting, the number per unit area is obtained from the difference of two counts. The variance of the number per unit area depends

on the sum of the variances of the two counts if they are independent samples, for example, if the observations are made on different tracks. On the other hand, if the observations are made on the same sample area the variance of the number per unit area depends on the variance of the total number of particles counted.

Let $M = \phi L$ denote the observed count, L being the length of scanning track. Consider the case where the number per unit area is obtained from a track scan at $p = 0$, ϕ being $N(w + \bar{x})$. Counts ϕ_A, ϕ_B are made at track widths w_A, w_B and N is calculated from $(\phi_A - \phi_B)/(w_A - w_B)$, which may be written

$$N = \frac{(M_A/L_A) - (M_B/L_B)}{w_A - w_B} \tag{32}$$

Suppose that L and w are known exactly and the variance of N is due solely to the variances of M_A, M_B. Then the variance of N, $V(N)$ is

$$V(N) = N^2 \frac{L_B^2 V(M_A) + L_A^2 V(M_A)}{(L_B M_A - L_A M_B)^2} \tag{33}$$

where $V(M_A)$, $V(M_B)$ are the (small) variances of M_A and M_B, provided the counts M_A and M_B are independent. Since the variance $V(M)$ is equal to M, and if the lengths of scan are equal $L_A = L_B = L$,

$$\frac{V(N)}{N^2} = \frac{M_A + M_B}{(M_A - M_B)^2} = \frac{(w_A + w_B + 2\bar{x})}{NL(w_A - w_B)^2} \tag{34}$$

The coefficient of variation of N, $C(N) = \sqrt{V(N)}/N$, is thus

$$C(N) = \frac{1}{\sqrt{NLw}} \cdot \frac{\sqrt{(2r + q + 1)}}{q - 1} \tag{35}$$

where w stands for the smaller track width w_B, r is the ratio $\bar{x}/w$, and q the ratio of larger to smaller track width ($q > 1$).

Similarly for the case of scanning at constant z (Section 3.1), the coefficient of variation of the number oversize z is

$$C(N) = \frac{1}{\sqrt{NLw}} \frac{\sqrt{(2r + q + 1 - 4p)}}{q - 1} \tag{36}$$

where r is $\bar{z}/w$, and p is z/w.

When the separate counts are not independent, for example, if $\phi_1 + \phi_2$ is recorded directly by a suitable guard spot system, then the coefficient of variation is simply

$$C(N) = 1/\sqrt{NLw} \tag{37}$$

The additional factor in equations (36) and (37), which always exceeds unity, is a measure of the increased count required for the same precision when the two scans are independent. In practice the scanning tracks of different widths will sample substantially the same particles, and there will be a large interdependence between the counts.

REFERENCES

(1) WICKSELL, S. *Biometrika*, **17**, p. 84 (1925).
(2) HAGERMAN, T. H. *Geol. Forenings, Stockholm, Forhand*, **46**, p. 325 (1924), with appendix by Odquist, F. K. G., at p. 343.
(3) KRUMBEIN, W. C., and PETTIJOHN, F. J. *Manual of Sedimentary Petrography*, p. 192 (New York: D. Appleton-Century Co., 1938).
(4) WILLIS, T. F. Disc. (p. 203) to Powers, T. C., *Proc. Highways Res. Board*, **29**, p. 184 (1949), reprinted in *Bull. Res. Lab. Portland Cement Assoc.*, No. 33, p. 20 (1950). See also Lord, G. W., and Willis, T. F. *Bull. Amer. Soc. Test. Mat.*, No. 177, p. 56 (1951).
(5) WICKSELL, S. *Biometrika*, **18**, p. 151 (1926).
(6) CROFTON, M. W. *Phil. Trans Roy. Soc.*, **158**, p. 181 (1868); *Encyclopaedia Britannica*, 9th Ed., **19**, p. 784 (1885).
(7) WILLIAMSON, B. *An elementary treatise on the integral calculus*, 3rd Ed., p. 313 (London: Longmans Green and Co., 1880).
(8) CZUBER, E. *Geometrische Wahrscheinlichkeiten und Mittelwerke* (Leipzig: Teubner, 1884).
(9) WALTON, W. H. *Nature* [*London*], **169**, p. 518 (1952).
(10) MARGENAU, H., and MURPHY, G. M. *The Mathematics of physics and chemistry*, p. 506 (New York: D. van Nostrand Co., 1943).
(11) PIGFORD, R. L. *Air Pollution: Proc. U.S. Tech. Conference on*, p. 672 (New York: McGraw-Hill Book Co. Inc., 1952).
(12) HAWKSLEY, P. G. W. *Nature* [*London*], **170**, p. 984 (1952).
(13) WOLFF, H. S. *Nature* [*London*], **165**, p. 967 (1950).
(14) LAGERCRANTZ, C. *Acta. Physiol. Scandinavica*, **26**, (1952), Supp. 93, p. 131.
(15) ROBERTS, F., and YOUNG, J. Z. *Nature* [*London*], **169**, p. 962 (1952).
(16) ARMITAGE, P. *Biometrika*, **36**, p. 257 (1949).

Paper F.2

Some fundamental aspects of particle counting and sizing by line scans

By J. W. PHILLIPS, B.Sc., Scientific Department, National Coal Board

Some of the simpler ways of using line scans are noted, particularly with reference to counting and sizing particles which approach the limits of optical resolution.

A general treatment relating derivable information to observed data of frequency of interception of particles by line scans and combinations of line scans is given, and it is shown that to achieve a desirable accuracy a large aperture must be used and the presence of particles which do not fill the whole aperture must be recognized; this is best done by using an aperture composed of a line of independent probes so that the field is scanned as with a comb. Other methods, favoured at present, which depend on the use of apertures or probes whose size and position must be known accurately, cannot realize the potential and desirable accuracy of counting and sizing owing to limits set by optical resolution.

Estimates are made of the increased counts required in statistical methods and also of the relative merits of criteria of association of signals in methods where particles are assessed individually.

The development of methods for the automatic counting of particles has been pursued with much skill and ingenuity, but little has been published of any general treatment of the subject such as would be expected to bring out the fundamental limitations and possibilities of the ideas. The discussion in this paper is confined to assessment of samples by simple scanning methods. Even within these limits the paper is not in any way comprehensive. Thus, for instance, no reference is made to methods in which varying degrees of obscuration of light are assessed. Briefly, the paper discusses scanning by a spot, or spots, or slit, operating a simple "on-off" detector. A practical system requires the detection of radiation and therefore the use of a system having a finite resolution. In some of the following discussion it is necessary to distinguish between the particle and its image. Unless such a distinction is made, the term particle is used here for both.

Methods of counting and sizing particles may be divided logically into two groups. In individual methods, particles are assessed separately and individually. Particles are not necessarily examined in sequence so that one is completely assessed before the next is examined, but all the information relating to any one particle is collected together before that particle is assessed. In statistical methods no attempt is made to identify items of information with particular particles or to correlate items of information from the same particle. In general, the type of information required in a statistical method is much easier to collect since no selecting or correlating of information is required. On the other hand, the quantity of information required is greater and may be of a different order of magnitude.

STATISTICAL METHODS

Scanning a line. The exact relative position of a scanning spot and the image of a particle when the presence of the image is first registered is a function of both the spot (which in practice must be of finite dimensions), and the image, but for a given spot and image and line of approach the relative position is unique and the boundary of the image can be defined as at the nominal centre of the spot when the image is first registered. The spot is then effectively dimensionless. By using the spot in a single line scan we can obtain:

(*a*) mean density of sample (by integration of intercept lengths);
(*b*) mean size of an image;
(*c*) frequency distribution of intercept lengths.

In theory at least, if (*c*) is known, and the frequency distribution of intercept lengths for a single image is known, the frequency distribution of image sizes can be obtained. Up to now such attempts have been, on the whole, unsuccessful except in a few favourable cases, as for instance when images are known to be circular. In view of the very different frequency distributions for images having rectilinear and curved profiles (see Fig. 1), it seems unlikely that a frequency distribution of intercept lengths for a particle of "average" shape can be assumed.

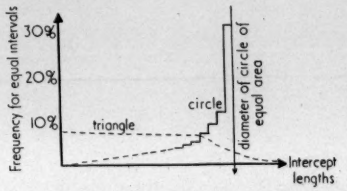

Fig. 1. Frequency distribution of intercept lengths for a circle and for a triangle (linear scales)

Scanning by a path of finite width. To extend the information provided by a spot scan, another dimension must be introduced into the scan, either by scanning with a pattern of spots, or by scanning with a single spot on parallel scan lines at a known separation and associating signals from different scans, or by using an aperture having a finite dimension perpendicular to the line of scan. The first two methods are for the present regarded as one. Various patterns of spots have been proposed for special applications, but it is not possible to discuss them in a short paper.

For the purposes of this discussion, a pair of spots scanning parallel lines is assumed, and the extension to scanning by an aperture is indicated where appropriate. Hawksley[1] has discussed this; an alternative and fuller treatment which relates the derivable information more directly to the observed data, is summarized below.

For all except circular particles (and a particular family of shapes bounded by circular arcs) the probability of interception of a particle varies with the orientation of the particle. Consider first, then, the case in which a pair of spots defining a path of nominal width w traverses a field of circular particles of various diameters.

Suppose the function defining the frequency distribution of particle diameters is $F(x)$ such that

$$\int_0^\infty F(x)dx = 1$$

All definitions of dimensions are nominal, in the sense indicated above. Expressions may be derived for the frequency of interception of particles by either or both spots. For instance, both spots are intercepted by particles of diameter $x > w$ having centres lying within a path of width $(x - w)$, and if the field of particles is of density N per unit area, the number of particles intercepted in this way per unit length of scan is

$$N \int_w^\infty (x - w)F(x)dx$$

Expressions for other types of interception are tabulated in the table, together with their first derivates with respect to w.

The useful expressions reduce to those set out under the next two headings.

Expressions representing various types of interception

Interceptions of circles by two parallel line scans or by an aperture.

n = number of particles intercepted per unit length of scan.
x = diameter of circle.
w = separation of scan lines, or width of aperture.
$n' = dn/dw$.

Type of interception	$x < w$	$x > w$
1. Single line scan	$n_1 = N \int_0^\infty xF(x)dx$ $n_1' = 0$	$n_1 = N \int_0^\infty xF(x)dx$ $n_1' = 0$
2. Two lines simultaneously, or wholly obscure an aperture	$n_2 = 0$	$n_2 = N \int_w^\infty (x - w)F(x)dx$ $n_2' = -N \int_w^\infty F(x)dx$
3. Either or both lines	$n_3 = 2N \int_0^w xF(x)dx$ $n_3' = 2NwF(w)$	$n_3 = N \int_w^\infty (x + w)F(x)dx$ $n_3' = N \int_w^\infty F(x)dx - 2NwF(w)$
4. Intercept a specified line, but not both $\frac{1}{2}(n_3 - n_2)$	$n_4 = N \int_0^w xF(x)dx$ $n_4' = NwF(w)$	$n_4 = Nw \int_w^\infty F(x)dx$ $n_4' = N \int_w^\infty F(x)dx - NwF(w)$
5. Fall between two lines or wholly within an aperture*	$n_5 = N \int_0^w (w - x)F(x)dx$ $n_5' = N \int_0^w F(x)dx$	$n_5 = 0$
6. Fall between two lines, or intercept either or both (intercept an aperture)	$n_6 = N \int_0^\infty (w + x)F(x)dx$ $n_6' = N \int_0^\infty F(x)dx = N$	$n_6 = N \int_0^\infty (w + x)F(x)dx$ $n_6' = N \int_0^\infty F(x)dx = N$

* To detect a particle falling wholly within an aperture implies more than the registering of a simple on-off signal. It could be done with a multi-line scan (see below).

Counting only by frequency of interception. It is required to obtain N, bearing in mind that

$$\int_0^\infty F(x)dx = 1$$

If particles are of all sizes, the various useful combinations of the expressions tabulated, e.g. $n_4 + n_5 = Nw$, $n_6 - n_1 = Nw$, $(n_6)_{w_1} - (n_6)_{w_2} = N(w_1 - w_2)$, $n'_6 = N$, etc., reduce to either: (*a*) counting particles which fall within a path, or overlap one specified edge (this is a standard counting practice), or (*b*) differencing counts of all particles intercepting two paths of different widths.

If particle sizes have a known lower limit, we can count the intercepts of only one specified line of two (n_4), the lines being at a separation smaller than the smallest particle. This is Dell's guard-spot method.[2,3] If the sizes have a known upper limit, we can count the particles falling between two lines or intercepting one specified line ($n_5 + n_1$), the lines being at a separation greater than the largest particle. Other equivalent expressions may be derived (e.g. $n_3 - n_1 = n_1 - n_2 = n_4$) or we can adapt one of the sizing methods below to give a single oversize or undersize count.

Counting and sizing by frequency of interception. Differencing methods, employing derivatives with respect to w, must be used when counting and sizing by frequency of interception.

Oversize counts at a size w are given by n'_2, n'_3, n'_4, i.e. difference the numbers of interceptions on two lines simultaneously, or the number on either or both of two lines, or the numbers on one specified line but not both, all at two nearly equal line separations w and $w + \Delta w$. The result is

$$N\Delta w \int_w^\infty F(x)dx$$

An undersize count is given by n'_5, i.e. differencing the numbers falling between two lines, giving

$$N\Delta w \int_0^w F(x)dx$$

By taking undersize or oversize counts at appropriate values of w a full size distribution can be obtained.

Some of these methods are more accurately described as individual since some association of signals is required, also some of them cannot be operated by a simple "on-off" detector in conjunction with a simple aperture or pair of spots.

Extension to non-circular particles. The extension of methods based on frequency interception of non-circular particles is discussed here as being typical. If a particle may be found in any orientation, the mean probability of interception is the same as that of a circle of equal perimeter and may be measured by the diameter of that circle, conventionally referred to as the perimeter diameter. For a non-re-entrant profile this is equal to the mean of the projected diameters, i.e. the separation of parallel tangents. In practice then similar particles variously oriented are represented in methods based on frequency of interception by values distributed about a mean which is the common perimeter diameter, and the apparent frequency distribution of a number of particles having various perimeter diameters is a broadened version of the true one. In certain orientations a re-entrant profile might be counted as two particles. In Fig. 2 the results of counting two particles by a recommended method involving differencing counts of total obscuration of a slit of variable width[1] are shown, the particles each being given many orientations. It may be seen that each particle appears as less than one full-size particle, together with positive and negative small particles. The distribution of projected diameters in various orientations is given for comparison.

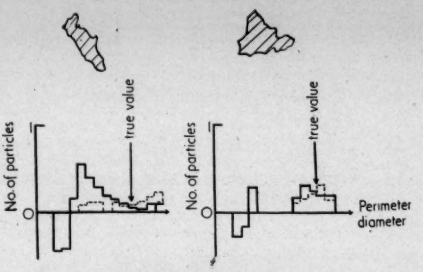

Fig. 2. Count of irregular shaped particles

———— by statistical analysis of frequency of intercepts
– – – – by projected diameters

INDIVIDUAL METHODS

Individual methods involve a means of identifying particles, so that all the information from repeated interception of the same particle can be associated, and also a method of assessment. Various parameters, appropriate to various methods of assessment, are available for an assembly of irregular particles; size orders according to these various parameters differ, but a high correlation between them is expected and it is probably immaterial which is used. The merits of the parameters are not considered further here.

The practicable means of identifying particles reduce to identifying and counting unique points on each particle. Certainly for irregular particles, and probably for others, the only readily identifiable points are the extremities in directions related to the direction of scan. Once a particle is identified, all information relating to it must be associated.

Criteria of association. The suggested criteria of association are: (i) A criterion of anticipation, in which signals from adjacent scans starting within a predetermined time interval of each other (after allowing for any time interval between scans) are assumed to derive from the same particle. (ii) An overlap criterion, in which signals from adjacent scans overlapping in time (again after allowing for any interval between scans) are assumed to derive from the same particle. The choice of the best criterion must be made on the grounds of the ease of application and of the amount of dead space involved.

Dead space associated with criteria of association. The overlap criterion in its most economical form, in which the comparison is made only with the signal from the adjacent scan, leads to a dead space in the form of a border round the particle of width equal to or less than the separation of adjacent scan lines. This is frequently the limit of resolution, and it then represents a minimum dead space.

If it is necessary to superimpose signals from adjacent scans (either to give a measure of particle size or to simplify the memory circuits) and to operate the criterion from this composite signal, then the dead space is the area of the shadow projected by the particle into a line which just fails to intercept

the particle (see Fig. 3). For a circular particle of radius R, this area is $0{\cdot}43R^2$.

The anticipation criterion leads to a dead space in the form of "steps" whose size depends on the variations in size and shape of the particles. For circular particles, the maximum anticipation is that dictated by the first-to-second scan of the largest particle (radius R_1), i.e. $1{\cdot}4\sqrt{R_1S}$, where S is the scan separation.

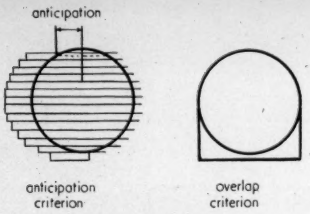

Fig. 3. Dead space

The dead space for a particle of radius R, which is taken to occur only on the leading edge, is approximately (see Fig. 3)

$$2R \times 1{\cdot}4\sqrt{R_1S} = 2{\cdot}8R\sqrt{R_1S}$$

Applying these results to a typical distribution curve of sizes with cuts at diameters of $0{\cdot}5\ \mu$ and $5\ \mu$, we find that dead spaces are equal in the two methods for $S = 0{\cdot}05\ \mu$ approximately. An increased separation of scan lines, or a greater spread in the size distribution, is favourable to the overlap criterion. Since the limit of resolution in any optical system is about $0{\cdot}25\ \mu$, then for circular particles the overlap criterion is the more favourable for likely scan separations and size distributions.

Some considerations of accuracy. In statistical methods, where results are obtained by combining independent counts, the standard errors are cumulative, and to achieve a given confidence limit larger individual counts must be made than if the result was obtained in a single count. Typically, a simple count (without sizing) may be obtained by a single operation, e.g. traversing the field with twin spots using the guard-spot technique (n_4 in the table) or by traversing the field twice; first with twin spots and then with one ($n_3 - n_1$ in the table). In the first technique it is required to use a criterion of association; in the second technique it is required to increase the length of scan by a factor of 6 compared with that in the first to achieve the same confidence limits in counting equal particles, or by 24 in counting particles in a typical size distribution. If sizing is included as well, then using a recommended statistical method[1] requires an increase in the length of scan by a factor of 40 compared with an individual method if a simple oversize count is enough, or by 120 if particles are to be sized within limits of $0{\cdot}5\ \mu$.

If the successive scans in a statistical method are not independent (e.g. if the single spot is designed to trace a path traced previously by one or two twin spots) then the increase in scan length is reduced, but the technique may be less simple to operate, and in fact tends to an individual method.

Another source of error is the discontinuous nature of line scanning. Classification into sizes must then give graded cuts. For instance, the first definable size contains particles which intercept two scan lines simultaneously. If the whole field is covered by the scan raster of line separation w (centre to centre) and effective line width p the probability of a circular particle of diameter x intercepting simultaneously two lines of the raster is $(x + p)/w - 1$ (see Fig. 4). This varies from 0 to 1 as x varies from $(w - p)$ to $(2w - p)$ and the "cut" is therefore a graded one having a 50% value at $x = 3w/2 - p$. It is of interest to note that, in theory at

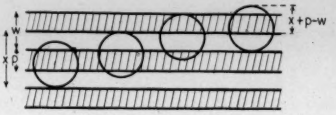

Fig. 4. Probability of intercepting two scan lines

least, particles can be classified as of diameter x by use of scan lines at a separation greater than x. In practice uncertainties in the effective value of p introduce difficulties, and also signal-to-noise ratios deteriorate. The next class, that of particles intercepting three scan lines simultaneously, is graded from $x = (2w - p)$ to $(3w - p)$.

There is a more serious source of error. All the methods summarized above require either: (*a*) recognizing particles which fall wholly within a path or traversing slit, and also recognizing as separate two or more particles intercepting a slit simultaneously, or (*b*) using at some stage an aperture or path width w which is smaller than the smallest particle present, and, in some cases, providing apertures which differ by a small known increment Δw.

In all cases of (*b*) the count obtained is directly proportional to the small width w or increment of width Δw, and any errors in estimates of either of these two quantities appear as at least proportionate errors in the final counts, and if a statistical method is employed in which counts are combined, the errors are cumulative and possibly exaggerated. Now in many applications of particle counting and sizing the range of size approaches the limits of optical resolution, and would no doubt be pressed further if a better resolution were available, as for instance by using radiation of a shorter wavelength. It follows that all these methods of type (*b*) require an accurate estimate of a size, or change in size, of an aperture or separation of spots, which size is itself required to be as small as or smaller than the limits of optical resolution. Moreover, the size which must be estimated is a function of the interaction of an aperture or spot with the image of a particle, and the effective size varies therefore as images are changed or substituted.

Now these large proportionate errors arising from working near the limits of optical resolution are perhaps inevitable in assessing the small images, but they are not necessary when large images are being scanned, where the necessary proportionate indeterminacy is small. In effect, these methods listed under (*b*) above view only the indeterminate fringe of image, and take no note of the main bulk which, for a large image, is easily observed. The effect may be illustrated by reference to counting by guard-spot; it was in this connexion that the weakness of methods involving the accurate estimation of small displacements was first pointed out by W. H. Walton.[4] In guard-spot techniques, the lines traced out by the spots form the two edges of a path, and all particles having one extremity (say the upper one) falling within that path are counted. The area scanned is the area of the path. It may be made up of a single length, or a number of disconnected lengths which may or may not be parallel and adjacent. This is still true when the paths are designed to be parallel and adjacent and to scan completely an area which is known

independently, for it cannot be known whether this object has been achieved unless the path width is known or, what is equivalent, the ratio of the path width to the width of the field to be scanned is known. If, due to an error, the edges of adjacent paths overlap, some particles are counted twice (see Fig. 5). The increase in the count is that due to the extra area scanned in the overlaps. Similarly, if the edges of the paths fail to meet, some particles are missed (see Fig. 5) and the count is too small by an amount appropriate to the missed

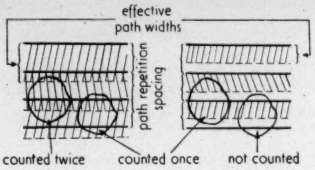

Fig. 5. The effective area scanned

area. Thus in all cases of counting by guard-spot, the accuracy is limited by the accuracy with which the nominal width of the path is determined, and any indeterminacy here appears as an indeterminacy in the final count. Moreover, this inaccuracy is dictated by the smallness of the smallest particles, and is perhaps inevitable there, but it appears equally in the count of the larger particles, where it is not necessary.

The only way of avoiding this error is to ensure that the spots are identical. This must be taken to include not only the light beams, but the detecting elements as well. In effect the only way to do this is to use one spot only, to convert signals to the on-off form, and to memorize successive traces.

Since the methods listed in (*b*) are not admissible, at least if the size range approaches the limits of optical resolution, we must examine the methods (*a*). The requirements for these cannot be met by a single simple on-off device, and only with difficulty by any other device, unless the scanning aperture consists of a line of detecting elements each capable of independent action—"a multi-line scan."[5] The multi-line scan could be produced by drawing a number of single line scans in succession and memorizing them (a magnetic memory is a convenient form of cyclic memory[6]), or by scanning the image simultaneously by a number of detecting heads with associated light-ducts. Flying-spot techniques applied to the sample or detectors applied to an enlarged moving image are both possibilities.[5] Whichever method is used the effect is to scan the sample with a comb of detecting heads.

The method has an incidental but important advantage that the problems of association of signals are much simplified since the leading edge of a particle is the first to be observed, and for all later signals from the same particle it is known at the inception of the signals whether they are to be associated with those already recorded, except for some, but not all, cases of particles having re-entrant profiles.

CONCLUSIONS

In the applications of automatic counting to particles that approach the limits of optical resolution, any method depending on defining accurately the relative positions and sizes of two or more closely spaced optical probes tends to be suspect. It would be required to match the probes (that is, two spots together with their associated projecting and detecting equipment) exactly. In practice this would be best achieved by using one probe only and comparing idealized signals recorded by a memory system. This elaboration discounts the advantages of statistical methods (which in any case introduce their own additional difficulties in the number of observations required to give statistically reliable results) and greatly reduces the advantage of simplicity in the guard-spot method. Methods requiring the comparison of small apertures are open to rather similar objections.

The alternative is to use an aperture so large that small errors of definition become negligible except for the smallest particles, where the errors are unavoidable. At the same time the presence of particles which do not fill the aperture must be recognized. This is most easily achieved by a multi-line scan.

A multi-line scan could be obtained by the use of a single probe and a memory system, or by simultaneous scanning of an enlarged image by an array of probes. The method lends itself to the use of the overlap criterion of association which is in any case the most economical.

ACKNOWLEDGEMENT

The author is indebted to Dr. W. Idris Jones, Director-General of Research in the National Coal Board, for permission to publish this paper; the views expressed are the author's, and not necessarily those of the Board.

REFERENCES

(1) HAWKSLEY, P. G. W. Private communication; *Nature [London]*, **17**, p. 984 (1952).
(2) DELL, H. A., and JONES, E. British Patent Application 5473/51.
(3) DELL, H. A. This Supplement: Paper G.4.
(4) WALTON, W. H. Private communication.
(5) PHILLIPS, J. W., THOMAS, D. G. A., and WALTON, W. H. British Patent Application 12789/53.
(6) WALTON, W. H., THOMAS, D. G. A., and PHILLIPS, J. W. British Patent Applications 29460/51 and 23720/52.

[*The discussions on Sessions F and G were taken together and will be found on pp.* S 175–S 180]

SESSION G. AUTOMATIZED COUNTING AND SIZING: PHOTOELECTRONIC MACHINES

Chairman: J. BRONOWSKI, M.A., Ph.D.

Paper G.1

A photoelectronic instrument for counting and sizing aerosol particles*

By Prof. F. T. GUCKER, JR., Ph.D., and D. G. ROSE, M.A., Ph.D.,† University of Indiana, Bloomington, Indiana, U.S.A.

The instrument described, using a new arrangement of stops, collects light scattered between 1 and 20° of the forward direction and focuses it upon a photomultiplier tube. The resulting electrical pulses are amplified, sorted with a single-channel pulse height selector, and counted. With an aerosol of refractive index 1·5, the instrument counts particles of 0·17 μ radius or larger, and its response is linear with radius over the range of 0·25 to 0·50 μ, with a sensitivity of 0·001 μ and a reproducibility of 0·01 μ. Data for a typical 16-step histogram, based upon 3350 counts covering a total range of 0·22 μ, were obtained in 40 min, and could be obtained in 2 min with a 16-channel pulse height selector.

In developing aerosol counters suitable for particle-size determination, we have calculated from Gustav Mie's[1] theory of colloidal light scattering the response to spherical isotropic particles in right- and forward-angle scattering systems. Space does not permit the presentation of our calculations, but they show that the response curves of right-angle scattering counters increase with particle size through a series of plateaux, between 0·15 and 0·50 μ, while those of forward-scattering counters increase regularly over this range. These calculations show the advantage of the forward-scattering system for particle size determination, allow us to estimate the most efficient lens system, and emphasize the importance of refining the dark-field system to minimize the difference in aperture between collecting lens and dark stop.

bright slit image, each particle is illuminated for an instant. The light pulses scattered in the forward direction are collected by a lens nearly filling the image of the dark stop, and strike the photocathode of a 1P21 photomultiplier. Thus each smoke particle passing through the counter causes the photomultiplier to emit an electrical pulse which is amplified, classified by height, and counted.

OPTICAL SYSTEM OF THE COUNTER

All components of the optical system shown in Fig. 1 are supported on an optical bench, either in standard carriages or in cradles which allow adjustment and focusing. The ribbon filament micro-illuminator A (by the General Electric

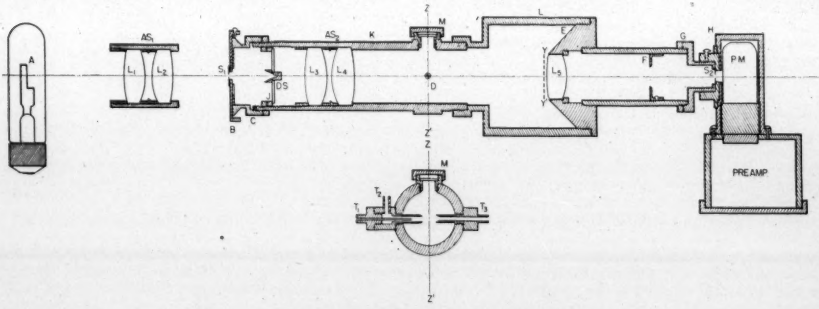

Fig. 1. Optical system of the counter

The present instrument resembles those which we have described previously,[2,3,4] differing from our first forward-scattering counter chiefly in the greatly improved dark-field illumination. The circular dark stop is placed between a brightly illuminated slit and an achromatic condensing pair which forms a sharp image of the dark stop beyond the bright image of the slit. As the aerosol stream flows through the Co. of Schenectady), operated at 6·3 V and 18 A from an Electro (Model B) filtered d.c. power supply, is surrounded by a glare shield through which cooling air is blown. An image of A is formed upon slit S_1 by the achromatic condensing pair L_1, L_2, of 46 mm diameter and 77 mm focal length. Scattering from the ground edges of the thick lenses, which produces a "halo" around the image, is prevented by a sharp stop AS_1 placed between the lenses. S_1, 2·7 × 0·5 mm, is cut with a sharp razor blade from 0·13 mm (0·005 in.) copper sheet, attached to a brass cap B fitting over a sleeve C

* Contribution No. 612 from the Department of Chemistry.

† Now at Applied Physics Laboratory, the Johns Hopkins University, Silver Spring, Maryland, U.S.A.

and held in place by three machine screws (one shown) engaging the 45° conical face of C; thus the slit can be focused by screwing C without rotating B, and centred by the screws. C is held in final position by a lock nut, as are the holders J, G, for the dark stop and the final slit, which also are threaded for focusing.

The condensing pair L_3, L_4, of 49 mm diameter and 75 mm focal length, form an image of S_1 in plane ZZ', containing the axis of the smoke and sheath air tubes, beyond which the diverging light strikes the round conical light trap E. A sharp stop AS_2, 40 mm in diameter, prevents light scattering from the ground edges of this pair of lenses and, being smaller than AS_1, acts as aperture stop for the system, giving a 15° half-angle of convergence.

The sharp-edged conical brass dark stop DS is sealed in the centre of a coated glass disk mounted on a threaded brass ring J. Lenses L_3, L_4, form an enlarged image of DS in plane YY', which actually coincides with the entrance pupil of lens L_5. The radius of the sharp retaining shoulder of the lens mount is 1 mm smaller than the image of DS; hence L_5 collects light scattered between 1 and 20° of the forward direction, and forms a secondary image of S_1 upon slit S_2 which is the same size as S_1. The location of the dark stop between S_1 and L_3 in this counter is vastly superior to the previous location at or near the second surface of L_4 which, with any finite light source, gives a dark cone surrounded by a penumbral half-shadow, requiring a collecting lens aperture 8° less than that of the stop, with correspondingly smaller light pulses.

In the design and construction of this optical system, every precaution was taken to reduce stray light, which ultimately limits the sensitivity of the instrument. All inner surfaces of the counter were coated with an optical black lacquer. A glare stop F, placed where L_5 forms an image of the ring of light scattered from the second surface of L_4, eliminates this light without reducing that scattered from a particle in the plane ZZ'.

Uniform illumination of the image space at D is necessary to allow correlation of pulse height and particle size. The image brightness, measured by a photoelectric probe with a 0·4 mm aperture built by O'Konski,[4] was found to vary $\pm 0{\cdot}6\%$ over a vertical distance of ± 3 mm from the axis, 1% over a horizontal distance of $\pm 0{\cdot}5$ mm in plane ZZ', and $\pm 3\%$ over a horizontal distance of $\pm 1{\cdot}65$ mm along the axis of the beam. Thus with a source slit up to 0·5 mm wide and a smoke tube diameter up to 2·3 mm, the variation in the illumination of the particles will not exceed $\pm 4\%$.

In the flow system shown in Fig. 1, the aerosol and the surrounding sheath of filtered air enter respectively through T_1 and T_2, at pressures slightly above atmospheric, and are exhausted through T_3 at a pressure slightly below atmospheric. This flow system differs from those in our previous counters[2–4] only in the dimensions which conform to the usable image size. With a central sample tube 2·26 mm in diameter, and a flow rate of 1 litre/min, the aerosol flow is 416 cm/sec, corresponding to a Reynolds' number of 602 (well below the turbulent region) and giving, with a slit 0·5 mm wide, a pulse length of 120 μsec. The outer tube diameter of 4·7 mm gives the sheath air the same linear flow rate at 3 litres/min.

ADJUSTMENT OF THE OPTICAL SYSTEM

The dark stop and slits S_1 and S_2 are adjusted and locked in place when the counter is assembled. First, the barrel K and cylinder L are screwed together and alined on the optical bench. A focusing jig screwed into the right end of L holds a ground-glass screen in the plane of the entrance pupil of L_5. Using any convenient light source, dark stop DS is adjusted to focus its image upon the screen. Next, the focusing jig is replaced by the light trap and viewing lens assembly E; the slit S_1, lenses L_1, L_2, and lamp A are put in place; and the filament is approximately focused on S_1. Now filtered air is passed through T_2 and concentrated cigarette smoke through T_1. When lamp A is turned on, sleeve C is screwed in or out until the image of S_1 is centred on the smoke stream, viewed through the hole in the barrel normally closed by cover M, and S_1 is adjusted by means of the three screws on cap B until the whole smoke stream appears illuminated when viewed through lens L_5. Next G is adjusted to focus the secondary image of S_1 sharply on a small glass reticle put in place of S_2. Finally S_2 is replaced, adjusted to allow the complete smoke stream to be seen, and fastened to G. The position of the phototube behind S_2 is not critical.

ELECTRONIC SYSTEM OF THE COUNTER

A block diagram of the electronic system is shown in Fig. 2. Commercial components were used wherever possible; but the preamplifier, amplifier, and integral pulse height selector were designed and built to meet the special requirements of

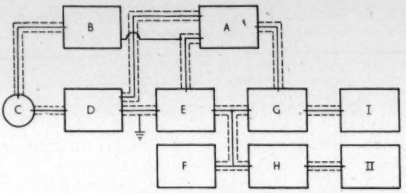

Fig. 2. Block diagram of the electronic system

A, anode and heater supply; *B*, high voltage supply; *C*, photomultiplier; *D*, preamplifier; *E*, amplifier; *F*, cathode-ray oscilloscope; *G*, integral pulse height selector; *H*, 1-channel pulse height selector; I, scaler I; II, scaler II.

this counter. The whole system was carefully earthed to reduce pickup in the early stage of the amplifier, which must include some method of differentiating against the noise from the photomultiplier, and be completely free of underswing and linear over the entire output range, 0–100 V in this instance. The output from the amplifier was fed to two channels: (1) the integral pulse height selector G, consisting of a Schmitt trigger circuit set at a low bias voltage to count all pulses, and (2) the Atomic Model 510 single channel pulse height selector H to determine the number of pulses in any particular voltage range. The ratio of the two counts gives the fraction of the total number of pulses lying within the chosen voltage range.

The detector, C, is a 1P21 photomultiplier tube with an S-4 photosurface having a bell-shaped spectral response curve between 3000 and 7000 Å, with a maximum at 5100 Å. A schematic diagram of the photomultiplier and preamplifier circuit is shown in Fig. 3. A Furst Electronics Model 810-P regulated power supply, continuously variable from -150 to -1500 V, provides the voltage drop of about -800 V across the dividing resistors connected to the dynodes of the photomultiplier. The capacitors C_1–C_4 maintain the voltages on the last four dynodes even when large current pulses flow

between them. The grid of the 6AK5 preamplifier V_1 operates at earth potential and the 1 MΩ grid resistor acts as load resistor for the photomultiplier. The 6AK5 preamplifier is pentode connected and operated as a cathode follower, but the cathode resistor is on the amplifier chassis. The heater and anode supplies and an earth lead are connected to the preamplifier through a four-conductor microphone connector. The photomultiplier supply and the output signal are brought through Amphenol single-conductor connectors. The output is connected to the amplifier chassis by about 3 ft of Amphenol RG58/U coaxial cable.

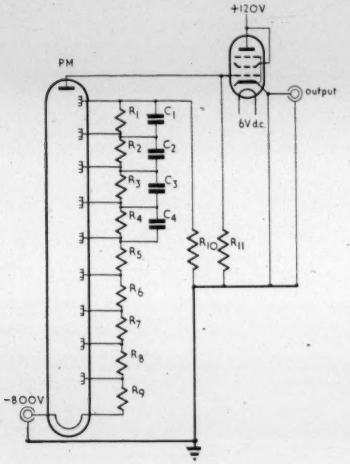

Fig. 3. Phototube and preamplifier circuit

R_1–R_9 = 100 kΩ
R_{10} = 100 kΩ
R_{11} = 1 MΩ
C_1–C_4 = 0·01 μF
V_1 = 6AK5
P.M. = 1P21

Fig. 4 is the schematic diagram of the amplifier and Schmitt trigger, mounted on a single chassis. The 2 kΩ Helipot gain control RV_1, which is the preamplifier cathode resistor, is connected to a simple RC integrating circuit consisting of an 820 Ω series resistor R_1 and 0·1 μF capacitor C_1 to earth, designed to attenuate the 0·01 μsec noise pulses in comparison with the 120 μsec signal pulses. Thomas and White[5] show that the best signal-to-noise ratio results when the time constant of the integrating circuit equals the length of the pulses. However, the other time constants of the circuit must be 100 times smaller, as shown by Elmore and Sands,[6] to avoid more than 1% underswing of the amplifier. The integrating circuit is coupled through a 0·1 μF capacitor C_2 to the first amplifier stage, a degenerate pentode, V_1, which is followed by a two-valve feedback loop, V_2, V_3. The maximum amplifier gain was 700, measured to 2% (with an oscilloscope standardized against a d.c. potential), by comparing the amplitude of 120 μsec negative square input pulses with the peak amplitude of the output pulses; the response was linear, and the rise time 115 μsec.

The low-frequency amplifier cut-off at about 20 c/s necessitated the following precautions to reduce the 120 c/s output ripple to a negligible 0·2 V at full gain: (1) the 6AK5 pentode heater was heated by a 6 V storage battery, (2) a 5693

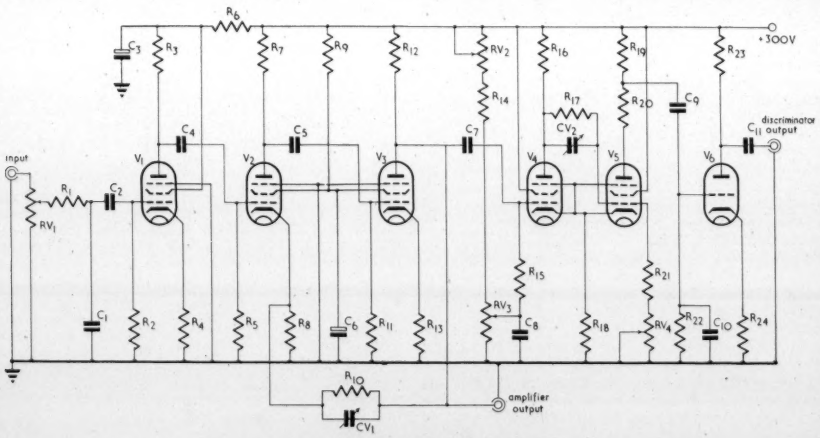

Fig. 4. Schematic diagram of the amplifier

R_1 = 820Ω
R_2 = 220 kΩ
R_3 = 6·8 kΩ
R_4 = 100 Ω
R_5 = 1 MΩ
R_6 = 20 kΩ, 10 W
R_7 = 18 kΩ, 2 W
R_8 = 150 Ω
R_9 = 2–33 kΩ, 2 W in parallel
R_{10} = 18 kΩ
R_{11} = 1 MΩ
R_{12} = 4–22 kΩ, 2 W in parallel
R_{13} = 150 Ω
R_{14} = 75 kΩ w.w.
R_{15} = 1 MΩ
R_{16} = 4 kΩ w.w.
R_{17} = 100 kΩ w.w.
R_{18} = 10 kΩ, 2 W
R_{19} = 560 Ω
R_{20} = 4·8 kΩ
R_{21} = 40 kΩ w.w.
R_{22} = 100 kΩ
R_{23} = 4·7 kΩ
R_{24} = 4·7 kΩ
RV_1 = 2 kΩ Helipot
RV_2 = 150 kΩ w.w.
RV_3 = 50 kΩ Helipot
RV_4 = 25 kΩ w.w.
V_1 = 5693
V_2 = 6AC7
V_3 = 6AC7
V_4 = 6AC7
V_5 = 6AC7
V_6 = 6J5
C_1 = 0·1 μF
C_2 = 0·1 μF
C_3 = 20 μF electrolytic
C_4 = 0·01 μF
C_5 = 0·01 μF
C_6 = 20 μF electrolytic
C_7 = 0·01 μF
C_8 = 0·01 μF
C_9 = 50 μμF
C_{10} = 20 μμF
C_{11} = 0·01 μF
CV_1 = 1·5–7 μμF
CV_2 = 25 μμF

pentode V_1 with more rugged construction and wider spacing between heater and cathode replaced a 6SJ7 pentode in the input stage, and (3) an earth lead was run directly from the photomultiplier power supply B to the amplifier earth as shown in Fig. 2.

The output from the anode of V_3 goes directly to the Atomic Model 510 single channel pulse height selector, the input circuit of which is a 0·01 μF capacitor and a 1 MΩ grid resistor. These same values were chosen for the coupling circuit of the Schmitt trigger, V_4, V_5, to match the input characteristics of the two instruments. The Schmitt trigger is like that described by Elmore,[7] with a 50 kΩ Helipot RV_3 as bias resistor for the first valve. The positive rectangular pulse from the second valve of the Schmitt trigger is taken over part of the anode resistor of V_5 and fed to a phase inverter, V_6, which gives the negative pulse necessary to operate the Berkeley Model 1000 recording scaler (I, Fig. 2), to which it is connected through a length of coaxial cable.

ADJUSTMENT OF THE ELECTRONIC SYSTEM

The capacitance of the variable capacitor in the feedback loop of the amplifier is increased until the output shows no tendency to overshoot. RV_2 in the Schmitt trigger is set to give 100 V across the 50 kΩ bias Helipot RV_3, and RV_4 is adjusted until the trigger "flips" as the Helipot slider is raised slowly to the top. When the slider is lowered, the Helipot reads directly the voltage of the minimum pulse which will fire the trigger, i.e. 100 V minus the grid bias of V_4.

In the Atomic single channel pulse height selector, base-line and channel-width potentiometers set the minimum voltage pulse counted and the counting range. Thus if these are set at 25 and 5 V respectively, pulses between 25 and 30 V will be counted. If the channel-width potentiometer is opened fully, the instrument passes all pulses above the base line. The counts are recorded on a Model DS-1 decade scaler (II, Fig. 2), by the Nuclear Measurements Corporation. This scaler and the integral scaler are operated from the same preset time clock. The variable bias resistor of the Atomic Model 510 pulse height selector was found to be accurately calibrated and, with the channel-width potentiometer fully open, our Schmitt trigger was adjusted by counting the amplified noise from the photomultiplier simultaneously with both instruments and changing RV_2 to equalize their counting rates at the same bias levels.

TESTS OF THE NEW COUNTER

The counter was calibrated with a series of DOP (dioctylphthalate) aerosols produced in modified La Mer–Sinclair generators.[8] The first (I) was built by G. J. Doyle[9] and the second (II) by P. Dorain. The particle size of each aerosol was determined by two methods based upon calculations from the Mie theory: (1) noting the number and angular positions of the red bands in the higher order Tyndall spectrum[8,10,11] and (2) determining the wavelength of the maximum in the absorption spectrum[10,12–14] with a Beckman Model DU spectrophotometer having a 10 cm gas cell.

The generators gave 1 to 10 $\times$ 10^5 particles per c.c. This concentration is necessary for the determinations of particle size, but requires dilution before entering the counter, which has a maximum counting rate of 3000 particles/litre, at 1 litre/min, for 1% or less coincidence. We used a quantitative Venturi diluter described by O'Konski,[15] consisting of one to four stages, having individual dilution factors between 25 and 60.

The counting efficiency of the instrument was found by determining the particulate concentration of an aerosol from the generator, then diluting and counting it. Following La Mer,[8,12–14] the particulate concentration is calculated from the optical density at the maximum of the absorption spectrum and the corresponding scattering cross-section obtained from the Mie theory for particles of the known size and refractive index. The scattering curve for an aerosol of refractive index 1·50 was taken from the calculations of Langmuir cited by La Mer.[16] Immediately after counting, the dilution factor of each stage was determined by comparing the inlet and outlet aerosol in a visual penetrometer, and the overall dilution ratio was calculated. This involves the greatest uncertainty in the measurement, with a standard deviation of 8%. We obtained a value of 95 ($\pm$8)% for the counting efficiency, and conclude that the instrument counts essentially all of the aerosol particles which pass through it.

To calibrate the counter, the size of each of a series of aerosols was measured, after which it was diluted and run through the counter to give a pulse-height distribution histogram. Two typical results are shown in Fig. 5. Curves

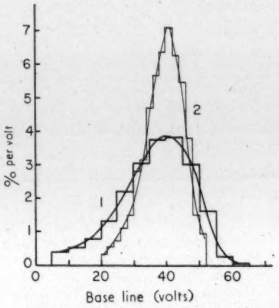

Fig. 5. Typical pulse-height histograms obtained with the counter

1 and 2, employing respectively 5 and 2 V windows, are normalized to the per cent of counts per volt window, to be directly comparable. They show clearly the greater homogeneity of the output of generator II. Curve 2 is based upon 3350 counts taken in 40 min. From such data we obtained the mean and the standard deviation of each pulse-height histogram. The calibration data are given in the table. The radii from absorption spectra average 0·02 μ larger than those from Tyndall spectra, which are used as abscissae in Fig. 6. This plot shows that the response of the counter, which must curve up from the origin, may be considered linear with particle size from about 0·25 to 0·50 μ, then goes through a maximum and decreases. Since the curve falls off above 0·50 μ, the pulse-height distribution of aerosols having a spectral radius above 0·45 μ is skewed to the left, and the mode is a better measure of central tendency than the mean. These modes are plotted as open circles in Fig. 6 and the curve is drawn through them. The standard deviation of the individual points from the linear portion of the curve is only 0·022 μ. Its slope is 140 V/μ; hence the 0·1 V electrical sensitivity of the instrument corresponds to less than 0·001 μ. Fig. 6 allows us to interpret voltage settings in terms of particle size provided no particles exceed 0·50 μ radius. During this work particles as small as 0·17 μ in radius were counted at a discriminator setting where the background averaged 3 counts per min.

Calibration data for the aerosol particle counter

Radius (μ)				
Tyndall spectra	*Absorption spectra*	*Δ*[b] *(μ)*	*Distribution mean (V)*	*Standard deviation (% of mean)*
0·25	—		14·7	48·9
0·32 (0·32, 0·32)[a]	0·35	0·03	25·1	43·9
0·32 (0·32, 0·32)[c]	—		24·9[c]	16·9[c]
0·36 (0·36, 0·36, 0·35)	0·35	−0·01	29·1	34·8
0·38 (0·39, 0·38, 0·38)	—		34·1	29·0
0·40 (0·40, 0·40, 0·39)	0·38	−0·02	36·6	28·7
0·40 (0·41, 0·40, 0·39)[c]	—		39·1[c]	15·8[c]
0·40 (0·40, 0·39, 0·40)[c]	—		45·4[c]	9·8[c]
0·41 (0·42, 0·40, 0·41)[c]	—		45·8[c]	9·1[c]
0·41 (0·42, 0·41, 0·40)	0·44	0·03	37·3	28·6
0·42 (0·42, 0·42, 0·42)	0·46	0·04	36·6	29·8
0·43 (0·43, 0·43, 0·43)	0·47	0·04	43·2	25·8
0·47 (0·47, 0·47, 0·45)	0·54	0·07	43·5	20·3
0·48 (0·48, 0·48, 0·48)[c]	—		50·2[c]	8·8[c]
0·50 (0·51, 0·52, 0·48, 0·50)	0·50	0·00	50·0	18·1
0·51 (0·51, 0·51, 0·48, 0·53)	0·50	−0·01	49·1	18·0
0·60 (0·60, 0·60, 0·60)	0·64	0·04	47·2	12·0

(*a*) The values in parentheses, following the average, were obtained from the positions of successive red bands, when more than one was observed.

(*b*) Δ is the difference between the radii determined from Tyndall and absorption spectra.

(*c*) These data are from generator II.

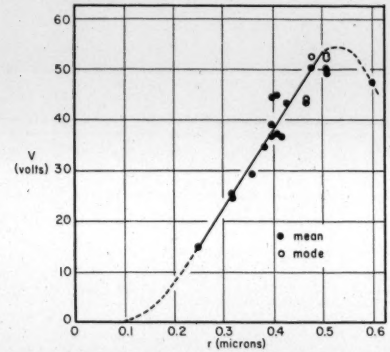

Fig. 6. Calibration curve for DOP ($m = 1{\cdot}49$)

The calibration curve for DOP parallels Sinclair's[17] total scattering curve for a refractive index of 1·50 reproduced in Fig. 7, but is somewhat smoother because white light is used in the counter. Use of one or more optical filters in the counter, to shift the response curve along the *r*-axis, should allow measurement of particle size in the range near 0·5 μ radius now inaccessible with white light. Fig. 7 shows that the range of applicability of the counter for measuring particle size increases with decreasing refractive index, and would extend up to about 0·8 μ radius for water fogs of refractive index 1·33, with green or white light.

Recently, R. Penndorf and B. Goldberg[18] have made more extended calculations of the scattering coefficients for spherical particles of several refractive indices over the range 0·1 (0·1) 30·0 in the parameter $\alpha = 2\pi r/\lambda$, the ratio of the circumference of the particle to the wavelength of the light. Their figures were used to calculate the total scattering of monochromatic blue, green, and red light by DOP particles up to 3·0 μ radius, with the results shown in Fig. 8. Parts of the scattering curves which increase monotonically are shown in full lines; the regions where they oscillate are dashed. Assuming that the small irregularities in the full curves are smoothed out somewhat by the band of wave-

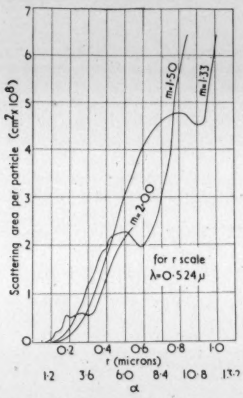

Fig. 7. Total scattering curves for aerosols of three different refractive indices [after Sinclair]

(Reproduced by permission of the Atomic Energy Commission, Washington)

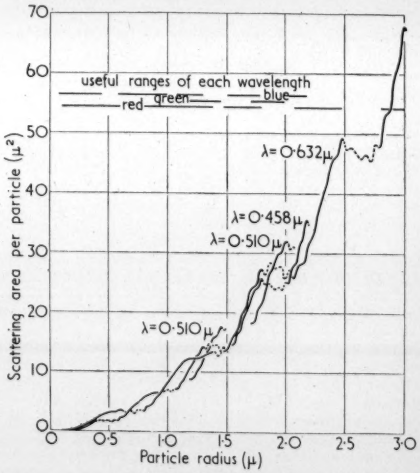

Fig. 8. Total scattering of blue, green and red light by DOP ($m = 1{\cdot}486$), based on calculations by R. Penndorf[18]

lengths passed by practical optical filters, it should be possible to measure particle size up to a radius of 2·5 μ by equipping the present counter having a response maximum in the green at $\lambda = 0{\cdot}510\ \mu$, with available red and blue filters having

peak transmissions at 0·632 and 0·458 μ respectively. The practicability of this system is being investigated in our Laboratory by Jesse E. White, to whom we are indebted for Fig. 8.

To minimize instrumental errors due to changes in light intensity we always ran the source at the same input power, and checked its constancy by measuring the steeply-rising integral background noise pulse distribution, which is sensitive to a change in the light level. No measurable change was observed over a period of 6 months. To avoid changes in photometric sensitivity, the amplifier was carefully designed for stability, and highly regulated power supplies were used for photomultiplier and amplifier. The largest known experimental uncertainty is about 4% in the illumination of the image space, which should be independent of particle size. This seems a reasonable estimate of the standard deviation of the instrument, since we found a standard deviation of only 9·1% for an aerosol of 0·4 μ radius from generator II, and previous experience with such generators indicates that at least half of this is due to the spread of particle size in the aerosol.

ACKNOWLEDGEMENTS

The research reported in this paper has been sponsored by the Geophysics Research Directorate of the Air Force Cambridge Research Center, Air Research and Development Command, under Contract No. AF 19(122)–375.

REFERENCES

(1) Mie, G. *Ann. Phys* [*Leipzig*], **25**, p. 377 (1908).
(2) Gucker, F. T., Jr., O'Konski, C. T., Pickard, H. B., and Pitts, J. N., Jr. *J. Amer. Chem. Soc.*, **69**, p. 2422 (1947).
(3) Gucker, F. T., Jr., and O'Konski, C. T. *Chem. Rev.*, **44**, p. 373 (1949).
(4) Gucker, F. T., Jr., and O'Konski, C. T. *J. Colloid Sci.*, **4**, p. 541 (1949).
(5) Thomas, A. L., and White, Locke, Jr. Final Rept., Oak Ridge National Laboratory, U.S. Atomic Energy Commission, from Southern Research Institute, Project 270, Report 6, 1952.
(6) Elmore, W. C., and Sands, M. L. *Electronics: Experimental Techniques*, p. 131 (New York: McGraw-Hill Book Co., Inc., 1949).
(7) Elmore, W. C. *Nucleonics*, No. 3, p. 16 (1948).
(8) Sinclair, D., and La Mer, V. K. *Chem. Rev.*, **44**, p. 245 (1949).
(9) Doyle, George J. *The Sonic Determination of Particle Size in Aerosols*, Ph.D. Thesis, Indiana University (May, 1952).
(10) La Mer, V. K., and Sinclair, D. OSRD Report No. 1668, August, 1943; issued as P. B. Report No. 32 200, Office of Publications Board, U.S. Department of Commerce.
(11) La Mer, V. K., and Gendron, P. R. *Chemistry for Canada*, **4**, No. 4, p. 44 (1952).
(12) Barnes, M. D., and La Mer, V. K. *J. Colloid Sci.*, **1**, p. 79 (1946).
(13) La Mer, V. K., Inn, E. C. Y., and Wilson, I. B. *J. Colloid Sci.*, **5**, p. 471 (1950).
(14) Inn, E. C. Y. *J. Colloid Sci.*, **6**, p. 368 (1951).
(15) O'Konski, C. T. *New Instrumental Methods in Aerosol Studies*, Ph.D. Dissertation, Northwestern University (1948).
(16) La Mer, V. K. OSRD Report No. 1857, 29 September, 1943; issued as P.B. Report No. 944, Office of Publications Board, U.S. Department of Commerce.
(17) Sinclair, D. "Optical Properties of Aerosols." Chapter 7 of *Handbook on Aerosols* (U.S. Atomic Energy Commission, Washington, D.C., 1950).
(18) Goldberg, B., and Penndorf, R. *New Tables of Mie Scattering Function for Spherical Particles*, to be published by the Geophysics Research Directorate of the Air Force Cambridge Research Center, Mass.

Paper G.2

The automatic size analysis of dust deposits by means of an illuminated slit

By L. Le Bouffant and J. L. Soulé, Centre d'Etudes et Recherches des Charbonnages de France
(Translated by R. J. Hamilton, B.Sc., A.Inst.P.)

The analysis of dust deposits by means of an illuminated slit allows simultaneous counting and size distribution analysis. For counting, it is possible to provide statistical compensation of errors due to fractional interception, overlapping, "coincidence," and lack of sensitivity by choice of an optimum slit length. Under these conditions classification by surface area gives accurate size distribution information. An apparatus designed to operate on these principles is described.

Many devices have been considered or built in order to provide automatic counting and size analysis of a sample of a product pulverized to microscopic sizes either by direct microscopy or from a photograph. A great number of these involve the scanning of the sample or its image by a flat pencil of light[1-4] (from an illuminated slit). The various methods based on this principle are compared in this paper.

PARTICLE COUNTING

All the processes are the same in principle, for particle counting, since each involves the counting of discrete light impulses detected by a receiving photocell. The basic problem concerns the errors which cause the number of light impulses to be unequal to the number of particles. It is possible to group these errors into four categories (see Fig. 1):

(i) *Fractional interception error.* Certain particles intercept two or more passages of the scanning beam.

(ii) *Overlap error.* Certain particles overlap each other in the projected image and are counted as one. Very often these errors will also be found in visual counting.

(iii) *Coincidence error.* Certain particles, quite distinct, are counted as one because their impulses overlap or are not far

enough apart for the apparatus to be able to separate them (size of scanning beam and "inertia" of the counting apparatus).

(iv) *Sensitivity error.* Certain particles (or edge fractions) are too small to be counted.

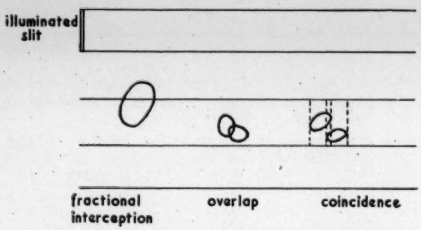

Fig. 1. Illustrating three of the errors present in particle counting

The use of a guard spot only permits the elimination of fractional interception errors under favourable conditions, and so does not entirely solve the problem, particularly when one wishes simultaneously to make a size distribution analysis.

It has appeared preferable to us to lean towards a statistical solution, remembering that the sample, however good it may be, is already subject to a statistical error (which follows Poisson's law) and therefore itself modifies the counting precision necessary.

It is possible to calculate the probability of the effects of the various errors.

(i) *Fractional interception errors.* If the length of the slit is d, a particle of apparent diameter D will give on average D/d additional transits. If the particles are orientated at random, D is on average P/π (P is the perimeter of the particle)[5]. We have $P/\pi = kx$, where x is the "equivalent" diameter (the diameter of the circle of the same area as the particle) and k a shape factor ($k \geqslant 1$). The extent of these errors will be on average then $\bar{k}\bar{x}/d$ (if the mean $\bar{k}$ is independent of size).

(ii) *Overlap errors.* Overlap errors have been studied for the case of particles deposited perfectly at random and independently for circular and rectangular shapes.[6] We have been able to extend the formula to the case of contours with any degree of convexity; the proportion of particles not counted owing to overlapping is:

$$\frac{N}{\Sigma}\left[\bar{S} + \frac{\pi}{4}(\bar{k}\bar{x})^2\right] \tag{1}$$

where $\bar{S}$ is the average surface area of the particles;
N is their number;
Σ the total area of the field

(neglecting the effect of overlapping of more than two particles at once).

(iii) *Coincidence errors.* Coincidence errors may be examined more easily by starting with a general expression in which they are not distinguished from overlapping errors. As a result of the fractional interceptions there are, for each unit of the scan length, on average:

$$n = \frac{dN}{\Sigma}\left(1 + \frac{\bar{k}\bar{x}}{d}\right) \tag{2}$$

particles or fractions encountered in random positions. It can be established that their mean length is

$$\bar{l} = \frac{\bar{k}\bar{x} + \bar{S}/d}{1 + \bar{k}\bar{x}/d} \tag{3}$$

In consequence of overlapping and coincidence, the proportion of particles and fractions counted amounts only to:

$$\exp(-n\bar{l}) = \exp\left[-\frac{dN}{\Sigma}(\bar{k}\bar{x} + \bar{S}/d)\right] \tag{4}$$

In order to correct for the dead time of the apparatus it is enough to add to $\bar{l}$ the length ϵ which is the minimum necessary to separate two signals so that they are counted separately.

(iv) *Sensitivity errors.* Sensitivity errors are a function of the apparatus. Very small particles will be covered entirely by the scanning beam; the extinction will in general be a function of surface area. On the other hand, fractions whose width is less than a certain value δ will not be counted: the proportion of "fractional" errors is then given by

$$(\bar{k}\bar{x} - 2\delta)/d \tag{5}$$

To sum up, if ϵ and δ are negligible, the ratio of the number of particles recorded to the real number of detectable particles will be, on average:

$$\left(1 + \frac{\bar{k}\bar{x}}{d}\right)\exp\left[-\frac{dN}{\Sigma}(\bar{k}\bar{x} + \bar{S}/d)\right] \tag{6}$$

It will be seen that the second term of the exponential corresponds to the first term of the overlapping errors. As a first approximation the expression for the average proportion of errors, as compared with visual examination (where overlapping errors are made) can be taken as

$$\frac{\bar{k}\bar{x}}{d} - \frac{dN}{\Sigma}\bar{k}\bar{x} \tag{7}$$

The form of this expression has suggested the elimination of errors by a statistical compensation. It will be seen that in effect it will be enough to take for this:

$$\frac{1}{d} = \frac{dN}{\Sigma} \quad \text{or} \quad d = \sqrt{\frac{\Sigma}{N}} \tag{8}$$

It is enough in this formula to introduce an approximate value for N (guessed, or obtained by visual examination) in order to decide the optimum width of scan. Conditions where δ and ϵ are not negligible lead to a smaller optimum value of d.

The errors occur practically independently: the fluctuations of their total number follow approximately Poisson's law. Under suitable conditions (the field of view not overcrowded) they will clearly be less numerous than the particles and their fluctuations will be smaller than that of the sampling. The total number of errors and thus the fluctuations of this total are at a minimum under conditions where they compensate for each other.

It has been implicitly assumed that scanning by contiguous traverses is being considered. Every other traverse of the scanning beam is evidently statistically equivalent, for the same area of scan.

SIZE ANALYSIS

The different methods whereby, starting from scanning by an illuminated slit, a size classification is obtained, consist in measuring various properties of the transmitted impulse, as follows:

(*a*) the apparent transverse diameter (maximum intensity of signal);

(*b*) the apparent longitudinal diameter (duration of signal);
(*c*) the surface area (the total intensity, integrated over the duration of the signal).

In fact, if we consider the object being classified, a dust particle, and the importance of its physical and chemical properties, it is clear that the essential geometrical parameter for classification is that of volume, followed by external surface area. In default of being able to measure these properties on a flat image, the best representative parameter remains projected area (for example, a needle-shaped particle will not be given an over-estimated "dimension"). In addition, the choice of surface area as a parameter eliminates the difficulty of orientation and the heterogeneity it introduces into size analysis. Finally, surface area, increasing as the square of the diameter, gives a more sensitive and therefore more exact measure.

The complication of the apparatus required to give this measure is not excessive. The need for perfect contrast in the image is shared with certain methods of classification by diameter.

The various kinds of error examined in connexion with counting also occur in size analysis, for which they can be calculated. A rigorous mathematical treatment is difficult, and this discussion is restricted to some general observations.

As with simple counting there is a tendency for compensation between fractional interception errors and coincidence errors. However, it is certain that for a narrow size range in the specimen the errors will tend to produce a spread (fractions appearing smaller than any whole particle, aggregates greater than any individual particle). In practice, the size distributions of dusts cover wide ranges (exponential distribution) and so this introduces no difficulty. According to this view the measurement of surface area has the advantage that, in spite of errors, it gives the total apparent surface area correctly and, therefore, if the exact number of particles is obtained, the mean surface area of the particles is given.

It seems clear to us that to apply a correction formula to the results in order to eliminate the errors on average would be an illusory complication, and that it is better to keep to this approximate compensation.

In the case where a precise size distribution over an extended range is required the use of two images at different magnifications will provide a satisfactory solution.

THE CONSTRUCTION AND PERFORMANCE OF AN APPARATUS FOR THE MEASUREMENT OF SURFACE AREA

The apparatus which has been constructed at this centre operates as follows.[3,7] A flat beam of light is projected on to a photographic plate which is moved to and fro with a lateral shift at the end of each traverse. The particles are reproduced in negative form, light on a dark background, and the light beam passes through the plate when it encounters the image of a particle. The luminous flux transmitted is proportional at each instant to the amount of beam limited by the profile of the spot. The light is focused on to a photocell. The "quantity of electricity" produced by this cell in the course of traverse of a particle is integrated by a condenser. The charge thus given to the condenser operates five counting circuits set at different levels. The classification operates thus as a function of the maximum charge obtained during the scan, which is practically proportional to the area of the spot, the time constant of the integrating circuit being high. The charge on the condenser is automatically removed after the scanning of each particle. In this way, a cumulative size distribution curve is obtained.

The apparatus is designed to analyse spots whose mean diameter is of the order of 1 mm. The photographic enlargement is chosen accordingly. It is possible thus to analyse samples of widely different particle size by magnification through a microscope (optical or electron) and by reduction if it is wished to examine macroscopic objects.

An experimental study of the possibilities of the apparatus has been carried out. The following points have been successively investigated on the actual prototype:

(*a*) each counter fluctuates with a scatter of less than 5% of the effective cut;
(*b*) the minimum size detected is 0·025 mm^2;
(*c*) the "resolving power" is about 0·5 mm, the width of the illuminated slit being 0·3 mm. (The improvement of these characteristics is in hand.)

Moreover, the size distributions obtained with the apparatus have been compared with true size distributions, on artificial plates (with geometrical shapes placed at random) and on photographs of dust samples. The validity of the preceding theoretical conclusions has been demonstrated, if the work is confined to samples with a particle surface covering not more than 5% of the field; thus it is possible to analyse correctly in number and size distribution a deposit of 400 dust particles on 70 cm^2, using a slit length of 3 mm.

CONCLUSIONS

The analysis of dust deposits by means of an illuminated slit allows simultaneous counting and size distribution analysis. For counting, the choice of an optimum slit length readily permits a statistical compensation of errors. Under these conditions classification by surface area provides precise size distribution information.

Note added 6 *May* 1954. I should like to give some details about the results as determined by our apparatus for particle sizing.[7] The value of the method has been checked by analysing artificial samples with geometrical shapes corresponding to the usual size distribution. One of the negatives analysed is shown in Fig. 2. The position and orientation of the rectangles have been chosen by lot. These samples have been analysed with variable slit lengths: 2,3,4 mm. The

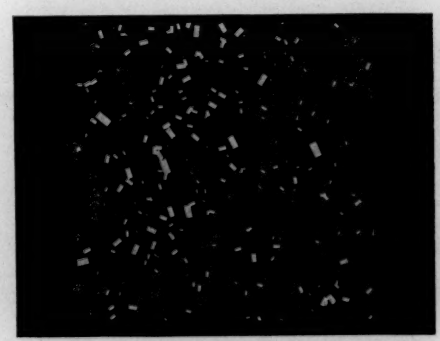

Fig. 2. Negative of geometrical shapes for test

direct results obtained with this negative give curves (Fig. 3) which surround the real curve obtained by visual counting. Here, the ideal slit would be 3·5 mm.

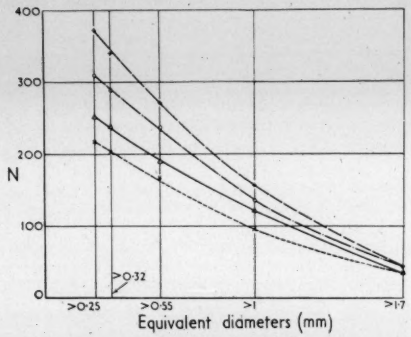

Fig. 3. Curves obtained from Fig. 2

—○— $d = 3$ mm —△— visual count
---×--- $d = 4$ mm —+— $d = 2$ mm

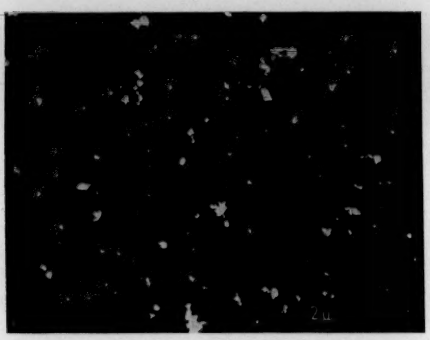

Fig. 4. Negative from electron micrograph of real dust sample

The experiments were repeated with real dust samples, such as with the plate shown in Fig. 4 taken with an electron microscope. The mean diameter is 1 μ and the magnification is ×1500. The curves are given in Fig. 5. Converted into percentages, these different curves show very slight variations about the real curve in spite of the important differences in the slit length used for scanning. The figure for the total

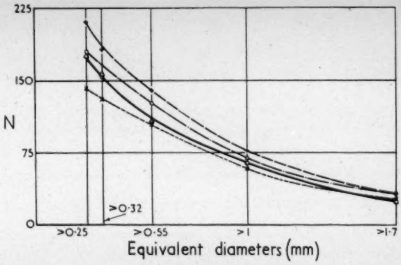

Fig. 5. Curves obtained from Fig. 4. (Key as for Fig. 3)

number of particles fits in well with the theory developed in this paper (taking into account δ and ϵ which in the present case are not negligible).

The method therefore seems to give precise results even for a small number of counted particles; the principle of a statistical compensation will fully operate only for a great number of particles (say more than 1000). The simplicity of the principle and its validity which has been experimentally established have led us to envisage the building of an improved prototype operating on films of 35 mm with a high speed of scanning.

REFERENCES

(1) WALTON, W. H. *Nature* [*London*], **169**, p. 518 (1952).
(2) LAGERCRANTZ, C. *Acta Physiologica Scandinavica*, **26**, Supp. 93 (1952).
(3) LE BOUFFANT, L., and SOULÉ, J. L. *C.R. Acad. Sci.* [*Paris*], **235**, p. 1207 (1952).
(4) HAWKSLEY, P. G. W. *Nature* [*London*], **170**, p. 984 (1952).
(5) BARBIER. *J. Liouville*, **5**, p. 273 (1860).
(6) ARMITAGE, P. *Biometrika*, **36**, p. 257 (1949).
(7) LE BOUFFANT, L., and SAILLARD, P. *Mesures et Controle Industriel*, **202**, p. 169 (1954).

DISCUSSION

Mr. P. G. W. Hawksley: In track scanning systems of the statistical type there is an error arising from coincidence of several particles. M. le Bouffant and M. Soulé in their ingenious method assume a random distribution of particle centres. In such a distribution there is in addition to coincidence, actual overlapping of particles and they work out the errors for both events. Whilst a random distribution may be true for thermal precipitator samples, it is not true in many other cases as shown by the absence of overlapping. In such cases it is not easy to work out the effect of coincidence. It is not sufficient to assume that the distribution is random because the magnitude of overlapping may be of the same order as that of coincidence. An experimental approach to coincidence correction seems necessary where a random distribution cannot be assumed.

Authors' reply: With methods using an illuminated slit, the law governing the geometrical distribution of the particles must be known in order to work out coincidence errors (whether they are eliminated by a mathematical treatment or by automatic compensation). For dust samples, it has been found that generally there is a random distribution (thermal precipitation, filtration, sedimentation, etc.). The only exceptions which we have encountered were certain deposits obtained by electrostatic precipitation (overlaps must not be confounded with pre-existing aggregates). It must be said at once that in the case where the particles are attracted towards each other in sampling, the deposit is not representative and has a chance of being unsuitable for examination. In addition to dust images, three-dimensional disperse systems all give (by projection or after sedimentation) random distributions (stars, blood cells).

On the other hand, plane sections (porous material, alloys,

inclusions) can give more regular distributions, as chance would do; particularly in these distributions overlapping is generally impossible. A tendency to regularity is found in dust samples where an electrical repulsion has occurred at the time of the deposit. Obviously such distributions must be considered in themselves as being better than random distributions, in so far as overlap errors are reduced.

In our study of automatic compensation, fractional interception errors are compensated by coincidence errors with the exception of overlap errors, in order to find with the apparatus the same results as by visual examination and not the theoretical values which are uncontrollable, especially when aggregates are present. It follows that our calculations are still valuable if there is a variation only in the overlap errors, i.e. if the distances between neighbouring elements are still random. If coincidence errors are also reduced, a study of the distribution law is necessary in order to determine the new compensation; this will be better, of course, than in the case of a random distribution.

Paper G.3

The automatic counting of red blood cells

By E. H. Cooke-Yarborough, M.A., A.M.I.E.E., and R. E. Whyard, B.Sc., Atomic Energy Research Establishment, Harwell, Berkshire

The paper considers automatic blood cell counting apparatus in which the cells are scanned by mechanical oscillation of a microscope stage. It is shown how errors can arise from various sources and how these errors may be minimized by use of suitable electronic circuits, by careful choice of parameters and by adopting a novel shape of scanning aperture.

Counting apparatus whose design follows these principles is described and the results are given of many experiments using this apparatus. These show that consistent results are obtainable which are largely independent of variations in light intensity, focus, cell size, amplifier and photocell sensitivity and of other variations likely to be encountered in practice.

1. Introduction

It is often necessary to count microscopic particles randomly distributed over a flat surface. Visual counting is slow, tedious and exacting; automatic counting is therefore very desirable.

Fortunately, red blood cells are almost circular in outline and their sizes fall within a fairly narrow range; in applying automatic counting techniques it is thus possible to avoid many of the difficulties[1] which arise when the particles are less uniform in shape and size. Nevertheless there are many factors which may cause errors. The more important of these are discussed in this paper and it is shown that the errors can be made satisfactorily small.

In visual counting by conventional means a sampling technique is employed; the particles are assumed to be randomly distributed over a flat surface and only those within one or more defined areas are counted. The problem then arises of deciding whether to count particles which straddle the boundaries of the counting area. The automatic counting methods described below present a problem which is similar but more acute, since it is necessary to scan the counting area in long, narrow strips.

In visual counting the difficulty is overcome by adopting certain conventions. Their effect is that a particle is only counted if an easily defined point on the particle (such as the centre or the left-hand or lower extremities) lies within the counting area. It is possible to do something very similar by electronic means[2] but where particle size discrimination is unimportant the simpler method described by Wolff and others[3, 4] and by Lagercrantz[5] is more attractive. In this method the counting area is scanned in strips of known width and total length. A second scan is then performed with strips of the same total length but having a different width. The number of cells counted in each case is the number whose centres lie within the strip, plus (or minus) an edge error determined by how much an average cell must overlap the edge of the strip in order to be counted. The edge error is the same in both cases (subject to the usual statistical uncertainties) if the sensitivity of the apparatus remains constant. Thus it is simple in principle to eliminate the edge error and so to deduce the true number of cells per unit area.

Practical difficulties encountered by the present authors led them to devise another method similar in principle but different in execution.

2. General design considerations

The apparatus of Wolff, Lagercrantz[3-5] and the present authors are basically very similar. In each case a dilute suspension of the blood cells is introduced into a glass counting chamber and the cells are allowed to settle to the bottom. The chamber is placed on a suitable stage under the objective of a microscope. The image of the counting chamber floor is focused on to a suitably shaped aperture which defines the area on the floor of the chamber seen at any instant by a photomultiplier situated behind the aperture. Scanning is effected by a suitable mechanical drive to the stage. Electrical pulses delivered by the photomultiplier are counted by an electronic scaler and a register.

An important question is that of the relative merits of dark ground illumination (used by Lagercrantz) as opposed to direct illumination (used by Wolff). The noise voltage at the output of an illuminated photomultiplier is due mainly to shot effect at the cathode and is therefore proportional to the square root of the light intensity at the cathode. With dark ground illumination this noise should be small and a good pulse to noise ratio is in principle obtainable. However, departures of the optical system or the photomultiplier from the ideal may cause a large increase in noise level. Moreover, changes in overall sensitivity (such as may be caused by changes of light intensity or of gain in the photomultiplier) can occur unnoticed and may cause inaccuracies in the edge error correction and, in extreme cases, the counting of noise pulses or the loss of genuine pulses.

With direct illumination the mean current passed by the

anode of the photomultiplier is a direct measure of the overall optical sensitivity of the system. This current may be amplified and used to control the gain of the photomultiplier so as to keep the mean anode current nearly constant. Then when a blood cell crosses the field of view, the magnitude of the resultant momentary fall in anode current is independent, within wide limits, of the light intensity or of the photomultiplier characteristics and depends only on the proportion of the light which is intercepted by the blood cell. Another advantage of direct illumination is that considerably less amplification is needed following the photomultiplier, since the amount of light intercepted by a blood cell with direct illumination is much larger than the amount scattered into the objective when dark ground illumination is used.

It was therefore considered that, if an adequate pulse to noise ratio could be obtained reliably, use of direct illumination would result in a more stable instrument of simpler design.

A disadvantage of the direct illumination method, whose importance was not at first realized, is its necessarily great sensitivity to small but rapid light fluctuations. The effects of external vibration can be serious if suitable precautions are not taken to minimize relative vibration of the various parts of the optical system. This consideration had an important influence on the mechanical design of the instrument.

3. THE METHOD OF SCANNING

3.1. *Length of scanned strip.* Linear scanning was adopted, rather than the spiral method of Lagercrantz, as a microscope stage of standard design can then be used. The scan is performed in longitudinal strips, the stage being shifted laterally at the end of each strip.

The minimum total length of the complete scan is dictated mainly by the cell diameter and by the desired statistical accuracy. Owing to the finite diameter of the cells, pairs of cells may be counted as one if the separation between their centres measured in the direction of the strip scan is of the order of the cell diameter or less. (This has been considered in detail by Lagercrantz.) Taking the mean effective cell diameter as 10^{-3} cm the loss due to this cause will be about 10% if the cells appear randomly along the strip at the rate of 100 per cm length. If suitable precautions are taken, reliable statistical corrections can be applied to losses of this order, but with larger losses the accuracy falls off rapidly. It is therefore desirable to limit the number of cells per centimetre strip to 100. For statistical reasons discussed in Section 4, about 20 000 cells should be counted. The total length of scan should therefore be at least 200 cm. The present instrument scans 200 strips each nominally $\sqrt{2}$ cm long.

3.2. *Shape of the scanning apertures.* In the scanning methods of Wolff and Lagercrantz the problem arises of changing the aperture width while keeping the area of the aperture the same. (This is essential if the mean photomultiplier current is used to stabilize the optical sensitivity.) Wolff achieves this by using a long rectangular aperture and orienting the long dimension successively perpendicular and parallel to the strip scan direction. With this method the cells remain in the field of view much longer in the second case and there is thus a greatly increased probability that two or more cells, none overlapping the scanned strip enough to be counted individually, may, through appearing simultaneously within the field of view, together generate a pulse large enough to be counted. A correction for the additional pulses thus produced is not readily applied.

A further objection is that the pulse durations are very different in the two cases and it is difficult to ensure that the pulses are dealt with in an identical manner by the electronic circuits, as is essential if the edge error is to be corrected with the necessary accuracy.

These objections are largely overcome by using the scanning apertures shown in Fig. 1. Aperture *A* scans strips of width

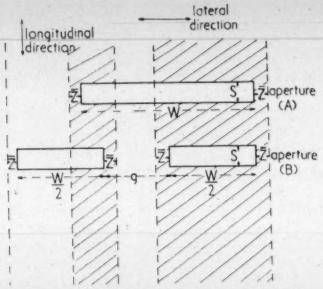

Fig. 1. Aperture for red blood cell counter

The longitudinal direction is the direction of oscillatory scan.

W in the usual manner and with the usual edge error. Aperture *B* has the same area as aperture *A* but scans pairs of strips, each of width *W*/2. The edge error is thus twice as great in the second case.

If the two counts obtained after correction of counting losses (Section 5) are N_1 and N_2 respectively, the true number *N* of cells whose centres lie within the strip of width *W* can, in principle, be obtained from the relation

$$N = N_1 - (N_2 - N_1)$$

or

$$N = 2N_1 - N_2$$

3.3. *Dimensions of the scanning apertures.* For convenience the aperture dimensions will be referred to the object plane of the microscope. The dimensions quoted are thus the actual aperture dimensions divided by the optical magnification (× 40).

It is proved in Appendix 1 that if it is assumed that the cells are disks having uniform light absorption and that the noise is shot noise at the photocathode, then the pulse to noise ratio is at an optimum for a given cell diameter when the aperture dimension *S* (Fig. 1) is 90% of the cell diameter. *S* will normally be chosen to have an optimum value for the smallest cells it is expected to encounter. Values of 8 μ and 4 μ have been used; the latter is to be preferred.

A compromise is involved in the choice of *W*. If *W* is made large in relation to the cell diameter, the proportion of cells partially overlapping the scanned strip and causing edge error is reduced, allowing a more precise correction. However, pulse to noise ratio deteriorates as *W* is increased, for reasons similar to those discussed in Appendix 1. A value of about 30 μ was found satisfactory.

The value of *W* influences the blood dilution factor, which must be made large enough (Section 8) to keep the number of cells counted per centimetre of scan fewer than 100 (Section 3.1).

The gap *g* between the two halves of the double aperture *B* (Fig. 1) must not be so small that a large particle can overlap both half apertures enough to register a count. Otherwise

the dimension is not critical, but a value of $W/2$ gives a desirably uniform statistical accuracy (Appendix 2).

4. STATISTICAL UNCERTAINTIES

In this section consideration is given only to the uncertainties that result from the assumption that the blood cells scanned are a random sample of the subject's blood.

Since the number of cells scanned lies between zero and a positive number approaching infinity, the results of counts performed on many specimens prepared from the same blood are expected to have a Poisson distribution about a mean value n and to have a standard deviation of $\sqrt{n}$. Since n is large the distribution is nearly Gaussian, so if the results of two independent counts are subtracted the standard errors add geometrically.

Such subtraction may occur in the process of eliminating edge errors and it can be shown that a result N thus obtained may have a standard error as large as $\sqrt{5N}$. The standard error can be reduced if the standard errors of the two counts are partly correlated by making the two scans cover substantially the same path. This is considered in Appendix 2 where it is shown that the error then becomes $\sqrt{[N(1 + 2g/W)]}$.

In cases where really accurate tracking between successive scans can be achieved and edge errors are small an alternative scanning method (Appendix 3) is inherently capable of higher statistical accuracy.

5. COUNTING LOSSES

The number of cells lost owing to two or more being simultaneously within the area covered by the aperture can be satisfactorily estimated if the cells are randomly distributed and if an accurate value can be obtained for the minimum distance between the centres of a pair of cells (measured in the direction of the scan) which allows them just to be resolved. This distance depends upon the cell diameter, the optical sensitivity of the apparatus and the transparency of the cells. It may also depend on the focusing of the microscope and on the time resolving power (i.e. the frequency response) of the amplifier following the photomultiplier.

Lagercrantz has estimated counting losses by use of data obtained from the measured edge errors. The accuracy of the method depends upon the frequency response of the pulse amplifier being wide enough to pass the pulse delivered by the photomultiplier without appreciable distortion. However, it is necessary to limit the amplifier frequency response in the interests of good pulse to noise ratio. Consequently a rather different method is adopted by the present authors. This takes advantage of a facility already available in the scaling unit used, namely a pulse amplitude discriminator[7] which becomes temporarily inoperative after being triggered by a pulse. The effect is that a succeeding pulse is not counted if it begins less than a predetermined time after the beginning of the earlier pulse. If this time exceeds the duration of the pulse caused by the passage of a single blood cell across the aperture, then counting losses involving only a pair of cells depend upon the duration of the inoperative period and upon the mean rate at which the cells are scanned, but are independent of cell dimensions and pulse duration.

Losses involving combinations of three or more cells are to some extent dependent on the latter quantities. Suppose, for example, that a pulse which operates the discriminator is followed by a second pulse which begins before, but ends after, the end of the inoperative period and that a third pulse begins after the end of this period but overlaps the end of the second pulse. Then the second and third pulses have the same effect as a long single pulse beginning before the end of the inoperative period and neither pulse is counted, although the third pulse begins after the end of this period. The probability of pulses overlapping in this manner clearly depends on pulse duration. However, the probability of losses occurring which involve combinations of three or more cells is relatively small so even a crude estimate of pulse duration allows the correction to be calculated with sufficient accuracy.

If a large proportion of pulses are lost, statistical errors will increase. The increase is not important in the present case and is neglected. In the present instrument the scanning movement is nearly sinusoidal, so the mean rate at which cells are scanned varies over the length of each scanned strip. Computation of counting losses thus becomes rather involved. Expressions are derived in Appendix 4 from which tables can be prepared. These are consulted to obtain the corrected result.

6. CONSTRUCTION OF APPARATUS

An important consideration in the construction of the present instrument was the reduction of the effects of mechanical vibration. To this end the optical path is made as short and as rigid as possible and the stage drive mechanism is well separated from the optical system and so mounted as to minimize the transmission of vibration.

Standard units are used where possible and the only specially constructed parts are the drive mechanism, the unit containing the photomultiplier and a small electronic unit containing three valves.

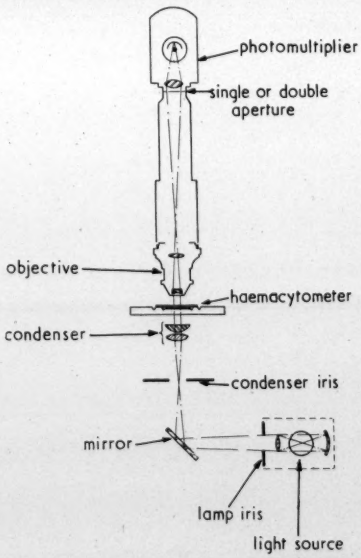

Fig. 2. Schematic layout of blood count microscope

6.1. *The optical system.* A standard microscope by Cooke, Troughton and Simms Ltd. is used with minor modifications. The optical system is shown in Fig. 2. The image of a small aperture at the lamp lens is focused on to the counting chamber floor by the condenser. (Owing to the thickness of the counting chamber used the focal length of the condenser had to be slightly lengthened by the addition of a weak concave lens.) The illuminated area need be little larger than the area "seen" by the scanning apertures and is kept to a minimum to reduce loss of contrast by scattering.

At the image plane of the objective there is a rectangular slit of width S and length $W+g$. This is crossed by a movable wire having a diameter g. The wire can either cross the slit at one end, exposing a single aperture of length W, or it can be made to cross the slit near the centre, exposing two apertures having a total length W. This arrangement ensures that the areas of the single and double apertures are equal without calling for excessively close dimensional tolerances. The slit and the mechanism for moving the wire are illustrated in Fig. 3. The eyepiece is removed and immediately above the slit is mounted a lens which focuses an image of the objective aperture on to the cathode of the photomultiplier. Thus a blood cell entering the field of view at any point causes a uniform reduction in light over the

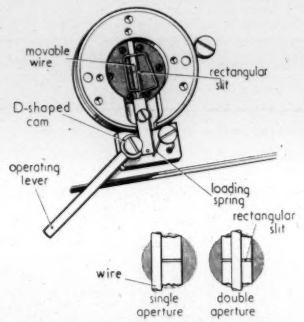

Fig. 3. Aperture control mechanism

whole of the illuminated area of the photocathode. This prevents lack of uniformity over the surface of the photocathode from causing variation in the sensitivity over the field of view. An eyepiece on a retractable side tube allows visual focusing to be carried out.

6.2. *The stage drive mechanism.* The operating knobs of standard stages move with the stage in the longitudinal direction. As it is difficult to design a satisfactory stage in which this does not occur, the drive mechanism is designed to cater for such movement. This is achieved by use of a slide which is oscillated by a crank and connecting rod so that its motion corresponds to the desired longitudinal motion of the stage (Fig. 4). A pinion on the slide meshes with a stationary rack, both being identical to the corresponding components in the microscope stage. Thus the linear and rotary motions of the drive pinion correspond to the desired motion of the stage pinion. A flexible coupling which transmits only the rotary motion from the drive pinion to the stage pinion thus causes the stage to reproduce the oscillatory motion of the slide. A second shaft on the slide is rotated through a small angle at the end of each sweep. This is coupled to the other shaft on the stage and causes the stage to be displaced laterally at the end of each sweep so that the scanned strips are separated by about 100 μ.

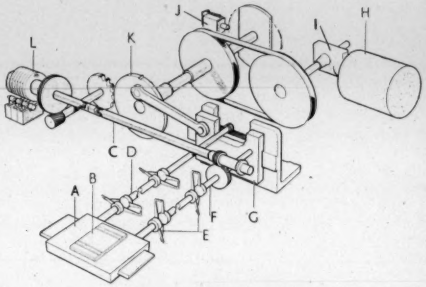

Fig. 4. Stage drive mechanism

A, microscope stage; *B*, haemacytometer; *C*, intermittent drive shaft for lateral shift; *D*, longitudinal drive shaft; *E*, flexible couplings; *F*, lateral drive shaft; *G*, reciprocating slide; *H*, driving motor; *I*, reduction gear; *J*, blanking switch; *K*, crank; *L*, revolution counter, cams and microswitches for controlling scan.

The full amplitude of the stage oscillation is 2 cm, but a contact renders the counting circuits inoperative for 45° of the crank rotation at the extremities of each sweep, making the effective length of each scanned strip 1·414 cm. After the first 100 strips have been scanned the mechanism automatically reverses and a further 100 strips are scanned. This returns the stage to its starting point and the mechanism stops automatically. The statistical accuracy is improved if the return scan follows a track different from that followed by the forward scan since the statistical errors in the two scans are then uncorrelated. In practice normal backlash in the lateral drive mechanism allows adequate displacement between scans. After 200 strips have been scanned in the above manner, to obtain N_1, the aperture is changed manually and N_2 is obtained by scanning a further 200 strips. These strips follow closely the track of the strips scanned previously.

The whole drive mechanism is flexibly mounted to minimize transmission of vibration to the microscope. The two pairs of flexible couplings to the microscope stage are specially designed to combine good torsional rigidity with great flexibility in other directions.

7. ELECTRONIC CIRCUITS

Most of the electronic circuits are part of the standard scaling unit which is employed. This uses two scale of ten stages and an electromechanical register and is similar to that described by Rotblat, Sayle and Thomas[6] but of a later design incorporating a stabilized high tension supply and a discriminator giving a predetermined inoperative period following each pulse which is counted.[7]

The special electronic circuits are built into a small unit which incorporates a d.c. supply for the microscope lamp, a high tension supply for the photomultiplier and three valves which amplify the pulses delivered by the photomultiplier and regulate the high tension supply. The valves obtain their own high tension from the stabilized supply in the scaler. The circuit of this unit is shown in Fig. 5. The

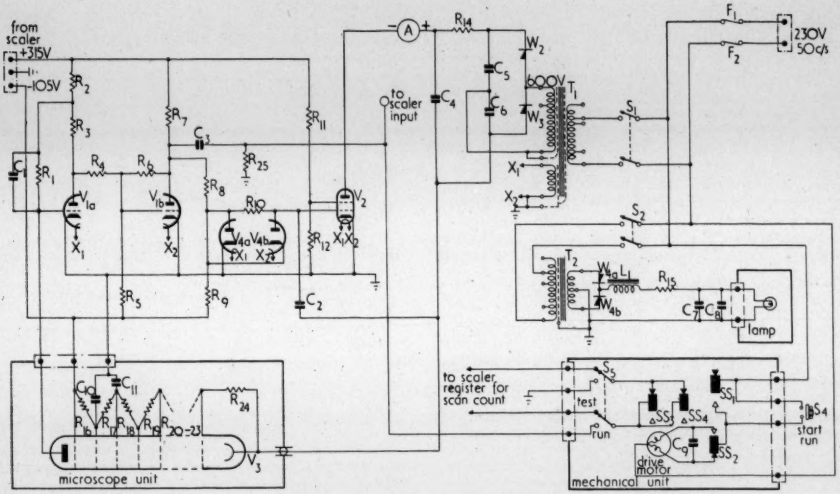

Fig. 5. Amplifier and control circuits

R_1 = 1·8 MΩ
R_2, R_3 = 47 kΩ
R_4 = 680 kΩ
R_5 = 330 kΩ
R_6 = 4·7 MΩ
R_7 = 100 kΩ
R_8 = 1·2 MΩ
R_9 = 1 MΩ
R_{10} = 2·7 MΩ
R_{11} = 560 kΩ
R_{12} = 22 kΩ
R_{14} = 1 MΩ
R_{15} = 4·7 Ω
R_{16}–R_{24} = 330 kΩ
R_{25} = 1 MΩ
C_1 = 56 pF
C_2 = 2000 pF
C_3 = 0·01 μF
C_4, C_5, C_6 = 0·1 μF
C_7, C_8 = 250 μF
C_9 = 1 μF
C_{10}, C_{11} = 0·02 μF
V_1 = CV455 (12AT7)
V_2 = CV276
V_3 = CV337 (931A)
V_4 = CV140
W_2, W_3 = 36EHT60
A = 500 μA
T_1 = 600 V, 1 mA, 6·3 V, 2 A
T_2 = 37·5–0–37·5 V, 0·35 A
L_1 = 0·5 H, 0·5 A

two halves of V_1 form a d.c. and pulse amplifier with heavy negative feedback. The output of this amplifier is d.c. coupled to the regulator valve V_2. The anode load of V_2 is made up of the floating high voltage supply in series with the potential divider R_{16} to R_{24} shunting the photomultiplier. The voltage appearing across this potential divider, and hence across the photomultiplier, is determined by the current passed by V_2. Thus V_1 and V_2 act to keep constant the mean anode current of the photomultiplier. If this regulating action were instantaneous sudden changes in light due to the passage of a cell past the aperture would cause only a negligible change in photomultiplier anode current. The action of the stabilizer is therefore slowed up by the feedback condenser C_2 so that a sudden change in light produces at the output point a sudden voltage change which dies away exponentially as the stabilizer takes control.

Assuming the circuit to be linear, sudden restoration of the light to its original intensity produces a similar pulse of reverse polarity. The circuit behaves in a similar way to a differentiating circuit comprising a capacitor and resistor, the effective time constant being determined by R_{10}, C_2 and the loop gain of the stabilizer. Thus low frequency disturbances, such as may be caused by mechanical vibration or any residual mains ripple appearing at the light source, can be attenuated by use of a short enough time constant. However, too short a time constant entails loss of pulse amplitude and large overshoots appear following the pulse. The value chosen causes little pulse attenuation and overshoots are minimized by V_{4a} which limits the amount by which a pulse disturbs the stabilizer and V_{4b} which speeds up the recovery of the stabilizer after the pulse.

Condenser C_1 lowers the upper frequency response of the system and thus reduces the effect of high frequency noise components.

The meter A gives a reading proportional to the voltage across the photomultiplier. The action of the stabilizer causes this to increase if the light intensity or the photomultiplier sensitivity decreases. The meter reading thus gives early warning of deterioration of the lamp or photomultiplier and is invaluable in setting up the optical system.

8. EXPERIMENTAL PROCEDURE

The experiments described in the next section were aimed at assessing the reliability and consistency of the results provided by the instrument. Consequently most of the experiments involved repeated counts of the same chamber filling or repeated fillings of the chamber from the same diluted sample. The experimental procedure therefore differs somewhat from that which would be adopted in routine work.

8.1. *Dilution.* The blood sample is measured with a pipette in the normal manner and is thoroughly mixed with a diluting fluid consisting of 0·1% iodine in isotonic potassium iodide plus 30 ml. per litre of 1% eosin. The staining of the cells caused by this fluid greatly improves the pulse to noise ratio.

It has already been pointed out that there should not be more than 100 cells per centimetre of scanned strip. The width W of the strip is 0·0315 mm and the depth of the counting chamber is 0·1 mm so a volume 0·0315 mm^3 is scanned per centimetre length of the scanned strip. If the number of cells counted in this length is to be less than 100,

the cell concentration in the dilute suspension must not exceed 3200 per mm^3. The cell concentration in normal undiluted blood is of the order of 5×10^6 per mm^3 so the dilution should be one in at least 1500. A dilution of 1 : 2500, giving about 60 cells per cm length is normally used; dilutions in the range 1 : 1500 to 1 : 4000 have been found satisfactory.

8.2. *Filling the chamber.* The counting chamber is similar to those used for visual counting but is larger (20×40 mm working area, 100 μ deep) and is not ruled. It is filled in the normal manner by introducing the suspension at the edge of the cover glass which is then drawn into the chamber by capillary attraction. Filling must be done with care if errors are to be avoided. If the chamber is underfilled, surface tension draws down the cover glass by as much as 10 μ near the centre, causing a 10% reduction in the depth of the chamber. Ideally the chamber should be slightly overfilled so that a convex meniscus exists at the edges of the cover glass. Overfilling should not be carried to the point that drops form in the channels as the cells appear to distribute themselves unevenly between such drops and the fluid in the main part of the counting chamber.

There is some evidence that when the fluid is introduced in the above manner the cells do not distribute themselves quite evenly over the chamber. This has not been investigated.

When many counts are to be performed with the same chamber filling, evaporation is reduced by sealing the edges of the cover glass with vaseline.

8.3. *Counting.* The procedure for doing this has already been described. Scanning occurs at the rate of about 100 strips per minute; successive runs with the single and double aperture take a total of about four minutes.

9. TEST RESULTS

No serious attempt has so far been made to assess the absolute accuracy of the instrument, mainly because alternative counting methods are tedious and of doubtful accuracy. At an earlier stage in the development of the instrument an attempt was made to check this by photographing a specimen scanned by the instrument and subsequently counting by eye the cells on the photograph. In almost all cases discrepancies between the automatic and visual results could be accounted for by the expected statistical errors of the visual method alone.

The tests described below were aimed mainly at showing that the results given by the instrument depend only upon the cell concentration and are unaffected by other factors. In most cases the tests were designed to eliminate the effects of errors arising in the preparation of the specimen, as this was regarded as a separate line of investigation which the authors were not qualified to pursue.

In all tests except the last, repeated scans were performed with the same specimen while one or more of the operating conditions were varied. Owing to the accuracy of the scanning mechanism, scans can be repeated over almost identical tracks so that random variations in the results are almost entirely absent. This is a most valuable feature of the instrument. Had every scan been subject to the full random error it would have been almost impossible to detect and rectify the many small systematic errors which occurred in the earlier stages of development.

9.1. *Effects of variations in discriminator bias.* It is important to ascertain that the corrected results are in fact unaffected by edge errors. A convenient way is to vary the sensitivity of the scaler by use of the calibrated discriminator bias control which is provided. This varies the amount by which a cell must overlap the aperture in order to be counted. A typical set of results is shown in Fig. 6. As would be expected the slope of the double aperture curve is about twice that of the single aperture and the slope of the corrected curve is quite small, showing that satisfactory edge correction has been achieved.

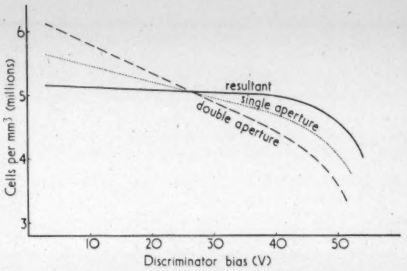

Fig. 6. Variation of result with discriminator bias volts

The residual slope of the resultant curve may be due to imperfect correction or it may be due to the presence of a few very small particles giving pulses too small to be counted at the higher bias levels. Apart from this slight slope the result is almost independent of bias voltage over a range of at least 10 : 1.

A flat curve of this nature is only obtained when most of the particles counted are larger than a certain minimum size. Particles having a continuous size distribution over a wide range would give a sloping bias curve and could not be counted reliably by this method.

9.2. *Effects of variation in focus.* Defocusing can affect the edge correction and may occur as a result of faulty adjustment or because of imperfections in the haemacytometer or the microscope stage. It is therefore important to ensure that the results are unaffected by moderate defocusing. Fig. 7 shows how the result varies with focus setting at discriminator bias levels of 10, 20 and 30 V. Defocusing causes

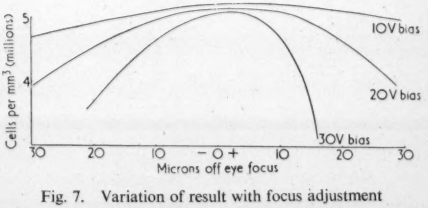

Fig. 7. Variation of result with focus adjustment

a fall in pulse amplitude and an increase in pulse length. The former causes large losses at the higher bias levels. At the lower bias levels the losses are probably caused by the pulse duration exceeding the dead time of the discriminator so that losses due to pulse overlap are increased. Fig. 7 shows that, at a bias of 10 V, a variation of 5 μ on either side of eye focus causes a total error of only about 1%.

Measurements of the contour of the floor of a haemacytometer mounted on the microscope stage showed that variations

over the whole area (4×2 cm) may be as large as $\pm 7\,\mu$. However, variations over the $1 \times 1{\cdot}4$ cm area used for counting are much smaller and it is reasonable to expect that errors due to this cause will be less than 1%.

9.3. *Effects of variation of light intensity.* Discriminator bias curves were taken with normal illumination and with the illumination reduced by factors of 2, 4 and 8 below the normal level. These curves are illustrated in Fig. 8. Owing

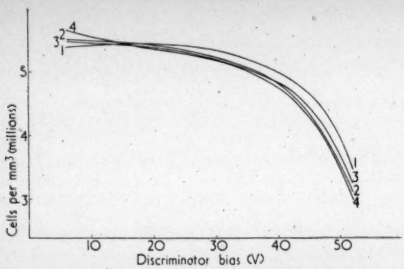

Fig. 8. Variation of result with light intensity

Curve	*Intensity*	*Meter reading*
1	Normal	225 μA
2	$\frac{1}{2}$ normal	250 μA
3	$\frac{1}{4}$ normal	275 μA
4	$\frac{1}{8}$ normal	300 μA

to the action of the automatic control circuit, a change of light intensity is compensated by an increase of photomultiplier gain and it will be seen that a fall of light intensity by a factor of 4 causes a change of less than 2% in the result obtained in the bias range 10 to 20 V. The increased count obtained at low bias voltages when the light is reduced by a factor of 8 is due to the presence of shot noise from the photomultiplier.

Similar results would be expected if the photomultiplier sensitivity fell by similar factors, except that there would not be an appreciable increase of noise unless most of the loss of sensitivity occurred at a very early stage in the photomultiplier.

It is concluded, therefore, that the results will be negligibly affected by the variations in light intensity or photomultiplier sensitivity which would be encountered in normal operation.

9.4. *Reproducibility of results.* Owing to the accuracy of the scanning mechanism, repeated counts performed on the same specimen have a standard deviation of less than 1%, which is considerably smaller than the statistical error discussed in Section 4. This is because nearly the same track is followed in performing each count.

While this does not increase the accuracy with which routine counts can be performed, it greatly helps in checking the performance of the instrument. The curves of Figs. 6, 7 and 8 would have been far less smooth, and far less significant, had every point been subject to the full statistical error.

Since the above results indicate that the instrument itself does not introduce appreciable random errors, other than the expected statistical ones, an attempt was made to assess the errors to be expected in routine counting.

Dilutions were prepared from samples of the blood of three individuals. Counts were performed on twelve specimens prepared from each of the three diluted samples. Four counting chambers were employed, so each was used three times with each diluted sample.

The results are tabulated below:

	Sample 1	*Sample* 2	*Sample* 3
Mean of counts in twelve specimens (millions of cells per mm³)	5·32	5·57	4·67
Standard deviation of twelve results	3·1%	3·6%	2·9%
Standard deviation corrected for chamber errors	2·6%	3·3%	2·3%

The expected statistical error is 1·1%, so the errors in the second row are rather large. The results were analysed to see if systematic errors were associated with individual counting chambers. It appeared that one of the four was giving results about 2% high and another 1·6% low, presumably because of dimensional errors. Correction of the results for these errors gave the standard deviations shown in the lowest row. These are still larger than expected and it is difficult to escape the conclusion that despite careful technique a random error of nearly 3% is introduced in the process of filling the counting chamber.

10. THE COUNTING OF OTHER PARTICLES

An attempt was made to count white cells by suppressing the much more numerous red cells. This was unsuccessful because the remains of the red cells caused a large background fluctuation from which the white cell pulses could not be satisfactorily separated. It is likely that better technique of specimen preparation would allow white cells to be counted successfully.

No serious attempts have been made to count other particles. As already mentioned serious difficulties arise if the size distribution is wide.

11. CONCLUSIONS

A method for automatically counting red blood cells has been described which is capable of providing results reproducible to within a standard deviation of $\pm 3\%$. It has been demonstrated that instrumental variations are unlikely to contribute seriously to the errors, which are mainly due to statistical uncertainties and to the preparation of the specimen. The former can be reduced by performing several counts on one specimen and it is hoped that the ease with which counts can be performed will facilitate experiments aimed at reducing the latter.

A comprehensive check of the absolute accuracy of the instrument has not been carried out because of the difficulty of performing the measurement by other means with sufficient accuracy, but it is difficult to see how absolute errors can be introduced by the instrument itself if all critical dimensions are accurately known.

In order to reduce cost the instrument has been designed so that the major components are standard production units.

12. ACKNOWLEDGEMENTS

The authors benefited greatly from discussions with Mr. H. S. Wolff, late of the Radcliffe Infirmary, Oxford, who demonstrated the practicability of the moving stage scanning method and suggested the composition of the diluting fluid. Dr. Macfarlane and his colleagues at the Radcliffe Infirmary

have also been very helpful and they suggested the method of changing from a single to a double aperture by use of a movable dividing mask.

The help of Dr. K. Williams and Mr. C. Sanders of the Medical Division, A.E.R.E., is gratefully acknowledged, the former for her advice and encouragement and the latter for much help in the preparation of specimens and for obtaining many of the results.

Thanks are due also to Mr. J. Henderson of the Electronics Division, A.E.R.E., for so diligently performing measurements, to Mr. R. E. Cox whose careful mechanical work contributed greatly to the success of the instrument and to Mr. M. C. B. Russell for help in preparing the paper.

REFERENCES

(1) WALTON, W. H. *Nature* [*London*], **169**, p. 518 (1952).
(2) COOKE-YARBOROUGH, E. H. British Patent Application No. 21937/51.
(3) WOLFF, H. S., STOREY, M. G., and BEHRENS, D. J. British Patent Application No. 595/50.
(4) WOLFF, H. S. *Nature* [*London*], **165**, p. 967 (1950).
(5) LAGERCRANTZ. *Acta Physiologica Scandanivica*, **26**, Supplementum 93 (1952).
(6) ROTBLAT, J., SAYLE, E. A., and THOMAS, D. G. A. *J. Sci. Instrum.*, **25**, p. 33 (1948).
(7) COOKE-YARBOROUGH, E. H. *J. Sci. Instrum.*, **26**, p. 96 (1949).

APPENDIX 1

Optimum aperture dimension in longitudinal direction

Let d = diameter of blood cell;
S = dimension of slit in longitudinal direction.

The change in photocurrent caused by the appearance of a blood cell is proportional to the maximum area of the aperture covered by the blood cell. This area is given by:

$$\tfrac{1}{2}S\sqrt{(d^2 - S^2)} + \tfrac{1}{2}d^2 \sin^{-1} S/d$$

(The light absorption is assumed to be uniform throughout the area of the cell.)

Noise in the photomultiplier is mainly due to shot effect in the photocurrent and is thus proportional to the square root of the photocurrent. It is thus proportional to $\sqrt{S}$. The pulse to noise ratio is therefore at a maximum when the ratio of the cell area covering the slit to $\sqrt{S}$ is a maximum.

The pulse to noise ratio is thus proportional to:

$$\frac{\sqrt{S}}{2} \cdot \sqrt{(d^2 - S^2)} + \frac{d^2}{2\sqrt{S}} \sin^{-1} \frac{S}{d}$$

Differentiation with respect to S gives:

$$\frac{(d^2 - 3S^2)}{4\sqrt{(d^2S - S^3)}} - \frac{d^2}{4S^{3/2}} \sin^{-1} \frac{S}{d} + \frac{d}{2\sqrt{[S - (S^3/d^2)]}}$$

After equating to 0 and rearranging, this expression becomes:

$$\frac{S}{d} = \sin\left[\frac{3S}{d}\sqrt{\left(1 - \frac{S^2}{d^2}\right)}\right]$$

This equation is satisfied by a value of S/d of 0·908.

Thus the dimension S should be about 90% of the diameter of the smallest cell it is desired to count.

APPENDIX 2

Standard error of result

Let $\bar{z}$ = the maximum distance the centre of an average cell may be outside the scanned strip, yet still be counted;
C = concentration of cells per unit area on the floor of the counting chamber;
g = gap between two half apertures;
l = total strip length.

Number N_1 of cells counted with single aperture
$= Cl(W + 2\bar{z})$
Standard error $= \sqrt{[Cl(W + 2\bar{z})]}$

Number N_2 of cells counted with double aperture
$= Cl(W + 4\bar{z})$
Standard error $= \sqrt{[Cl(W + 4\bar{z})]}$

The edge error is obtained by subtracting N_2 from N_1. If the scans with single and double apertures covered totally different parts of the counting chamber, the standard error in the estimate of edge error would be the geometric sum of the two standard errors given above. If, however, the two scans cover substantially the same track, much of the area scanned by the single aperture will be scanned again by the double aperture. The area scanned twice is indicated by the shaded strips in Fig. 1. Statistical errors owing to cells lying in this area are indentical in both scans and therefore cancel when the two counts are subtracted. The standard error in estimating the edge error is thus the geometric sum of the standard errors in counting the cells lying in the two unshaded strips. The total width of these strips is $2g - 2\bar{z}$, so the standard error is $\sqrt{[Cl(2g - 2\bar{z})]}$.

Thus when the total number N of cells lying within a strip of width W is obtained by subtracting $(N_2 - N_1)$ from N_1 the standard error of the result is the geometric sum of $\sqrt{[Cl(W + 2\bar{z})]}$ and $\sqrt{Cl(2g - 2\bar{z})}$, or $\sqrt{[Cl(W + 2g)]}$. Since $ClW = N$, the standard error is thus $\sqrt{[N(1 + 2g/W)]}$.

Inspection of Fig. 1 shows that if g is made equal to $W/2$, the double aperture may be displaced laterally relative to the single aperture over a total range of $1{\cdot}5W$ without changing by more than $2\bar{z}$ the total width of the strips which are scanned by both single and double apertures. Thus the standard error has a value of approximately $\sqrt{2N}$ which remains nearly constant despite quite large tracking errors between the single aperture and double aperture scans.

APPENDIX 3

Alternative arrangement of apertures

Notation is the same as in Appendix 2.

The apertures are arranged as shown in Fig. 9.

Every cell counted by the single aperture is counted also by the double aperture. However, each cell whose centre lies in the shaded strip is counted once by the single aperture and twice by the double aperture.

The number of cells lying in this area $= 2Cl\bar{z}$.

This number is equal to the edge error.

With perfect tracking between single and double scans the counts N_1 and N_2 are fully correlated. However, because in the double scan the cells in the shaded area are counted twice,

$N_2 - N_1 = 2Cl\bar{z}$.

The standard error of this difference is $\sqrt{(2Cl\bar{z})}$.

$N_1 = Cl(W + 2\bar{z})$: the standard error is $\sqrt{[Cl(W + 2\bar{z})]}$.

$N = Cl(W + 2\bar{z}) - 2Cl\bar{z}$.
$= ClW$: the standard error is $\sqrt{[Cl(W + 4\bar{z})]}$
$= \sqrt{[N + (4N\bar{z}/W)]}$.

In cases where good tracking between single and double aperture scans is assured and where the conditions can be so chosen that $\bar{z}$ is small compared with W, this method is inherently capable of greater statistical accuracy than that discussed in Appendix 2.

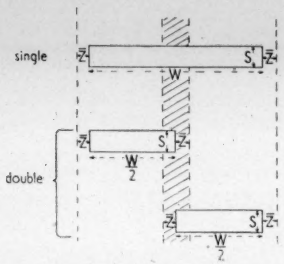

Fig. 9. Alternative arrangement of apertures

APPENDIX 4

Determination of the number of cells per cubic millimetre from experimental results

Let M = the number of cells per cubic millimetre in the original blood sample;
k = the dilution factor;
L = the length (in millimetres) of the connecting rod coupling the crank to the microscope stage;
R = the radius (in millimetres) of the crank driving the stage;
ω = the angular velocity of the crank (assumed to be constant);
ϕ = the masking angle measured relative to the horizontal plane in which the microscope stage is moved;
T = the total number of strips scanned;
d = the depth (in millimetres) of the counting chamber;
t_d = duration of the artificially imposed paralysis time following the counting of a pulse.

N_1' and N_2' = the total number of counts registered with the single and double apertures respectively before application of counting loss corrections. The other symbols are as previously defined.

The value of M, which it is required to determine finally, may be expressed as

$$M = k(2N_1 - N_2)/ldW \tag{1}$$

Where N_1 and N_2 are, as previously defined, the total number of cells lying within the strips scanned by the single and double apertures respectively, and l, W and d are expressed in millimetres.

The values of N_1 and N_2 are obtained by applying corrections to N_1' and N_2' respectively for the probable counting losses due to closely spaced cells.

The correction for the paralysis time t_d is made as follows:

The velocity of the cells at any instant, when the crank arm makes an angle θ_1 with the plane in which the cells are moved, is given by

$$V_1 = \omega R\left(\sin\theta_1 - \frac{R}{2L}\sin 2\theta_1\right) \tag{2}$$

where it is assumed that $L \gg R$ so that terms involving higher orders of L/R may be neglected.

If N_a is the total number of cells in the total strip length scanned by an aperture the probability p that a cell enters the field of view in an interval of time dt, at the position corresponding to θ_1, is

$$p = \frac{N_a R}{l}\left(\sin\theta_1 - \frac{R}{2L}\sin 2\theta_1\right)d\theta \tag{3}$$

since $\omega dt = d\theta$.

If p_1 is the probability of counting a cell which enters the field of view in the vicinity of the position corresponding to θ_1, the probability p_c of a count being registered in the interval dt at $\theta = \theta_1$ is pp_1 or

$$p_c = p_1(N_a R/l)\left(\sin\theta_1 - \frac{R}{2L}\sin 2\theta_1\right)d\theta \tag{4}$$

The probability p_t that a count is registered in the interval from $\theta = \theta_1 - \omega t_d$ to $\theta = \theta_1$, where the angle ωt_d is small is

$$p_t = p_1(N_a R\omega t_d/l)\left(\sin\theta_1 - \frac{R}{2L}\sin 2\theta_1\right) \tag{5}$$

Since $(1 - p_t)$ is the probability p_1 that a count is registered if a cell enters the field of view in the interval dt, at $\theta = \theta_1$

$$p_1 = \left[1 + (N_a R\omega t_d/l)\left(\sin\theta_1 - \frac{R}{2L}\sin 2\theta_1\right)\right]^{-1} \tag{6}$$

Hence it follows from equation (4) that the probable count registered N_c is given by

$$N_c = T\int_{\phi}^{\pi-\phi} \frac{(N_a R/l)\left(\sin\theta_1 - \frac{R}{2L}\sin 2\theta_1\right)d\theta}{1 + (N_a R\omega t_d/l)\left(\sin\theta_1 - \frac{R}{2L}\sin 2\theta_1\right)} \tag{7}$$

Since $N_a R\omega t_d/l < 1$, the integral in equation (7) may be expanded as an infinite series, the terms of which decrease rapidly in magnitude, so that only the first few terms (depending on the value of N) need be considered. On integrating the resulting series term by term it is found that terms in R/L vanish and

$$N_c = \frac{N_a RT}{l}\left[2\cos\phi - \left(\frac{\pi}{2} + \sin 2\phi\right)\frac{N_a R\omega t_d}{l} + (2\cos\phi - \tfrac{2}{3}\cos^3\phi)\frac{(N_a R\omega t_d)^2}{l^2} - (\tfrac{3}{8}\pi + \tfrac{1}{2}\sin 2\phi - \tfrac{1}{16}\sin 4\phi)\frac{(N_a R\omega t_d)^3}{l^3} + (2\cos\phi - \tfrac{4}{3}\cos^3\phi - \tfrac{2}{5}\cos^5\phi)\frac{(N_a R\omega t_d)^4}{l^4} - \ldots\right] \tag{8}$$

A table can be prepared using equation (8) from which the value of N_a corresponding to a known count N_c may be ascertained. It is convenient, however, to multiply the values of N_a by the factor k/ldW (see equation 1) so that the apparent value of M corresponding to a known value of N_c may be found.

Then if M_1 and M_2 are the apparent values of M corresponding to counts N_1' and N_2' taken with the single and double apertures respectively, the value of M required is found simply by the relationship

$$M = 2M_1 - M_2 \tag{9}$$

On the A.E.R.E. experimental equipment described the various parameters employed have the following values:

$L = 80$ mm;
$R = 10{\cdot}057$ mm;
$\omega = 5{\cdot}79$ radians/sec;
$\phi = 0{\cdot}7715$ radian $= 44{\cdot}2°$ approx. (The nominal value of ϕ is $\pi/4$ radians);
$T = 200$;
$d = 0{\cdot}1$ mm;
$b = 0{\cdot}031\,75$ mm;
$t_d = 500\ \mu$sec.

The dilution factor k normally employed is 2500 although experiments have been made in the range $k = 1500$ to $k = 4000$. The value of $k = 2500$ gives a suitable rate of counting, and a mean separation between cells entering the field of view of approximately 20 times the average cell diameter; with the dead time used counting losses are of the order of 12% of the true number of cells lying in the scanned path.

Paper G.4

Stages in the development of an arrested scan type microscopic particle counter

By H. A. Dell, A.R.C.S., D.I.C., Ph.D., The Mullard Research Laboratories, Redhill, Surrey

The most detailed analysis of the particles of dust deposited on a plane surface is possible when the surface considered is examined point by point by a spot scanning system. Techniques are described using line-to-line memory systems which provide a single impulse for each particle in each field of scan. These impulses can be used to arrest the normal scanning motion of the spot, which can then explore each particle in turn as it is discovered. The mode of exploration chosen can be designed to exhibit the features of the particles which are of interest. Some simple modes are described.

The aspect of particle counting that has been investigated is that of numbering and finding the size distribution of a collection of dust particles of random size and shape deposited on a plane surface.

The development of automatic techniques for these purposes was undertaken at the suggestion of the National Coal Board who have a very large standing requirement for airborne dust counts using thermal precipitators. This need largely determined the course of the work.

Optical techniques have been developed by which dust particles greater than 1 μ in mean diameter may be both counted and sized in a variety of ways.

METHODS OF MEASUREMENT

There are two basic scanning methods of specimen examination. (i) If an illuminated slit is used which is swept across the specimen,[1] the total length of the particle intercepts on the line at any instant may be found from the light transmitted. Information about distribution within the line is lost. Particles can therefore be measured individually only if single interceptions occur, and even then end effects must be obviated.[2,3] (ii) If an illuminated spot is scanned across the specimen in a series of parallel tracks, the transparency of each point of the whole specimen may be found, averaged only over the elemental spot area. Within certain limits of resolution due to this area, these measurements must contain all information about the particles present, for a specimen image can be reconstructed from them (*cf.* phototelegraphy). Unfortunately information about particle numbers and sizes can only be extracted with difficulty.

Thermal precipitator slides contain very high concentrations of particles of widely differing shape and even of varying degrees of transparency. It is thus almost impossible to maintain the conditions necessary for slit scan. Only the second method therefore offered any hope of providing a reliable technique of analysis in spite of its greater complexity.

The difficulties which this method introduces are illustrated diagrammatically in Fig. 1. This shows [Fig. 1(*a*)] four particles in a field of view scanned in a series of lines by an ideally small spot. The transparency found as scanning proceeds is illustrated in Fig. 1(*b*).

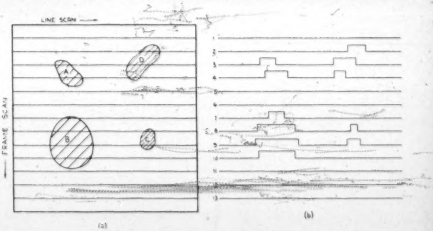

Fig. 1. Spot scan method: (*a*) specimen with horizontal lines traced by spot, (*b*) signals

Large particles which overlap several lines of scan produce a change of transparency on each interception. In a particle counter it is therefore necessary to recognize this condition. If the size of each particle is required, it is necessary in addition to store up the intercept information due to any one particle. On completing the scan either the number or the magnitude of the intercepts on each particle may then be determined.

This has been avoided in some instruments (Dawes; Hawksley[4]) by a statistical analysis of the intercept lengths found, irrespective of their association. Only in the case of regular particles (e.g. circles) is this a reliable method.

An alternative method of avoiding storage is possible if a scanning counter is so constructed that when a particle is first intercepted the scanning spot is immobilized. An

auxiliary scan can then be generated which causes the spot to explore only the particle which it has discovered. Having completed that exploration, normal scanning can be resumed. Subsequent interceptions of that particle in following lines of scan can be made to have no effect. Each particle can thus be explored once and once only, and by observing the activity of the auxiliary scan generator alone the particle sizes present may be determined irrespective of their position.

This arrested scan technique is particularly valuable as it makes a very wide variety of exploratory scans possible. The auxiliary scan used can therefore be devised to exhibit clearly the features of the particles which are of interest.

COURSE OF DEVELOPMENT

Field of investigation

When the development work was begun in 1950 it was decided to concentrate on the investigation of techniques of specimen scanning and signal handling rather than the amassing of results using any one method. The double-spot scanner and the arrested scan technique of sizing appeared as a result of this.

Methods of scanning specimens

Specimen examination by spot scan can be carried out in many ways. Of the scanning devices considered, the cathode-ray tube flying-spot scanner appeared the most suitable.

The ultimate resolution of 1 μ particles which was needed implied that the scanner should work either with photomicrographic enlargements of dust specimens or should scan a specimen directly *via* some optical reducing system.[5] Experimental work was based on both these methods, and the necessary resolution was achieved.

Line to line signal association

It was pointed out by Gillings[6] that if either counting or sizing is to be carried out, it is necessary to lay down some criterion by which the signals may be judged to decide whether multiple interceptions of a single particle have taken place or not.

Two different criteria have been considered so far. The first, called the "anticipation-tolerance" criterion,[6] states that a signal in any line of scan must be regarded as due to a large particle overlapping the previous line of scan only if a signal occurred in the previous line which, as measured along the line, lay within a predetermined dimensional tolerance of the later signal.

In the instance illustrated (Fig. 1) a dimensional tolerance may be selected which would, for example, correctly associate the first signal in line 8 with that in line 7, but which would rightly exclude the second signal in line 8, recognizing it as due to a separate particle. If particles exist having extended edges nearly parallel to the lines of scan, a large tolerance is necessary. It may then be very difficult to avoid incorrectly associating signals due to separate but nearby particles.

The second, the "overlap" criterion (the advantages of which were first emphasized by Roberts[7]) states that a signal in any line of scan must be regarded as due to a large particle overlapping the previous line of scan only if a signal occurred in the previous line some part of which lay the same distance along the line as some part of the later signal (i.e. some signal overlap existed). When a light spot of finite size is used scanning lines separated by approximately the spot radius, it can be shown that the overlap criterion will correctly interpret all signals down to a resolving limit of about the spot diameter. The false association possibility of the anticipation-tolerance criterion, which may be a very real danger when dense specimens are considered, has no counterpart in this case.

The overlap criterion is the superior when only counting is required, but if sizing by intercept summation is to be carried out it has a great disadvantage. Consider, for example, the signals due to the particle *D* in Fig. 1. In the second line of scan the first intercept signal from this particle occurs and must be suitably stored away. In the third line of scan, the second intercept will occur, but only when it is more than half over will association with the first intercept be recognized. All of the signal must be stored correctly, however, for otherwise a later signal, as that in the fourth line, may never be recognized as due to part of the particle. Some temporary store is thus necessary in which all signals can be held until their ultimate destination is known. This difficulty does not arise with the anticipation-tolerance criterion. A signal in any line of scan either lies within the tolerance zone of a previous interception when the correct destination is known, or it lies outside all such zones when it must represent a new particle. In either case the appropriate action is established from the beginning of the signal. For this reason, all the intercept summing sizing counters so far suggested use the anticipation-tolerance criterion.[6,8,9]

Line to line memory

Whichever criterion of signal association is used some form of memory is necessary in which it is possible to record the signals generated by the scanning system. During the scanning of any line this record must then be read so that a representation of the signals generated one line previously is available for comparison with the current signal output. In a particle counter these remembered signals may be made to annul coherent scanner impulses. Only at the first intercept of each particle therefore, when the memory is blank, is a counting pulse emitted. When intercept summation is required, additional memory devices must be used (sometimes of the same form as the line to line memory) to sum the signals from each particle.[6,9] No practical work has been done on integrators and they will not be further described here. Several different line to line memories, variously suggested, have been tried by us; some of these are described below. In all of them, adequate resolution must be provided so that signal degradation may not occur.

Electronic memory elements. Electronic elements may be used,[6,8] each remembering the position of one signal in terms of time or potential. At least as many elements must be provided as particle intercepts occur in any single line, and a complex routing switch is necessary. Units of this type have not so far been constructed, but resolution adequate for a 100 picture point line scan is available.

Magnetic drum and tape recordings. Magnetic drum and tape recordings[9] have been tried on a limited scale and offer possible solutions. The former is essential if high line scan speeds are used (as, for example, when simultaneous image display is required), but produces a large attenuation of signals. The latter has rather less attenuation, but can only give adequate resolution at low line scan speeds. Tape-wear is a disadvantage.

Magnetostrictive delay lines. Magnetostrictive delay lines[10] have been used, and give both an adequate resolution at high speeds and a lower attenuation than the magnetic drum. The absence of moving parts is an advantage.

Electrostatic cathode-ray tube store. An electrostatic cathode-ray tube storage system[11] has been tried, but the

very low geometrical resolution obtainable from the tube increases the complexity. A very large attenuation of signals occurs, but the mobility of the reading electron stream is attractive.

Double spot pseudo-memory. In addition to the true memory systems described, a double spot pseudo-memory[12] has also been extensively used. In this the specimen is scanned by two similar but identifiable light spots and the opacities experienced at the two scanning points indicated in two separate circuits. If as one spot scans the nth line of the raster, the other spot similarly scans the $(n-1)$th line, signals are available in the two channels which correspond to those which a single spot scanner and a memory would produce.

This simple method of imitating the action of a memory suffers from an important disadvantage first pointed out by Walton in a private communication. The signal delivered by the secondary trailing scanning spot is not the remembered signal which the leading spot delivered; it is only a signal reconstructed by inference. If, therefore, the secondary spot either takes a rather different path than the primary spot, or possesses a slightly different signal sensitivity (both conditions very difficult to avoid in practice) the reconstructed signal may be false. The result of this potential fallibility is that in certain instances particles may be counted twice or missed altogether.

Although in use care was taken to control accurately the two factors referred to it was found in a simple counter using ideal specimens that about 1% of the particles were missed or double counted. In spite of this possibility, the specification of a machine working on these principles has been agreed with the National Coal Board and two machines are under construction.

Arrested scan method

Both the general difficulties of intercept summation and the particular problems of the overlap criterion when sizing is attempted can be overcome by using the arrested scan technique.[13] The basic components of this system applied to a cathode-ray tube flying-spot scanner are illustrated in Fig. 2.

A scanning generator provides deflexions for the scanner which examines the specimen point by point. A detector

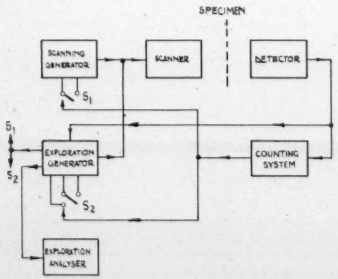

Fig. 2. Basic components of arrested scan system

provides output signals corresponding to the opacity of the specimen found at each point. Signals from the detector are fed to a counting system, which may best be of the overlap type. When the counter indicates the contact of the scanning spot with a particle (i.e. first intercept), a signal is fed out in such a form that it can open the switch S_1 which is attached to the scanning generator. If this switch (normally closed) is opened, the scanning generator is arrested, and the scanning spot stands still. At the same instant the switch S_2 is operated, starting the exploration generator. This develops exploration signals which are superimposed on the momentarily static scanning signals and cause the spot to explore the particle discovered. Meanwhile signals from the detector control the exploration generator and indicate the features of the particle as they are explored. When exploration is complete, the generator reverts to its original condition and emits a signal which resets the switches S_1 and S_2 to their original condition. Normal scanning therefore re-starts from the point at which it was arrested. The exploration generator meanwhile is arranged to feed out to some analyser quantitative signals which indicate the features of the particle discovered.

Necessary properties of counting system. It can be seen that the primary counting system must have certain properties not always needed in such apparatus. Firstly, the scanning generator must be capable of being halted in mid-flight, and must then maintain its signal to a high degree of accuracy. Secondly, the scanner used must be of a type which gives a fair signal under both normal scanning and exploring conditions. A flying-spot scanner falls into this category. Thirdly, the scanner-detector combination must be capable of discovering the features of the particles which are of interest. This often implies some form of multiple exploring spot, or spot balancing as is common in curve following systems.[14,15] Fourthly, the counter must be capable of being stopped in mid-flight without losing control of the system when it is restarted once more. Thus, if it includes any memory system, this must be halted too.

Practical systems

The best combination of techniques for a practical arrested scan system is still being investigated, but simplified model counters have been made. The scanning generators used were of the Miller type.[16] They were arrested by reducing the condenser charging current to a very low value. The residual drift remaining was by this means reduced to 1/10 000 of the normal scan speed, a figure found to be adequate. The scanner included an electrostatic cathode-ray tube which was particularly easy to control in the required manner. A brighter magnetic tube may be used in the future.

The form of particle exploration chosen for the first instrument was simple. On first finding a particle the scanning spot was caused to explore in a straight line at right angles to the normal direction of line scan. After reaching the remote edge of the particle the exploration ceased and normal scanning was resumed. A typical chord of each particle was thus measured and corresponding impulses were available from the exploration generator.

It is not in fact necessary, as at first was thought, to have a counter with a memory which can be stopped abruptly when an exploration is begun. Instead during exploration, the remembered signals can be re-cycled. After the exploration is over the scanning spot can pause at the starting point. When the circulating memory is again in the starting condition, re-cycling can be interrupted and normal scanning resumed. By this means a magnetic drum or a delay line can be used satisfactorily.[17]

For simplicity, the counter used initially was actually of the double spot type and had the disadvantages of that technique. The development of an instrument using a true

memory and with other forms of exploration is proceeding. Details of some of these exploration methods appear in the Appendix.

CONCLUSIONS

The arrested scan technique makes possible an automatic dust particle sizer which can handle rigorously specimens of great density. In addition, by using this system there is the utmost flexibility in the type of exploration to be adopted. Whatever technique is chosen, it only involves the addition of electronic units to a simple counting system.

At the time of writing (October 1953), prototype instruments are being constructed along these lines.

ACKNOWLEDGEMENTS

This work, carried out at Mullard Research Laboratories, for the National Coal Board, is published by kind permission of both organizations. The author wishes to acknowledge with thanks the great assistance which his colleagues at both of these organizations have given him. He must thank in particular Mr. M. A. Snelling, of the former laboratories, who has so consistently turned ideas into realities.

REFERENCES

(1) COOKE-YARBOROUGH, E. H., and WOLFF, H. S., reported by Walton, W. H., in *C.R.E. Report No.* 79 *of National Coal Board*, p. 6 (1951).
(2) WOLFF, H. S. *Nature* [*London*], **165,** p. 967 (1950).
(3) MEYER, E. W. British Patent Application 25647/51.
(4) DAWES, J. G.; HAWKSLEY, P. G. W., reported by Walton, W. H., in *C.R.E. Report No.* 79 *of National Coal Board*, pp. 7, 8 (1951).
(5) YOUNG, J. Z., and ROBERTS, F. *Nature* [*London*], **167,** p. 231 (1951).
(6) GILLINGS, D. W. British Patent Application 11078/50.
(7) ROBERTS, F., reported by Walton, W. H., in *Nature* [*London*], **169,** p. 518 (1952).
(8) BAREFORD, C. F., and DELL, H. A. British Patent Application 5473/51.
(9) WALTON, W. H., THOMAS, D. G. A., and PHILLIPS, J. W. British Patent Application 29460/51.
(10) BRADBURD, E. M. *Elect. Comm.*, **28,** p. 46 (1951).
(11) WILLIAMS. F. C., and MOODY, N. F. *J. Instn Elect. Engrs*, **93,** p. 1188 (1946).
(12) DELL, H. A., and JONES, E. British Patent Application 15311/51.
(13) DELL, H. A., and BROCKELSBY, C. F. British Patent Application 17206/52.
(14) HAZEN, H. L., JAEGER, J. J., and BROWN, G. S. *Rev. Sci. Instrum.*, **7,** p. 353 (1936).
(15) NEWTON, H. E. *Metropolitan-Vickers Gaz.*, **24,** p. 207 (1952).
(16) WILLIAMS, F. C., and KILBURN, T. *Proc. Instn Elect. Engrs*, **96,** Pt. III, p. 81 (1949).
(17) DELL, H. A. British Patent Application 7985/53.
(18) SCOTT, W. E., and MURPHY, B. *British Patent* 690426 (1953).

APPENDIX

Some suggested methods of particle exploration possible with an arrested scan sizer are described here. Owing to resolution limitations the more complex forms are only suitable for large particles, but they indicate the possibilities of the technique.

Exploration of particle chord. The exploration of the chords of two ideal particles is illustrated diagrammatically in Fig. 3. The paths explored are AB on P_1 and CD on P_2. The apparatus necessary is illustrated schematically in Fig. 4. A line to line memory and a signal comparator

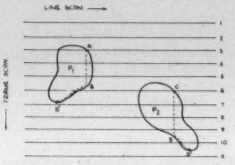

Fig. 3. Particle exploration by chord and y-axis measurement

together form a counter. The memory is assumed to be of the delay line type. Output signals from the comparator indicating first interception of particles are fed to two switch units. Mechanical switches are illustrated, but in practice electronic switch units would be used if the highest speed were necessary. The spot on the tube is deflected in the x-direction by the output from the line scan generator, while the y-deflection is generated by the frame scan generator. Each

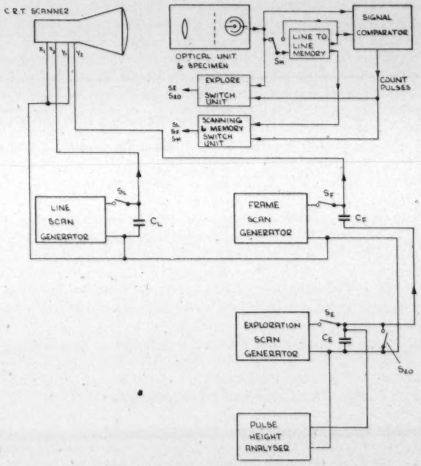

Fig. 4. Arrested scan sizer with measurement of particle chord

of these generators contains some condenser system whose periodic charge and discharge produces the necessary potential waveforms to deflect the cathode-ray tube beam. The condensers, C_L and C_F, are shown in the output circuits, but they would normally be followed by buffer amplifiers. Each condenser is connected to the generator by a switch, S_L and S_F, by which the source of charging current can be cut off. Normally S_L and S_F are closed, current flows into the condensers and time base waveforms are generated. The

cathode-ray tube spot therefore produces a raster. As soon as a count pulse appears indicating that the first interception of a particle has occurred (e.g. at *A* on line 3 of the raster in Fig. 3) the switch units operate. The lower unit controls S_L and S_F which then open, immobilizing the spot. At the same time S_M is operated. This connects the output of the memory to the input so that circulation begins.

In series with the frame condenser C_F is a switch S_{E0}, normally in the closed position. This shunts a condenser C_E belonging to the exploration scan generator which can be charged up to generate a special time base when S_E (normally open) is closed. When the upper switch unit is operated S_{E0} is opened and S_E is closed. The condenser C_E charges up and superimposes a potential on the now static charge in the frame condenser C_F. Thus, although the scan has been arrested and the original arrested position can be retrieved whenever required, an additional deflexion has been superimposed on the cathode-ray spot. In this instance the exploration scan generator moves the cathode-ray spot vertically downwards (Fig. 3 from *A* to *B*).

The upper switch unit can only be re-set by a signal from the scanner. The spot is obscured by the particle between *A* and *B*, but at *B* a signal appears, the upper switch re-sets, S_E opens and S_{E0} closes, and the spot returns to *A*.

At some later time the memory is again in the state at which exploration began (i.e. after a whole number of circulations). An output pulse is then emitted, the lower switch is re-set and S_L and S_F are closed so that scanning begins again. S_M is also operated by this switch so that circulation is stopped and normal counting is resumed. Later intercepts on P_1 produce no effect as the memory prevents the generation of a count pulse. The particle P_2 would be similarly discovered at *C* and explored from *C* to *D*. A conventional pulse height analyser connected to C_E records the particle sizes discovered.

Exploration of particle y-axis. An improvement in the chord measurement is possible if the maximum dimension of each particle at right angles to the direction of scan is found. This can be achieved if the exploring spot has an additional small rapid oscillatory motion superimposed on it in the direction of line scan. On reaching a point such as *B* in particle P_1 (Fig. 3) the spot will first emerge only at the right-hand limits of its oscillation. This can be made to generate a potential, superimposed on the line condenser C_L, which drives the oscillating spot back into the particle. It therefore drifts downwards along the path *BB'*. At the lower limit of the particle, the spot wholely emerges indicating the completion of the exploration. In the same way particle P_2 would be explored along *CD*, when the spot would emerge on the left-hand limits of oscillation. This would force it to the right so that it would explore along *DD'*.

Exploration of particle area. Particle area may be found by causing the spot to explore horizontally back and forth over the particle in a number of equally spaced lines. If the spot motion is reversed and stepped down in the frame direction at each emergence, the total length of track is proportional to the area of the particle.

Exploration of particle mean diameter. The mean diameter of particles may be found approximately by superimposing on each in turn a spot tracing out a circle of ever increasing radius. The emergence of the spot must be arranged to provide self-centring shift potentials to the system so that as much of the circular track as possible lies on the particle. Eventually, in spite of this, half the track will lie off the edge of the particle when exploration can be considered complete. The diameter of the final circle is approximately that of a disk having an area equal to that of the particle.

Exploration of particle perimeter. The perimeter of a particle may be explored by means of a spot rapidly tracing out a small circle of constant radius. This must be constrained both to move along and to remain in contact with the particle edge *P* (Fig. 5). A mechanical method of doing this at slow exploring speeds has been described.[18]

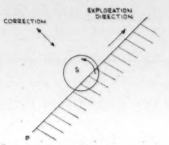

Fig. 5. Motion required for particle perimeter exploration

The time for one complete circuit of a particle can be made proportional to the perimeter length. The activity of a servo-driven shaft controlling the direction of exploration can indicate particle shape.

DISCUSSION

Mr. E. H. Cooke-Yarborough: It has been pointed out that guard spot systems fail if the two scanning spots do not have identical characteristics. This objection has been overcome in Mr. Dell's apparatus by using a single spot and comparing what it sees with what it saw one line scan earlier. This involves storing the whole of one line scan on acoustic delay lines.

It seems to me that there is fundamentally no need to store so much information and I would draw attention to a proposal I made in 1951* and which is referred to briefly in our paper (G.3).

This scheme proposes use of rapid repetitive sawtooth scans, which we will call minor scans, perpendicular to the line scan, having an amplitude of a few spot diameters and a period of a few microseconds. A coincidence circuit associated with a short electrical delay line ensures that a pulse is only obtained if an object appears in corresponding positions on two or more successive minor scans. An electronic gate causes any part of this pulse which occurs within a defined period near

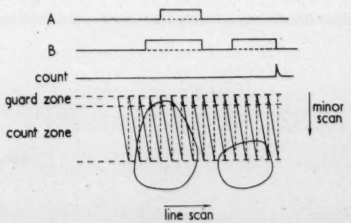

Illustrating use of repetitive sawtooth scans in a particle-counting machine

* British Patent Application 21937/51.

the beginning of the scan to trigger a bistable circuit *A*. This establishes a guard zone as shown in the figure. Any part of the pulse which occurs during the remainder of the minor scan triggers a second bistable circuit *B*. This establishes the count zone. The first occurrence of a complete minor scan period without a signal resets *B* and also resets *A* if this has been triggered. If *B* resets without *A*, this means that an object has been in the count zone for two or more successive scans and has been scanned through without being in the guard zone for two or more successive scans. This condition causes a count to be registered, or could cause the scan to be arrested and the object to be explored as in Mr. Dell's scheme.

An advantage of this arrangement is that it places a fairly well defined lower limit on the diameter of the particles counted, since the particle must be large enough to cover two successive minor scans (this was the original object of the scheme). For the present purpose its greatest advantage seems to be that it requires a memory delay circuit only a few microseconds long (equal to the duration of a minor scan), which could be provided rather simply by an electrical delay line.

I believe that this system need not suffer from the disadvantages of the double spot pseudo-memory mentioned in the paper and I would be interested to have Mr. Dell's comments.

Author's reply: Consider a field scanned once by a single spot system with some line-to-line memory device. The area examined as each line of scan proceeds is that enclosed between the line scanned and the previous line, wherever it was. Within the usual resolution limits, the field can therefore be covered uniquely by ensuring only that the scanning lines never cross. When a double spot pseudo-memory system is used, on the other hand, the area examined as each line proceeds is that enclosed between the tracks of the two spots. If the field is to be covered uniquely, it is therefore necessary that the leading spot in one line of scan and the trailing spot in the next line of scan should follow identical paths. It is the practical difficulty of achieving this that introduces the overlap and underlap miscounting phenomena. In the method described by Mr. Cooke-Yarborough, the scanning spot oscillates rapidly at small amplitude (minor scan) normal to the direction of progression in the line direction (major scan). At one extreme of the oscillatory motion it is given the properties of a "guard" spot, and at the other a "counting" spot. The area of the specimen examined as a major scan proceeds is that swept out by the "counting" fraction of the minor scan. If a field is to be uniquely covered it is therefore necessary that the counting areas swept out in each major scan are truly contiguous. Thus in practice the same difficulties will exist as with other pseudo-memory devices. Using isolated traverses, the method described would undoubtedly give good results where only a statistical examination of a specimen area is required.

Paper G.5

Testing a counting machine

By R. J. Courshee, B.Sc., National Institute of Agricultural Engineering, Silsoe, Bedfordshire

The method and results of measuring the accuracy of a particle sizing and counting machine are described and compared with the results obtained when sizing with a microscope. Machine counting appears to be quicker and more consistent and accurate than counting by eye.

It is important for certain methods of agricultural spraying to be able to measure the sizes of the drops formed by a nozzle and landing on a plant. For this purpose a black dye is added to the spray and a deposit record in the form of black circular stains on a white background is obtained. Since numerous samples need to be examined a machine was made to size and count the stains.[1,2]

The method known as intercept sizing was used as this leads to a simple machine. Consider a set of thin lines which are parallel and equally spaced drawn across a set of circles of several sizes. The family of chords thus obtained characterizes the family of circles. The machine measures the size frequency distribution of chords obtained in a similar way by moving the spray stains at uniform velocity in front of a light sensitive detector. The chord length and linear velocity of scan determine the duration of the signal corresponding to a black, scanned surface.

Each stain of a given size gives a characteristic number and size distribution of chords. Therefore given the total numbers of chords in each of several size ranges it is possible to compute approximately the number of circular stains from which they were derived.[3,4]

When the particle counting machine first went into action, however, there were surprising differences between the measurements made by eye and with the machine. There seemed to be no good reason for the differences and no indication was available to indicate which, eye or machine counting, was right or more nearly right. Accordingly, we tried to measure for our methods of sizing spray drops how accurate were the several stages: sampling, sizing (including the small number counting error) and the reduction of the measurements made to convenient parameters.

Sampling an inhomogeneous population can lead to very large errors as when, for example, a single sampling cell is placed in one part of the spray from a nozzle which is distributed in the manner shown in Fig. 1. Sampling is not usually done under isokinetic conditions since the spray drops are normally large enough for errors introduced in this way to be negligible. Occasionally they are not, as in Fig. 2, which shows how the smaller drops tend to land only on the edges of a slide held by hand in the path of a cloud of fine spray. Sizing is sufficiently accurate and the sizing machine is more accurate than eye counting, the latter being faulty partly because of the tedium of the work. It is rarely convenient to size the spherical spray drops and the impressions left by them on a plane receiving surface are measured instead. The correlation between the size of the parent drop and the size of these impressions, or in our case, stains on a glass slide coated with a silicone, has been studied and since the relationship is expressed graphically an error of 1% at this stage cannot be avoided. The statistical counting error has been considered by many people and the only additional

comment I wish to make is that the criterion of accuracy accepted determines how many particles need to be counted in each size group. For our own work we need to know surface area accurately rather than mass.

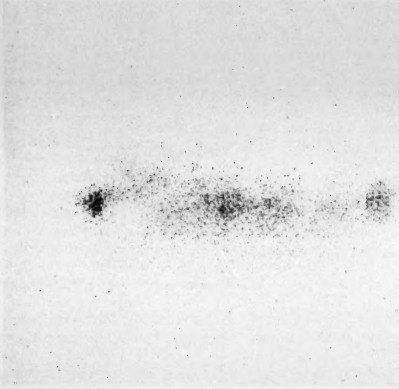

Fig. 1. Distribution of drop size within the spray from a fine nozzle

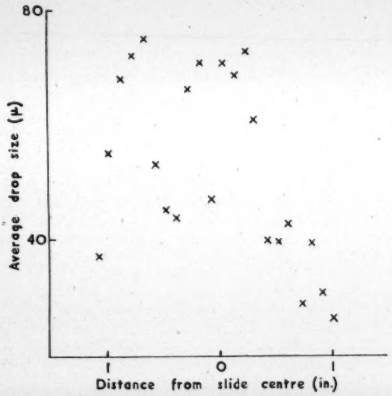

Fig. 2. Distribution of drops on a slide in the path of a cloud of fine spray

Finally having done all the work it is possible to introduce quite large errors in reducing the experimental results as has been shown by Joyce in a Shell Oil Company Technical Bulletin, when, for example, the surface area of spray per unit mass is estimated by graphical methods which, largely owing to their insensitiveness, only appear to fit the experimental results. To quote R. A. Fisher, "A quantity of data which usually by its mere bulk is incapable of entering the mind is to be replaced by relatively few quantities which shall adequately represent the whole." To do this we use only numerical methods.

Of these experimental errors which are likely to be encountered when measuring the sizes of drops formed by a nozzle one, sizing and counting, is considered more fully in the following paragraphs.

EQUIPMENT

The equipment is formed in two units: the scanner and the analyser. The most convenient readily available equipment for scanning the sample was a Muirhead picture telegraph transmitter.[5] The spray deposit record is wound on to a cylindrical drum which moves so that the record is scanned in a spiral path by the microscope and photoelectric detector. The output of the transmitter, consisting of a series of pulses of various durations, is fed to the analyser.

For the duration of each pulse a voltage is increased linearly with time and applied simultaneously to ten counters each of which is set to count once when the applied voltage reaches a prescribed level. A cumulative, that is integral, count is thereby obtained of chord intercepts. The decade counters used have a capacity of 99 999 and using Dekatron valves can handle signals at the rate of 1500 a minute.

Early tests appeared to show wide differences between the count obtained with the machine and that given by eye counting. For this reason a more complete test of eye counting was made and the meaning of the word accuracy when applied to a frequency histogram further considered. The limitations of the intercept method of sizing circular stains became more apparent as a result of these tests.

CHORD INTERCEPT SIZING

Consider the number of chords per unit range of chord length which will be obtained from a stain of diameter D. It is clear that if the scanning lines cross a circle within the bands a–b or c–d (Fig. 3) a chord of the required length L results. The number of such chords is $2ab/t$ where the interval between scanning lines is t. Such chords will be obtained from all stains larger in diameter than the length L.

Therefore as dL tends to zero

$$G(L) = \frac{L}{t}\int_{L}^{\infty} (D^2 - L^2)^{-\frac{1}{2}} \cdot f(D)dD \qquad (1)$$

where $G(L)$ is the frequency function for chord lengths and $f(D)$ that for stain diameters.

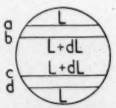

Fig. 3. Chord intercept sizing

Conversely from the measured value of $G(L)$, the approximate value of $f(D)$ may be obtained.

The numbers of such chord lengths lying within ten size ranges are recorded by the analyser and it is assumed that the frequency distribution of chord lengths can be defined with sufficient accuracy for many purposes by only ten size groups.

SIGNAL GENERATION

As the scanning spot edge crosses the stain edge the amount of light reflected to the detector begins to decrease and reaches a minimum value when the eclipse is complete. The

true chord length is the distance between the two positions where the scanning spot centre lies on the scanned stain edge. This is approximately equal to the distance between the two points when the scanning spot is half obscured.

The signal generated is not therefore rectangular and so the duration attributed to it depends upon the point where it is measured. A level equal to half the maximum level of the signal is therefore selected. The duration of signals formed by scanning across black bands of known width was measured with a millisecond chronometer controlled by a quartz crystal source to ensure that the correct signal duration was obtained.

SIGNAL MEASUREMENT

Pulses of known duration, measured with the chronometer, were fed to the analyser to ensure that the integrator period, which determines the time rate of growth of the voltage applied to the counters, and the counter settings and sensitivities were correct.

The combination of the two tests of signal generation and measurement show that the scanner and analyser together measure and record the lengths of intercepts on the scanned pattern accurately.

SPRAY DEPOSIT MEASUREMENTS

An artificial sample representing a spray deposit was used for the majority of the tests described. It was made with black, punched disks mounted on white card. The frequency distribution curve should consist of a series of peaks centred on the size of each punch.

The tests and their results were as follows:

(1) One observer sized the pattern by eye, using two standard methods: (*a*) comparison of the stains with a set of circles of standard size (magnification unity); (*b*) measurement with a linear graticule (× 10). The answers for mean linear diameter were 1·86 mm and 1·94 mm respectively. (The class interval medians were used to estimate the mean.)

(2) A second observer was called upon to repeat the first measurement using the comparison circles and found a mean linear diameter 2·10 mm (compared with 1·86 mm).

(3) A third observer repeated the second measurement made by the first observer and obtained an answer 2·06 mm (compared with 1·94 mm).

(4) Finally the first observer was asked after a period of a few weeks to repeat his second measurement and obtained the answer 1·90 mm compared with the previous value of 1·94 mm.

(5) The counting machine was then used to size the same sample. Two runs were made with an interval of several days between them and the values 2·01 and 2·01 mm were obtained. The average machine value was 2·01 mm and the average of the several counts made by eye was 1·97 mm.

(6) The time taken was approximately 7 hours per sample of 2000 stains for each count made by eye. Scanning time was negligible when sizing by machine but about thirty minutes was required for (*a*) photographing the original record and preparing a print suitable in size and contrast for machine analysis, and (*b*) the arithmetic involved to translate the chord count into a stain frequency distribution count.

ERRORS

The most important errors of the method are due to: (i) the machine estimating incorrectly the length of a chord, and (ii) the necessity, for practical reasons, of estimating the frequency distributions with only a small number of size ranges.

Errors of measurement. It was found that the relatively small errors of chord measurement (usually less than 1% of the range) caused large errors in estimating the frequency of occurrence of diameters in the lower size ranges which are near the mode of the distribution and where the size rate of change of frequency of occurrence is great. It was concluded that the integral frequency distribution curve is usually more suitable for illustrating the form of distribution with the 1% accuracy which is required, than the frequency histogram. From equation (1) it may be shown that

$$\bar{D} \text{ i.e. } \frac{\int_0^\infty Df(D)dD}{\int_0^\infty f(D)dD} = \frac{\pi}{2}\frac{\int_0^\infty G(L)dL}{\int_0^\infty L^{-1}G(L)dL} \qquad (2)$$

If the machine underestimates the length of each chord it will underestimate the total number of chords greater than the minimum measurable size, the numerator of equation (2), because those chords which occur but are not recorded are judged by the machine to be less than the minimum. The underestimation of each chord length results in a decrease in the estimated chord harmonic mean and an increase in the denominator in equation (2). The net result is a greater error of the same sign in estimating the mean diameter. The error in estimating the mean stain diameter has usually been greater than twice the error in measuring the mean chord length. The average of the measurements made by eye was taken as a standard of correct measurement for the estimation of error.

Errors of analysis. $G(L)$ is estimated by recording the numbers of chords falling within a set of size ranges. Chords greater than a length L, but which may have a length anywhere in the range L to $L + dL$ where $dL = (2^{\frac{1}{2}} - 1)L$, can only be obtained by scanning stains with diameters greater than L. If the stain diameter $= 2^{\frac{1}{2}}L$ the average number of chords of length greater than L which will be obtained per stain is $0{\cdot}64\ L/t$. Whereas if the stain diameter is $2^{\frac{1}{2}}L$ the average numbers of chords of length greater than L which will be obtained per stain is L/t.

The process of measuring the number of chords in a size range and estimating the number of stains from which they were derived depends upon assuming a value for the average number of chords obtained per stain. This average may be obtained on the basis of several alternative assumptions concerning the distribution of stain diameters inside one machine measuring range.

Early samples used to test the machine were made with stains formed by a spinning disk nozzle which gives at one setting stains of closely similar sizes. The nozzle was used at several settings to give several sets of stains each of a narrow size range. Errors were met because of the way in which these arbitrarily chosen stain sizes coincide with the upper and lower limits of a size measuring range and gave rise to numbers of chords different from the number expected from a rectangular distribution of stain sizes.

It is convenient to assume either that the stains are concentrated at the mid point of each measuring range or that

they occur with equal frequency throughout each measuring range. Some such assumption is necessary to compute the average number of chords expected per stain. This subject has been treated more fully by Thompson and Acton.[3]

CONCLUSIONS

It is concluded:

(1) That the experimental error associated with eye counting is larger than is often assumed in accepting this method as a comparison standard.

(2) That the counting machine measures quickly and with an accuracy better than 1% of the range.

(3) That chord intercept measurement errors tend to result in greater errors in the estimation of stain mean diameters.

(4) That the interpretation of the measurements made is not accurate unless the stain diameter distribution is represented with sufficient accuracy by a histogram with size limits arranged in steps the same as the chord length limits of the machine and, therefore, multimodal distributions are unsuitable for testing the present arrangement of this type of counting machine.

REFERENCES

(1) Trickett, E. S., and Courshee, R. J. *Nat. Inst. Agric. Eng.*, Report No. 27 (1953).
(2) Trickett, E. S., and Wheeler, L. K. *Post Office Engineering Department*, Report No. 13397 (1952).
(3) Thompson, W. E., and Acton, R. A. *Post Office Engineering Department*, Report No. 13355 (1952).
(4) Grundy, P. M. Private communications.
(5) *Operating instructions for picture transmitter type D6281.* (Beckenham: Muirhead and Co. Ltd.)

DISCUSSION

Mr. P. G. W. Hawksley: The line intercept method of sizing as discussed by Mr. Courshee, has the advantage, in contrast with track scanning methods, that coincidence errors are negligibly small but suffers from the severe drawback that the available theoretical treatments are limited to circular particles. The following gives an extension to elliptical particles. An expression is obtained for the frequency distribution of intercept lengths in terms of the frequency distribution of ellipse sizes (defined by the diameter of a circle having the same perimeter as the ellipse). It has not proved possible to solve this integral equation, but numerical solutions can be constructed for any specified eccentricity.

Denote the size distribution of ellipses by $f(t)$, where t is the diameter of a circle having the same perimeter as the ellipse. Let a and b be the smallest and largest ellipses present and let $\int_a^b f(t)dt = 1$. Let $\psi(y)$ denote the frequency distribution of chord lengths y with $\int_0^{y_{max}} \psi(y)dy = 1$, where y_{max} is the largest possible chord. For convenience we put the number of ellipses per unit area equal to unity. The number per unit area of size t to $t + dt$ is then $f(t)dt$. For any given ellipse let θ be the angle between its major axis and the perpendicular to the intercepting line and let x be the projection of the ellipse on this perpendicular.

Now if we assume the ellipses are orientated at random, the number per unit area of ellipses of size t having major axes lying between θ and $\theta + d\theta$ is

$$\frac{1}{2\pi} f(t)dtd\theta$$

The probability that the straight line will intercept an ellipse of size t orientated at angle θ and having a projection x, relative to the probability of intercepting ellipses of all sizes and all orientations is $x/\bar{x}$, where $\bar{x}$ is the mean value of the projections of all sizes in all orientations. Thus the number per unit area of size t intercepted and orientated at angle θ and having a projection x is

$$\frac{1}{2\pi}\frac{x}{\bar{x}} f(t)dtd\theta$$

Now let $z(< x/2)$ be the perpendicular distance from the chord (of length y) to the centre of the ellipse. The intercepting line is equally likely to lie (for a random line) at any given distance z as at any other distance in the range $z = 0$ to $z = x/2$ and the probability that the intercepting line giving a chord y lies at a distance between z and $z + dz$ from the centre of the ellipse is therefore $2dz/x$.

Thus the number per unit area of ellipses of size t, orientated at angle θ, having a projection x and giving a chord y is

$$\frac{1}{\pi\bar{x}} f(t)dtd\theta dz$$

Let y_0 denote the central chord through the centre of the ellipse and parallel to the chord y. Then from the geometry of the ellipse,

$$y_0 = Bt/(1 + k^2\cos^2\theta)^{\frac{1}{2}}$$

$$x = Bte(1 + k^2\cos^2\theta)^{\frac{1}{2}}/k$$

where $k = e/(1 - e^2)^{\frac{1}{2}}$. $B = \pi/2E(\sin^{-1} e)$, e being the eccentricity and $E(\sin^{-1} e)$ the complete elliptic integral of the second kind with argument $\sin^{-1} e$.

Since from the geometry of the ellipse, we have also

$$y^2 = y_0^2(x^2 - 4z^2)/x^2$$

it is easily shown that, on differentiating and substituting for y_0 and x,

$$\frac{dz}{dy} = -\frac{y(1 - e^2)^{\frac{1}{2}}(1 + k^2\cos^2\theta)^{\frac{1}{2}}}{2[B^2t^2 - (1 + k^2\cos^2\theta)y^2]^{\frac{1}{2}}}$$

Hence the number of ellipses of size t, per unit area, orientated at angle θ and giving a chord of length y is, dropping the minus sign to keep the probabilities positive,

$$\frac{(1 - e^2)^{\frac{1}{2}}}{2\pi\bar{x}} \cdot \frac{y(1 + k^2\cos^2\theta)^{\frac{1}{2}} f(t)dtd\theta dy}{[B^2t^2 - (1 + k^2\cos^2\theta)y^2]^{\frac{1}{2}}}$$

Now for ellipses orientated at angle θ, chords of length y will be given by all sizes of ellipse whose central chord y_0 is equal to or greater than y, that is for sizes t, equal to or greater than $t_0 = y(1 + k^2\cos^2\theta)^{\frac{1}{2}}/B$. Thus the total number of chords of length y due to ellipses of all sizes orientated at angle θ is

$$\frac{(1 - e^2)^{\frac{1}{2}}}{2\pi\bar{x}} \cdot ydy(1 + k^2\cos^2\theta)^{\frac{1}{2}}d\theta \int_{t_0}^{b} \frac{f(t)dt}{[B^2t^2 - (1 + k^2\cos^2\theta)y^2]^{\frac{1}{2}}}$$

where $t_0 = y(1 + k^2\cos^2\theta)^{\frac{1}{2}}/B$.

The frequency distribution $\psi(y)$ due to all sizes of ellipse $t \geqslant t_0$, for all orientations θ is obtained by integrating over

$\theta = 0$ to $\theta = 2\pi$, which is equivalent to four times the integration for 0 to $\pi/2$. Thus

$$f(y) = \frac{2(1-e^2)^{\frac{1}{2}}}{\pi\bar{x}} \cdot y \int_0^{\pi/2} (1 + k^2\cos^2\theta)^{\frac{1}{2}} d\theta \times \times \int_{t_0}^{b} \frac{f(t)dt}{[B^2t^2 - (1 + k^2\cos^2\theta)y^2]^{\frac{1}{2}}}$$

The mean projection $\bar{x}$ is equal to the mean perimeter diameter $\bar{t}$, and, making this substitution, changing the order of integration and writing $u = y/B$, we have

$$\psi(y) = \psi(Bu) = \frac{2(1-e^2)^{\frac{1}{2}}}{\pi\bar{t}} u \times \times \int_u^b \frac{f(t)dt}{(t^2-u^2)^{\frac{1}{2}}} \int_{\cos^{-1}(1/s^2)}^{\pi/2} \frac{(1 + k^2\cos^2\theta)^{\frac{1}{2}} d\theta}{(1 - s^2\cos^2\theta)^{\frac{1}{2}}}$$

where $s = ku/(t^2 - u^2)^{\frac{1}{2}}$.

It has not proved possible to solve this integral equation for $\psi(y)$ nor to carry out the integration under the integral. However, numerical methods may be employed in any particular case. For very small eccentricities $|k^2| < 1$, $|s^2| \ll 1$, the series in the integrand can be expanded and integrated term by term. Including only terms in k^2 and s^2 gives

$$\psi(Bu) = \frac{(1-e^2)^{\frac{1}{2}}}{\bar{t}} u \int_u^b \frac{f(t)}{(t^2-u^2)^{\frac{1}{2}}} \times \times \left[1 + \frac{s^2 + 3k^2}{4} - \frac{2}{\pi}\cos^{-1}\left(\frac{1}{s^2}\right)\left(\frac{s^2 + 3k^2 + 4}{4}\right)\right] dt$$

In the case of circles, since $e = 0$, $k = 0$, $E(\sin^{-1} e) = \pi/2$, $B = 1$, $u = y$, this reduces to Wicksell's* solution

$$\psi(y) = \frac{y}{\bar{t}} \int_y^b \frac{f(t)dt}{(t^2-u^2)^{\frac{1}{2}}}$$

* WICKSELL, S. *Biometrika*, **17**, p. 84 (1925).

Author's reply: Although the intercept method of sizing cannot be used at present (except by graphical methods) to measure the size distribution of irregularly shaped particles it has advantages over other sizing methods when applied to measuring the deposition of sprays on agricultural crops even if the stains left by the spray are not circular.

The size of the drops forming a spray are one of several factors influencing its toxicity. But sizing, i.e. measuring the full size distribution of a spray, is only one means of deriving the parameters which have a more direct influence on toxic activity. These are readily measured directly by a chord intercept sizer and are listed below to show that although the drop size distribution could be used to provide the figures required we must not in this example of particle sizing work, and possibly in many others, be misled into pursuing too closely sizing as an end in itself.

The factors thought at present to influence the effectiveness of many types of spray deposit are (1) the cover of the target (fraction of the leaf area contaminated with spray), (2) the size of the unsprayed intervals between spray particles, and (3) the quantity per unit area of toxin however it is distributed. The first and second determine the likelihood of contact between toxin and pest and the third both whether or not the pest is killed if contact occurs and also the durability of the exposed deposit.

These are measured with a chord intercept counter in the following manner. The fraction of the unit area scanned which is covered with spray is equal to the total intercept length multiplied by the distance between scanning lines. The time interval between consecutive signals denoting interceptions is measured (exactly as the time duration of signals is measured) to show how large are the distances between spray stains in the direction of the scanning line. The dose per unit area follows from a measurement of the cover. The relationship between the two is measured empirically at present. (It is determined by the Sauter mean diameter of the drops forming the spray and their contact angle on the plant surface.)

Paper G.6

The design and construction of a photoelectronic scanning machine for sizing microscopic particles

By P. G. W. HAWKSLEY and J. H. BLACKETT, British Coal Utilisation Research Association, Leatherhead, Surrey; E. W. MEYER and A. E. FITZSIMMONS, Casella (Electronics) Ltd., London

The design of photoelectronic scanning machines for counting and sizing particles is discussed. Data are presented on the performance of a machine constructed for sizing particles dispersed on microscope slides. The size distribution of a sample of coal particles down to 5 μ as determined by the scanning machine agrees with that from a visual count.

In recent years a number of photoelectronic scanning machines have been developed for the automatic counting and sizing of particles dispersed in a plane field of view. Wide[1] or track scan methods have been employed for the counting of red blood cells (Lagercrantz,[2] Wolff,[3] MacFarlane and Poole[4] and Cooke-Yarborough and Whyard[5]); double spot counting of microscopic particles, which is a special case of track scanning, is being investigated by Roberts and Young[6] and by Dell[7] using the flying spot scanning technique of Young and Roberts.[8] Track scanning can however be employed for particle sizing (Hawksley[9,10]), and one method has been investigated by Pigford[11] for sizing photographic images at millimetre sizes. Narrow spot or line scan methods—chord intercept sizing—provide the basis of machines for sizing photographic images, developed by Hoare[12] in collaboration with Wheeler and Trickett[13] and Courshee,[14] and by Adler, Mark, Marshall and Parent.[15]

An attempt has been made to develop a machine not only for counting but also for sizing microscopic particles directly, without the intermediate photographic enlargement stage used in the sizing machines described so far. A flexible construction has been employed so that both track and line scanning methods can be investigated. At present the experimental work has been restricted to confirming the theory of

track scanning given by Hawksley.[10] This requires for its simplest practical application that the particles be of constant optical density and attention has been confined to the sizing of coal particles. Double spot sizing (Hawksley[9,10]), can be used where the optical density is not constant.

The present indications are that observations from the direct scanning of particles smaller than about 5 μ cannot be interpreted unless account is taken of diffraction effects present at such sizes. This does not rule out the sizing and counting of particles near the limit of optical resolution by means of an appropriate calibration or by the development of more elaborate scanning machines.

1. DESIGN CRITERIA

The essential features of a photoelectronic scanning machine are shown in Fig. 1. An illuminated aperture S_1 is imaged by a lens system C on the field of particles F, which in turn is imaged by a lens system O on a second aperture S_2, behind which is placed the cathode K of a photocell. The area of the field viewed by the photocell is determined by whichever aperture S_1 or S_2 acts as the field stop of the system. The field is scanned by moving it relatively to the field stop S_1 or S_2. The light flux falling on the cathode generates a photocurrent which produces a voltage across the load resistor R. When the field is scanned, the changes of light flux resulting from the passage of particles across the field of view of the photocell, produce pulses of proportionate magnitude, which after amplification are fed to an amplitude discriminator. The discriminator gives a standard output pulse whenever the input pulse height exceeds a predetermined trigger level. The standard pulses are counted by a scaler.

The details of the arrangement are not important for the following discussion, although some arrangements are in practice preferable to others. It does not matter whether the area viewed by the photocell is determined by S_1 or S_2 or by both together. The aperture S_1 may be Kohler illuminated as shown in Fig. 1 or the source of light itself (a solid filament,

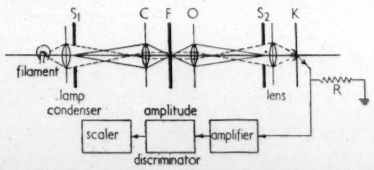

Fig. 1. Diagram of photoelectronic scanning machine

diffusing screen or the flying spot on a cathode-ray tube) may be placed at S_1. The cathode K may be placed directly at S_2 or, as shown in Fig. 1, the exit pupil of the lens system O may be imaged on the cathode by a lens at S_2. The field may be scanned by moving the slide F carrying the particles or by moving either S_1 and its illuminating system or S_2 together with the cathode. The flying spot microscope system,[8] in which the illuminated aperture S_1 is a flying spot on a cathode-ray tube, may be employed. Although the case of particles viewed by transmitted light is discussed below, the arguments apply in general also for dark field illumination.

1.1. *Methods of counting and sizing.* There is no essential difference between counting and sizing. Sizing is the measurement of the number of particles, per unit reference area, between specified limits of particle size; counting is the same measurement for all sizes of particle present in the field. Scanning methods, in their simplest form, give the number of particles per unit area larger than a size z determined by the setting of the amplitude discriminator ("discriminator bias" or "trigger level"). With a suitable shape of scanning aperture (e.g. a slit), the discriminator bias may be made proportional to the size z, and sizing carried out by making a series of counts at different trigger levels. Counting, for example, of red blood cells, is relatively simple because the size z may be chosen anywhere below the lower limit of particle sizes present. In many practical cases, however, the particle size distribution extends down to sizes below the limit of detection; the "counting" of particles down to some fixed size, for example of a thermal precipitator sample down to $\frac{1}{4}$ μ, requires a machine designed for sizing.

There are two scanning methods: (*a*) track and (*b*) line scanning. The number of particles per unit area of size greater than a specified size z is deduced from observations:

(*a*) in track scanning, of the number $\phi(w, z)$ of particles, per unit length of track, that reach into the track of width w, by distances h greater than a distance z (see Fig. 2). The theory has been given by Hawksley,[10] who lists a variety of special cases. Here it is sufficient to note that, for z = constant,

$$\phi(w, z = \text{const.}) = (w + \bar{z} - 2z)NF(z) \qquad (1)$$

where $NF(z)$ denotes the number per unit area of particles oversize z, and $\bar{z}$ is the mean size of particles larger than z. The number oversize z is found from counts at constant z but two different track widths. The oversize distribution is obtained from a series of such pairs of counts at several values of z.

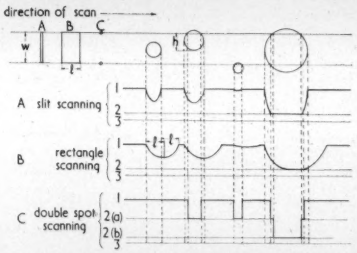

Fig. 2. Track scanning: pulse heights

1, full light; 2, full obscuration; 2(*a*), full obscuration one spot; 2(*b*), full obscuration both spots; 3, blackness.

(*b*) in line scanning, of the number $\psi(u)$ of particles intercepted per unit length of scan and giving intercept lengths y greater than u (see Fig. 3). The theory of line scanning has been worked out only for circular particles[15–17], and in that case, the number of particles per unit area larger than z is

$$NF(z) = \frac{2}{\pi}\int_z^b (u^2 - z^2)^{-\frac{1}{2}}\psi'(u)du \qquad (2)$$

where the prime denotes differentiation with respect to u and b is the largest diameter present.

1.2. *Shape of scanning aperture.* In track scanning the pulse height depends on the shape of the scanning aperture as well as on the size and position of the particle in the track.

The number ϕ is most easily measured by scanning with a slit-shaped aperture (*A*, Fig. 2), whose length *l* in the direction of scan is negligibly small. In that case the maximum height of any pulse is proportional, for circular particles, to the distance *h* by which the particle extends into the track, independent of the size of the particle; for non-circular particles, the pulse height depends on the maximum distance within the track which is not necessarily equal to *h*; the error in taking the pulse height equal to *h* will be small except for extreme shapes and when *h* is comparable with the track width *w*. Slit scanning is the method adopted in the present investigation. If the scanning aperture is rectangular and its length *l* is not negligibly small (*B*, Fig. 2), as is the case in the machines[2–5] employed for blood cell counting, the maximum pulse height varies with both *h* and the size of the particle relative to the dimensions *w* and *l* of the scanning aperture. If, however, the particles are all the same size the pulse height varies with *h*, but not proportionally. In double spot scanning (*C*, Fig. 2), pulses of constant height result from full obscuration of the spot apertures.

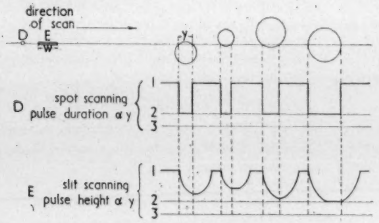

Fig. 3. Line scanning
1, full light; 2, full obscuration; 3, blackness.

In line scanning there are two possible arrangements. If a spot aperture is employed as in the machines constructed by Hoare and others[12–15] the pulse height is constant but its duration is proportional to the intercept length *y*. The number $\psi(u)$ is then found by including in the electronic circuit a device for producing, for presentation to the discriminator, pulses of height proportional to the duration of the output pulses from the photocell. It is also possible to determine $\psi(u)$ by using a slit-shaped scanning aperture (*E*, Fig. 3), orientated parallel to the direction of scan. The pulse height is then proportional to the intercept length *y*. A slit scanning machine may be used for both track and line scanning by simply turning the scanning slit through 90°.

1.3. *Pulse height and signal to noise ratio.* The design of any photoelectronic scanning machine is governed by a number of inter-related conditions partly electronic and partly optical. The two most important are the signal to noise ratio and the lower limit set by diffraction to the effective scanning area at the field. The first is considered here and the second in the following section.

1.3.1. *Maximum pulse height.* If *F* denotes the light flux falling on the cathode of sensitivity *k*, the resulting photocurrent is *kF*. The amplified output current from the photocell produces a voltage kG_PRF across the load *R*, G_P being the (linear) current gain of the (electron multiplier) photocell. The voltage *V* at the output of the amplifier of (linear) voltage gain G_A is

$$V = G_A G_P R k F \tag{3}$$

Now the flux F_0 through the field stop *S* unobstructed by any particles in the field is, providing the source and field radiate diffusely

$$F_0 = \pi K B N_e^2 A \tag{4}$$

where *A* is the area of the scanning aperture at the field (the actual area of the field stop S_1 or S_2 in Fig. 1 divided by the square of the linear magnification *M* of the lens system *C* or 0), *B* is the brightness of the source (filament, diffusing screen or flying spot), N_e is the effective numerical aperture of the system (determined by whatever constitutes the aperture stop) and *K* is the transmission factor, $(1 - K)$ being the fractional energy lost by absorption and reflexion in the optical system from source to cathode. It is assumed in equation (4) that the media on either side of the field have the same refractive index. The equation applies strictly only for a point on the optical axis; *K* is effectively smaller for off-axis parts of the field stop.

The flux F_1 through the field stop when a particle of uniform optical density *D* is interposed at the field (for the moment this is supposed to be a particle large compared with the area *A*) is $F_0(1 - D)$ so that the maximum change $(F_0 - F_1)$ in flux reaching the cathode is $\pi K B N_e^2 D A$.

The maximum change in voltage $(V_0 - V_1)$, denoted by ΔV, corresponding to the maximum change $(F_0 - F_1)$ in the flux falling on the cathode is, from equations (3) and (4),

$$\begin{aligned}\Delta V &= G_A G_P R D k F_0 \\ &= \pi k K N_e^2 B G_A G_P R D A\end{aligned} \tag{5}$$

This is the maximum output signal or pulse height, for any photoelectronic scanning machine, obtained when the field stop of area M^2A is fully obscured by a particle of optical density *D*.

1.3.2. *Signal to noise ratio.* Noise fluctuations superimposed on the pulses modify their height. A pulse whose peak height does not reach the trigger level may be raised above it and a pulse exceeding the trigger level may be depressed below it. The effective pulse height may thus differ from its nominal value and the discriminator may also be fired more than once. Multiple firing is readily prevented either by paralysing the scaler for longer than the time that peak noise fluctuations lie within reach of the trigger level, or by arranging that the discriminator is not reset until the signal has fallen below the trigger level by more than the peak noise value. It is less easy to correct for the change of pulse height due to noise and it is simplest to employ a signal to noise ratio so large that there is a negligible alteration in the pulse height.

In scanning with a multiplier photocell, it is easy to arrange that sources of noise other than the shot noise of the photocurrent and of thermionic emission are negligibly small. Again thermionic emission noise can be neglected except at the very lowest light levels. It is easily shown that the r.m.s. voltage fluctuation at the output of the amplifier superimposed on the output voltage *V*, due to the photocurrent *kF*, is

$$s(V) = G_A G_P R \sqrt{(2e\Delta f)} \sqrt{(kF)} \tag{6}$$

where *e* is the electron charge and Δf the effective bandwidth of photomultiplier and amplifier circuit. $s(V)$ will be slightly increased in practice above the value given by equation (6) by the thermionic emission noise, the thermal noise of the load resistor and the amplifier noise.

To ensure that there is a negligible difference between the nominal and effective pulse height, $s(V)$ must be sufficiently small. The largest value $s(V_0)$ occurs with the unobscured scanning aperture at $V = V_0$. It is convenient to express

$s(V_0)$ as a fraction of the maximum signal ΔV and to define a signal to noise ratio S_0 as

$$S_0 = \Delta V/s(V_0) = D\sqrt{(kF_0)}/\sqrt{(2e\Delta f)} \quad (7)$$

The value of F_0 may be inserted from equation (4). S_0^2 is seen to vary directly as k, B and N_e^2 and inversely as Δf. The bandwidth depends on the time constant of the photomultiplier load circuit and the amplifier frequency response, which in turn are dictated by the desired rate of counting.

1.4. *Effective area of scanning aperture at the field.* The expressions above refer to the light flux passing through the field stop of area M^2A. This flux is not necessarily contained in the area A at the field; nor need it be uniformly distributed. The effective scanning area is, owing to diffraction, always larger than the geometrical image area A. The difference is negligible when the dimensions of A are large compared with λ/N_e, λ being the wavelength of the light; at the other extreme, when A tends towards a point-area, the flux F_0, although still given by equation (4), is distributed in a diffraction pattern, 84% lying within the Airy disk of radius $0{\cdot}3\lambda/N_e$.

Thus for track scanning, the effective track width will approximate the nominal width w, provided w exceeds λ/N_e by a sufficient amount. The length l of the scanning aperture is not so important; the effect of diffraction in this direction is that particles are seen by the photocell before they enter the scanning aperture. If, however, the length is not too small, a partial obscuration of the scanning area will give a proportional change in the flux and the pulse heights when expressed as a fraction of the maximum pulse height, will correspond to the fractional amounts that particles cover the scanning aperture. The limiting condition $l \geqslant 0{\cdot}3\lambda/N_e$ may be suggested. Since in slit scanning w should exceed l by a factor of say 10 so that the fractional obscurations of the scanning area approximate the fractional amounts by which particles reach into the track, the least length of the slit determines the smallest usable track width. This may be put at $w \geqslant 3\lambda/N_e$. Similarly for spot scanning the smallest effective spot diameter is of the order of $0{\cdot}3\lambda/N_e$.

Consequently the smallest particle that can be counted or sized by simple scanning methods is of the order $3\lambda/N_e$. Now the maximum numerical aperture is determined by the depth of field needed for focusing particles covering a range of sizes and perhaps also not lying in the same plane. Since the depth of field is of order λ/N_e^2 and since it is not an excessively severe condition to require that the field depth should exceed the size $(3\lambda/N_e)$ of the smallest particles that can be counted, there is an upper limit of N_e of about $\frac{1}{3}$. The smallest particle that can be sized is then about 5 μ.

The above discussion does not exclude the possibility of correcting the observations when scanning at smaller track widths or spot sizes for the difference between nominal and effective track width and for the non-uniformity of the distribution of light flux. The lower limit of 5 μ is imposed only by the requirement that the observations shall be easily interpreted.

1.5. *Total time of scanning.* The total time of scanning depends on the maximum speed of scanning and the desired precision of the measurement of the number of oversize particles per unit area.

1.5.1. *Maximum scanning speed.* The maximum scanning speed is determined by the time constants of the photomultiplier and amplifier circuits and the permissible attenuation of the pulse height. The determining factor is the time constant RC of the photocell load circuit, C being the interelectrode capitance of the photocell plus stray capitance in parallel with the load R. The pulse rise time or its residence time at the peak height must be large compared with RC, if the attenuation is to be small (about 5 RC for 1% attenuation). The restriction on scanning speed is most severe for a slit-shaped aperture. In counting particles oversize z, the shortest rise or residence time of recorded pulses occurs for particles of size z and is $z/2v$, v being the scanning speed. The maximum scanning speed for 1% attenuation is therefore given by

$$v < z/10\,RC \quad (8)$$

The overall rise time of the system will in practice be longer than that of the RC input circuit, depending on the frequency response of the amplifier; and the maximum scanning speed should be smaller than that given by equation (8).

With a rectangular aperture somewhat higher scanning speeds are permissible when the length exceeds z. In spot scanning the residence time is z/v and the scanning may be twice as fast as that given by equation (8); still higher speeds can be used in double spot scanning since there is no need to preserve the pulse height accurately.

1.5.2. *Sampling error.* A lower limit to the precision of determining the number per unit area is set by the inherent error of counting only a sample out of the total number of particles. The error can be estimated if it is assumed that the particles are distributed at random. The number oversize, denoted by N for brevity, is from equation (1),

$$N = (M_2 - M_1)/Lz(1/p_2 - 1/p_1) \quad (9)$$

where M_1, M_2 are the recorded count for a track length L and z/p is substituted for the track width w, p_1, p_2 being the fractional discriminator levels. The variance of N, denoted by $s^2(N)$, depends on the variances of quantities M, L, p and z (or w). That part $s_M^2(N)$ of the total variance due to the variance of M is shown[10] in the appendix to be given by

$$\frac{s_M^2(N)}{N^2} = \frac{p_1(2p_1 s - 4p_1 + q + 1)}{NLz(q-1)^2} \quad (10)$$

where q is the ratio p_1/p_2 and s the ratio $\bar{z}/z$. The left-hand side of equation (10) is the square of the coefficient of variation.

For a given field of particles (so that N, $\bar{z}$ and z are fixed), the precision of N increases with increasing L and q and with decreasing p_1. The total length of scan may be estimated from equation (10) for the conditions of any particular case and by using equation (8) the minimum total time of scanning may be found.

1.6. *Overall precision.* In addition to the sampling error, there is a contribution to the total variance $s^2(N)$ arising from lack of reproducibility of the discriminator level p. We can suppose that the remaining two quantities, L and z (or w), in equation (9) are constant and do not contribute towards the total variance. The additional variance $s_p^2(N)$ is shown in the appendix to be

$$\frac{s_p^2(N)}{N^2} = \frac{s^2(p_1)(q^4+1)}{p_1^2(q-1)^2} \quad (11)$$

where $s^2(p_1)$ is the variance of the trigger level, assumed to be the same for both p_1 and p_2. The right-hand side of equation (11) has a minimum at q approximately equal to 2; it decreases with increase in p_1. Even under the best conditions of $q \simeq 2$ and $p_1 = 1$, the coefficient of variation of N is some four times that of p.

The overall precision is estimated by adding the contributions $s_M^2(N)$ and $s_p^2(N)$ from equations (10) and (11). It should be noted that there is no advantage in increasing the length of track beyond the point where $s_M^2(N)$ is reduced to $s_p^2(N)$.

2. ARRANGEMENT OF SCANNING MACHINE

A conventional microscope arrangement is employed: the field stop is a scanning aperture S_2 in front of a photomultiplier cell (Fig. 1) and particles dispersed on a microscope slide are scanned by a reciprocating mechanical stage. Various methods of scanning—track, double spot, line—can be studied by using scanning apertures of suitable shape but only track scanning by a slit has been investigated at present.

2.1. *Optical arrangement and light source.* The optical arrangement is shown in Fig. 4. Standard microscope components are used. The source is a tungsten filament coil (2 mm diameter and 3 mm long) of rated brightness 8×10^{-6} candle/μ^2 (6 V – 48 W projection bulb of 100 h life). It is imaged by an achro-aplanatic lamp condenser (30 mm focal length 19 mm diameter) in the first focal plane of a dry achro-aplanatic substage condenser (1·0 N.A. 13 mm diameter). The lamp condenser is of sufficiently short focal length to fill the whole aperture of the objective thread condenser at 300 mm distance. A 45° silvered prism is used as a mirror; an ordinary microscope mirror is unsuitable because the multiple images of the lamp iris in the field of view introduce undesirable stray light. (In use the lamp iris is stopped down to illuminate an area a little larger than that of the scanning aperture at the field.)

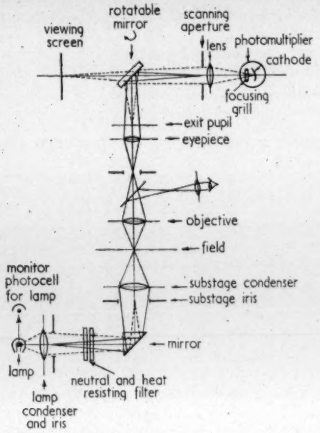

Fig. 4. Optical arrangement of scanning machine

The field is viewed by an objective (an 8 mm 0·5 N.A. achromat has mostly been used) and eyepiece at a mechanical tube length of about 160 mm. The image of the field is projected by means of a front surface mirror that can be rotated about a vertical axis, either on to a viewing screen or on to the scanning slit, the screen and slit being at the same distance from the mirror axis. The distance of throw is 250 mm. A lens (similar to lamp condenser) behind the slit focuses an image of the exit pupil of the microscope on the cathode of a 931 A photomultiplier. The cathode cannot be placed immediately behind the slit because it is not uniformly sensitive and obscuration of different parts of the slit does not give a constant photocurrent; there is also a danger of false counts due to the passage of the particle images across the wire grid of this type of photomultiplier.

The scanning slit is adjustable from 0–10 mm in both length and breadth by micrometer screws. It opens symmetrically and is alined on the optical axis of the system. All internal surfaces are painted with optical black and stops are placed to minimize scattering of stray light. The measured transmission of the system, at 0·5 N.A., is $K \simeq \frac{1}{4}$.

The maximum field of view at the viewing screen is only about 3 cm dia. and for convenience in setting up, a viewing tube consisting of front surface mirror and eyepiece is mounted on the body tube and may be inserted to intercept the beam from the objective. This is employed only for general inspection of the field. Focusing is carried out on the projected image.

The light source is driven by a special stabilizing unit. (Batteries drift too much over the long periods of operation of the machine.) It consists of a 2 kc/s oscillator and driver stage followed by a power amplifier giving 48 W at 6 V. The light source is viewed by a vacuum photocell whose output is fed back *via* an amplifier to the screen grid of the oscillator valve to oppose changes in the light flux falling on the photocell. The stability is such that a 10% change in mains input produces approximately 0·9% change in light flux.

2.2. *Reciprocating mechanical stage.* The mechanical stage is kinematically mounted on rolling spheres and reciprocated by a motor-driven cam shaped to give a moderately uniform stage velocity over a travel of about 7 mm. The stage remains in focus over the scanning area, the vertical shift being less than 2 μ. At the end of each stroke the stage is displaced laterally by a ratchet arrangement adjustable by increments of 10 μ to a maximum of 50 μ per step. The stage speed v over the central 7 mm travel averages 2·5 cm/sec. The rate of traversing is, however, only one stroke per second; rather more than half the total time is not used. Vibration has proved too severe to employ appreciably higher traversing rates, which are needed to make full use of the possible counting rate (Section 3.1). There is some vibration at reversal, which may result in multiple counting of a particle lying at the end of a traverse. The scaler is therefore electromechanically gated within the length of the traverse. Alternatively the field of particles has been specially prepared to lie within the traverse length. The particles are dispersed in Durofix diluted with acetone, which dries to an optically clear film. It is cut with a razor blade to give a field of particles about 7 mm square. A cover glass is cemented on with Canada balsam. The field area can also be defined by masking out all but a square in the centre of the cover glass.

2.3. *Photomultiplier, amplifier and discriminator circuits.* The amplifying and discriminating circuits are shown in Fig. 5. These are the circuits employed in obtaining the data given in Section 3. They have been superseded by improved (but untested) designs and the following description serves only to illustrate the principle of the machine. Negative going particle pulses from the photomultiplier are passed to a fixed gain d.c. amplifier V_2, V_3 and V_4 *via* a cathode follower V_1. The input of V_1 is also fed with a variable negative voltage controlled by a potentiometer P_2. The amplifier output indicated on meter M is directly coupled to a Schmitt trigger circuit V_6 and V_7 provided with a graduated bias control P_4. Positive trigger pulses from amplifier V_8 drive a scaler.

2.3.1. *Photomultiplier and cathode follower.* An R.C.A. 931 A photomultiplier is used with the anode pin removed to reduce base leakage and stabilize the dark current. The

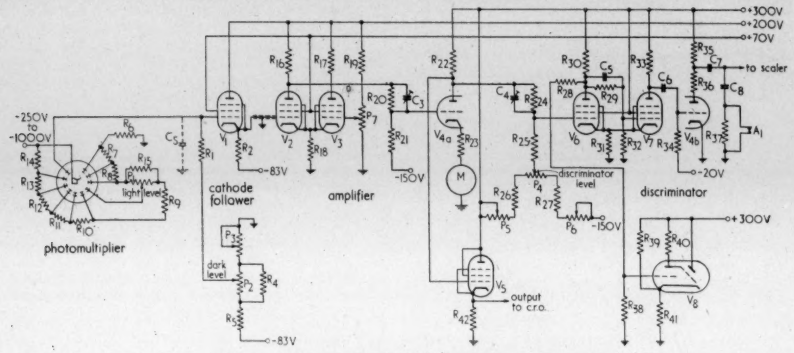

Fig. 5. Photomultiplier amplifier and discriminator circuit

RESISTORS

R_1 = 1 MΩ, ½ W 1% H.S.
R_2 = 100 kΩ, ½ W 1% H.S.
R_4 = 2·7 kΩ, ½ W 1% H.S.
R_5 = 150 kΩ, ½ W 1% H.S.
R_6–R_{14} = 30 kΩ, ½ W 1% H.S.
R_{15} = 56 kΩ, ½ W 1% H.S.
R_{16}–R_{17} = 100 kΩ, ½ W 1% H.S.
R_{18} = 1 kΩ, ½ W 1% H.S.
R_{19} = 1 MΩ, ½ W 1% H.S.
R_{20} = 500 kΩ, ½ W 1% H.S.
R_{21} = 1 MΩ, ½ W 1% H.S.
R_{22} = 15 kΩ, ½ W 1% H.S.
R_{23} = 500 kΩ, ½ W 1% H.S.
R_{24}–R_{25} = 2 MΩ, ½ W 1% H.S.
R_{26} = 150 kΩ, ½ W 1% H.S.
R_{27} = 25 kΩ, ½ W 1% H.S.
R_{28} = 1 MΩ, ½ W 10% H.S.
R_{29} = 100 kΩ, ½ W 1% H.S.
R_{30} = 15 kΩ, ½ W 1% H.S.
R_{31} = 25 kΩ, ½ W 1% H.S.
R_{32}–R_{33} = 50 kΩ, ½ W 1% H.S.
R_{34} = 47 kΩ, ½ W 10% H.S.
R_{35} = 47 kΩ, ½ W 10% H.S.
R_{36} = 33 kΩ, ½ W 10% H.S.
R_{37} = 220 kΩ, ½ W 10% H.S.
R_{38} = 1 MΩ, ½ W 10% H.S.
R_{39} = 100 kΩ, ½ W 10% H.S.
R_{40} = 1·2 MΩ, ½ W 10% H.S.
R_{41} = 30 kΩ, ½ W 10% H.S.
R_{42} = 470 kΩ, ½ W 10% H.S.

CONDENSERS

C_3 = 60–100 μF, mica trimmer
C_4 = 3–30 μF, mica trimmer
C_5 = 50 μF, silvered mica
C_6 = 2000 μF, silvered mica
C_7 = 100 μF, silvered mica
C_8 = 0·1 μF, 350 V.d.c.

METER

M = 0–5 M.A.

POTENTIOMETERS

P_1 = 50 kΩ, wire wound
P_2 = 10 kΩ, wire wound

POTENTIOMETERS (*contd.*)

P_3 = 10 kΩ, wire wound
P_4 = 50 kΩ, 3½ in. dia. 1% linearity
P_5 = 50 kΩ, wire wound
P_6 = 10 kΩ, wire wound
P_7 = 50 kΩ, wire wound

VALVES

V_1 = 6 BR 7
V_2 = 6 BR 7
V_3 = 6 BR 7
V_4 = 12 AU 7
V_5 = 6 BR 7
V_6 = 6 AM 6
V_7 = 6 AM 6
V_8 = 6 M 1

glass envelope has a conducting graphite coating to prevent the build-up of static charges.[18] The gain of the photomultiplier is controlled by a variable e.h.t. supply adjustable from −250 to −1000 V. This enables the output voltage appearing across the load resistor R_1 to be set (when the slit is unobscured and the full light falls on the cathode) to a fixed value corresponding to the firing point of the discriminator with the bias control P_4 at 0% obscuration. A fine gain control is obtained by varying the potential on one of the dynodes by means of potentiometer P_1, which is known as the light level control. The linearity of the photomultiplier is not impaired unless the stage voltage is reduced greatly.

An alternative method of setting the full light output to a fixed value employed in an earlier design, is to make the load R variable. This has the disadvantage that the time constant RC which controls the maximum stage speed, equation (8), varies with the operating conditions. Moreover, stray capacities raised C to an undesirably high value (100 pF). By mounting a cathode follower directly on the photomultiplier house the total capacitance C in parallel with R has been reduced to 15 pF. The measured capacitance of the photomultiplier is 7·5 pF.

The input voltage to V_1 is set (when the slit is obscured by a particle of optical density D) to a second fixed value corresponding to the firing point of the discriminator with the bias control P_4 at 100% obscuration by means of the potentiometer P_2, which is known as the dark level control.

Both light and dark level controls are provided with epicyclic drives. The reliability of the instrument depends in large part on the accuracy of setting these controls (Section 1.6). Their operation is not independent and they are adjusted alternately until both are correctly set.

2.3.2. *Amplifier.* The amplifier has a gain of about 140 providing an output swing of 96 V suitable for the operation of the trigger circuit from an input voltage change of 0·7 V. The first stage uses two similar valves with a common cathode load to minimize the effects of residual fluctuations on the stabilized lines. A capacity corrected potential divider is used as the coupling to triode V_4, R_6 providing a small amount of negative feedback to improve the linearity. The output is indicated by the meter M (3 in. scale 0–10 mA).

The trimmer condensers C_3 and C_4 are adjusted for minimum distortion of rectangular pulses (0·1 μ sec rise time) injected at the amplifier input. The adjusted system passes 35 μ sec pulses with negligible attenuation. The effective band width Δf for estimating the signal to noise ratio, equation (7), is approximately 10 kc/s; this figure was calculated from the measured frequency response curve of the amplifier and the input time constant $RC = 15$ μ sec. The upper half-power frequency f_2 is approximately 9 kc and the overall rise time, taken[19] as $\frac{1}{3} f_2$, is 37 μ sec.

2.3.3. *Amplitude discriminator and scaler.* The discriminator is an adaptation of the Schmitt trigger described by Elmore and Sands,[19] directly coupled through a capacity corrected potential divider to the amplifier output. The lower end of the potential divider is returned to a variable bias controlled by P_4 the trigger potentiometer (4 in. diameter scale divided into 100 divisions). The stage of the trigger circuit is shown by a cathode-ray tuning indicator V_9. This is employed in setting the 0 and 100% positions of P_4, by means of P_5 and P_6, to correspond with the light and dark level settings (8.2 and 1·8 mA) indicated on the meter M.

Positive going pulses from the discriminator are taken from the anode of the amplifier V_8 to the scaler input. V_8 is maintained at cut-off bias to remove the negative half of the differentiated square pulse from R_{21} and C_5. Except in some tests at very low counting rates, scalers having a resolving time of better than 35 μ sec have been used. Relay

A_1 operated by the gating contacts at the stage mutes the scaler at the end of each line.

The value of the common cathode resistor R_4 determines the hysteresis or backlash voltage (the amount by which the input signal must drop below the firing point before the circuit returns to its initial state and can accept a subsequent signal). There is no paralysis in the circuit. To avoid multiple counting of noise present on the pulses, the backlash voltage has been made larger than the peak to peak noise fluctuations. A value corresponding to about 8% of the trigger dial is given with $R_4 = 25\ \text{k}\Omega$ and this condition has been used in most of the tests. In consequence the lowest usable trigger setting is 16%.

2.3.4. *Power supplies.* The +300 V and +200 V lines are stabilized to $\pm 0{\cdot}2$ V and $\pm 0{\cdot}02$ V respectively. The +70 V line is taken from a neon stabilizer fed from the +300 V line. The −83 V and −150 V supplies are drawn from reference neon tubes of rated stabilities $\pm 0{\cdot}01$ V and $\pm 0{\cdot}2$ V supplied from a well stabilized −400 V line. The e.h.t. supply is stable to $\pm 0{\cdot}05$ V. The heaters of V_1 to V_4 are run in series with a barretter from a smoothed d.c. source fed from a constant voltage transformer, which also supplies all the other heaters in the equipment.

The overall stability of the machine including the light stabilizing unit is such that ± 10 V mains change results in less than $\pm 0{\cdot}05$ mA change at the output meter M. It is estimated that the discriminator level does not in normal operation vary between repeated tests by more than $\pm \frac{1}{2}\%$.

3. PERFORMANCE OF SCANNING MACHINE

3.1. *Computed performance.* The following quantities constitute machine constants and their numerical values may be inserted in equations (4–11) for the computation of the performance of the apparatus.

Lamp brightness	$B = 8 \times 10^{-6}$ candle/μ^2 (rated)
Transmission factor	$K \simeq \frac{1}{2}$ (measured)
Cathode sensitivity	$k = 10^{-5}$ A/lumen (rated)
Photocell load	$R = 10^6\ \Omega \pm 1\%$
Capacitance in parallel with R	$C \simeq 15 \times 10^{-12}$ F (measured)
Amplifier gain	$G_A = 140$ (measured)
Output voltage range	$\Delta V = 96$ V (measured)
Effective bandwidth	$\Delta f \simeq 10^4$ c/sec (measured and computed)
Stage speed	$v = 2{\cdot}5$ cm/sec

The photomultiplier gain G_P is adjusted so that equation (5) is satisfied for the particular optical density D and field area A. It is limited to a maximum (rated) value of 10^6. A further condition is that the photomultiplier output current $G_P k F_0$ must not exceed some limiting value, tentatively put at 10 μA, if fatigue is to be negligibly small. In the tests reported below the effective numerical aperture was $N_e = 0{\cdot}2$.

We define the aspect ratio r of the scanning aperture as w/l. In counting particles oversize z observations are made at track widths w equal to z/p, p being the fractional discriminator setting. Hence we put for the scanning area $A = wl = w^2/r = z^2/p^2 r$. All values of w, l and z below are expressed in microns.

3.1.1. *Photomultiplier gain and signal to noise ratio.* From equation (5) the photomultiplier gain required is $10^6\ p^2/z^2 D$, where as aspect ratio of $r = 7$ has been assumed. Since the gain is limited to 10^6, the value of z must always exceed $p/\sqrt{D}$. Since the output current is limited 10 μA, we have also from equation (5), that D must exceed 7%. The signal to noise ratio S_0 from equation (7), is $15\ Dz/p$. Experimental tests have shown a negligible change in the effective pulse height at a signal to noise ratio of 60 calculated as above ($D \simeq 1$, $z \simeq 4\ \mu$, $p \simeq 1$). The r.m.s. noise has not been measured but the peak pulses, for the same conditions, amounted to about one-twelfth of the signal, that is about five times the calculated r.m.s. value.

3.1.2. *Total time of scanning.* From equation (8), the maximum scanning speed is $0{\cdot}7\ z$ cm/sec. The actual stage speed of $2\frac{1}{2}$ cm/sec is suitable for scanning particles of 4 μ; for larger particles proportionally higher stage speeds are needed to make full use of the possible speed of scanning.

The reproducibility of a determination of the number oversize, due to machine errors, is estimated (from equation (11) taking $s(p) = \frac{1}{2}\%$) to be $\pm 2\%$ under the best conditions of $p_1 = 1$ and $q = 2$. There is no point in reducing the sampling error much below the same figure of $\pm 2\%$; the overall precision is then $\pm 2{\cdot}8\%$. For a sampling error of 2% or smaller, the track length L must from equation (10) be greater than $0{\cdot}8/Nz$ cm/sec when $p_1 = 1$, $q = 2$, and $s \simeq 2$. The minimum scanning time is thus $1{\cdot}1/Nz^2$ sec. The value of Nz^2 for fields of density suitable for scanning is of the order of $\frac{1}{2}\%$ or smaller and the minimum scanning time is at least $3\frac{1}{2}$ min. A total time of 7 min will be needed for the two scans giving the number of particles oversize z. This estimate assumes the sampling errors in the two scans are uncorrelated; scanning along the same track could reduce the time by a factor of $\sqrt{3}$, but any non-uniformity in the distribution of particles on the slide would offset this gain. In the present machine a large part of the traverse is ineffective and the total scanning time required is rather more than twice the above figures. Furthermore, the actual scanning speed is smaller than the maximum value for all values of z larger than 4 μ.

3.2. *Experimental data*

3.2.1. *Focusing.* The observed count (of pulses) in scanning with a slit-shaped aperture passes through a maximum as the focus is varied. The position of maximum count agrees with that of visual focus of the image projected on the viewing screen. (It is impractical to focus on the image seen down the microscope viewing tube.) The position of visual focus varies with the particle size; for particles 5 to 40 μ (at × 200 using 0·5 N.A. objective stopped down 9/10) the overall variation was up to 10 μ. But particles of the same size in different parts of the field appeared to be in focus within 1 or 2 μ depth on most carefully prepared slides. It was sometimes necessary to pack the slide with plasticine to obtain this degree of flatness.

Since a single focus position must be employed for the whole field of particles of all sizes, it has been necessary to increase the depth of focus by stopping down the substage condenser. For scanning particles of 5 to 40 μ an effective numerical aperture of 0·2 ensures that the count is independent of the position of focus within $\pm 6\ \mu$. Such an aperture, although low by conventional standards, is adequate for scanning where fine detail is unnecessary. On the other hand the Airy disk diameter is then some $1\frac{1}{2}\ \mu$ and it may be doubted whether particles as small as 5 μ can be correctly sized at this numerical aperture.

3.2.2. *Scanning tests.* The first test was designed to find whether for a constant value of z, the count ϕ was linear against w. Observations were made on a field of circular black disks in the size range 10 to 100 μ. The slide was prepared by spraying a solution of colloidal graphite in water. The disks were, with few exceptions, circular and of uniform

optical density ($D \simeq 0{\cdot}95$). Since the available stage speed is inadequate for sampling the whole slide in a reasonably short time, the observations were confined to a selected area, which was scanned with five groups of 100 traverses of 7 mm length, successive traverses being displaced by 50 μ and each group being displaced 10 μ from the start of the previous group. The total time of counting was just over 8 min for the 500 scans.

The data are plotted in Fig. 6 as number of pulses $\phi(w, z)$ per 500 scans (total track length 355 cm) against the track width w for several fractional discriminator settings p between 0·95 and 0·25. The track widths w were chosen so that counts ϕ were obtained for a number of values of z ($= pw$) from 11 to 88 μ. The graph has the expected pattern (compare Fig. 3 of reference 10). For each value of z, the count ϕ is linear against w.

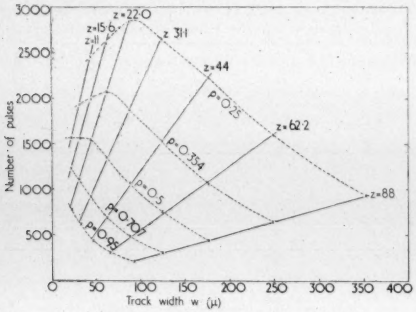

Fig. 6. Sizing of circular particles

The relationship was next investigated for non-circular profiles. For this purpose a well-dispersed low density slide of coal particles was prepared as described in Section 2.2. The area of the rectangular sample was about 65 mm^2: the sizes ranged from 80 μ down to below the limit of resolution. As can be seen from Fig. 7 ϕ was again linear with w except at the highest p values.

According to the theory the slope of the line of constant z gives the number of particles oversize z per unit area. The accuracy of the machine has not yet been investigated in detail, but some results obtained with the slide of coal particles are included as an indication that there is a tolerable measure of agreement between visual and machine counts. Oversize counts have been made at four values of z from 5·5 to 15·6 μ. The table gives the number N oversize z per unit area and the mean size z together with the standard error of N calculated from the regression of count on track width. The table gives also the corresponding visual counts together with their calculated random sampling errors; the sampling errors are underestimated since the particle distribution was not uniform along the slide. The differences between machine

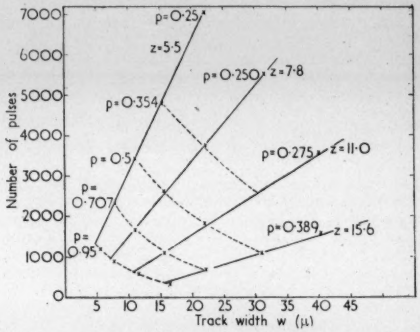

Fig. 7. Sizing of coal particles

and visual counts range from 3 to 30% but, in view of the large coefficient of variation (2 to 14% for machine counts, 4–5% for visual counts), the differences are not significant at a probability level of 0·05. The lack of precision of the machine count is largely due to sampling errors; for the length of track scanned (162 cm) the coefficient of variation due to random sampling errors, calculated from equation (10), ranges from 2 to 7½% and, in view of the non-uniform density of the slide, the actual sampling errors may be higher.

3.2.3. *Discussion.* The data presented above indicate that slit scanning is a practical method of sizing particles. A number of points require further investigation. There is a tendency (see Figs. 6 and 7) for the count to be low at the larger values of p. The errors cannot be symmetrically distributed near $p = 1$ and an undercount is to be expected. Further study is needed of the effective slit size and the depth of field; it is desirable to increase the numerical aperture above the value of 0·2 employed. Only limited data is available on the effects of coincidence of two or more particles. In the tests reported visual checks indicated a negligible amount of coincidence. Scanning at high field densities shows that the lines of constant z first curve upwards as p is decreased, indicating an overcount due to the recording of coincident pulses from particles that separately could not reach the discriminator level. At still smaller values the line curves downwards as coincidence results in loss of particles. In the extreme case with very large track widths and small values of p, the count tends to zero.

Comparison of machine and visual sizing of coal particles

	Machine count			*Visual count*		
Size z (μ)	*Number N oversize* z/μ^2 ($\times 10^6$)	*Mean size z of oversize z* (μ)	*Standard* error of N*	*Number N oversize* z/μ^2 ($\times 10^6$)	*Mean size z of oversize z* (μ)	*Sampling standard error of N*
5·5	204	9·7	5·6	210	10	8·6
7·8	115	14	1·9	110	13	4·6
11·0	60·0	18	4·6	48	18	2·4
15·6	29·1	24	4·0	20	24	0·81

* Number of degrees of freedom is 1 for $z = 15{\cdot}6$ and 2 in other cases.

4. ACKNOWLEDGEMENTS

The authors gratefully acknowledge the assistance given at various stages by R. P. Abraham of C. F. Casella and Co. Ltd., and of Mr. B. B. Morgan and Miss J. M. Coleman of the British Coal Utilisation Research Association.

REFERENCES

(1) WALTON, W. H. *Nature* [*London*], **169**, p. 518 (1952).
(2) LAGERCRANTZ, C. *Acta Physiologica Scandinavica*, **26**, Supplement 93 (1952).
(3) WOLFF, H. S. *Nature* [*London*], **165**, p. 967 (1950).
(4) MACFARLANE, R. G., and POOLE, J. F. C. See reference 1.
(5) COOKE-YARBOROUGH, E., and WHYARD, R. E. This Supplement: Paper G.3.
(6) ROBERTS, F., and YOUNG, J. Z. *Nature* [*London*], **169**, p. 962 (1952).
(7) DELL, H. A. See reference 1; also this Supplement: Paper G.4.
(8) YOUNG, J. Z., and ROBERTS, F. *Nature* [*London*], **167**, p. 231 (1951).
(9) HAWKSLEY, P. G. W. *Nature* [*London*], **170**, p. 984 (1952).
(10) HAWKSLEY, P. G. W. This Supplement: Paper F1.
(11) PIGFORD, R. L. *Proc. U.S. Tech. Conference on Air Pollution*, p. 672 (New York: McGraw Hill Book Co. Inc., 1952).
(12) HOARE, E. R. See reference 1.
(13) WHEELER, L. K., and TRICKETT, E. S. *Electronic Engng*, **25**, p. 402 (1953).
(14) COURSHEE, R. J. This Supplement: Paper G.5.
(15) ADLER, C. R., MARK, A. M., MARSHALL, W. R., and PARENT, R. J. *Chem. Engng Progr.*, **50**, p. 14 (1954).
(16) WICKSELL, S. *Biometrika*, **17**, p. 84 (1925).
(17) DAWES, J. G. *Safety Mines Res. Estab. Res. Rep.* No. 54 (1952).
(18) TAYLOR, C. J. *Phys. Radium*, **10**, p. 255 (1949).
(19) ELMORE, W. C., and SANDS, M. *Electronics: Experimental Techniques*, p. 203 (New York: McGraw-Hill Book Co. Inc., 1949).

APPENDIX

Derivation of equations (10) *and* (11)

From equation (1) the count M obtained in a track length L with discriminator setting p, the track width being z/p, is

$$M = NLz(1/p + s - 2)$$

where s is the ratio $\bar{z}/z$. Hence if counts are made at two track widths, the number per unit area is

$$N = (M_2/L_2 - M_1/L_1)/z(1/p_2 - 1/p_1)$$

which reduces to equation (9) for $L_1 = L_2 = L$.

The variance $s^2(N)$ of N depends on the variances of the quantities M, L, z, p. Suppose L and z are known exactly and $s^2(M)$ and $s^2(p)$ denote the variances of M and p. Then for small values,

$$s^2(N) = \left(\frac{\partial N}{\partial M_2}\right)^2 s^2(M_2) + \left(\frac{\partial N}{\partial M_1}\right)^2 s^2(M_1) + \left(\frac{\partial N}{\partial p_2}\right)^2 s^2(p_2) + \left(\frac{\partial N}{\partial p_1}\right)^2 s^2(p_1)$$

and it is easily shown that, if $s^2(M) = M$,

$$\frac{s^2(N)}{N^2} = p_1\frac{[(t+1)(p_1 s - 2p_1) + tq + 1]}{NLz(q-1)^2} + \frac{q^4 s^2(p_2) + s^2(p_1)}{p_1^2(q-1)^2}$$

where $t = L_1/L_2$, $q = p_1/p_2$, $s = \bar{z}/z$. The first term is the sampling error contribution $s^2_M(N)$ and, for equal track lengths $t = 1$, reduces to equation (10). The second term is the contribution $s^2_p(N)$ due to lack of reproducibility of the discriminator levels and, for equal variances $s^2(p_1) = s^2(p_2)$ reduces to equation (11).

Paper G.7

An automatic system for obtaining particle size distributions with the aid of the flying spot microscope

By W. K. TAYLOR, M.Sc., University College, London

A method is described that enables an automatic count to be made of the number of particles within a microscope field that have a maximum dimension, in any chosen direction, exceeding a calibrated reference dimension. The method thus enables a histogram of size distribution to be constructed for any convenient grouping, and by rotating the area it is possible to detect whether unsymmetrical particles show a tendency to aline themselves in a particular direction.

BASIC REQUIREMENTS

In the method considered in this paper the physical property that defines the position of the particles with greater accuracy (e.g. density, colour, reflective power) is converted into a voltage waveform by scanning the field with a spot of light and obtaining the voltage output from a suitably placed photocell.* The field is scanned by a television type of raster and the size distribution is obtained by comparing two consecutive lines of the output voltage at the same instant of time. One method of obtaining these voltages is to use two spots of light separated by one line* and another method is to delay each line waveform by a time interval equal to the duration of the line. A variable calibrated delay unit is used to modify the line waveforms until they correspond to those that would be obtained by scanning an imaginary modified field, consisting of those portions of the particles in the actual field that are in excess of a given size in the direction of scan. Thus if a particle is less than the given size in any chosen direction it would not appear at all in the modified field, and if a particle is greater than the given size, only those portions of it that are in excess would appear

* ROBERTS, F., and YOUNG, J. Z. *Proc. Instn Elect. Engrs*, **99**, Pt. IIIA, p. 747 (1952).

in the modified field. This is illustrated in Fig. 1, which shows five particles outlined by the full black lines. The numbered horizontal lines represent the path of the scanning spot of light. From each line four principal waveforms are obtained. Taking line number 14 as an example, the first waveform is 14_0, which represents the output from the photocell after it has been through a clipping amplifier. The latter

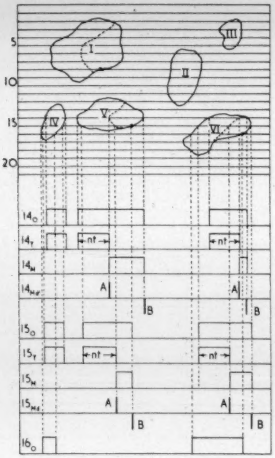

Fig. 1. Waveforms for particle size analysis

selects those portions of the signal that have an amplitude greater than a fixed clipping level and converts them into the rectangular waves shown. The second waveform (14_T) goes positive at the same instant as 14_0 but returns to zero after a time nt has elapsed, or when 14_0 returns to earth, depending on which interval is shorter. The third waveform 14_M is obtained by subtracting 14_T from 14_0 and constitutes the modified field waveform. It is the waveform that would be obtained from the photocell if only those portions of the original particles enclosed by the dotted lines and the right-hand boundary of the original particles were present. The last waveform 14_{Md} is obtained by differentiating 14_M.

The counting of the particles in the modified field will now be described. Because the waveforms of two consecutive lines are required simultaneously it is necessary to delay each line by the duration of one line or to use two scanning spots separated by one line. Consider first the waveform 14_{Md} and assume that it has been made to occur at the same time as the waveform 15_M. The A pulses of waveform 14_{Md} are used to change the state of a storage device (e.g. a condenser or a two-state device), and the B pulses to restore the state to its original value, and at the same time produce an output pulse. Any portion of the waveform 15_M, however, is also capable of restoring the state and if it does so before B occurs then B does not produce an output pulse and there is no count. Thus for the lines 14_{Md} and 15_M there is no output pulse but the next pair of waveforms 15_{Md} and 16_M produce one output pulse which represents the counting of particle V. Particles I, V and VI are thus counted because their greatest length in the direction of the scan is greater than the distance which corresponds to the duration nt, and particles II, III and IV are not counted since they do not fulfil this condition. If nt is made zero then all the particles will be counted and if nt is greater than the largest particle duration the count will be zero.

METHOD OF CALIBRATION

Referring to Fig. 2(*a*), the ordinates at n represent the number of particles in the field that have sizes greater than $n\delta$ ($n = 0, 1, 2, \ldots N$) and are read off the counter, one ordinate being obtained for each frame of scan. If the velocity of the spot of light crossing the particles is v then the time taken to travel a distance $n\delta$ is $n\delta/v$. For a given value

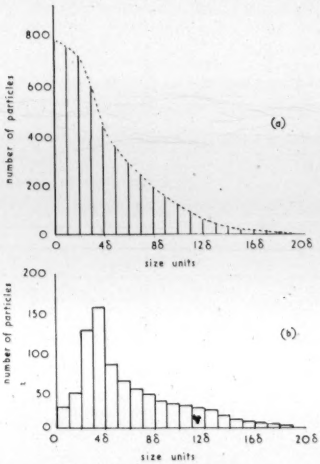

Fig. 2. Method of calibration

of δ, a variable time delay $nt = n\delta/v$ is required, which can be increased in steps of t from zero to Nt. Should a histogram giving the number of particles with sizes between $n\delta$ and $(n + 1)\delta$ ($n = 0, 1 \ldots N$) be required it is easily obtained from the above results by taking the differences between adjacent ordinates as shown in Fig. 2(*b*). This latter operation could also be done automatically if required.

DESCRIPTION OF BLOCK DIAGRAM

A block diagram of the essential elements in the particle sizing system is shown in Fig. 3. One of two alternative methods of obtaining the signals may be used, the selection being made by the switch S. When this switch is in position 1 the waveform 14_0 (for example) is obtained from a second spot situated above the one producing waveform 15_0.* The second switch position gives the same result so far as the

* ROBERTS, F., and YOUNG, J. Z. *Proc. Instn Elect. Engrs*, **99**, Pt. IIIA, p. 747 (1952).

functioning of the rest of the system is concerned, but in this case the waveform 14_0 is delayed by one line and is therefore available at the same time as waveform 15_0.

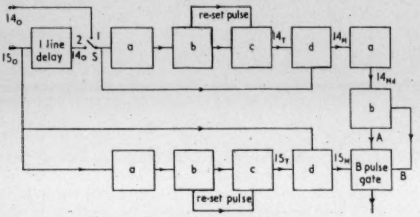

Fig. 3. Block diagram of essential elements in particle sizing system

a, diffr.; *b*, pulse separator; *c*, variable delay, *nt*; *d*, subtractor; *B* pulse out if 15_M waveform is zero between the *A* and *B* pulses

Reference to the section on basic requirements will show that the rest of the system fulfils the conditions described. To assist reference to the example given in Fig. 1, the points at which the waveforms of lines 14 and 15 appear to have been numbered. It will be noted that for the delay shown in Fig. 1, there will be output pulses from particles I, V and VI as required. The positions of these three pulses are indicated by the black dots in Fig. 1.

A limitation of the system is that it will not give accurate results for certain irregularly shaped particles (e.g. S shapes), but these probably constitute a small proportion of the particles encountered in practice.

ACKNOWLEDGEMENTS

This research was carried out in the Department of Anatomy, University College, London, and the author is grateful to Professor J. Z. Young for advice and encouragement, and to Mr. D. J. Causley who constructed most of the equipment and contributed many ideas.

DISCUSSION

Dr. H. A. Dell: The method of particle sizing which has been described by Mr. Taylor is commendable for its simplicity, but it does seem to be potentially fallible in one important respect. When particles with indented edges have to be dealt with, the delay technique which is described has the effect of breaking up large particles into numbers of small ones. Thus with a particle very little more re-entrant than, say, No. VI in Fig. 1, a time delay can be found which effectively divides it into two particles. This would mar the size distribution inferred since it not only falsely increases the numbers of particles assumed to be large, but at the same time it reduces the number assumed to be small. It would therefore be rather worse than merely misjudging the size of one of the particles. I should be interested to hear whether this in fact contributes a significant error to the system. An additional slight disadvantage would appear to be that a complete analysis of the particles in a field can only be carried out after repeatedly scanning the specimen with different time delays in circuit.

Author's reply: The observation made by Dr. Dell is quite correct in that particles with indented edges could be counted more than once. Even without the sizing, however, it would seem that there will always exist a set of particle shapes that cannot be counted accurately by any system which employs the single line storage or double spot method. The range of such shapes could presumably be reduced by increasing the amount of stored information or the effective number of scanning spots, but only at the expense of simplicity. Since our experience has been mainly with spray droplets and biological material, we have not encountered particles with indented edges and cannot give figures for the error which they would introduce.

In reply to Dr. Dell's last point, the time taken for repeated scannings is still short compared with the time spent in adjusting the position of the slide and setting the controls. There would be little advantage, therefore, in using more elaborate electronics to reduce the scanning time.

GENERAL DISCUSSION ON SESSIONS F AND G

Mr. W. H. Walton: In my introductory survey to Session F I referred to the possible use of intermediate photography as an aid to the development of automatic counting and sizing machines for particles of very small size. It is not necessary to use photographs of large dimensions, modern fine-grain films will record detail as small as 0·01 mm so that 1 or $\frac{1}{2}\,\mu$ diameter particles can be adequately recorded at a magnification of about $\times 50$ on the film. This allows a field of view equivalent to that seen by eye using a 2 mm objective to be recorded on 16 mm film, which has a frame size of approximately $7{\cdot}5 \times 10$ mm. The cost of such film (including processing) is about 40*s*. per 100 ft and 40 frames are recorded per foot of film. Thus 100 fields of view can be recorded at a cost of 1*s*. Mr. F. G. Hermges has investigated the recording of thermal precipitator samples of airborne coal dust in the above manner. The apparatus consisted of a 150 c.p. Pointo-light lamp, an ordinary bench microscope, a viewing and focusing attachment with shutter (Leitz Micro-Ibso) and 16 mm Ciné-camera arranged for single frame exposures. The microscope has an 8 mm achromatic objective N.A. 0·5 and $\times 10$ eyepiece. This arrangement was found to give the best compromise between resolving power and depth of focus. The resolving limit is about $0{\cdot}5\,\mu$. The overall magnification on the film is $\times 55$, and the exposure time $\frac{1}{2}$ sec on the film used (Kodak "16 mm film for Ciné photo-micrography.") Typical photographs obtained with this arrangement, enlarged from the 16 mm film negatives, are shown in the accompanying figures. Fig. 1 was obtained at normal contrast and closely represents what the eye sees down the microscope. The background illumination is of rather variable density and particles are surrounded by diffraction rings. Fig. 2 shows a similar field of view, but with the film developed to higher contrast, $\gamma = 2{\cdot}5$. It will be seen that this removes the background variations and sharpens the edges of the particles,

producing a picture which is much better suited to automatic counting, for which purpose the original 16 mm negative would be used (Fig. 2 is the positive).

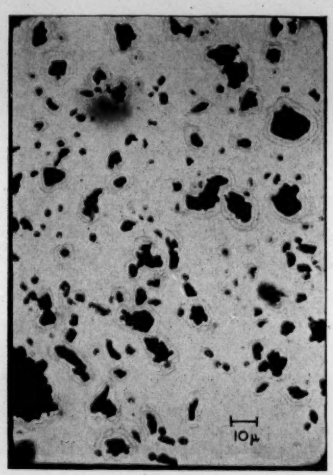

Fig. 1. Photomicrograph of coal dust enlarged from a 16 mm negative: normal contrast

Fig. 2. Similar field of view to Fig. 1, but developed to a higher contrast ($\gamma = 2{\cdot}5$)

Mr. E. W. Meyer: The photographs shown to us by Mr. Walton do assist obviously in making the instrumentation of particle counting easier, but in only one aspect and that is to overcome the difficulty of sensitivity of the instrument. By sensitivity is meant the signal-to-noise relationship. Because of the larger images more light is available and therefore the signal-to-noise relationship is much increased. However, a more sensitive photo-cathode would give the same results. It must be clearly understood that no advantage is obtained either from the optical application such as an improvement of image, depth of focus or resolving power. Actually there is a loss as this is another process. This loss, though, may be of a very small order and considering the other errors it may not be significant.

The field of automatic particle counting has a strong bias because of the interest shown by the National Coal Board and its activities in this field. This has produced instruments for rather specific application and the size range is of the order of between 5 and 1 μ. It is important for other people with their own problems of particle counting to inform the makers of these machines of their problems and of the type they would like. This will enable their design to cover a wider field and in all probability hasten their application.

Mr. B. J. Mason: I should like to mention a rather different application of the automatic counting techniques from those described by other speakers. At Imperial College in London we have been concerned with obtaining an automatic and continuous recording of the size distribution of falling raindrops. An instrument has been built[1] in which the drops are allowed to fall through a rectangular, parallel light beam, 5 cm wide and 0·5 cm in depth, produced by a stabilized high-pressure mercury arc and a collimator system. Drops falling through the beam scatter light in all directions, some of which is collected by a telescope system and focused on the cathode of a photo-multiplier. Each raindrop therefore produces a light pulse at the photo-multiplier where it is converted into a voltage pulse of amplitude roughly proportional to the square of the drop radius. The voltage pulses corresponding to various drop sizes are sorted electronically into eight different size groups, the number in each group being recorded on a four-figure telephone message register. The bank of registers together with the recorder of a very sensitive rain gauge and a clock are photographed at minute intervals.

The instrument is calibrated with artificially produced drops of known size and is set to detect drops of radius greater than 100 μ. The sampling area is 72 cm^2. Some of the major advantages of this instrument are: (*a*) the sampling area is optically defined so that the results are not vitiated by splashing which occurs in mechanically defined systems; (*b*) the sampling area is well defined and a drop of given size produces the same response at all points in the sensitive area, except, of course, at the very edges; (*c*) the sampling area is large enough to record a representative sample of drops in a ten-minute shower but not so large that coincident counts will be numerous; (*d*) use of the instrument is not restricted to vertically falling rain; (*e*) the sorting and recording is entirely automatic, avoiding the immense labour involved in previous techniques.

Mr. M. A. Strivens: No mention has been made in this Conference of the electrostatic method of particle analysis published by Guyton,[2] Kunkel and others.[3,4] The method is similar in set-up to that of Professor Gucker, except that the particle stream instead of interrupting a beam of light, is first charged electrostatically and then impinged upon the grid lead of a sensitive valve. The individual pulses are then amplified and passed through the usual discriminator circuits and counted.

The method seems to provide a surface area-frequency distribution. I would propose for consideration the combination of Gucker's method and Guyton's method, using a dual tube in which the particles first interrupt a light beam and then impinge on the grid lead, the relevant counts being made in separate circuits. This would give an immediate experimental correlation between the projected diameter and surface area of a given powder, which is apparently much desired. It is understood that the Medical Research Council has carried out some work in connexion with Guyton's method.

Dr. F. T. Gucker, Jr.: I am pleased to learn that Guyton's electrostatic method of particle counting is under investigation by the Medical Research Council. Dr. C. T. O'Konski studied this method while he was developing the first photoelectronic counter in our laboratory, and we published a brief comparison of the two methods some years ago.[5] Guyton's original counter was limited to aerosol particles with a diameter of approximately 3 μ or more, and we concluded that it would be impossible to reduce the limit below about 1 μ by any improvement in the design of the amplifier; hence a comparison of the electrostatic and photoelectronic methods would not be possible below this size.

It does not seem that the combination of these two methods suggested by Mr. Strivens would necessarily give a correlation between the projected diameter and surface area of a particle. Dr. Rose found empirically a linear relation between pulse height and particle radius over the range between 0·50 and 1·0 μ diameter in our counter, but in general light scattering is proportional to $\pi r^2 K$ where r is the radius of the particle and K is the scattering coefficient. Therefore where the fluctuations of K with particle size can be neglected, the light scattering, like the electrostatic response, is proportional to the cross-section or surface of the particle. However, since Guyton found characteristic differences between the pulses given by solid and liquid aerosol particles, his type of counter used in conjunction with a photoelectronic one might throw some light upon the nature of the particles as well as their size and number.

Dr. H. Heywood: Dr. Bronowski asked whether anyone could comment upon automatic star counting methods: although I cannot say what methods were used for this purpose, there was an interesting similarity between star and particle counting results when the limit of visibility was approached. Early records of microscopical counts, when extended to the extreme limit of resolution, showed a false maximum frequency at a particle size just greater than the lower limit, whereas it is now known that the numerical frequency for normal dusts increases continuously as the particle size decreases. Star counts made by unaided vision about 300 years ago showed a maximum frequency at about 4th magnitude, the limit of such vision being about 6th magnitude. With the aid of telescopes it was easily shown that the numerical frequency of stars increased as the magnitude increased, i.e. brightness decreased. The important feature of this comparison was that false effects might be observed if any counting process was worked to the extreme limit of its capabilities.

Dr. D. W. Gillings: I have been rather detached from active work in this field for a little over a year, and it is some measure of the rate of development that comment based in detail on ideas of so short a time ago presents some difficulty. I have, however, been struck by the emphasis laid by several speakers on the importance of exact electrical and optical equivalence of scanning spot and signal characteristics, when any simultaneous measurements are based on signals from two spots. In particular, correct performance of a "guardspot" system may be dependent on such exact equivalence.

In our early study of the scanning process used in all this work, we thought it wise to assume that there should be the least possible dependence on any measurement of signal strength, and we discarded some methods of automatic sample assessment which depended on measurement of intensity of signal from scanning to give data on particle size. It has been accepted as sounder practice, to design so that scanning any part of an image leads to a signal of definite magnitude. All counting and sizing operations are then dependent only on the detection of uniform signals, and the time at which such signals are generated during scanning. Thus a single spot giving a signal of magnitude independent of image or sample characteristics can be used with a memory device to enable sequences of signals from one particle to be related to that particle alone. The "arrested scan" proposal described by Dr. Dell can incorporate such a "line-to-line memory" device, which ensures that any particle image yields not more than one signal registering its existence. Such a device can also ensure that if a particle is missed on the first line interception it can give signals with certainty on subsequent interceptions. This avoids the possibility already mentioned of missing a particle on the first interception of a "guardspot" and thus missing the particle altogether.

On an entirely different point of detail, I should have expected rather more to be made at this stage of the possibilities of using ultra-violet microscopy with the scanning microscope. This would appear to avoid some of the elaboration needed for direct viewing and ought to minimize some of the difficulties feared when very small particles have to be assessed either automatically or visually.

Dr. N. H. Chamberlain: In cases where the measurement of two parameters only, namely the average projected diameter and the total number of particles, is required from a particle array, it is possible to make use of a simple procedure which has not so far received specific mention.

If the array is scanned by means of a light slit of length l, as shown in Fig. 3(*a*), the distance between successive scan

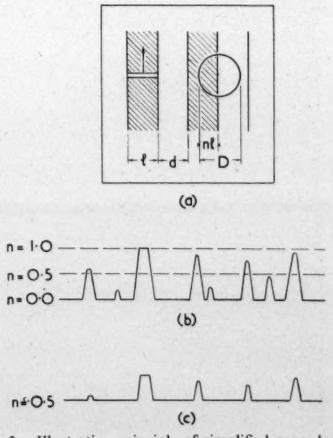

Fig. 3. Illustrating principle of simplified procedure of counting by machine

tracks being d, the output from the photoelectric scanning head consists of a series of pulses of varying height, as shown by the heavy line in Fig. 3(*b*). The greatest pulse height will correspond to complete cut-off of the light, and the number of pulses will in general be greater than the number of particles present. This signal may now be fed to an amplitude discriminator (a simple biased diode clipping circuit may be used) which rejects all the signal falling below a certain predetermined level.

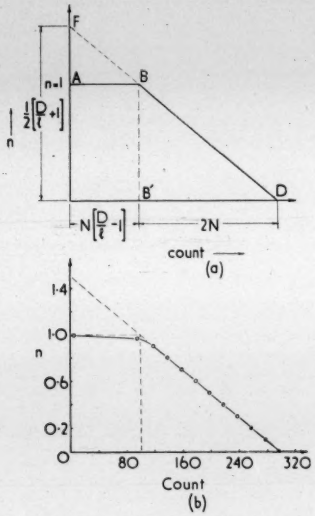

Fig. 4. Relation between number of particles in array N and fractional clipping level: (*a*) theoretical; (*b*) experimental results

This level is designated n, and varies between 0 and 1·0, so that when $n = 0$ no clipping occurs, and when $n = 1{\cdot}0$ the highest pulse is just clipped out and the signal vanishes. [Fig. 1(*c*) shows the form of the original signal, for example, after clipping at $n = 0{\cdot}5$.] The clipped signal is then fed to a counter in the usual manner.

It may easily be shown that under these conditions

$$\frac{C}{N} = \frac{l + D - 2nl}{d + l}$$

where N = total number of particles in the array;
n = fractional clipping level as defined above;
C = total experimental count;
D = average projected diameter of particles;
d = width of unscanned track;
l = width of scanned track;

always providing that the diameter of the smallest particle present is not less than the width of the scanning track. If $d = 0$, i.e. if the scanned tracks just coincide at the edges so that the whole field is scanned,

$$\frac{C}{N} = 1 + \frac{D}{l} - 2n$$

and there is no sampling error.

By counting the sample at a series of values of n, and plotting the count obtained, C, against n, the curve obtained should be that shown at ABD in Fig. 4(*a*). By producing DB to cut the axis of ordinates at F, the intercept OF is obtained, which gives D in terms of l. Similarly, the distance $B'D$ is equal to $2N$. The two parameters required are therefore obtained directly if l is known. This proposition is contained

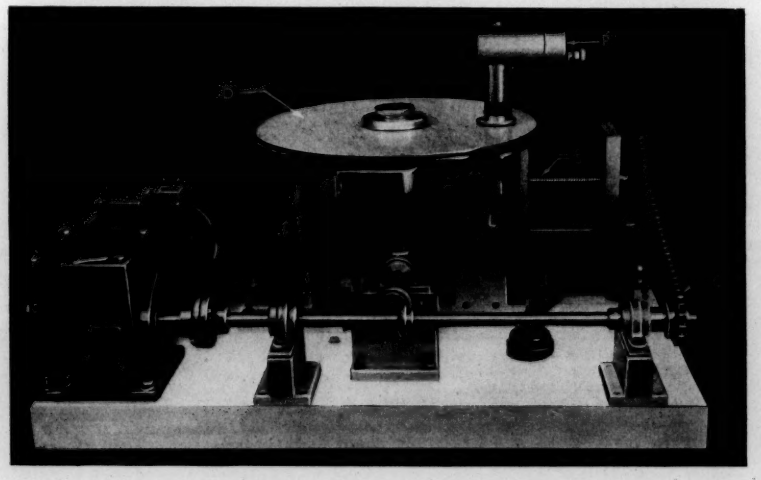

Fig. 5. Scanning part of machine for counting neps in carded fibre webs

in the general theory put forward by Hawksley, but is perhaps not immediately apparent from his presentation of it.

The theory has been tested during the design of an apparatus for the automatic counting of neps in carded fibre webs (neps are small tight balls of fibre fragments embedded in the web, and give rise to much trouble in subsequent spinning operations). The scanning part of this apparatus is shown in Fig. 5. The web is sandwiched between two plate-glass disks *D* which rotate together in a horizontal plane, and the sample is scanned by a light source *L* and photocell *P* mounted on a scanning head which is moved in radially by a lead-screw *S* as the disks revolve. The scan pattern is therefore a spiral whose pitch can be altered at will by changing the ratio of the chain-drive *C*.

With this apparatus, a number of "ideal" samples consisting of numbers of small punched disks of black paper, of accurately known diameter, randomly dispersed between the plates, were investigated. A typical count curve is shown in Fig. 4(*b*), and is seen to conform very closely to theoretical shape. There is some rounding of the corner at *B*, caused by undercounting at high values of *n*; Hawksley has noted the same phenomenon. This error does not in any way interfere with the use of the curve in the manner already indicated. The subjoined table gives the results obtained for four different arrays, varying in number from 30 to 100 particles, some being homogeneous as regards diameter, and some containing disks of two or three different diameters. In every case the estimated number and diameter are within ±3% of the true values.

Counting of "ideal" sample arrays

	Actual array tested		*Experimental values obtained*			
Details of array examined	*N (total)*	$\bar{D}$ *(in.)*	*N (total)*	$\bar{D}$ *(in.)*	*% error of N*	*% error of D*
100 of diameter 0·1 in.	100	0·100	101·1	0·098 (7)	+1·1	−1·3
30 of diameter 0·1 in.	30	0·100	29·5	0·100 (2)	−1·6	+0·2
30 of diameter 0·1 in. 30 of diameter 0·1275 in. 10 of diameter 0·084 in.	60	0·113 (7)	61·2	0·110 (8)	+2·0	−2·5
10 of diameter 0·100 in. 10 of diameter 0·1275 in.	30	0·104	29·1	0·104 (8)	−3·0	+0·8

The method does not, of course, enable the distribution of particle sizes to be obtained, but it is simple and rapid in use, and in cases where only average particle size and particle number are important, or in preliminary sorting tests, before more elaborate estimations are undertaken, it may prove to be of some general interest. If the particles concerned are very small, there is difficulty in fulfilling the condition that the width of the scan track must not exceed the diameter of the smallest particle; but if, as is foreshadowed, intermediate photographic enlargement before counting becomes more generally practised, this difficulty will be eliminated.

Mr. P. G. W. Hawksley: With regard to Dr. Chamberlain's theoretical discussion, it is perhaps worth noting that his condition that the diameter *a* of the smallest particle present shall not be less than the width *l* of the track, is unnecessarily stringent. His equation corresponds to equation (22*b*) of my paper (F.1) which is subject to the requirement that the track width *l* shall be smaller than the size *a* of the smallest particle divided by the fractional clipping level *n*. Thus, up to $n = 1/10$, *l* may be $10a$; up to $n = \frac{1}{4}$, *l* may be $2a$ and so on. A rounding of the corner *B*, Fig. 4(*b*), will start at the value $n = a/l$; but this does not affect the slope of the straight line portion for smaller values of *n*, which still gives correctly the total number of particles.

Mr. E. V. Reeves (*written contribution*): Where the number of particles to be counted and sized is large the technique of scanning microscope slides can be used, but where the number is small, this method introduces a large sampling error. One of the papers mentioned 20 000 particles as the minimum for counting on one slide, to reduce sampling errors to an acceptable value.

The particles which I have in mind are not only small in number, but are contained in a liquid of high viscosity and of the same density as the particles, thus preventing any relative motion between the particles and the liquid. With these restrictions given, a method adopted to deal with the counting and sizing of these particles utilizes a narrow rectangular channel, through which the liquid is passed under pressure, the thickness (or depth) of the channel being of the order 0·25 to 1·0 mm. Light from a microscope lamp is focused on to part of this channel, and a microscope with a depth of field almost equal to the depth of the channel focuses the image of the moving particles on to a slit covering a photomultiplier. The flow channel is normally made of glass (or Perspex), and introduces the effect of a thick cover glass.

With this type of flow, there is the inherent disadvantage of the viscous drag at the walls. To overcome this, and to lessen the effect of noise in the electronic circuit, the amplifier may be made an a.c. one, with a low frequency cut off, for frequencies corresponding to particle speeds a little inside the two planes *a*, *b* (Fig. 6) defining the depth of field of the microscope, *cd* being the planes defining the frequency selectivity of the amplifier.

Due to the relatively small number of particles existing the photo-multiplier slit has to be longer than those normally used. This implies a lower signal/noise ratio, which is partly compensated by negative feed-back and l.f. cut off. Although

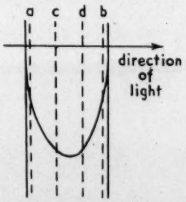

Fig. 6. Illustrating design of amplifier

the system is different from that used in the track scanning systems described in the papers, there is still the possibility of a particle being only partly on the slit when it is counted and hence being sized wrongly.

A correction for this possibility may be applied to the

count obtained as follows. If the particles are assumed spherical, and at the region of observation, the light beam is assumed to be parallel, the loss of light caused by the passage

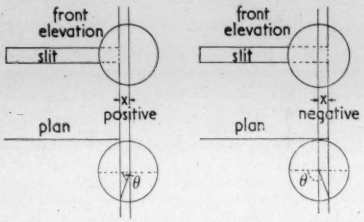

Fig. 7. Illustrating loss of light caused by particle

of a particle at its diameter (which determines the pulse height) will be given by

$$\Delta s = \beta a r^2(\theta - \tfrac{1}{2}\sin 2\theta) \tag{1}$$

where β is a constant and a is the width of the slit; this is illustrated in Fig. 7, which may be written in turn as

$$\Delta s = \beta a r^2\left[\cos^{-1}\frac{x}{r} - \frac{x^2}{r^2}\left(\frac{r^2}{x^2} - 1\right)^{\frac{1}{2}}\right] \tag{2}$$

and a count will be made at counting level L_n if

$$\beta a r^2\left[\cos^{-1}\frac{x}{r} - \frac{x^2}{r^2}\left(\frac{r^2}{x^2} - 1\right)^{\frac{1}{2}}\right] \geqslant L_n \tag{3}$$

that is if

$$r^2\left[\cos^{-1}\frac{x}{r} - \frac{x^2}{r^2}\left(\frac{r^2}{x^2} - 1\right)^{\frac{1}{2}}\right] \geqslant K_n \tag{4}$$

where $K_n = L_n/\beta a$, where L_n is a counting level divided by photo-multiplier and amplifier constants, corresponding to loss of light Δs.

Thus

$$r^2\left[\cos^{-1}\frac{x_n}{r} - \frac{x_n^2}{r^2}\left(\frac{r^2}{x_n^2} - 1\right)^{\frac{1}{2}}\right] = K_n \tag{5}$$

where x_n is that value of x which for a particle of radius r will cause a count to be made at level L_n. To make such a count, the particle may be anywhere within the length l_n (Fig. 8) given by

$$l_n = b + 2(r + x_n) \tag{6}$$

and the probability that it is completely on the slit when the count is made is given by

$$P_n^r = \frac{b}{l_n} = \frac{1}{1 + 2\frac{r}{b}\left(1 + \frac{x_n}{r}\right)} \tag{7}$$

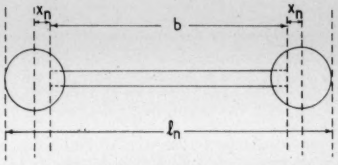

Fig. 8. Defining l_n within which particle must be, to count

From this, curves similar to those in Fig. 9 may be drawn, showing the probability that a particle of radius r is completely on the slit when a count is made at level L_n. Particles greater than 20 μ and less than 5 μ diameter do not matter, the former being almost non-existent. From Fig. 9, correction values may be obtained, when arriving at the final size distribution.

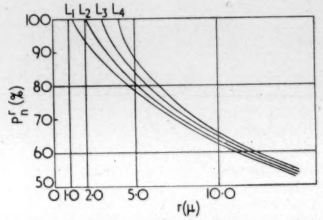

Fig. 9. Curves showing the probability that a particle is completely on the slit (for slit 6·25 × 0·15 mm)

REFERENCES

(1) MASON and RAMANADHAN. *Quart. J. Roy. Met. Soc.*, **79**, p. 490 (1953).
(2) GUYTON. *J. Ind. Hyg. Toxicol.*, **28**, p. 133 (1946).
(3) KUNKEL and HANSEN. *Rev. Sci. Instrum.*, **21**, p. 308 (1950).
(4) KUNKEL. *J. Appl. Phys.*, **21**, pp. 820, 833 (1950).
(5) GUCKER and O'KONSKI. *Chem. Rev.*, **44**, p. 373 (1949).

SESSION H. GENERAL

Chairman: H. HEYWOOD, A.C.G.I., D.Sc., M.I.Mech.E., M.I.Chem.E.

Paper H.1

The application of methods of particle size and surface area measurement to whiting

By G. E. BESSEY, M.Sc., F.R.I.C., and D. C. SOUL, B.Sc., A.R.I.C., A.R.C.S., British Whiting Research Laboratories, Bedford

The application to whiting (calcium carbonate) of various methods of determining particle size distributions and surface area is considered and results by various methods are compared. Techniques for determining sieve residues on fine sieves and particle size distribution by sedimentation are described. These methods, together with surface area measurements by air permeability are considered to give data on whitings adequate for most purposes.

PHYSICAL CHARACTERISTICS AND PARTICLE SHAPE

Whiting is made up of particles roughly within the size range of 0·1 μ to 200 μ, with the bulk of particles between 1 and 10 μ. Fig. 1 is a photomicrograph of a ground whiting which shows the typical particle shape, with some circular coccoliths.

One would expect to obtain angular shaped particles by grinding a friable material. The shape of most of the smaller whiting particles (up to 2 μ) approximates to cubes but both electron photomicrographs and optical photographs show the larger particles to be of irregular shapes formed of whole or part fossil remains or of irregular clusters of smaller particles weakly cemented together. No work has been done on assessing the effect of these irregularly shaped particles on the general properties of whiting but they will clearly have a higher specific surface value than would simple cubes, and the true specific surface will thus be greater than values calculated from size distribution data assuming cubes with a surface (shape) factor of 6 cm^2/c.c. Delfosse[1] has calculated a shape factor of 6·4 cm^2/c.c. from microscopic studies of French (Champagne) whiting.

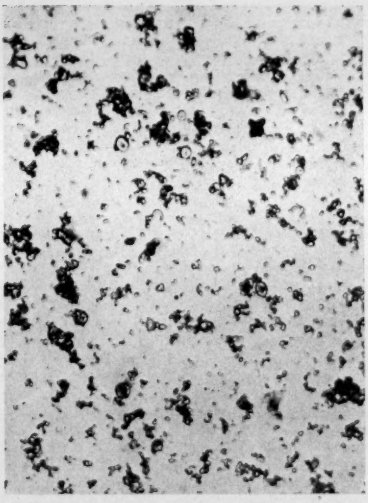

[Reproduced from *Chemistry and Industry*]

Fig. 1. Photomicrograph of a whiting, magnification ×340

As whiting consists mainly of calcite, the physical characteristics are similar to those of this mineral. The specific gravity varies little from 2·71. Appreciable variations have been found in the compressive strength of chalk samples from different localities, due apparently to differing amounts of secondary calcite cementing the primary material, but no attempt has yet been made to correlate the strength of the raw chalk with the type of particle size distribution of the ground whiting. The factors affecting flocculation are being studied.

COARSE PARTICLES: SIEVE RESIDUES

The technique used in determining residues on fine test sieves may have considerable influence on the results. A standardized procedure has been evolved for obtaining the coarse particle contents of whiting by wet sieving. The sample, usually 100 g, is shaken with water in a stoppered flask and washed through a 3 in. B.S. test sieve. Lumps on the sieve are washed back into the flask and broken down with gentle pressure from a rubber-tipped rod, and then washed back through the sieve. The powder on the sieve is washed with a 3 ft head of water passing through $\frac{1}{4}$ in. rubber tubing fixed with a standard washbottle jet. Complete separation of irregularly shaped particles is very difficult in sieve analysis, and so the washing is continued until negligible amounts of powder pass through. It is often of assistance in deciding when the washing is complete to immerse the sieve, held at a slight angle, in a beaker of water of 4 in. (or greater) diameter and to raise and lower the sieve gently. This greatly facilitates the passage of near-sieve sizes, particularly those particles which may have temporarily stuck in the mesh. The complete washings through the sieve are collected and washed through the next smaller mesh sieve in use. The residues are usually washed into sintered glass crucibles (porosity 3), dried and weighed. Washing with alcohol and ether enables the drying process to be speeded up if a result is required quickly. Replicate determinations, usually by two different operators, of 240 mesh sieve residues on about 300 samples have been studied to obtain statistical evaluation of the reproducibility

of results over a range of values. The values of the difference of the individual determinations y plotted against the mean of the pair of determinations x were plotted on a log-log scale, and the straight line of best fit to the points calculated by the method of least squares. The standard deviation σ_y of the points from the line was then calculated and the line corresponding to the previous straight line $+2\,\sigma_y$ was drawn. This line should give the maximum differences from the true value in 98% of determinations. The equation obtained is:

$$y = 0{\cdot}164R^{0{\cdot}715}$$

Where y is the maximum difference from the true value probable in 98% determinations,

and R is the probable true value.

This equation is representative of the sum of errors which apply to sieve residue determinations, as made in these laboratories. It includes the purely personal errors of two or more operatives, with their variable time and technique of washing and the variation of sieve cloth between different sieves. It should be noted that the residue is that amount retained on a wet sieve which, if dried, will pass more powder.

A convenient method for demonstrating the efficiency of sieving is to project the magnified image of the sieve cloth and residue separately on to photographic paper or plate. Fig. 2

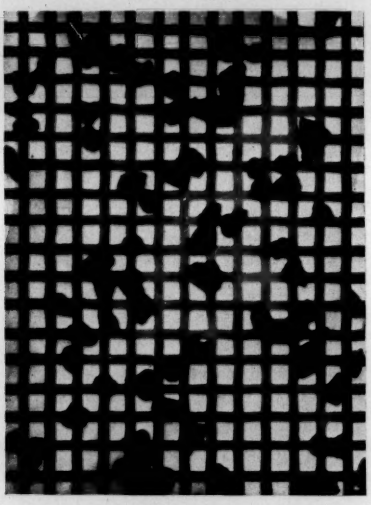

Fig. 2. Residue retained on B.S. 240 mesh cloth, magnification $\times 50$

was obtained with a projection microscope using a magnification of $\times 50$. An image of a small piece of sieve cloth was focused on to a sheet of hard (No. 4 Kodak) bromide paper or a B4 plate, and a suitable exposure was made. A sample of the sieve residue was prepared by dropping the powder on to a slide coated with a thin layer of Vaseline, this giving random orientation of the particles. The slide was fitted into a microscope which was then refocused, and a second exposure made on to the same paper or plate which was developed to give maximum contrast.

Fig. 2 also shows clearly the variation in quality of sieve cloth in the finer mesh. At the present time the tolerances which have to be allowed for successful manufacture of fine cloth are sufficient to give appreciable variations in results with test sieves of the same nominal aperture. The limitations of the method of sieving are twofold; with increasing fineness the errors of the sieve cloth increase and the time taken to obtain complete washing is appreciable, particularly for high residues on the finest sieves. Samples smaller than 100 g are taken with coarse whitings where the residue is expected to be more than several per cent, but this in turn reduces the accuracy.

PARTICLE SIZE DISTRIBUTION BY SEDIMENTATION

Andreasen method. The proportion of whiting particles above 43 μ is usually only a fraction of 1% and only in the coarsest grades amounts to several per cent. Although exact knowledge of this proportion of coarse particles is important for many uses, it gives no information about the bulk of the powder, and other methods of examining particle size characteristics are therefore necessary. The Andreasen method of test by sedimentation in water has been successfully applied to whiting suspensions for determining the size distribution from 25–1 μ.

Investigations with some of the many dispersing agents available have shown that several are quite suitable, and good results have been obtained with Dispersol T, a non-foaming water solution of the sodium salt of a formaldehyde/naphthalene sulphonic acid condensate (Imperial Chemical Industries Ltd., Dyestuffs Division). A millilitre of the Dispersol T 50% solution is added to 600 ml of distilled water for the suspending liquid. Efficient dispersion is obtained by high-speed stirring for $\frac{1}{2}$ h followed by remixing with a plunger when the suspension has regained the temperature of the thermostat bath.

The optimum concentration for the sedimentation of whiting in water was found by the usual method of decreasing the concentration of solids in test suspensions until constant results were obtained for particle size distribution. There was no significant change in results with dilution below 5·5 g/l or nearly 0·2% by volume. This concentration figure of 0·2% agrees with that found by Stairmand[2] to give good agreement of results for size distribution of fine chalk when determined by a modified Andreasen water sedimentation method or by his precise method of photosedimentation.[3] Most of our work has been done with the apparatus commonly in use for this determination. A thermostatically controlled water-bath held at 25° C $\pm$ 0·2° C with the samples contained in cylindrical gas jars of 600 ml capacity are the main items of equipment. Samples are withdrawn at 10 cm depth with a 10 c.c. pipette at time intervals calculated to obtain the percentage of particles finer than 25, 10, 5, 3, 2 and 1 μ. The weights of the fractions were originally determined by a rather lengthy method of evaporation to dryness and correcting for the weight of dispersing agent, but a titration method has been found to be quicker and less liable to manipulative errors. The 10 ml portions extracted from the jars are pipetted into titration flasks containing excess hydrochloric acid. The pipette is rinsed with distilled water to wash out particles adhering to the walls. Whiting reacts easily with hydrochloric acid, but some limestones need gentle heating to obtain complete solution. The excess acid is titrated with

standard sodium carbonate using Hoppner's indicator,[4] a mixture of dimethyl yellow and cresol green. As whitings have a slightly variable carbonate content a blank determination is made with the original powder.

Another method for determining small weights of calcium carbonate is based on the colorimetric determination of calcium with chloranilic acid,[5] the red colour of the reagent being measured with the Spekker absorptiometer using yellow-green filters (Ilford No. 605). This takes longer than the titration method but it is very useful when only small quantities of sample are available.

By using either micro-titration or the above colorimetric method, determinations have been made with suspensions containing only 0·01% by volume of solids. At this concentration the particles have an average separation of 17 diameters (calculated on spherical shape), a condition which should give unhindered settling. The results were in good agreement with those obtained for sedimentation at 0·2% volume concentration thus showing that there is no flocculation at the latter concentration.

Hypodermic syringes of 2 and 5 ml capacity fitted with 10 cm serum needles have been successfully used as alternatives to a pipette for withdrawing samples in the Andreasen method.

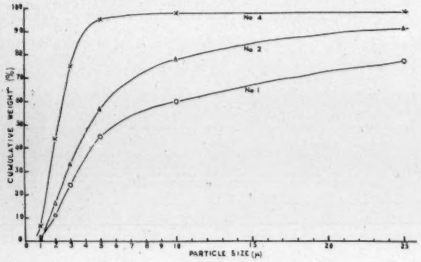

Fig. 3. Cumulative size distributions of whitings Nos. 1, 2 and 4

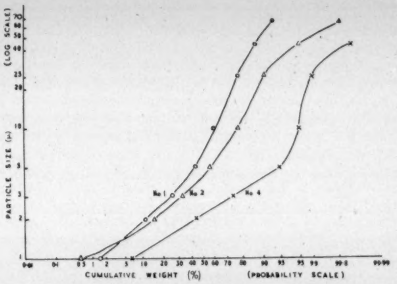

Fig. 4. Cumulative size distributions of whitings Nos. 1, 2 and 4 on log-probability graph paper

When a limited size distribution is required, which only takes 1 h (5 μ), it has been found quite satisfactory to carry out the sedimentation in a wide-necked vacuum flask, used previously, for example, by Andreasen.[6] If the suspension is shielded from air draughts and the temperature measured, good agreement is obtained with results from the thermostat bath sedimentation. The simple arrangement is very convenient for use in works, particularly when only one sample is to be tested at a time.

Particle size distribution and specific surface of a range of whitings

Whiting sample number	1	2	3	4	5	6	7	8	9
Sieve residues									
Per cent retained B.S. 100 mesh	0·02	0·01	0·01	0·03	0·01	0·85	0·02	0·01	0·02
Per cent retained B.S. 240, passing B.S. 100 mesh	7·3	0·15	0·08	0·02	0·05	4·7	7·3	0·03	0·05
Per cent retained A.S.T.M. 325, passing B.S. 240 mesh	5·2	1·76	0·33	0·03	0·09	4·2	8·6	0·44	0·98
Size distribution (by sedimentation)									
Per cent finer than 25 μ	78	92	96	99	98	80	73	94	89
Per cent finer than 10 μ	60	78	87	98	95	68	59	80	80
Per cent finer than 5 μ	45	57	68	95	90	53	42	59	60
Per cent finer than 3 μ	24	33	49	75	68	32	25	41	40
Per cent finer than 2 μ	11	16	31	44	39	16	13	25	21
Per cent finer than 1 μ	2	0·5	5	7	5	1	0·7	1	0·5
Centrifugal sedimentation, finer than 1 μ	—	—	—	10	13	—	—	—	—
Specific surface (in cm^2/g)									
(1) Nitrogen adsorption method	12 950	18 700	15 700	19 200	18 200	14 300	11 700	14 350	18 600
(2) Light (Spekker) absorption method	10 650	14 150	10 300	15 750	14 350	11 350	9 000	12 250	11 600
(3) Air permeability method	7 500	10 000	9 900	11 850	12 300	8 350	7 050	9 850	10 300
(4) Air permeability (Rose's correction)	9 400	12 450	12 250	14 750	15 650	10 300	8 550	12 350	12 800
(5) Calculated from size distribution	5 300	6 300	9 600	12 450	11 150	6 000	5 000	7 350	6 900
(6) Calculated from log-probability distribution	—	—	9 800	11 700	10 900	—	—	—	—
Geometric mean diameter d_g (μ)	6·2	4·15	3·0	2·15	2·3	4·75	6·8	3·8	3·8
15·8% *content diameter* d (μ)	—	—	1·4	1·3	1·4	—	—	—	—
Standard deviation σ_g	—	—	2·14	1·65	1·64	—	—	—	—

In all methods described above, the average range for replicate tests is 3%. Fig. 3 shows the cumulative size distributions for three typical grades of whiting. The sedimentation analysis is seldom carried below 2 μ, although figures obtained for 1 μ contents appear reasonable when plotted in the size distribution curve on log-probability graph paper, Fig. 4. The limitations of the Andreasen method are well known, but it has been found to be a most useful method for whiting since the greater proportion of particles are within the size range (2–25 μ) to which the method is most applicable.

Centrifugal sedimentation. Several techniques have been investigated to obtain the contents of 1·5, 1 and 0·5 μ size particles by accelerated (centrifugal) sedimentation.

Using a centrifuge with 100 ml capacity tubes and speeds up to 1000 r.p.m., measured accurately with a tachometer applied directly on to the centrifugal axle, it has been confirmed that a simple adaptation of the Andreasen technique of withdrawing 2 ml samples at 10 cm depth at time intervals calculated from the Stokes' equation, amended for centrifugal sedimentations, does not give correct results. This is almost certainly due to the Coriolis[7] effect produced by the retardation of the horizontally spinning tube falling to its final stationary vertical position. The results obtained were all high, as would be expected if the suspension had been stirred by the induced circular flow along the length of the tube.

Some results have been obtained using a procedure based on Stokes' law and Oden's method of tangential intercepts described by Jacobsen and Sullivan,[8] and Callaway Brown.[9] Suspensions of various heights were centrifuged at constant speed and time, and the total weight fraction of powder falling to the flat bottom of the tube was measured. A plot was made of the weight per cent in suspension against the depth of suspension. By drawing tangents to the curve and measuring the intercepts on the weight per cent axis, a size distribution graph was obtained, or single point determinations were calculated corresponding to the percentage of any required size of particle within the range covered by the determination.

Fair agreement was obtained for the less than 1 μ content of whitings with values obtained by the Andreasen sedimentation, but, due to the rapid rate of change of slope on the curve in the size range 1–3 μ, tangents cannot be drawn with accuracy. Some of the results obtained for the 1 μ content are given in the table.

ELECTRON MICROGRAPHS

A number of electron micrographs of the particles finer than 5 μ, separated from whitings by repeated decantation of samples dispersed in water, have been taken for the authors by the Paint Research Station (Research Association of the British Paint, Colour and Varnish Manufacturers). The sample for the electron micrograph was prepared by adding a dilute suspension in oil to a nitro-cellulose supporting film on water. The film was washed free from oil with white spirit, and then shadowed with a gold–palladium beam at an angle of 24°. Two of these electron micrographs are shown in Figs. 5 and 6. Fig. 5 has been chosen to show a particular type of whiting containing some clearly defined large fragments of fossil coccoliths and particles of about 1 μ which are mainly individual segments of the coccoliths. Fig. 6 shows a larger number of particles, including a few stick-shaped fragments of a different type of coccolith. Examination of these and other electron micrographs shows a few particles below 1 μ and the lower limit of size to be about 0·1 μ. Both these sizes correlate well with figures obtained from the extrapolation of size distribution curves plotted on log-probability paper.

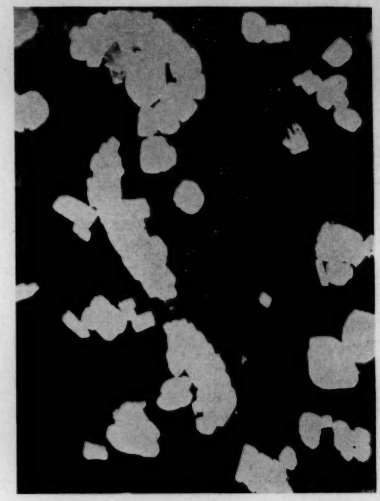

[Reproduced from *Chemistry and Industry*]

Fig. 5. Electron photomicrograph of a whiting *A* magnification ×8000

Fig. 6. Electron photomicrograph of a whiting *B* magnification ×8000

PRESENTATION OF THE SIZE DISTRIBUTION DATA

The presentation of data obtained by the various methods of determining size distribution can be made in a variety of ways. The most commonly used methods of plotting size distribution are of the cumulative weights of material on arithmetic, log-log (Gaudin function), log-log reciprocal (Rosin–Rammler function) and log probability (Gaussian or normal probability distribution) scales. Whiting is a material produced by a variety of methods of grinding and classification, wet and dry; it is not to be expected, therefore, that any one distribution function will apply to all grades of whiting. One type of whiting made by dry grinding and with air classification to remove the coarse fractions (Nos. 3 and 4) has a cumulative size distribution which follows closely the log-normal probability function (see table). Several other types form S-shaped curves when plotted with this type of co-ordinate and are typical of wet ground-levigated powders. The Rosin–Rammler function, which was developed to describe the size distribution of ground coal, and also found to be suitable for many other friable materials, has not been found to fit any of the size distribution of whitings examined so far.

It is convenient for whitings and other ground materials which follow a log-normal weight distribution to adopt the method proposed by Hatch and Choate in 1929 to describe the mathematical function of the size distribution by giving the values of geometric mean diameter (50% of weight value) and the standard deviation σ_g.[10] The standard deviation σ_g is obtained from the graph by reading off the diameters of particles at a certain percentage contents by weight, thus:

$$\sigma_g = 84{\cdot}13\%\ \text{size}/50\%\ \text{size} = 50\%\ \text{size}/15{\cdot}87\%\ \text{size}.$$

This type of plot on "probability" paper is useful for extrapolation to obtain the percentage contents of 1 μ and smaller particles, and in addition can be used to calculate the specific surface as described in this paper.

SURFACE AREA MEASUREMENT AND CALCULATIONS

Numerous methods have been proposed for determining the surface areas of fine powders.[11] Some of them are specific for certain materials such as the determination by rate of dissolution or the absorption of dyestuffs on particle surfaces, but most attention has been paid to evolving methods intended to have general application.

Nitrogen adsorption. In recent years the determination of the low temperature adsorption isotherm of nitrogen by the powder has gained the position of being considered the "reference" method of evaluating specific surface. The method of determining the monolayer capacity of a powder for adsorbed gas molecules according to Brunauer, Emmett and Teller[12] from a sigmoid-shaped isotherm is generally adopted. Results of a number of determinations of specific surface of whiting by nitrogen adsorption at the temperature of liquid oxygen made by the Building Research Station in the course of the present work, are given in the table; the figures shown are in all instances the mean of two determinations.

Air permeability. Determinations of the specific surface of whitings have been made using a Lea and Nurse apparatus as described in B.S. 12: 1947,[13] with a slightly finer bore capillary tube to the flowmeter to give suitable readings with powders having apparent surface areas ranging from 7000–14 000 cm^2/g.

It is generally recognized that the air permeability method does not give true specific surface values for powders with values much beyond 5000 cm^2/g, and that the error increases with the specific surface. When air flows through a bed of very fine particles the dimensions of the capillary spaces approach in value the mean free path of the gas molecules, and the type of air flow through the bed changes from normal viscous flow to molecular streaming. Carman and Malherbe[14] proposed an equation to allow for the slip correction due to the latter type of flow and results obtained by them seemed to indicate that their method gave better values for the specific surface. Some work in these laboratories, using their type of apparatus and calculations, has confirmed that the values obtained are in closer agreement with those obtained from nitrogen adsorption determinations, but are very dependent on the porosity of the bed of powder under test.

A different approach to the calculation of results obtained by the air permeability apparatus of Lea and Nurse has recently been described by H. E. Rose.[15] Rose proposes that, by introducing an empirical factor into the voidage function and then calculating the parameters from test data, results can be obtained which are in closer agreement with values from nitrogen adsorption and photo-extinction data. Values obtained by using this type of correction are shown in the table.

Optical method. The optical method of determination of specific surface by measurement of the light absorbed in passing through a dilute suspension of the powder was originally described by Wagner[16] and increasing attention has been paid to the theory and practical applications of this method during recent years. Sharratt and his co-workers[17] described a simple adaptation of this method using a Spekker photoelectric absorptiometer to pass a beam of white light through a suspension of powder contained in a 1 cm glass cell, the light absorbed being measured by the usual technique of adjusting the aperture of the instrument, which is calibrated on a logarithmetic scale to base 10. The specific surface is calculated from the following simplified equation based on Lambert's law and the Cauchy relationship for a random distribution of convex particles.

$$S_W = 9{\cdot}21(\theta_0 - \theta_1)/C.L.$$

Where S_W is specific surface in g/cm^3.
θ_0 and θ_1 are the absorptiometer drum readings for the clear medium and suspension respectively.
C is the suspension concentration in g/cm^3.
L is the length of light path through the suspension in cm.

This equation assumes that the particles are completely opaque and that their projected area is directly proportional to the amount of light absorbed, irrespective of the size of the particles and the wavelength of the incident light. Forward reflected and diffracted light give errors depending upon the dimensions and design of the optical system used; with the Spekker absorptiometer these errors are likely to be significant.

A more generalized relationship can be used introducing a term known as the extinction coefficient, which is affected by the above-mentioned variables. The extinction coefficient is asymptotic with increasing particle size, and Rose and French,[18] for example, have shown that it varies in a complex manner with a size of particles up to at least 20 μ in diameter, whilst Andreasen and co-workers[7] have demonstrated that the coefficient varies with the wavelength of the incident light, with a maximum value when the wavelength is of the same dimensions as the particle diameter. Jopling[19] and Leech and co-workers[20] have recently reported that this optical method gives good agreement with other methods of surface area determination.

As whitings normally consist of particles within the size range of powders used by the above-mentioned authors employing the Spekker absorptiometer, it seemed to be worth while comparing results on a range of whitings with surface area data obtained by other methods. In view of the large proportion of particles just above 1 μ in size it seemed advisable to use a light of fairly low wavelength to reduce the effect of the maxima of the extinction coefficients for particles above 1 μ. The use of an 0·01% aqueous suspension of whiting with 0·1% "Alcopol O" as dispersing agent with green light from an Ilford No. 604 filter (approximately 0·55 μ wavelength) were the main differences in procedure from that described by Sharratt and co-workers.[17] The results are given in the table (item 2).

DISCUSSIONS AND CONCLUSIONS

The coarse particle contents obtainable with test sieves down to the limit of 43 μ still provide adequate size data for some uses of whiting where only the absence or limitation of coarse particle content is important. The water sedimentation of whiting using the Andreasen technique, has been shown to give practically complete data on the size distribution of most whitings, the percentage finer than 1 μ Stokes' diameter, which is the practical limit for this method, usually being very small. Whilst centrifugal sedimentation has been found to give fair agreement with the Andreasen method for the proportion of particles finer than 1 μ, the method needs further investigation before it can be regarded as giving any useful extension of information on whiting beyond that given by the Andreasen method. It is considered that the wet sieving and Andreasen sedimentation procedures described above, together give adequate and reliable data for the size distributions of whitings.

The relative value of the various methods of determining specific surface depends largely on the purpose for which the data are needed. It is clear from the table that, although the various methods all give results of the same order, the agreement is poor and the correlation is moderate. It is generally assumed that the nitrogen adsorption method gives the true specific surface value and that it includes "internal" surfaces which are accessible to the nitrogen gas molecules. This method can be considered as absolute, but is lengthy and the value found is not necessarily the best measure of fineness in relation to all uses of the powder. It might be preferable for some purposes to measure the adsorption of a much larger molecule to obtain a measure of the outer effective surface. The air permeability method has two main advantages: it is a simple and rapid determination, and the results are a measure of the effective external surface. The corrections proposed by Rose,[15] whilst giving results nearer to the nitrogen adsorption values, do not improve the correlation. Results by the air permeability method are not expected to be as high as values obtained by gas adsorption, but there is fairly good correlation between both the corrected and uncorrected air permeability values (items 4 and 3 in the table) and the nitrogen adsorption figures.

The specific surface values obtained by the optical method using the Spekker absorptiometer do not show good correlation with any other method. This is not a surprising result for fine powders, because the method is somewhat arbitrary in its conditions and assumptions. The specific surface values calculated from particle size distribution data are significantly lower than the air permeability values, except for the three samples which have nearly a log-normal (Gaussian) particle size distribution. The relations observed are understandable since values calculated from particle size distributions entirely ignore internal surface, the irregularity of surface and particle shape where the surface/volume ratio is greater than that of a cube. The two values calculated by different methods from size distribution data for each of samples Nos. 3 to 5 are in good agreement with each other and with air permeability values. Whilst only these three samples among those shown follow a log-normal (Gaussian) size distribution, they are whitings produced from three different types of chalk. This may indicate that log-normal distribution is of fairly frequent occurrence.

Where specific surface is required merely for comparison of "average" particle size or as a simple index of the overall fineness of whiting, the air permeability method has been found useful and adequate. If a rough guide to the true (nitrogen adsorption) surface is required, it can be obtained by multiplying the air permeability value by 1·6.

ACKNOWLEDGEMENTS

The present work is published by permission of the Research Council of the British Whiting Federation. The authors wish to acknowledge the help afforded by Dr. L. A. Jordan, Director of the Paint Research Station, in taking the electron micrographs, and Dr. F. M. Lea, Director of the Building Research Station, for the facilities afforded for nitrogen adsorption surface area measurements.

REFERENCES

(1) DELFOSSE, P. *Peintures–Pigments–Vernis*, **28,** p. 774 (1952).
(2) STAIRMAND, C. J. *Instn Chem. Engrs Symposium on Particle Size Analysis*, p. 77 (1947).
(3) CAREY, W. F., and STAIRMAND, C. J. *Trans Instn Chem. Engrs*, **16,** p. 57 (1938).
(4) HOPPNER, K. *Dtsch. Zuckerindustr.*, **61,** p. 361 (1936).
(5) FROST-JONES, R. E. U., and YARDLEY, J. T. *Analyst*, **77,** p. 468 (1952).
(6) ANDREASEN, A. H. M., KREBS, K., DALSGAARD-PEDERSON, N., CAMRADT-PETERSEN, E., and KJAER, B. *J. Soc. Chem. Ind.*, **69,** p. 312 (1950).
(7) JOOS, G. *Theoretical Physics*, p. 221 (London: Blackie and Son Ltd., 1934).
(8) JACOBSEN, H. E., and SULLIVAN, W. F. *Industr. Engng Chem.* (Anal. Ed.), **18,** p. 360 (1946).
(9) BROWN, CALLAWAY. *J. Phys. Chem.*, **48,** p. 246 (1944).
(10) HATCH, T., and CHOATE, S. P. *J. Franklin Inst.*, **207,** p. 369 (1929); **210,** p. 793 (1930).
(11) *Bibliography on Particle Size and Surface Area Determination with brief abstracts.* No. 1 May 1950, No. 1A December 1951, Research Council of the British Whiting Federation, Bedford.
(12) BRUNAUER, S., EMMETT, P. H., and TELLER, E. *J. Amer. Chem. Soc.*, **60,** p. 309 (1938).
(13) B.S. 12: 1947, *Portland Cement (Ordinary and Rapid Hardening).*
(14) CARMAN, P. C., and MALHERBE, P. LE R. *J. Soc. Chem. Ind.*, **69,** p. 134 (1950).
(15) ROSE, H. E. *J. Appl. Chem.*, **2,** p. 511 (1952).
(16) WAGNER, L. A. *Proc. Amer. Soc. Test. Mater.*, **32,** p. 553 (1933).
(17) SHARRATT, E., VAN SOMEREN, E. H. S., and ROLLASON, E. C. *J. Soc. Chem. Ind.*, **64,** p. 73 (1945).
(18) ROSE, H. E., and FRENCH, C. C. J. *J. Soc. Chem. Ind.*, **67,** p. 283 (1948).
(19) JOPLING, D. W. *J. Appl. Chem.*, **2,** p. 642 (1952).
(20) LEECH, L. G., RATCLIFFE, S. W., and GERMAN, W. L. *Trans Brit. Ceram. Soc.*, **52,** p. 145 (1953).

DISCUSSION

Mr. G. W. Mack: The method of determining sieve residues involves breaking down lumps with gentle pressure from a rubber-tipped rod. Have the authors any experience of variability arising from different interpretation by different operators?

Does the carbonate content of whitings vary between fractions of different coarseness, particularly in those whitings whose carbonate content may vary?

Surface areas for the whitings by nitrogen absorption are roughly 1·6 times those by the Lea and Nurse method, varying between 1·46 and 1·87. Is there any relation between the exact ratio and the appearance of the micrographs, particularly in relation to the type of coccolith or particle shape?

Dr. H. Heywood: Centrifugal sedimentation of small particles in a liquid had the same relationship to gravitational sedimentation as the electron microscope had to the optical microscope. The brief reference to this method by Mr. Soul did not indicate very satisfactory results, but several papers on this subject have been published and the fundamental principles are well established. Further research seems necessary, however, to develop a technique for size analyses below 1 μ, and it seems that the method of sampling whilst the sedimentation vessel was rotating would probably be most successful.

Mr. R. Johnson: I was surprised to see in Paper H.1 that centrifugal sedimentation gave finer results than gravitational sedimentation. As mentioned in connexion with Paper A.4, there are doubts about pipette sampling results being correct since these results depend on: (*a*) speed of sampling and (*b*) the design of sampling device. Consequently, I cannot accept the statement that centrifuge results are incorrect because they do not agree with pipette sampling results.

At the British Ceramic Research Association we have compared centrifugal and gravitational sedimentation and found that gravitational sedimentation invariably gives finer results for materials such as ball clay and china clay. For ground flint, whose fineness is similar to that of whiting, we have had fairly good agreement between results by centrifugal sedimentation and diver results.

Mr. T. G. Callcott: Although many size analyses are made by one or other method of sieving, this aspect of particle sizing has not been extensively considered at this Conference. Mr. Bessey and Mr. Soul, in mentioning some initial sieving procedures in Paper H.1, relegate sieving to the less interesting part of their studies. I would like to present the following data as suggestive of some possibilities and as a method of investigation of sieving theory and practice. It is important that the latter aspects be considered since for the immense majority of laboratories, sieves are the basic equipment used in size analyses of particles greater than about 70–80 μ.

The numerous investigations into size analyses by sieving have led essentially to a definition of the maximum size of particle passing the sieve in terms of a mean aperture. All particles just less than the mean aperture are said to have passed the sieve if the rate of sieving is less than a certain value, usually 0·1 g/min. That both the mean aperture, e.g. that of a calibration by the National Physical Laboratory, and the limiting rate of sieving may be irrelevant to the definition of particle size, has been generally ignored. The studies of Carpenter and Deitz* show that an empirical approach may supply the solution to many problems.

Experiments were done with Carpenter and Deitz's glass spheres. The first test concerns simply the calibration of sieves; second, the meaning of particle size or of a size analysis curve obtained by sieving. Samples of glass beads of known size distribution and sizes from 70–1100 μ approximately were used in a designed experiment to determine the "effective aperture" of the sieves. Two samples of spheres were sieved by a routine procedure on four banks of sieves each containing six sieves. Four replicates of each sieving test were done.

The effective aperture in microns was obtained from the weight of spheres passing the sieve. Two features stand out from the statistical analysis: first, the reproducibility of a determination was very good—the coefficient of variation of a determination was less than $\pm 1\%$ even though it depended on the sieve and its condition. With a 16-mesh B.S. sieve, the standard error of an observation was $\pm 5{\cdot}8$ μ, 12 degrees of freedom, and for a 150-mesh sieve the standard error of an observation was $\pm 0{\cdot}8$ μ, 12 degrees of freedom. Second, the weight of spheres passing a given sieve depends not only on the duration of sieving, but also on the composition of the bank of sieves, on the weight of spheres on the sieve, on size distribution of the spheres on the sieve.

Now these tests considered a particular method of sieving only, namely 10 minutes sieving in a machine, then cleaning by brushing and then another 10 minutes of sieving, a final cleaning in order to obtain the weights passing and retained. Carpenter and Deitz believed the end point of sieving was reached in about 8 minutes with the glass spheres since by this time less than 0·1 g/min passed a sieve. The dependence of the amount passing on the factors mentioned above indicates Carpenter and Deitz's notion was not very good. Further studies showed that the 0·1 g/min criterion for an end point was not a satisfactory criterion of the practical elimination of not only "near mesh" but even smaller particles.

Consider Fig. 1, where the weight of spheres passing is plotted against the duration of sieving for a 25 B.S. sieve. Curve *A* shows the behaviour with a full sample of glass spheres added to the 25 B.S. sieve. The sieve was cleaned at

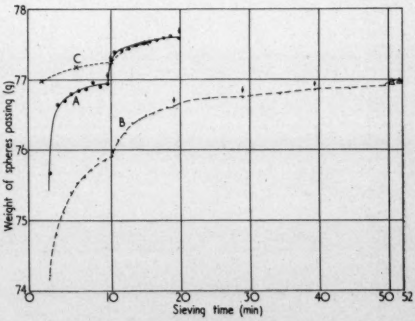

Fig. 1. Relation between weight passing and time for a 25 B.S. sieve

○ Test A. ● Test B. × Test C.
↓ Sieve cleaned after this reading.
△ halfpenny on sieve followed by the 28·34 g of +25 B.S. sieve spheres from Test A added.

* Carpenter and Deitz. *J. Res. Nat. Bur. Stand.*, **47**, p. 139 (1951).

10 and 20 min, then the spheres that had passed the sieve were placed on the cleaned sieve, whilst the +25 B.S. sieve spheres were kept in the clean sample jar. Curve *B* shows the course of the sieving of the −25 B.S. sieve spheres. After nearly 50 min sieving and 4 cleanings, the weight of spheres passing was less than after 10 min for curve *A*, although after 7 and 14 min of sieving the rate of passage was less than 0·1 g/min. After 52 min sieving the +25 spheres were added, and the relation between the weight passing and time (curve *C*) found. Very soon, the amount passing had returned to a corresponding position on the original curve *A*. Similar phenomena were found for the 44 and 100 mesh sieves. These data can neither be predicted nor be calculated from any of the present theories of sieving. Carpenter and Deitz's explanations are also inadequate. We may conveniently, but not necessarily accurately, divide sieving characteristics into three classes, those where less than an "optimum weight" of material is on the sieve, those with the "optimum weight," and those with "excessive weights." For each class, we can quite definitely state that when 0·1 g/min passes the sieve we have not necessarily achieved a true *end point**: for example, for the tests of Fig. 1 this sieving rate was achieved within 4–6 min in each case.

The principal object of this presentation of the data is to indicate that "end points," times of sieving, etc., are quite irrelevant when obtaining a size analysis of a material, provided one does not define the cut sizes of a sieve by the mean aperture of the mesh and does not expect practically all near mesh particles to have passed when 0·1 g/min is attained. If the "cut size" or the effective aperture of a sieve is defined by the glass bead technique, it should be, firstly, reproducible for a given method of sieving; secondly, any material sieved in a number of ways should have a unique size analysis since variations in the effective aperture should be measurable and should account for the variations in weight passing; thirdly, it should have a better relationship with theoretical studies

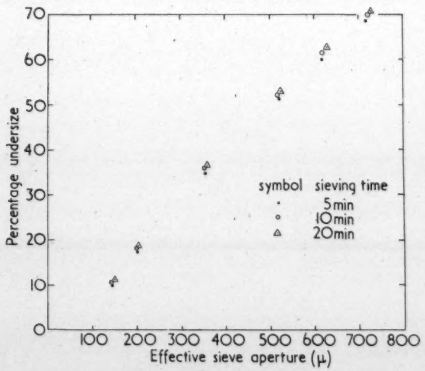

Fig. 2. Percentage undersize in relation to effective aperture for a sample of coal

than N.P.L. calibrations or such. A sieve used in different ways gives different, but reproducible, effective apertures. For example, a particular 22 B.S. sieve had, for three methods of sieving, the following mean effective apertures: 718, 720·5, and 728·5 μ, all within about ±½ μ.

A sample of coal ground so that all passed a 14-mesh sieve, was sieved in three ways. Fig. 2 shows the size analysis. For two ways a single curve is found, the third way is slightly different but is actually within experimental error; hence the "effective apertures" of sieves to glass spheres may be a simple empirical solution to size analysis by sieving. In Fig. 3, the dotted curve represents the plot of the size analysis

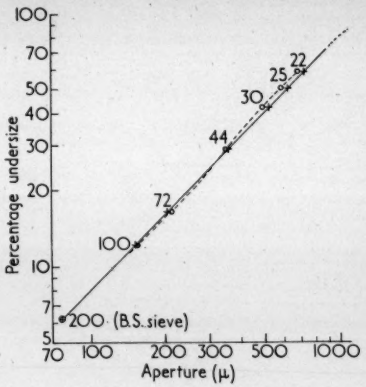

Fig. 3. Comparison of nominal and effective apertures

of a sample of coal using sieve apertures from N.P.L. calibrations and end point sieving and the full line, the size analysis using the "effective" apertures. The coal sample had been broken in such a way that the plot was expected to be linear in the range considered and of nearly unit slope. Obviously, the full line agrees far more with the theoretical expectations. Data such as this latter have been accumulated for several hundreds of tests.

In conclusion, I would like to return to my initial thoughts. Sieve analysis is important if only because many people do it. Present-day specifications of sieving apertures, methods of sieving are unsatisfactory, as also are the theoretical aspects. It seems very important that some considerable study be made of test sieves and their modes of operation and also that *new* simple definitions of the truly relevant features be given. Personally I feel that many of the previous studies have, unfortunately, been rather beside the point, which is, essentially, the establishment of a single or unique size analysis curve for a single sample irrespective of the sieving procedures.

Mr. C. J. Stairmand: Referring to Mr. Callcott's remarks on sieving, I would say that part of the trouble might be due to sticking of the particles, even though spherical particles were employed in the tests. I have had similar trouble, and have partly avoided it by putting a dozen or so nylon fibres on each sieve, which gave a controlled degree of de-aggregation without excessive breakdown of the particles, and could subsequently be separated very easily before weighing the fractions.

Authors' reply: In reply to Mr. Mack's question with regard to the interpretation by various operators of the instruction to break down lumps in sieve residue determination with a rubber-tipped rod, we have not found that

* See *British Standard* 1796: 1952.

this gives rise to any difficulty. The rubber-tipped rod does not give any significant pressure upon the small particles of 100 mesh size downwards, and very little of such treatment is needed with whiting.

On his question regarding carbonate content of the various particle size fractions, this depends upon the nature of the impurity in the whiting. The total impurity amounts only to some 1–4%. Most of this consists of clay mineral with, in some instances, some finely crushed flint. Where the latter is present, it will be concentrated in the coarser fractions thus reducing their calcium carbonate content, but the clay mineral, being inherently fine, does not concentrate in this way.

No relation has been found between the ratio of nitrogen absorption surface areas to air permeability surface areas and the particle shape, etc., of the whitings. One might expect that the ratio would be greatest when the proportion of whole or partially broken coccoliths was high, but the number of samples examined by both methods is inadequate to determine the effect of this factor amongst the other likely variables.

We agree with Dr. Heywood that in the centrifugal sedimentation method, the method of sampling whilst the sedimentation vessel is rotating is most likely to be successful. We also agree with Mr. Johnson that in gravitational sedimentation the results will depend to some extent upon sampling technique; equally in the centrifugal method the results depend upon technique, and only direct measurement of particle size by optical or electronmicrographs can be used to establish ultimately which technique gives the more accurate result.

Mr. Callcott's contribution on sieve analysis is most useful and interesting. We agree with him on the importance of this question but have given more attention in our paper to other methods, since for whiting the proportion retained on sieves is so small. Whilst effective aperture of a sieve as defined by the glass bead technique is of interest, it seems doubtful to us whether it is much less arbitrary than the average sieve aperture, as defined in the British Standard. The effective aperture will, in practice, vary according to the particle shape of the material under test and any precise interpretation of sieve residue will entail not only the question of effective aperture but also of effective particle diameter where the particles differ widely from the spherical form. The use of sieve tests is generally for purpose of comparison rather than separation at a precise particle size, so that if the sieves are accurately defined and the procedure of test is closely reproducible the objectives of testing should be achieved. We have found that even these limited requirements are not easy to achieve. The tolerances of British Standard sieves, particularly with the very fine sieves with which we have been concerned, are sufficient to give appreciable differences in some instances between results with one standard sieve and another, and it is important in any specifications involving limitation of sieve residues that the tolerances submitted should be sufficient to allow for this factor.

Paper H.2

A microscope method of measuring thicknesses of fine particles

By W. H. M. Robins, B.Sc., Scientific Department, National Coal Board

The principle of the method is to bring the particle into the space beneath a lens, resting on a plane surface, until the particle is in contact with both lens and plane. The particle's thickness is then calculated from a knowledge of the radius of curvature of the lens and the distance of the particle from the point of contact of lens and plane. The lens, of suitable curvature, forms part of an attachment to the sub-stage condenser mount of a microscope, preferably of the inverted type. A wide range of thicknesses (100 to 3 μ) can be measured. The method has been checked using microscopic spherical particles and the results showed that thicknesses are measured with an accuracy of the order of 10%.

Measurements of the thickness of an irregularly shaped particle, and of the dimensions of its projected image, provide a measure of the particle shape. Whilst the projected dimensions are readily found, few methods are available for determining the thickness, especially for fine particles of micron sizes. A new method for measuring the thicknesses of individual fine particles has been described for the optical microscope.[1] The dimensions of the particles' images can also be measured and their shape factors can then be estimated. The new method for particle thickness measurement was suggested by the "crushing" lens technique employed by Boddy[2] in his studies of the fracture and flow of microscopic particles.

Description of Method

The principle of the method is to bring the particle into the space beneath a lens resting on a plane surface until the particle is in contact with both lens and plane (Fig. 1).

The particle's thickness T is then calculated from a knowledge of the radius of curvature R of the lens and the distance r of the particle from the point of contact of lens and plane

$$T = r^2/2R \text{ providing } R \gg T$$

The particle's highest point can occur anywhere over its image, but it is sufficiently accurate to measure the distance r

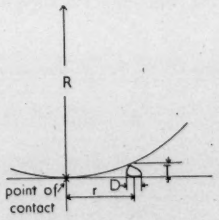

Fig. 1. Principle of microscope method of measuring thickness of particles

from the centre of the particle image, providing r is large compared with the "projected" size D of the particle (measured along the line r). The maximum error in the thickness arises when the peak height occurs at the distance $r \pm D/2$ instead of at the distance r; for $r/D = 10$, the maximum error is $\pm 10\%$.

The observations are made with a microscope. A lens of suitable curvature, carried on the sub-stage condenser mount (in place of the condenser) is brought lightly into contact with a microscope slide. Particles dispersed on the slide (on the sub-stage side) are brought into the contact region by traversing the mechanical stage. It is convenient to use a microscope of the inverted type. The particles may then be mounted dry on the upper (condenser) side of the slide and viewed through the slide, with objectives of sufficiently long working distance (e.g. standard objectives of 8 mm, or longer focal lengths). For objectives of shorter focal length, the particles are mounted on No. 1 cover slips instead of microscope slides. The point of contact of the lens and slide is located at the centre of the system of Newton's rings (Fig. 2).

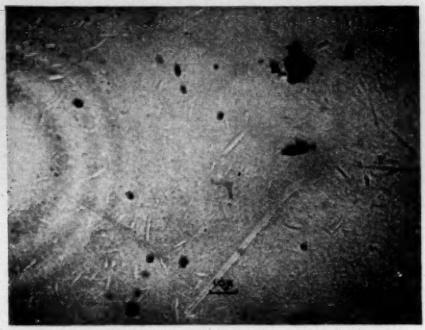

Fig. 2. Image of coal particle B ($11{\cdot}6 \times 9{\cdot}5 \times 4{\cdot}3\ \mu$) when it meets the lens (3 mm diameter)

The lens acts partially as a condenser and the particle images are of reasonable quality.

The construction of the lens attachment to the sub-stage condenser mount is shown in Fig. 3. A is a hollow cylindrical collar, which replaces the barrel of lenses of an Abbé type sub-stage condenser, the iris being retained. B is a sleeve that slips freely, without rocking, over A. To B is attached one of three interchangeable caps C which carries the quartz lens E held firm by the locking plate D. Quartz lenses are used, as they are resistant to scratching.

The method of making measurements is as follows: the condenser is racked down until the pole of the lens is about 5 mm from the slide. The objective is focused on the field of particles, and the mechanical stage traversed to select a region free of particles. The sleeve B is unscrewed from the collar A (Fig. 3) and slips down until the lens E makes contact with the slide. The sleeve of the attachment slips freely over the collar so that permanent contact is ensured against the slide without excessive pressure. The Newton's rings round the point of contact are focused; the image of the iris (closed to pin-hole size) should be nearly in focus at the centre of the rings. In order to make use of the whole field of view, the point of contact is moved (by means of the sub-stage centring screws) to one edge of the field, say the left-hand side. The stage is now traversed slowly, so that particles are brought in from the right-hand side until they make contact

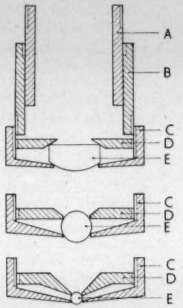

Fig. 3. Section (actual size) through optical axis of condenser attachment

with the lens. The distance r, from the position of contact to the centre of the Newton's rings, is measured for each particle in turn and their thicknesses T calculated.

To assist in measuring the distance r, an eyepiece graticule (or a graticule screen for projection microscopes) may be constructed as shown in Fig. 4. The image of the Newton's rings is arranged to lie with 0 as their centre. The arcs are

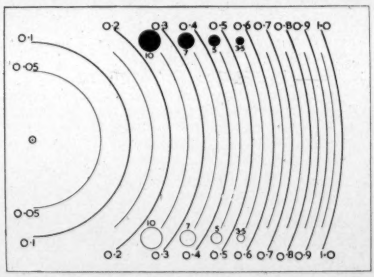

Fig. 4. Graticule for direct reading of particle thickness

parts of concentric circles centred at 0. The arcs' radii are chosen so that the thickness along each arc is a known fraction of the thickness along the arc of largest radius. These are numbered accordingly. The diameters of the reference circles are in geometric progression with a common ratio $\sqrt{2}$, as in the Fairs[3] graticule. A comparison of a particle's image area with the areas of the circles will enable the observer to decide whether the particle should be examined.

In order to cover a wide range of thickness measurements, several lenses of different radius of curvature are needed: lenses of about 9, 3 and 1 mm radius will be suitable for thickness measurements from 3 to 100 μ.

The pressure of the condenser attachment, although light, is sufficient to produce an indentation of the slide, and

allowance for this must be made when measuring the thickness of the smallest particles. The depth of indentation can be found by measuring the radii of the Newton's rings. A plot of the square of ring radius against ring number, which should be linear through the origin, gave in measurements with a 3 mm lens, a positive intercept on the ordinate, from which it was calculated that the depth of indentation was 0·14 μ. The weight of the sleeve and lens was 40 g.

It has been observed that particles resting in an unstable position on the slide are pushed over on meeting the lens, so that their least dimension is vertical. Elongated particles were observed to orientate themselves on meeting the lens, so that their longest dimension was perpendicular to the radius proportional to their thickness.

EXPERIMENTAL VERIFICATION OF METHOD WITH MICROSCOPIC SPHERES

As a check of the accuracy of the method, measurements have been made of the thickness of microscopic spherical particles. Three lenses of suitable radii, which would have covered the complete range of the light microscope, were not available to the writer, but an artificial transparent sapphire sphere, 3 mm diameter, served to cover a range of 4 to 25 μ.

With this lens the thickness T was calculated from the observation of the distance r using a value for the radius R of curvature of the lens obtained by micrometer measurement of its diameter. The diameter D of the projected image of the sphere, which should be equal to T, was measured simultaneously. The table gives the mean value of the differences $(D - T)$ for observations on 20 particles in each of three size intervals, together with the standard error of the differences. Application of Student's t test shows that the mean difference for each size interval is not significantly different from zero, the probability of the differences occurring by chance being greater than 0·05 for the 19 degrees of freedom. It is concluded that the method gives a reliable measure of the thickness T.

The observed differences might arise from many causes, including not only errors of the method, but also variation in the sphericity of the spheres. If we assume the particles to be perfectly spherical and no error occurred in the measurement of D, the standard error of the difference $(D - T)$ provides an estimate of the reproducibility of a thickness measurement. The standard error, expressed as a percentage of the mean value of the thickness in each size interval, is given in the table under the heading "Coefficient of variation." Differences of more than 2·1 (for 19 degrees of freedom) times the standard error (or the coefficient of variation) are not likely to occur more than five times in a hundred. In broad terms, we can say the method measures thickness with an accuracy of the order of 9–10%, the error being due to inaccuracies in the measurement of r and variation in the curvature of the lens.

Comparison of thickness T and projected diameter D for microscopic spheres

Size interval (μ)	Difference $(D-T)$ between projected diameter and thickness: Mean	Standard error	No. of degrees of freedom	Mean value of thickness T (μ)	Coefficient of variation
24·5–14	+0·1	±0·54	19	16·9	±3·2%
14–8	0·0	±0·44	19	10·6	±4·2%
8–4	−0·03	±0·26	19	5·55	±4·6%

CONCLUSIONS

Thicknesses of sub-sieve particles of projected diameters down to 4 μ can be measured with a modified optical microscope to an accuracy of about 10% throughout. The method is eminently suitable for microscopes of the inverted type, such as the Vickers Projection Microscope.

ACKNOWLEDGEMENTS

I am indebted to Dr. A. Crawford, Divisional Chief Scientist, North-Western Division, National Coal Board, for laboratory facilities needed for the investigations.

I owe gratitude to Dr. R. G. H. B. Boddy of the Medical Research Council and Mr. H. H. Watson of the Canadian Defence Research Board, for interest and encouragement and also for supplying materials essential to the investigations.

The apparatus required for particle thickness measurements is to be manufactured by The Singer Instrument Co. Ltd., of Reading, Berks.

REFERENCES

(1) Robins, W. H. M. *Nature* [*London*], **170**, p. 583 (1952). British Patent 21335 (1951).
(2) Boddy, R. G. H. B. *Fuel*, **32**, p. 310 (1953).
(3) Fairs, G. L. *Chem. Ind.*, **62**, p. 374 (1943).

DISCUSSION

Dr. R. G. H. B. Boddy: In preparing samples of dust for size analysis I use a technique described in 1953.* A cloud of dust is raised in a rotating drum and dusty air is drawn from it along a horizontal settling dust and the settling is watched through the microscope. On occasion, most surprising aggregates have been noted—a mixture of coal and acrylic plastic spheres gave rise to hedgehog-like aggregates, consisting of a large, plastic sphere to which were attached radial strings of fine coal particles. The position in the duct at which the aggregate was deposited showed that its apparent density was very much less than the density of either the coal or the plastic.

The plastic spheres can be used to check the height of the coal dust particles. A crushing lens of large radius is used to crush the mixture of dusts. The point of contact of the crushing lens with the particles can be detected in reflected light because a mirror reflexion is set up as the particle begins to squash, and as crushing continues the reflecting area enlarges. The plastic spheres crush to form disks of equal height, but coal dust particles become ovoids, these differences being indicated by the position and colours of the Newton's rings. Figs. 1, 2 and 3 illustrate these effects. The particles were photographed with a 16 mm objective so that the position of Newton's rings, both in the air-film and in the particles, could readily be seen. Compared with Fig. 1, the particles in Fig. 2 are much larger and easier to see. It will be noted that the crushed plastic spheres are of uniform colour whilst the coal particles are dark in the centre. Fig. 3 shows the same field in reflected light. The larger interference rings are in the air-film and again it can be seen that the plastic particles are uniformly coloured whilst the coal shows rings. These phenomena suggest that the coal and acrylic spheres

* Boddy. *Fuel*, **32**, p. 310 (1953).

react differently when crushed though both are plastics. In the crushing technique, the objective is focused through the microscope slide and in order to extend it to small particles Messrs. R. and J. Beck Ltd. have made a 4 mm lens for me at high magnifications without the need of special objectives, for example, after the photomicrograph shown in Fig. 2 of my paper had been taken (2 mm oil immersion objective used), the slide was further traversed and the particle im-

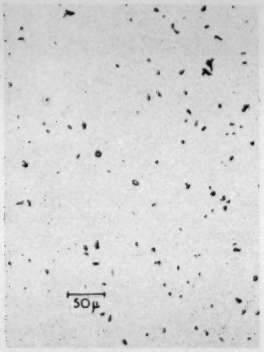

Fig. 1. Photomicrograph by transmitted light of an elutriated sample of coal and plastic spheres

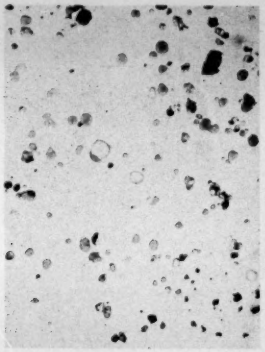

Fig. 2. Same field as Fig. 1 after crushing. The plastic spheres have spread to disks of uniform colour; the coal has rings of different colour

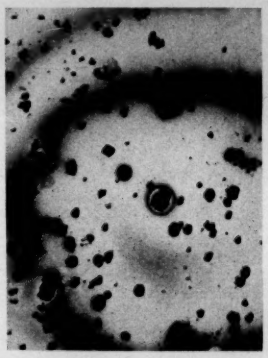

Fig. 3. Same field as Fig. 1 by reflected light to show the large interference rings in the air-film and the small ones in the coal

which has been computed for use with a cover-glass of 1 mm thickness. When used with the appropriate crushing lens this combination can be used for examining dry mounts of dusts and gives as high a resolution as is optically possible.

Author's reply: The method of particle thickness measurement was suggested by Dr. Boddy's crushing technique and, as can be expected, similar effects occur in both methods. I observed that the smaller particles of a material were sheared between the lens and slide into thin films when continuing to traverse the slide, after the particles had met the lens. There appeared to be a critical size below which the particles sheared and this size might be related to the material's grindability.

In the case of coal, translucent films are produced, which give rise to interference fringes when viewed by reflected light, suggesting a method of investigating the optical properties of coals.

The crushed particles are of known geometric shape, and their dimensions, and hence their volume, can be determined in the same way as for uncrushed particles. This volume could be compared with the volume of the particles uncrushed, calculated from empirical formulae, if the porosity of the particles is negligible.

This method of deforming particles provides means of investigating the rheological properties of polymeric and metal particles. The method has the advantage of being used mediately below "B" was sheared to form the thin film "C" seen in Fig. 4.

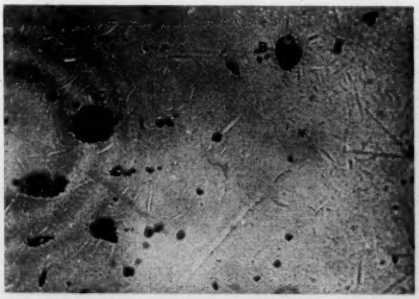

Fig. 4. Coal particle below *B* in Fig. 2 of Paper H.2 has sheared to form thin film *C*

These observations form the basis of my prospective investigations.

Paper H.3

Some methods of dispersing difficult powders

By M. G. Harwood, B.Sc., A.Inst.P., Philips Electrical Ltd., Mitcham Junction, Surrey

Methods are described for making suitable microscopic slides for particle size distribution analysis on two types of powders found difficult to do by the usual methods. One involves the use of electrical charges to repel the particles and fixing the aqueous suspension with a gelatine-coated slide to overcome Brownian movement. The other, for magnetic materials, involves heating the sample to a temperature above the Curie point, dispersing and fixing them on a slide before they cool.

Some powders consist of aggregates of crystals sintered, cemented or grown together in one way or another. Projections which are sometimes present in these crystals increase the difficulty of separating neighbouring aggregates from one another. A common method of doing this is to mix them with a highly viscous medium and rely on the transmission of external forces through the medium to separate the particles.

When the use of a jelly is necessary it has been found that the sliding of a cover slip to and fro is attended with a partial separation of the fine from the coarse material. The former tends to remain at the centre and the latter to migrate to the edge. This can be overcome at times by replacing the mechanical separating forces by electrical ones. Peptising agents are used to this end.

Charges are formed of like sign on all the particles and electrostatic repulsion causes a separation to take place. However, for a microscopic determination of particle size distribution the particles have to be fixed in space. Most peptising solutions are dilute and aqueous. The viscosity is low and Brownian movement of the fine material inhibits accurate counting.

To overcome this difficulty the following method has been adopted. The powder and peptising solution are shaken up in a small tube, and a drop is extracted and placed on a clean cover glass. If a wetter has been added this will readily cover the whole glass.

A slide coated with a layer of dry gelatine is placed on the slip with the gelatine side towards it. It is essential to make contact quickly between the two glasses as the water is rapidly taken up by the gelatine and a poor distribution of the sample may result. If the suspension originally covered the slip a well fixed and distributed sample results. The slip adheres rigidly to the slide with the gelatine between them, the whole arrangement becoming semi-permanent. This method has been used many times with great success, especially for weakly magnetic materials.

For strongly magnetic materials which do not disperse well in either jelly or a peptising solution another method has been adopted. This involves heating the sample to some few degrees above the Curie point and dispersing it on a slide before the magnetic forces again operate. For this a small tubular furnace was wound.

If the material can be heated in air to the Curie temperature without causing oxidation or any other change, so much the better. In this case a small platform is mounted on a swivel in the centre of the furnace which is mounted vertically. A slide is coated with Canada balsam and placed on a hotplate near the bottom end of the tube. The temperature of the hotplate is just enough to soften the balsam. The sample is placed on the platform in the furnace and heated.

When it reaches the desired temperature it is flicked off by rotation of an arm fixed to the mounting of the platform. The powder is thoroughly dispersed by this process for two reasons. Firstly, it is projected in all directions, the centrifugal force varying across the platform, so that a cloud of dispersed powder results; secondly, contact with, and subsequent reflexion from, the walls of the tube takes place for particles moving in directions subtending fairly large angles with the axis of the tube. Of course the heavier particles tend to arrive on the slide first but this is of no great consequence as the whole sample settles before the slide is withdrawn. No evidence of reaggregation due to magnetic forces could be observed in any of the samples examined even when the slide was left for 1 or 2 minutes to make sure all the material had been deposited.

If it is found that, owing to the fineness of the powder a long time must elapse before withdrawing the slide, it is best to have the balsam tacky, otherwise aggregations of the larger particles may occur. This will involve, however, sizes requiring electron microscopic examination and is beyond the intended scope of this method.

Some such method seems to be absolutely essential if the size of the smaller particles is of the same order as that of the magnetic domains. It is useful for other types of samples also.

ACKNOWLEDGEMENTS

I wish to thank Mr. J. A. M. van Moll and the Directors of Philips Electrical Ltd. for permission to present this paper.

DISCUSSION

Mr. D. J. Colwill: We are interested in a wide range of materials, including insecticides, fungicides, ceramics, pigments, fillers, extenders and pharmaceuticals. We are accustomed to handling these materials in the sub-sieve range between 1 and 30 μ. The Conference seems to have agreed that the preparation of a slide for powder examination is as much an art as a science and the particular technique that we employ is as follows. A suitable fluid, essentially of a viscous nature such as mineral oil, castor oil, naphthenic acid, immersion oil, etc. etc., is selected by trial and error. A small drop of this fluid is deposited in the centre of the slide and serves to moisten the tip of a clean, dry, fine camel-hair brush. A tiny quantity of the specimen powder adheres to the treated area of the brush on contact and can thus be readily transferred to the slide and worked into the dispersion medium. The best objective-eyepiece combination that is consistent with overall definition is used to obtain a magnified image. This is then projected on to a ground glass screen which also has superimposed upon it the image of a scale graticule contained in the microscope eyepiece. Since this scale can be readily calibrated for any setting of the microscope against a standard ruled graticule (0·01 mm divisions) the instrument

automatically becomes a direct micron sizer. Permanent records may also be taken photographically if desired.

Author's reply: The dispersants quoted by Mr. Colwill are in common use and variations on the method of introduction of the powder into them are many. The use of a projected image while, possibly, being less trying to the eyes than monocular vision is nevertheless accompanied by an overall definition and contrast which is lower than that normally secured by direct viewing. As a consequence the finer particles, at times, remain undetected.

Paper H.4

The adhesion of dust particles

By D. W. JORDAN, B.Sc., Medical Research Council's Environmental Hygiene Research Unit, London School of Hygiene and Tropical Medicine, London, W.C.1

An important factor in the handling of dust is the fact that the particles will adhere to each other and to solid surfaces. The mechanism by which this takes place is discussed and some quantitative results are given. It is shown that the intermolecular force between the surfaces in contact is large enough to account for this phenomenon of adhesion, although in some cases electrical forces and other processes may operate giving considerably greater attraction. An application to dust sampling problems is also mentioned.

A factor of great practical importance in the handling of airborne dust is the adhesion of dust particles to solid surfaces, and their mutual adhesion to form aggregates. The reasons for adhesion are frequently not understood, and it is the purpose of this paper to describe the forces involved and to mention their influence on the efficiency of dust sampling instruments.

These forces are not generally electrical in nature—they act between the molecules of the surfaces in contact and are of the same type as those involved in surface tension and the tensile strength of materials. They can be shown to be sufficient in themselves to account for the retention of particles on smooth, clean surfaces, and for the stability of aggregates undergoing Brownian motion or rotating due to eddies in the air.

Lennard-Jones[1] describes the way in which forces operate between molecules. The force between two molecules consists of an attraction

$$F = \lambda/r^7 \tag{1}$$

and a repulsion

$$-\mu/r^m \tag{2}$$

where r is the separation of their centres and λ, μ, are constants. The attracting force λ/r^7 is named after van der Waals. The precise form of the repulsion is doubtful, but it accounts for the fact that despite collisions between atoms and molecules and their close proximity in, for example, the liquid state, the nuclei do not in fact fly together and form a dense rigid mass as they would if the attractive force held right up to the nucleus. The repulsive force is only appreciable when the molecules are very close, and will not be considered. The attraction also falls off very rapidly with distance but is effective within a few molecular diameters. Two molecules are considered to touch when they are so close that the repulsive force operates, and the separation then is one molecular diameter.

The forces are like gravitation in that the attraction between two elements of volume is not affected by the presence of the other elements, whereas with charged bodies this does not hold. Hence the attraction between two bodies containing a great number of molecules can be obtained by adding the attractions between the individual molecules.

Bradley[2] and Hamaker[3] calculated the attraction between two solid spheres and obtained the equation

$$F = \frac{\pi^2\lambda q^2}{24h^2} \cdot \frac{d_1 d_2}{d_1 + d_2} \tag{3}$$

where d_1, d_2 are the sphere diameters, h is the separation (supposed to be about 5 Å when the spheres are in contact), λ is the constant involved in the law of force and q is the number of molecules per cubic centimetre. ($\pi^2\lambda q^2$ is of the order 10^{-12} or 10^{-13}.) For spheres of varying sizes in contact

$$\pi^2\lambda q^2/24h^2 = A \text{ in C.G.S. units} \tag{4}$$

where A is a constant, and for a sphere of diameter d resting on a plane the equation becomes

$$F = Ad \text{ dynes} \tag{5}$$

A in fact equals $2\pi \times$ the total surface energy of the spheres.

Bradley tested this formula experimentally. He constructed a microbalance consisting of a spiral spring whose extension could be observed with a travelling microscope. On the lower end he fused quartz spheres of various sizes. Another such sphere was attached to a fine capillary tube and brought up to the first, then drawn away from it until they parted. The attraction between them was obtained from the extension of the spring at the moment separation occurred. Agreement with theory was very good over the range of sizes tested, which seemed to cover spheres from 0·4 to 1 mm diameter. The constant A was found to be 212, thus for quartz spheres

$$F = 212\, d_1 d_2/(d_1 + d_2) \text{ dynes} \tag{6}$$

when d is measured in centimetres.

The apparatus could be evacuated, and special precautions were taken to eliminate possible electric charges and the effects of contaminating materials such as adsorbed water vapour. The attraction was the same whether the apparatus was evacuated or not, and Bradley concluded that adsorbed gas molecules were squeezed out by the pressure. The admission of water vapour, however, gave an increased attraction.

Beischer[4] formed long thread-like aggregates of various chemical substances by allowing the aggregation to take place

in an electric field. The threads hung from the electrodes and they could be detached to measure the rupture strength. He found that the forces acting depended greatly on the physical nature of the substance investigated, and upon the shape of the constituent particles. Diffusion may lead to the formation of a welded joint, and a substance such as ammonium chloride, with a low but appreciable vapour pressure, was found to have a fibre strength about ten times as great as iron oxide, which has negligible vapour pressure. If permanent electric polarization exists, the forces may be many times greater. Beischer's result with iron oxide particles of diameter about 0·5 μ corresponded to a value for A of about 3 c.g.s. units, so it may be that the value for quartz is exceptionally high.

Lowe and Lucas[5] suggest another method for estimating the attraction by comparing it with the tensile strength, U, of the material acting over a certain area. If two spheres are in contact, the opposing areas where the molecules are within a distance h of each other is given by

$$\text{area} = \pi h\, d_1 d_2/(d_1 + d_2) \tag{7}$$

Assume the force across the area to be of the same order as the tensile strength of the material, and put $h = 10^{-8}$ cm. Then we obtain

$$F = 10^{-8}\pi U\, d_1 d_2/(d_1 + d_2) \tag{8}$$

which is in the same form as Bradley's formula. The tensile strength of quartz filaments is 10^{10} dynes/cm^2 so the constant corresponding to A has the value 314, compared with Bradley's value 212. Hence, having found a physically reasonable value for h which gives roughly the right results for quartz, it is at least possible that this value may be carried over to other substances with an appropriate value for the tensile strength, provided it was determined with the substance in a homogeneous, non-porous condition. These considerations again suggest that the value for quartz is too high to be typical, since its tensile strength is very great.

It is known that airborne dust is charged, and Kunkel[6] has measured the charge on artificially dispersed powders. The net charge on a cloud is zero, and the larger the particle the higher the charge: in one experiment 10 μ quartz particles had an average charge of 600 electron units each. Thus it seems possible that the principal force binding aggregates may be electrical. However, charges of this order would not be large enough to play an appreciable part. The force between two electron units of charge ($4{\cdot}77 \times 10^{-10}$ e.s.u.), at a distance of R μ, is $22{\cdot}75 \times 10^{-12}/R^2$ dynes. Comparing this with the van der Waals attraction for two d μ particles, $212 \times 10^{-4}\, d$ dynes, it is seen that the latter is of greater order of magnitude. In the case of two 10 μ particles, charge 600 units; if the electrostatic attraction is to equal the molecular attraction, all the charge must be concentrated within 0·01 μ of the point of contact.

We shall now consider some numerical examples of the practical effects of the van der Waals attraction. The van der Waals force becomes more important as the particles considered become smaller. Forces tending to detach particles from a surface, for example, usually depend on the mass of the particles (as when the surface vibrates and the force is mass × the normal acceleration), or on the surface area (as in the case of the aerodynamic drag due to a wind across it); that is, upon d^3 or d^2. The van der Waals force is proportional to d, so this will come to predominate as d gets smaller.

A practical case worked out by Bradley[2], where the argument appears to work in reverse, is the possibility of the breaking-up of airborne aggregates due to Brownian rotation. Here the centripetal force tends to separate the particles. For the equal particles of diameter d the centripetal force is $\pi\rho d^4\omega^2/12$ (where ω is the angular velocity of the rotation and ρ the density). This is proportional to d^4, so the argument above might seem to apply. However, as the particles become smaller the Brownian rotation becomes more violent, ω being proportional to $d^{-5/2}$, so that the centripetal force is proportional to $1/d$. Since the van der Waals force depends on d, the aggregates become unstable as they become smaller. However, when the problem is worked out numerically, it is found that impossibly high temperatures would be required to disrupt aggregates of dust or even of the finest particles occurring in smokes.

If a quartz particle is suspended upside down from a plate the force of gravity w is $mg = 981 \times \frac{1}{6}\pi\rho d^3$ and the van der Waals force $F = 212d$. The particle will stick if F is greater than w, i.e. if $212d$ is greater than $981 \times \frac{1}{6}\pi\rho d^3$ or d less than 0·46 cm (for $\rho = 2$ g/cm^3). For any natural particle of this size contact between sphere and plate would be very imperfect due to roughness of the surface, so that in fact such a sphere would undoubtedly fall off. However, as sizes become measurable in microns the irregularities become less important and better adhesion is possible.

Some idea of the effect of shaking and concussion in removing small particles from surfaces can be obtained as follows. If the acceleration perpendicular to the surface is a, the dislodging force is

$$ma = \tfrac{1}{6}\pi\rho d^3 a \tag{9}$$

Hence the particle leaves the plate when $212d = \frac{1}{6}\pi\rho d^3 a$ or $a = 200/d^2$ (putting $\rho = 2$ g/cm^3). Thus, if $d = 1$ μ the necessary acceleration is 250 000 g and if $d = 100$ μ it is 2000 g. It is thus impossible to remove such particles by shaking. A sharp blow may remove them, however. For example, if a plate moving at 10 m/sec is stopped in 1/10 mm the acceleration is about 10^8 cm/sec^2 and such a bang would remove particles above about 10 μ.

When dust is carried on to the sampling plate of an impingement dust sampling instrument at great speed, it might be expected that it would bounce off and be carried away by the air stream immediately. On the other hand, smaller particles may be held by the plate and either remain fixed to it or slide away (see Fig. 1). A rough calculation

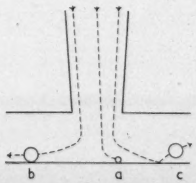

Fig. 1. Illustrating the behaviour of particles upon striking the collecting plate of a sampling instrument

(*a*) particle sticks, (*b*) particle slides, (*c*) particle bounces.

giving the maximum speed of approach of a spherical particle if it is to stick to the plate after falling upon it might be made as follows.

When the particle (Fig. 2) mass m, diameter d (supposed spherical), is at A, some distance from the plate and outside the range of the van der Waals force, we suppose it to be approaching the plate with speed w and at an angle θ with

the horizontal, rotating with angular velocity ω. At B it is drawn sharply towards the plate due to the van der Waals force F. At the point of contact it receives an impulse from the plate with a horizontal component sufficient to bring the point of contact of the particle to rest and thus to alter its

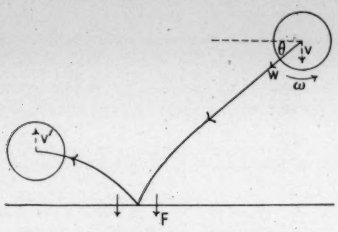

Fig. 2. Track of a sphere striking a plate

spin and the horizontal component of velocity, and a vertical component measured by the coefficient of restitution e of the particle, supposed independent of the other impulse and such that

$$\frac{\text{vertical component of velocity after contact}}{\text{vertical component of velocity before contact}} = e$$

After the collision the particle has reduced kinetic energy, which is further reduced by the action of F. Since F only acts very close to the plate we may say that if, on leaving the field of influence of F, the particle still has any upward velocity, then it bounces. If it has not it probably slides.

According to Bradley the potential energy P of a particle diameter d at a distance h from the surface is nearly

$$P = -\pi^2\lambda q^2 d/12h \tag{10}$$

We know that the force on the particle is

$$F = \pi^2\lambda q^2 d/12h^2 = 212d \text{ (for quartz)} \tag{11}$$

so therefore

$$P = -212hd \tag{12}$$

and for a particle touching the surface we put $h = 5 \times 10^{-8}$ cm.

We may now use the equations of energy and linear and angular momentum to work out the track of the particle, assuming the nature of the collision with the surface to be as mentioned above. This is a simple problem in mechanics and the result is that the particle will bounce when the initial vertical component of velocity v is such that

$$v^2 > \frac{2P}{m} \cdot \frac{1 - e^2}{e^2} \tag{13}$$

This is the same result as would be obtained if the particle were initially falling vertically and had no spin, a fact which is due to the assumption that the change in the vertical component is independent of the change in the horizontal component when the impact takes place.

If we now put $e = 0{\cdot}8$, $h = 5 \times 10^{-8}$ cm and $\rho = 2$ g/cm^3 and substitute for P and m, then if d is measured in microns we find that the particle will stick only if

$$v < (30/d) \text{ cm/sec}$$

The critical velocity is proportional to $1/d$, so that for two particles of different size approaching the plate, the smaller is more likely to stick. The speed is very small compared with the speeds of impingement used in sampling instruments, therefore most of the particles will not remain on the sampling plate unless an adhesive is used.

It seems possible that those particles which are at first retained will roll or slide away owing to drag of the air (Fig. 1). Retention will still be better for small particles, firstly because they are subjected to smaller average air speeds owing to the presence of the boundary layer, and secondly because the air drag depends on d^2, whereas the retaining force, and hence presumably the friction, depends on d, so for small enough particles the friction will be great enough to resist the air drag.

Some experiments will now be described which supplement an investigation on the efficiency of impingement sampling instruments by Davies, Aylward and Leacey.[7] It was found there that unless an adhesive was used on the sampling plate the proportion of particles caught was very low. The loss of particles was evidently due to their being blown away or bouncing off on collision with the sampling plate. These experiments were carried out to see to what extent the blowing away of particles took place.

A model, slit-shaped jet was constructed with slightly tapering sides and chamfered edges to produce a steady streamline flow of air (Fig. 3). Above it was fixed a plate to

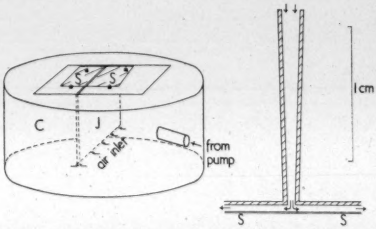

Fig. 3. Experimental arrangement. C airtight chamber, J jet, SS cover slip. The detail of the jet design is shown on the right

which could be attached the dusty cover slip under test. The jet was fed with filtered compressed air and a flow meter was connected in the air circuit. The procedure was to sediment dust upon several cover slips at once in a sedimentation chamber; the deposits being supposed equal. One was kept

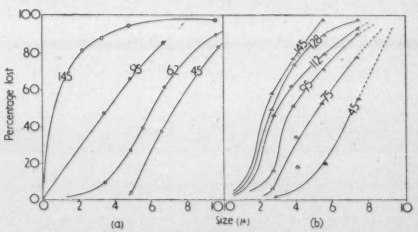

Fig. 4. Percentage of particles removed at various air speeds

(*a*) glass dust, (*b*) quartz dust. Air speeds down the jet are indicated in m/sec on each curve (the dotted lines represent extrapolations used for constructing Fig. 5).

as a control, the others were fixed in turn above the jet and subjected for about 2 sec to various air speeds, comparable to those speeds used in practical instruments. Afterwards counts were made along the line directly below the jet to see what dust had been blown away. Experiments were done with quartz dust and ground glass, and the results are plotted on Fig. 4.

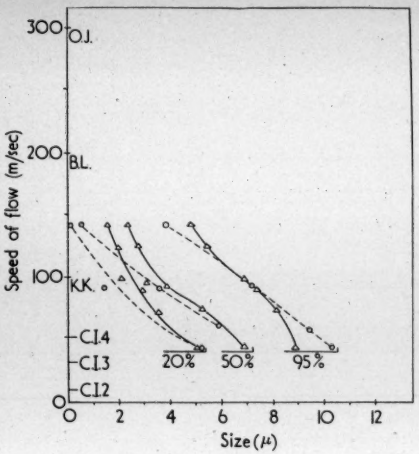

Fig. 5. Air speeds required to remove 20%, 50% and 95% respectively of particles from the plate

O.J. = Owens jet dust counter; *B.L.* = Bausch and Lomb dust counter; *K.K.* = Kotzé Konimeter; *C.I.* 2, 3, 4 = cascade impactor, jets 2, 3 and 4.

– – ○ – – glass —△— quartz

Fig. 5 gives the speeds for which 20%, 50% and 95% respectively of particles were detached. The speeds of flow down the jets of some sampling instruments—May's cascade impactor, jets 2, 3 and 4; the Kotzé konimeter; the Bausch and Lomb and the Owens jet dust counters—are indicated for comparison purposes. It will be seen that very few particles above 10 μ will remain on a dry sampling plate even for the very moderate speeds of blowing used in the cascade impactor, and for the Owens jet dust counter very little of any size will remain, as in fact was noticed in reference (7).

Another question connected with air sampling which may be mentioned here is whether or not thermal precipitator samples may be sent by post without losing a significant proportion of the sample. The acceleration required to detach a 10 μ quartz particle from the plate is 10^8 cm/sec^2. Such an acceleration would be produced by stopping the package within 1 mm after its having fallen 600 ft. It is not expected that it would encounter such violence, so we may suppose that the samples would not be seriously affected in the post, which is in fact confirmed in practice.

Lastly it must be stressed that all the calculations in this paper refer to spheres only, and cannot be applied even in order of magnitude to large irregular particles which may make contact at only a few points.

REFERENCES

(1) Lennard-Jones. *Proc. Phys. Soc.* [*London*], **43,** p. 461 (1931).

(2) Bradley, R. S. *Phil. Mag.*, **13,** p. 853 (1932); *Trans Faraday Soc.*, **32,** p. 1088 (1936).

(3) Hamaker, H. C. *Physica*, **4,** p. 1058 (1937).

(4) Beischer, D. *Koll Zeits.*, **89,** p. 215 (1939).

(5) Lowe, H. J., and Lucas, D. H. *Static Electrification, Brit. J. Appl. Phys.*, Supplement No. 2, p. S 40 (1953).

(6) Kunkel, W. B. *J. Appl. Phys.*, **21,** p. 821 (1950).

(7) Davies, Aylward and Leacey. *Arch. Ind. Hygiene and Occupational Medicine*, **4,** p. 354 (1951).

DISCUSSION

Mr. D. H. Lucas: Mr. Jordan has been kind enough to refer to the work I did on particle adhesion some time ago[1] on the ideal case of perfect spheres. He has not, however, mentioned that I extended the theoretical study to more practical cases. Since the application of ideal results to real situations is sometimes a dangerous cause of error, I would like to point out that the range of action of molecular forces is very small, even compared with the smallest particles we are considering, and it is the "diameter of curvature" in the region of contact rather than the diameter of the particle which should be substituted in the formula. In the case of a perfect sphere the two diameters are equal. In practical cases the radius of curvature at the point of contact is likely to be much less than the radius of the particle, either because of shape factors or because of surface roughness. It is therefore very dangerous to estimate an adhesive force in terms of the size of the particle. It is a fact of experience that angular material such as carborundum is much more free running than glass spheres of the same size range and this illustrates the point.

Mr. W. R. Lane: The calculations of Bradley and Hamaker referred to in Paper H.4 illustrate the role of van der Waals forces in the adhesion of clean, dry, spherical microscopic particles to each other and to smooth, dry, clean surfaces. In practice, however, it seems likely that moisture has a significant effect in the sense that an adsorbed layer of polar molecules may give rise to much larger forces of adhesion. This view receives support from the observation that the inter-particle adhesion of many powders can be greatly reduced by coating the particles with a thin hydrophobic layer. A film of a silicone polymer, for example, of a few molecules in thickness, is remarkably effective in reducing the tendency of the particles of many fine powders and dusts to clump together.

Mr. R. P. Abraham: About 25 years ago the late Dr. Owens devised a simple method of holding large particles on to a cover glass. 10% Canada balsam dissolved in xylol gives a thin coat of balsam after evaporation. When particles are in place a vapour of xylol will soften the balsam and hold the particles without altering their position. The vapour can be easily produced by inverting a dish containing blotting paper on to which a few drops of xylol have been placed.

Dr. H. Heywood: The classical systems of packing spheres for minimum voidage are well known, but the work of Mr. S. Melmore in devising geometrical systems of open packings are worth studying.[2] These systems had porosities of 94 to 96%, and compared remarkably well with electron

microscope photographs of carbon black and magnesium oxide smoke. Although the latter did not possess geometrical regularity, as did the systems devised by Mr. Melmore, the general similarity of chain structure was remarkable.

REFERENCES

(1) Lowe and Lucas. *Static Electrification, Brit. J. Appl. Phys.*, Supplement No. 2, p. S 40 (1953).
(2) Melmore. *Nature*, **149**, pp. 412, 669 (1942).

Paper H.5

The aggregation of aerosols

By J. M. DallaValle, Sc.D., Clyde Orr, Jr., Ph.D., and B. L. Hinkle, Ph.D., The Georgia Institute of Technology, Engineering Experiment Station, Atlanta, Georgia, U.S.A.

Aggregation of the individual particles composing an aerosol is a phenomenon of primary importance in the aging of the aerosol. The influence of electrification and foreign vapours on the aggregation process has been investigated. Results indicate that electrification amounting to a few electron charges per particle has little effect on the rate of aggregation, but has a decided influence on the shapes of the aggregates. In the case of aerosols whose particles have a significant vapour pressure, certain substances which lower this vapour pressure have been found to increase the rate of aggregation, presumably by reducing the vapour cushion surrounding the particles. When the particles are readily soluble in a substance whose vapour is present, the rate of aggregation also appears to be increased because of reduction of the vapour layer about the particles.

The aggregation of aerosol particles on aging is a complex process governed by mechanisms which sometimes defy prediction. Smoluchowski's theory for the coagulation of monodisperse sols has been extended to the analysis of the behaviour of aerosols, but conditions satisfying the theoretical assumptions are seldom met in practice. For example, most natural aerosols exhibit a high degree of polydispersity and are seldom free from thermal or turbulence effects. In addition, the effect of an aerosol's electrification on its aggregation has been a subject of considerable interest and controversy.

The recent studies of Kunkel,[1] in agreement with the earlier work of Whytlaw-Gray[2] and associates, indicate that the electrification of an aerosol does not alter the aggregation rate. Gillespie,[3] however, examined aerosols whose particles carried many electron charges and found that the aggregation rate increased as the magnitude of the charges was increased.

The conclusions drawn by some investigators concerning the effect of certain vapours on the aggregation of aerosols are often diametrically opposed to the experimental observations of other investigators. Smirnov and Solntseva[4] report the effectiveness of water vapour and butyric acid as aggregants for an ammonium chloride aerosol, but Samokvalov and Kozhukhova[5] state that water and octyl alcohol in low concentrations act as stabilizers, rather than aggregants, for ammonium chloride. Samokvalov[6] suggests that if the vapour of a substance with a high dipole moment is introduced into a nonpolar medium such as air, the polar substance undergoes oriented adsorption on the dispersed particles and thus stabilizes the dispersion. Radushkevich and Chugunova[7] have found that the rate of coagulation of an ammonium chloride aerosol was reduced by phenol, and was unaffected by methyl alcohol, ethyl alcohol and oleic acid. Petryanov and his co-workers,[8] however, report that phenol vapours had no effect on the aggregation of a ferric oxide aerosol. Fujitani[9] found, by measuring the sedimentation velocity, that a fog produced from an aqueous ammonium chloride solution was stabilized by acetone while carbon tetrachloride acted in the opposite way. Although some of the apparent discrepancies have been traced to differences in experimental technique, it is obvious that many of the phenomena require further study before clarity of generalized statements on aging can be realized.

The purpose of the present study was to investigate some of the aspects of aggregation with emphasis devoted to the role of electrification and to the effects of foreign vapours in the aerosol system. Because of the apparent disagreement concerning aerosol behaviour as reported in the literature, many of the results of this work, while serving as confirmation of some studies, also serve as refutation of other studies. Therefore, it is advisable to qualify present results as pertaining only to the materials and conditions employed.

ELECTRIFICATION

Before any systematic study of the effect of electrification on an aerosol's aggregation could be made, it was necessary to devise a technique which would give accurate, reproducible measurements of the nature and magnitude of the electrical charge carried by the particles and a technique with which the charge on the particles could be altered.

Apparatus for charge analysis. A variety of apparatus has been used by previous investigators. The apparatus of Wells and Gerke[10] subjected airborne particles to an alternating electrical field, thereby causing charged particles to oscillate and to move in zigzag paths when the particles were passed through the field. The results were recorded photographically. White and Hill[11] used the method of Wells and Gerke to obtain the charge on each particle from the amplitude of its vibration, but could not distinguish between positively and negatively charged particles.

The apparatus of Kunkel[1] and Kunkel and Hansen,[12] recorded photographically successive positions of individual particles settling under the influence of gravity through a horizontal electrical field. The charge on each particle was then determined from the path taken by the particle. Apart from being a tedious and time-consuming analysis for obtaining statistically precise results, the technique had one serious limitation. Small convection currents resulting from temperature differences between the wall or ends of the settling chamber could easily invalidate the results.

Gillespie[3] and Gillespie and Langstroth[13] used an

instrument in which a thin stream of particles and air were drawn in a sleeve of clean air between two parallel vertical electrodes maintained at a high potential difference. The charged particles were deposited on microscope slides placed on the inner surfaces of the electrodes, while the neutral particles passed through the apparatus and were collected in a thermal precipitator. The electric charge distribution was then obtained from a microscopic analysis of the deposits.

An instrument, though somewhat similar to the one of Gillespie and Langstroth, was developed independently in this work. It employed a stream of aerosol particles moving at a relatively slow velocity but moving at a velocity compared to which convection currents were insignificant. The behaviour of a great number of particles was analysed so that statistically acceptable results were obtained in a short time. While the apparatus to be described here was, therefore, not subject to many of the limitations of previous apparatus, it had limitations which will be discussed later.

The main component of the apparatus is shown in Fig. 1. The aerosol to be examined entered the aerosol chamber

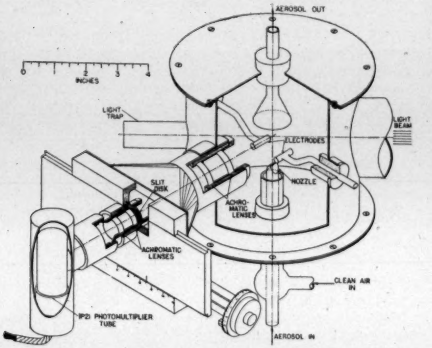

Fig. 1. Diagram of aerosol charge analyser

through a special nozzle at the bottom centre, flowed vertically upward and exhausted from the top centre. (The flow may be either upward or downward.) An upward flow has been found to be more satisfactory with very small particles, while a downward flow is better with the larger particles sizes. When a downward flow is used, the electrodes are rotated 180° about the axis of their supporting arms from their position in Fig. 1. The significant feature of the system through which the aerosol entered the chamber was a slit orientated so that the narrowest dimension of the resulting stream (approximately 0·5 mm) was presented to an observation port. Electrodes were located so that the electrical field, when established, was at right angles to this plane of observation. A collimated beam of light entered the chamber horizontally through a port located at angles of 45° and 135°, respectively, with the plane of the electrodes and the plane of observation. A light trap was provided 180° from the port through which the light entered. The interior of the chamber was blackened to eliminate light reflexions. In early models, a camera was mounted at the observation port, and the deflexions of the particle stream were recorded photographically. In later models, a twice-magnified image of a small horizontal section of the particle stream was formed by a lens system in the observation port at the plane of a movable vertical slit. The slit was 0·1 mm wide. An image of the slit was in turn formed on the sensitive element of a 1P21 photomultiplier tube. The output of the photomultiplier tube registered on a meter. Moving the photomultiplier tube across the plane of observation and noting the meter readings constituted one determination.

A stream having an elongated cross-section was used so that, from the position of observation, the stream would appear to originate from a narrow zone and yet would contain sufficient particles to produce a bright image when dispersed by the electrical field. A stream of clean air flowing at about the same rate surrounded the aerosol stream. By preventing the stream's coming into contact with the stagnant body of air in the chamber, this sheath of air prevented the spread of the particle stream when there was no electrical field. When the electrical field was energized, the surrounding sheath of air acted as a zone into which charged particles might move without undergoing change in vertical velocity. The electrodes were shaped and located as shown in the figure to avoid interference with the light field. They were also polished to eliminate sharp points and edges.

The major pieces of auxiliary equipment were a high voltage source, a pump and a power supply for the photomultiplier tube. The high voltage supply used in this work was capable of generating a potential difference between the electrodes from 0 to 20 000 V, and was constructed so that, when one electrode was positive, the other was negative by the same amount. Gradients between the electrodes of about 4000 V/cm were generally employed. The pump was obtained from George A. Thiberg, Cedar Knolls, N.J., and was originally designed for the aeration of small fish ponds. It was altered to provide a suction port. An ordinary microscope lamp provided the illumination. Since the pieces of auxiliary equipment are either commercial items or may be built according to standard circuits from commercially available components, further discussion of them is not required.

Technique of charge analysis. This description will suppose a smoke, e.g. tobacco smoke, has been generated and is contained in some sort of reservoir.

Obtaining the proper smoke flow rate and a compatible flow of pure air in the sheath to give laminar flow conditions of the desired magnitude through the analysing chamber sometimes requires rather careful adjustment. Hence, it has been found advantageous to employ a pump having an adjustable pumping rate and also to provide a by-pass valve. The pump, as used in this investigation, provided a slight suction and was, therefore, attached so as to exhaust the analysing chamber. Additional valves were provided on the line between the smoke reservoir and the analysing chamber and on the air sheath inlet. It was found expedient to remove the photomultiplier tube (including the housing and the slit) while adjusting the flow so that the effect of each adjustment could be visually observed.

After a sharply defined smoke stream had been obtained and while the stream was being viewed, the voltage on the electrodes was increased until the desired spreading of the smoke resulted. The spreading employed was that which would not produce appreciable corona discharge and which would give maximum separation of the smoke without causing the stream to disperse to such a degree that large parts of it became faint. A spreading of the original smoke stream to ten times its original width was regarded as the minimum necessary to give adequate resolution. When the instrument was thus adjusted for measurements, the photomultiplier tube was put in place.

Making the measurement merely required moving the photomultiplier tube across the image of the smoke stream with the electrical field energized and recording the photomultiplier tube output as a function of position. These data were then plotted. When the smoke stream appeared as it is shown in the lower half of Fig. 2, a curve such as shown in Fig. 3 resulted. Scanning the negative, from which the print of Fig. 2 was made, with a photodensitometer gave a

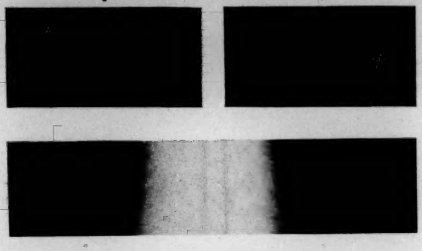

Fig. 2. Behaviour of tobacco smoke particles, above, passing through no electrical field, and, below, passing through a gradient of 5000 V/cm

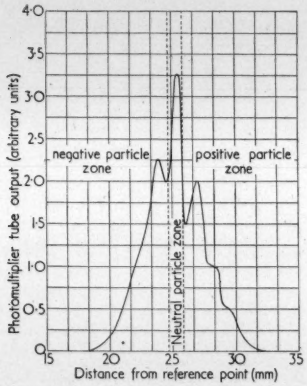

Fig. 3. Distribution of the charges on tobacco smoke particles

similar curve. Generally, curves having a single mode were obtained; the significance of the multimodal curve is discussed later.

Results of charge analysis. Before a curve, such as that given in Fig. 3, can be used, several factors need to be considered. First, is the charge on the particles changed by friction with the tube or nozzle wall or is it changed by passage through the electrical field? Charging due to the friction of passage through ducts appears to depend directly on particle velocity.[14] Since low aerosol velocities (of the order of 1–3 cm/sec) were used through all conduits, an appreciable generation of charges because of friction was quite improbable. Rapid charging of particles in an electrical field occurs when corona discharge takes place, but the voltage gradient was kept below that giving significant corona discharge. Such voltage gradients were found satisfactory for spreading the aerosol. The conclusion was reached that the apparatus and the method of analysis do not change the charge distribution of the aerosol particles when proper care is exercised. This conclusion was verified by examining a stearic acid smoke generated by the method of La Mer.[15] Nearly all of the particles of such a smoke have been shown by White and Hill[11] to be uncharged at generation. They were found to be almost completely uncharged when analysed with the apparatus described here.

The second factor requiring consideration is the effect of multiple light scattering, i.e. is the light scattered in a particular direction by the smoke equal to the sum of the light scattered by the individual particles in that direction? According to Sinclair,[16] particles scatter light essentially independently of one another when the distance between the particles is 100 times the radius of the particles. This condition is fulfilled by a smoke having particles with a radius of 1 μ and a number concentration of 10^6 particles/cm^3, a rather dense smoke. While this effect fixes an upper acceptable concentration, the concentration is so great that little limitation is imposed.

The 1P21 photomultiplier tube gives a very nearly linear electrical response to radiation in the range of white light. Therefore, a curve such as Fig. 3, if it had been obtained for a monodisperse smoke, would represent the charge distribution of the smoke. When monodispersity does not exist, the curve obtained affords a measure of the fraction of the particles charged negatively, the fraction charged positively and the fraction neutral. The apparatus is regarded as capable of giving such results within an error of $\pm 5\%$. Figs. 2 and 3 present results obtained with tobacco smoke. Classification of the particles on the basis of electrical charge into three rather distinct groups is evident. It is further evident that one group of particles did not deviate from its course, while the other groups moved to the right and to the left, leaving, in this particular case, a zone of largely free space between themselves and the neutral, central zone.

Complete analysis of the charge associated with the aerosol particles entails consideration of several factors. The amount of lateral deflexion of a particle, in the system described, is a function of the mass of the particle, the charge, the field strength and the flow rate of the aerosol stream through the electrification chamber. An analysis of the electrical field between cylindrical electrodes has been summarized by Harnwell.[17] If the boundary conditions imposed by the design of the apparatus and by the experimental technique are applied, an expression may be derived which relates the deflexion of the particle passing through the field to the charge of the particle. Thus,

$$x = \frac{(1{\cdot}6 \times 10^{-12})Vq}{6\pi\mu r V_0 w}\left(\tan^{-1}\frac{2y_1}{c} + \tan^{-1}\frac{2y_0}{c}\right) \qquad (1)$$

where x = horizontal deflexion of particle, cm
v = potential difference, V
q = charge of particle, electrons
μ = viscosity of medium, P
r = particle radius, cm
V_0 = vertical velocity of particle, cm/sec
y_1 = vertical distance from plane of electrodes to point of observation, cm
y_0 = vertical distance from aerosol inlet to plane of electrodes
$w = \ln c/2b + 1/2\,(c/b)^2 - 4$
c = separation between electrode centres, cm, and
b = electrode radius, cm

The minimum deflexion, determined from the width of the relatively dark space between the central stream and the charged particle area in Fig. 3, corresponds to tobacco smoke particles with a maximum diameter of the order of 0·6 μ, carrying charges of one electron. This result is in agreement with the data of several investigators who found that the charge carried by those particles which are charged is roughly proportional to surface area, and that very small particles seldom carry multiple charges. According to equation (1), an electrified smoke perfectly homogeneous with respect to particle size would give a curve exhibiting a series of maxima and minima in the charged particle area, each peak corresponding to a different multiple charge on the particle. Therefore, the departure from this predicted peaked curve to a curve showing only a hint of multimodality indicates non-homogeneity of particle size. Calculations by equation (1) may be based on a median particle size, thus permitting estimations of the fractions of particles carrying multiple charges, but the accuracy of the estimation depends upon the deviation of the distribution of particle sizes from the median value. For the tobacco smoke aerosols used in the present study, it was found that the deflexion from the central stream to the peak of the curve in the charged particle area corresponded to singly charged particles from 0·1 μ to 0·25 μ in diameter. This result, in excellent agreement with the observations of Gibbs,[18] Sinclair[16] and others on the size of tobacco smoke particles, is evidence that the relatively clear zone between neutral and charged particle areas arises because these charged particles must carry at least a single electronic charge.

Equation (1) has been used to calculate the average charge carried by particles in several different aerosols. The results are summarized in Table 1. Table 2 presents data obtained on the fractions charged and uncharged of a number of aerosols.

The multiple charges carried by magnesium oxide particles may be attributed to the violent reactions which occur during the combustion of magnesium ribbon. It is interesting to note that the average charge of clay particles is essentially the same value reported by Kunkel[1] for a quartz dust of corresponding particle size. The charges on particles in a certain aerosol were found to increase somewhat more slowly than the surface area, as in Kunkel's studies. Gillespie,[3] however, found that the charge on a particle increased as the diameter increased. The results showing that generally a single electronic charge is carried by the charged particles in aerosols formed with the La Mer generator confirms the work of White and Hill.[11]

Apparatus for charge alteration. To investigate the effect of electrical charge on the aggregation of aerosol particles, it was necessary to devise a means for changing the charge, so that measurements could be made on the original and the altered aerosol. Several methods were investigated, including the corona discharge technique of La Mer,[20] and irradiation was found to be the most satisfactory method for the charging of aerosol particles. In the present investigation, the aerosol to be charged was passed through a tube containing either radioactive polonium or radium. The aerosol particles passing through the ionized zone about the radioactive source picked up both positively and negatively ionized air molecules and became charged.

Table 1. *Electron charge on aerosol particles soon after generation*

Aerosol	*Method of formation*	*Particle diameter*	*Particle charge*
Tobacco smoke	Burning	0·1–0·25 μ	1–2 electrons
Magnesium oxide	Burning	0·8–1·5	8–12
Clay	Elutriation	2–4	20–40
Stearic acid	La Mer generator	0·2	1
Ammonium chloride	La Mer generator	0·2	1
Ammonium chloride (irradiated)	La Mer generator	0·2	1–3
Ammonium chloride	Atomization of an alcoholic solution	0·8–1·5	12–15

Table 2. *Electrical charge data for various aerosols soon after generation*

Aerosol	*Method of formation*	*Particle diameter*	*Fraction positive*	*Fraction negative*	*Fraction neutral*
Tobacco	Burning	0·1–0·25	40	34	26
Magnesium oxide	Burning magnesium ribbon	0·8–1·5	44	42	14
Magnesium oxide	Burning magnesium ribbon	—	48*	43*	9*
Clay	Elutriation	3–5	47	44	9
Stearic acid	La Mer generator	0·2	2	2	96
Stearic acid	Low-temperature volatilization	—	3*	4*	93*
Ammonium chloride	La Mer generator	0·2	2	2	96
Ammonium chloride	Low-temperature volatilization	—	—	—	95*
Ammonium chloride	Dispersed from alcoholic solution by atomizer	0·8–1·5	40	40	20
Ammonium chloride (irradiated)	La Mer generator	0·2	26	25	49
Sugar	Dispersed from alcoholic solution by atomizer	0·8–1·5	40	39	21

* Data of Whytlaw-Gray and co-workers.[2,19]

METHODS FOR EVALUATING AGGREGATION

Characterizing the degree of aggregation is a problem in itself. Several methods for assessing aggregation might be suggested: light scattering techniques, sedimentation rate measurements, photography and microscopy. Each of the methods has certain advantages and certain limitations; therefore it was deemed advisable, whenever possible, to use

all the techniques in the final interpretation of the aggregation state.

Actually, none of these techniques is considered to be a direct measure of aggregation. Light-scattering and sedimentation-rate studies give indications which must be interpreted in terms of physical laws to determine whether such indications can be attributed to aggregation. Photographic and microscopic methods allow a visual interpretation of aggregation, but are somewhat open to question because the particles being examined are no longer a constituent of the aerosol.

Sedimentation method. Two sedimentation chambers were used to determine the rates at which aerosol particles settled out of suspension. The first was a glass cylindrical tube with brass top and bottom sections. A removable sliding section in the bottom plate of the chamber was constructed with circular slots into which glass plates were fitted. In making a sedimentation analysis, the glass plates were exposed periodically, and the quantity of particles which settled during the time interval of the exposure was determined by methods described in more detail in the following sections. The sedimentation chamber was fashioned from a glass tube having an inside diameter of 15 cm and a height of 80 cm. The glass collector plates were 7·5 cm in diameter.

The second sedimentation chamber was a cubical box constructed from transparent plastic. The length of a side was 20 in. giving it a total surface area of approximately 17 ft^2, as compared with less than 5 ft^2 for the cylindrical chamber. A circular door 12 in. in diameter was cut in one of the sides of the plastic box to permit easy access to the inside. Sedimented samples were again collected on slides 7·5 cm in diameter.

The procedure for introducing an aerosol into either sedimentation chamber varied with the aerosol being examined. Ammonium chloride aerosols were formed with a LaMer generator having a spark discharge ion source and blown directly into the sedimentation chamber through a port in the base. When the chamber had been filled with the aerosol, collector slides were put in place in the bottom of the chamber, and samples were taken after periods of 5, 15, 30, 60, 90 and 150 min and again after 24 h. The time involved in changing plates between samples was only a few seconds and was disregarded.

Magnesium oxide aerosols were formed by burning a specified amount of magnesium ribbon in a flask and transferring the contents of the flask into the sedimentation chamber. Approximately 2 min were required to burn the ribbon and transfer the smoke to the sedimentation chamber, after which samples were collected as described above.

When the effects of electrical charge were being investigated, the aerosol was passed over the radioactive source before being introduced into the chamber.

The effect of vapours on the sedimentation rate of aerosols was determined by introducing the vapour and the aerosol into a sedimentation chamber and measuring the amount of aerosol settled with time by the chemical methods to be described. In the case of an ammonium chloride smoke formed continuously with the La Mer generator, the main aerosol stream was mixed with a diluent air stream which was introduced either directly or after passage through a gas-washing bottle containing the liquid whose vapour was to be investigated. Thus, by controlling the flow rates of the various streams, it was possible to subject an aerosol to atmosphere varying from one nearly void of any vapour to one nearly saturated. Because the formation of magnesium oxide aerosols by burning was an intermittent process, the vapours to be investigated in this case were applied in a different manner. The magnesium oxide smoke resulting from the burning of a specified amount of ribbon was collected in a large flask and blown with dry air into the sedimentation chamber, where the atmosphere had been previously conditioned with the desired vapour. Generation of this vapour was accomplished by vaporizing a quantity of liquid, calculated to bring the atmosphere of the chamber to the desired relative saturation, in a small heating tube located in the sedimentation chamber.

Because electron photomicrographs of aerosol particles, in various stages of aggregation, showed the greatest effect with propylene glycol and water vapour, these two substances were emphasized in the sedimentation studies.

Methods of analysis. Sedimentation experiments have been conducted with aerosols of magnesium oxide and ammonium chloride. Since the samples taken in the analyses were very small in quantity, chemical methods were employed to obtain quantitative results. In addition, electron photomicrographs were taken of samples of the settled particles. When magnesium oxide was being investigated, the magnesium content of a sample was determined by the versenate technique which consists essentially of the following analytical steps: first, dissolving in hydrochloric acid the sample which has been collected; next, adjusting the pH of the solution to 10 with ammonium hydroxide; and finally, titrating with versenate (solution of the disodium salt of tetra-acetic acid), using Eriochromeschartz T as the indicator. The amount of ammonium chloride settled in an increment of time was determined through measurements of the chloride content by Fajan's method. This technique consists of dissolving the sample in distilled water and titrating with a silver nitrate solution, using dichlorofluorescein as the indicator. A silver nitrate solution approximately one-hundredth normal has been found suitable as the titrating reagent. With the versenate technique, the end point is evidenced by the change of the solution from a pink to a blue colour, while with Fajan's method, the end point is evidenced by the sudden change of the solution from colourless to red or rose.

Light scattering method. While difficulties are encountered in generating an aerosol having the same characteristics, e.g. particle size, distribution, concentration, etc., from one day to the next, it is relatively easy to generate an aerosol having constant characteristics for a few minutes. The principal advantage of the light-scattering technique used by these investigators lay in the fact that results were indicated in a matter of minutes. Analysis of the data depended on an interpretation of the Tyndall meter measurements in conjunction with electron photomicrographs of precipitated samples. This system was used primarily for the purpose of estimating the effect of foreign vapours on an aerosol's behaviour and was found to be quite sensitive to such effects.

Aerosols formed with the La Mer generator were used in this method. The principal components of the system included, in addition to the generator, a Tyndall-meter with a light scattering chamber, an aerosol mixing chamber, wet- and dry-bulb thermometers, a chamber where foreign vapours might be introduced into the aerosol stream, and a thermal precipitator.

The Tyndall meter and auxiliary light-scattering chamber were designed to permit direct mounting of the chamber on a spectrometer tripod. The photocell was mounted in the normal position of the telescopic eyepiece, and a microscope projection lamp served as a light source. Fluctuations of voltage to both the light source and phototube circuits of the Tyndall meter were minimized through the use of a voltage

stabilizer. A spherical 5 litre flask provided a suitable aerosol reservoir and chamber where mixing between the aerosol and foreign vapours could take place. Contact of foreign vapours with the air stream was generally accomplished by bubbling the air through a porous plate immersed in the liquid whose vapours were to be investigated. The thermal precipitator was provided with a special aerosol inlet so that samples could be taken directly from the aerosol stream issuing from the light-scattering chamber. The aerosol stream at the point of leaving the condensing column of the La Mer generator was diluted immediately with a stream of dry air, and was then diluted a second time just prior to entering the aerosol mixing chamber. This design permitted the introduction of either pure air or vapour-laden air at the second dilution point, while the first dilution ensured an aerosol sufficiently dispersed to be quite stable. Vapours in the desired concentration could be introduced into the main aerosol stream of constant particle concentration by adjusting the flow rates in the various diluent streams. A wet- and dry-bulb thermometer in the exit stream indicated the relative saturation at all times. All tubes were made as short as possible. In general, the only agitation in the mixing chamber was produced by the turbulence of the incoming and outgoing aerosol streams. The stream leaving the mixing chamber was passed through another small chamber where a light beam was partially scattered by the aerosol particles. The scattering (at an angle of 140° with the incident light beam) was detected by the phototube and indicated by a microammeter.

A change in the light scattered by the aerosol because of the presence of the vapour was clearly apparent about 6 min after introducing the vapour. Calculations showed that this time interval is sufficient for the vapour-laden atmosphere to replace most of the former contents of the mixing chamber. In air devoid of aerosol, the contribution of vapour to scattering was undetectable; therefore the change in scattered light was believed to be related to aggregation. This matter will be discussed further in a later section. Since only a short period of time was required to obtain the indication, the limitation of time-consuming measurements was avoided; that is, the probability of a change in the aerosol due to causes other than those resulting from the introduction of vapour or other change was small.

Determinations of the effect of the change in question were made by recording the scattered light intensity before, during and after the change. Electron micrographs were taken of the aerosol particles from a dry atmosphere (relative humidity less than 5%) and from a vapour-laden atmosphere. The thermal precipitator was used to obtain samples of the aerosols for the electron microscope studies.

Vapours of water, propylene glycol, glycerol, methanol, ethanol, phenol, carbon tetrachloride, oleic acid, acetic acid, 5% sodium chloride solution, 30% ferric chloride solution and nitrobenzene were tested on aerosols of ammonium chloride, propylene glycol, stearic acid, β-napthol and tin chloride. In most cases, the relative saturation of the vapour in the system was kept at 40%, though the actual concentration of the foreign vapours in the aerosol differed widely because of the differences in vapour pressure (higher vapour pressures meaning greater concentration).

Calculations for ammonium chloride particles and light from a tungsten filament lamp, using a publication of the National Bureau of Standards,[21] indicate that aggregation of an aerosol whose individual particles are less than 0·75% in diameter would increase the light-scattering power of the aerosol until the diameter of the particles exceeded about 0·75 μ. The particles of the ammonium chloride aerosols used in this study had a mean diameter of about 0·22 μ, and all of the other aerosols exhibited average particle diameters smaller than 0·5 μ. Since the vapour itself produced no measurable light scattering, the increased scattering in the presence of the aerosol particles could either be attributed to (1) particle growth as a result of the adsorption of the vapour, (2) particle aggregation, or (3) to a changed scattering effectiveness of the particles due to vapour adsorbed on their surfaces.

The growth of the particles in humidities of the magnitude employed seems to be so small as to be quite insignificant. For example, calculations according to the method of Neiburger and Wurtele[22] showed that an ammonium chloride particle with a diameter of 0·22 μ in a dry atmosphere would grow to 0·23 μ in an atmosphere of 40% relative humidity. The possibility of a change in scattering action due to a change in the humidity of the air about aerosol particles was investigated. A tiny glass rod with small ammonium chloride crystals stuck on it was mounted in the light-scattering chamber in such a way that a light beam played on the crystals and some of the scattered light was picked up by a phototube. It was found that wide relative humidity changes (between 30 and 80%) produced no measurable change in the amount of light scattered. Indications from the light-scattering portion of this investigation are therefore strong that aggregation of the aerosol particles was the principal result of the vapours in many cases. In general this was borne out by electron micrographs of aerosol particles collected from the various vapours.

The greatest aggregation found was that produced by water vapour and an aerosol of ammonium chloride. This result is probably explained by the mechanism suggested in the recent studies of Fedoseev, Manakin and Domentianova[23]; i.e. substances which lower the vapour pressure of the aerosol constituent can significantly increase the collision probability by removal of the vapour cushion surrounding a particle. That is, ammonium chloride, being hygroscopic, causes the water molecules to be less in number near each ammonium chloride aerosol particle than in the main body of the air, which results in a somewhat reduced pressure in the vicinity of the particles and makes it somewhat easier for two particles to collide.

Light-scattering measurements indicated that propylene glycol also increased the aggregation rate of ammonium chloride particles, but this was contradicted by sedimentation studies. How this situation will eventually be resolved is not known; however, great differences in the packing of aggregates have been observed and this fact may contribute to the solution. It is probable that a loosely packed aggregate, while settling slowly, would scatter light differently from a tightly packed aggregate which would settle relatively rapidly.

The effect of electrical charges on the aerosol particles is uncertain from light-scattering measurements, probably because the slope and tightness of the aggregates must again be considered.

RESULTS

Little change in the charge distribution of a magnesium oxide aerosol (charged by thermal emission in the process of generation) was evident after the aerosol had aged in the presence of radioactive polonium. This result may be explained on the basis of the random charging by the air ions resulting from α-radiation, i.e. a particle, whether charged or not and whether charged positively or negatively, is about as likely to pick up a positive as a negative ion. On the other hand, approximately half the particles of an

ammonium chloride aerosol generated with a La Mer generator, and hence essentially uncharged, became charged after being subjected for a short time to the α-radiation of the polonium. Subsequent experiments showed that ammonium chloride aerosols could be charged by passage near either the polonium of radium sources and that, in contrast to corona discharge methods, deposition on the tube walls about the radioactive source was insignificant. Only one or two electronic charges were picked up by the charged particles, however, so that although a large fraction of the particles became charged, the magnitude of the charge was small.

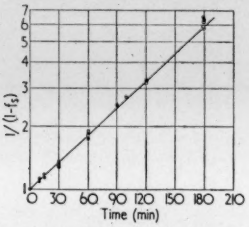

Fig. 4. The sedimentation of charged and uncharged ammonium chloride particles

● = uncharged; ○ = charged by irradiation.

The sedimentation of ammonium chloride aerosols, uncharged and charged by radioactive means, was measured, and results are presented in Fig. 4. It is evident that the fraction of ammonium chloride aerosol settled at any particular time was not measurably changed by charging the particles. It is interesting to note that although the sedimentation rates of the uncharged and the charged ammonium chloride aerosols were equal, the shape of the charged particle aggregates differed markedly from the shape of the uncharged aggregates. The aggregates of charged particles showed a pronounced tendency to be oriented in a chainwise fashion, indicating polarization, while the aggregates of uncharged particles showed more random packing. Photographs of settled samples of uncharged and charged ammonium chloride particles are given in Fig. 5. From a number of such photomicrographs it was possible to compare the number of particles joined in an aggregate for the cases of the charged and uncharged aerosols. These results are presented in Fig. 6. Whytlaw-Gray[2] also found that charging had no

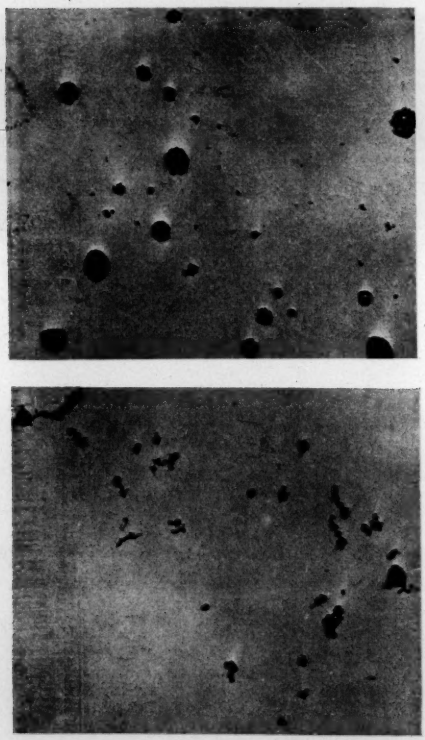

Fig. 5. Photomicrographs of aggregated ammonium chloride particles. *Above:* aggregates of uncharged particles; *below:* aggregates of charged particles

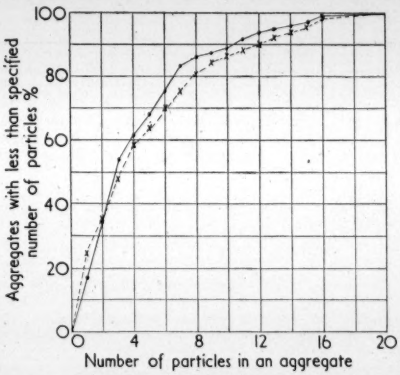

Fig. 6. Comparison of the number of particles comprising an aggregate for uncharged and charged ammonium chloride aerosols

● = charged; × = uncharged.

effect on the aggregation of aerosol particles. Gillespie,[3] however, studying larger particles with much greater charges, found the aggregation rate to be increased as the charging was increased. Light-scattering measurements as conducted in this investigation indicated a possibility of a small degree of aggregation. The measurements were quite sensitive. However, in the case of the sedimentation measurements as well as in light-scattering work, the shape of the aggregate may have had more effect than the degree of aggregation.

The effect of vapours on the sedimentatjon of magnesium oxide and ammonium chloride aerosols is shown in Fig. 7.

In the figure, the ordinate is a function of the fraction settled, f_s. It appears that in both cases the sedimentation rate is increased by the presence of water vapour and reduced by the presence of propylene glycol vapours. To clarify the relationship between sedimentation rate and aggregation, electron microscope slides were placed in the bottom of the sedimentation chamber, and samples of the aerosols were taken at various times. The aggregates of magnesium oxide particles in a humid atmosphere appeared to be more compact and dense than the dry aggregates, and hence would be expected to settle faster. Aggregates in an atmosphere of propylene glycol also appeared to be more compact than the dry aggregates and, on that basis alone, would be expected to settle faster than the dry aggregates. Close examination

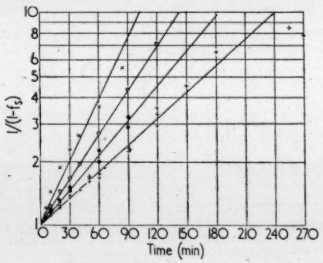

Fig. 7. The sedimentation of a magnesium oxide aerosol in various atmospheres

× = 98% R.H.; ○ = 80% R.H.; • = dry; + = 98% saturated with propylene glycol.

of the electron micrographs showed that there were more small, discrete aggregates in the case of the propylene glycol atmosphere. Since from Stokes' law the terminal settling velocity is proportional to the square of the diameter, it follows that, on the basis of size, the magnesium oxide aggregates in the presence of propylene glycol vapours would settle at a slower rate, the result which was determined experimentally. Measurements with the aerosol charge analyser have shown that the presence of water vapour or propylene glycol vapour has no effect on the charge distribution of either a magnesium oxide or an ammonium chloride aerosol. Further clarification of this effect is necessary, since it appears that these may be a change in the effective density of the aggregates. As Whytlaw-Gray[2] points out, many aggregates contain pockets of occluded air, which effectively lowers the density of the clumps, leading to slower settling rates. The recent studies of Artemov[24] describe the influence of vapours on the shape of aggregates and the effect of particle shape and sedimentation rate. It is interesting to note that this same investigator, Artemov,[25] had stated earlier that foreign vapours have no effect on aggregation and that contrary data are due to errors of technique. In addition to a possible relation between particle shape and sedimentation rate, the shape of a particle influences the light-scattering properties of an aerosol. Further, adsorbed vapours, or increased particle size due to certain atmospheres, also effect the light scattering. Fig. 8, for example, shows the effect of water vapour on the light-scattering characteristics of an ammonium chloride aerosol and the effects of some other changes to the aerosol system. In the case of ammonium chloride, electron micrographs have indicated that such changes in the light scattering were largely the result of aggregation.

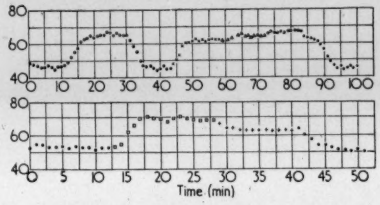

Fig. 8. Effect of variation in the method of generating an atmosphere of 40% R.H. on light scattered from an ammonium chloride aerosol

• = dry aerosol; ○ = diluent air bubbled through cold water; × = diluent air passed over hot water; △ = diluent air bubbled through hot water; □ = diluent air bubbled through water; + = diluent air bubbled through water and octyl alcohol.

CONCLUSIONS

As noted elsewhere, the literature reveals many cases of apparent disagreement concerning aerosol behaviour. Because of this discord, many of the results of this work, while serving as confirmation of some studies, also serve as refutation of other studies. Therefore, it is necessary to qualify most of the following conclusions as pertaining only to the materials and conditions employed in the present work.

(1) The ultimate or "equilibrium" electrification of aerosol particles is a function of the particle size. That is, the magnitude of the charge carried by an aerosol particle apparently increases roughly as the diameter increases.

(2) The shape of aggregates of aerosol particles is related to the electrical charge carried by the particles. Charged particles showed a pronounced tendency to form chain-like clumps or groups suggesting polarization, while aggregates of uncharged particles exhibited more random clumping.

(3) Electrification, in the degree attained by the charging methods employed and by the natural ionization of the atmosphere, is of minor importance in the aggregation of an aerosol. The sedimentation rate of an aerosol was unchanged by charging the particles, and the light-scattering measurements showed only a slight change, a part of which was possibly due to a change in the shape of the aggregates rather than to change in their size as determined by sedimentation.

(4) The effect of electrification on aggregation has not been clearly distinguished from the effect on the shape of the aggregate. Since aggregation, sedimentation rate and light scattering are all affected by the shape of the particles, it is necessary to examine the effect of particle shape on the methods of aggregation measurement (sedimentation, light scattering) before assessing any effects on the aggregation process itself.

(5) The charge-analysing apparatus developed in this work affords a convenient and rapid measure of the degree of an aerosol's electrification.

(6) Some vapours change the aggregation rates of certain aerosols, as evidenced from sedimentation and light-scattering measurements in conjunction with electron micrographs. The particular influence of the vapour depends on the aerosol system and the nature of the vapour; at present there is little information upon which accurate predictions can be made

regarding the degree or type of influence, e.g. aggregation or stabilization. Recent studies, however, indicate that substances which lower the vapour pressure of the suspended particles increase the probability of collision by removal of the "vapour cushion" surrounding a particle.

REFERENCES

(1) KUNKEL, W. B. *J. Appl. Phys.*, **21**, p. 820 (1950).
(2) WHYTLAW-GRAY, R., and PATTERSON, H. S. *Smoke* (London: Edward Arnold and Co., 1932).
(3) GILLESPIE, T. *Porton Tech. Paper No.* 289 (1952), Chemical Defence Experimental Establishment, Porton, Wilts., England.
(4) SMIRNOV, L. V., and SOLNTSEVA, V. H. *Colloid J.* [*U.S.S.R.*], **4**, p. 401 (1938).
(5) SAMOKVALOV, K., and KOZHUKHOVA, O. S. *J. Phys. Chem.* [*U.S.S.R.*], **8**, p. 420 (1936).
(6) SAMOKVALOV, K. *J. Phys. Chem.* [*U.S.S.R.*], **10**, p. 489 (1937).
(7) RADUSHKEVICH, L. V., and CHUGUNOVA, O. K. *J. Phys. Chem.* [*U.S.S.R.*], **15**, p. 811 (1941).
(8) PETRYANOV, I. V., and co-workers. *J. Phys. Chem.* [*U.S.S.R.*], **12**, p. 34 (1938).
(9) FUJITANI, V. *J. Chem. Soc.* [*Japan*], **73**, p. 817 (1952).
(10) WELLS, P. V., and GERKE, R. H. *J. Amer. Chem. Soc.*, **41**, p. 312 (1919).
(11) WHITE, L., and HILL, D. G. *J. Colloid Sci.*, **3**, p. 251 (1948).
(12) KUNKEL, W. B., and HANSEN, J. W. *Rev. Sci. Instrum.*, **21**, p. 308 (1950).
(13) GILLESPIE, T., and LANGSTROTH, G. O. *Canad. J. Chem.*, **30**, p. 1056 (1952).
(14) DALLAVALLE, J. M. *Micromeritics* (New York: Pitman Publishing Co., 1948).
(15) LA MER, V. K. *Proceedings First National Air Pollution Symposium* (1949), Stanford Research Institute, Stanford, California.
(16) SINCLAIR, D. *Handbook on Aerosols*, Chap. 7. (1950), Summary Tech. Rep., Division 10, National Defense Research Committee, U.S. Atomic Energy Commission, Washington, D.C.
(17) HARNWELL, G. P. *Principles of Electricity and Electromagnetism* (New York: McGraw-Hill Book Co., Inc., 1938).
(18) GIBBS, W. E. *Clouds and Smokes* (Philadelphia: P. Blackiston's Son and Co., 1924).
(19) PATTERSON, H. S., WHYTLAW-GRAY, R., and CAWOOD, W. *Proc. Roy. Soc. A*, **124**, p. 523 (1929).
(20) LA MER, V. K., GOYER, G., GRUEN, R., and KRUGER, J. *Report NYO-514 U.S. Atomic Energy Commission*, Oak Ridge, Tennessee.
(21) *Tables of Scattering Functions for Spherical Particles* (Washington: U.S. Government Printing Office, 1949).
(22) NEIBURGER, M., and WURTELE, M. G. *Chem. Rev.*, **44**, p. 321 (1949).
(23) FEDOSEEV, V. A., MANAKIN, B. A., and DOMENTIANOVA, Z. M. *Kolloid Zhur*, **14**, p. 420 (1952).
(24) ARTEMOV, I. S. *Kolloid Zhur*, **9**, p. 225 (1947).
(25) ARTEMOV, I. S. *J. Phys. Chem.* [*U.S.S.R.*], **20**, p. 553 (1946).

DISCUSSION

Dr. C. N. Davies: Aggregation and disaggregation of colloidal solutions is controlled by the medium because this has a high dielectric constant which makes possible the establishment of an electrical double layer at the particle surface. Each particle can therefore be surrounded by a diffuse cloud of charge of the same sign which prevents the particles from approaching close enough to adhere to one another by van der Waals forces when they diffuse together.

The dielectric constant of air is too low to permit this to happen and the charge on aerosols resides on the particles. Hence aggregation is a question of particle collisions; in the vast majority of cases the charge does not have much effect.

Collisions are promoted by inertia effects such as acoustic vibration, turbulence, impingement, etc. In the absence of this factor they are due to Smoluchowski coagulation. This is independent of particle size, except for the increasing Cunningham slip effect below about 1 μ, because change in particle mobility is balanced by collision cross-section.

Coagulation depends primarily upon number concentration. If it is to be avoided the concentration of particles at the earliest moment of their existence must be kept low. As a cloud coagulates the number of particles automatically drops and aggregation ceases.

Mr. W. H. Walton: Professor DallaValle has emphasized the importance of aggregates in determining the properties of an aerosol and has pointed out that misleading results may be obtained if only the actual sizes of the constituent particles are measured. This has long been recognized in studies of the health hazard of dust clouds and has contributed to the popularity of the thermal precipitator as a standard sampling instrument in this country. When it is desired to separate dust clouds into size fractions, for example, to separate the respirable particles for chemical analysis, it is very important that the separation should be carried out on the original cloud and not after redispersal of the particles in air or in liquid. The impinger, which is widely used as a sampling instrument for air hygiene purposes in some countries, is subject to the criticism that particles which are aggregated in the air become dispersed in the liquid collecting medium before they are examined.

GENERAL DISCUSSION ON SESSION H

Mr. C. J. Stairmand: The aggregation of particles often has a profound effect on the interpretation of size analysis results. Theoretical studies might show how aggregation took place in a fluid-borne suspension, but would give little indication of the strength of the aggregates. If terminal velocities are required, great difficulty is experienced in extracting a sample and subsequently sizing the aggregates without destroying their form. Some of the clusters are extremely fragile and break up on settling on a slide, even if no centrifugal force is employed to enhance the settling rate. Clearly, the dispersed size of the fragments gives little indication of the true nature of the cluster, and in many cases direct determination of the terminal velocity in the suspended fluid under its actual working conditions is necessary. While, therefore, the work on shape factor and particle height referred to by previous speakers might be of great importance in a fundamental sense, I think that greater attention should be given to the direct determination of terminal velocities. It is important to use an apparatus which reproduces as closely as possible the actual conditions under which the particles are working. For

example, an air elutriation or sedimentation method is essential for particles suspended in gases, and water elutriation or sedimentation is essential for particles suspended in water or similar fluids.

Referring to the various papers dealing with the development of methods of size analysis, I wish to emphasize that it is most unlikely that any single instrument will be developed to deal with even the majority of dusts. Every dust has its own characteristics, and it is important to consider the precise nature of the information required before attempts are made to develop measuring instruments. Mr. Walton clearly had this in mind in developing special sampling hoods, but the point is not always borne in mind.

It is not possible to sample stagnant gases isokinetically, since the sampling velocity would be zero. It appears that there are two schools of thought on this matter, one of which maintains that sampling should be carried out at as low a velocity as possible, i.e. as near as possible to isokinetic, and the other thinks that sampling speeds far in excess of the terminal velocity of the largest particles should be employed. Could Mr. Walton offer any interim advice on this problem?

Mr. W. H. Walton: Mr. Stairmand asks how to sample in still air. If sampling is carried out at a fairly low velocity so that the effects of particle inertia can be neglected, i.e. so that the stopping distance of the particles at the sampling velocity is small compared with the aperture of the sampling instrument, then the number of particles collected by an upward facing sampling tube will be equal to the product of the cloud concentration and the volume of air sampled, plus the number of particles that would have fallen into the orifice if there had been no sampling flow. A sampling orifice with an opening in the vertical plane could also be used, in which case there would be no correction for particles sedimenting into the apparatus under still air conditions. In this case, however, care should be taken that there are no overhanging components of the sampling apparatus which will create dust shadows from which air free of particles could be drawn.

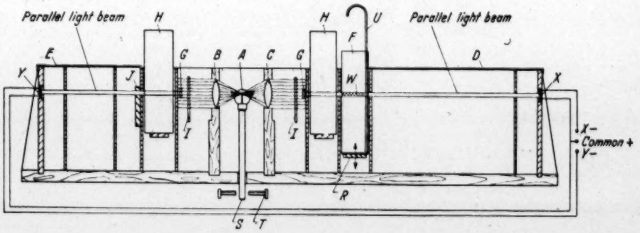

Fig. 1. Section through optical unit of photosedimentometer

A, light source; *B* and *C*, condenser lenses; *D* and *E*, top covers; *F*, sedimentation tank; *G*, infra-red absorption filters; *H*, dummy tank; *I*, optical density filters; *J*, cut-off device; *R*, adjustable platform; *S*, bulb holder; *T*, centring bolts; *U*, stirrer; *W*, illuminated volume; *X* and *Y*, photocells.

This condition would be met by a vertical sampling tube which the dust cloud entered through holes in the vertical wall. As a guide to the conditions in which inertia effects are negligible, the stopping distance of a 10 μ diameter particle of approximately unit density at a velocity of 5 m/sec is about 2 mm. The opening of a sampling system into which air is drawn at this speed should, therefore, be at least a centimetre across to avoid errors in sampling particles up to 10 μ diameter.

Mr. V. T. Morgan: The Conference may be interested in the instrument developed by Bound Brook Bearings Ltd. for the automatic recording of photo-extinction sedimentation. Fig. 1 shows diagrammatically the construction of the apparatus. A central light source produces two flat rectangular beams of light in opposite directions. The sedimentation cell (with provision for adjustment of the height of fall during settling) is placed in one of these beams. The ratio of the output of the two photocells is therefore proportional to the opacity of illuminated volume within the sedimentation cell. This ratio is measured potentiometrically on a modified industrial recorder calibrated in logarithmic units, so that a graph of optical density against time is automatically obtained.

Knowledge of the absolute size of particles is of no value in itself to industrial processes, but it is important that an accurate comparative assessment of particulate materials can be made quickly and cheaply. The recorder charts obtained from a sample of graphite having a median size of about 8 μ shows that after 45 min 96% of the sample had settled out (i.e. all above 2 μ) and for a sample of tin powder, median size 16 μ, when the tank lowering device is used, 99·5% of the sample was analysed in 28 min sedimentation. Fig. 2 shows the comparative results obtained on a sample of tin powder using the Roller air elutriator, Andreasen pipette sedimentometer, the Andrews water elutriator, and photosedimentometer described above. The curves have also been given for the fraction above 43 μ which could be tested by sieving. It will be noticed that the photo-extinction analysis gives a finer result than the other methods, but agrees reasonably well with the sieve curves upon extrapolation.

Mr. L. A. Peletier: I wish to draw attention to the air elutriation method of particle size analsyis.* The Gonell apparatus is well known, but the Bahco analyser developed in Sweden is not so well known. This apparatus, which is illustrated in Fig. 3, is a centrifugal classifier. The dust is fed through a vibrator on to a flat circular disk rotating at 3000 r.p.m. The airflow drag which is proportional to the particle size tends to force the particle to the periphery while the centrifugal force, which is proportional to the cube of the particle size, acts in the opposite direction. The larger particles will thus travel outwards and the smaller ones inwards. A fan draws an airstream from the circumference to the centre. By changing the size of the annular inlet the airspeed can be controlled and therefore the position of the "cut size," i.e. the size of the particle which is just in equilibrium under the drag and the centrifugal forces. The analyser is designed for the range 4–50 μ for a dust of unit density. We have used this apparatus in the Bureau van Tongeren N.V. in Holland for about two years and are well satisfied with its performance. An analysis takes about two hours and no special skill is required.

* Gustavsson. *Tekn. Tidskr.*, **38**, p. 667 (1948).

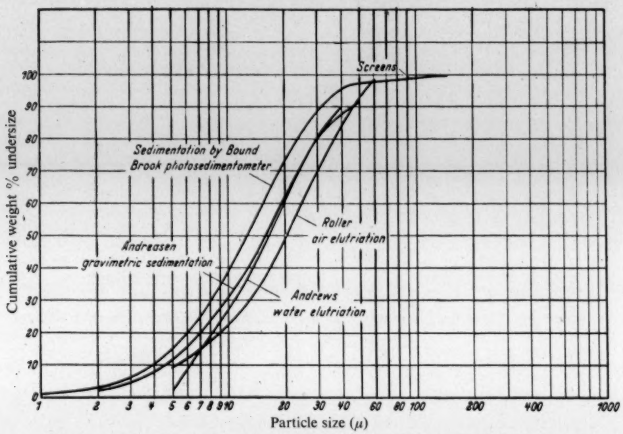

Fig. 2. Comparison of various methods of particle size analysis of tin powder

Dr. E. G. Berns: The Bahco analyser is being successfully used in several factories. It separates particles by Stokes' diameters into fractions that may be examined microscopically and analysed, for example, by projected diameter. Samples of $CaHPO_4$ were analysed by another laboratory and their results were in good agreement with ours. From

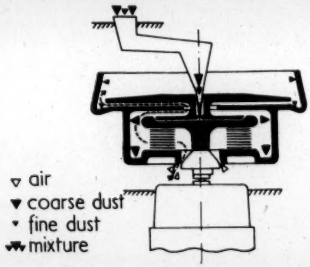

Fig. 3. Bahco particle size analyser

our microphotographs of powders, it appears that the separation of the fractions by this analyser is very good. Moreover, a change in the shape of the crystal accompanying a change of particle size can easily be observed.

Dr. J. Labeyrie: When a radioactive gas, such as radon, is diluted in very minute amounts (less than 10^{-7} c/l) in relatively dust-free air (containing less than 0·01 mg/m^3), the decay products (RaA, B, C, C′) are in the form of very fine solid particles, containing only one atom of RaA, etc., as will be observed by collecting them on nuclear photographic emulsions.

Owing to their strong electrostatic positive charge (due to the α-ray emitted from the mother product) these very fine particles move towards the walls of the vessel or of the room containing the mixture of air and radon; therefore, because an unknown fraction of these particles escapes collection, it is very difficult to measure their concentration by the ordinary methods of air filtration. On the other hand, the method of collecting these particles in an electrical field created throughout the vessel is not very practicable, because an unknown fraction of the fine particles becomes attached to the dust particles always present in the air; this attachment gives to the charged fine particles a very low mobility, and, subsequently, a quasi-total independence with respect to the electrical field.

We have carried out some experiments in order to test a method which permits quantitative measurements of the concentration of the fine particles of RaA, etc. This consists in adding to the air containing the radon a small quantity of a normal aerosol, such as iron oxide fumes (mean diameter: around 0·1 μ), which "adsorbs" the atoms of RaA, etc., and stops their migration towards the wall. After about one hour, the mixture is filtered on paper, and the filter is examined on an α-ray detecting device (proportional counter, scintillation counter, or nuclear emulsion). The experiments show that for spherical volumes of the order of 10 litres, and for a concentration of fume of the order of 1 μg/l, about 100% of the RaA produced is captured, provided that no electrical field of strength greater than about 100 V/m is present. The necessary concentration of fume for 100% capture seems to be inversely proportional to the average dimension of the volume which limits the mixture; in a room of 100 m^3, for instance, fume or fine dusts concentrations around 0·05 mg/m^3 are sufficient for the complete collection of the RaA. Because such concentrations are often spontaneously present in atmospheres, it is thus possible, by this method, to measure with some accuracy the radium A concentration (and consequently the radon concentration) in these atmospheres.

M. C. E. N. Saclay has been associated with me in this work.

Summary of conference and concluding remarks

By H. Heywood, A.C.G.I., D.Sc., M.I.Mech.E., M.I.Chem.E., Imperial College of Science and Technology, London

It is my privilege to make the concluding remarks at this Conference, and I should first like to say a little about the early developments in this field of study, which has now reached an advanced status, and indeed has attained the degree of respectability which enables it to have a history. I am not referring so much to the use of powdered materials in the Arts and Technology, which has been prevalent since prehistoric times, but to the scientific study of the fundamental properties of such materials. Possibly one of the earliest mentions of such studies is to be found in Hooke's *Micrographia* of 1665, in which he refers to observations on the molten globules obtained by striking a steel with flint, and upon the shape of sand particles—in his own words: spherical, oval, pyramidal, conical and prismatical—a remarkable anticipation of some of the present work. The real flux of scientific investigations in this field started about 1920, and the majority of the papers published during this period were written by those concerned with the practical applications of particulate materials; mining engineers, chemists, soil scientists. This would be expected, for particle size analysis is but a means to an end, and "necessity being the mother of invention" it was those who wished to know more about the properties of the materials they were handling who started measuring particle size and surface area. Many of the experimental procedures developed during this early stage were somewhat crude, though often very ingenious, and it was the fuller realization of the intricate nature of the problems involved that has brought this field of study so intimately within the scope of the physicist, who now employs all the facilities of modern science to extend knowledge of particulate materials.

The importance to science and industry of a knowledge of the properties of particulate material is shown by the succession of conferences which have been organized at intervals during the last six years. The purposes of such conferences and symposia are to take stock of existing knowledge of the subject and to present the latest developments. The organizers of the present Conference have wisely concentrated on the latter feature, and all the papers that have been presented describe researches previously unpublished.

Two new forms of equipment have recently become available or are being developed for the extension of research on fine dusts—the electron microscope and the automatic particle counting and measuring machine. These supplement the optical microscope, which for obvious reasons was one of the first methods of particle size measurement, and is still the preferred method for the minute samples of fine dust collected from the atmosphere. The limitations of the optical microscope, both as regards the smallest particle resolvable and the fact that for statistical accuracy of measurement many thousands of particles should be observed, may now be overcome by these two new developments. Sessions F and G of this Conference, devoted to electronic particle counting, represent a notable milestone in progress, and may well restore the optical microscopical method of measurement to a predominant position in certain fields of particle size analysis. Session E, on microscope techniques, produced a very keen discussion, not without some criticism of existing procedures, and showed that available instruments are not completely satisfactory in all respects. Session D on shape factors marked a revival of interest in this subject, rendered necessary in order to determine the free-falling velocity of particles from microscopical measurements. The dynamics of particle motion in air has been another very important section of the Conference. This fundamental work applies not only to dust sampling, which if ineffective vitiates the whole of the subsequent work, but also to the design of large-scale industrial collectors and the prevention of dust emission from machinery. The complexities of surface measurements and of the optical properties of dust clouds and suspensions have been brought into prominence. The study of aggregations of dust particles has also been emphasized, which is somewhat ironical, for chemists have devoted much endeavour to the effective dispersion of dust samples into a suspension of discrete particles for the purpose of size analysis. It is now realized that separated fine particles are rarely present in aerosols and that the aggregated state predominates. One field of study which has received rather scant attention at the Conference concerns the size analysis of the powdered materials which are the final manufactured product in many industrial processes. Such materials are usually analysed by sedimentation in a liquid, and perhaps it is considered that this field of study comes more into the domain of the chemist rather than that of the physicist.

The Conference Committee considered at an early stage in the organization whether any attempt could be made to standardize terms and symbols for various particle dimensions and properties. It was decided that it would have been impossible to effect this in the time available before the preparation of the papers, nevertheless, this problem will need to be solved eventually. The British Standards Institution has recently appointed committees to consider this, though I cannot state at the moment the extent of detail which will be covered as the committees have only just been formed. It is obvious, however, that the comparison of papers by different authors would be greatly facilitated if a uniform system of symbols for the various mean diameters that characterize a particle or a system of particles could be established.

Since the Conference of the Institution of Chemical Engineers and the Society of Chemical Industry in 1947 there has been a marked extension in the scope of particle size studies. We have to consider not only the health hazards due to dust in the mining and other industries, but the very large range of industries in which powdered materials are the main products or enter into manufacturing processes. Also, although particulate systems most commonly consist of solid particles dispersed in gases or liquids, it must be noted that many of the same physical principles apply to liquid drops in air—either natural mists or artificial sprays—to emulsions of one liquid in another and to small gas bubbles in liquids. Whilst the fundamental papers that have been presented at this Conference on the dynamics of particles, on surface measurements and on optical properties are of the greatest value, I think that the authors would agree that this is only the first stage of investigation, and that the second stage of applying these researches to the practical design and operation of industrial equipment is equally important. It has been mentioned in the discussion that particle size analysis methods have in many cases been developed to a degree of accuracy which is sufficient for the practical application concerned. Whilst every effort will continue to improve particle size

analysis methods, I think that the needs for the immediate future are to concentrate upon such applications.

Every industry concerned with particulate materials has its own peculiar problems, yet there are also many problems that are common to all. There is much to be gained by improving the co-operation between all the professional scientific and technical societies concerned, and this can only be accomplished by conferences such as the present one. I feel sure that the keen response to this one will encourage the organization of others at suitable intervals to promote the general study of particulate materials in the widest sense.

THE DEMONSTRATIONS

The following demonstrations of automatized particle counting and sizing machines were given in the physics laboratories (by kind permission of Prof. L. F. Bates).

ATOMIC ENERGY RESEARCH ESTABLISHMENT, HARWELL, BERKS.

Mr. E. H. Cooke-Yarborough and Mr. R. E. Whyard

Harwell automatic red blood cell counter. Red blood cells are scanned by mechanical oscillation of a microscope stage. The counting chamber is similar to those used for visual counting but is larger and unruled; it is filled with a blood sample diluted about 2500 times. Errors are minimized by use of suitable electronic circuits, by careful choice of parameters and by adopting a novel shape of scanning aperture. Consistent results are obtained which are largely independent of variations in light intensity, focus, cell size, amplifier or photocell sensitivity. The count which is displayed on a standard scaler is converted to cells per cubic millimetre by reference to a conversion table.

Mr. J. M. Hutcheon and Mr. T. Beirne

Automatic particle counter. A photoelectric particle counter has been designed for the rapid determination of the number of particles per gramme in sieved fractions of powders. The particles are drawn through a small capillary which allows them to be presented singly to a photomultiplier and by means of five interchangeable capillaries, a size range of 20–240 mesh can be counted.

A projected area measuring unit has been developed in conjunction with the particle counter to provide information for shape factor calculations. A known weight of powder is dispersed on a slide with all the particles in their most stable positions. By directing a uniform collimated beam of light perpendicular to the slide and focusing the transmitted light on to a photocell, the fraction of light extinguished by the particles is measured. From these results, the projected area per gramme is calculated.

BRITISH COAL UTILISATION RESEARCH ASSOCIATION, LEATHERHEAD, SURREY, and CASELLA (ELECTRONICS) LTD., LONDON, N.W.1

Mr. E. W. Meyer and Mr. J. H. Blackett

Slit scanning particle sizer. The machine, employing a conventional microscope arrangement, is designed to count and size particles down to 5 μ. A microscope slide is mounted on a reciprocating mechanical stage. The projected images of the particles are scanned by a slit placed in front of a photocell. A scaler records pulses passed by an amplitude discriminator. Sizing may be carried out by either track scanning or chord intercept method.

UNIVERSITY OF LEEDS, DEPARTMENT OF TEXTILE INDUSTRIES

Dr. N. H. Chamberlain

Automatic counting of neps in carded webs. Neps are small tight bunches of entangled fibres which remain as faults in an opened web after the carding process in the manufacture of textile yarns. The present apparatus is designed to estimate the number and average diameter of the neps in a given area of carded web, by mounting the specimen between two glass disks and scanning it spirally by means of a light beam of known dimensions. Photoelectronic counting, and graphic evaluation of the results obtained, enables both the number of neps present and their average diameter to be determined with an accuracy of $\pm 3\%$.

THE MULLARD RESEARCH LABORATORIES, SALFORDS, SURREY

Dr. H. A. Dell

Flying-spot arrested scan type particle sizer. The apparatus demonstrates the principles of the arrested scan technique of particle sizing. The specimen is examined by a flying-spot cathode-ray tube scanner, the motion of which is arrested on first contact with a particle. A subsidiary scan generator then causes the spot to explore the particle discovered. After exploration the spot resumes normal scanning. A memory system ensures that each particle is explored once only. Many forms of exploration are possible. The one demonstrated is that in which a chord of each particle is measured, at right angles to the normal direction of scan.

NATIONAL INSTITUTE OF AGRICULTURAL ENGINEERING, SILSOE, BEDFORDSHIRE

Mr. E. S. Trickett

Chord intercept particle sizer. The machine, comprising a scanner and analyser, sizes, by the chord or line intercept method, circular stains of insecticidal spray droplets or photographs of droplets. With the picture telegraph scanner unit exhibited, a spray pattern up to 10 in. square is scanned in about 10 min and the particles classified into 10 size grades between $\frac{1}{2}$ and 8 mm diameter.